

Series in Plasma Physics

Plasma Waves, 2nd Edition

D Gary Swanson

Auburn University, USA

IOP

Institute of Physics Publishing
Bristol and Philadelphia

© IOP Publishing Ltd 2003

All rights reserved. No part of this publication may be reproduced, stored in a retrieval system or transmitted in any form or by any means, electronic, mechanical, photocopying, recording or otherwise, without the prior permission of the publisher. Multiple copying is permitted in accordance with the terms of licences issued by the Copyright Licensing Agency under the terms of its agreement with Universities UK (UUK).

D G Swanson has asserted his moral rights under the Copyright, Designs and Patents Act 1998 to be identified as the author of this work.

British Library Cataloguing-in-Publication Data

A catalogue record for this book is available from the British Library.

ISBN 0 7503 0927 X

Library of Congress Cataloging-in-Publication Data are available

First Edition published by Academic Press, New York, 1989

Commissioning Editor: John Navas

Production Editor: Simon Laurenson

Production Control: Sarah Plenty

Cover Design: Victoria Le Billon

Marketing: Nicola Newey and Verity Cooke

Published by Institute of Physics Publishing, wholly owned by The Institute of Physics, London

Institute of Physics Publishing, Dirac House, Temple Back, Bristol BS1 6BE, UK

US Office: Institute of Physics Publishing, The Public Ledger Building, Suite 929, 150 South Independence Mall West, Philadelphia, PA 19106, USA

Typeset in L^AT_EX 2_E by Text 2 Text, Torquay, Devon

Printed in the UK by MPG Books Ltd, Bodmin, Cornwall

Contents

Preface to the first edition

Preface to the second edition

Acknowledgements

Acronyms

1 Introduction

1.1 Properties of plasmas

 1.1.1 Unmagnetized plasmas

 1.1.2 Magnetized plasmas

 1.1.3 Thermal plasmas

1.2 Plasma wave applications

 1.2.1 Plasma waves in ionospheric physics

 1.2.2 Plasma waves in astrophysics

 1.2.3 Plasma waves in magnetized fusion plasmas

 1.2.4 Plasma waves in laser-produced plasmas

1.3 Review of electromagnetic wave propagation

 1.3.1 The Maxwell equations

 1.3.2 Properties of the Helmholtz equation

 1.3.3 Conservation laws for electromagnetic fields

 1.3.4 Conservation laws with Fourier amplitudes

 1.3.5 Methods of geometric optics from WKB theory

1.4 Statistical mechanics of plasmas

1.5 Overview of the plasma wave zoo

2 Waves in a cold uniform plasma

2.1 The cold plasma dispersion relation

 2.1.1 Equations of motion

 2.1.2 Cold plasma dielectric tensor

 2.1.3 Forms of the dispersion relation

2.2 The CMA diagram

 2.2.1 Principal solutions—parallel propagation

 2.2.2 Principal solutions—perpendicular propagation

- 2.2.3 CMA boundaries—cutoffs and resonances
- 2.2.4 Wave normal surface topology—spheroids and lemniscoids
- 2.2.5 Labeling—left and right, ordinary and extraordinary
- 2.2.6 The CMA diagram for a one-ion species plasma
- 2.3 Phase and group velocity in three-dimensions
 - 2.3.1 The one-dimensional case
 - 2.3.2 The three-dimensional case
 - 2.3.3 Group velocity surfaces
- 2.4 $\omega(k, \theta)$ dispersion surfaces
 - 2.4.1 Underdense case, $\omega_p/\omega_{ce} = 0.32$
 - 2.4.2 Overdense case, $\omega_p/\omega_{ce} = 3.2$
- 2.5 Examples of propagation at arbitrary θ
 - 2.5.1 Low frequency waves
 - 2.5.2 Intermediate frequency waves—whistlers
- 2.6 Faraday rotation
 - 2.6.1 High frequency limit—region 1
 - 2.6.2 Low frequency limit—region 13
- 2.7 Plasma interferometry
 - 2.7.1 Detecting the signal
 - 2.7.2 Interpreting the signal when $\omega \gg \omega_p$
 - 2.7.3 Interpreting the signal when $\omega \sim \omega_{p0}$
- 2.8 Electrostatic waves
 - 2.8.1 Validity conditions for the electrostatic approximation
 - 2.8.2 Lower hybrid waves
 - 2.8.3 Resonance cones
- 2.9 Particle motions near resonance
 - 2.9.1 Lower hybrid resonance (high density case)
 - 2.9.2 Upper hybrid resonance
 - 2.9.3 Cyclotron resonances

3 Waves in fluid plasmas

- 3.1 Moments of the distribution function
 - 3.1.1 The moment equations
 - 3.1.2 Longitudinal plasma oscillations from the moment equations
- 3.2 The fluid equations
- 3.3 Low frequency waves
 - 3.3.1 The low-frequency dispersion relation
 - 3.3.2 Stringer diagrams of the LFDR
 - 3.3.3 Approximate dispersion relations and transitions
 - 3.3.4 Parallel and perpendicular propagation
 - 3.3.5 High frequency waves
 - 3.3.6 Summary of fluid waves
- 3.4 Partially ionized plasmas and collisions

- 3.4.1 Neutral collisions
 - 3.4.2 Electron–ion collisions
 - 3.5 Amplifying waves and instabilities
 - 3.5.1 Classification of instabilities
 - 3.5.2 Streaming instabilities
 - 3.6 Power and energy flow in fluid plasmas
- ## 4 Kinetic theory of plasma waves
- 4.1 The basic equations
 - 4.1.1 The Boltzmann equation
 - 4.1.2 Collisions and the Fokker–Planck equation
 - 4.1.3 BBGKY theory
 - 4.1.4 The Vlasov equations
 - 4.2 Waves in a thermal, unmagnetized plasma
 - 4.2.1 Vlasov method
 - 4.2.2 Landau solution
 - 4.2.3 A Physical picture of Landau damping
 - 4.2.4 Conventional descriptions of Landau damping
 - 4.2.5 Ion acoustic waves and ion Landau damping
 - 4.2.6 Effects of collisions on Landau damping
 - 4.3 Waves in a magnetized hot plasma
 - 4.3.1 The evolution of the distribution function
 - 4.3.2 Integrating along the unperturbed orbits
 - 4.3.3 General $f_0(v_\perp, v_z)$
 - 4.3.4 Maxwellian distributions
 - 4.3.5 The dielectric tensor
 - 4.3.6 The hot plasma dispersion relation
 - 4.3.7 Examples of hot plasma wave effects
 - 4.4 Electrostatic waves
 - 4.4.1 Perpendicular propagation–Bernstein modes
 - 4.4.2 High-order Bernstein modes
 - 4.5 Velocity space instabilities
 - 4.5.1 Anisotropic temperature
 - 4.6 Conservation of energy and power flow
 - 4.6.1 Poynting’s theorem for kinetic waves
 - 4.6.2 Group velocity and kinetic flux
 - 4.7 Relativistic plasma effects
 - 4.7.1 The relativistic dielectric tensor
 - 4.7.2 The relativistic dielectric tensor without sums
 - 4.7.3 The weakly relativistic dielectric tensor
 - 4.7.4 Moderately relativistic expressions
 - 4.7.5 Exact expressions with $n_{\parallel} = 0$
 - 4.7.6 The relativistic X-wave

5 Bounded homogeneous plasmas

- 5.1 Introduction
- 5.2 Boundary conditions
 - 5.2.1 Conducting boundary
 - 5.2.2 Plasma–vacuum (or dielectric) interface
- 5.3 Unmagnetized plasmas
 - 5.3.1 Scattering from a plasma column
 - 5.3.2 Surface waves in a partially-filled plasma waveguide
- 5.4 Electrostatic waves on a plasma column in a magnetic field
- 5.5 Cold plasma-filled waveguide
 - 5.5.1 The dispersion relation
 - 5.5.2 Wave fields and boundary conditions
 - 5.5.3 MHD approximation— $\omega \ll \omega_{ci}$
 - 5.5.4 Intermediate frequency case— $\omega \simeq \omega_{ci} \ll \omega_p$
 - 5.5.5 Mode orthogonality and power flow
 - 5.5.6 Antenna problems
 - 5.5.7 Experiments in plasma-filled waveguides
- 5.6 Conducting wall with vacuum layer, $m = 0, \pm 1$
- 5.7 Infinite magnetic field approximation
 - 5.7.1 Cold plasma-filled waveguide in an infinite magnetic field
 - 5.7.2 Hot plasma-filled waveguide

6 Waves in inhomogeneous plasmas

- 6.1 Introduction
- 6.2 WKB method for one-dimensional inhomogeneities
 - 6.2.1 Behavior near a cutoff
 - 6.2.2 Tunneling between back-to-back cutoffs
 - 6.2.3 Behavior near an isolated resonance
 - 6.2.4 Behavior near a resonance–cutoff pair
- 6.3 Mode conversion theory
 - 6.3.1 The mode conversion theorem
 - 6.3.2 Solution of the tunneling equation
 - 6.3.3 Mode conversion examples
 - 6.3.4 Conservation of energy
- 6.4 Absorption and emission
 - 6.4.1 Generalized Kirchhoff's law
 - 6.4.2 Absorption and mode conversion
- 6.5 WKB Method for three-dimensional inhomogeneous plasmas—ray tracing
 - 6.5.1 The ray equations
 - 6.5.2 The inhomogeneous plasma dispersion relation
 - 6.5.3 The amplitude equations
- 6.6 Drift waves and instabilities
 - 6.6.1 Introduction—drift waves

- 6.6.2 The drift resistive instability
- 6.6.3 Kinetic theory of drift waves

7 Quasilinear theory

- 7.1 Introduction
- 7.2 Quasilinear theory
 - 7.2.1 Basic equations
 - 7.2.2 Conservation laws
 - 7.2.3 Velocity space diffusion in a magnetic field
 - 7.2.4 H-theorem for quasilinear theory
 - 7.2.5 Weak bump-on-the-tail instability
 - 7.2.6 Effects of collisions
- 7.3 Nonlinear wave–particle–wave applications
 - 7.3.1 Plasma wave echoes

8 Finite amplitude plasma waves

- 8.1 Nonlinear mechanisms in plasmas
 - 8.1.1 Ponderomotive effects
- 8.2 Solitary waves and solitons
 - 8.2.1 Ion-acoustic solitary wave
 - 8.2.2 The Korteweg–de Vries (KdV) equation
 - 8.2.3 Ion acoustic solitons
 - 8.2.4 Alfvén wave solitons
 - 8.2.5 Nonlinear Schrödinger equation
- 8.3 Trapped particle effects
 - 8.3.1 Nonlinear Landau damping
 - 8.3.2 Bernstein–Greene–Kruskal (BGK) modes
- 8.4 Parametric instabilities
 - 8.4.1 The modulated harmonic oscillator model
 - 8.4.2 Excitation of coupled mode oscillations
 - 8.4.3 Effects of finite pump wavelength
 - 8.4.4 Unmagnetized plasma examples

A Complex variables

- A.1 Contour integrals
- A.2 Analytic continuation
- A.3 The method of steepest descents—saddle point method
 - A.3.1 Steepest descents with saddle points along the real axis
 - A.3.2 Saddle point method
 - A.3.3 Spatial Landau damping example

B Special functions in plasma physics

- B.1 Plasma dispersion function, $Z(\zeta)$
 - B.1.1 Properties of the plasma dispersion function
 - B.1.2 Generalized dispersion functions and the Gordeyev integrals

- B.1.3 Relation to the error function for complex argument
 - B.1.4 Relation to the Y function
 - B.1.5 Relation to the W function
 - B.2 Weakly relativistic plasma dispersion function, $F_q(z)$
 - B.2.1 Relation to other functions
 - B.2.2 Properties of $F_q(z)$
 - B.3 Generalized relativistic plasma dispersion function, $\mathcal{F}_q(z, a)$
 - B.3.1 Properties of $\mathcal{F}_q(z, a)$
 - B.3.2 Relation to $Z(\zeta)$
 - B.4 Gamma function, $\Gamma(z)$
 - B.5 Generalized hypergeometric functions
 - B.5.1 Integrals leading to hypergeometric functions of the first type
 - B.5.2 Integrals leading to hypergeometric functions of the second type
- C The amplitude equations of geometric optics**
- C.1 The current density
 - C.2 The wave equation
 - C.3 The amplitude equation
 - C.4 Energy density conservation
- D Answers to selected problems**
- References**

Preface to the first edition

This book is an advanced text for first or second year graduate students who have had an introductory plasma course at some level. While largely self-contained, so that it could precede a general introductory course, the full background of kinetic theory and collisions is incomplete in this text, and the mathematical skills required in the later chapters go beyond what is usually expected in a senior level course. It may also be used as an adjunct to a more general text for those who choose to emphasize plasma waves in a first year graduate course.

Despite the presumptuous title, this book is not the last word in plasma waves, as there are many topics upon which entire books have been written, several of which were partial sources for this book. It is comprehensive, however, in the sense that few wave topics are not at least introduced, and it does not treat every subject in an introductory manner. The general philosophy has been to include the basic development and formulas for as many aspects of plasma waves as possible, and develop more fully those topics which have not been treated in other texts. This leads to nonuniform depth of coverage, but other texts are presumably available for the instructor to expand on favorite topics. Because of the uneven coverage, some may find their favorite topic treated either in a cavalier fashion or not at all. In order to produce the book at a reasonable length and price, however, I have attempted to include only a few examples after the general development of each topic, leaving the instructor to develop other examples. Some additional topics are included in the problems, but probably not enough to indicate the breadth of possible applications. Answers to some of the problems are included in [appendix D](#), and an instructor may obtain a solutions manual directly from the author.

Since my own background has been almost exclusively in laboratory plasma physics, both theoretical and experimental, a large part of which has been fusion related, the book is primarily addressed to this audience. As such, the original ambition of making a book that ionospheric and astrophysical scientists could also use is unsatisfied, but I believe there is much here from which the latter audience may benefit, since not all of these topics are well covered in their literature.

This book has many beginnings¹, starting from notes on a course by

¹ Since my own career has largely been devoted to wave heating for fusion applications, and hence to the heating of deuterium, it could be said that the Genesis of this book is Deuteronomy.

R W Gould, following through notes on a course I taught at the University of Texas from Stix's book (which is undoubtedly the book to which I am most indebted), and culminating with a review article I wrote on mode conversion and ion wave heating. But the determination to actually write the book came from conversations with D Q Hwang, with whom I originally began to write the book. We had determined the time was right for a general book on plasma waves, and I took a six months sabbatical in 1987 at U C Davis, Livermore, so I could write it with him. Unfortunately, the Livermore Laboratory did not permit him the time to pursue this adventure, so he had to withdraw from the project, extending the time an extra six months while I learned and wrote what was to have been his contribution.

In addition to D Q Hwang, I would like to acknowledge the patience and helpfulness of my colleagues, J-M Wersinger, J D Hanson and R F Gandy, who have had to carry the major responsibility for our mutual projects during the preparation of this book, and to my former student, Suwon Cho, who assisted me and helped keep some of my research alive during this period. I would also like to thank Walter Sadowski for stimulating and supporting the earlier review, and for his patience and support during the preparation of this book. Finally, I would like to thank Leslie Lamport and Donald Knuth for their development of L^AT_EX and T_EX, respectively, without which I would never have attempted to write this book, much less prepare it camera ready.

D Gary Swanson
Department of Physics
Auburn University, AL 36849-5311

Preface to the second edition

In this second edition, a large number of errors have been corrected, most of which were typos in the original edition, but some of which were actual errors or very poor representations. In addition, absorption is included as a new section in inhomogeneous plasmas. In nearly all cases, the figures are improved so that they are real plots whereas some of the originals were merely topologically correct. Many more figures are included where parameter ranges may be so broad that a single figure fails to build intuition adequately. The appendices are expanded, especially for the relativistic plasma dispersion functions.

D Gary Swanson
Department of Physics
Auburn University, AL 36849-5311
16 September 2002

Acknowledgements

In addition to Mike Ngan (Y C Ngan), others who have worked closely in this development have been Suwon Cho, who was both student and postdoctoral fellow; Vadim Shvets, a research fellow; and recent students Jianlong Hu and C S Ng, all of whom have contributed to this work. There were also collaborations with C K Phillips, R Kashuba, and P L Colestock, and through them, some others. I am grateful to all of them for their encouragement and stimulation. I would also like to acknowledge the support of Walter Sadowski of the US Department of Energy through much of this period. I would especially like to thank V F Shvets for reading the manuscript in its formative stage and for suggesting many valuable changes. The preparation of this book was supported by Auburn University and the US Department of Energy.

Acronyms

BGDR Bohm–Gross dispersion relation

BGK Bernstein–Green–Kruskal

CMA Clemmow–Mullaly–Allis

CPDR cold plasma dispersion relation

ESDR electrostatic dispersion relation

FLR finite Larmor radius

GKL generalized Kirchhoff’s law

HPDR hot plasma dispersion relation

LFDR low frequency dispersion relation

MHD magnetohydrodynamic

PDF plasma dispersion function

TE tunneling equation

WKB Wentzel–Kramers–Brillouin

WNS wave normal surface

WPDR warm plasma dispersion relation

Chapter 1

Introduction

1.1 Properties of plasmas

The plasma state is a characterization of matter where long range electromagnetic interactions dominate the short range interatomic or intermolecular forces among a large number of particles. Plasmas are generally high temperature entities, and some of the properties of a plasma are connected with thermal effects, and among the wave types we shall discuss are sound waves. We define the thermal speed to be the *most probable speed* in a Maxwellian distribution,

$$v_j = \sqrt{\frac{2\mathcal{K}T_j}{m_j}} \quad j = e, i \quad (1.1)$$

for electrons or ions.¹ In addition to the thermal speeds for electrons and ions, however, there are two other fundamental parameters which characterize a plasma in the absence of a magnetic field, and these are the plasma frequency and the Debye length. The plasma frequency is the oscillation frequency of a simple unmagnetized plasma when the charge distribution is locally perturbed from its equilibrium, and is given for electrons by

$$\omega_{pe} = \sqrt{\frac{n_e e^2}{m_e \epsilon_0}}. \quad (1.2)$$

The Debye length is the distance a thermal particle travels during a plasma period. Its definition is

$$\lambda_{De} \equiv \sqrt{\frac{\epsilon_0 \mathcal{K}T_e}{n_e e^2}} = \frac{v_e}{\sqrt{2}\omega_{pe}}. \quad (1.3)$$

In fact, unless an assembly of charged particles is large enough that it is many Debye lengths in size, and of such a density that there are many particles in a

¹ Many authors delete the factor of two in their definition of thermal speed. The definition here differs from v_{rms} by only 13% instead of the 60% difference without the factor of two.

Debye sphere, we do not call the assembly a plasma. It is thus apparent that plasma waves are fundamental to the very definition of a plasma.

1.1.1 Unmagnetized plasmas

Unmagnetized plasmas are generally the first to be studied because they are isotropic, i.e. the properties are the same in all directions. The waves that such a plasma will support are either high frequency electromagnetic waves which see the plasma as a simple dielectric due to the response of the electrons to the wave (by comparison the ions are generally immobile), or sound-type waves. In a cold plasma, these latter waves become a simple oscillation at the plasma frequency, below which the electromagnetic waves do not propagate. In a thermal plasma, however, there are sound-like waves near this frequency, and in a plasma with disparate electron and ion temperatures with $T_e \gg T_i$, there is even a kind of hybrid sound wave that depends on the electron temperature and the ion mass. These waves even damp through a non-dissipative process. While these several kinds of behavior are already much more complicated than waves in ordinary fluids, they are very simple compared to the complexities added by a magnetic field. Even the kinds of nonlinearities in this simple plasma are richer in both diversity and complexity than in fluid dynamics where only averages over the velocity distribution are analyzed. Compared to ordinary fluids, plasmas even have an additional kind of turbulence, called microturbulence, which has many kinds of sources.

1.1.2 Magnetized plasmas

The addition of magnetic field effects to the subject of plasma waves adds a host of new phenomena, among which are: anisotropy, since there is now a preferred direction; new kinds of transverse waves existing only in magnetized plasmas, which we call Alfvén waves; finite Larmor orbit effects due to thermal motions about the magnetic field lines; and many other kinds of waves which are either totally new or greatly modified. Because of the anisotropy, the description of these effects is inevitably complicated algebraically, and this tends sometimes to obscure the physics. We shall, however, try to give the general descriptions, which are formidable, and show enough special cases to illustrate the richness of wave phenomena which are found in a magnetized plasma. Even in a cold plasma where thermal effects are absent, the number of wave types added by the inclusion of the magnetic field is large, and wave types vary greatly with the angle of propagation with respect to the magnetic field. We find waves which are guided by the magnetic field in certain frequency ranges, and cases where the phase and group velocities are nearly normal to one another. Whereas in a cold unmagnetized plasma, the only parameter that may lead to inhomogeneities is the plasma density, the magnetic field not only adds a possible new source of inhomogeneity, but the gradients may appear in different directions. Since

nearly all of the realistic plasmas, both in the laboratory and in ionospheric and astrophysical plasmas, have a magnetic field, we shall expend considerable effort studying these effects and attempt to sort out the somewhat bewildering array of phenomena.

1.1.3 Thermal plasmas

When thermal effects are added to the cold plasma effects, the new phenomena can be grouped into two general categories: acoustic wave phenomena due to various kinds of sound waves; and kinetic phenomena due to the fact that in a thermal or near thermal distribution, there are some particles moving at or near the phase velocity. These particles have resonant interactions with the waves due to their long interaction time with the wave. These interactions can lead to either collisionless wave damping or to instabilities and wave growth. When coupled with magnetic field effects, finite Larmor orbit effects lead to even more new wave types and instabilities.

We shall first examine the wave types in a cold, magnetized plasma in [chapter 2](#), and then introduce the thermal effects, analyzing the acoustic phenomena through the fluid model of a plasma in [chapter 3](#), and the kinetic effects in [chapter 4](#). In the subsequent chapters, we shall examine the effects of adding sharp boundaries, slowly varying inhomogeneities, and nonlinearities at several levels, but will stop short of fully turbulent plasmas.

1.2 Plasma wave applications

Some of the earliest applications of plasma physics were related to gaseous electronics and the study of positive columns for device applications. While these investigations contributed significantly to the early development of plasma physics, most of those applications have either been superseded by solid state devices or involve no wave phenomena, and are hence of no interest in the context of this book. We thus turn our attention to several applications which both contributed to the development of the field, helping us to understand that plasmas indeed form the ‘fourth state of matter’ and which are the active areas of research today.

1.2.1 Plasma waves in ionospheric physics

It was apparent from the very early days of radio that some poorly understood phenomenon was occurring in the upper atmosphere which was affecting radio propagation in a nontrivial manner. By 1932, when Appleton published what came to be known as the ‘Appleton–Hartree Dispersion Relation’ (which we will henceforth refer to as the ‘Altar–Appleton Dispersion Relation’ for reasons discussed in section 2.1), there was a significant amount of data indicating the location and nature of the ionospheric plasma and many of the observed effects

on radio wave propagation were understood. Those studies have continued to uncover new phenomena and refine the picture of the ionosphere, and continue to influence our communications through the ionosphere. Beginning with passive characterization of the wave propagation characteristics of the ionosphere, we have moved on to active modification of the ionosphere through nonlinear plasma wave interactions, and we attempt to model the potential modifications to the propagation characteristics which might follow a major disruption of the ionosphere due either to a large solar flare or to human intervention.

1.2.2 Plasma waves in astrophysics

In astrophysics, plasma waves are ubiquitous, providing the basis for understanding many types of energy transport and plasma instabilities, both linear and nonlinear. Wave transport of both energy and momentum leads to plasma heating and modification of the velocity distribution. Conversely, nonequilibrium velocity distributions lead to plasma instabilities which convert particle energy to wave energy then back to particle energy. While wave–particle interactions may dominate the interest in astrophysical plasma waves, the propagation and characterization of linear waves lie at the root of all nonlinear interactions, and the various competing mechanisms for wave dissipation and wave generation or growth must be thoroughly understood first. While the scale of astrophysical plasmas is large, suggesting that uniform plasma theory might suffice, it is the weakly inhomogeneous effects which transport waves through propagating regions to a resonance region where the wave–particle effects lead to energy exchange between the particles and waves, or else block the propagation through a caustic or reflection layer.

1.2.3 Plasma waves in magnetized fusion plasmas

A major impetus for research in plasma waves has been the international effort to realize controlled thermonuclear fusion. Since plasma waves determine the magnetohydrodynamic (MHD) instability time scale, and fusion plasmas are perennially fraught with micro-instabilities and the ensuing microturbulence, understanding both linear and nonlinear instabilities has always been a driving force in the development of wave theory. Plasma wave heating has also recently come to the forefront, leading to even more refinement in wave theory as one tries to model successfully the scenarios for using plasma waves to raise the plasma temperature to ignition levels. This effort includes more detailed descriptions of propagation in inhomogeneous plasmas as the wave energy must travel from the edge to the center, and then more sophisticated models of the wave absorption processes which finally transfer the wave energy to the plasma particles. The emission of waves from hot plasmas is also used to measure the temperature of thermal plasmas; and the use of the generalized Kirchhoff law (GKL) to describe this phenomenon appears here for the first time in a textbook. The

use of waves to generate a plasma current, where wave momentum is converted to particle momentum through nonlinear wave–particle interactions, has led to further developments in nonlinear theory. Many of the examples in this book have potential magnetic fusion applications, but they are certainly not limited to such a narrow scope.

1.2.4 Plasma waves in laser-produced plasmas

Another area where wave–plasma interactions drive the physics is the realm of laser-produced plasmas, principally those related to inertial confinement fusion. In this application, the electromagnetic waves are so intense that the plasma response is not only nonlinear, but relativistic, as electrons can gain a reasonable fraction of their rest energy in one cycle of the incident wave. In addition, there are other kinds of nonlinearities which produce sideband waves and shock waves. While these plasmas have no intrinsic magnetic field, wave-driven currents sometimes produce one. In these plasmas, the steep gradients in the plasma parameters stretch the weakly inhomogeneous models, and the strong fields lead to strong nonlinearities, both areas which go beyond the scope of this book. While some of the examples herein may give a qualitative guide to the kinds of behavior to expect in such plasmas, the parameters are sufficiently extreme in many cases that qualitatively different phenomena can and do occur.

1.3 Review of electromagnetic wave propagation

1.3.1 The Maxwell equations

The propagation of electromagnetic waves in all physical media for all frequency ranges from zero frequency to gamma rays are governed by the Maxwell equations. Moreover, we are particularly interested in wave propagation in a material medium, namely a plasma, which is usually treated in a slightly different manner from general dielectric media such as insulating materials. Throughout this text, SI units will be employed so the field equations are:

$$\nabla \times \mathbf{E} = - \frac{\partial \mathbf{B}}{\partial t} \quad (1.4)$$

$$\nabla \times \mathbf{H} = \mathbf{J} + \frac{\partial \mathbf{D}}{\partial t} \quad (1.5)$$

$$\nabla \cdot \mathbf{B} = 0 \quad (1.6)$$

$$\nabla \cdot \mathbf{D} = \rho \quad (1.7)$$

where all quantities are functions of space and time, e.g. $\mathbf{J} = \mathbf{J}(\mathbf{r}, t)$. These quantities are the standard electromagnetic fields plus the current and charge density.

- (i) \mathbf{E} is the electric field intensity in Volt/m or Newton/Coulomb.

- (ii) \mathbf{D} is the electric displacement vector or $\mathbf{D} = \epsilon \mathbf{E}$ in a standard isotropic dielectric medium characterized by a scalar dielectric permittivity. If the medium is anisotropic, the medium is characterized by a tensor dielectric permittivity, ϵ , and $\mathbf{D} = \epsilon \cdot \mathbf{E}$.
- (iii) \mathbf{B} is the magnetic induction in Tesla.
- (iv) \mathbf{H} is the magnetic intensity, and \mathbf{B} and \mathbf{H} are related by $\mathbf{B} = \mu \mathbf{H}$ where μ is the magnetic permeability of the medium. For plasmas, we shall take $\mu = \mu_0$ where μ_0 is the permeability of free space.
- (v) ρ is the electrical charge density in Coulomb/m³.
- (vi) \mathbf{J} is the electrical current density in Ampere/m².

As a consequence of these equations, the charge density ρ and the current density \mathbf{J} are related through the continuity equation:

$$\nabla \cdot \mathbf{J} + \frac{\partial \rho}{\partial t} = 0. \quad (1.8)$$

Another relation which is very important in dealing with conductive media such as plasmas (as we will show in subsequent chapters) is the conductivity σ which is defined such that

$$\mathbf{J} = \sigma \cdot \mathbf{E} \quad (1.9)$$

where the dot product indicates that in general σ is a tensor which we shall characterize either by a 3×3 matrix or as the scalar σ . As will be demonstrated in [chapter 3](#), the physical properties of the medium are manifested through the quantities ϵ , μ , and σ . In an isotropic medium, these are all scalar quantities, denoted by ϵ , μ , σ , while in an anisotropic medium they may all become tensors denoted by ϵ , μ , σ .

In an insulating dielectric medium, another vector field is usually used to relate the properties of the medium to the electric intensity, namely the electric polarization \mathbf{P} , where

$$\mathbf{P} = \epsilon_0 \chi \cdot \mathbf{E} \quad (1.10)$$

where χ is the susceptibility tensor of the material. The convenience of defining the electric susceptibility is to obtain a divergence-free electric displacement in the medium or

$$\nabla \cdot \mathbf{D} = 0. \quad (1.11)$$

Since the charges in the medium are bound, it is possible to write

$$\rho = -\nabla \cdot \mathbf{P} \quad (1.12)$$

or from equation (1.7), we have

$$\nabla \cdot (\epsilon_0 \mathbf{E}) = \rho = -\nabla \cdot \mathbf{P} \quad (1.13)$$

$$\nabla \cdot (\epsilon_0 \mathbf{E} + \mathbf{P}) = 0. \quad (1.14)$$

Now let $\mathbf{D} = \epsilon_0 \mathbf{E} + \mathbf{P}$, and since $\mathbf{D} = \epsilon \cdot \mathbf{E}$, we have

$$\epsilon = \epsilon_0(\mathbf{I} + \boldsymbol{\chi}) \quad (1.15)$$

where $\boldsymbol{\chi}$ is in general a 3×3 matrix and \mathbf{I} is the unit 3×3 matrix.

For a plasma, the currents are related to the various physical properties of the medium and can be used to define an *effective* dielectric constant (or tensor). External currents, however, must be dealt with explicitly, and may not be incorporated into a characterization of the medium through an effective dielectric constant. For a homogeneous plasma, we may Fourier transform in both time and space so that the fields vary as $\exp(i\mathbf{k} \cdot \mathbf{r} - i\omega t)$, so that we may define

$$\mathbf{D} = \epsilon \mathbf{E} = \epsilon_0 \mathbf{E} - \mathbf{J}/i\omega = (\epsilon_0 - \sigma/i\omega) \mathbf{E} \quad (1.16)$$

where we have used equation (1.9) (scalar form) with the result

$$\begin{aligned} \epsilon &= \epsilon_0 - \sigma/i\omega && \text{scalar dielectric permittivity} \\ \epsilon &= \epsilon_0 \mathbf{I} - \boldsymbol{\sigma}/i\omega && \text{effective dielectric permittivity tensor} \end{aligned} \quad (1.17)$$

and in terms of the dimensionless dielectric constant, where $\epsilon = \epsilon_0 K$,

$$K = 1 - \frac{\sigma}{i\omega\epsilon_0} \quad \text{the effective dielectric constant} \quad (1.18)$$

$$\mathbf{K} = \mathbf{I} - \frac{\boldsymbol{\sigma}}{i\omega\epsilon_0} \quad \text{the effective dielectric tensor.} \quad (1.19)$$

Thus a good conducting medium at low frequency, such as a plasma, or water with an electrolyte, will have a very high dielectric constant as well. Hence the dielectric constant of a medium is related to the polarizability of an insulator, as in equation (1.15), or the mobility of the charges in a plasma, as will be shown in chapter 2.

Problem 1.3.1. Incorporating the current into the dielectric constant. Show that equation (1.16) comes from equation (1.5) where the current has been incorporated into ϵ .

1.3.2 Properties of the Helmholtz equation

Again let us consider electromagnetic waves in free space where $\mu_0 \equiv 4\pi \times 10^{-7}$ Henry/m and $\epsilon_0 = 8.854 \times 10^{-12}$ Farad/m, or in a dielectric medium characterized by a dielectric constant K . The speed of light may be written in terms of the free space constants as $1/c^2 = \mu_0\epsilon_0$. We can combine equation (1.4) and equation (1.5) for free space and obtain the general Helmholtz equation for free space or use $\mathbf{D} = \epsilon_0 K \mathbf{E}$ to represent the homogeneous, isotropic medium. We use the various quantities used in section 1.3.1 to obtain

$$\nabla \times (\nabla \times \mathbf{E}) + \mu_0 \frac{\partial}{\partial t} \mathbf{J} + \frac{K}{c^2} \frac{\partial^2}{\partial t^2} \mathbf{E} = 0 \quad (1.20)$$

where now \mathbf{J} represents *external* currents, so with no external currents, we have the Helmholtz or wave equation:

$$\nabla \times (\nabla \times \mathbf{E}) + \frac{K}{c^2} \frac{\partial^2}{\partial t^2} \mathbf{E} = 0. \quad (1.21)$$

This result is valid either for free space, where $K = 1$ or in an insulating medium or in a plasma which is represented by an effective dielectric constant.

If we use the vector identity

$$\nabla \times (\nabla \times \mathbf{A}) = \nabla(\nabla \cdot \mathbf{A}) - \nabla^2 \mathbf{A}$$

and take the case $\nabla \cdot \mathbf{E} = 0$ so that there is no net free charge, we have the simplified wave equation

$$\nabla^2 \mathbf{E} - \frac{K}{c^2} \frac{\partial^2}{\partial t^2} \mathbf{E} = 0. \quad (1.22)$$

These same basic techniques can be used to write a wave equation for \mathbf{H} as

$$\nabla \times (\nabla \times \mathbf{H}) + \frac{K}{c^2} \frac{\partial^2}{\partial t^2} \mathbf{H} = \nabla \times \mathbf{J} \quad (1.23)$$

where again \mathbf{J} represents external currents, since internal currents have been incorporated into K . Thus with no external currents, equation (1.23) is equivalent to equation (1.22) so that \mathbf{E} and \mathbf{H} satisfy the same equation.

Let us first consider some simple cases of the wave equation. For simplicity, consider only the scalar wave equation, equation (1.22), in a homogeneous, isotropic, nondispersive medium. The most common solution of the scalar equation

$$\nabla^2 f - \frac{K}{c^2} \frac{\partial^2}{\partial t^2} f = 0$$

is the plane wave solution, or

$$f = A e^{i\theta} = A e^{i(k \cdot r - \omega t)} \quad (1.24)$$

since any other solution can be constructed by Fourier synthesis, so the solution is a complex function with a scalar amplitude A and phase θ , where

$$\theta = \mathbf{k} \cdot \mathbf{r} - \omega t. \quad (1.25)$$

Here, \mathbf{k} is known as the wavevector, and ω is the angular frequency, measured in radians per second. The homogeneous assumption implies that k is not a function of r , the isotropic assumption implies that it is not a function of direction, and the nondispersive assumption implies that it is not a function of ω . The surface where θ is a constant is known as the surface of constant phase, or if an observer

moves with the wave in the k -direction, the phase is constant. Taking differentials of equation (1.25), we have

$$\delta\theta = \mathbf{k} \cdot \delta\mathbf{r} - \omega\delta t$$

and for constant phase we demand $\delta\theta = 0$, so

$$0 = \mathbf{k} \cdot \delta\mathbf{r} - \omega\delta t$$

which leads to

$$\frac{d\mathbf{r}}{dt} = \frac{\omega}{|\mathbf{k}|} \hat{\mathbf{e}}_k = \mathbf{v}_p. \quad (1.26)$$

The quantity \mathbf{v}_p is known as the phase velocity of the wave and points in the \mathbf{k} -direction, and its magnitude v_p is the phase speed. The other physical quantities of interest in the study of waves are the wavelength λ and the period τ . The wavelength is the distance traveled by the wave when the phase has increased by 2π with t constant, so that

$$\lambda = \frac{2\pi}{|\mathbf{k}|} \quad (1.27)$$

and the period is the time elapsed for a 2π phase shift at constant \mathbf{r} , or

$$\tau = \frac{2\pi}{\omega}. \quad (1.28)$$

The wave frequency is simply the inverse of τ or

$$f = \frac{1}{\tau} = \frac{\omega}{2\pi}. \quad (1.29)$$

Another quantity that can be used to simplify the form of the wave equation is the vector index of refraction \mathbf{n} given by

$$\mathbf{n} = \frac{\mathbf{k}c}{\omega}. \quad (1.30)$$

The physical meaning of $n = |\mathbf{n}|$ is that it represents the ratio of the speed of light in free space to the phase speed of the wave. Hence if $n > 1$, it means that the phase speed of the wave is slower than the speed of light, and if $n < 1$, it means it is faster. Using \mathbf{n} , equation (1.22) becomes

$$\mathbf{n} \times (\mathbf{n} \times \mathbf{E}) - K\mathbf{E} = 0 \quad (1.31)$$

and if $\nabla \cdot \mathbf{E} = 0$ (which is typically true for transverse waves but not for longitudinal waves), then this leads to

$$n^2 - K = 0 \Rightarrow n = \pm\sqrt{K}. \quad (1.32)$$

The index of refraction for free space is thus $n = \pm 1$ since $K = 1$ for free space, and differs from unity for general media.

It is clear from the nature of the vector equations that whenever the medium is *not* isotropic, the tensor character of the effective dielectric tensor will require the index of refraction to be different in different directions, and the algebra will be more formidable than shown here. Nevertheless, the Helmholtz equation may be written for stationary ($\partial K/\partial t = 0$), homogeneous ($\partial K/\partial r = 0$), anisotropic media as

$$\mathbf{n} \times (\mathbf{n} \times \mathbf{E}) - K \cdot \mathbf{E} = 0. \quad (1.33)$$

In addition to the phase velocity, we will often need to know the velocity of a *wave packet* which is called the *group velocity*. This velocity gives information about the movement of energy and information, and may be either faster or slower than the phase velocity, and frequently travels in a different direction. In a homogeneous, isotropic plasma, the group velocity is given by

$$v_g = \frac{d\omega}{dk} \quad (1.34)$$

and travels either parallel or antiparallel to the phase velocity. In more general plasmas, the vector expression is

$$v_g = \frac{d\omega}{dk} = \nabla_k \omega. \quad (1.35)$$

This phenomenon will be examined more thoroughly in [chapter 2](#).

1.3.3 Conservation laws for electromagnetic fields

The flow of electromagnetic energy is a balance between the power leaving a bounded volume through its surface, the power dissipated in the volume (transferred to mechanical or other non-electromagnetic energy), and the energy stored in the electromagnetic fields (\mathbf{E} and \mathbf{H}). It is this energy balance that is the content of Poynting's theorem. We begin with the definition of the Poynting vector which describes the electromagnetic energy flux,

$$\mathbf{P} = \mathbf{E} \times \mathbf{H} \quad (1.36)$$

along with equations (1.4) and (1.5). Taking the divergence of \mathbf{P} and using the vector identity,

$$\nabla \cdot (\mathbf{A} \times \mathbf{B}) = -\mathbf{A} \cdot (\nabla \times \mathbf{B}) + \mathbf{B} \cdot (\nabla \times \mathbf{A})$$

then

$$\begin{aligned} \nabla \cdot \mathbf{P} &= \mathbf{H} \cdot (\nabla \times \mathbf{E}) - \mathbf{E} \cdot (\nabla \times \mathbf{H}) \\ &= -\mathbf{H} \frac{\partial \mathbf{B}}{\partial t} - \mathbf{E} \cdot \mathbf{J} - \mathbf{E} \cdot \frac{\partial \mathbf{D}}{\partial t}. \end{aligned} \quad (1.37)$$

If we take the magnetic permeability μ to be constant and the dielectric permittivity ϵ to be time independent, we may write this result as

$$\nabla \cdot \mathbf{P} = -\frac{\partial U}{\partial t} - \mathbf{J} \cdot \mathbf{E} \quad (1.38)$$

where U is an energy density given by

$$U = \frac{1}{2} \mathbf{E} \cdot \mathbf{D} + \frac{1}{2} \mathbf{B} \cdot \mathbf{H} \quad (1.39)$$

and where \mathbf{D} includes the loss-free portion of the dielectric tensor (the Hermitian part of \mathbf{K}) and $\mathbf{J} = -i\omega\epsilon_0\mathbf{K}^A$ (where \mathbf{K}^A is the anti-Hermitian part of \mathbf{K}). The various terms in (1.38) and (1.39) simply reflect the different components of the energy balance. The total energy balance can be found by integrating equation (1.38) over a volume V bounded by a surface S so that by using the divergence theorem

$$\int_V \nabla \cdot \mathbf{P} \, dV = \oint_S \mathbf{P} \cdot d\mathbf{A}$$

we obtain

$$\oint_S \mathbf{P} \cdot d\mathbf{A} = -\frac{\partial}{\partial t} \int_V U \, dV - \int_V \mathbf{J} \cdot \mathbf{E} \, dV. \quad (1.40)$$

From this equation, we identify the stored electromagnetic energy as being comprised of an electric and a magnetic term, given in terms of the energy densities (in Joule/m³)

$$U_E = \frac{1}{2} \mathbf{E} \cdot \mathbf{D} \quad (1.41)$$

$$U_M = \frac{1}{2} \mathbf{B} \cdot \mathbf{H} \quad (1.42)$$

and the volume-averaged power dissipation term is

$$\mathcal{D} = \int_V \mathbf{J} \cdot \mathbf{E} \, dV. \quad (1.43)$$

Integrating over the volume, the total field energy is

$$W = \int_V U_E \, dV + \int_V U_M \, dV \quad (1.44)$$

so the energy balance equation may be written as

$$\oint_S \mathbf{P} \cdot d\mathbf{A} = -\frac{\partial W}{\partial t} - \mathcal{D}. \quad (1.45)$$

This conservation law, which is called Poynting's theorem, indicates that the energy flux through the surface, represented by the first term in equation (1.45), is equal to the rate at which energy is lost in the volume, either by a decrease in the stored energy or by dissipation. It is important to note that both U_E and U_M are nonlinear functions of the fields and thus for energy balance with material media through wave interactions, the conservation laws will be nonlinear (see chapter 7).

1.3.4 Conservation laws with Fourier amplitudes

In studying wave physics, the wave fields and other variables are generally harmonic in both time and space, or very nearly so. For this reason it is common to represent the wave fields in terms of the Fourier amplitudes which are complex quantities. For a harmonic time dependence, for example, we let the electric field be represented by

$$\mathbf{E}(t) = \operatorname{Re}[\hat{\mathbf{E}}(\omega)e^{-i\omega t}]$$

where the hat reminds us that $\hat{\mathbf{E}}$ is a complex number and is the Fourier amplitude for \mathbf{E} . Throughout the book we use Re to denote the real part and Im to denote the imaginary part of whatever follows. While this recipe is rather obvious for linear equations (multiply by $e^{-i\omega t}$ and take the real part), it is less obvious for products of two complex amplitudes. If we represent the product of any two functions of time by $[\mathbf{A}][\mathbf{B}]$ where this could represent the product of two scalars, a scalar and a vector, or a scalar or vector product of two vectors, then we have

$$\begin{aligned} [\mathbf{A}][\mathbf{B}] &= \operatorname{Re}[\hat{\mathbf{A}}e^{-i\omega t}]\operatorname{Re}[\hat{\mathbf{B}}e^{-i\omega t}] \\ &= \frac{1}{2}[\hat{\mathbf{A}}e^{-i\omega t} + \hat{\mathbf{A}}^*e^{i\omega t}]\frac{1}{2}[\hat{\mathbf{B}}e^{-i\omega t} + \hat{\mathbf{B}}^*e^{i\omega t}] \\ &= \frac{1}{4}([\hat{\mathbf{A}}][\hat{\mathbf{B}}]e^{-2i\omega t} + [\hat{\mathbf{A}}][\hat{\mathbf{B}}^*] + [\hat{\mathbf{A}}^*][\hat{\mathbf{B}}] + [\hat{\mathbf{A}}^*][\hat{\mathbf{B}}^*]e^{2i\omega t}). \end{aligned}$$

While this time dependence is very cumbersome, if we ask for the *time average over a period* rather than the instantaneous time behavior, then for real ω this reduces to

$$\begin{aligned} \frac{1}{\tau} \int_0^\tau [\mathbf{A}][\mathbf{B}] dt &= \frac{1}{4}([\hat{\mathbf{A}}][\hat{\mathbf{B}}^*] + [\hat{\mathbf{A}}^*][\hat{\mathbf{B}}]) \\ &= \frac{1}{2}\operatorname{Re}([\hat{\mathbf{A}}][\hat{\mathbf{B}}^*]) \end{aligned} \quad (1.46)$$

where $\tau = 2\pi/\omega$. The complex Poynting vector is obtained from the set of curl equations:

$$\begin{aligned} \nabla \times \hat{\mathbf{E}} &= i\omega\mu_0 \hat{\mathbf{H}} & \nabla \times \hat{\mathbf{E}}^* &= -i\omega\mu_0 \hat{\mathbf{H}}^* \\ \nabla \times \hat{\mathbf{H}} &= \hat{\mathbf{J}} - i\omega\epsilon_0 \hat{\mathbf{E}} & \nabla \times \hat{\mathbf{H}}^* &= \hat{\mathbf{J}}^* + i\omega\epsilon_0 \hat{\mathbf{E}}^* \end{aligned} \quad (1.47)$$

with the result

$$\nabla \cdot (\hat{\mathbf{E}} \times \hat{\mathbf{H}}^* + \hat{\mathbf{E}}^* \times \hat{\mathbf{H}}) = -(\hat{\mathbf{E}} \cdot \hat{\mathbf{J}}^* + \hat{\mathbf{E}}^* \cdot \hat{\mathbf{J}}). \quad (1.48)$$

If we integrate this over the volume, then the result may be expressed as

$$-\oint_S \mathbf{P} \cdot d\mathbf{S} = \mathcal{D} \quad (1.49)$$

where

$$\mathbf{P} = \frac{1}{2}\operatorname{Re}(\hat{\mathbf{E}} \times \hat{\mathbf{H}}^*) \quad (1.50)$$

$$\mathcal{D} = \frac{1}{2}\operatorname{Re} \int_V (\hat{\mathbf{E}} \cdot \hat{\mathbf{J}}^*) dV \quad (1.51)$$

so we can identify \mathbf{P} as the Poynting vector and \mathcal{D} as the volume averaged dissipation. Equation (1.49) tells us that the power flowing *in* through the surface is equal to the rate of loss of power inside through dissipation. In the lossless plasma, we shall find that $\text{Re}(\hat{\mathbf{E}} \cdot \hat{\mathbf{J}}^*) = 0$, so there is no dissipation and no net power flow averaged over a cycle.

When ω is complex, with $\omega = \omega_r + i\omega_i$, then equation (1.48) has an additional term such that

$$\nabla \cdot (\hat{\mathbf{E}} \times \hat{\mathbf{H}}^* + \hat{\mathbf{E}}^* \times \hat{\mathbf{H}}) = -(\hat{\mathbf{E}} \cdot \hat{\mathbf{J}}^* + \hat{\mathbf{E}}^* \cdot \hat{\mathbf{J}}) - 2\omega_i(\mu_0|\hat{\mathbf{H}}|^2 + \epsilon_0|\hat{\mathbf{E}}|^2) \quad (1.52)$$

and this additional term represents the energy stored in the electromagnetic fields, which can decay if the plasma is lossy or grow if the plasma is unstable.

1.3.5 Methods of geometric optics from WKB theory

In a stationary, infinite, homogeneous, isotropic medium, the wave equation, equation (1.22), may be written as a scalar wave equation of the form,

$$\frac{d^2y}{dx^2} + k^2 y = 0 \quad (1.53)$$

where k is the wavenumber, and $n = kc/\omega$ is the index of refraction in the x -direction. In an anisotropic medium, k depends on the direction, and there may be more than one value of k to describe the propagation. The solutions are simple plane waves, described by equation (1.24).

For an inhomogeneous (but still isotropic) plasma, however, the simple plane wave solutions are only approximations to the actual solutions. If the medium is sufficiently slowly varying, however, they represent a good starting point. If we restrict our inhomogeneity to one dimension, then equation (1.53) can be generalized to

$$\frac{d^2y}{dx^2} + k^2(x)y = 0 \quad (1.54)$$

where now $k(x)$ is determined by the properties of the medium and we require $k(x)$ to vary little over a wavelength. If we assume that the solution is nearly a plane wave, then we can choose to represent the solution as an *eikonal* of the form

$$y(x) = A(x)e^{iS(x)} \quad (1.55)$$

where $A(x)$ is assumed to vary slowly while $S(x)$ varies rapidly ($S(x) = kx$ in homogeneous media). If we insert this solution into equation (1.54), we find

$$[A'' + 2iA'S' + A(k^2 - S'^2 + iS'')]e^{iS} = 0$$

so the dominant terms (with no derivatives of A and neglecting S'') give

$$S' = \frac{dS}{dx} = \pm k(x) \quad \text{so} \quad S(x) = \pm \int^x k(x') dx'. \quad (1.56)$$

To the next order, we keep A' and S'' but neglect A'' to obtain

$$2iS'A' + iS''A = 0 \quad \text{with solution} \quad A = \frac{A_0}{\sqrt{k(x)}}. \quad (1.57)$$

The eikonal solution of this simple wave equation is thus (through first order)

$$y(x) = \frac{A_0}{\sqrt{k(x)}} \exp \left[\pm i \int^x k(x') dx' \right]. \quad (1.58)$$

This method of dealing with wave equations of the type equation (1.54) was introduced by Jeffreys [1] and developed for quantum mechanics and the Schrödinger equation by Wentzel, Kramers, and Brillouin [2] and is commonly called the WKB or WKBJ method. The method is sometimes taken to include only this eikonal solution where the variation is slow, and sometimes taken to refer to the matching of these solutions to solutions valid near a local cutoff ($k(x_c) = 0$) where the matching is done far enough from the cutoff that the eikonal solutions are valid, but near enough that the local solution is still valid.

We shall find occasion to use solutions of this type in both one dimension and in three dimensions where the waves are still nearly plane waves, but the direction of the waves changes continuously in space as the wave propagates. The trajectory of the group velocity is called a *ray* and the solution of the equations governing the trajectory is called *ray tracing*. We will also need to find local solutions near both cutoffs ($k(x_c) = 0$) and resonances ($k(x_r) \rightarrow \infty$) and back-to-back cutoffs and resonances, since examples of all these types of behavior are encountered in plasmas. These methods and their conditions for validity, along with numerous examples, are described in [chapter 6](#), but we shall occasionally refer to the eikonal solutions in the intervening chapters.

1.4 Statistical mechanics of plasmas

A plasma is a collection of ionized gas particles such that the overall charge of the system is zero and whose principal interactions between the particles are due to the Coulomb interaction. We refer to the condition on the overall charge as the quasineutrality condition, since we allow local or periodic deviations from exact neutrality. The condition may be written

$$\sum_{j=1}^N n_j q_j = n_e e \quad (1.59)$$

where n_j is the ion charge density for species j and q_j is the charge for that species and the sum is over the N ionic species. We assume that the only negatively charged particles are electrons, so that n_e is the electron density. We recognize that in some weakly ionized plasmas the possibility of negative ions

would require changes in this and other conditions, since we always take the electron mass to be much smaller than the ion mass and this would be violated if negative ions constituted a nontrivial portion of the negative charge in the plasma. In dusty plasmas, the right-hand side of equation (1.59) must be replaced by a sum over the dust particles species that are typically highly charged.

Usually, plasmas are not in true thermal equilibrium, so that some standard statistical mechanical methods cannot be applied. However, each particle species, such as electrons and ions, closely approximates a local equilibrium state, so the usual treatment of the plasma involves several species with independent thermal equilibria. The conventional description of a thermal dynamic system is in terms of its particle distribution function, $f(\mathbf{r}, \mathbf{v}, t)$, where \mathbf{r} is the configuration space coordinate, \mathbf{v} is the velocity space coordinate, and the combination is called the phase space which is a space with six dimensions plus time. The distribution function is an averaged quantity and is hence interpreted as a probability density of finding a particle in a prescribed volume of the phase space.

The starting point of the statistical description of the plasma in phase space is the Boltzmann equation with the interactions dominated by electromagnetic forces. The statistical approach deals either with the description of a collection of individual particles (a microscopic distribution) or with a description of an average over a collection of particles (a macroscopic distribution). The microscopic description of the particles involves a set of point charges located at a point in phase space $(\mathbf{r}_j, \mathbf{v}_j)$ so that the density of particles in this case can be written as a function of the instantaneous location of each particle or

$$N(\mathbf{r}_1, \mathbf{r}_2, \dots, \mathbf{r}_N, \mathbf{v}_1, \mathbf{v}_2, \dots, \mathbf{v}_N, t) = \prod_{j=1}^N \delta[\mathbf{r} - \mathbf{r}_j(t)] \delta[\mathbf{v} - \mathbf{v}_j(t)].$$

This description is complete but of little use since it requires knowledge of the position and velocity of each particle in the phase space which may involve the solution of 10^{20} equations.

A more tractable description is the macroscopic distribution method where a physical quantity is averaged over the microscopic distribution function $f(\mathbf{r}, \mathbf{v}, t)$. For example, the particle density in configuration space, $n(\mathbf{r}, t)$, is

$$n(\mathbf{r}, t) = \int f(\mathbf{r}, \mathbf{v}, t) d^3 v \quad (1.60)$$

where we frequently use the abbreviated notation, $d^3 v = dv_x dv_y dv_z$. The averaging in velocity space is sometimes called the fluid model approach since the various macroscopic moments of the distribution function correspond to treating the plasma as a fluid and the various quantities as fluid elements. The first few moments after equation (1.60) (the zeroth moment) are the momentum density (the first moment)

$$m\mathbf{u} = m \int \mathbf{v} f d^3 v \quad (1.61)$$

and the energy density (the second moment)

$$\mathcal{E} = \frac{1}{2}m \int v^2 f d^3v. \quad (1.62)$$

The evolution of the distribution function in phase space is governed by the Boltzmann equation

$$\frac{\partial f}{\partial t} + \mathbf{v} \cdot \nabla f + \frac{\mathbf{F}}{m} \cdot \nabla_v f = \left(\frac{\partial f}{\partial t} \right)_{\text{coll.}} \quad (1.63)$$

where \mathbf{F} is the force due to electric and magnetic fields and ∇_v is the gradient in velocity space. This is essentially a conservation law describing a trajectory in phase space, and the collision term amounts to the annihilation of a particle at one point and its corresponding creation at another point because the actual trajectory appears discontinuous in phase space due to the (assumed) short range of the collision. These collisions tend to relax the distribution function to thermal equilibrium, but the collisions between different species which tend to bring the entire plasma to thermal equilibrium are not included here. The collisional term can be approximated in various ways, the simplest of which is to assume that it vanishes in the collisionless model. The collisionless Boltzmann equation,

$$\frac{\partial f}{\partial t} + \mathbf{v} \cdot \nabla f + \frac{q}{m} (\mathbf{E} + \mathbf{v} \times \mathbf{B}) \cdot \nabla_v f = 0 \quad (1.64)$$

along with the Maxwell equations are called the Vlasov equations, although occasionally equation (1.64) alone is referred to as the Vlasov equation. We shall generally refer to equation (1.64) as the *kinetic equation*. Without any collisions, of course, every phenomenon described by the Vlasov equations is reversible, so no loss of information can occur within this simplest approximation. The simplest nontrivial approximation to the collision term is the Krook model where

$$\left(\frac{\partial f}{\partial t} \right)_{\text{coll.}} = -\nu(f - f_0) \quad (1.65)$$

where ν is the collision frequency and f_0 is the steady-state equilibrium distribution function. In order to conserve particles in this model, we demand $\int f_1 d^3v d^3x = 0$, where $f_1 = f - f_0$, since f_1 will eventually decay away, and any particles associated with f_1 will disappear. However, it will relax the distribution towards equilibrium with an increase in entropy, so it does allow irreversible processes and loss of information. If we speak of a true equilibrium distribution function, then we necessarily must take f_0 to be a Maxwellian, described by

$$f_0(\mathbf{r}, \mathbf{v}) = A e^{-E/\kappa T}$$

where E is the sum of the kinetic energy and the potential energy, $E = \frac{1}{2}mv^2 + q\varphi(\mathbf{r})$, A is a normalization constant, κ is Boltzmann's constant, and T is the

thermodynamic temperature. We will occasionally refer to other functions $f_0(\mathbf{v})$ in later chapters, but the concept of temperature is unique to the Maxwellian distribution and the alternative functions are used either to simplify a calculation to demonstrate a point or represent a nonthermal distribution which may still be stationary on the wave time scale. Moreover, the value of A is obtained by the conservation of particles. If N is the total number of particles of the particular species, then we have

$$N = A \int d^3x \int d^3v e^{-E/\kappa T}$$

or

$$A = \frac{N}{\int d^3x \int d^3v e^{-E/\kappa T}}.$$

Since, as we noted earlier, the various plasma species are not in thermal equilibrium with one another, it is usually necessary to define a temperature for each plasma species. It is quite common, for example, for the electron temperature to be much higher than the ion temperature in an electron-ion plasma. We occasionally will even refer to two temperatures for a single species, since thermal effects for motion parallel to a magnetic field are very different from motions perpendicular to the field, so a parallel temperature distinct from a perpendicular temperature can be defined, but these only rarely are substantially different from one another or else the plasma becomes unstable.

1.5 Overview of the plasma wave zoo

In the chapters ahead, the general trend is from simple to complex, but even in the next chapter on cold plasmas, the anisotropy introduced by the magnetic field will introduce great complexity. The general development begins with a cold, infinite, homogeneous, and linear plasma, and then these constraints are relaxed one by one. The anisotropy due to the magnetic field is so fundamental to so many applications that it will be included throughout the linear development, but few examples are given in the more complicated nonlinear chapters.

[Chapter 2](#) introduces the basic dielectric tensor formalism with which we deal with cold plasma waves propagating in a magnetized plasma. With no thermal motions to complicate the picture, we discover the kinds of waves which may propagate in different regions of parameter space, and their different properties in different directions are so numerous we appear to be in a plasma wave ‘zoo’, where we must identify and classify the various wave types carefully. This is largely done through the Clemon–Mullaly–Allis (CMA) diagram (you may wish to turn to [figure 2.8](#) while you read the remainder of this paragraph) where boundaries or ‘fences’ keep each wave ‘animal’ in its own ‘cage’, so that we can analyze one (or two since sometimes two waves share the same cage) at a time. Without a magnetic field, there is a single ‘fence’ (the vertical line in

[figure 2.8](#)) and on one side it is empty and on the other side there is only one ‘animal’ characterized by a sphere. With a magnetic field, there are suddenly 13 ‘cages’, some with subregions inside! In these numerous regions, we may study the taxonomy where the waves may be characterized as spheroids or lemniscoids (two types), so that we may see relationships among the various subspecies in our zoo. One ‘cage’ is still empty, some have only one inhabitant (spheroid or lemniscoid), some have two spheroids while others have one of each (two lemniscoids cannot occur simultaneously). The ‘fences’ have peculiar properties also, since for some places one of the inhabitants can pass through one of the fences while the other cannot.

We discover that phase and group velocities are more complicated in three-dimensions with a magnetic field, and resonances which occur at specific angles with respect to the magnetic field lead to resonance cones and interesting particle motions. We also discover that some cages are so large that a wave near one boundary appears so different from its twin at the other boundary that it merits a new name. Thus it is not surprising that the *nomenclature* is a ‘zoo’ in its own right, there being separate histories from different communities with their own naming conventions which are quite incompatible, sometimes resulting in the same name describing different waves and different names describing the same wave.

In [chapter 3](#), we introduce the first thermal corrections, where effectively we allow the plasma to have a finite pressure and, later, drift velocities. These are described through the fluid equations which require the phase velocity to be large compared to the thermal velocity. This addition adds new animals to each cage, the acoustic or sound waves, which are sometimes unique new wave types and sometimes serve only to modify one of the cold plasma waves. Sometimes they provide a coupling between different cold plasma waves, and these couplings are generally found to be very dependent on angle. We try to organize these waves through Stringer diagrams, since they refuse to be bound by the fences of the cold plasma wave zoo. We also introduce collisions, though they could have been introduced to cold plasmas. Finally, the introduction of drift velocities leads to a variety of instabilities, so the classification of the types of instabilities is studied here along with several examples.

The restriction on the phase velocity is removed in [chapter 4](#) through the use of kinetic theory, where we allow the effects of particles traveling near the phase velocity to influence wave propagation and damping. The kinetic theory treatment of plasma waves is the most comprehensive description, but also the most complex. The fences of the CMA diagram may become fuzzy, and many of the couplings in the Stringer diagrams are found to be effectively eliminated through collisionless damping. Here we discover the effects of Landau damping, where the slope of the distribution function at the phase velocity can lead either to collisionless damping or instability. We explore the nature of this new damping without collisions, since it may cause the wave to damp away, but without any loss of information, characteristics which at first appear contradictory. The

same basic phenomenon in a magnetized plasma leads to cyclotron damping, and the effects of finite Larmor radii (usually but not always small compared to the wavelength) lead to cyclotron harmonic effects and an entirely new set of waves propagating nearly normally to the field which we call the Bernstein modes after their discoverer. By now, we have expanded the zoo and modified each of its species to such an extent that we can only look closely at the new arrivals and a few representative cases. Although the development from kinetic theory can treat any distribution function, the analysis is generally restricted to Maxwellian distributions except for illustrative examples and for the relativistic case. The general analysis for the relativistic case is included, with yet more new phenomena, but we examine only a few examples where the relativistic effects make a qualitative difference in the wave behavior, namely the appearance of collisionless damping exactly normal to the field. Because of the relativistic mass increase, even the fences move if the relativistic effects are strong enough, and these effects have been observed in high intensity laser irradiation.

The addition of physical boundaries in [chapter 5](#) restricts the spectrum of wavevectors which was unbounded in the infinite plasma. We treat only uniform plasmas within these boundaries, but point out an example where inhomogeneity affects the result significantly. In the bounded plasma we find waveguide-type cutoffs, discrete eigenmodes, geometry-dependent scattering resonances, and surface waves that propagate in one dimension but decay in the radial direction. While each wave type arises from one of the original animals in our zoo, it takes on a new look in the bounded plasma. This chapter also includes a discussion of mode orthogonality in a plasma-filled waveguide and the only antenna calculation.

While we could consider chapter 5 to deal with plasmas with a step function inhomogeneity (rapid change in plasma parameters over a wavelength), [chapter 6](#) deals with weak inhomogeneities (small change in plasma parameters over a wavelength). Following a wave through a slowly varying inhomogeneous plasma amounts to following a trajectory through the plasma zoo, often crossing fences (mode conversion) and occasionally passing through empty cages (tunneling). Away from these boundaries, not all of which are CMA boundaries since many of the transitions are from cold to hot plasma waves which did not appear in the cold plasma, the description of waves by WKB theory is relatively easy in one dimension. Most of the effort is then directed at the transitional coupling, where there may be transmission (tunneling through a resonance to a wave of the same type), reflection, mode conversion (to a wave of a different type), and absorption. An inevitable companion of absorption is radiation, since the two are coupled by Kirchhoff's law, and in this edition, emission is discussed in detail after generalizing Kirchhoff's law to include the variety of plasma wave types that are coupled in absorption and radiation zones. Beyond the one-dimensional inhomogeneities, we examine the nontrivial extension of WKB theory to three dimensions where the trajectory of the wave energy (following the group velocity) is influenced by gradients of plasma parameters in arbitrary directions. Finally,

we examine a class of instabilities called drift waves which arise from the fact that an inhomogeneous plasma is not in equilibrium, and hence has a source of free energy.

In the last two chapters, we finally relax the last restriction of linearity, and first examine weakly nonlinear effects ([chapter 7](#)) that include the effects of waves on the distribution function through quasilinear theory, and the resonant effects of waves coupling with other waves to produce a third wave. [Chapter 8](#) goes on to treat stronger nonlinear effects, where we deal with solitary waves and solitons, the effects of trapped particles, and finally the parametric instabilities. This latter topic couples animals from the same or different cages through a variety of possible nonlinear mechanisms, and is another zoo of its own because of the many possible combinations. Here we only lay out some of the general framework and examine a small (unmagnetized) corner of this zoo.

Chapter 2

Waves in a cold uniform plasma

The ABCs of plasma waves are linear cold plasma waves in an infinite, homogeneous plasma. The plasma is not isotropic, however, since the presence of a magnetic field provides one preferred direction. Without the magnetic field, the plasma may be represented by a simple dielectric constant and the only wave solution is a simple electromagnetic wave that propagates above the plasma frequency, ω_{pe} . This virtually trivial result will be included as a special case in our treatment of the finite magnetic field case, but we begin immediately with the more general and nontrivial case. By cold plasma, we mean a collection of charged particles without any net charge, and the particles are at rest except when they are induced to move through the action of the self-consistent electric and magnetic fields of the wave or, in other words, the particles have no kinetic thermal motion of their own.

In this chapter, we will examine several forms of the *dispersion relation*, the function that relates the frequency and the wavevector, that characterizes each wave type and leads to the labels for the various types. We will then examine some of the general properties of these various types of waves and examine a few special cases in more detail in order to illustrate the features of the various categories.

The labeling may be the most confusing part of this chapter, and indeed throughout the book, since there is virtually no overlap in the nomenclature used by laboratory plasma physicists and that used in ionospheric and astrophysical plasma waves. Even within these two major groups, there are sometimes several distinct names for exactly the same wave, depending on the history of the wave or the wave feature to be emphasized. For example, the fast Alfvén wave is the compressional Alfvén wave is the magnetohydrodynamic wave is the whistler wave is the ... (and the list goes on). Throughout the body of the text, the variety of names for a single wave will be severely restricted, but as each wave is introduced, or as a new aspect of the wave is unveiled, the multiplicity of names will be noted, although exhaustive lists are both unlikely and unhelpful. Whenever one is uncertain about which wave is referenced in the literature, it is best to determine

which wave it is by noting its characteristics, since it even happens that different groups use exactly the same names to mean totally different waves.

2.1 The cold plasma dispersion relation

The cold plasma dispersion relation (CPDR) was first published by Appleton in two stages: the result in 1927 [3] and the derivation in 1932 [4]. Because Hartree influenced the publication of the 1932 derivation, although he added nothing to the result, it is sometimes called the Appleton–Hartree dispersion relation. Following the historical study by Gillmor [5], however, where it was discovered among Appleton's own personal papers that Wilhelm Altar, while working with Appleton, first calculated the dispersion relation in 1926, it would be more appropriate to call it the Altar–Appleton dispersion relation. These early forms neglected ion motions but did include electron–neutral collisions.

2.1.1 Equations of motion

The calculation begins with the equation of motion for a single particle of species j in an electromagnetic field,

$$m_j \frac{d\mathbf{v}_j}{dt} = q_j(\mathbf{E} + \mathbf{v}_j \times \mathbf{B}) \quad (2.1)$$

along with the Maxwell equations,

$$\begin{aligned} \nabla \times \mathbf{E} &= -\frac{\partial \mathbf{B}}{\partial t} \\ \nabla \times \mathbf{B} &= \mu_0 \left(\mathbf{j} + \epsilon_0 \frac{\partial \mathbf{E}}{\partial t} \right) \end{aligned} \quad (2.2)$$

and the expression for the total current,

$$\mathbf{j} = \sum_j n_j q_j \mathbf{v}_j$$

where the sum is over the species. Since the plasma has been presumed to be uniform and homogeneous in both space and time, we may Fourier transform these equations or what is equivalent, assume that

$$\begin{aligned} \mathbf{E} &= \mathbf{E}_1 e^{i(\mathbf{k} \cdot \mathbf{r} - \omega t)} \\ \mathbf{B} &= \mathbf{B}_0 + \mathbf{B}_1 e^{i(\mathbf{k} \cdot \mathbf{r} - \omega t)} \\ \mathbf{v} &= \mathbf{v}_1 e^{i(\mathbf{k} \cdot \mathbf{r} - \omega t)} \end{aligned} \quad (2.3)$$

and \mathbf{B}_0 is the static magnetic field and is taken to be in the z -direction, and $|\mathbf{B}_1| \ll |\mathbf{B}_0|$. With these inserted into equation (2.1), we may rewrite that equation in linear form as

$$-i\omega m_j \mathbf{v}_{1j} = q_j(\mathbf{E}_1 + \mathbf{v}_{1j} \times \mathbf{B}_0) \quad (2.4)$$

where the second order terms have been neglected because we have assumed the waves are of sufficiently low amplitude that the linear approximation is valid. The solution of equation (2.4) for the velocity is

$$\begin{aligned} v_{xj} &= \frac{iq_j}{m_j(\omega^2 - \omega_{cj}^2)} (\omega E_x + i\epsilon_j \omega_{cj} E_y) \\ v_{yj} &= \frac{iq_j}{m_j(\omega^2 - \omega_{cj}^2)} (-i\epsilon_j \omega_{cj} E_x + \omega E_y) \\ v_{zj} &= \frac{iq_j}{m_j \omega} E_z. \end{aligned} \quad (2.5)$$

Here we have introduced the definitions $\epsilon_j \equiv q_j/|q_j|$ to denote the sign of the charge for species j and $\omega_{cj} \equiv |q_j|B_0/m_j$ is the cyclotron frequency for species j .¹ The first two of these may be simplified by introducing rotating coordinates such that $v_{\pm} = v_x \pm iv_y$ and $E_{\pm} = E_x \pm iE_y$. Then we may write both of these components as

$$v_{\pm} = \frac{iq_j}{m_j(\omega \mp \epsilon_j \omega_{cj})} E_{\pm}. \quad (2.6)$$

Similarly, the current density may be written as

$$\begin{aligned} J_{\pm} &= i\epsilon_0 \sum_j \frac{\omega_{pj}^2}{(\omega \mp \epsilon_j \omega_{cj})} E_{\pm} \\ J_z &= i\epsilon_0 \sum_j \frac{\omega_{pj}^2}{\omega} E_z \end{aligned} \quad (2.7)$$

where ω_{pj} is the plasma frequency for species j , given by

$$\omega_{pj}^2 = \frac{n_j q_j^2}{m_j \epsilon_0}. \quad (2.8)$$

2.1.1.1 Particle motions

In Fourier transform space, integrating the velocity equations to obtain the coordinates is done by simply dividing by $-i\omega$. For a simple case where $E_y = E_z = 0$ so that \mathbf{E} has only an x -component, we find

$$\begin{aligned} x_j &= -\frac{q_j E_x}{m_j(\omega^2 - \omega_{cj}^2)} \\ y_j &= \frac{\epsilon_j \omega_{cj}}{i\omega} x_j \end{aligned} \quad (2.9)$$

so that in general, the trajectory is elliptical. For $\omega \ll \omega_{cj}$, we find $x_j \ll y_j$, so the motion is principally across both the \mathbf{E} and \mathbf{B}_0 directions. However, for

¹ Some authors define $\omega_{cj} \equiv q_j B_0/m_j$ so that it is negative for electrons.

$\omega \gg \omega_{cj}$, $x_j \gg y_j$ and the motion is principally parallel to the electric field. In this latter case, we would call the particles unmagnetized, since the magnetic influence is small. Since it is possible for the wave frequency to be well above the ion cyclotron frequency at the same time it is well below the electron cyclotron frequency, it is possible for ions to be effectively unmagnetized while electrons are magnetized.

When $\omega \simeq \omega_{cj}$, then the linear solutions exhibit resonance effects with large amplitudes, and at resonance, the radius increases uniformly in time and no steady-state solution exists. In this vicinity, we expect the cold plasma approximation to fail and either thermal, inhomogeneous, or nonlinear effects to dominate the dynamics.

Problem 2.1.1. Cold plasma conductivity tensor.

- (i) Derive the elements of the conductivity tensor σ where $j = \sigma \cdot E$.
- (ii) Show that there is no dissipation associated with this conductivity. (Hint: Show that $\text{Re}(E^* \cdot j) = 0$, and then note how this result demonstrates the absence of dissipation, where E^* is the complex conjugate of E .)

2.1.2 Cold plasma dielectric tensor

If we now combine the plasma current and the displacement current such that

$$j - i\omega\epsilon_0 E \equiv -i\omega\epsilon_0 \mathbf{K} \cdot \mathbf{E}$$

then the resulting equivalent dielectric tensor is given by

$$\mathbf{K} = \begin{pmatrix} S & -iD & 0 \\ iD & S & 0 \\ 0 & 0 & P \end{pmatrix} = \begin{pmatrix} K_1 & K_2 & 0 \\ -K_2 & K_1 & 0 \\ 0 & 0 & K_3 \end{pmatrix} \quad (2.10)$$

where the dielectric tensor elements are defined by

$$K_1 \equiv S \equiv \frac{1}{2}(R + L) = 1 - \sum_j \frac{\omega_{pj}^2}{\omega^2 - \omega_{cj}^2} \quad (2.11)$$

$$iK_2 \equiv D \equiv \frac{1}{2}(R - L) = \sum_j \frac{\epsilon_j \omega_{cj} \omega_{pj}^2}{\omega(\omega^2 - \omega_{cj}^2)} \quad (2.12)$$

$$K_3 \equiv P = 1 - \sum_j \frac{\omega_{pj}^2}{\omega^2} \quad (2.13)$$

$$K_1 + iK_2 \equiv R \equiv S + D = 1 - \sum_j \frac{\omega_{pj}^2}{\omega(\omega + \epsilon_j \omega_{cj})} \quad (2.14)$$

$$K_1 - iK_2 \equiv L \equiv S - D = 1 - \sum_j \frac{\omega_{pj}^2}{\omega(\omega - \epsilon_j \omega_{cj})}. \quad (2.15)$$

The two equivalent sets of tensor elements in equations (2.11) through (2.15) are the familiar S , D , R , L , and P notation of Stix [6] and the cold plasma limit of the more general dielectric tensor to be developed in later chapters. The Stix labels are mnemonics for the Sum, Difference, Right, Left, and Plasma terms, respectively. In the subsequent sections, we will occasionally use the Stix notation to refer explicitly to the cold plasma terms *only*, while the more general notation may refer either to the cold plasma limit or include warm or hot plasma terms. The original Altar–Appleton dispersion relation neglected the ion terms, and the simplified dielectric tensor elements were then given by

$$\begin{aligned} K_1 &= 1 - \frac{X}{1 - Y^2} \\ K_2 &= \frac{iXY}{1 - Y^2} \\ K_3 &= 1 - X \end{aligned} \quad (2.16)$$

where $X = \omega_{pe}^2/\omega^2$ and $Y = \omega_{ce}/\omega$, except that collisions were included in the original work. The discussion of collisions is deferred until [chapter 3](#). This particular notation is common in discussing ionospheric phenomena, but is rarely used to discuss laboratory plasma waves.

Problem 2.1.2. Zeros of D .

- (i) Show that D cannot vanish at any frequency in a plasma with only one ion species (only one q_j/m_j ratio) and electrons with finite density and magnetic field.
- (ii) Show that there is one zero in D for each *additional* ion species (different q_j/m_j) added and that the zeros lie between each adjacent pair of ion cyclotron frequencies. (Hint: Do not try to find these frequencies, only prove that they exist.)

2.1.3 Forms of the dispersion relation

The Maxwell equations of equation (2.2) are now written as

$$\begin{aligned} ik \times \mathbf{E} &= i\omega \mathbf{B} \\ ik \times \mathbf{B} &= -i\omega \epsilon_0 \mu_0 \mathbf{K} \cdot \mathbf{E} \end{aligned} \quad (2.17)$$

with the resulting wave equation

$$\mathbf{n} \times (\mathbf{n} \times \mathbf{E}) + \mathbf{K} \cdot \mathbf{E} = 0 \quad (2.18)$$

where

$$\mathbf{n} = \frac{\mathbf{k}c}{\omega} \quad (2.19)$$

is the index of refraction vector whose direction is the direction of the wavevector \mathbf{k} and whose magnitude is the index of refraction. If we now choose \mathbf{n} to lie in

the x - z plane, and since we have already chosen \mathbf{B}_0 to be in the z -direction, then equation (2.18) becomes

$$\begin{pmatrix} S - n^2 \cos^2 \theta & -iD & n^2 \cos \theta \sin \theta \\ iD & S - n^2 & 0 \\ n^2 \cos \theta \sin \theta & 0 & P - n^2 \sin^2 \theta \end{pmatrix} \begin{pmatrix} E_x \\ E_y \\ E_z \end{pmatrix} = 0 \quad (2.20)$$

where θ is the angle between \mathbf{k} and the z -axis. In order to have a nontrivial solution, one requires that the determinant of coefficients vanish. This condition gives the cold plasma dispersion relation (CPDR),

$$An^4 - Bn^2 + C = 0 \quad (2.21)$$

where

$$\begin{aligned} A &= S \sin^2 \theta + P \cos^2 \theta \\ B &= RL \sin^2 \theta + PS(1 + \cos^2 \theta) \\ C &= PRL. \end{aligned} \quad (2.22)$$

The solutions of equation (2.21) may be written in either of two forms, first as a quadratic in n^2 ,

$$n^2 = \frac{B \pm F}{2A} \quad F^2 = B^2 - 4AC \quad (2.23)$$

where F^2 may be written in the form,

$$F^2 = (RL - PS)^2 \sin^4 \theta + 4P^2 D^2 \cos^2 \theta \quad (2.24)$$

or alternatively in terms of the angle,

$$\tan^2 \theta = -\frac{P(n^2 - R)(n^2 - L)}{(Sn^2 - RL)(n^2 - P)}. \quad (2.25)$$

The general condition for a resonance, where $n^2 \rightarrow \infty$, or where $A \rightarrow 0$, is given by equation (2.23) or equation (2.25) as

$$\tan^2 \theta = -P/S \quad \text{general resonance condition} \quad (2.26)$$

and the general cutoff condition, where $n = 0$, is given by equation (2.21) as

$$C = PRL = 0 \quad \text{general cutoff condition.} \quad (2.27)$$

We note some special cases at this point which we will take up in more detail in the following sections.

- (i) Propagation parallel to \mathbf{B}_0 , $\theta = 0$. (The numerator of equation (2.25) must vanish.)
 - (a) $P = K_3 = 0$ plasma oscillations.

- (b) $n^2 = R = K_1 + iK_2$ wave with right-handed polarization.
- (c) $n^2 = L = K_1 - iK_2$ wave with left-handed polarization.
- (ii) Propagation perpendicular to \mathbf{B}_0 , $\theta = \pi/2$. (The denominator of equation (2.25) must vanish.)
 - (a) $n^2 = P = K_3$ ordinary wave.
 - (b) $n^2 = RL/S = (K_1^2 + K_2^2)/K_1$ extraordinary wave.

Problem 2.1.3. Show that F^2 is positive definite, i.e. show that F^2 may be written in the form of equation (2.24).

2.2 The CMA diagram

Because of the number of different solutions and their behavior at various angles and in different frequency bands, this simplest of plasma wave problems (cold plasma only) has become significantly complicated. There are various ways of tabulating the characteristics of the waves in various regions of parameter space, and we shall include several. The starting point is the Clemmow–Mullaly–Allis (CMA) diagram and the associated wave normal surface (WNS) topology. This method of tabulating shows at a glance whether one or two waves (or none) propagate, whether a resonance occurs, which wave is fast or slow, and shows the connections between the right- and left-handed waves and the ordinary and extraordinary waves as the angle changes from 0 to $\pi/2$.

As we establish conditions for the boundaries and determine the topology of the WNSs for each region of the CMA diagram, we will also show dispersion curves that represent selected slices through the CMA diagram, and offer interpretations of the topological features.

2.2.1 Principal solutions—parallel propagation

We first define the *principal resonances* to be those which occur at $\theta = 0$ and $\theta = \pi/2$. The general condition for a resonance ($n^2 \rightarrow \infty$) is evident from equation (2.25) which becomes

$$\tan^2 \theta = -P/S. \quad (2.28)$$

Hence, for $\theta \rightarrow 0$, we require $S \rightarrow \infty$ since $P = 0$ is a cutoff. Since $S = \frac{1}{2}(R + L)$, this can be satisfied for either

$$R \rightarrow \infty \text{ (electron cyclotron resonance)}$$

or

$$L \rightarrow \infty \text{ (ion cyclotron resonance).}$$

2.2.1.1 The right-handed wave

For a simple plasma of electrons and one ion species, the dispersion relation for the right-handed wave, $n_R^2 = R$, which propagates parallel to \mathbf{B}_0 is given by equation (2.14) as

$$n_R^2 = R = 1 - \frac{\omega_{pi}^2}{\omega(\omega + \omega_{ci})} - \frac{\omega_{pe}^2}{\omega(\omega - \omega_{ce})} \quad (2.29)$$

so the resonance is clearly at $\omega = \omega_{ce}$. The cutoff frequency, where $n^2 = R = 0$, is given by

$$\omega_R = \frac{\omega_{ce} - \omega_{ci}}{2} + \left[\left(\frac{\omega_{ce} + \omega_{ci}}{2} \right)^2 + \omega_p^2 \right]^{1/2} \quad (2.30)$$

where we have defined the composite quantity

$$\omega_p^2 \equiv \omega_{pe}^2 + \omega_{pi}^2.$$

For low and high density limits, the cutoff frequency may be approximated by

$$\omega_R \simeq \begin{cases} \omega_{ce} \left(1 + \frac{\omega_{pe}^2}{\omega_{ce}^2} \right) & R\text{-wave cutoff—low density} \\ \omega_{pe} + \frac{1}{2}\omega_{ce} & R\text{-wave cutoff—high density} \end{cases} \quad (2.31)$$

where we have assumed $m_e \ll m_i$, which is always valid except in electron–hole or electron–positron plasmas (except that in partially ionized plasmas, electron attachment may lead to negative ions with $m_- \sim m_+$).

For low and high frequencies, the index of refraction approaches the limits

$$n_R^2 \simeq \begin{cases} 1 + \frac{\omega_{pi}^2}{\omega_{ci}^2} \equiv \frac{c^2}{V_A^2} & \text{as } \omega \rightarrow 0 \\ 1 - \frac{\omega_{pe}^2}{\omega^2} & \text{as } \omega \rightarrow \infty. \end{cases} \quad (2.32)$$

where V_A is the Alfvén speed. The dispersion relation for the right-handed wave is plotted for high and low density cases in figure 2.1.

2.2.1.2 The left-handed wave

The dispersion relation for the left-handed wave, $n_L^2 = L$, is also given by equation (2.15) as

$$n_L^2 = L = 1 - \frac{\omega_{pi}^2}{\omega(\omega - \omega_{ci})} - \frac{\omega_{pe}^2}{\omega(\omega + \omega_{ce})} \quad (2.33)$$

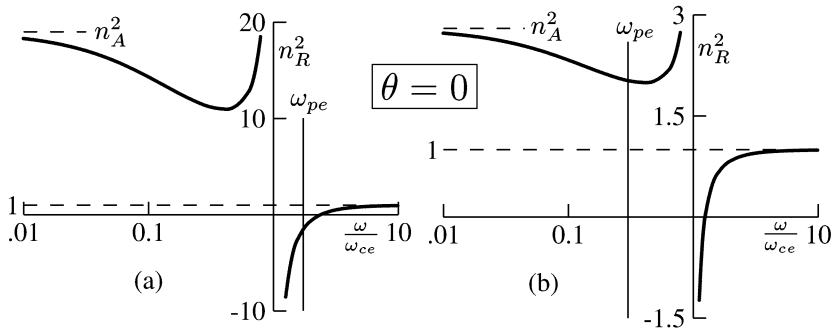


Figure 2.1. Dispersion relation for R -wave: (a) high density case, $\omega_{pe}^2/\omega_{ce}^2 = 3$; (b) low density case, $\omega_{pe}^2/\omega_{ce}^2 = 0.3$ ($m_i/m_e = 5$).

so the resonance in this case is clearly at $\omega = \omega_{ci}$. The cutoff frequency, where $n^2 = L = 0$ is given by

$$\omega_L = \frac{\omega_{ci} - \omega_{ce}}{2} + \left[\left(\frac{\omega_{ci} + \omega_{ce}}{2} \right)^2 + \omega_p^2 \right]^{1/2}. \quad (2.34)$$

For low and high densities, the cutoff frequency may be approximated by

$$\omega_L \simeq \begin{cases} \omega_{ci} + \frac{\omega_{pi}^2}{\omega_{ci}} & L\text{-wave cutoff—low density} \\ \omega_{pe} - \frac{1}{2}\omega_{ce} & L\text{-wave cutoff—high density} \end{cases} \quad (2.35)$$

where we have again assumed $m_e \ll m_i$.

For low and high frequencies, the index of refraction approaches the limits

$$n_L^2 \simeq \begin{cases} 1 + \frac{\omega_{pi}^2}{\omega_{ci}^2} \equiv \frac{c^2}{V_A^2} & \text{as } \omega \rightarrow 0 \\ 1 - \frac{\omega_{pe}^2}{\omega^2} & \text{as } \omega \rightarrow \infty. \end{cases} \quad (2.36)$$

The dispersion relation for the left-handed wave is plotted for high and low density cases in figure 2.2. Except for the large difference between the two cyclotron frequencies, it is apparent that the propagation characteristics are very similar to the R -wave dispersion relation with identical asymptotes at low and high frequency.

2.2.2 Principal solutions—perpendicular propagation

As $\theta \rightarrow \pi/2$, $P/S \rightarrow \infty$, and since $P \rightarrow \infty$ is a trivial solution (either $\omega \rightarrow 0$, so no wave at all, or $\omega_p \rightarrow \infty$, which is impossible), we require $S \rightarrow 0$. These

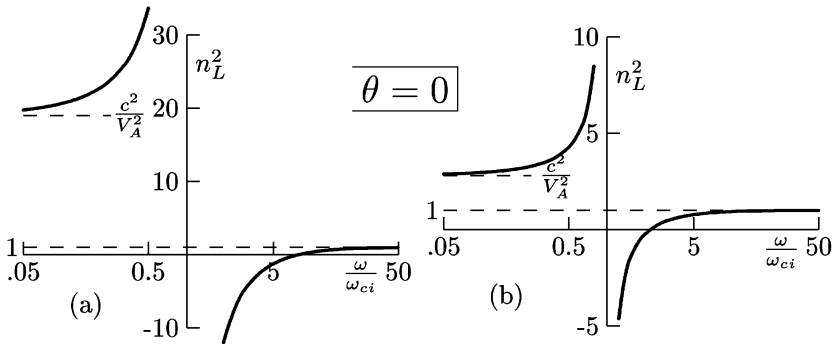


Figure 2.2. Dispersion relation for L -wave: (a) high density case, $\omega_{pe}^2/\omega_{ce}^2 = 3$; (b) low density case, $\omega_{pe}^2/\omega_{ce}^2 = 0.3$ ($m_i/m_e = 5$).

resonances are called hybrid resonances because they generally involve some combination of ω_c and ω_p . The solutions for perpendicular propagation are the ordinary and extraordinary waves.²

2.2.2.1 The ordinary wave

The dispersion relation for the ordinary wave is the same as in an unmagnetized plasma, and is given simply by

$$n_O^2 = P = 1 - \frac{\omega_{pe}^2}{\omega^2} - \frac{\omega_{pi}^2}{\omega^2} = 1 - \frac{\omega_p^2}{\omega^2} \quad (2.37)$$

for a single-ion species plasma, and it is immediately apparent that this wave has no dependence on the magnetic field at all. As will be shown later as we look at the polarization of the various solutions, this wave has E parallel to B_0 , so the particles do not experience any effects of the magnetic field. It is clear that there is no resonance and that the cutoff is at $\omega = \omega_p$. There is no propagation below ω_p and $n^2 \rightarrow 1$ as $\omega \rightarrow \infty$, so the dispersion relation is very simple in a cold plasma.

Problem 2.2.1. The ordinary wave. Show that for the ordinary wave (O -wave), $v_p v_g = c^2$, or that the product of the phase velocity and the group velocity is equal to the square of the velocity of light. What does this imply about the relationship between the phase velocity and the velocity of light for the O -wave?

Problem 2.2.2. Reflection from the ionosphere. Since AM broadcast (and ham band) waves reflect from the ionosphere ($\omega_p > \omega$), permitting long range

² For space and ionospheric applications, their ordinary wave is our R -wave and our X -wave is their Z -mode.

communication, whereas FM waves propagate through the ionosphere, limiting the range to line-of-sight, estimate the electron density in the ionosphere.

2.2.2.2 The extraordinary wave

The dispersion relation for the extraordinary wave, given by

$$n_X^2 = \frac{RL}{S} = \frac{[(\omega + \omega_{ci})(\omega - \omega_{ce}) - \omega_p^2][(\omega - \omega_{ci})(\omega + \omega_{ce}) - \omega_p^2]}{(\omega^2 - \omega_{ci}^2)(\omega^2 - \omega_{ce}^2) + \omega_p^2(\omega_{ce}\omega_{ci} - \omega^2)} \quad (2.38)$$

is the most complicated of these simplified dispersion relations, since neither the resonances nor the cutoffs have simple expressions. The resonances are given by the zeros of the denominator, which lead to the quadratic roots

$$\omega^2 = \frac{\omega_e^2 + \omega_i^2}{2} \pm \left[\left(\frac{\omega_e^2 - \omega_i^2}{2} \right)^2 + \omega_{pe}^2 \omega_{pi}^2 \right]^{1/2} \quad (2.39)$$

where we have defined the composite frequencies

$$\omega_j^2 \equiv \omega_{pj}^2 + \omega_{cj}^2 \quad j = e, i.$$

One of the roots is simply given (neglecting m_e/m_i) by ω_e , the Pythagorean sum of the electron cyclotron frequency and the electron plasma frequency, namely

$$\omega_{UH}^2 = \omega_{pe}^2 + \omega_{ce}^2 \quad [\text{upper hybrid resonance}]. \quad (2.40)$$

The extraordinary wave is sometimes called the Z-mode, especially in space applications.

The other root is more complicated, but again neglecting terms of order m_e/m_i ,

$$\omega_{LH}^2 = \omega_{ce}\omega_{ci} \left(\frac{\omega_{pe}^2 + \omega_{ce}\omega_{ci}}{\omega_{pe}^2 + \omega_{ce}^2} \right) \quad [\text{lower hybrid resonance}] \quad (2.41)$$

so the lower hybrid resonance occurs at the geometric mean of the two cyclotron frequencies in the high density limit and at ω_i , the Pythagorean sum of the ion cyclotron frequency and the ion plasma frequency in the low density limit.

Problem 2.2.3. The hybrid resonances.

- (i) Show that equations (2.38) and (2.39) are exact.
- (ii) Show that the given hybrid resonance frequencies are accurate to order m_e/m_i . (Hint: After factoring out $(\omega_e^2 - \omega_i^2)/2$ from the radical of equation (2.39), expand the radical and show that all terms after the first

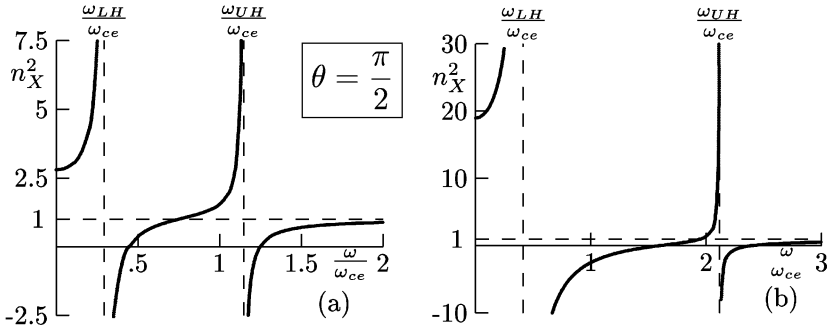


Figure 2.3. Dispersion relation for the extraordinary wave (X -mode): (a) low density case, $\omega_{pe}^2/\omega_{ce}^2 = 0.3$; (b) high density case, $\omega_{pe}^2/\omega_{ce}^2 = 3$ ($m_i/m_e = 5$).

order term are higher order in m_e/m_i . Then show how the zero and first order terms lead to the listed results.)

- (iii) Show that the low density expression for the lower hybrid resonance is the Pythagorean sum indicated.

The cutoffs for the extraordinary wave are given by the roots of the numerator of equation (2.38), again leading to quadratic roots of the form

$$\omega_X = \left[\left(\frac{\omega_{ce} + \omega_{ci}}{2} \right)^2 + \omega_p^2 \right]^{1/2} \pm \frac{\omega_{ce} - \omega_{ci}}{2} \quad (2.42)$$

where two negative roots have been discarded. For the high density limit, the two cutoffs are at

$$\omega_X \simeq \omega_{pe} \pm \frac{1}{2}\omega_{ce} \quad \text{X-wave cutoff—high density.} \quad (2.43)$$

For the low density limit, the two cutoffs are located at

$$\omega_X \simeq \begin{cases} \omega_{ce} + \frac{\omega_{pe}^2}{\omega_{ce}} & \text{X-wave cutoff—low density.} \\ \omega_{ci} + \frac{\omega_{pe}^2}{\omega_{ce}} \end{cases} \quad (2.44)$$

The low frequency limit ($\omega \rightarrow 0$) again leads us to the case

$$n^2 \rightarrow 1 + \frac{\omega_{pi}^2}{\omega_{ci}^2} = \frac{c^2}{V_A^2} \quad \text{as } \omega \rightarrow 0 \quad (2.45)$$

as in the R - and L -wave cases. In the high frequency limit, $n^2 \rightarrow 1$ as $\omega \rightarrow \infty$. With these features established, the dispersion relation for the extraordinary wave is plotted in figure 2.3 for the low and high density cases.

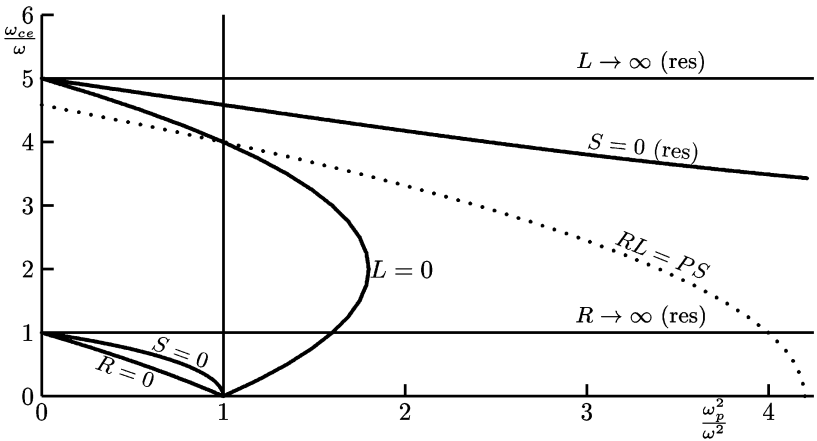


Figure 2.4. Principal axes and boundaries of the CMA diagram (to scale with $m_i/m_e = 5$).

2.2.3 CMA boundaries—cutoffs and resonances

Having established some of the features of the principal waves, we wish now to plot the principal resonances and cutoffs as a function of density and magnetic field. We use as the coordinates for this plot the normalized magnetic field, $\omega_{ce}/\omega = Y$, versus the density, $\omega_p^2/\omega^2 \equiv X$, where X and Y are the variables in the Altar–Appleton dispersion relation. These axes are linear in density to the right and linear in the magnetic field in the vertical direction. Noting first just the principal boundaries, the electron and ion cyclotron frequencies and the plasma frequency are the horizontal and vertical lines in figure 2.4.

It is clear from the spacing that this figure is not to scale for a real plasma since the ratio, $\omega_{ce}/\omega_{ci} \gg 1$, is so large for realistic plasma parameters that the two cyclotron resonances could not be shown in a reasonable fashion. Using this distorted scale ($m_i = 5m_e$), we then add all of the principal resonances and cutoffs. With the axes chosen to vary inversely with ω , the high frequency region is in the lower left corner, approaching the origin as $\omega \rightarrow \infty$, and the low frequency region is in the upper right section.

We note that the $R = 0$ boundary is a straight line with this choice of axes ($S = 0$ would be a straight line if we used ω_{ce}^2/ω^2 for the vertical axis, but it lies above $R = 0$ in either case). It is easily shown that near the bottom of the figure, $L = 0$ and $R = 0$ are described by $X = 1 \pm Y$, so both converge to $X = 1$ at the bottom. At $\omega = \omega_{ce}$, it may be shown that the $L = 0$ boundary crosses the $R \rightarrow \infty$ boundary at $X = 2(m_i - m_e)/m_i \rightarrow 2$ as $m_e/m_i \rightarrow 0$. The two cutoffs have already been shown to approach their respective cyclotron frequencies as $\omega_p \rightarrow 0$, so the paths of $R = 0$ and $L = 0$ are defined. The upper hybrid resonance (the *lower* $S = 0$ curve) has the same end points as the

$R = 0$ curve, and lies above it, so its character is determined. The lower hybrid resonance (the *upper S = 0* curve) approaches the ion cyclotron resonance in the low density limit (the left edge), and the geometric mean $\sqrt{\omega_{ce}\omega_{ci}}$ in the high density limit, so it asymptotes to a value between the cyclotron resonances to the right. It always lies above the $L = 0$ curve, so its character is determined. The boundaries between propagating and nonpropagating waves for the principal solutions are thus shown in figure 2.4. The significance of the $RL = PS$ boundary is that the distinction between the ordinary wave and the extraordinary wave is lost since both have $n^2 = P$ on this boundary where the solutions cross.

Problem 2.2.4. $RL = PS$ and $S = 0$ boundary crossings.

- (i) Prove that the $RL = PS$ boundary crosses the $P = 0$ axis at $\omega_{ce}/\omega = m_i/m_e - 1$ (exact).
- (ii) Prove that $\omega_{ce}/\omega \rightarrow m_i/m_e - \frac{1}{2}$ for the $RL = PS$ boundary as $\omega_p \rightarrow 0$ for $m_i \gg m_e$.
- (iii) Prove that the $S = 0$ curve crosses the $P = 0$ boundary at $\omega_{ce}/\omega = m_i/m_e - \frac{1}{2}$ for $m_i \gg m_e$.

2.2.4 Wave normal surface topology—spheroids and lemniscoids

The wave normal surfaces (WNSs) are plots of the phase velocity in each domain of the CMA diagram. Their topological features are invariant inside each region and change as each boundary is crossed. In order to establish the WNS topology in each region and to establish the significance of the boundaries of the CMA diagram, since they have been drawn only for $\theta = 0, \pi/2$ while the dispersion relation involves general angles, we will first prove some properties of the solutions and the CMA diagram boundaries.

2.2.4.1 Theorems on WNS topology and CMA diagram boundaries

CMA Theorem 1. Inside any bounded volume of the CMA diagram, $n \neq 0$.

Proof. The condition for $n = 0$ is $PRL = 0$ from equation (2.27) so this occurs only for $P = 0$, $R = 0$, or $L = 0$, and these are all bounding surfaces.

CMA Theorem 2. If $n \rightarrow \infty$ at any point inside a bounded volume, then there exist angles θ_{res} and $\pi - \theta_{\text{res}}$ at every point inside the volume where $n \rightarrow \infty$.

Proof. The condition for resonance, $\tan^2 \theta = -P/S$, is given by equation (2.26). Since P and S are real and single-valued, if P/S is negative anywhere in a volume, it is negative everywhere in the volume since both P and S can change sign only at one of the boundaries (P is bounded for finite plasma density, so it can only change sign at $P = 0$. $S = \frac{1}{2}(R + L)$ can change sign at $S = 0$ and where $R \rightarrow \infty$ or $L \rightarrow \infty$). For each value of $P/S < 0$, there exists an angle

θ_{res} and its supplement $\pi - \theta_{\text{res}}$ where $n^2 \rightarrow \infty$. We note that this angle cannot equal 0 or $\pi/2$ except on the boundary.

CMA Theorem 3. For any real angle within an interval where $n \neq 0$ and bounded, a single branch of n will be either real or imaginary throughout the interval.

Proof. From Problem 2.1.3, $F^2 \geq 0$, so n^2 is real everywhere, and hence n is either purely real or imaginary, and can only change over the interval in θ when n^2 passes through 0 or ∞ .

CMA Theorem 4. When n is real, it is symmetric about the z -axis ($\theta = 0$) and about the midplane ($\theta = \pi/2$).

Proof. The symmetry derives from the physics of the wave problem, since the dispersion relation does not depend on the sign of B_0 . The symmetry is apparent from equation (2.22) where the coefficients in the dispersion relation depend only on $\sin^2 \theta$ and $\cos^2 \theta$, both of which are symmetric about 0 and $\pi/2$.

CMA Theorem 5. Two solutions can coincide only at $\theta = 0$ or $\theta = \pi/2$, except where $RL = PS$ and $PD = 0$.

Proof. Solutions coincide only when $F = 0$, from equation (2.23), which requires $PD = 0$ and $RL = PS$ since each term in equation (2.24) is individually positive definite. At this point they coincide at all angles.

With only one ion species, it may be noted that $D \neq 0$ (except for the trivial case where $n_e \rightarrow 0$ or $B_0 \rightarrow 0$). For a multiple species CMA diagram, an additional boundary should be added for each additional ion species to show $D = 0$, particularly at the intersection with the $RL = PS$ surface.

2.2.4.2 The wave normal surfaces (WNSs)

We form the WNSs by plotting the phase velocity, $u = \omega/k = c/n$, versus θ . The surfaces are of three types: spheroids, dumbbell lemniscoids, and wheel lemniscoids.

Spheroids. If P and S have the same sign, then by theorem 2, $u \neq 0$ everywhere in the volume. By theorem 1, u cannot go to ∞ in the volume. Then by theorem 3, if u is real anywhere, it is real everywhere. Topologically, then, this is a spheroid. We do not distinguish between prolate and oblate spheroids.

Lemniscoids. If $P/S < 0$, then by theorem 2, at least one branch has $u \rightarrow 0$ at θ_{res} and its supplement everywhere in the volume. The cross generated near $u = 0$ by these angles rotated about the vertical axis forms a pair of cones touching vertex to vertex. By theorem 1, u cannot go to ∞ , and by theorem 2 cannot go to 0 at any other angle. Thus u is finite everywhere except at the vertex of the cones. By theorem 3, u must be real inside the cones and imaginary outside or vice versa. If it is real inside the cone, we have a dumbbell lemniscoid, and if

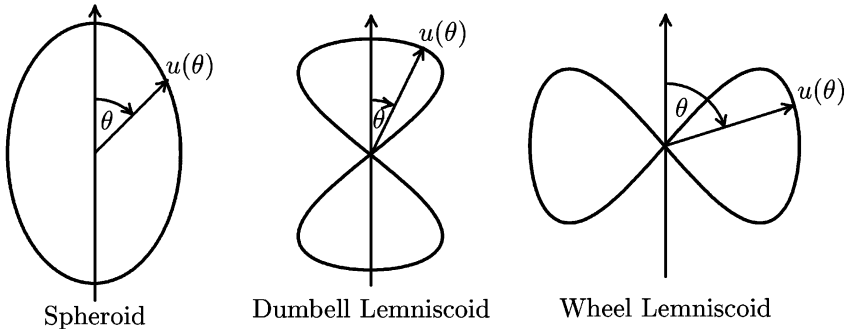


Figure 2.5. The three topological varieties of wave normal surfaces.

it is real outside the cone, we have a wheel lemniscoid. These are illustrated in figure 2.5.

In general, there are two solutions for u , and we must consider the possibilities for the second solution. Clearly, if $P/S > 0$, there can only be spheroids. From theorem 3, there can be either one, two, or none in this case. From theorem 5, they cannot touch inside a region, so if there are two, they are nested in the same order throughout the volume (except along the surface $RL = PS$ where they cross and the labels change).

For the case when $P/S < 0$, the second solution, if it has real u , is a spheroid. This may be demonstrated by examining the dispersion relation in the vicinity of θ_{res} where $A = 0$ in equation (2.21). Using this condition to eliminate the n^4 term, the remaining solution is given by

$$u^2 \simeq \frac{B}{C} \simeq \frac{S^2 + D^2 \cos^2 \theta}{RLS} \quad (2.46)$$

where we have used $\sin^2 \theta \simeq -(P/S) \cos^2 \theta$. This solution is nonzero within any volume, so it represents a spheroid. We also note that if there is both a lemniscoid and a spheroid in the same volume, the spheroid must enclose the lemniscoid by theorem 5.

2.2.5 Labeling—left and right, ordinary and extraordinary

One of the most confusing aspects of reading the plasma literature is the nomenclature used to describe the various waves. Some of the confusion arose when E Astrom [7] called the two low-frequency waves (upper right in the CMA diagram) the ordinary and extraordinary waves because the former is a spheroid (spherical as $\omega \rightarrow 0$). Later W P Allis [8] decided to call the solution $n^2 = P$ at $\theta = \pi/2$ the ‘ordinary’ wave because it was unaffected by the magnetic field. These two definitions remain in conflict and both are in present use. Without

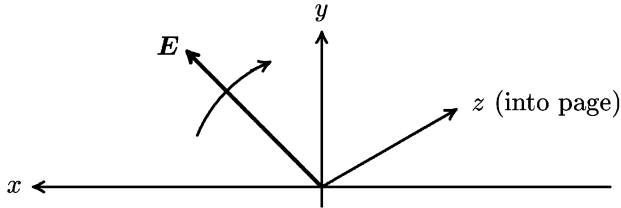


Figure 2.6. Clockwise rotation of the electric field.

the additional $RL = PS$ boundary, the Allis notation even had the disadvantage that the labels could change within a bounded volume, since X changes to O as this boundary is crossed, but that difficulty has been removed with this additional surface. Because the character of these various waves changes so much as one goes from $\theta = 0$ to $\theta = \pi/2$, it is difficult to choose a labeling system which adequately describes a good physical property of the solutions over the entire range of parameters within a bounded volume except for the fast and slow labels. We thus will label the waves first in terms of their behavior at $\theta = 0$ and then at $\theta = \pi/2$ as a separate label. Then we will discuss other possible schemes.

2.2.5.1 Polarization for propagation at $\theta = 0$

We define the terms right-handed and left-handed in terms of the rotation of the electric field vector as a wave propagates parallel to the magnetic field. If the electric vector rotates clockwise as we look along the B -field direction, then this is a right-handed wave, and the left-handed wave rotates counterclockwise. To see what this implies, we consider a wave with complex E_x and E_y that represents a circularly polarized R -wave by requiring

$$\begin{aligned}\operatorname{Re}(E_x) &= a \cos(-\omega t) = \operatorname{Re}(ae^{-i\omega t}) \\ \operatorname{Re}(E_y) &= -a \sin(-\omega t) = \operatorname{Re}(iae^{-i\omega t})\end{aligned}\quad (2.47)$$

and from figure 2.6, it is clear that the measurable fields represented by equation (2.47) with real a rotate clockwise. Thus it follows that the phases of the waves are given by

$$\begin{aligned}iE_x &= E_y && R\text{-wave} \\ iE_x &= -E_y && L\text{-wave.}\end{aligned}\quad (2.48)$$

In order to connect this result with the plasma waves, we note that the middle equation of equation (2.20) leads to

$$\frac{iE_x}{E_y} = \frac{n^2 - S}{D} = \pm 1\quad (2.49)$$

by letting $n^2 = R, L$. This verifies our labeling of the waves as being right- or left-handed. Even this labeling is not consistent as the angle varies, since if the angle given by $\sin^2 \theta_c = P/S$ is a real angle, then $n^2 = S$ at that angle and the polarization changes direction (see problem 2.2.5). Thus the polarization labels apply only at $\theta = 0$.

The ordinary and extraordinary labels have no physical significance except that the ordinary wave, with $n^2 = P$, is independent of the magnetic field, as noted by Allis, and has no resonance. The extraordinary wave, in contrast, has two resonances and depends strongly on both the magnetic field and the density.

The final label, which is the most useful topological designation since it applies everywhere inside a volume and at all angles, is the fast (*F*) or slow (*S*) label, which simply means that the fast wave has a higher phase velocity than the slow wave. From theorem 5, this labeling is valid throughout the volume and independent of the angle.

We can now establish which regions have which kinds of waves by noting whether these principal solutions exist in the various regions and whether there is a resonance (lemniscoid) in the region. Referring to figure 2.7, the shaded regions show where the various quantities are negative, hence there can be no *O*-wave to the right of the $P = 0$ boundary, no *L*-wave to the right of the $L = 0$ boundary and below the $L \rightarrow \infty$ line, and no *R* wave to the right of the $R = 0$ boundary and below the $R \rightarrow \infty$ line. In figure 2.7(*d*), the shaded regions must have a lemniscoid, while the unshaded regions may have spheroids only, but need not have any.

Problem 2.2.5. Change of polarization. Show that if the angle defined by $\sin^2 \theta_c = P/S$ is a real angle, then the polarization changes at that angle from right to left or vice versa.

2.2.6 The CMA diagram for a one-ion species plasma

In order to fill in the regions of the CMA diagram with the appropriate WNSs, and at the same time get a fuller appreciation of their structure, we will take a tour through the diagram, filling in the surfaces and labels, using the properties at the boundaries to enable us to resolve which is the appropriate label for which surface.

2.2.6.1 Transitions across boundaries

We first establish the character of a boundary crossing, where by definition, some wave either ceases to propagate or begins to propagate, or at least changes labels. From the property that the phase velocity $u = c/n$, it follows that every cutoff means the phase velocity for the wave experiencing the cutoff tends toward infinity. For the same reasons, a wave experiencing a resonance has the phase velocity approach zero, at least at the appropriate angle.

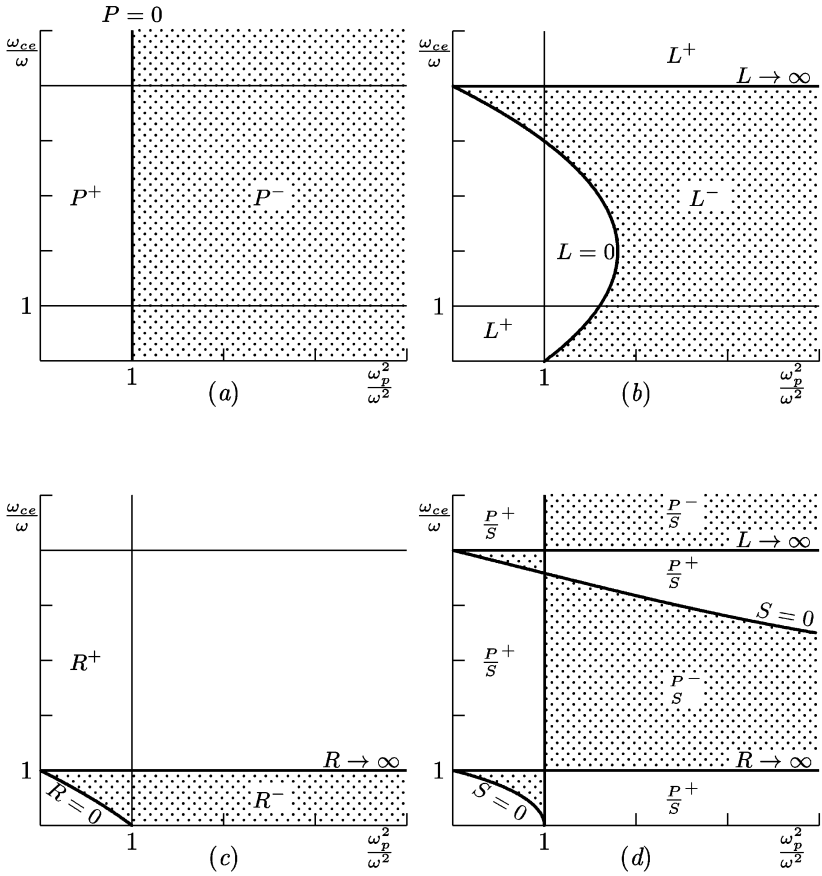


Figure 2.7. (a) O -waves propagate in P^+ regions. (b) L -waves propagate in L^+ regions. (c) R -waves propagate in R^+ regions. (d) Spheroids only in $(P/S)^+$ regions. One lemniscoid in $(P/S)^-$ regions.

2.2.6.2 Touring the CMA diagram

We begin with the high frequency limit, which is the lower left-hand corner of the CMA diagram, and we call this region 1. From figure 2.7(a), The O -wave propagates in this region, and from figures 2.7(b) and 2.7(c), both the R - and L -waves propagate. In fact, since in the extreme high frequency limit the plasma does not respond at all, it is clear that two waves propagate in both directions, so we must have the X -wave also. Using figure 2.7(d) establishes that $S > 0$, so we can determine the same result from $RL/S > 0$. This same figure establishes that there are spheroids only, and since both the R - and L -waves propagate, there must be two spheroids, so the result may be established in many ways. We now

use that fact that both the R - and X -waves have a cutoff at the $R = 0$ boundary, sending the phase velocity to infinity, so the $R-X$ spheroid must be the fast wave and the $L-O$ spheroid the slow wave, as in [figure 2.8](#).

Crossing the $R = 0$ boundary to region 2, the $R-X$ spheroid disappears as both are cutoff, while the $L-O$ spheroid is topologically unchanged.

Crossing the $S = 0$ boundary into region 3, there is now a lemniscoid from [figure 2.7\(d\)](#), and since we passed through the extraordinary wave resonance, the lemniscoid introduces an X -wave on the inside of the $L-O$ spheroid, which is again topologically unchanged. Because it is an X -wave lemniscoid, it is a wheel lemniscoid, propagating at $\theta = \pi/2$.

The transition as we cross the $P = 0$ boundary to region 4 is less obvious, except that of course the O -wave disappears and the L -wave survives. Figure 2.7(d) indicates that there is no lemniscoid, so a single $L-X$ spheroid is the only possibility.

Crossing the $L = 0$ boundary into region 5a, this is a cutoff for both the L - and X -waves, so both disappear. There is no O - or R -wave either from figures 2.7(a) and (b), so this region is empty and nothing propagates. Region 5b is distinct because we have crossed the $RL = PS$ boundary, but still nothing propagates.

Crossing the $R \rightarrow \infty$ boundary from region 3 to region 6a, the R -wave begins to propagate, and is the slow wave. The X -wave continues to propagate as this boundary is crossed, since the resonance is both in the numerator and denominator, so the two spheroids have opposite labels from those in region 1.

Crossing the $P = 0$ boundary into region 7, there is now a lemniscoid from [figure 2.7\(d\)](#), but both the R - and L -waves are unaffected. There is no O -wave from [figure 2.7\(a\)](#), so the surviving spheroid must be an $L-X$ spheroid.

Moving across the $L = 0$ boundary into region 8a, both the L - and X -waves pass a cutoff, so the $L-X$ spheroid has moved off to infinity and the dumbbell lemniscoid of the R -wave is unchanged. The transition across the $RL = PS$ boundary into region 8b means nothing here, since there is neither an X - nor an O -wave.

Moving from region 6a to 6b across the $RL = PS$ boundary, however, does make a nontrivial difference, since both an O - and X -wave are present. In this case the O -wave is the fast wave in region 6a, and the X -wave is the fast wave in region 6b.

Crossing the $L = 0$ boundary into region 9, the $L-X$ spheroid moves off to infinity, leaving the $R-O$ spheroid only. We could also have reached this conclusion by crossing the $P = 0$ boundary from region 8b, where the crossing removes the lemniscoid and introduces the O -wave.

Crossing the $S = 0$ boundary into region 10, the $R-O$ spheroid is unaffected, but a lemniscoid is added from [figure 2.7\(d\)](#). The $S = 0$ boundary is a resonance for the X -wave, so the X -wave now propagates as a wheel lemniscoid.

Moving up across the $L \rightarrow \infty$ boundary into region 12, the $R-O$ spheroid is unaffected, while the L -wave is added, opening up the lemniscoid into the $L-X$

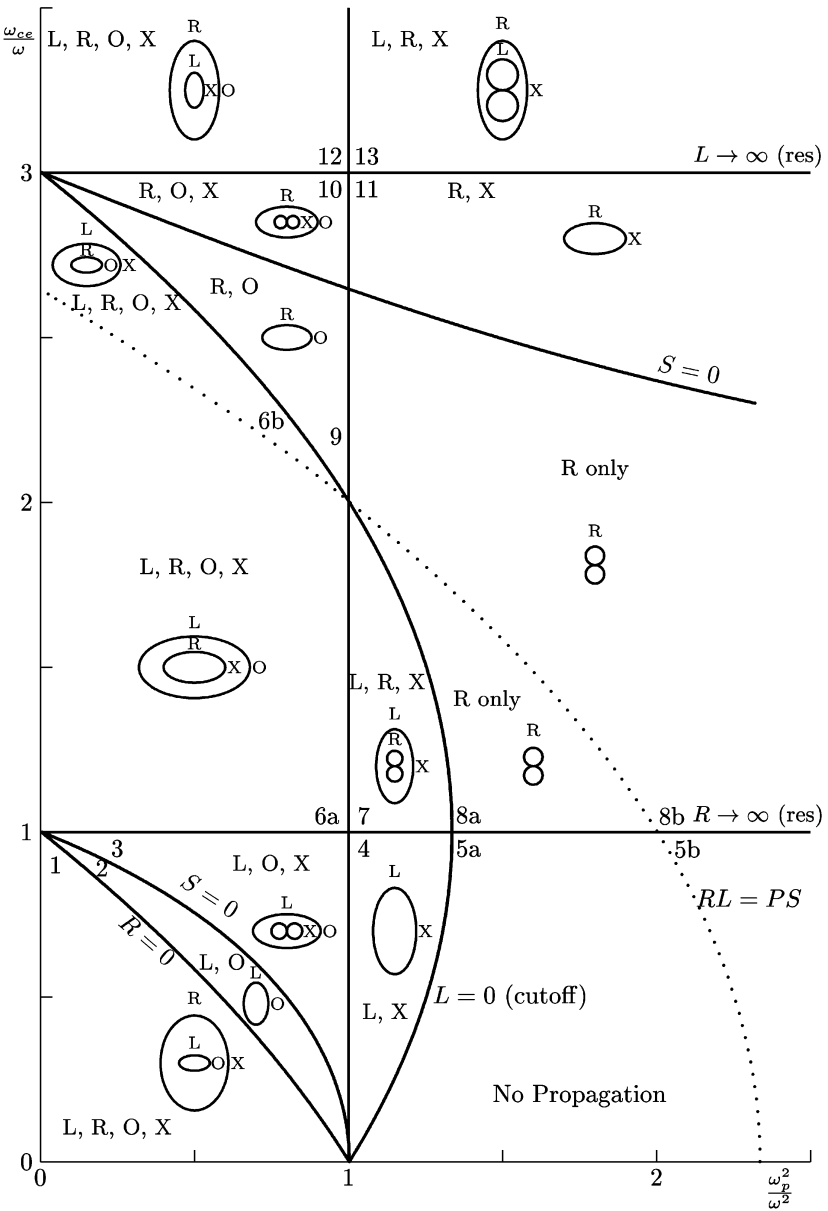


Figure 2.8. CMA diagram with all boundaries and wave normal surfaces (to scale with $m_i/m_e = 3$).

spheroid which is the slow wave.

Moving now across the $P = 0$ boundary, the O -wave disappears and a lemniscoid appears. Since the R -wave is still the fast wave compared to the L -wave, the spheroid must be an R - X spheroid, and the L -wave is the dumbbell lemniscoid.

Finally, crossing the $L \rightarrow \infty$ boundary again into region 11, the R - X spheroid is unchanged, but the L -wave lemniscoid shrinks and disappears.

An examination of [figure 2.8](#), where all the WNSs are sketched, shows that there are no two regions that have identical labeling except the trivial ones where nothing propagates (5a and 5b) or where neither the O - nor X -wave is present (8a and 8b).

2.2.6.3 Interpreting WNSs

In order to interpret these WNSs, the CMA diagram is sometimes likened to a ‘plasma pond’ where a pebble sends out ripples from a center. In such a case, the WNSs represent the phase fronts or the patterns of the individual waves as they radiate out from the disturbance. The outer perimeter of the waves propagates at the group velocity, and the CMA diagram does not directly give information on that part of the picture.

While figure 2.8 shows which regions have spheroids and lemniscoids, there are usually significant changes in these spheroids and lemniscoids as one moves around in a region, especially as one approaches a boundary. Some of this type of variation is illustrated for a few regions in [figure 2.9](#). In region 12, there are only spheroids, but near the bottom of the region, approaching region 10, the *inner* spheroid collapses to a lemniscoid as it crosses the lower boundary in [figure 2.9\(a\)](#). Moving to the right toward region 13, however, the *outer* spheroid tends toward infinity as the boundary is approached. After the crossing into region 13, a lemniscoid appears inside the surviving spheroid, and as one moves to the upper right (MHD region), the pair of surfaces approaches the limiting form of [figure 2.25](#).

In the lower half of [figure 2.9](#), we see the variations as we move around in regions 1 through 4 (region 5 is empty). The scales for the phase velocity surfaces differ only by a factor of two between the upper and lower sections, but the factor would be much larger if the mass ratio (here only a factor of three) were more realistic.

2.3 Phase and group velocity in three-dimensions

The concept of group velocity arises from the notion of a wave packet made of a group of waves with a range of phase velocities but the amplitudes of the components are grouped about a particular phase velocity. In the continuous

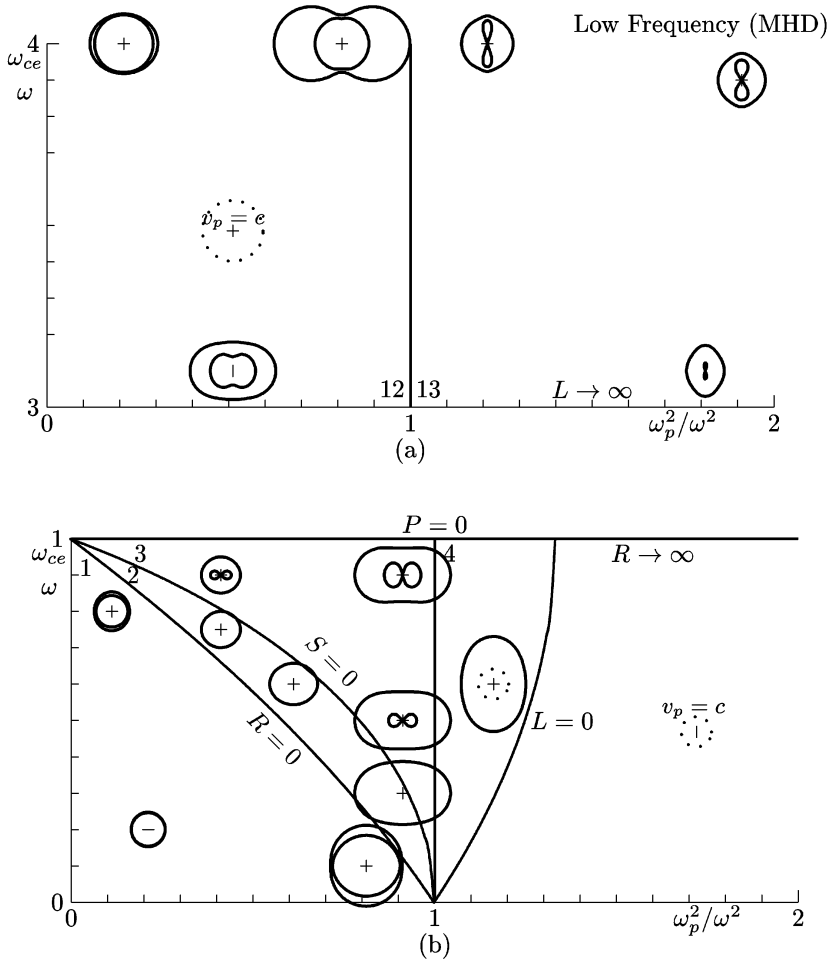


Figure 2.9. Variation of the wave normal surfaces as they move around in various regions of the CMA diagram with $m_i/m_e = 3$. (a) Spheroids in region 12 and combination spheroids and lemniscoids in region 13, all to the same arbitrary scale. (b) Various wave normal surfaces in regions 1, 2, 3 and 4 to the same scale (but half the scale of (a)). The velocity of light circles are shown for reference.

spectrum case, this wave packet is represented by the integral,

$$f(\mathbf{r}, t) = \int A(\mathbf{k}) e^{i(\mathbf{k} \cdot \mathbf{r} - \omega t)} \frac{d^3 k}{(2\pi)^3} \quad (2.50)$$

where we require $|A(\mathbf{k})| \rightarrow 0$ as $|\mathbf{k} - \mathbf{k}_0|$ becomes large with \mathbf{k}_0 being the value of \mathbf{k} where the wave group is centered in \mathbf{k} -space. If $|\Delta \mathbf{k}|_{\max}$ is a measure of

the spread in \mathbf{k} about \mathbf{k}_0 , then $1/|\Delta\mathbf{k}|_{\max}$ is a measure of the size of the packet. Introducing $\Delta\mathbf{k} \equiv \mathbf{k} - \mathbf{k}_0$, then at time $t = 0$, the integral becomes

$$f(\mathbf{r}, 0) = e^{i\mathbf{k}_0 \cdot \mathbf{r}} \int A(\mathbf{k}) e^{i\Delta\mathbf{k} \cdot \mathbf{r}} \frac{d^3 k}{(2\pi)^3} = e^{i\mathbf{k}_0 \cdot \mathbf{r}} F(\mathbf{r})$$

so the wave packet is some function of space localized about the origin with a phase factor.

For the propagation in time, since we may expand

$$\omega(\mathbf{k}) = \omega(\mathbf{k}_0) + \Delta\mathbf{k} \cdot \frac{\partial\omega}{\partial\mathbf{k}} \Big|_{\mathbf{k}_0} + \mathcal{O}(\Delta\mathbf{k}^2)$$

where $\partial\omega/\partial\mathbf{k}|_{\mathbf{k}_0}$ is equivalent to $\nabla_{\mathbf{k}}\omega(\mathbf{k})$ evaluated at \mathbf{k}_0 , then for $t > 0$, we obtain through first order in $\Delta\mathbf{k}$,

$$f(\mathbf{r}, t) = e^{i(\mathbf{k}_0 \cdot \mathbf{r} - \omega t)} \int A(\mathbf{k}) \exp \left[i\Delta\mathbf{k} \cdot \left(\mathbf{r} - \frac{\partial\omega}{\partial\mathbf{k}} \Big|_{\mathbf{k}_0} t \right) \right] \frac{d^3 k}{(2\pi)^3}. \quad (2.51)$$

The structure of equation (2.51) is that of a phase factor and an amplitude function. The leading phase factor determines the phase velocity to be

$$v_p = \frac{\omega}{|\mathbf{k}_0|} \quad (2.52)$$

in the direction of \mathbf{k}_0 . The principal contribution of the integral will occur near where the quantity in parentheses vanishes since the remainder will phase mix away. The position in space where this maximum occurs will move at the group velocity which is defined as the velocity of the amplitude envelope maximum. Hence,

$$\mathbf{v}_g = \frac{\partial\omega}{\partial\mathbf{k}} \Big|_{\mathbf{k}_0} = \nabla_{\mathbf{k}}\omega(\mathbf{k})|_{\mathbf{k}_0} \quad (2.53)$$

so $v_{gx} = \partial\omega/\partial k_x$, etc. The higher order terms principally change the shape of the wave packet, rather than its location.

2.3.1 The one-dimensional case

In one dimension, the group velocity becomes simply $v_g = \partial\omega/\partial k$ and both the phase velocity and the group velocity may be determined graphically from a simple plot of the dispersion relation as shown in figure 2.10 which is plotted for the simple dispersion relation

$$n^2 = 1 - \frac{\omega_p^2}{\omega^2}$$

that may also be written in the form

$$\omega^2 = \omega_p^2 + k^2 c^2.$$

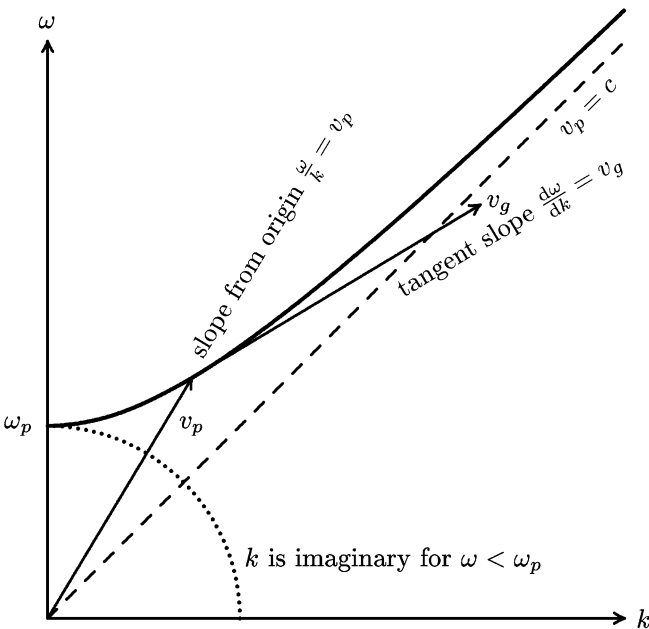


Figure 2.10. Phase and group velocity in one-dimension.

In this plot, the slope of the line from the origin to a point on the curve is the phase velocity, and the slope of a line tangent to the curve at that point of intersection is the group velocity. For this example, it is apparent that $v_p > c$ and $v_g < c$. In fact, for this simple dispersion relation, $v_p v_g = c^2$, so the inequalities apply everywhere the wave propagates. For $\omega < \omega_p$, the wave is not propagating, k is purely imaginary, and neither the phase velocity nor the group velocity is defined.

2.3.2 The three-dimensional case

For the more complicated case of 3-dimensional propagation, we can use the symmetries of the spheroids and lemniscoids about the z -axis to represent the phase and group velocity in terms of a polar plot. The coordinates and angles are shown in figure 2.11(a) where θ is the previously defined angle between the magnetic axis and the \mathbf{k} vector and α is the angle between the group velocity and the phase velocity. The angle α may be determined by writing the frequency in terms of the polar variables such that $\omega = \omega(k, \theta)$ where the group velocity becomes

$$\mathbf{v}_g = \nabla_k \omega = \frac{\partial \omega}{\partial k} \Big|_{\theta} \hat{e}_k + \frac{1}{k} \frac{\partial \omega}{\partial \theta} \Big|_k \hat{e}_{\theta} \quad (2.54)$$

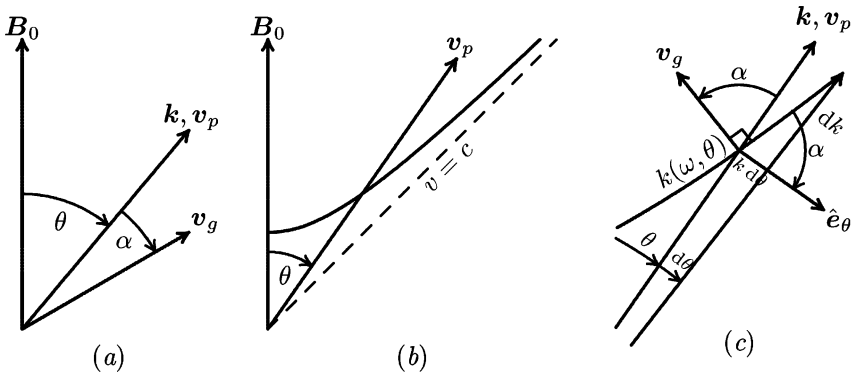


Figure 2.11. Phase and group velocity in three-dimensions: (a) definition of coordinates; (b) polar plot of $k(\omega, \theta)$ versus θ ; and (c) detail of (b) showing the directions of \mathbf{k} , \mathbf{v}_g , $\hat{\mathbf{e}}_k$, and $\hat{\mathbf{e}}_\theta$.

where $\hat{\mathbf{e}}_k = \mathbf{k}/|\mathbf{k}|$ and $\hat{\mathbf{e}}_\theta$ is everywhere normal to $\hat{\mathbf{e}}_k$. In view of this, the angle α is given by

$$\tan \alpha = \frac{\text{θ component}}{\text{k component}} = \frac{\frac{1}{k} \frac{\partial \omega}{\partial \theta} \Big|_k}{\frac{\partial \omega}{\partial k} \Big|_\theta} = -\frac{1}{k} \frac{\partial k}{\partial \theta} \Big|_\omega. \quad (2.55)$$

From this last equality, we draw a sketch of k versus θ in figure 2.11(b) and note the direction of the phase velocity relative to the surface. From the detailed construction of figure 2.11(c), it is apparent that traveling a distance $k d\theta$ in the $\hat{\mathbf{e}}_\theta$ direction from an arbitrary point on the surface, and then a distance dk in the $\hat{\mathbf{e}}_k$ direction returns one to the surface. Thus the $\hat{\mathbf{e}}_\theta$ direction is at an angle α below the surface. With both dk and $k d\theta$ positive, α is negative from equation (2.55), so the group velocity angle is *less than* the phase velocity angle in this example. Furthermore, since the phase velocity surface is at an angle α from the $\hat{\mathbf{e}}_\theta$ direction, and \mathbf{v}_g is also at the angle α from the $\hat{\mathbf{e}}_k$ direction, it follows that the group velocity is normal to the k -surface as noted in figure 2.11(c).

Problem 2.3.1. Group velocity angle. Show that equation (2.55) may be written as

$$\tan \alpha = \frac{1}{v_p} \frac{\partial v_p}{\partial \theta} \Big|_\omega = -\frac{1}{2n^2} \frac{\partial n^2}{\partial \theta} \Big|_\omega. \quad (2.56)$$

2.3.3 Group velocity surfaces

It is possible to construct group velocity surfaces that are analogous to the wave normal surfaces. Topologically, the group velocity surfaces are the same as the WNSs, consisting of the same number of spheroids and lemniscoids in each

region, since a spheroidal WNS will correspond to a spheroidal group velocity surface, and similarly with a lemniscoidal surface. In order to better envision the way a WNS may translate to a group velocity surface, however, figure 2.12 shows the group velocity surfaces that correspond to the wave normal surfaces in figure 2.9. The expression for the group velocity surfaces may be obtained by first writing the CPDR as

$$D[k, \omega(k, \theta), \theta] = An^4 - Bn^2 + C = 0 \quad (2.57)$$

from equations (2.21) and (2.22). We may then write

$$\frac{\partial D}{\partial k} + \frac{\partial D}{\partial \omega} \frac{\partial \omega}{\partial k} = 0 \quad \text{and} \quad \frac{\partial D}{\partial \theta} + \frac{\partial D}{\partial \omega} \frac{\partial \omega}{\partial \theta} = 0 \quad (2.58)$$

so that

$$\frac{\partial \omega}{\partial k} = -\frac{\partial D}{\partial k} \left(\frac{\partial D}{\partial \omega} \right)^{-1} \quad (2.59)$$

and

$$\frac{\partial \omega}{\partial \theta} = -\frac{\partial D}{\partial \theta} \left(\frac{\partial D}{\partial \omega} \right)^{-1}. \quad (2.60)$$

The magnitude of the group velocity may then be obtained from equation (2.54) as

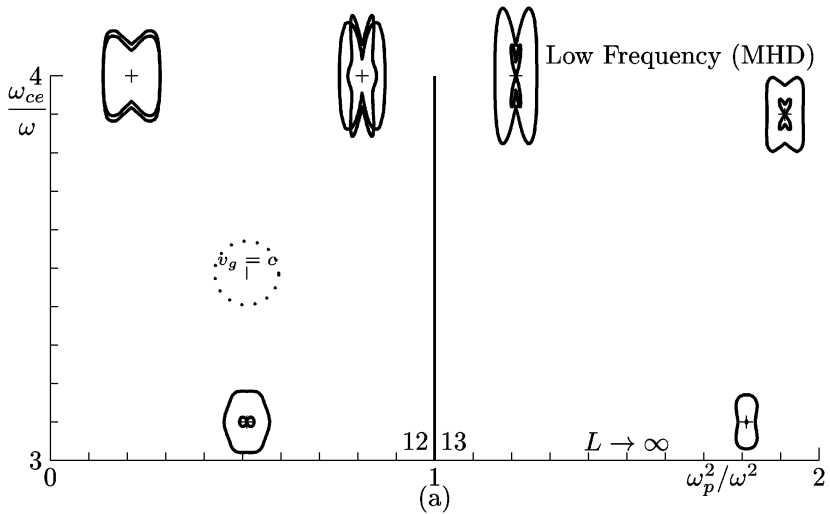
$$v_g^2 = \left(\frac{\partial \omega}{\partial k} \right)^2 + \left(\frac{1}{k} \frac{\partial \omega}{\partial \theta} \right)^2 = \left[\left(\frac{\partial D}{\partial k} \right)^2 + \left(\frac{1}{k} \frac{\partial D}{\partial \theta} \right)^2 \right] \left(\frac{\partial D}{\partial \omega} \right)^{-2}. \quad (2.61)$$

Problem 2.3.2. Group velocity surfaces. Show that using equation (2.57), equation (2.61) may be written as

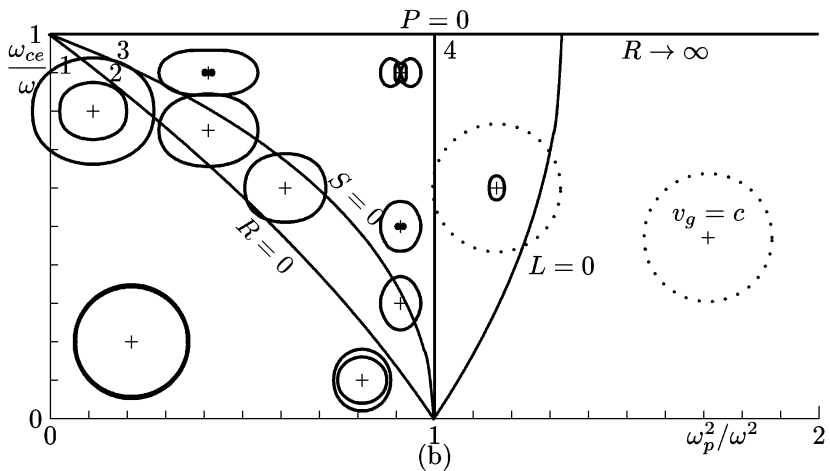
$$\frac{v_g^2}{c^2} = \frac{\left\{ \left[16A^2 + \left(\frac{\partial A}{\partial \theta} \right)^2 \right] n^4 - \left(16AB + \frac{\partial A}{\partial \theta} \frac{\partial B}{\partial \theta} \right) n^2 + 4B^2 + \left(\frac{\partial B}{\partial \theta} \right)^2 \right\} n^2}{\left[\left(\omega \frac{\partial A}{\partial \omega} - 4A \right) n^4 + \left(2B - \omega \frac{\partial B}{\partial \omega} \right) n^2 + \omega \frac{\partial C}{\partial \omega} \right]^2}. \quad (2.62)$$

Problem 2.3.3. Group velocity surface components.

- (i) Find expressions for all of the partial derivatives in equation (2.62) in terms of θ , R , L , P , S , and their derivatives.
- (ii) Defining $X \equiv \omega_p^2/\omega^2$ and $Y \equiv \omega_{ce}/\omega$ with $\mu = m_i/m_e$ (remembering that $\omega_p^2 = \omega_{pe}^2 + \omega_{pi}^2$), find expressions for $\omega \partial P / \partial \omega$, $\omega \partial R / \partial \omega$, $\omega \partial L / \partial \omega$, and $\omega \partial S / \partial \omega$ (using $S = \frac{1}{2}(R + L)$) in terms of X , Y , and μ .
- (iii) Calculate and plot both the WNSs and the group velocity surfaces in region 7 of the CMA diagram for $X = 1.1$, $Y = 1.2$ with $\mu = 3$.



(a)



(b)

Figure 2.12. Variation of the group velocity surfaces as they move around in various regions of the CMA diagram with $m_i/m_e = 3$. Each surface represents the group velocity counterpart to the corresponding wave normal surface in figure 2.9. (a) Spheroids in region 12 and combination spheroids and lemniscoids in region 13, all to the same arbitrary scale. (b) Various group velocity surfaces in regions 1, 2, 3 and 4 to the same scale (twice the scale of (a)). Speed of light circles are shown for reference.

2.4 $\omega(k, \theta)$ dispersion surfaces

Another way of representing the dispersion relation is to plot ω as a function of k and θ . This is traditionally done with either $\theta = 0$, so the plot is of ω versus

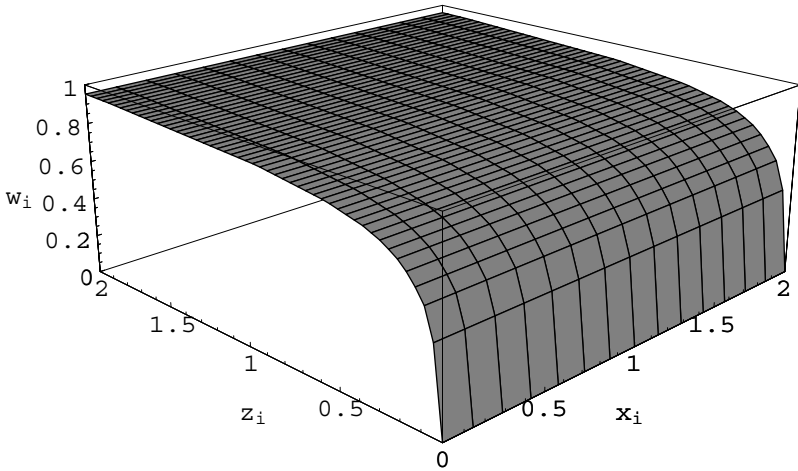


Figure 2.13. Surface plot of $w_i = \omega/\omega_{ci}$ versus $z_i = k_z c/\omega_{ci}$ to the left and for $x_i = k_x c/\omega_{ci}$ to the right. This surface corresponds to the lemniscoid in region 13 of the CMA diagram for an underdense plasma ($\omega_p/\omega_{ce} = 0.32$).

k_{\parallel} , or with $\theta = \pi/2$, so the plot is of ω versus k_{\perp} . Written as a polynomial for $\omega(k, \theta)$, the polynomial is fifth order in ω^2 , and may be written:

$$\begin{aligned}
 & \omega^{10} - \omega^8(2k^2c^2 + \omega_{ce}^2 + \omega_{ci}^2 + 3\omega_p^2) \\
 & + \omega^6[k^4c^4 + (2k^2c^2 + \omega_p^2)(\omega_{ce}^2 + \omega_{ci}^2 + 2\omega_p^2) + (\omega_p^2 + \omega_{ce}\omega_{ci})^2] \\
 & - \omega^4[k^4c^4(\omega_{ce}^2 + \omega_{ci}^2 + \omega_p^2) + 2k^2c^2(\omega_p^2 + \omega_{ce}\omega_{ci})^2] \\
 & + k^2c^2\omega_p^2(\omega_{ce}^2 + \omega_{ci}^2 - \omega_{ce}\omega_{ci})(1 + \cos^2\theta) + \omega_p^2(\omega_p^2 + \omega_{ce}\omega_{ci})^2] \\
 & + \omega^2[k^4c^4[\omega_p^2(\omega_{ce}^2 + \omega_{ci}^2 - \omega_{ce}\omega_{ci})\cos^2\theta + \omega_{ce}\omega_{ci}(\omega_p^2 + \omega_{ce}\omega_{ci})]] \\
 & + k^2c^2\omega_p^2\omega_{ce}\omega_{ci}(\omega_p^2 + \omega_{ce}\omega_{ci})(1 + \cos^2\theta)] \\
 & - k^4c^4\omega_{ce}^2\omega_{ci}^2\omega_p^2\cos^2\theta = 0.
 \end{aligned} \tag{2.63}$$

2.4.1 Underdense case, $\omega_p/\omega_{ce} = 0.32$

The fact that the CPDR is quadratic in n^2 , from equation (2.21), while quintic in ω^2 from equation (2.63) means that if a cut were made horizontally in a figure such as figure 2.13, only two crossings would be encountered, while a vertical cut would have five crossings. Figure 2.13 shows the surface for the slow or left-handed Alfvén wave which is the lowest surface. In contrast, figure 2.14 shows the opposite limit and corresponds to the spheroid from region 1 of figure 2.8 and on the left-hand face is the high frequency branch of the R-wave while

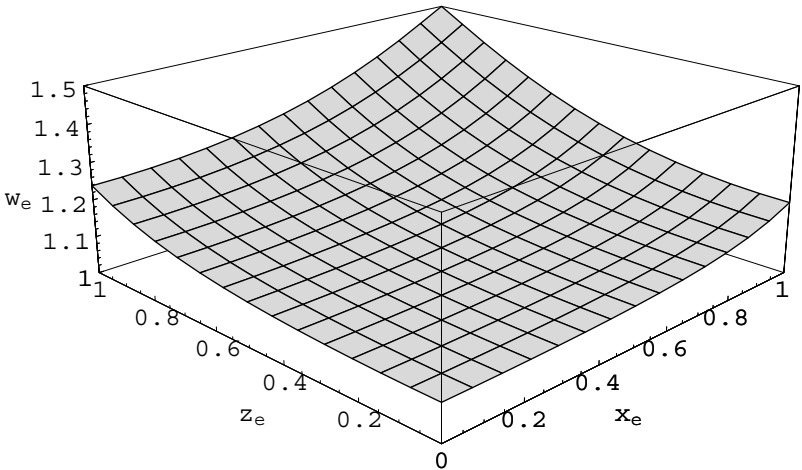


Figure 2.14. Surface plot of $w_e = \omega/\omega_{ce}$ versus $z_e = k_z c/\omega_{ce}$ to the left and for $x_e = k_x c/\omega_{ce}$ to the right. This surface corresponds to the spheroid in region 1 of the CMA diagram.

on the right-hand face it is the high frequency branch of the X -wave. The rise at the back of the surface asymptotes to a cone that represents the velocity of light. The value at the origin corresponds to the upper cutoff frequencies $\omega_R/\omega_{ce} = \omega_X/\omega_{ce} = 1.094$ with $\omega_p/\omega_{ce} = 0.32$ and $m_i/m_e = 1836$.

In between these two limits are three surfaces that represent the R - and L -waves (along with plasma oscillations with $P = 0$) on the left-hand edge and the X - and O -waves along the right-hand edge. The three surfaces are shown together in figure 2.15 where the lowest surface begins as an R -wave on the left and an X -wave on the right near the origin and then saturates at the plasma frequency on the left. Exactly on the left-hand edge corresponds to $k_x = 0$ so that the R -wave is uncoupled to any other wave, but as soon as one moves to finite k_x , there is coupling near the plasma frequency. In order to illustrate this coupling, we examine a simple plot near this edge in figure 2.16 that shows both the R - and L -waves with boxes highlighting the regions where these cross the plasma frequency. In figures 2.17 and 2.18 the boxes in figure 2.16 are magnified so one can see the coupling as $x_i \equiv k_x c/\omega_{ce}$ is varied from 0 (uncoupled case) to 0.002 (weakly coupled) to 0.02 where the coupling is evident. For $k_x > 0$, then, the branch that begins as an L -wave flattens and follows the plasma frequency for a short distance and then follows the R -wave branch for higher frequencies. This implies rapid changes in polarization from a left-handed wave to a longitudinal wave to a right-handed wave where the changes become increasingly rapid as $k_x \rightarrow 0$.

There is no corresponding coupling on the other edge where $k_z = 0$. This is

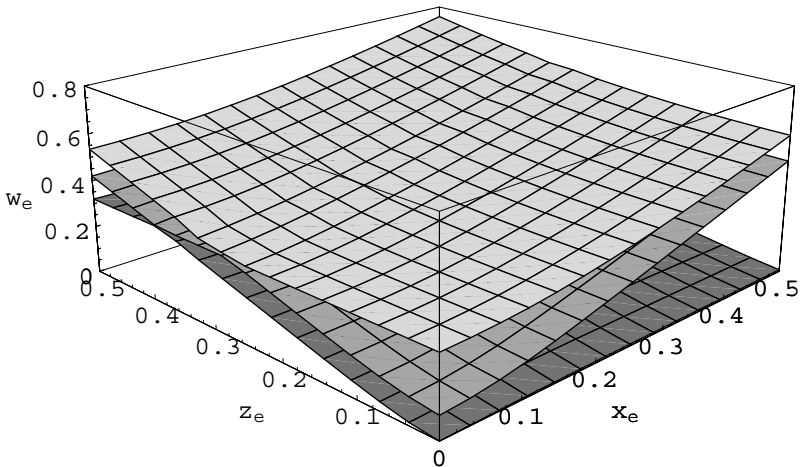


Figure 2.15. Surface plot of $w_e = \omega/\omega_{ce}$ versus $z_e = k_z c/\omega_{ce}$ to the left and $x_e = k_x c/\omega_{ce}$ to the right. These surfaces have two apparent confluences on the left face where the R - and L -wave surfaces cross the $P = 0$ (plasma oscillations at $\omega = \omega_p$) surface.

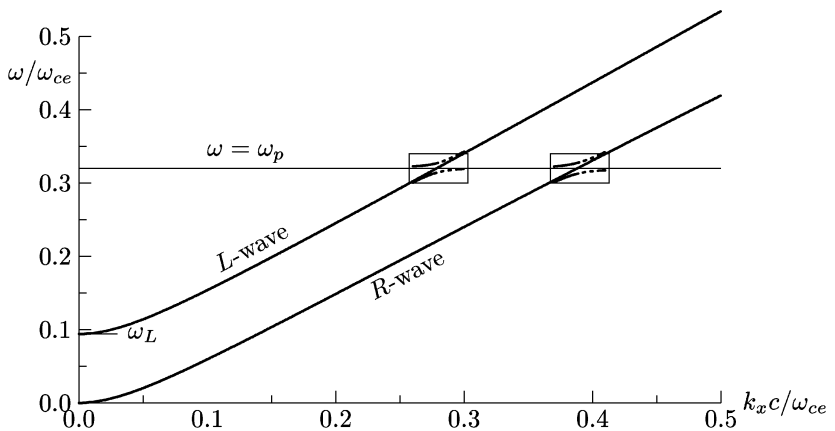


Figure 2.16. Coupling of the P -, R - and L -waves near $k_x = 0$. In this case, plasma oscillations couple to the R - and L -waves with $k_z > 0$. The coupling in the boxed areas that is barely perceptible with $k_x c/\omega_{ce} = 0.02$ is shown with the $-\cdots-$ pattern. These boxes are magnified in figures 2.17 and 2.18.

illustrated in figure 2.19 where the range of $x_e \equiv k_x c/\omega_{ce}$ is extended relative to figure 2.16. In this case, the lower curve is simply the lower X -wave, the middle

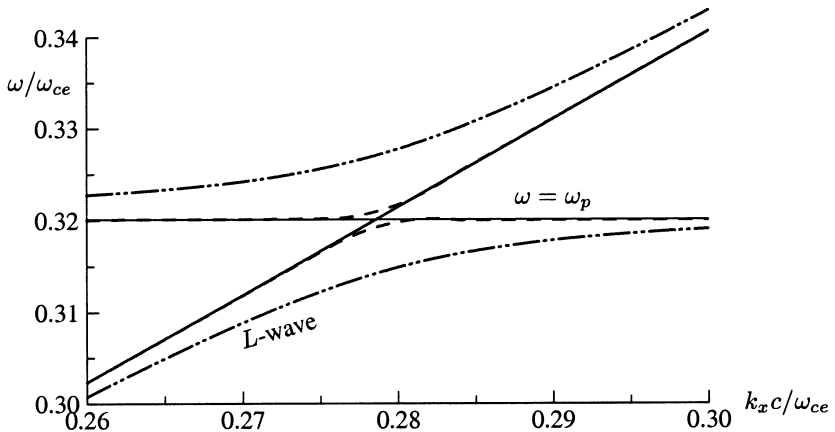


Figure 2.17. Magnified area of first box in figure 2.16. The full lines are the *L*-wave and the plasma frequency, the dashed line is with $k_x c/\omega_{ce} = 0.002$, and $-\cdots-$ is with $k_x c/\omega_{ce} = 0.02$.

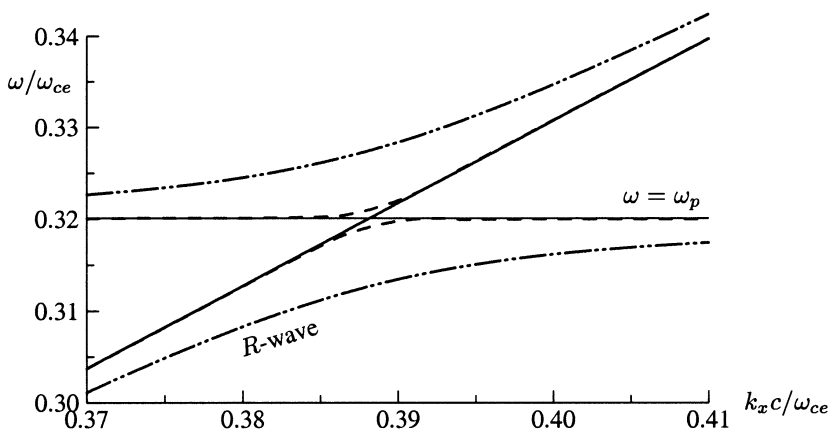


Figure 2.18. Magnified area of second box in figure 2.16. The full lines are the *R*-wave and the plasma frequency, the dashed line is with $k_x c/\omega_{ce} = 0.002$, and $-\cdots-$ is with $k_x c/\omega_{ce} = 0.02$.

curve is the *O*-wave, and the upper curve is the upper *X*-wave. The *O*- and upper *X*-waves merge as $k_x \rightarrow \infty$ and the phase velocity approaches the velocity of light. The lower *X*-wave asymptotes to the upper hybrid resonance. The lowest surface of figure 2.16 asymptotes to the lower hybrid resonance on the right edge, and is not shown in figure 2.19.

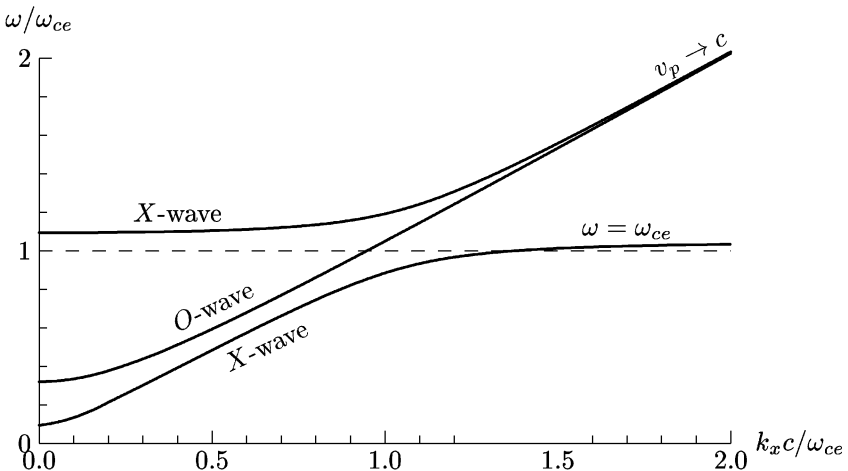


Figure 2.19. The right-hand edge of figure 2.15 shows the behavior of the *O*- and *X*-waves with $k_z = 0$ in an underdense plasma. On this edge, the *X*-waves and the *O*-wave remain uncoupled.

2.4.2 Overdense case, $\omega_p/\omega_{ce} = 3.2$

For the overdense case, some of the surfaces remain similar while others change significantly. One of the coupling regions on the left-hand edge of figure 2.15 disappears, since the *R*-wave has a resonance below the plasma frequency and hence never crosses the plasma frequency. The coupling of the *L*-wave at the plasma frequency is similar, however, and is illustrated in figures 2.20(*a*) and (*b*), where the latter figure expands the coupling region in the former.

The two lowest surfaces in the overdense case correspond to the lemniscoid (figure 2.21) and the spheroid (figure 2.22) of region 13 of the CMA diagram. The intermediate and higher frequencies of figure 2.22 correspond to the whistler region while the low frequency section is the fast Alfvén wave.

The second lowest surface in figure 2.23, which begins near the origin as the *L*-wave on the left, is remarkably flat over the entire surface, ranging from 2.74 to 3.29 over the range shown. The portion of the *L*-wave that continues above the plasma frequency couples to the *O*-wave on the right. The top surface is the *R*-wave on the left and the high frequency *X*-wave on the right, both of which asymptote to the speed of light.

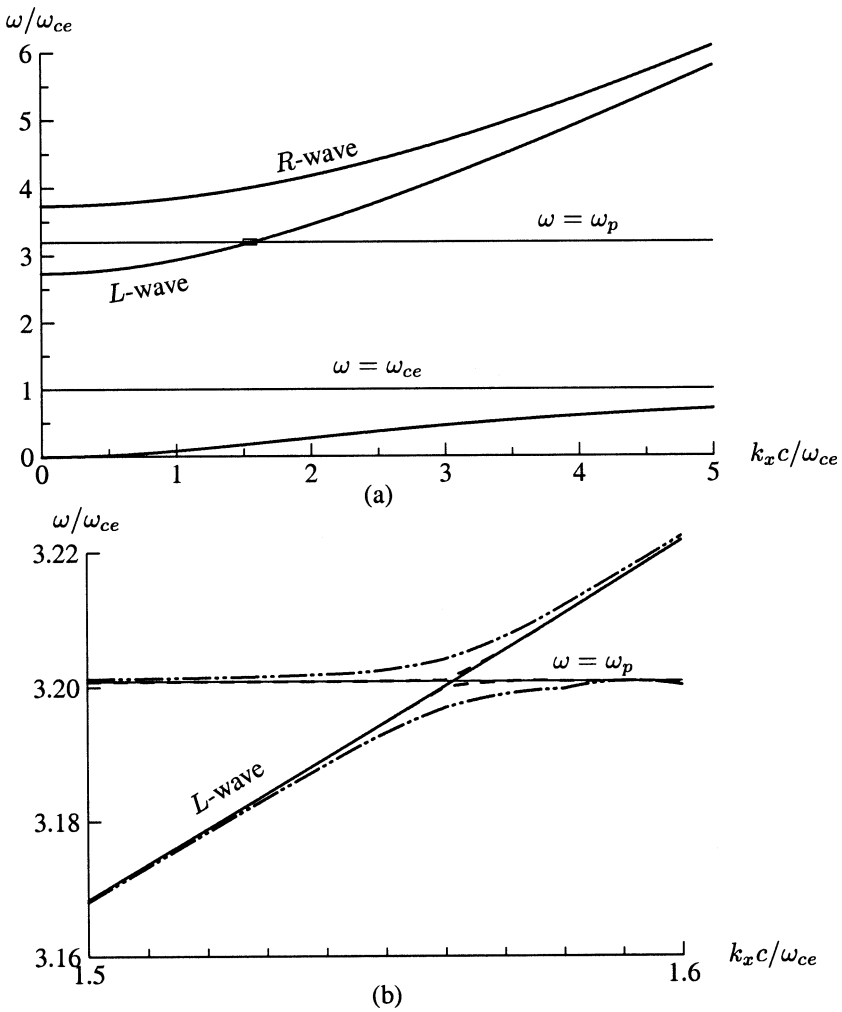


Figure 2.20. (a) Coupling of the P - and L -waves near $k_x = 0$ for an overdense plasma. In this case, plasma oscillations couple to the L -wave only with $k_z > 0$. The coupling in the boxed area is imperceptible even with $k_x c/\omega_{ce} = 0.02$. This box is magnified in (b) where the lines are the L -wave and the plasma frequency, the dashed line is with $k_x c/\omega_{ce} = 0.002$, and $- \cdots -$ is with $k_x c/\omega_{ce} = 0.02$.

2.5 Examples of propagation at arbitrary θ

2.5.1 Low frequency waves

In the very low frequency limit, which corresponds to the upper right corner of the CMA diagram, the dielectric tensor is simple enough that we can

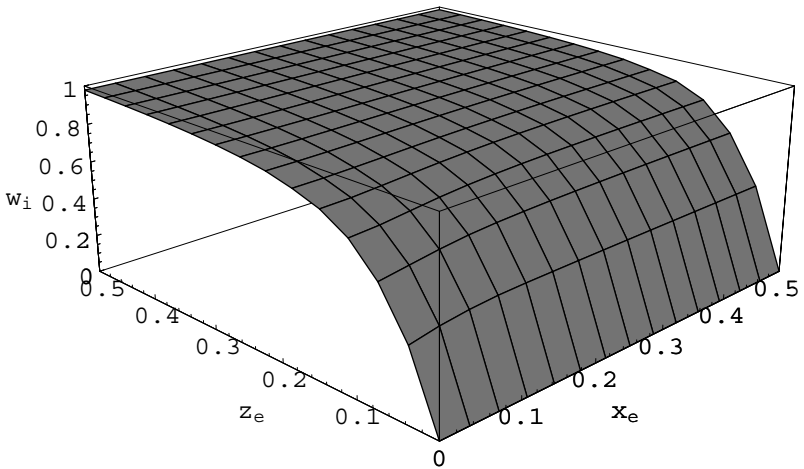


Figure 2.21. Surface plot of $w_i = \omega/\omega_{ci}$ versus $z_e = k_z c/\omega_{ce}$ to the left and $x_e = k_x c/\omega_{ce}$ to the right for the overdense case. This surface is similar to figure 2.13 except that the approach to the ion cyclotron frequency is much slower (note that k_x and k_z are scaled to ω_{ce} in this case). It corresponds to the lemniscoid in region 13 of the CMA diagram.

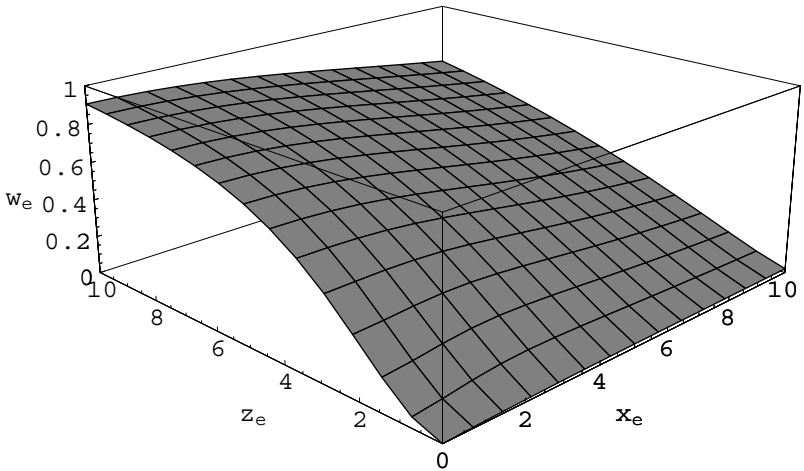


Figure 2.22. Surface plot of $w_e = \omega/\omega_{ce}$ versus $z_e = k_z c/\omega_{ce}$ to the left and $x_e = k_x c/\omega_{ce}$ to the right for the overdense case. This surface is the right-handed wave on the left-hand face and the low frequency branch of the X-wave on the right-hand face. It corresponds to the spheroid in region 13 of the CMA diagram.

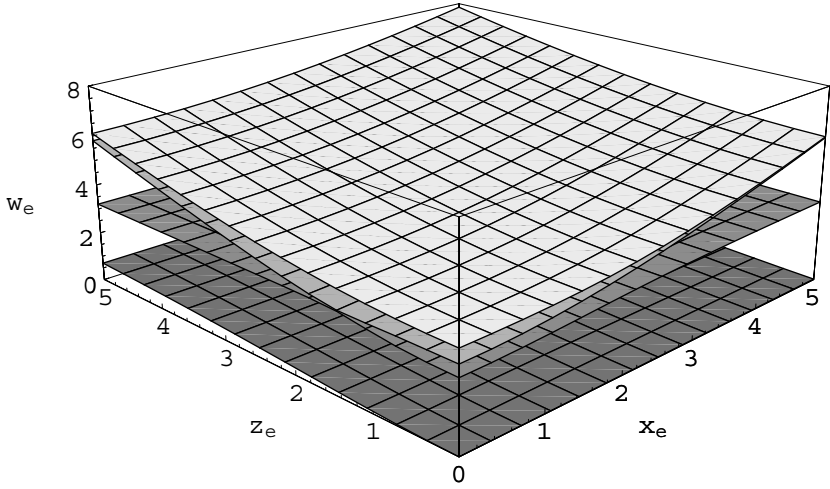


Figure 2.23. Surface plot of $w_e = \omega/\omega_{ce}$ versus $z_e = k_z c/\omega_{ce}$ to the left and $x_e = k_x c/\omega_{ce}$ to the right for the overdense case. The lowest surface is the same surface as in figure 2.22. The next two surfaces show the coupling of the L -wave with the plasma frequency for $k_x > 0$ on the left face that is illustrated in more detail in figures 2.20(a) and (b).

examine propagation at an arbitrary angle in order to gain further insight into the propagation characteristics of a region which has one spheroid and one lemniscoid. The approximation is that $\omega \ll \omega_{ci}$, which is the MHD approximation, since the waves are characteristic of a perfectly conducting fluid in a magnetic field and are often called magnetohydrodynamic (MHD) waves. Neglecting terms of order m_e/m_i , the dielectric tensor elements are:

$$\begin{aligned} K_{xx} = S &= 1 + \frac{\omega_{pi}^2}{\omega_{ci}^2 - \omega^2} + \frac{\omega_{pe}^2}{\omega_{ce}^2 - \omega^2} \simeq 1 + \frac{\omega_{pi}^2}{\omega_{ci}^2} \\ &= 1 + \frac{c^2}{V_A^2} \equiv K_A \end{aligned} \quad (2.64)$$

$$\begin{aligned} K_{xy} = -iD &= \frac{i\omega_{ci}\omega_{pi}^2}{\omega(\omega_{ci}^2 - \omega^2)} - \frac{i\omega_{ce}\omega_{pe}^2}{\omega(\omega_{ce}^2 - \omega^2)} \simeq \frac{i\omega}{\omega_{ci}} \frac{c^2}{V_A^2} \\ &\simeq 0 \end{aligned} \quad (2.65)$$

$$\begin{aligned} K_{zz} = P &= 1 - \frac{\omega_{pi}^2 + \omega_{pe}^2}{\omega^2} \simeq 1 - \frac{c^2}{V_A^2} \frac{\omega_{ci}\omega_{ce}}{\omega^2} \\ &\rightarrow \infty \end{aligned} \quad (2.66)$$

so equation (2.20) reduces to the set of equations

$$\begin{aligned} (-n^2 \cos^2 \theta + K_A) E_x &= 0 \\ (-n^2 + K_A) E_y &= 0 \\ (\infty) E_z &= 0. \end{aligned} \quad (2.67)$$

The last equation is trivial, leading to $E_z = 0$ (E_z is of order m_e/m_i compared to the other fields, and hence neglected). The other two solutions we will investigate individually.

2.5.1.1 Torsional Alfvén waves

The first solution, with $E_x \neq 0$ and $E_y = 0$, has the dispersion relation,

$$n^2 \cos^2 \theta = K_A \quad (2.68)$$

leading to

$$v_p^2 = \frac{c^2 \cos^2 \theta}{K_A} \simeq V_A^2 \cos^2 \theta \quad (2.69)$$

if $V_A \ll c$. Using equation (2.56) with this result, we have

$$\tan \alpha = \frac{1}{v_p} \frac{\partial v_p}{\partial \theta} = -\tan \theta$$

so $\alpha = -\theta$ and the group velocity is parallel to \mathbf{B}_0 . We can obtain this result another way by noting from the Maxwell equations (2.17),

$$\mathbf{B} = \frac{\mathbf{k} \times \mathbf{E}}{\omega} = B_y \hat{e}_y$$

for the wave magnetic field so the Poynting vector is

$$\mathbf{P} = \frac{\mathbf{E} \times \mathbf{B}}{\mu_0} = P_z \hat{e}_z. \quad (2.70)$$

The respective directions are illustrated in figure 2.24(a).

From the equation of motion, since $\omega \ll \omega_{ci}$, we have $\mathbf{E} = -\mathbf{v} \times \mathbf{B}$ so that

$$\mathbf{v} = v_y \hat{e}_y = -\frac{E_x}{B_0} \hat{e}_y.$$

Using this result in the continuity equation, we discover that

$$\mathbf{k} \cdot \mathbf{v} = \frac{i\omega\rho}{Nq} = 0 \quad (2.71)$$

where ρ is the charge density, so there is no fluctuating charge with this wave. For this reason we call it the shear Alfvén wave or the torsional Alfvén wave since the magnetic field lines twist relative to one another but do not compress.

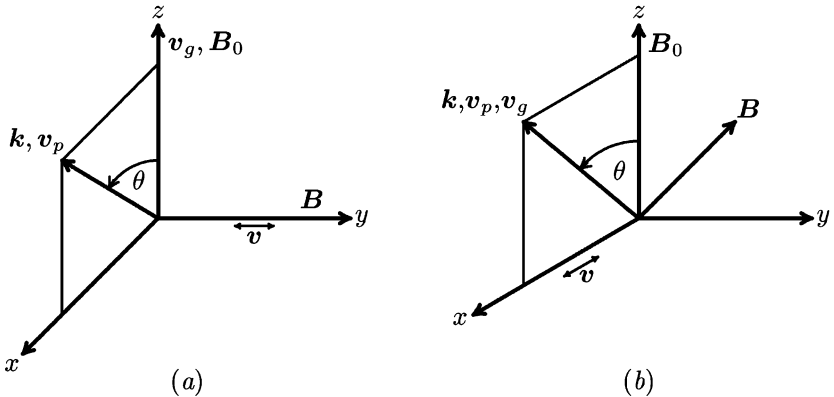


Figure 2.24. Relative directions for the phase velocity, group velocity, and particle velocities for low-frequency Alfvén waves: (a) shear or torsional Alfvén wave; and (b) compressional Alfvén wave.

For these very low frequencies, another intuitive derivation leads to this same result [9]. If we imagine that the charged particles are ‘tied’ to a local magnetic field line, in the sense that they can move along the field line but not across it, and this is a good approximation for $\omega \ll \omega_{ci}$, then the field lines have an effective mass density. From the Maxwell stress tensor, the field lines are under tension/unit area of B_0^2/μ_0 , so by analogy with waves on a stretched string,

$$v = \sqrt{\frac{T}{\rho_\ell}} = \sqrt{\frac{B_0^2}{\mu_0 \rho_m}} \equiv V_A \quad (2.72)$$

where ρ_ℓ is the mass/length of the string and $\rho_m \simeq n_i m_i$ is the mass density of the plasma. The analogy with waves on a stretched string also indicates the transverse nature of the perturbation.

2.5.1.2 Compressional Alfvén waves

The second solution of equation (2.68) has $E_y \neq 0$, $E_x = 0$, and the dispersion relation,

$$n^2 = K_A \quad (2.73)$$

so the phase velocity is given by

$$v_p^2 = \frac{c^2}{K_A} \simeq V_A^2. \quad (2.74)$$

Since there is no dependence on angle, $\alpha = 0$ and the phase and group velocities always point in the same direction. As in the torsional wave case, the result may

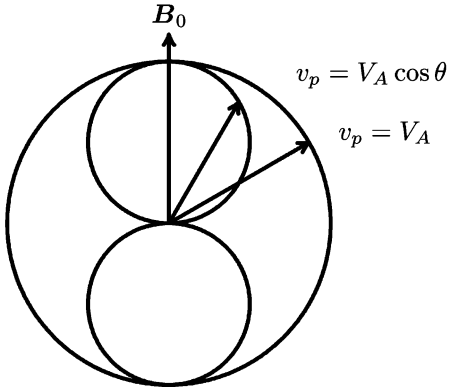


Figure 2.25. Wave normal surfaces for low-frequency Alfvén waves. The dumbbell lemniscoid is the shear or slow Alfvén wave and the outer sphere is the compressional or fast Alfvén wave.

also be seen from the wave field,

$$\mathbf{B} = \frac{\mathbf{k} \times \mathbf{E}}{\omega} \rightarrow \mathbf{B} \text{ is in the } x-z \text{ plane,}$$

and hence the Poynting vector,

$$\mathbf{P} = \frac{\mathbf{E} \times \mathbf{B}}{\mu_0} = P_k \hat{e}_k$$

is parallel to the phase velocity as in figure 2.24(a) so the wave energy flows in the direction of \mathbf{k} .

Looking again at the particle motions, we find $\mathbf{E} = E_y \hat{e}_y = -\mathbf{v} \times \mathbf{B}_0$ so

$$\mathbf{v} = v_x \hat{e}_x = \frac{E_y}{B_0} \hat{e}_x \quad (\mathbf{v} \text{ is normal to } \mathbf{B}_0, \mathbf{E})$$

so in this case $\mathbf{k} \cdot \mathbf{v} \neq 0$ since \mathbf{k} has a component along \mathbf{v} . This means the particles bunch so the magnetic field lines (tied to the particles) are compressed, hence the name of compressional Alfvén waves. This wave is also called the fast Alfvén wave, since the phase velocity is higher than the phase velocity for the torsional wave. This is illustrated in the plot of the WNSs for the two waves in figure 2.25 where all surfaces are spheres, but the slow or torsional wave dumbbell lemniscoid is formed by two adjacent spheres and the fast or compressional wave sphere surrounds both.

Just as the analogy between the torsional Alfvén wave and waves on a stretched string gave a simple interpretation of the slow wave, a similar analogy for the fast wave exists and gives some insight into its character. For this case we

use the result from the Maxwell stress tensor that a magnetic field has an effective pressure given by $p_m = B_0^2/2\mu_0$. With the mass density again tied to the field lines, the analogy with sound waves gives

$$v_s = \sqrt{\frac{\gamma p}{\rho_m}} = \sqrt{\frac{\gamma B_0^2}{2\mu_0\rho_m}} = V_A \quad (2.75)$$

where we have taken $\gamma = 2$. This analogy gives the same Alfvén speed and indicates both a longitudinal component to the motion and a possible connection to ordinary sound waves, a connection that will be made explicit in the next chapter. Also we see that while the pressure is isotropic, leading to the spherical WNS, tension is highly directional so that the torsional wave energy propagates along the magnetic field. Exciting a torsional wave is like ‘plucking’ a magnetic field line, while exciting the compressional wave is like ‘squeezing’ a group of field lines.

2.5.2 Intermediate frequency waves—whistlers

Ionospheric whistlers were discovered during the first World War while German radio monitors were trying to intercept Allied radio transmissions [10]. Without narrow band tuners, the whistlers occurred as declining tones in the audio band. They were later traced to lightning and propagation in the ionosphere and the magnetosphere [11]. In order to see the characteristics of this mode of propagation, we first note that it occurs in regions 8a,b of the CMA diagram, and to simplify the analysis, we assume that $\omega_{ci} \ll \omega \ll \omega_{ce} \sim \omega_{pe}$, so we are above the lower hybrid resonance but well below the electron cyclotron resonance.

2.5.2.1 Propagation parallel to the magnetic field

Looking first at propagation along the field, the dispersion relation is

$$\begin{aligned} n^2 = R &= 1 - \frac{\omega_{pi}^2}{\omega(\omega + \omega_{ci})} - \frac{\omega_{pe}^2}{\omega(\omega - \omega_{ce})} \simeq 1 - \frac{\omega_{pi}^2}{\omega^2} + \frac{\omega_{pe}^2}{\omega\omega_{ce}} \\ &\simeq \frac{\omega_{pe}^2}{\omega\omega_{ce}} \end{aligned} \quad (2.76)$$

so that $k = \omega n/c = (\omega_{pe}/c)\sqrt{\omega/\omega_{ce}}$ or $\omega = k^2 c^2 \omega_{ce}/\omega_{pe}^2$ and the phase and group velocities are

$$\begin{aligned} v_p &= \frac{c}{n} = c \sqrt{\frac{\omega\omega_{ce}}{\omega_{pe}^2}} = \frac{kc^2\omega_{ce}}{\omega_{pe}^2} \\ v_g &= \frac{d\omega}{dk} = \frac{2kc^2\omega_{ce}}{\omega_{pe}^2} = 2v_p = 2c \sqrt{\frac{\omega\omega_{ce}}{\omega_{pe}^2}}. \end{aligned} \quad (2.77)$$

This wave is very dispersive because both the phase and group velocities vary as $\sqrt{\omega}$ which causes high frequencies to propagate faster along the magnetic field lines. The whistlers in the audio range in the northern hemisphere are most commonly caused by lightning strokes in the southern hemisphere (and vice versa) which are guided by the earth's magnetic field, and the dispersion led to the detection of a declining tone which was heard as a whistle. Occasionally, lightning strokes in the northern hemisphere which reflected from the conjugate point in the southern hemisphere were detected, but were much fainter and had slower declining tones in the whistle.

2.5.2.2 The guidance of whistler waves

In order to see that the waves are indeed guided by the earth's field, we must examine the direction of the group velocity. For this we need the approximate dispersion relation for arbitrary angle. For this we first examine the ordering of the dielectric tensor elements. For K_{xx} , we may approximate

$$K_{xx} = 1 - \frac{\omega_{pi}^2}{\omega^2 - \omega_{ci}^2} - \frac{\omega_{pe}^2}{\omega^2 - \omega_{ce}^2} \simeq 1 - \frac{\omega_{pi}^2}{\omega^2} + \frac{\omega_{pe}^2}{\omega_{ce}^2}$$

so K_{xx} is of the order of $\omega_{pe}^2/\omega_{ce}^2$ or less. For K_{xy} ,

$$K_{xy} = \frac{i\omega_{pi}^2 \omega_{ci}}{\omega(\omega_{ci}^2 - \omega^2)} - \frac{i\omega_{pe}^2 \omega_{ce}}{\omega(\omega_{ce}^2 - \omega^2)} \simeq -\frac{i\omega_{pe}^2}{\omega \omega_{ce}}.$$

Then for K_{zz} we have

$$K_{zz} = 1 - \frac{\omega_{pi}^2 + \omega_{pe}^2}{\omega^2} \simeq -\frac{\omega_{pe}^2}{\omega^2}$$

so we may order these such that $|K_{zz}| \gg |K_{xy}| \gg |K_{xx}|$. Looking at equation (2.20), we let $E_z \rightarrow 0$ because $K_{zz} = P$ is so much larger than the other elements. Then the remaining determinant,

$$\begin{vmatrix} K_{xx} - n^2 \cos^2 \theta & K_{xy} \\ -K_{xy} & K_{xx} - n^2 \end{vmatrix} = 0$$

reduces to

$$n^4 \cos^2 \theta = -K_{xy}^2 = D^2 \quad (\text{unless } \theta \simeq \pi/2)$$

from which we obtain

$$\omega = \frac{k^2 c^2 \omega_{ce} \cos \theta}{\omega_{pe}^2}. \quad (2.78)$$

From this result and equation (2.55), we can obtain the angle for the group's velocity angle as

$$\tan \alpha = \frac{\frac{1}{k} \frac{\partial \omega}{\partial \theta} |_k}{\frac{\partial \omega}{\partial k} |_\theta} = \frac{-kc^2 \omega_{ce} \sin \theta / \omega_{pe}^2}{2kc^2 \omega_{ce} \cos \theta / \omega_{pe}^2} = -\frac{1}{2} \tan \theta \quad (2.79)$$

so \mathbf{v}_g always lies between \mathbf{B}_0 and \mathbf{v}_p . The angle between \mathbf{B}_0 and \mathbf{v}_g is then given by

$$\tan(\theta + \alpha) = \frac{\tan \theta}{2 + \tan^2 \theta} \quad (2.80)$$

which has a maximum since for small θ , $\tan(\theta + \alpha) \sim \tan \theta / 2$ while for larger θ , $\tan(\theta + \alpha) \sim 1 / \tan \theta \rightarrow 0$. Setting the derivative of $\tan(\theta + \alpha)$ with respect to θ to 0, the maximum angle occurs for $\tan^2 \theta = 2$ so

$$\tan(\theta + \alpha)_{\max} = \frac{\tan \theta}{2 + \tan^2 \theta} = \frac{\sqrt{2}}{2 + 2} = \frac{1}{\sqrt{8}}$$

with the result,

$$(\theta + \alpha)_{\max} = \tan^{-1} \frac{1}{\sqrt{8}} = 19.5^\circ. \quad (2.81)$$

In words, this means that the energy flows within a cone of 19.5° around \mathbf{B}_0 . In the earth's magnetosphere, the energy flow is not precisely along the magnetic field due to the magnetic curvature, so the source of a whistler is not exactly at the conjugate magnetic field point, but these points have been found to be relatively close to the magnetic conjugate points, so the wave is strongly guided by the field.

Problem 2.5.1. The whistler wave.

- (i) Fill in the steps leading to equation (2.81).
- (ii) Show that $|v_g| = (kc^2 \omega_{ce}^2 / \omega_{pe}^2) \sqrt{1 + 3 \cos^2 \theta}$.
- (iii) Sketch the WNS lemniscoid and the corresponding polar plot of $v_g(\theta + \alpha)$.
- (iv) These approximate expressions are not valid as $\theta \rightarrow \pi/2$. What happens in this limit?

2.6 Faraday rotation

An important feature of magnetoactive media is that they lead to Faraday rotation. In order to analyze this feature of wave propagation, we shall limit the analysis to $\theta = 0$ where the Maxwell equations become:

$$\begin{aligned} -k_z E_y &= \omega B_x \\ k_z E_x &= \omega B_y \\ -k_z B_y &= -\frac{\omega}{c^2} (K_{xx} E_x + K_{xy} E_y) \\ k_z B_x &= -\frac{\omega}{c^2} (-K_{xy} E_x + K_{xx} E_y). \end{aligned} \quad (2.82)$$

We then define the rotating coordinates variables,

$$\begin{aligned} E_\pm &= E_x \pm iE_y \\ B_\pm &= B_x \pm iB_y \\ K_\pm &= K_{xx} \pm iK_{xy} = R, L \end{aligned} \quad (2.83)$$

so that equation (2.82) can be reduced to

$$\begin{aligned} k_z E_{\pm} &= \mp i\omega B_{\pm} \\ k_z B_{\pm} &= \pm (i\omega/c^2) E_{\pm} K_{\mp}. \end{aligned} \quad (2.84)$$

These may be solved to obtain the result

$$(n^2 - K_{\mp}) E_{\pm} = 0 \quad (2.85)$$

which has two solutions.

- (i) Suppose $E_+ \neq 0$. Then $n^2 = L$ and $E_- = 0$ so $E_x = iE_y$, which confirms our identification of this as the L -wave. The E_+ field may then be represented by

$$E_+ = \hat{E}_+ \exp \left[i \left(\frac{\omega}{c} n_L z - \omega t \right) \right]$$

where \hat{E}_+ is the complex amplitude.

- (ii) Suppose $E_- \neq 0$. Then $n^2 = R$ and $E_+ = 0$ so $E_x = -iE_y$, which confirms our identification of this as the R -wave. The E_- field may then be represented by

$$E_- = \hat{E}_- \exp \left[i \left(\frac{\omega}{c} n_R z - \omega t \right) \right]$$

where again \hat{E}_- is the complex amplitude.

Constructing the measurable fields, E_x and E_y , from these, we obtain

$$\begin{aligned} \operatorname{Re}(E_x) &= \operatorname{Re} \left(\frac{E_+ + E_-}{2} \right) = \frac{1}{2} \operatorname{Re} \{ \hat{E}_+ e^{[i(\omega n_L z / c - \omega t)]} + \hat{E}_- e^{[i(\omega n_R z / c - \omega t)]} \} \\ \operatorname{Re}(E_y) &= \operatorname{Re} \left(\frac{E_+ - E_-}{2i} \right) = \frac{1}{2} \operatorname{Re} \{ -i \hat{E}_+ e^{[i(\omega n_L z / c - \omega t)]} + i \hat{E}_- e^{[i(\omega n_R z / c - \omega t)]} \}. \end{aligned} \quad (2.86)$$

If we now take $\operatorname{Re}[E_y(0, t)] = 0$ so that the electric field is aligned with the x -axis at $z = 0$, then this demands that $\hat{E}_+ = \hat{E}_- = E_0$ which we take to be real. We may then factor out a common term and write the result as

$$\begin{aligned} \operatorname{Re}(E_x) &= E_0 \cos \left(\frac{\Delta n}{2} \frac{\omega}{c} z \right) \operatorname{Re} \left[e^{i(\omega \bar{n} z / c - \omega t)} \right] \\ \operatorname{Re}(E_y) &= E_0 \sin \left(\frac{\Delta n}{2} \frac{\omega}{c} z \right) \operatorname{Re} \left[e^{i(\omega \bar{n} z / c - \omega t)} \right] \end{aligned} \quad (2.87)$$

where

$$\bar{n} = \frac{1}{2} (n_L + n_R)$$

$$\Delta n = n_L - n_R > 0.$$

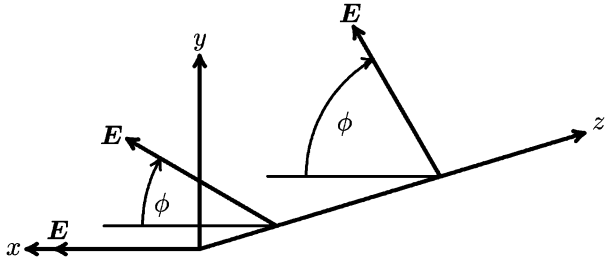


Figure 2.26. Faraday rotation of the electric field.

From this it is apparent that E_x and E_y are being modulated by the sine and cosine terms while the phase velocity of the composite wave is determined from the exponential term which yields a phase velocity of $v_p = c/\bar{n}$. Choosing a point of constant phase, the total electric field rotates in space as the wave propagates, as shown in figure 2.26. If we take the angle of rotation to be ϕ , then the rate of rotation of the E -field vector is given by

$$\frac{d\phi}{dz} = \frac{d}{dz} \left(\frac{\Delta n}{2} \frac{\omega}{c} z \right) = \frac{\omega}{2c} (n_L - n_R). \quad (2.88)$$

2.6.1 High frequency limit—region 1

In order to estimate the amount of Faraday rotation for frequencies $\omega \gg \omega_{ce} \gg \omega_{ci}$, we begin with the dispersion relations for the R -wave from equation (2.29) and the L -wave from equation (2.33),

$$n_{R,L}^2 = 1 - \frac{\omega_{pi}^2}{\omega(\omega \pm \omega_{ci})} - \frac{\omega_{pe}^2}{\omega(\omega \mp \omega_{ce})} \simeq 1 - \frac{\omega_{pe}^2}{\omega^2} \mp \frac{\omega_{pe}^2 \omega_{ce}}{\omega^2}. \quad (2.89)$$

This dispersion relation is compared with the definitions

$$n_{R,L}^2 \equiv (\bar{n} \mp \frac{1}{2}\Delta n)^2 \simeq \bar{n}^2 \mp \bar{n}\Delta n \quad (2.90)$$

where the comparison yields the results

$$\begin{aligned} \bar{n}^2 &= 1 - \frac{\omega_{pe}^2}{\omega^2} \simeq 1 && \text{(approximately free space propagation)} \\ \bar{n}\Delta n &\simeq \Delta n = \frac{\omega_{pe}^2}{\omega^2} \frac{\omega_{ce}}{\omega}. \end{aligned} \quad (2.91)$$

These results, along with equation (2.88), then give the rate of rotation as

$$\frac{d\phi}{dz} = \frac{\Delta n}{2} \frac{\omega}{c} = \frac{\omega_{pe}^2 \omega_{ce}}{2\omega^2 c} \propto \lambda^2 n_e B_0 \quad (2.92)$$

where λ is the free space wavelength. The total rotation angle then is given by

$$\phi \propto \lambda^2 \int_0^L n_e(z) B_0(z) dz. \quad (2.93)$$

If the Faraday rotation is used as a diagnostic for estimating the magnetic field in a plasma, it is preferable to use long wavelengths (since $\phi \propto \lambda^2$), but one must still keep $\omega \gg \omega_{ce} \sim \omega_{pe}$ in order to get a significant rotation. Since the rotation is proportional to both density and magnetic field strength, one must be known to determine the other, and some idea of the variation along the path is necessary.

Simultaneous measurement of the phase can give some additional information, since \bar{n} differs some from unity. The phase is given by

$$\phi = \frac{\omega}{c} \int_0^L (1 - \bar{n}) dz \simeq \frac{\omega}{c} \int_0^L \frac{\omega_{pe}^2}{2\omega^2} dz \propto \lambda \int_0^L n_e(z) dz \quad (2.94)$$

since $\bar{n} \simeq 1 - \omega_{pe}^2/2\omega^2$. Thus measurement of both the phase and rotation can give estimates of both the mean density and mean magnetic field along the path of integration.

Problem 2.6.1. Faraday rotation. Estimate the electron density required to produce 1 radian of Faraday rotation for a wave passing through the Crab nebula if the path length is estimated to be $L = 3 \times 10^{19}$ m, the magnetic field is assumed to be $B = 10^{-9}$ T and the observation is made with $\lambda = 21$ cm radiation.

2.6.2 Low frequency limit—region 13

Following a similar analysis to that used in the high frequency case, except that now we assume $\omega \ll \omega_{ci} \ll \omega_{ce} \sim \omega_{pe}$, the dispersion relations for the R - and L -waves can be approximated by

$$n_{R,L}^2 \simeq 1 + \frac{\omega_{pe}^2}{\omega_{ce}\omega_{ci}} \left(1 \mp \frac{\omega}{\omega_{ci}} \right). \quad (2.95)$$

Hence, from our definition of \bar{n} and Δn with $|\Delta n| \ll \bar{n}$, we can compare terms in

$$\bar{n}^2 \mp \bar{n}\Delta n \simeq 1 + \frac{\omega_{pe}^2}{\omega_{ce}\omega_{ci}} \pm \frac{\omega}{\omega_{ci}} \frac{\omega_{pe}^2}{\omega_{ce}\omega_{ci}}$$

and find

$$\bar{n}^2 = 1 + \frac{\omega_{pe}^2}{\omega_{ce}\omega_{ci}} = 1 + \frac{c^2}{V_A^2} = K_A. \quad (2.96)$$

If $V_A \ll c$, as is often the case, then the 1 may be neglected in equation (2.96) so that

$$\begin{aligned}\bar{n} &= \frac{c}{V_A} \\ \bar{n}\Delta n &= \frac{\omega}{\omega_{ci}} \frac{\omega_{pe}^2}{\omega_{ce}\omega_{ci}} \simeq \frac{\omega}{\omega_{ci}} \bar{n}^2 \\ \Delta n &= \bar{n} \frac{\omega}{\omega_{ci}}.\end{aligned}\quad (2.97)$$

The rotation is then given by combining equations (2.88) and (2.97) to obtain

$$\begin{aligned}\frac{d\phi}{dz} &= \frac{\Delta n}{2} \frac{\omega}{c} \simeq \frac{1}{2} \frac{\omega}{\omega_{ci}} \frac{\omega}{V_A} \\ &= (\text{constant}) \left(\frac{\sqrt{n_e}\omega^2}{B_0^2} \right).\end{aligned}\quad (2.98)$$

For the low frequency limit, then, the angle of rotation decreases as the frequency or density gets small, and increases as B_0 gets small, but one must maintain $\omega \ll \omega_{ci}$.

2.7 Plasma interferometry

The O -wave is often used as a plasma diagnostic to measure the plasma density, either by itself or in conjunction with a Faraday rotation measurement so that both the density and magnetic field may be determined.

By using a comparison between a wave traveling through a plasma and a reference wave which does not travel through the plasma, the phase difference can be used as a measure of the plasma density. We assume the signal through the plasma may be represented by

$$S_p = A_p e^{i\phi_p - i\omega t}$$

and the reference wave may be represented by

$$S_r = A_r e^{i\phi_r - i\omega t}$$

and we measure the sum of these signals,

$$S = S_r + S_i = (A_p e^{i\phi_p} + A_r e^{i\phi_r}) e^{-i\omega t}. \quad (2.99)$$

If we adjust the phase and amplitude of the reference signal so that $S = 0$ when there is no plasma, then we require

$$A_p = -A_r = A \quad \phi_0 = \phi_r$$

where ϕ_0 is the phase of the plasma path in vacuum. In general, the phase in the plasma will depend on time as the density varies according to

$$\begin{aligned}\phi(t) &= \int_{-L/2}^{L/2} k_z(z, t) dz - \int_{-L/2}^{L/2} k_0 dz \\ &= \frac{\omega}{c} \int_{-L/2}^{L/2} [n(z, t) - 1] dz \\ &= \frac{\omega}{c} \int_{-L/2}^{L/2} \left[\sqrt{1 - \frac{\omega_p^2(z, t)}{\omega^2}} - 1 \right] dz.\end{aligned}\quad (2.100)$$

2.7.1 Detecting the signal

If there is no attenuation in the plasma, then the detected signal may be expressed as

$$\begin{aligned}S &= A(e^{i\phi} - 1)e^{i\phi_0 - i\omega t} \\ &= Ae^{i\frac{1}{2}\phi}(e^{i\frac{1}{2}\phi} - e^{-i\frac{1}{2}\phi})e^{i\phi_0 - i\omega t} \\ &= 2iA \sin \frac{1}{2}\phi e^{i\frac{1}{2}\phi} e^{i\phi_0 - i\omega t}.\end{aligned}$$

For microwave signals, the simplest detectors are generally square-law detectors, so the received signal is

$$|S|^2 = 4A^2 \sin^2 \frac{1}{2}\phi. \quad (2.101)$$

An example of a plasma whose density rises in time from zero density to a maximum where $\omega_p > \omega$ and then falls again to zero is shown in figure 2.27.

2.7.2 Interpreting the signal when $\omega \gg \omega_p$

When the wave frequency is much greater than the maximum plasma frequency, such as is the usual case when either optical or far infrared waves are employed, then we may expand the root in equation (2.100) to obtain

$$\phi = -\frac{\omega_p^2}{2\omega c} \int_{-L/2}^{L/2} f(z) dz = -\frac{\overline{\omega_p^2} L}{2\omega c} \propto \bar{n} L \lambda_0 \quad (2.102)$$

where λ_0 is the free space wavelength, \bar{n} is the average plasma density, and $\omega_p^2(z) = \omega_p^2 f(z)$. It is clear that to find the peak density, one must know the profile $f(z)$ and the column width L . If the column is cylindrical, one may measure the phase shift at a series of chords and then use an Abel inversion to obtain the profile (the frequency must be far enough above the maximum plasma frequency that refractive effects do not distort the path along the various chords). Otherwise one must make an independent measurement of the profile.

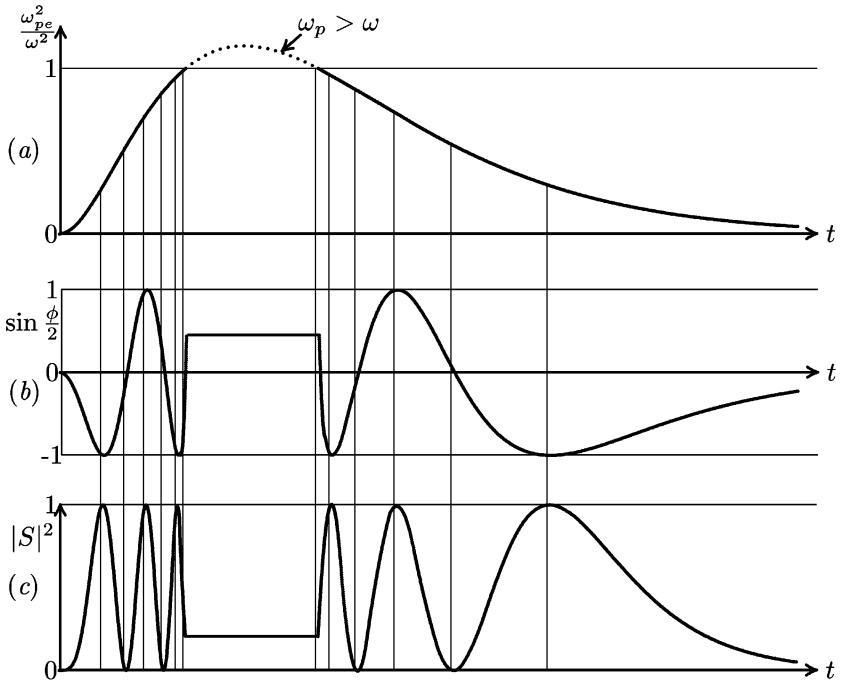


Figure 2.27. Plasma density microwave interferometer: (a) plasma density (ω_{pe}^2/ω^2) versus t ; (b) phase signal versus time; and (c) detected signal versus time.

2.7.3 Interpreting the signal when $\omega \sim \omega_{p0}$

When the plasma frequency approaches, or even surpasses, the wave frequency, then the expansion of the square root is a poor approximation and equation (2.102) is inappropriate. Then the general expression from equation (2.100),

$$\phi = \frac{\omega}{c} \int_{-L/2}^{L/2} \left[\sqrt{1 - \frac{\omega_{p0}^2}{\omega^2} f(z)} - 1 \right] dz \quad (2.103)$$

is appropriate. This is trivial when $f(z) = 1$, $-L/2 < z < L/2$, but nontrivial otherwise. It is sometimes possible to use the cutoff condition when $\omega = \omega_{p0}$ to determine the column width L . At cutoff, the phase is

$$\phi = \frac{\omega}{c} \int_{-L/2}^{L/2} \left[\sqrt{1 - f(z)} - 1 \right] dz. \quad (2.104)$$

For the trivial case (square plasma profile), we have $\phi = -\omega L/c$, so if $m = |\phi|/2\pi$ is the number of cycles (the example in figure 2.27(c) has $\phi = -6.3\pi$ at

cutoff so $m \simeq 3.2$) in the detected signal, then $L = \lambda_0 m$. If, however, we assume the density profile is parabolic, with $f(z) = 1 - (2z/L)^2$, then $L = 2\lambda_0 m$. Thus we see that the interpretation of the width depends on the profile and knowledge of the width and phase shift can help to estimate the profile.

Problem 2.7.1. Phase shift with nonuniform density profile.

- (i) Find an expression for the phase shift as a function of $\alpha = \omega_{p0}/\omega \leq 1$ for a parabolic profile $f(z) = 1 - (2z/L)^2$.
- (ii) Find an expression for the phase shift as a function of $\alpha = \omega_{p0}/\omega \leq 1$ for a cosine profile, $f(z) = \cos^2(\pi z/L)$.

2.8 Electrostatic waves

Electrostatic waves form a special subset of plasma waves where the wavelength is short and the phase velocity is low. For these cases, the waves are longitudinal and we may represent the electric field by a scalar potential so that

$$\mathbf{E} = -\nabla\phi = -ik\phi. \quad (2.105)$$

When the plasma charge and current are incorporated into the effective dielectric tensor, then Gauss' law inside the plasma gives from equation (1.11),

$$\nabla \cdot \mathbf{D} = 0$$

which reduces to the electrostatic dispersion relation (ESDR),

$$\mathbf{k} \cdot \mathbf{K} \cdot \mathbf{k} = 0. \quad (2.106)$$

In cold plasmas, this dispersion relation reduces further to

$$k_\perp^2 K_1 + k_\parallel^2 K_3 = 0 \quad (2.107)$$

which is sufficiently simplified that many exact results may be readily obtained. We recognize at once that for parallel propagation, this leads to $K_3 = P = 0$ so the plasma wave is clearly an electrostatic wave. For $k^2 \rightarrow \infty$, we previously had the resonance condition of equation (2.26), but for electrostatic waves, we see that this relationship is always true, and we can understand this as taking the large- k limit of the dispersion relation. After examining the conditions for the validity of this approximation, we examine a special case which will be treated now for a cold uniform plasma but will be visited again in later chapters as other effects are added.

2.8.1 Validity conditions for the electrostatic approximation

Following Stix' [6] general development we break the electric field vector into parallel and perpendicular components with respect to \mathbf{k} so that we may determine how nearly longitudinal the wave is, such that

$$\mathbf{E} = \mathbf{E}_{\parallel} + \mathbf{E}_{\perp}$$

where

$$\begin{aligned}\mathbf{E}_{\parallel} &= \frac{\mathbf{n}(\mathbf{n} \cdot \mathbf{E})}{n^2} \\ \mathbf{E}_{\perp} &= -\frac{\mathbf{n} \times (\mathbf{n} \times \mathbf{E})}{n^2}\end{aligned}$$

which we insert into the wave equation, equation (2.18), in the form

$$\mathbf{n} \times (\mathbf{n} \times \mathbf{E}) + \mathbf{K} \cdot \mathbf{E} = 0. \quad (2.108)$$

If we take the scalar product of equation (2.108) with \mathbf{n} , we obtain the result that

$$\mathbf{n} \cdot \mathbf{K} \cdot (\mathbf{E}_{\parallel} + \mathbf{E}_{\perp}) = 0$$

which reduces to the ESDR of equation (2.106) if $|\mathbf{E}_{\parallel}| \gg |\mathbf{E}_{\perp}|$, which means the electric field is *dominantly* longitudinal. Equation (2.105) indicates the wave is *exactly* longitudinal, but we broaden the definition here to include the *nearly* longitudinal field case. If we now take the scalar product of equation (2.108) with \mathbf{E} , then we may write the result as

$$(n^2 - \mathbf{K} \cdot \mathbf{E}_{\perp}) \mathbf{E}_{\perp} = \mathbf{K} \cdot \mathbf{E}_{\parallel}. \quad (2.109)$$

We can see that for large enough n , $|\mathbf{E}_{\perp}|/|\mathbf{E}_{\parallel}|$ can be made as small as one chooses. From this comparison, we can give a *sufficient condition* for the validity of the electrostatic approximation as

$$n^2 \gg |K_{ij}| \quad (2.110)$$

or that the index of refraction should be large compared to all of the dielectric tensor elements. Thus the cyclotron resonances, where $n^2 \rightarrow \infty$ because the dielectric tensor elements tend toward infinity, are not necessarily electrostatic. However, this is not a necessary condition, since plasma oscillations are electrostatic, and n^2 is not even defined in the cold plasma approximation for this case.

Problem 2.8.1. Cold electrostatic waves. Show that near either hybrid resonance, the waves are electrostatic.

2.8.2 Lower hybrid waves

One example of electrostatic waves occurs when a wave is propagating close to the lower hybrid resonance, since in this case k is large because of a zero in a dielectric tensor element ($K_1 = S \simeq 0$). We shall assume for this case that $\omega_{ci} \ll \omega \ll \omega_{ce}, \omega_{pe}$ so the dispersion relation, which we write as

$$k_\perp^2 = -k_\parallel^2 K_3 / K_1$$

where

$$\begin{aligned} K_1 &\simeq 1 - \frac{\omega_{pi}^2}{\omega^2} + \frac{\omega_{pe}^2}{\omega_{ce}^2} \\ K_3 &\simeq -\frac{\omega_{pe}^2}{\omega^2} \end{aligned}$$

becomes

$$k_\perp^2 \simeq \frac{k_\parallel^2 \omega_{pe}^2 \omega_{ce}^2}{(\omega_{pe}^2 + \omega_{ce}^2)(\omega^2 - \omega_{LH}^2)} \quad (2.111)$$

where

$$\omega_{LH}^2 = \omega_{ce} \omega_{ci} / (1 + \omega_{ce}^2 / \omega_{pe}^2).$$

Here we see that for fixed k_\parallel , k_\perp grows arbitrarily large as we approach the hybrid resonance, so the electrostatic approximation is validated.

This case has interesting behavior with respect to its phase and group velocity. If we solve for $\omega(k, \theta)$, we find

$$\omega^2 = \omega_{LH}^2 + \frac{k_\parallel^2 \omega_{pe}^2 \omega_{ce}^2}{k_\perp^2 (\omega_{pe}^2 + \omega_{ce}^2)} = \omega_{LH}^2 + \frac{\omega_{pe}^2 \omega_{ce}^2}{(\omega_{pe}^2 + \omega_{ce}^2)} \cot^2 \theta \quad (2.112)$$

so ω does not depend explicitly on k . If we consider $\omega(k_\parallel, k_\perp)$, however, then we find that

$$\begin{aligned} \left. \frac{\partial \omega}{\partial k_\parallel} \right|_{k_\perp} &= \frac{1}{k_\parallel} \left(\frac{\omega^2 - \omega_{LH}^2}{\omega} \right) \\ \left. \frac{\partial \omega}{\partial k_\perp} \right|_{k_\parallel} &= -\frac{1}{k_\perp} \left(\frac{\omega^2 - \omega_{LH}^2}{\omega} \right). \end{aligned} \quad (2.113)$$

With the group velocity angle ϕ with respect to the magnetic field defined in this case as

$$\tan \phi = \left. \frac{\partial \omega}{\partial k_\perp} \right|_{k_\parallel} \left(\left. \frac{\partial \omega}{\partial k_\parallel} \right|_{k_\perp} \right)^{-1} = -\left. \frac{\partial k_\parallel}{\partial k_\perp} \right|_\omega \quad (2.114)$$

then the group velocity is found to be precisely perpendicular to the phase velocity.

Another feature which will be important later is that if we consider k_{\parallel} to be fixed, then the wave is a backward wave, in the sense that the phase velocity and the group velocity are in opposite directions. If, however, k_{\perp} is taken as fixed, then it is a forward wave. This wave is frequently launched across a magnetic field into a plasma of varying magnetic field and density in the perpendicular direction but with no variation in the parallel direction, so k_{\parallel} is determined by the launch structure only and the wave is taken to propagate nearly in the perpendicular direction (but at a finite angle from perpendicular, since it does not propagate at all with $k_{\parallel} = 0$) where it is a backward wave. The effects of the variation of plasma parameters will be taken up in [chapter 6](#).

2.8.3 Resonance cones

If one excites a wave in an anisotropic plasma from a point source, then the radiation pattern is generally not symmetric in space, especially in those regions of parameter space where the wave normal surfaces are lemniscoids, since waves do not even propagate in all directions. In fact, in regions of the CMA diagram which have resonance angles, the propagation is strongly influenced by the resonance and has been shown both theoretically [12] and experimentally [13] to give rise to resonance cones, so-called because virtually all of the wave energy is propagated from the point source in cones with a fixed angle with respect to the magnetic field. To see how this occurs, we again consider electrostatic waves near the lower hybrid resonance.

We first represent the source as an oscillating point source described by $\rho(\mathbf{r}, t) = \delta(\mathbf{r})e^{-i\omega t}$ so the spatial Fourier transform of the source is given by $\rho(\mathbf{k}) = 1$. This may be considered to be a Green function from which we construct a distributed source, but as long as the source extent is small compared to the distances where measurements are to be made, this provides an adequate description of the source. The Fourier transform of the resulting potential is given by Poisson's equation so that

$$\Phi(\mathbf{k}) = \rho(\mathbf{k})/\epsilon_0 D(k_{\perp}^2, k_z) \quad (2.115)$$

where $D(k_{\perp}^2, k_z) = \mathbf{k} \cdot \mathbf{K} \cdot \mathbf{k}$. In cylindrical coordinates in k -space with the axis aligned with the magnetic field, the inverse Fourier transform gives

$$\begin{aligned} \varphi(\mathbf{r}) &= \frac{1}{(2\pi)^3} \int_{-\infty}^{\infty} d^3k \Phi(\mathbf{k}) e^{i\mathbf{k} \cdot \mathbf{r}} \\ &= \frac{1}{4\pi^2 \epsilon_0} \int_{-\infty}^{\infty} dk_z e^{ik_z z} \int_0^{\infty} dk_{\perp} k_{\perp} \frac{J_0(k_{\perp} \rho)}{D(k_{\perp}^2, k_z)} \end{aligned} \quad (2.116)$$

where we have used the identity,

$$\int_0^{2\pi} d\psi e^{ik_{\perp}\rho \cos(\psi - \theta)} = 2\pi J_0(k_{\perp}\rho)$$

to do the integral over the angle ψ in k -space and where the coordinates in configuration space are ρ , θ , and z . Using the Bessel identity

$$J_0(x) = \frac{1}{2}[H_0^{(1)}(x) + H_0^{(2)}(x)]$$

where $H_0^{(1)}(x)$ and $H_0^{(2)}(x)$ are Hankel functions of order zero of the first and second kind, we may make the further change in the perpendicular integral such that

$$\begin{aligned} \int_0^\infty dk \frac{k J_0(k\rho)}{D(k^2)} &= \frac{1}{2} \int_0^\infty dk \frac{k H_0^{(1)}(k\rho)}{D(k^2)} + \frac{1}{2} \int_0^\infty dk \frac{k H_0^{(2)}(k\rho)}{D(k^2)} \\ &= \frac{1}{2} \int_{-\infty}^\infty dk \frac{k H_0^{(1)}(k\rho)}{D(k^2)} \end{aligned} \quad (2.117)$$

where we have used the reflection symmetry that $H_0^{(2)}(ze^{-i\pi}) = -H_0^{(1)}(z)$ to extend the range of the integral to $[-\infty, \infty]$. In terms of the original variables, the potential is then given by

$$\varphi(\mathbf{r}) = \frac{1}{8\pi^2\epsilon_0} \int_{-\infty}^\infty dk_z e^{ik_z z} \int_{-\infty}^\infty dk_\perp k_\perp \frac{H_0^{(1)}(k_\perp \rho)}{D(k_\perp^2, k_z)}. \quad (2.118)$$

Having extended the range of integration, we can now evaluate the second integral by contour integration, closing in the upper half-plane where $H_0^{(1)}$ is small. In general, this contour will pick up contributions from all of the zeros of the dispersion relation which lie in the upper half-plane, but for electrostatic waves in a cold plasma, there are only two poles. These are located at

$$k_\perp = \pm k_{\perp 0} \quad k_{\perp 0} = k_z \sqrt{-K_3/K_1} \quad (2.119)$$

only one of which can be above the real axis. If we assume $\text{Im}(k_{\perp 0}) > 0$, then the pole corresponding to the upper sign gives

$$\varphi(\mathbf{r}) = \frac{i}{8\pi\epsilon_0 K_1} \int_{-\infty}^\infty dk_z e^{ik_z z} H_0^{(1)}(k_{\perp 0} \rho). \quad (2.120)$$

Now for general values of ρ , this is difficult to evaluate but for large $|\rho|$, we may use the asymptotic form, $H_0^{(1)}(x) \sim \sqrt{2/\pi x} e^{i(x-\pi/4)}$, so the exponent in equation (2.120) is approximately

$$i(k_z z + \rho k_{\perp 0}) = i \left(k_z z + k_z \frac{\partial k_{\perp 0}}{\partial k_z} \rho \right) = ik_z(z - \rho \cot \phi)$$

where the middle step has used the expansion

$$k_{\perp 0}(k_z) = k_{\perp 0}(0) + \left. \frac{\partial k_{\perp 0}}{\partial k_z} \right|_{k_z=0} k_z + \dots$$

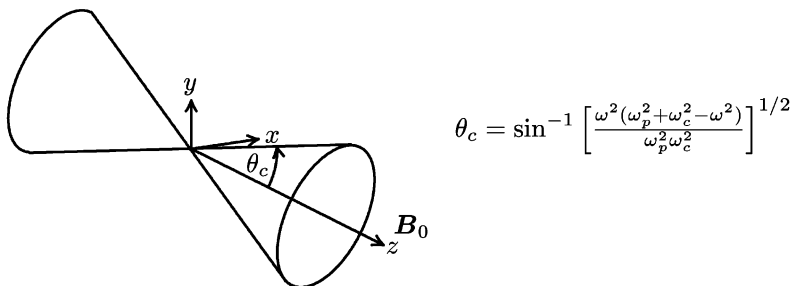


Figure 2.28. Geometry of resonance cones for a lower hybrid wave showing cone angle θ_c for a point source at the origin. The z -axis is in the direction of \mathbf{B}_0 . (from reference [14]).

which is trivial for a cold plasma but important for warm plasmas, and the last step has used equation (2.114). The integral is then a delta function, evaluating the integrand at $z = \rho \cot \phi$ or at $\rho = z \tan \phi$. From the analysis leading to equation (2.114), ϕ is the angle of the group velocity at resonance, so the only disturbance far from the source occurs at this particular cone angle. The pole we did not use earlier leads to a complementary cone in the negative z -direction, so it yields no new information.

The conclusion of this section is that in frequency ranges where electrostatic waves propagate with $K_1/K_3 < 0$, and we used lower hybrid waves as an example of this, then the radiated energy far from the source is found only on cones whose angle is given by

$$\phi_c = \tan^{-1} \sqrt{-K_1/K_3}. \quad (2.121)$$

This conclusion will of course be modified by real plasma effects, such as finite temperature effects and weak inhomogeneities, but the resonance cone effect has been observed where the response of a localized source peaks on these cones. The thermal effects, among other things, tend to broaden the cone and even give thermal interference fringes just inside of the cone angle [12, 13]. These cones are illustrated in figure 2.28 where the geometry is evident.

Problem 2.8.2. Resonance cones.

- (i) Fill in the missing steps leading to equations (2.118) and (2.121).
- (ii) What if $K_1/K_3 > 0$? Show why this case has no resonance cones.

2.9 Particle motions near resonance

The motions of the electrons and ions for general cases are complicated and give insight into the wave motion only in special cases. We have already treated the particle motions for low-frequency Alfvén waves in section 2.5.1. In this section we examine the particle motions near resonance, because the concept of

resonance invariably suggests that something is singular and requires more careful examination in order to understand the physics of the phenomenon. We will examine this notion in more detail in chapter 6 where resonances are approached in space in an inhomogeneous plasma but we look first at the principal resonances in a cold, uniform plasma.

2.9.1 Lower hybrid resonance (high density case)

If we examine again the X -wave near the lower hybrid resonance, looking in particular at the electric fields, currents, and particle motions, we note first from the first equation of the set equation (2.20) that at $\theta = \pi/2$,

$$SE_x - iDE_y = 0 \quad (2.122)$$

and since at resonance $S = 0$, and $D \neq 0$, we find that $E_y = 0$, while $E_x \neq 0$. Then since the conductivity tensor component $\sigma_{xx} = i\omega\epsilon_0(S - 1) \rightarrow -i\omega\epsilon_0$, and since *except* at resonance, $|S| \gg 1$ in the high density limit, then we can take $|\sigma_{xx}|$ to be negligible compared to $|\sigma_{xy}|$. This leads to

$$J_x = \sigma_{xx}E_x + \sigma_{xy}E_y \simeq 0 \quad (2.123)$$

$$J_y = -\sigma_{xy}E_x + \sigma_{xx}E_y \neq 0 \quad (2.124)$$

since both $\sigma_{xx} \simeq 0$ and $E_y = 0$ in equation (2.123) lead to $J_x \simeq 0$ and $\sigma_{xy} \neq 0$ and $E_x \neq 0$ in equation (2.124) lead to $J_y \neq 0$. We note at once from the charge continuity equation that

$$\mathbf{k} \cdot \mathbf{j} = \omega\rho = 0 \quad (2.125)$$

since \mathbf{k} is perpendicular to \mathbf{j} , with the result that there is no charge fluctuation in this electrostatic ($\mathbf{E} = E_x\hat{\mathbf{e}}_x$, $\mathbf{k} = k_x\hat{\mathbf{e}}_x$) wave.

The electron equation of motion for this wave is

$$-i\omega_{LH}\mathbf{v}_e = -\frac{e}{m_e}(\mathbf{E} + \mathbf{v}_e \times \mathbf{B}_0) = -\frac{e}{m_e}\mathbf{E} - \omega_{ce}\mathbf{v}_e \times \hat{\mathbf{e}}_z. \quad (2.126)$$

The left-hand side of equation (2.126) is $\sqrt{m_e/m_i}$ smaller than the second term on the right, so we neglect it, with the result that

$$\mathbf{E} + \mathbf{v}_e \times \mathbf{B}_0 = 0$$

so that \mathbf{v}_e is perpendicular to both \mathbf{E} and \mathbf{B}_0 . Solving for the velocity, we obtain

$$\mathbf{v}_e = -\frac{E_x}{B_0}\hat{\mathbf{e}}_y = \frac{e}{m_i}\frac{E_x}{\omega_{ci}}\hat{\mathbf{e}}_y. \quad (2.127)$$

For ions, we have

$$-i\omega_{LH}\mathbf{v}_i = \frac{e}{m_i}(\mathbf{E} + \mathbf{v}_i \times \mathbf{B}_0) = \frac{e}{m_i}\mathbf{E} + \omega_{ci}\mathbf{v}_i \times \hat{\mathbf{e}}_z. \quad (2.128)$$

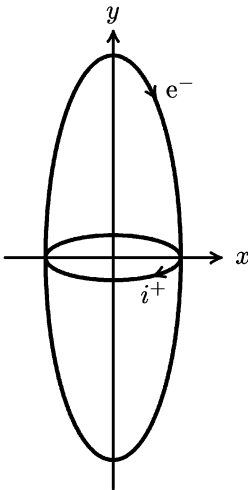


Figure 2.29. Electron and ion motions near the lower hybrid frequency.

In this equation, we can neglect the term involving ω_{ci} since it is small compared to $\omega_{LH} \simeq \sqrt{\omega_{ce}\omega_{ci}}$. Then,

$$\mathbf{v}_i = \frac{e}{m_i} \frac{\mathbf{iE}}{\omega_{LH}} = \frac{e}{m_i} \frac{\mathbf{iE}_x}{\omega_{LH}} \hat{\mathbf{e}}_x. \quad (2.129)$$

From these velocity estimates, it is apparent that the electrons have a much larger velocity than the ions but in a different direction. The orbits are found by dividing the velocities by $-i\omega_{LH}$, which does not change the ratio, so the electron orbit is much larger than the ion orbit. We sketch these orbits in figure 2.29 where it is apparent that the orbits are ellipses due to the terms of order $\sqrt{m_e/m_i}$ which were previously neglected.

From the figure it is apparent that the electron and ion currents cancel in the x -direction and add in the y -direction. It is this absence of J_x with finite E_x simultaneously with the production of finite J_y with no E_y component which is unique to the hybrid resonances.

The energy of the electrons and the ions can be calculated from the expressions for their respective velocities, with the result that $\frac{1}{2}m_e v_e^2 = \frac{1}{2}m_i v_i^2$. This equivalence of kinetic energy between the two species is another characteristic of the lower hybrid resonance, and demonstrates in yet another way its hybrid character.

In summary, we have seen that the lower hybrid resonance may lead to a resonance in the index of refraction or the wavevector but no singularities have been encountered in the particle motions.

Problem 2.9.1. Particle Orbits near the lower hybrid resonance. For a wave

propagating at $\theta = \pi/2$ near the lower hybrid resonance:

- (i) Show that the particle orbits are ellipses and find the ratio of their major and minor axes (in the high density limit).
- (ii) Show that $J_x = i\omega\epsilon_0 E_x$ (not only at resonance).
- (iii) Show that the kinetic energies of the electrons and ions are equal.

Problem 2.9.2. Particle orbits near the two-ion hybrid resonance. For a wave propagating at $\theta = \pi/2$ near the two-ion hybrid resonance ($\omega_{c1} < \omega_{ii} < \omega_{c2}$) in a high density plasma of 50% hydrogen and 50% deuterium:

- (i) Find the major and minor axes of the ion orbits.
- (ii) Sketch the particle orbits.
- (iii) Find the kinetic energies of each species.

2.9.2 Upper hybrid resonance

The particle motions near the upper hybrid resonance are even easier to analyze than near the lower hybrid resonance, because we can neglect the ion motions completely. The relation between the electric field components given by equation (2.122) still applies to the upper hybrid resonance, and we still have $S \rightarrow 0$, so we also have $E_x \neq 0$ and $E_y = 0$ for this case. Looking then at the electron equation of motion,

$$-i\omega_{UH} \mathbf{v}_e = -\frac{e}{m_e} (E_x \hat{\mathbf{e}}_x + \mathbf{v}_e \times \mathbf{B}_0)$$

leads to the velocity component expressions,

$$v_x = \frac{e\omega_{UH} E_x}{im_e \omega_{pe}^2} \quad v_y = \frac{e\omega_{ce} E_x}{m_e \omega_{pe}^2} \quad (2.130)$$

where we have used $\omega_{UH}^2 - \omega_{ce}^2 = \omega_{pe}^2$. From these we obtain the current components,

$$\begin{aligned} J_x &= i\omega_{UH} \epsilon_0 E_x \\ J_y &= -\omega_{ce} \epsilon_0 E_x. \end{aligned} \quad (2.131)$$

It now becomes apparent from equation (2.131) that when we add the plasma current to the displacement current, the x -component cancels and there will be no source term for the x -component, a result similar to the lower hybrid case. We again find no singularity in any of the particle motions, and we find relationships between the currents and fields that are similar to those in the lower hybrid case.

2.9.3 Cyclotron resonances

The particle motions at the cyclotron resonances are different from those at the hybrid resonances, and must be treated differently. As an example of this kind of resonance, we will examine the electron cyclotron resonance for the *R*-wave but we will not take Fourier transforms. Looking only at the transverse motions of the electrons, the components of the equations of motion give

$$\frac{dv_x}{dt} = -\frac{e}{m_e}(E_x + v_y B_0) \quad (2.132)$$

$$\frac{dv_y}{dt} = -\frac{e}{m_e}(E_y - v_x B_0). \quad (2.133)$$

By taking the derivative of equation (2.132) and using equation (2.133) to eliminate dv_y/dt , we may write the single second-order inhomogeneous differential equation for v_x ,

$$\frac{d^2v_x}{dt^2} + \omega_{ce}^2 v_x = -\frac{e}{m_e} \left(\frac{dE_x}{dt} - \omega_{ce} E_y \right). \quad (2.134)$$

For the *R*-wave polarization, we take the electric field to be circularly polarized such that

$$\begin{aligned} E_x &= E_0 \cos \omega_{cet} t \\ E_y &= E_0 \sin \omega_{cet} t \end{aligned} \quad (2.135)$$

so equation (2.134) becomes

$$\frac{d^2v_x}{dt^2} + \omega_{ce}^2 v_x = \frac{2eE_0\omega_{ce}}{m_e} \sin \omega_{cet}. \quad (2.136)$$

The homogeneous solution of equation (2.136) and the corresponding solution for v_y are given by

$$\begin{aligned} v_x &= v_0 \cos(\omega_{cet} t + \phi) \\ v_y &= v_0 \sin(\omega_{cet} t + \phi) \end{aligned} \quad (2.137)$$

where v_0 and ϕ are arbitrary amplitude and phase constants, but the inhomogeneous solutions are given by

$$v_x = -\frac{E_0}{B_0} \omega_{cet} \cos \omega_{cet} t \quad (2.138)$$

$$v_y = -\frac{E_0}{B_0} \omega_{cet} \sin \omega_{cet} t \quad (2.139)$$

so the magnitude of the velocity increases linearly in time. The kinetic energy is given by

$$\frac{1}{2} m_e v^2 = \frac{1}{2} m_e v_0^2 + \frac{(eE_0 t)^2}{2m_e} - v_0 e E_0 t \cos \phi \quad (2.140)$$

so the energy increases without bound in time and there is no steady-state solution. This is why we avoided using the Fourier transform, since that method assumes that steady-state amplitudes exist.

The conclusion from this section, then, is that cyclotron motions are truly singular in uniform cold plasma theory without collisions, and we must look either to collisions, thermal effects, inhomogeneity effects, or nonlinear effects to resolve these singularities, since truly unbounded motions are unacceptable physical solutions. We can easily imagine how an inhomogeneity in the magnetic field might affect our result, since with a finite velocity in the z -direction, a particle will spend only a finite time in the resonance region if the magnetic field also varies in the z -direction.

Problem 2.9.3. Ion cyclotron resonance. Fill in the steps leading to the result of equation (2.140) corresponding to the ion cyclotron resonance driven by an L -wave.

Problem 2.9.4. Localized resonance. Suppose an electron drifts through the resonance zone with a fixed v_z where $B(z) = B_0(1 - z/L) = B_0(1 - v_z t/L) = B_0(t)$.

- (i) Show that equations (2.132) and (2.133) may be written in dimensionless coordinates as

$$\begin{aligned}\frac{dv_x}{d\tau} &= -v_0 \cos \tau - v_y \left(1 - \frac{\tau}{\alpha}\right) \\ \frac{dv_y}{d\tau} &= -v_0 \sin \tau + v_x \left(1 - \frac{\tau}{\alpha}\right)\end{aligned}$$

where $v_0 = E_0/B_0$ and $\tau = \omega_{cet}t$.

- (ii) Use the Mathematica program

```
a=110;
v0=1;
eqone=vx'[t]==-v0 Cos[t]-vy[t] (1-t/a);
eqtwo=vy'[t]==-v0 Sin[t]+vx[t] (1-t/a);
sol=NDSolve[{eqone,eqtwo,vx[-40]==vy[-40]==1},
{vx[t],vy[t]}, {t,100}]
Plot[vx[t]^2+vy[t]^2 /. sol,{t,-40,100}]
```

to estimate the gain in the energy by finding the ratio of $\langle v^2 \rangle/v_0^2$ by trying several values of v_0 .

This calculation is only illustrative of the energy gain, since the wave amplitude should decay exponentially in z as it does not propagate above the resonance. The assumption of constant v_z is also a crude approximation since there are forces due to the gradient in B . The real problem is highly nonlinear.

Chapter 3

Waves in fluid plasmas

The analysis of cold plasma waves, although very complicated already, leaves out all of the physics that relates to finite temperature effects. These effects may be included in varying degrees of approximation, and it is instructive to include at this stage only the simplest thermal correction terms through the inclusion of a finite pressure term. This term appears in the *fluid equations*, which come from a moment expansion of equation (1.63), the Boltzmann equation,

$$\frac{\partial f}{\partial t} + \mathbf{v} \cdot \nabla f + \mathbf{A} \cdot \nabla_{\mathbf{v}} f = \left. \frac{df}{dt} \right|_{\text{coll.}} \quad (3.1)$$

where \mathbf{A} is the acceleration due to electric and magnetic fields through the Lorentz force. Introduced in [chapter 1](#), this basic equation and its interpretation will be discussed further in [chapter 4](#).

Whereas in the cold plasma we talked about motions of individual particles and then added up the motions of all of them to find the currents, in the fluid plasma we describe the motion of a fluid element which is an average over many particles of the same species and we assume that the separate fluid elements for each species move freely among one another, except as collisions exchange momentum between them. The averaging process we shall use here is to expand the Boltzmann equation for each species in a velocity moment expansion, truncating the expansion at some suitable level, depending on the particular problem. Collisions, which were neglected in the cold plasma, will be discussed in section 3.4. Instabilities which may arise from counterstreaming fluid elements and their classification are included in section 3.5.

3.1 Moments of the distribution function

3.1.1 The moment equations

If we neglect collisions for the moment, then equation (3.1) can also be written as

$$\frac{\partial f}{\partial t} + \nabla \cdot (\mathbf{v} f) + \nabla_{\mathbf{v}} \cdot (\mathbf{A} f) = 0 \quad (3.2)$$

since $f \nabla \cdot \mathbf{v} = 0$ and $f \nabla_v \cdot \mathbf{A} = 0$ since \mathbf{r} and \mathbf{v} are independent variables. We then introduce a scalar function of velocity, $Q(\mathbf{v})$, and define the moment process by an average over the velocity as

$$\begin{aligned}\langle Q(\mathbf{v}) \rangle &= Q(\mathbf{v}) \quad \text{averaged over velocity} \\ &= \frac{\int Q f d^3 v}{\int f d^3 v} = \frac{1}{n} \int Q f d^3 v\end{aligned}\quad (3.3)$$

where $n(\mathbf{r}) = \int f(\mathbf{r}, \mathbf{v}) d^3 v$ is the density in configuration space.

If we now multiply equation (3.2) by Q and integrate over velocity, we have

$$\int Q \frac{\partial f}{\partial t} d^3 v + \int Q \nabla \cdot \mathbf{v} f d^3 v + \int Q \nabla_v \cdot \mathbf{A} f d^3 v = 0.$$

Since Q is a function of \mathbf{v} only, this becomes

$$\frac{\partial}{\partial t} \int Q f d^3 v + \nabla \cdot \int Q \mathbf{v} f d^3 v + \int Q \nabla_v \cdot \mathbf{A} f d^3 v = 0. \quad (3.4)$$

The first term of equation (3.4) is simply $\partial(n(Q))/\partial t$ while the second is $\nabla \cdot (n(Q\mathbf{v}))$. The third term expands to

$$\begin{aligned}\int Q \nabla_v \cdot \mathbf{A} f d^3 v &= \int [\nabla_v \cdot (Q \mathbf{A} f) - f \mathbf{A} \cdot \nabla_v Q] d^3 v \\ &= \oint_{S_v} (Q \mathbf{A} f) \cdot d\mathbf{S}_v - \int f \mathbf{A} \cdot \nabla_v Q d^3 v\end{aligned}$$

and the surface integral in velocity space vanishes because we assume the distribution vanishes for $v \rightarrow \infty$. We can then write equation (3.4) as

$$\frac{\partial}{\partial t} (n(Q)) + \nabla \cdot (n(Q\mathbf{v})) - n \langle \mathbf{A} \cdot \nabla_v Q \rangle = 0. \quad (3.5)$$

3.1.1.1 Zeroth moment

Let $Q = 1$. Then $\langle Q \rangle = 1$ and $\langle Q\mathbf{v} \rangle = \langle \mathbf{v} \rangle \equiv \mathbf{u}$ where \mathbf{u} is the mean or average velocity of the fluid element. Then equation (3.5) leads to

$$\frac{\partial n}{\partial t} + \nabla \cdot (n\mathbf{u}) = 0 \quad \text{the continuity equation.} \quad (3.6)$$

3.1.1.2 First moment

Let $Q = m v_x$. Then $\langle Q \rangle = m u_x$ and $\nabla_v Q = m \hat{\mathbf{e}}_{v_x}$ so $\langle \mathbf{A} \cdot \nabla_v Q \rangle = m \langle a_x \rangle$. This leads to

$$\frac{\partial}{\partial t} (n m u_x) + \nabla \cdot (n m \langle \mathbf{v} v_x \rangle) - n m \langle a_x \rangle = 0.$$

Now we let $\mathbf{v} = \mathbf{u} + \mathbf{w}$, where \mathbf{w} measures the perturbation from the average velocity ($\langle \mathbf{w} \rangle = 0$). Then

$$\langle \mathbf{v} v_x \rangle = \langle (\mathbf{u} + \mathbf{w})(u_x + w_x) \rangle = \mathbf{u} u_x + \langle \mathbf{w} w_x \rangle.$$

We then call $nm\langle \mathbf{w} \mathbf{w} \rangle$ the stress tensor Ψ . The last term is

$$\begin{aligned} nm\langle a_x \rangle &= q \int (\mathbf{E} + \mathbf{v} \times \mathbf{B})_x f d^3 v \\ &= nq(\mathbf{E} + \mathbf{u} \times \mathbf{B})_x \end{aligned}$$

so that by taking all three such component equations from letting $Q = mv_x, mv_y, mv_z$, we obtain the first moment equation

$$\frac{\partial}{\partial t}(nm\mathbf{u}) + \nabla \cdot (nm\mathbf{u}\mathbf{u}) + \nabla \cdot \Psi - nq(\mathbf{E} + \mathbf{u} \times \mathbf{B}) = 0. \quad (3.7)$$

This equation is generally written, using equation (3.6) and the identity

$$\nabla \cdot (nm\mathbf{u}\mathbf{u}) = nm(\mathbf{u} \cdot \nabla)\mathbf{u} + m\mathbf{u}\nabla \cdot (n\mathbf{u})$$

as

$$nm \left[\frac{\partial \mathbf{u}}{\partial t} + (\mathbf{u} \cdot \nabla)\mathbf{u} \right] + \nabla \cdot \Psi - nq(\mathbf{E} + \mathbf{u} \times \mathbf{B}) = 0. \quad (3.8)$$

This is the first moment of the Boltzmann equation, and represents the conservation of momentum in the plasma:

$$\frac{\partial}{\partial t}(\text{momentum density}) + \text{flux of momentum density} = \text{force density}.$$

3.1.1.3 Higher moments

Equation (3.6) gave the evolution of n as a function of \mathbf{u} , equation (3.8) gave the evolution of \mathbf{u} as a function of Ψ , and to find the evolution of Ψ , one needs the next higher moment, etc. This process must be truncated in order to use the moment equations. If we assume the higher rank tensor (which would appear in the second moment equation) vanishes, then we may represent the stress tensor by a scalar pressure so that $\nabla \cdot \Psi = \nabla p = \nabla(n\kappa T)$.

3.1.2 Longitudinal plasma oscillations from the moment equations

In order to both illustrate the moment expansion method and to resolve an ambiguity in cold plasma waves, we shall investigate plasma oscillations in an unmagnetized plasma. The ambiguity came about from the fact that $P = 0$ was both a cutoff ($PRL = 0$ defined the cutoffs where $n^2 = 0$) and a resonance ($\tan^2 \theta = -P/S$ is the resonance condition, and $\theta = 0$ leads to $P = 0$). Part of

this difficulty was that $P = 0$ leads to $\omega = \omega_p$ and no phase or group velocity was defined since k was not involved.

For this case, we assume \mathbf{k} is parallel to \mathbf{E} , $\mathbf{E} = E\hat{\mathbf{e}}_x$ so that $\mathbf{k} = k\hat{\mathbf{e}}_x$, and $\mathbf{B}_0 = 0$. The moment expansion for the α th moment is obtained by multiplying the Boltzmann equation by v^α and integrating:

$$\frac{\partial}{\partial t} \int_{-\infty}^{\infty} v^\alpha f \, dv + \frac{\partial}{\partial x} \int_{-\infty}^{\infty} v^{\alpha+1} f \, dv + \frac{q}{m} E \int_{-\infty}^{\infty} v^\alpha \frac{\partial f}{\partial v} \, dv = 0.$$

Integrating the last term by parts leads to

$$\frac{\partial}{\partial t} \int_{-\infty}^{\infty} v^\alpha f \, dv + \frac{\partial}{\partial x} \int_{-\infty}^{\infty} v^{\alpha+1} f \, dv - \frac{\alpha q E}{m} \int_{-\infty}^{\infty} v^{\alpha-1} f \, dv = 0. \quad (3.9)$$

We then define the various integral terms by

$$F^{(\alpha)} = \int v^\alpha f(v) \, dv \quad (3.10)$$

where the velocity $v = u + w$ is comprised of the average velocity, $\langle v \rangle \equiv u$, and the random part, w . If we look at the first few moments, we find

$$\begin{aligned} F^{(0)} &= n \\ F^{(1)} &= nu \\ F^{(2)} &= nu^2 + M^{(2)} \\ F^{(3)} &= nu^3 + 3uM^{(2)} + M^{(3)} \\ F^{(4)} &= nu^4 + 6u^2M^{(2)} + 4uM^{(3)} + M^{(4)} \end{aligned}$$

where we have introduced modified moments depending only on the random part of v ,

$$M^{(\alpha)} \equiv \int w^\alpha f(v) \, dv. \quad (3.11)$$

The first few of these moments are $M^{(0)} = n$, $M^{(1)} = 0$, and $mM^{(2)} = p$. Since we wish to linearize the moment equations, and since u is a first order quantity, we may write the linearized moments as

$$\begin{aligned} F^{(2k)} &= \tilde{M}^{(2k)} + \tilde{M}^{(2k)} \\ &= \frac{(2k-1)!! \bar{n} v_t^{2k}}{2^k} + \tilde{M}^{(2k)} \end{aligned} \quad (3.12)$$

$$\begin{aligned} F^{(2k+1)} &= (2k+1)\tilde{M}^{(2k)}\tilde{u} + \tilde{M}^{(2k+1)} \\ &= \frac{(2k+1)!! \bar{n} v_t^{2k}}{2^k} \tilde{u} + \tilde{M}^{(2k+1)} \end{aligned} \quad (3.13)$$

where $\tilde{u} = \tilde{u} e^{i(kz - \omega t)}$, etc and we have used a Maxwellian distribution to obtain

$$\tilde{M}^{(\alpha)} = \frac{\bar{n}}{\sqrt{\pi} v_t} \int_{-\infty}^{\infty} w^\alpha e^{-w^2/v_t^2} \, dw = \frac{\bar{n} v_t^\alpha (\alpha-1)!!}{2^{\alpha/2}} \quad (3.14)$$

for even α with $v_t = \sqrt{2kT/m}$ and $(-1)!! = 1$. It is evident from equations (3.12) and (3.13) that for α even, there is a zero order and a first order term, while for α odd, there are only first order terms.

We then write equation (3.9) in terms of the $F^{(\alpha)}$ with the result

$$\frac{\partial}{\partial t} F^{(\alpha)} + \frac{\partial}{\partial z} F^{(\alpha+1)} - \frac{\alpha q}{m} E_z F^{(\alpha-1)} = 0. \quad (3.15)$$

Assuming E is first order and that n has both zero and first order terms, the linearized moment equations for $\alpha = 0$ through $\alpha = 4$ are (with $\partial/\partial z \rightarrow ik$ and $\partial/\partial t \rightarrow -i\omega$)

$$-i\omega \tilde{n} + ik\bar{n}\tilde{u} = 0 \quad \alpha = 0 \quad (3.16)$$

$$-i\omega \bar{n}\tilde{u} + ik\tilde{M}^{(2)} - \frac{q}{m}\bar{n}\tilde{E} = 0 \quad \alpha = 1 \quad (3.17)$$

$$-i\omega \tilde{M}^{(2)} + \left(\frac{3\bar{n}v_t^2}{2}\tilde{u} + \tilde{M}^{(3)} \right) = 0 \quad \alpha = 2 \quad (3.18)$$

$$-i\omega \left(\frac{3\bar{n}v_t^2}{2}\tilde{u} + \tilde{M}^{(3)} \right) + ik\tilde{M}^{(4)} - \frac{3q\bar{n}v_t^2}{2m}\tilde{E} = 0 \quad \alpha = 3 \quad (3.19)$$

$$-i\omega \tilde{M}^{(4)} + ik \left(\frac{5!!\bar{n}v_t^4}{4}\tilde{u} + \tilde{M}^{(5)} \right) = 0 \quad \alpha = 4. \quad (3.20)$$

The subsequent terms can be obtained from the two general expressions for α even and α odd:

$$-i\omega \tilde{M}^{(\alpha)} + ik \left[\frac{(\alpha+1)!!\bar{n}v_t^\alpha}{2^{\alpha/2}}\tilde{u} + \tilde{M}^{(\alpha+1)} \right] = 0 \quad \alpha \text{ even} \quad (3.21)$$

$$-i\omega \left[\frac{\alpha!!\bar{n}v_t^{\alpha-1}}{2^{(\alpha-1)/2}}\tilde{u} + \tilde{M}^{(\alpha)} \right] + ik\tilde{M}^{(\alpha+1)} - \frac{q\alpha!!\bar{n}v_t^{\alpha-1}}{m2^{(\alpha-1)/2}}\tilde{E} = 0 \quad \alpha \text{ odd.} \quad (3.22)$$

We may then use equation (3.16), written as $\tilde{u} = (\omega/k)\tilde{n}/\bar{n}$, to eliminate \tilde{u} in equation (3.21) so that the pair may be written as

$$-i\omega \left[\tilde{M}^{(\alpha)} - \frac{(\alpha+1)!!v_t^\alpha}{2^{\alpha/2}}\bar{n} \right] + ik\tilde{M}^{(\alpha+1)} = 0 \quad \alpha \text{ even} \quad (3.23)$$

$$-i\omega \tilde{M}^{(\alpha)} + ik\tilde{M}^{(\alpha+1)} + \frac{\alpha!!\bar{n}v_t^{\alpha-1}}{2^{(\alpha-1)/2}} \left(-i\omega \bar{n} - \frac{q}{m} \tilde{E} \right) = 0 \quad \alpha \text{ odd.} \quad (3.24)$$

By taking these equations two at a time, we may generate higher and higher order approximations in a systematic manner. Defining

$$\tilde{f} \equiv -i\omega \tilde{u} - \frac{q}{m} \tilde{E} \quad (3.25)$$

and using equation (3.24) with $\alpha = 1$, we first obtain

$$\tilde{f} = -\frac{ik}{\bar{n}} \tilde{M}^{(2)}. \quad (3.26)$$

Then taking the $\alpha = 2$ and $\alpha = 3$ cases together,

$$\begin{aligned} -i\omega \tilde{M}^{(2)} + ik \tilde{M}^{(3)} + i\omega \frac{3!!v_t^2}{2} \tilde{n} &= 0 \\ -i\omega \tilde{M}^{(3)} + ik \tilde{M}^{(4)} + \frac{3!!\bar{n}v_t^2}{2} \tilde{f} &= 0 \end{aligned}$$

and eliminating $\tilde{M}^{(3)}$ between them, we find

$$\tilde{f} \left(1 + \frac{3!!}{2\theta^2} \right) = -\frac{ik}{\bar{n}} \left(\frac{3!!v_t^2}{2} \tilde{n} + \frac{k^2}{\omega^2} \tilde{M}^{(4)} \right). \quad (3.27)$$

Continuing with two at a time, the result may be written as

$$S_m \tilde{f} = -\frac{ik}{\bar{n}} \left[v_t^2 \theta^2 (S_m - 1) \tilde{n} + \left(\frac{k}{\omega} \right)^{2m} \tilde{M}^{(2m+2)} \right] \quad (3.28)$$

where equation (3.26) is the result for $m = 0$, equation (3.27) is the result for $m = 1$, and

$$S_m(\theta) = \sum_{j=0}^m \frac{(2j+1)!!}{2^j \theta^{2j}} \quad \theta \gg 1 \quad (3.29)$$

where $\theta \equiv \omega/kv_t$. This equation of motion must now be solved along with Poisson's equation,

$$ik \tilde{E} = \frac{q\tilde{n}}{\epsilon_0}. \quad (3.30)$$

Using equation (3.30), we may write \tilde{f} as

$$\tilde{f} = -\frac{i}{k\bar{n}} (\omega^2 - \omega_p^2) \tilde{n}.$$

Using this result along with equation (3.28) results in

$$\omega^2 = \omega_p^2 S_m(\theta) + k^2 \left(\frac{k}{\omega} \right)^{2m} \frac{\tilde{M}^{(2m+2)}}{\tilde{n}}. \quad (3.31)$$

This is an asymptotic series in θ with the remainder term set to zero for some m . No matter how many terms are kept, there will never be any imaginary part. As more terms are kept, θ must be larger and larger since each term must be smaller than the previous term.

The lowest nontrivial approximation is to let $\tilde{M}^{(4)} = 0$ to obtain

$$\omega^2 = \omega_{pe}^2 \left[1 + \frac{3}{2} \left(\frac{v_e}{v_p} \right)^2 \right] \quad (3.32)$$

which is called the Bohm–Gross dispersion relation¹ [15] (BGDR) where we have defined the electron thermal speed as $v_e^2 \equiv 2\kappa T_e/m_e$. Keeping $\tilde{M}^{(4)}$ but setting $\tilde{M}^{(6)} = 0$, the result is

$$\omega^2 = \omega_{pe}^2 \left[1 + \frac{3}{2} \left(\frac{v_e}{v_p} \right)^2 + \frac{15}{4} \left(\frac{v_e}{v_p} \right)^4 \right] \quad (3.33)$$

so it is apparent that *the moment expansion is an expansion in the ratio of the thermal velocity to the phase velocity*. The BGDR now resolves the ambiguity in cold plasma theory and supports the notion that $P = 0$ in cold plasma is a cutoff rather than a resonance, since this dispersion relation describes a wave with a cutoff at ω_{pe} that propagates near the electron thermal speed for high frequencies.

We have thus learned from this example that the fluid equations which are based on moment expansions are valid as long as the phase velocity is large compared to the thermal speed. When this approximation fails, then we must solve the equations without expansion, and techniques for this approach will be discussed in the next chapter.

Problem 3.1.1. Moment expansions.

- (i) *Zeroth order moments.* Verify equation (3.14).
- (ii) *Moment pairs.* Fill in the steps leading to equations (3.23) and (3.24).
- (iii) *Fifth moment.* Continue with the $\alpha = 4$ and $\alpha = 5$ terms beyond equation (3.27) and verify that equation (3.28) is valid for $m = 2$.
- (iv) Using Poisson's equation, complete the steps from equation (3.28) to equation (3.31).

3.2 The fluid equations

Having used the notation in the previous section that \mathbf{v} is an independent variable and that \mathbf{u} is the velocity of a fluid element, we now switch definitions to the more traditional notation where the fluid velocity is denoted by \mathbf{v}_j since now it relates to a specific species j . We shall also use the definition of the mass density as $\rho_j = n_j m_j$ which is the mass per unit volume for a fluid element of species j . With these definitions, the fluid equations are:

$$\frac{\partial \rho_j}{\partial t} + \nabla \cdot (\rho_j \mathbf{v}_j) = Z_j \quad (\text{continuity equation}) \quad (3.34)$$

¹ Technically, the BGDR is equation (3.32) with $\omega = \omega_{pe}$ in the correction term. This leads to $\omega^2 = \omega_{pe}^2 (1 + 3k^2 \lambda_{De}^2)$ for the BGDR.

where Z_j is the ionization rate for species j and

$$\rho_j \left[\frac{\partial \mathbf{v}_j}{\partial t} + (\mathbf{v}_j \cdot \nabla) \mathbf{v}_j \right] = q_j n_j (\mathbf{E} + \mathbf{v}_j \times \mathbf{B}) - \nabla p_j \quad (\text{momentum equation}) \quad (3.35)$$

where collisions have been neglected for now. For particle conservation, the ionization rates among the various species (including neutrals) must satisfy

$$\sum_j Z_j = 0.$$

The linearized fluid equations are:

$$\frac{\partial \rho_{1j}}{\partial t} + \rho_{0j} \nabla \cdot \mathbf{v}_{1j} = 0 \quad (\text{continuity equation}) \quad (3.36)$$

where ionization has been neglected and

$$\rho_{0j} \frac{\partial \mathbf{v}_{1j}}{\partial t} = q_j n_{0j} (\mathbf{E}_0 + \mathbf{v}_{1j} \times \mathbf{B}_0) - \nabla p_{1j} \quad (\text{momentum equation}) \quad (3.37)$$

since all zero order quantities are assumed to be constant in space and time and we are taking $\mathbf{E}_0 = \mathbf{v}_{0j} = 0$ for the moment. We shall consider the effects due to collisions and $\mathbf{v}_{0j} \neq 0$ later in this chapter, and consider $\mathbf{E}_0 \neq 0$ in [chapter 6](#) when we deal with drift waves in inhomogeneous plasmas.

Problem 3.2.1. Fluid equations with zero order drifts and fields. Write the zeroth and first order continuity and momentum equations when $\mathbf{v}_{0j} \neq 0$ and $\mathbf{E}_0 \neq 0$.

3.3 Low frequency waves

The waves from the fluid equations conveniently break up into two regions when $m_e \ll m_i$. For the high frequency waves, ion motions are completely neglected, while in the low frequency region, we neglect terms of order m_e/m_i .

3.3.1 The low-frequency dispersion relation

Beginning with the linearized fluid equations for electrons and one species only of singly charged ions, following Stringer's development [16], we write for each species the continuity equation

$$\frac{\partial \rho_{1j}}{\partial t} + \rho_{0j} \nabla \cdot \mathbf{v}_{1j} = 0 \quad (3.38)$$

and the momentum equation

$$\rho_{0j} \frac{\partial \mathbf{v}_{1j}}{\partial t} = q_j n_{0j} (\mathbf{E} + \mathbf{v}_{1j} \times \mathbf{B}_0) - \nabla p_{1j}. \quad (3.39)$$

By adding the momentum equations for electrons and ions, we obtain the result

$$\rho_0 \frac{\partial \mathbf{v}}{\partial t} = \mathbf{j} \times \mathbf{B}_0 - \nabla p \quad (3.40)$$

where $\rho_0 = \rho_{0i} + \rho_{0e}$, $p = p_i + p_e$, and

$$\mathbf{v} = \frac{\rho_{0i}\mathbf{v}_{1i} + \rho_{0e}\mathbf{v}_{1e}}{\rho_{0i} + \rho_{0e}} \quad \mathbf{j} = n_0 e (\mathbf{v}_{1i} - \mathbf{v}_{1e}).$$

The other fluid equation is obtained by multiplying each of the momentum equations by q_j/m_j with $q_i = e$, $q_e = -e$, and adding, whereby the result may be expressed as

$$\frac{m_e}{n_0 e^2} \frac{\partial \mathbf{j}}{\partial t} = \mathbf{E} + \mathbf{v} \times \mathbf{B}_0 - \frac{m_i}{e} \frac{\partial \mathbf{v}}{\partial t} - \frac{1}{n_0 e} \nabla p_i \quad (3.41)$$

where terms of order m_e/m_i have been neglected.

We next assume that all first order quantities vary as $\exp(i\mathbf{k} \cdot \mathbf{r} - i\omega t)$ so that the Maxwell equations lead to the wave equation

$$k^2 \left(1 - \frac{\omega^2}{k^2 c^2} \right) \mathbf{E} - \mathbf{k}(\mathbf{k} \cdot \mathbf{E}) = i\omega \mu_0 \mathbf{j}. \quad (3.42)$$

Introducing the thermal speeds, defined by $c_j^2 \equiv \gamma_j \mathcal{K} T_j / m_j$, where γ_j is the ratio of specific heats for species j and comes from the equation of state (an alternative to truncating the moment equations), we may relate the pressure and density as $p_j = c_j^2 \rho_{1j}$ so the continuity equations give

$$p_i = \frac{n_0 m_i c_i^2 (\mathbf{k} \cdot \mathbf{v}_i)}{\omega} = \frac{g n_0 m_i c_s^2 (\mathbf{k} \cdot \mathbf{v}_i)}{\omega} \simeq \frac{g n_0 m_i c_s^2}{\omega} \mathbf{k} \cdot \mathbf{v} \quad (3.43)$$

$$\begin{aligned} p &= \frac{n_0 c_s^2 (m_i + m_e)}{\omega} \mathbf{k} \cdot \mathbf{v} - \frac{(1-g)c_s^2 m_i}{\omega e} \left(1 - \frac{c_i^2}{c_e^2} \right) \mathbf{k} \cdot \mathbf{j} \\ &\simeq \frac{n_0 c_s^2 m_i}{\omega} \mathbf{k} \cdot \mathbf{v} - \frac{(1-g)c_s^2 m_i}{\omega e} \mathbf{k} \cdot \mathbf{j} \end{aligned} \quad (3.44)$$

where

$$g \equiv \frac{\gamma_i T_i}{\gamma_i T_i + \gamma_e T_e} \quad c_s^2 \equiv \frac{\gamma_e \mathcal{K} T_e + \gamma_i \mathcal{K} T_i}{m_e + m_i} \quad (3.45)$$

and c_s is called the ion acoustic speed.

If we now solve equation (3.40) for \mathbf{v} , using equation (3.44) to eliminate p we obtain

$$\begin{aligned} \mathbf{v} &= \frac{1}{\omega^2 \mu_0 \rho_0} \left[k^2 \left(1 - \frac{\omega^2}{k^2 c^2} \right) (\mathbf{E} \times \mathbf{B}_0) - (\mathbf{k} \cdot \mathbf{E})(\mathbf{k} \times \mathbf{B}_0) \right] \\ &\quad + \frac{c_s^2}{\omega^2} (\mathbf{k} \cdot \mathbf{v}) \mathbf{k} - \frac{i \epsilon_0 (1-g) c_s^2}{n_0 e \omega} (\mathbf{k} \cdot \mathbf{E}) \mathbf{k} \end{aligned}$$

but if $\mathbf{v} = \mathbf{u} + \alpha(\mathbf{k} \cdot \mathbf{v})\mathbf{k}$, where \mathbf{u} is any vector, then $\mathbf{v} \equiv \mathbf{u} + \alpha(\mathbf{k} \cdot \mathbf{u})\mathbf{k}/(1 - \alpha k^2)$, so we may write

$$\begin{aligned}\mathbf{v} &= \frac{1}{\omega^2 \mu_0 \rho_0} \left[k^2 \left(1 + \frac{c_s^2 \mathbf{k} \cdot \mathbf{k}}{\omega^2 - k^2 c_s^2} \right) (\mathbf{E} \times \mathbf{B}_0) - (\mathbf{k} \cdot \mathbf{E})(\mathbf{k} \times \mathbf{B}_0) \right] \\ &\quad - \frac{i\omega\epsilon_0(1-g)c_s^2}{n_0e(\omega^2 - k^2 c_s^2)} (\mathbf{k} \cdot \mathbf{E})\mathbf{k}\end{aligned}\quad (3.46)$$

where we have neglected $\omega^2/k^2 c^2$ compared to unity. If we make this same approximation in equation (3.42), then $\mathbf{k} \cdot \mathbf{j} = 0$ and the last term in equation (3.46) disappears, with the result

$$\mathbf{v} = \frac{1}{\omega^2 \mu_0 \rho_0} \left[k^2 \left(1 + \frac{c_s^2 \mathbf{k} \cdot \mathbf{k}}{\omega^2 - k^2 c_s^2} \right) (\mathbf{E} \times \mathbf{B}_0) - (\mathbf{k} \cdot \mathbf{E})(\mathbf{k} \times \mathbf{B}_0) \right]. \quad (3.47)$$

We then use this equation for \mathbf{v} and equation (3.42) for \mathbf{j} and equation (3.43) for p_i in equation (3.41) to obtain

$$\begin{aligned}&\left(1 + \frac{k^2 c^2}{\omega_{pe}^2} - \frac{k^2 V_A^2}{\omega^2} \right) \mathbf{E} + \frac{iV_A^2}{\omega\omega_{ci}} [k^2 (\mathbf{E} \times \hat{\mathbf{e}}_z) - (\mathbf{k} \cdot \mathbf{E})(\mathbf{k} \times \hat{\mathbf{e}}_z)] \\ &+ \left(\frac{V_A^2}{\omega^2} - \frac{c^2}{\omega_{pe}^2} \right) (\mathbf{k} \cdot \mathbf{E})\mathbf{k} + \frac{V_A^2}{\omega^2} [k^2 E_z - (\mathbf{k} \cdot \mathbf{E})k_z] \hat{\mathbf{e}}_z \\ &- \frac{k^2 c_s^2}{\omega^2 - k^2 c_s^2} \left[\frac{V_A^2}{\omega^2} \mathbf{E} \cdot (\mathbf{k} \times \hat{\mathbf{e}}_z)(\mathbf{k} \times \hat{\mathbf{e}}_z) + \frac{iV_A^2(1-g)}{\omega\omega_{ci}} \mathbf{E} \cdot (\mathbf{k} \times \hat{\mathbf{e}}_z)\mathbf{k} \right] = 0\end{aligned}\quad (3.48)$$

where V_A is the Alfvén speed and where we have chosen $\mathbf{B}_0 = B_0 \hat{\mathbf{e}}_z$. We can now multiply equation (3.48) successively by \mathbf{k} , $\hat{\mathbf{e}}_z$, and $\mathbf{k} \times \hat{\mathbf{e}}_z$ to form the set of equations which if its determinant of coefficients is set to zero,

$$\begin{vmatrix} \frac{k^2 V_A^2}{\omega^2} k_z & -\frac{ik^2 V_A^2(\omega^2 - g k^2 c_s^2)}{\omega \omega_{ci} (\omega^2 - k^2 c_s^2)} & 1 - \frac{k_z^2 V_A^2}{\omega^2} \\ 1 + \frac{k^2 c^2}{\omega_{pe}^2} & -\frac{ik_z V_A^2(1-g) k^2 c_s^2}{\omega \omega_{ci} (\omega^2 - k^2 c_s^2)} & -\frac{k_z c^2}{\omega_{pe}^2} \\ -\frac{ik^2 V_A^2}{\omega \omega_{ci}} k_z & 1 + \frac{k^2 c^2}{\omega_{pe}^2} - \frac{k^2 V_A^2}{\omega^2 - k^2 c_s^2} \left(1 - \frac{k_z^2 c_s^2}{\omega^2} \right) & \frac{ik_z^2 V_A^2}{\omega \omega_{ci}} \end{vmatrix} = 0 \quad (3.49)$$

leads to the low frequency dispersion relation (LFDR),

$$\begin{aligned} & \left(1 - \frac{\omega^2}{k^2 V_A^2} - \frac{\omega^2}{\omega_{ce} \omega_{ci}} + \frac{k^2 c_s^2 \sin^2 \theta}{\omega^2 - k^2 c_s^2}\right) \left(\cos^2 \theta - \frac{\omega^2}{k^2 V_A^2} - \frac{\omega^2}{\omega_{ce} \omega_{ci}}\right) \\ &= \frac{\omega^2 \cos^2 \theta}{\omega_{ci}^2} \end{aligned} \quad (3.50)$$

where θ is the angle between the direction of propagation and the static magnetic field. This dispersion relation is equivalent to that given by Stringer [16] and Braginskii [17].

Problem 3.3.1. Fluid equations. Show that equation (3.41) may be written exactly as

$$\frac{m_e}{n_0 e^2 (1 + \epsilon)} \frac{\partial \mathbf{j}}{\partial t} = \mathbf{E} + \mathbf{v} \times \mathbf{B}_0 - \frac{m_i}{e} (1 - \epsilon) \frac{\partial \mathbf{v}}{\partial t} - \frac{1}{n_0 e (1 + \epsilon)} \nabla (p_i + \epsilon p_e)$$

where $\epsilon = m_e/m_i$, so the approximation includes neglecting ϵp_e compared to p_i as well as neglecting ϵ compared to unity.

Problem 3.3.2. Derivation of the low frequency dispersion relation. Show that equation (3.49) leads to equation (3.50).

3.3.2 Stringer diagrams of the LFDR

Plots of the LFDR which exhibit the character of the various waves in the low frequency region have been given by Stringer [16]. In these plots, ω/ω_{ci} is plotted against $k c_s / \omega_{ci}$ on logarithmic scales so that regions of constant phase velocity appear as straight lines.

3.3.2.1 Overdense case

Figure 3.1 shows the three roots of the LFDR (full curves) in a low β hydrogen plasma ($c_s^2/V_A^2 = \beta = 0.01$, $m_i/m_e = 1836$) which is overdense ($\omega_{pe} > \omega_{ce}$) such that $c/V_A = 10^3$. The general character for a broad range of angles is represented by this plot at $\theta = \pi/4$. Since equation (3.50) is cubic in ω^2 , there are only three branches. In the following sections, we shall investigate some of the special cases and transitions as well as the limits as $\theta \rightarrow 0$ or $\theta \rightarrow \pi/2$.

We can identify the R - X wave as the branch beginning at O_1 where it is a compressional Alfvén wave until A , after which it gradually changes slope until B where it enters the whistler wave region until it reaches C where it has a resonance. There is an apparent crossing of an ion acoustic branch at D . In the original Stringer diagrams, these branches do not cross, since the ion acoustic mode bends over and tends toward L while the first branch turns upward toward E , but they are not resolvable from equation (3.50).

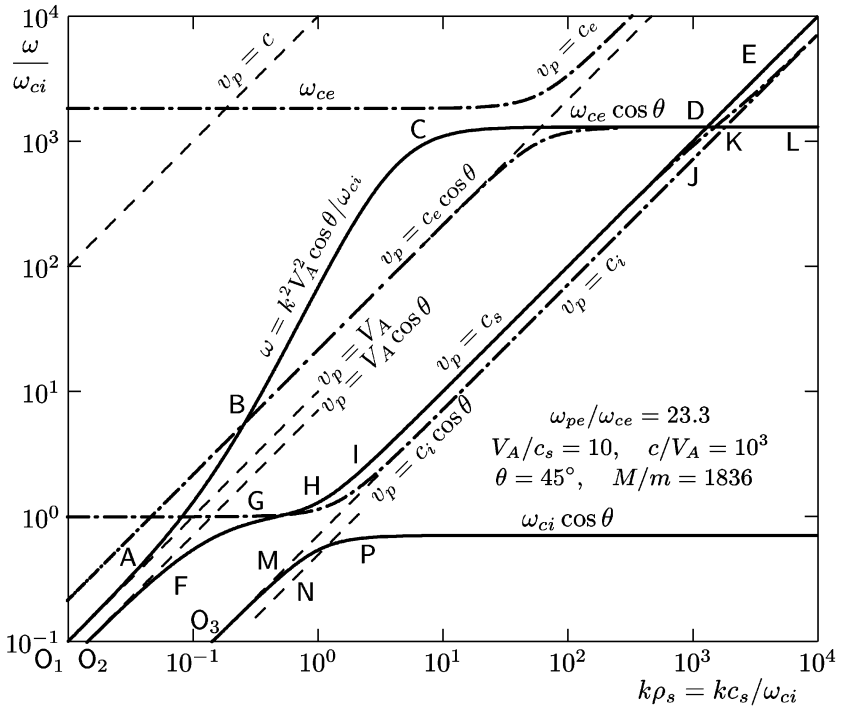


Figure 3.1. Dispersion curves for an overdense plasma. Full curves are from the low frequency dispersion relation, equation (3.50), while the dot-dash lines are from the warm plasma dispersion relation, equation (3.78).

The torsional Alfvén wave runs from O_2 to F where it approaches the ion cyclotron resonance at G , but for these parameters, it quickly couples to the ion-acoustic branch at H and is a simple ion-acoustic wave from I to D where it apparently crosses the first branch. The third branch that starts at O_3 does not occur in a cold plasma and is an ion sound wave below M and approaches a resonance beyond P .

The warm plasma dispersion relation (WPDR), given by equation (3.78) with both electron and ion terms, is shown in figures 3.1 and 3.2 by the dot-dash lines. The corresponding roots of the WPDR generally follow those of the LFDR, but several additional roots are shown (the WPDR with both ions and electrons is 15th order in ω^2 , but many roots are virtual double roots, so only seven are distinct in this case). One additional root begins near O_3 as a magnetized ion sound wave that experiences the resonance at the ion cyclotron frequency. Another begins at the ion cyclotron frequency and then becomes an unmagnetized ion sound wave. Yet another is a magnetized electron sound wave until it experiences the electron cyclotron resonance. The highest frequency branch shown begins at the electron

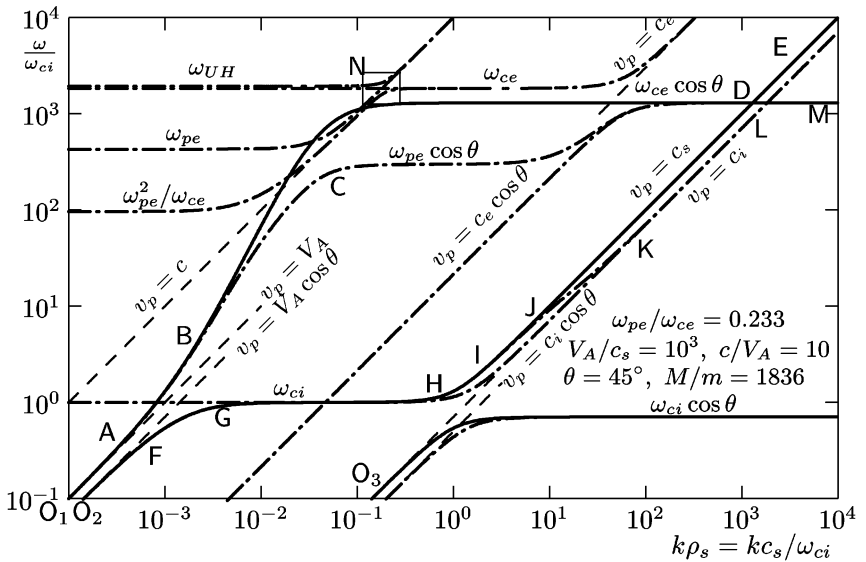


Figure 3.2. Dispersion curves for an underdense plasma. Full curves are from the low frequency dispersion relation, equation (3.50), while the dot-dash lines are from the warm plasma dispersion relation, equation (3.78). The box is magnified in [figure 3.3](#).

cyclotron frequency and then follows the electron sound wave. Three more higher modes are beyond the range of the figure.

One important difference between the LFDR and the WPDR is evident as one follows the LFDR (full curve) above I. As this root approaches J, the WPDR indicates a gradual transition from an ion acoustic wave to an ion sound wave, so the LFDR is unreliable in describing this high frequency region.

3.3.2.2 Underdense case

For an underdense plasma ($\omega_{pe} < \omega_{ce}$), the roots of both the LFDR and the WPDR are shown in figure 3.2 where now we have $c_s/V_A = 10^{-3}$ and $c/V_A = 10$. For this case, the first branch is little changed except that above B the LFDR indicates that the phase velocity exceeds c so the neglect of those terms of order ω/kc is not valid in this region. Here the LFDR continues to the electron cyclotron resonance while the WPDR indicates that this root bends over near C to follow the electron plasma frequency until it makes an additional pair of transitions, first to the magnetized electron sound wave and finally to the electron cyclotron frequency. The other significant deviation from the LFDR is the transition from an ion acoustic wave to an ion sound wave in the region between J and K which occurred at a much higher frequency in the overdense case of [figure 3.1](#). The figure is somewhat confusing near D, where it shows a

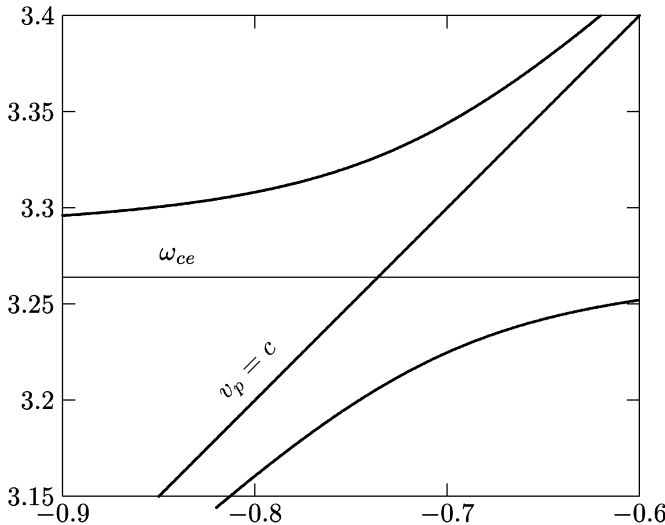


Figure 3.3. Magnified area near N from the warm plasma dispersion relation in [figure 3.2](#).

crossing of two LFDR roots, but as noted earlier, the rising branch has already moved over to the ion sound root, so no crossing occurs near D. The crossing does occur just to the right of D, and even the WPDR cannot distinguish between a crossing and a transition (there are five separate roots in this vicinity, and some are barely distinct, but no transition is evident even at high precision).

The third branch of the LFDR is basically unchanged from the overdense case, since the acoustic waves are relatively insensitive to changes in the density. The three additional high-frequency branches of the WPDR which were off scale for the overdense case are seen here. The highest frequency branch makes a transition to $v_p = c$ at N which is seen more clearly in figure 3.3 which is a magnification of the box in figure 3.2.

Two distinct roots are barely resolvable in the figure, the lower of which was also present in the overdense case. The two lower branches begin to asymptote to the velocity of light, but the upper one crosses the electron cyclotron resonance while the lower one experiences the resonance, finally making a transition to the electron sound wave.

Both [figures 3.1](#) and [3.2](#) are similar to figures given by Stringer [16], but differ in some important ways. Some transitions which occur slowly in the original diagrams occur much more rapidly here or not at all, so the nature of the transitions is less evident. Several transitions in the original figures are not due to the equations given here.

The significance of a crossing of two roots as opposed to a transition with roots avoiding one another is that a crossing indicates there is no coupling

between the waves in that region, while a transition indicates there is coupling. A purely longitudinal wave has no coupling to a purely transverse wave, so the corresponding roots may cross, but even with a little mixture, a transition will normally occur. The distinction is sharp in a uniform plasma, but with even small inhomogeneities, the distinction becomes fuzzy, since partial transmission (crossing or tunneling, see section 6.3) and partial conversion (transition or mode conversion) is possible unless strong absorption occurs in the coupling region. For the indicated crossings and transitions, however, one should recall that when the phase velocity is near a thermal velocity, absorption is likely and kinetic theory is required.

3.3.2.3 Electrostatic limit

When $k\lambda_{De} \geq 1$, equation (3.50) is inaccurate because of the neglect of space charge effects through the neglect of the $\mathbf{k} \cdot \mathbf{j}$ term. We could include this term through the charge continuity equation, whereby $\mathbf{k} \cdot \mathbf{j} = \omega\rho = \omega e(n_{1i} - n_{1e})$, but it is easier to use the electrostatic dispersion relation (ESDR) where the electric field is derived from a scalar potential. The large- k limit, or low phase velocity limit, leads us to the sufficient condition for the electrostatic approximation of equation (2.110) which we found in [chapter 2](#).

For this analysis, we may write the momentum equation for each species as

$$-i\omega m_j \mathbf{v}_j = q_j \left[-ik \left(\frac{p_j}{n_0 q_j} + \varphi \right) + \mathbf{v}_j \times \mathbf{B}_0 \right] \quad (3.51)$$

where φ is the scalar potential. This may be solved for the velocity components with $\mathbf{B}_0 = B_0 \hat{\mathbf{e}}_z$ such that

$$\mathbf{k} \cdot \mathbf{v}_j = \frac{1}{\omega m_j} \left(\frac{p_j}{n_0} + q_j \varphi \right) \left[\frac{k_x^2 + k_y^2}{1 - \omega_{cj}^2/\omega^2} + k_z^2 \right]. \quad (3.52)$$

Then using the continuity equation and gas law ($p_j = c_j^2 \rho_{1j}$) for each species, this may be written as

$$\mathbf{k} \cdot \mathbf{v}_j \left[1 - c_j^2 \left(\frac{k_\perp^2}{\omega^2 - \omega_{cj}^2} + \frac{k_z^2}{\omega^2} \right) \right] = \frac{\omega q_j \varphi}{m_j} \left(\frac{k_\perp^2}{\omega^2 - \omega_{cj}^2} + \frac{k_z^2}{\omega^2} \right). \quad (3.53)$$

We may combine these expressions for each species through Poisson's equation

$$k^2 \varphi = \frac{n_0 e}{\omega \epsilon_0} (\mathbf{k} \cdot \mathbf{v}_i - \mathbf{k} \cdot \mathbf{v}_e)$$

and the result may be written as

$$1 + \frac{1}{k^2 \lambda_{Di}^2} + \frac{1}{k^2 \lambda_{De}^2} = \frac{1}{k^2 \lambda_{Di}^2 \left[1 - k^2 c_i^2 \left(\frac{\sin^2 \theta}{\omega^2 - \omega_{ci}^2} + \frac{\cos^2 \theta}{\omega^2} \right) \right]}$$

$$+ \frac{1}{k^2 \lambda_{De}^2 \left[1 - k^2 c_e^2 \left(\frac{\sin^2 \theta}{\omega^2 - \omega_{ce}^2} + \frac{\cos^2 \theta}{\omega^2} \right) \right]} \quad (3.54)$$

where $\lambda_{Dj} = c_j / \omega_{pj}$. This dispersion relation is quartic in ω^2 , but one root is the electron plasma wave and not a low frequency wave, so as long as $\omega \ll kc_e$, we may neglect the last term and reduce the dispersion relation to a quadratic in ω^2 . This reduced dispersion relation may be used to plot the regions beyond D and H in both [figure 3.1](#) and [figure 3.2](#), but only the LFDR and the WPDR are actually plotted.

Problem 3.3.3. Electrostatic dispersion relation. Fill in the steps leading to equation (3.54).

3.3.3 Approximate dispersion relations and transitions

The LFDR, equation (3.50), is cubic in ω^2 , but by dividing up the parameter space into several regions, one root can be eliminated or factored in each region, reducing it to a quadratic, where we can more easily identify the properties of the solutions.

3.3.3.1 MHD Region

For the very low frequency case, where $\omega \ll \omega_{ci}$, the right-hand side of equation (3.50) may be neglected along with $\omega^2/\omega_{ce}\omega_{ci}$, so it reduces to

$$\left(1 - \frac{\omega^2}{k^2 V_A^2} + \frac{k^2 c_s^2 \sin^2 \theta}{\omega^2 - k^2 c_s^2} \right) \left(\cos^2 \theta - \frac{\omega^2}{k^2 V_A^2} \right) = 0. \quad (3.55)$$

The second factor gives the cold torsional wave root

$$\omega^2 = k^2 V_A^2 \cos^2 \theta \quad (3.56)$$

which is unaffected by the finite temperature terms. This branch is plotted from O₂ to F in figures 3.1 and 3.2 where it reaches a transition at ω_{ci} .

The remaining factor leads to the quadratic

$$\omega^4 - k^2 (V_A^2 + c_s^2) \omega^2 + k^4 V_A^2 c_s^2 \cos^2 \theta = 0$$

with approximate roots (for $c_s \ll V_A$)

$$\omega^2 = k^2 (V_A^2 + c_s^2 \sin^2 \theta) \quad (3.57)$$

and

$$\omega^2 = k^2 c_s^2 \cos^2 \theta. \quad (3.58)$$

This last root is a sound wave whose phase velocity is equal to the ion thermal speed as it propagates along the magnetic field and does not propagate across the

magnetic field (a dumbbell lemniscoid). It follows path O_3 to M in figure 3.1 and then approaches the resonance.

The first root, from equation (3.57), is more interesting, since now the cold compressional wave is coupled to the ion acoustic wave. For this reason, this wave that begins at O_1 is often called the magnetoacoustic wave or the magnetosonic wave since it is coupled to acoustic modes in the low frequency limit. It is clear from the dispersion relation that the magnetoacoustic wave is equivalent to the cold plasma compressional Alfvén wave when $V_A \gg c_s$, and that the phase and group velocities are parallel in that limit, but when V_A is comparable to c_s , then the phase and group velocities are no longer parallel, since the acoustic wave component of the dispersion relation tends to guide the wave away from the direction of the magnetic field. This same branch is thus partially guided across the field at very low frequencies if acoustic effects are important, isotropic if acoustic effects are negligible, and then at intermediate frequencies is guided along the field as the whistler wave beyond B , and carries a variety of names, depending on the approximation ($V_A \gg c_s$ or $V_A \ll c_s$), the frequency ($\omega \ll \omega_{ci}$ or $\omega_{ci} \ll \omega \ll \omega_{ce}$), and the angle (R -wave for $\theta = 0$, X -wave for $\theta = \pi/2$ up to ω_{LH}).

Problem 3.3.4. Magnetoacoustic wave.

- (i) Find an expression for $\tan \alpha$ where α is the angle between the phase velocity and the group velocity for the magnetoacoustic wave described by equation (3.57).
- (ii) Show that $\tan(\theta + \alpha) = (1 + c_s^2/V_A^2) \tan \theta$.
- (iii) Sketch α versus θ for $0 \leq \theta \leq \pi/2$ for $c_s = 2V_A$.
- (iv) For what angle θ_m is the ratio of the group velocity to the phase velocity maximum (as a function of c_s/V_A). Evaluate this angle for $c_s = 2V_A$.

3.3.3.2 High phase velocity region

In this region, we assume $v_p > \sqrt{V_A c_s}$ so we may neglect the $k^2 c_s^2/\omega^2$ terms compared to unity, with the resulting simpler quadratic dispersion relation,

$$\left(1 - \frac{\omega^2}{k^2 V_A^2} - \frac{\omega^2}{\omega_{ce} \omega_{ci}}\right) \left(\cos^2 \theta - \frac{\omega^2}{k^2 V_A^2} - \frac{\omega^2}{\omega_{ce} \omega_{ci}}\right) = \frac{\omega^2}{\omega_{ci}^2} \cos^2 \theta. \quad (3.59)$$

If we introduce the quantity,

$$\frac{1}{R} = \frac{\omega_{ci}^2}{k^2 V_A^2} \left(1 + \frac{k^2 c^2}{\omega_{pe}^2}\right) = \frac{\omega_{ci}^2}{k^2 V_A^2} + \frac{m_e}{m_i}$$

then the roots of equation (3.59) may be expressed as

$$\omega^2 = \frac{1}{2} R \omega_{ci}^2 \left[1 + \cos^2 \theta (1 + R) \pm \sqrt{[1 + \cos^2 \theta (1 + R)]^2 - 4 \cos^2 \theta}\right] \quad (3.60)$$

so the **A**–**B** transition occurs near where $R \cos^2 \theta \simeq 1$, or approximating R by $k^2 V_A^2 / \omega_{ci}^2$, it is near

$$kV_A \simeq \omega_{ci} \sec \theta.$$

Since R becomes large as we move up the curve beyond **B**, we may approximate one root by

$$\omega \simeq \omega_{ci} \sqrt{R(1 + R \cos^2 \theta)} \quad (3.61)$$

that for $k \ll \omega_{pe}/c$ leads to

$$\omega \simeq R\omega_{ci} \cos \theta \simeq \frac{k^2 V_A^2}{\omega_{ci}} \cos \theta \quad (3.62)$$

which is the same as equation (2.78), the whistler dispersion relation. The limits of validity for this case are that $\omega_{ci} \sec \theta / V_A \ll k \ll \omega_{pe}/c$, where the first ensures that we are above the lower transition, and the second validates our approximation for R . For the limit where $k \gg \omega_{pe}/c$, then $R \simeq m_i/m_e$, and the dispersion relation simplifies to

$$\omega \simeq \omega_{ce} \cos \theta \quad (3.63)$$

for $\cos^2 \theta > m_e/m_i$. This dispersion relation is independent of k , and represents a resonance as $k \rightarrow \infty$. Of course, as k gets very large, we leave the region of validity of equation (3.59) as we move beyond **C**. Just as the LFDR failed in the underdense case of figure 3.2, so this approximate analysis of the transition fails in the underdense case.

The second root in this region is $\omega \simeq \omega_{ci}$, which is the ion cyclotron resonance for the torsional branch and is plotted from **G** to **H** in the diagrams.

3.3.3.3 Low phase velocity, low frequency region

In this region, we take $v_p < \sqrt{V_A c_s}$ but also choose $\omega < \sqrt{\omega_{ce} \omega_{ci}} \cos \theta$ so that we may neglect both $\omega^2/k^2 V_A^2$ and $\omega^2/\omega_{ce} \omega_{ci}$ ($R \rightarrow \infty$ approx.) in equation (3.50) to obtain

$$\omega^4 - (k^2 c_s^2 + \omega_{ci}^2) \omega^2 + k^2 c_s^2 \omega_{ci}^2 \cos^2 \theta = 0. \quad (3.64)$$

The roots are given by

$$\omega^2 = \frac{1}{2} \left[k^2 c_s^2 + \omega_{ci}^2 \pm \sqrt{(k^2 c_s^2 + \omega_{ci}^2)^2 - 4k^2 c_s^2 \omega_{ci}^2 \cos^2 \theta} \right]$$

and the lower root, which we designate the electron-acoustic branch, may be represented by

$$\omega \simeq \frac{k c_s \cos \theta}{\sqrt{1 + k^2 \rho_s^2}} \simeq \begin{cases} k c_s \cos \theta & k \rho_s \ll 1 \\ \omega_{ci} \cos \theta & k \rho_s \gg 1 \end{cases} \quad (3.65)$$

where $\rho_s = c_s/\omega_{ci}$ is almost the ion Larmor radius, and where the first expression is valid between O₃ and M and the second beyond M in figure 3.1 and the transition occurs near $k\rho_s \sim 1$. The phase velocity below M is numerically equal to c_i , but this is an *accident*, since c_i and $c_s \cos \theta$ (the proper expression for the phase velocity of this lower curve) are equivalent when $\theta = 45^\circ$ and $T_e = T_i$ as assumed here. For different temperatures or a different angle, the two phase velocities would not coincide.

The upper root is

$$\omega^2 = \omega_{ci}^2 + k^2 c_s^2 \quad (3.66)$$

which gives the ion cyclotron resonance for $kc_s \ll \omega_{ci}$, the region between G and H for $kc_s \sim \omega_{ci}$, and the transition to the ion-acoustic branch near H which it follows from I to D, where $kc_s \gg \omega_{ci}$ and $v_p = c_s$.

3.3.3.4 Low phase velocity, high frequency region

In this region, we also take $v_p < \sqrt{V_A c_s}$ but now choose $\omega > \sqrt{\omega_{ce}\omega_{ci}} \cos \theta$ so that we may neglect the $\cos^2 \theta$ term in the second factor of equation (3.50). Then we may write the quadratic as

$$\omega^4 - [k^2 c_s^2 + \omega_{ci}^2 R(1 + R \cos^2 \theta)]\omega^2 + k^2 c_s^2 \omega_{ci}^2 R(1 + R) \cos^2 \theta = 0 \quad (3.67)$$

with roots

$$\omega^2 = \frac{1}{2} \omega_{ci}^2 R^2 \cos^2 \theta \left\{ 1 + \frac{k^2 \rho_s^2 \sec^2 \theta}{R^2} + \frac{\sec^2 \theta}{R} \right. \\ \left. \pm \left[\left(1 - \frac{k^2 \rho_s^2 \sec^2 \theta}{R^2} + \frac{\sec^2 \theta}{R} \right)^2 + \frac{4k^2 \rho_s^2 \sec^2 \theta \tan^2 \theta}{R^3} \right]^{1/2} \right\} \quad (3.68)$$

The higher root of equation (3.68) is either the whistler dispersion relation of equation (3.62) with $kc \ll \omega_{pe}$ or the cyclotron resonance of equation (3.63) with $kc \gg \omega_{pe}$. In order to find the higher frequency transitions for this branch, we need the ESDR, equation (3.54).

The lower root gives $\omega = kc_s$ to lowest order unless $kc_s \gg \omega_{ce} \cos \theta$, where again we need to examine the ESDR for large k .

3.3.3.5 Electrostatic region

For the region which has both high frequency and large k , we may neglect ω_{ci} compared to ω and also take $\omega \ll kc_e$ (except where $\omega \simeq \omega_{ce} \cos \theta$). In this case equation (3.54) reduces to

$$\frac{\omega^2}{k^2 \lambda_{Di}^2 (\omega^2 - k^2 c_i^2)} = 1 + \frac{1}{k^2 (\lambda_{Di}^2 + \lambda_{De}^2)} \quad (3.69)$$

with solution

$$\omega^2 = k^2 c_i^2 \left[1 + \frac{T_e}{T_i(1 + k^2 \lambda_{De}^2)} \right]. \quad (3.70)$$

This gives $\omega = kc_s$ for $k\lambda_{De} \ll 1$ and $\omega = kc_i$ for $k\lambda_{De} \gg 1$. The transition occurs when $k\rho_s \sim c/V_A$ which is equivalent to $k\lambda_{De} = 1$. This transition is evident in both figure 3.1 with $k\rho_s = c/V_A = 10^3$ and figure 3.2 with $k\rho_s = c/V_A = 10$. This transition is missing from the LFDR, but evident from either the ESDR or the WPDR.

The other root behaves as $\omega = \omega_{ce} \cos \theta$ as $k \rightarrow \infty$, which is the K to L $\rightarrow \infty$ branch in figure 3.1. This may be seen by multiplying equation (3.54) by $k^2 \lambda_{De}^2$ and letting $k^2 \rightarrow \infty$ (holding ω fixed) whereupon the left-hand side tends towards infinity as $k^2 \lambda_{De}^2$, the first term on the right tends toward zero, and the second term also tends towards zero unless the denominator vanishes, so we have

$$\omega^2 \simeq \omega_{ce}^2 \cos^2 \theta - \frac{\omega^2(\omega_{ce}^2 - \omega^2)}{k^2 c_e^2} \simeq \omega_{ce}^2 \cos^2 \theta \left[1 - \frac{\omega_{ce}^2 \sin^2 \theta}{k^2 c_e^2} \right]. \quad (3.71)$$

3.3.4 Parallel and perpendicular propagation

The general character of the waves does not change greatly from our previous results until $\theta \rightarrow 0$ or $\theta \rightarrow \pi/2$. As the angle of propagation approaches zero, the only significant change is that the transition regions become more localized and the transitions become sharper so that the coupling between the cold plasma waves and the thermal waves occurs only when the phase velocity is very close to one of the acoustic speeds. At $\theta = 0$, the R- and L-waves are decoupled from thermal motions, but the plasma wave (a high frequency mode) remains coupled.

As the angle $\theta \rightarrow \pi/2$, the lowest frequency branch is essentially unchanged except that the resonant frequency $\omega = \omega_{ci} \cos \theta \rightarrow 0$ as $\cos \theta \rightarrow 0$.

The intermediate frequency branch, however, which is the shear Alfvén wave at the low frequency end with $\omega/k = V_A \cos \theta$ never experiences the ion cyclotron resonance when $V_A \cos \theta < c_s$ and propagates relatively smoothly up to its resonance at $\omega = \omega_{ce} \cos \theta \ll \omega_{ce}$ where it makes a transition to resonance.

The higher frequency branch, which is the magnetoacoustic branch at low frequencies, propagates at the Alfvén speed until it reaches the greater of $\omega_{ce} \cos \theta$ or the lower hybrid frequency where it makes a transition over to the ion acoustic wave with $v_p = c_s$, or in the extreme case, to c_i .

3.3.5 High frequency waves

While some of the branches in the dispersion relations of the preceding section were followed to higher frequency, there are several more branches which were excluded in the LFDR of equation (3.50). The ESDR of equation (3.54) did not use any low frequency approximation, however, so it continues to be valid at high frequencies whenever the electrostatic approximation is appropriate.

3.3.5.1 The warm plasma dispersion relation

For high frequencies, we may use the warm plasma dispersion relation (WPDR) neglecting ion motions entirely. We do this by effectively letting $m_i \rightarrow \infty$, which is usually called the neglect of electron inertia. Using only the fluid equations for electrons and deleting the subscript denoting the species (except for c_e), the linearized time and space harmonic fluid equations are

$$-\mathrm{i}\omega\rho_1 + \rho_0\mathbf{i}\mathbf{k} \cdot \mathbf{v}_1 = 0 \quad (3.72)$$

and

$$-\mathrm{i}\omega\rho_0\mathbf{v}_1 = -en_0(\mathbf{E} + \mathbf{v}_1 \times \mathbf{B}_0) - \mathbf{i}\mathbf{k}p_1 \quad (3.73)$$

along with the equation of state, $p_1 = c_e^2\rho_1$. These may be combined to give an expression for the velocity as

$$\mathbf{v}_1 = \frac{e}{\mathrm{i}\omega m}(\mathbf{E} + \mathbf{v}_1 \times \mathbf{B}_0) + \frac{c_e^2}{\omega^2}(\mathbf{k} \cdot \mathbf{v}_1)\mathbf{k}. \quad (3.74)$$

Solving for the components of \mathbf{v}_1 , we find, after some tedious algebra,

$$\begin{aligned} v_{1x} &= \frac{e}{\mathrm{i}\omega D}[(\omega E_x - \mathrm{i}\omega_{ce}E_y)(\omega^2 - k^2c_e^2\cos^2\theta) + \omega E_zk^2c_e^2\cos\theta\sin\theta] \\ v_{1y} &= \frac{e}{\mathrm{i}\omega D}[\omega E_y(\omega^2 - k^2c_e^2) + \mathrm{i}\omega_{ce}E_x(\omega^2 - k^2c_e^2\cos^2\theta) \\ &\quad + \mathrm{i}\omega_{ce}E_zk^2c_e^2\cos\theta\sin\theta] \\ v_{1z} &= \frac{e}{\mathrm{i}\omega D}[\omega E_z(\omega^2 - \omega_{ce}^2 - k^2c_e^2\sin^2\theta) + k^2c_e^2\cos\theta\sin\theta(\omega E_x - \mathrm{i}\omega_{ce}E_y)] \end{aligned}$$

where $D = \omega^2(\omega^2 - k^2c_e^2) - \omega_{ce}^2(\omega^2 - k^2c_e^2\cos^2\theta)$. Using $\mathbf{j} = -n_0e\mathbf{v}_1 = \boldsymbol{\sigma} \cdot \mathbf{E}$ and $\mathbf{K} = \mathbf{I} - \boldsymbol{\sigma}/\mathrm{i}\omega\epsilon_0$, the dielectric tensor has the form

$$\mathbf{K} = \begin{pmatrix} K_{xx} & K_{xy} & K_{xz} \\ -K_{xy} & K_{yy} & K_{yz} \\ K_{xz} & -K_{yz} & K_{zz} \end{pmatrix} \quad (3.75)$$

where

$$\begin{aligned} K_{xx} &= 1 - \frac{\omega_{pe}^2(\omega^2 - k^2c_e^2\cos^2\theta)}{D} \\ K_{xy} &= \frac{\mathrm{i}\omega_{ce}\omega_{pe}^2(\omega^2 - k^2c_e^2\cos^2\theta)}{\omega D} \\ K_{xz} &= -\frac{\omega_{pe}^2k^2c_e^2\cos\theta\sin\theta}{D} \\ K_{yy} &= 1 - \frac{\omega_{pe}^2(\omega^2 - k^2c_e^2)}{D} \end{aligned}$$

$$K_{yz} = -\frac{i\omega_{ce}\omega_{pe}^2 k^2 c_e^2 \cos \theta \sin \theta}{\omega D}$$

$$K_{zz} = -\frac{\omega_{pe}^2 (\omega^2 - \omega_{ce}^2 - k^2 c_e^2 \sin^2 \theta)}{D}. \quad (3.76)$$

These dielectric tensor elements may easily be extended to include ions (letting $\omega_{ce} \rightarrow -\omega_{ci}$) by making a sum over species, but are very complicated for general use, except that they are valid in both electrostatic and electromagnetic regions. For cases where more than one ion species is involved, however, both the one-fluid model and the WPDR are very complicated with simple dispersion relations difficult to obtain, but the straightforwardness of the dielectric tensor method may be preferred for numerical work. In [figure 3.1](#), both ion and electron terms are included for comparison with the LFDR using the WPDR, equation (3.78), indicated by the dot-dash lines.

With this dielectric tensor, which has all nine components (although only six are independent), the wave equation of equation (2.20) generalizes to

$$\begin{pmatrix} K_{xx} - n^2 \cos^2 \theta & K_{xy} & n^2 \cos \theta \sin \theta + K_{xz} \\ -K_{xy} & K_{yy} - n^2 & K_{yz} \\ n^2 \cos \theta \sin \theta + K_{xz} & -K_{yz} & K_{zz} - n^2 \sin^2 \theta \end{pmatrix} \begin{pmatrix} E_x \\ E_y \\ E_z \end{pmatrix} = 0 \quad (3.77)$$

where $n = kc/\omega$. The determinant of coefficients of equation (3.77) gives the WPDR, which is considerably more complicated than the CPDR, but may be written as

$$[(K_{xx} - n^2 \cos^2 \theta)(K_{yy} - n^2) + K_{xy}^2]K_{zz} - n^2 \sin^2 \theta [K_{xx}(K_{yy} - n^2) + K_{xy}^2]$$

$$+ (2n^2 \cos \theta \sin \theta + K_{xz})[K_{xy}K_{yz} - K_{xz}(K_{yy} - n^2)]$$

$$+ K_{xy}K_{yz}K_{xz} + K_{yz}^2(K_{xx} - n^2 \cos^2 \theta) = 0. \quad (3.78)$$

This WPDR is very formidable, but simplifies in certain limits. Its general form is identical to that of the hot plasma dispersion relation (HPDR) which includes finite temperature effects through kinetic theory and is the subject of [chapter 4](#).

Problem 3.3.5. Derivation of the HFDR. Fill in the steps from equation (3.72) to equations (3.76) and (3.78).

3.3.5.2 Parallel propagation

When $\theta = 0$, the tensor elements simplify greatly, such that $K_{xx} = K_{yy} = S$, $K_{xy} = -iD$, $K_{xz} = K_{yz} = 0$, so the L- and R-waves are unchanged from the cold plasma results (with $m_i \rightarrow \infty$ for the high frequency cases described here) by the fluid pressure terms. There is only one change, namely that

$$K_{zz} = 1 - \frac{\omega_{pe}^2}{\omega^2 - k^2 c_e^2} \quad (3.79)$$

so the $P = 0$ root leads now to

$$\omega^2 = \omega_{pe}^2 + k^2 c_e^2 \quad (3.80)$$

which is equivalent to the BGDR for plasma waves if we take $\gamma_e = 3$ and the thermal speed is small compared to the phase velocity.

3.3.5.3 Perpendicular propagation

When $\theta \rightarrow \pi/2$, we have $K_{xz} = K_{yz} = 0$ and now $K_{zz} = P$ so the ordinary wave is unchanged, but

$$\begin{aligned} K_{xx} &= 1 - \frac{\omega_{pe}^2}{\omega^2 - \omega_{ce}^2 - k^2 c_e^2} \\ K_{yy} &= 1 - \frac{\omega_{pe}^2 (\omega^2 - k^2 c_e^2)}{\omega (\omega^2 - \omega_{ce}^2 - k^2 c_e^2)} \\ K_{xy} &= \frac{i \omega_{ce} \omega_{pe}^2}{\omega (\omega^2 - \omega_{ce}^2 - k^2 c_e^2)} \end{aligned} \quad (3.81)$$

so that the extraordinary wave (X -wave) is now given by

$$n_X^2 = \frac{K_{xx} K_{yy} + K_{xy}^2}{K_{xx}} = \frac{(\omega^2 - \omega_{pe}^2)(\omega^2 - \omega_e^2 - k^2 c_e^2) - \omega_{pe}^2 \omega_{ce}^2}{\omega^2 (\omega^2 - \omega_e^2 - k^2 c_e^2)} \quad (3.82)$$

where the upper hybrid resonance has been eliminated by the thermal term. The cutoff is unaffected by the thermal terms, so equations (2.42)–(2.44) are still valid (for the higher frequency cutoff). The upper branch of the extraordinary wave then propagates from its cutoff up to the upper hybrid resonance as in the cold plasma X -wave, but when it reaches $v_p \sim k c_e$, it couples to the electron sound wave.

3.3.5.4 Arbitrary angle

The general WPDR is very complicated, but it may be approximated in certain regions. The cutoffs, of course, do not depend on the angle. Away from the cutoffs, we may approximate the high frequency branch of the $R-X$ wave by

$$\omega^2 \simeq \omega_{ce}^2 \left(1 + \frac{\omega_{pe}^2 (1 + \cos^2 \theta)}{\omega_{ce}^2 - \omega_{pe}^2 - k^2 c_e^2} \right) + k^2 c_e^2 \sin^2 \theta \quad (3.83)$$

provided the denominator is not too small. The $O-P$ wave branch may be approximated by a similar expression

$$\omega^2 \simeq \omega_{pe}^2 \left(1 + \frac{\omega_{ce}^2 \sin^2 \theta}{\omega_{pe}^2 - \omega_{ce}^2 + k^2 c_e^2 \sin^2 \theta} \right) + k^2 c_e^2 \sin^2 \theta + k^2 c_e^2 \cos^2 \theta. \quad (3.84)$$

These are sketched for an overdense plasma in [figure 3.1](#) and for an underdense plasma in [figure 3.2](#).

3.3.6 Summary of fluid waves

The differences between the cold plasma waves and the fluid plasma waves may now be seen to be due to the coupling of acoustic branches with the cold plasma waves. The L , R , and X waves simply tend towards infinity as they approach resonance, and the new feature is an acoustic wave with much lower phase velocity than the Alfvén wave which would cross these resonances if there were no coupling. The coupling, however, prevents a simple crossing and instead takes each resonant cold wave and converts it to an acoustic wave, and the original acoustic wave then converts to the resonant wave. Whether the acoustic wave propagates at the ion acoustic speed c_s or the ion thermal speed (or for the high frequency branches, the electron thermal speed) is less obvious, and depends on the details of the dispersion relation.

In a homogeneous plasma, these waves are all linearly independent and energy does not couple from one branch to another in the transition regions. In inhomogeneous plasmas, however, where a transition region is approached in space, the waves are no longer independent and energy is coupled from one branch to another. For example, wave energy originating on branch O_3 , the low-frequency ion acoustic branch, may couple some energy across from L to I by tunneling across the transition zone, and the remaining energy proceeds along the normal branch towards M . We will discuss this kind of coupling in [chapter 6](#) where it is called linear mode conversion. One should not presume that because the homogeneous solutions are no longer linearly independent that linearly independent solutions no longer occur, but that the linearly independent solutions are now composed of more than one branch, and the branching ratios depend on which way the wave propagates.

We also note that each of the transition regions violates the conditions for the validity of the fluid equations, except for the ion-acoustic-wave transitions with $T_e \gg T_i$, since the moment expansion depended on the phase velocity being large compared to the thermal speed. Thus we would expect significant modifications of the dispersion relation near these regions from a full kinetic analysis, and we shall see in [chapter 4](#) that both collisionless damping and modification of the dispersion do indeed occur when thermal effects are kept to higher order. The value of the fluid equations thus lies more in their ability to indicate the kinds of cold plasma wave–acoustic wave couplings that do occur than in an accurate description of all the thermal effects.

3.4 Partially ionized plasmas and collisions

For partially ionized plasmas, two things must be considered in addition to those things characteristic of the fully ionized, collisionless plasmas. First, in a partially ionized plasma, ionizing collisions and charge-transfer collisions give rise to creation and annihilation processes for individual species, so we need the creation

rate Z_j for each species, noting that conservation of particles requires

$$\sum_j Z_j = 0. \quad (3.85)$$

Secondly, the neutral particles are neither influenced by the electric and magnetic fields, nor do they contribute to them, so they only interact through collisions among themselves and with other species of the plasma. This means we must include a collision frequency for each species with every other species, and as they exchange momentum among themselves, we must conserve the total momentum. Thus we require

$$\sum_{j,i} \rho_j \langle v_{ji} (\mathbf{v}_i - \mathbf{v}_j) \rangle = 0 \quad (3.86)$$

where v_{ji} is the collision frequency for particles of species j with particles of species i (the reciprocal of the mean time for a particle of species j to make a collision with a particle of species i). These depend on velocity and in general, $v_{ji} \neq v_{ij}$.

3.4.1 Neutral collisions

3.4.1.1 Ion neutral charge exchange collisions

If we consider a case where the principal collisions are between ions and neutrals, and consider only charge exchange collisions, which act like a head-on collision between particles of equal mass, then the average in equation (3.86) is trivial and the brackets may be dropped. We need the equation of motion for the neutrals, which we take as the linearized momentum equation (neglecting neutral pressure gradients) with collisional momentum transfer as

$$\rho_{n0} \frac{\partial \mathbf{v}_n}{\partial t} = \rho_{n0} (\mathbf{v}_i - \mathbf{v}_n) v_{ni}. \quad (3.87)$$

For harmonic time dependence, this may be solved for \mathbf{v}_n as

$$\mathbf{v}_n = \mathbf{v}_i / (1 - i\omega\tau_{ni}) \quad (3.88)$$

where τ_{ni} is the reciprocal of v_{ni} . Then using the equation of motion for the ions with its collision term (again with harmonic time dependence)

$$-i\omega\rho_{i0}\mathbf{v}_i = e n_{i0}(\mathbf{E} + \mathbf{v}_i \times \mathbf{B}_0) - \nabla p_i + \rho_{i0}(\mathbf{v}_n - \mathbf{v}_i)v_{in} \quad (3.89)$$

where $v_{in} \neq v_{ni}$, but $\rho_n v_{ni} = \rho_i v_{in}$ to conserve momentum. Using this relationship and equation (3.88), and assuming $m_n = m_i$, the collision term may be combined with the left-hand term of equation (3.89) with the result written as

$$-i\omega\rho_{i0}^* \mathbf{v}_i = e n_{i0}(\mathbf{E} + \mathbf{v}_i \times \mathbf{B}_0) - \nabla p_i \quad (3.90)$$

where

$$\rho_{i0}^* = \rho_{i0} \left[1 + \frac{n_{n0}}{n_{i0}(1 - i\omega\tau_{ni})} \right]. \quad (3.91)$$

We can see from equation (3.91) that this pseudo-ion mass density reduces to the usual ion mass density as $v_{ni} \rightarrow 0$ ($\tau_{ni} \rightarrow \infty$), but becomes equal to the total ion density plus neutral density either at low frequency or high collisionality. This is due to the fact that when collisions are very frequent, the neutrals are dragged along with the ions. In between, the pseudo-ion mass density is complex and leads to damping of the wave motion. The form of the dispersion relation is unchanged if one simply uses a pseudo-ion cyclotron frequency and a pseudo-ion plasma frequency.

3.4.1.2 Electron–neutral collisions

For electron–neutral collisions, the neutral velocities may always be neglected, so the electron momentum equation uses the Krook model of equation (1.65) with the momentum equation becoming

$$\rho_e \left[\frac{\partial \mathbf{v}_e}{\partial t} + \mathbf{v}_e \cdot \nabla \mathbf{v}_e \right] = -en_e(\mathbf{E} + \mathbf{v}_e \times \mathbf{B}) - \nabla p_e - \rho_e \mathbf{v}_e v_{en}. \quad (3.92)$$

Using harmonic time dependence in the linearized equation, this may be written as

$$(v - i\omega)\rho_e \mathbf{v}_e = -en_e(\mathbf{E} + \mathbf{v}_e \times \mathbf{B}) - \nabla p_e \quad (3.93)$$

where we have dropped the subscript on the collision frequency as there is only one involved. It would appear that one could simply replace $\omega \rightarrow \omega + iv$ in the cold plasma equations to include collisions, but there is an ω that comes from the Maxwell equations which should not include the collision term, so the replacement is rather for the mass term such that

$$m_e \rightarrow m_e(1 + iv/\omega).$$

Using this kind of Krook model for both ions and electrons for a cold plasma, the dielectric tensor elements which are the analogs of equations (2.11) through (2.15) are:

$$K_1 \equiv S \equiv \frac{1}{2}(R + L) = 1 - \sum_j \frac{\omega_{pj}^2(\omega + iv_j)}{\omega[(\omega + iv_j)^2 - \omega_{cj}^2]} \quad (3.94)$$

$$iK_2 \equiv D \equiv \frac{1}{2}(R - L) = \sum_j \frac{\epsilon_j \omega_{cj} \omega_{pj}^2}{\omega[(\omega + iv_j)^2 - \omega_{cj}^2]} \quad (3.95)$$

$$K_3 \equiv P \equiv 1 - \sum_j \frac{\omega_{pj}^2}{\omega(\omega + iv_j)} \quad (3.96)$$

$$K_1 + iK_2 \equiv R \equiv 1 - \sum_j \frac{\omega_{pj}^2}{\omega(\omega + iv_j + \epsilon_j \omega_{cj})} \quad (3.97)$$

$$K_1 - iK_2 \equiv L \equiv 1 - \sum_j \frac{\omega_{pj}^2}{\omega(\omega + iv_j - \epsilon_j \omega_{cj})}. \quad (3.98)$$

We can also keep the ionospheric notation of equation (2.16) for electrons only if we let

$$X = \frac{\omega_{pe}^2}{\omega(\omega + iv_e)} \quad \text{and} \quad Y = \frac{\omega_{ce}}{\omega + iv_e}. \quad (3.99)$$

These collisional corrections invariably contribute a negative imaginary part to ω , so they lead to decay in time, and since the plasma is passive (no free energy in the previous models), the proper root for k leads to decay in space away from a source.

Problem 3.4.1. Collisional damping of the L-wave. Neglecting electron collisions and using the Krook model for the ions,

- (i) Show that the dispersion relation for the *L*-wave for frequencies $\omega \sim \omega_{ci} < v_e \ll \omega_{ce}$ is given by

$$n_L^2 \simeq 1 - \frac{\omega_{pi}^2(\omega + iv_i)}{\omega\omega_{ci}(\omega + iv_i - \omega_{ci})}.$$

- (ii) Assuming $c^2/V_A^2 \gg 1$, $v_i \ll \omega_{ci}$, and $v_i \ll |\omega - \omega_{ci}|$, find the damping length for the *L*-wave (real ω).

- (iii) For the same assumptions, find the approximate decay time for the *L*-wave (real k).

3.4.2 Electron–ion collisions

For electron–ion collisions, the simple Krook model is less adequate, since the effective collision frequency is not an isotropic scalar quantity. For the basic collision frequencies, Braginskii finds [18]

$$\tau_e = \frac{3(2\pi)^{3/2}\sqrt{m_e}\epsilon_0^2(\kappa T_e)^{3/2}}{\ln \Lambda e^4 Z n_e} = \frac{3.4 \times 10^{11} T_e^{3/2}}{\ln \Lambda Z n_0} \quad (3.100)$$

$$\tau_i = \frac{12(\pi)^{3/2}\sqrt{m_i}\epsilon_0^2(\kappa T_i)^{3/2}}{\ln \Lambda e^4 Z^4 n_i} = \frac{2.1 \times 10^{13} \sqrt{A} T_i^{3/2}}{\ln \Lambda Z^3 n_0} \quad (3.101)$$

where SI units are used in the first expressions, and the temperatures are expressed in eV in the simplified expressions with $n_e = n_0 = Z n_i$ and A is the atomic mass number of the ion. The quantity Λ is approximately given by $\Lambda \simeq 9N_D$ where N_D is the number of particles in a Debye sphere (some authors have slightly

different coefficients, but since the dependence is only logarithmic, it matters little).

In terms of these collision frequencies, the frictional drag for $Z = 1$ and $\omega_{ce}\tau_e \gg 1$ is expressed in terms of $\mathbf{u} = \mathbf{v}_e - \mathbf{v}_i$ by the quantity

$$\mathbf{r}u = -\frac{m_en_e}{\tau_e}(0.51\mathbf{u}_{\parallel} + \mathbf{u}_{\perp}) = -ne\left(\frac{\mathbf{j}_{\parallel}}{\sigma_{\parallel}} + \frac{\mathbf{j}_{\perp}}{\sigma_{\perp}}\right) \quad (3.102)$$

where the perpendicular and parallel conductivities are given by

$$\sigma_{\perp} = \frac{n_e e^2 \tau_e}{m_e} \quad \sigma_{\parallel} = 1.96\sigma_{\perp}. \quad (3.103)$$

For $Z = 2$ the coefficients $0.51 (= 1/1.96) \rightarrow 0.44 (= 1/2.27)$, etc. Whenever $\omega_{ce}\tau_e \ll 1$, σ_{\perp} increases to the value of σ_{\parallel} .

These expressions may be incorporated into the fluid equations either by adding or subtracting the drag term of equation (3.102) to the individual species terms, since the momentum gained by the ions from collisions with electrons is equal and opposite the momentum gained by the electrons. Thus equation (3.40) is unchanged since the drag term cancels, while equation (3.41) becomes (neglecting m_e/m_i as before)

$$\frac{m_e}{n_0 e^2} \frac{\partial \mathbf{j}}{\partial t} = \mathbf{E} + \mathbf{v} \times \mathbf{B}_0 - \frac{m_i}{e} \frac{\partial \mathbf{v}}{\partial t} - \frac{1}{n_0 e} \nabla p_i - \frac{\mathbf{j}_{\parallel}}{\sigma_{\parallel}} - \frac{\mathbf{j}_{\perp}}{\sigma_{\perp}}. \quad (3.104)$$

Incorporating these into the LFDR, equation (3.50) becomes

$$\begin{aligned} & \left(1 - \frac{\omega^2}{k^2 V_A^2} - \frac{\omega(\omega + iv_{\perp})}{\omega_{ce}\omega_{ci}} + \frac{k^2 c_s^2 \sin^2 \theta}{\omega^2 - k^2 c_s^2}\right) \\ & \times \left(\cos^2 \theta - \frac{\omega^2}{k^2 V_A^2} - \frac{\omega(\omega + iv_{\parallel} \sin^2 \theta + iv_{\perp} \cos^2 \theta)}{\omega_{ce}\omega_{ci}}\right) = \frac{\omega^2}{\omega_{ci}^2} \cos^2 \theta \end{aligned} \quad (3.105)$$

where we have defined

$$v_{\perp} \equiv \frac{ne^2}{m_e \sigma_{\perp}} = \tau_e^{-1} \quad v_{\parallel} \equiv \frac{ne^2}{m_e \sigma_{\parallel}} = 0.51 \tau_e^{-1}.$$

Problem 3.4.2. LFDR with collisions.

- (i) Show that the changes in equation (3.104) lead to the result of equation (3.105).
- (ii) Assuming $v_{\perp}, v_{\parallel} \ll \omega$, find the corrections to equations (3.56), (3.57), and (3.58).

3.5 Amplifying waves and instabilities

3.5.1 Classification of instabilities

The literature of plasma physics includes innumerable examples of instabilities, some of which involve gross motion of the plasma, such as MHD instabilities, but for waves in plasmas, there are generally two classes of instabilities. We shall restrict the discussion to these two classes and analyze the criteria for distinguishing between them. The history of this problem is long, the distinction between the two classes having been noted by Twiss [19], Landau and Lifshitz [20], Sturrock [21], and by Briggs [22], whose development we shall follow most closely.

3.5.1.1 Convective and absolute instabilities

Whenever we have a

$$D(k, \omega) = 0 \quad (3.106)$$

which has either complex k for real ω , or complex ω for real k , then the wave may be described as either *stable* or *unstable* depending on whether the wave grows or decays in space or time. Unfortunately, however, the distinction is not always that simple, for there exist classes where a wave may grow in space but decay in time at a fixed point. We shall use the nomenclature that a wave is *unstable* if for some real k , with $\omega = \omega_r + i\omega_i$ ω has a positive imaginary part, or $\omega_i > 0$. We shall call a wave with complex $k = k_r + ik_i$ for real ω an *amplifying* wave if the wave grows in space *in the direction of energy flow* and *evanescent* if the wave decays in space *in the direction of energy flow*. It is not sufficient to find only the sign of the imaginary part of k , since growth in the direction of the phase velocity may be decay in the direction of the group velocity, as for a backward wave. A further distinction is that if a finite source (in space and time) leads to growth in time at *every* point in space, we call this an *absolute* instability. A different kind of instability occurs when a growing disturbance propagates in space ('convection') such that at a fixed point in space, the wave eventually decays in time, and we call this a *convective* instability. This distinction is clearly not observer independent, since an observer moving along with the growing disturbance would see it growing everywhere, so it would appear to him to be an absolute instability, while a stationary observer would call it a convective instability. Examples of these two types of instabilities are illustrated in [figure 3.4](#) by showing snapshots at successive times for some hypothetical unstable system with a pulsed local source.

Sturrock [21] concluded that the convective instability is essentially the same type as the amplifying wave, so that spatial amplification is due to a form of 'spatial instability' of the system. We will see that this interpretation is borne out in the following discussion.

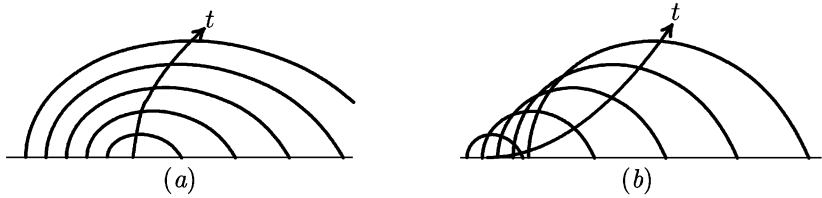


Figure 3.4. Evolution of a pulse disturbance in (a) an absolutely unstable system and (b) a convectively unstable system.

3.5.1.2 Green's function representation of localized sources

The analysis of the types of instability described in the previous section will be implemented by the introduction of a localized source so that the physical interpretation may be explicit. We shall assume the system is infinite and uniform in the z -direction, but that the source is bounded so that $g(z) = 1$ for $-a \leq z \leq a$ and zero otherwise. Using Fourier transforms in space, a unit amplitude source in this region can be represented by

$$g(k) = \int_{-\infty}^{\infty} g(z) e^{-ikz} dz = \frac{2 \sin ka}{k}. \quad (3.107)$$

In time, we shall use Laplace transforms so that we may represent a source which vanishes for $t < 0$. The Laplace transforms will be described by

$$f(t) = \int_{-\infty+i\sigma}^{\infty+i\sigma} f(\omega) e^{-i\omega t} \frac{d\omega}{2\pi} \quad (3.108)$$

$$f(\omega) = \int_0^{\infty} f(t) e^{i\omega t} dt \quad (3.109)$$

where the path of integration in equation (3.108) must lie *above* all the singularities of $f(\omega)$ in order to guarantee that $f(t) = 0$ for $t < 0$.

In order to distinguish between amplifying and evanescent waves at some real frequency ω_0 , we will assume a steady state source of the form

$$f(t) = e^{-i\omega_0 t} \quad (3.110)$$

so that

$$f(\omega) = \frac{i}{\omega - \omega_0}. \quad (3.111)$$

The response of the plasma to the source, denoted by $\psi(z, t)$, may be represented in terms of a Green's function of the form

$$\psi(z, t) = \int G(z - z', t - t') g(z') f(t') dz' dt' \quad (3.112)$$

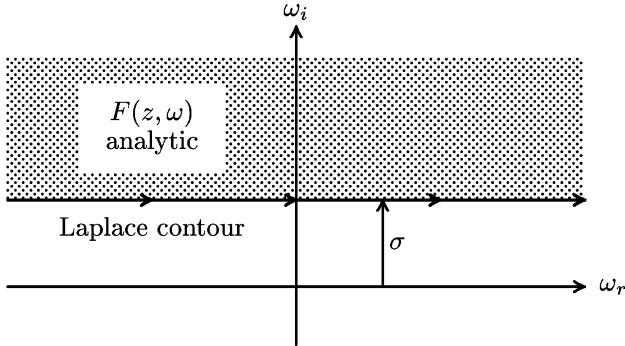


Figure 3.5. Analytic region of $F(z, \omega)$.

or in terms of the transform of the Green's function, $G(k, \omega)$,

$$\psi(z, t) = \int_{-\infty}^{\infty} \frac{dk}{2\pi} \int_{-\infty+i\sigma}^{\infty+i\sigma} \frac{d\omega}{2\pi} G(k, \omega) g(k) f(\omega) e^{i(kz - \omega t)}. \quad (3.113)$$

This analysis can be generalized to include transverse effects, but these effects do not influence the criteria we are trying to establish about the nature of the instability.

3.5.1.3 Establishment of instability criteria

Treating the time and space problems separately for the moment, we may write equation (3.113) as

$$\psi(z, t) = \int_{-\infty+i\sigma}^{\infty+i\sigma} F(z, \omega) f(\omega) e^{-i\omega t} \frac{d\omega}{2\pi} \quad (3.114)$$

with

$$F(z, \omega) = \int_{-\infty}^{\infty} G(k, \omega) g(k) e^{ikz} \frac{dk}{2\pi} \quad (3.115)$$

where $f(\omega)$ and $g(k)$ are given by equations 3.111 and 3.107, respectively.

In order to establish *causality*, we require that $F(z, \omega)$ be analytic in the shaded region of figure 3.5, since we chose σ to extend the path *above* all singularities.

Interpretation of $F(z, \omega)$. The z -dependence of the response is contained in the function $F(z, \omega)$. Since the system is source free for $|z| > a$, the response must be given in terms of the normal modes of the system or the undriven modes. These are just the roots of the dispersion relation of equation (3.106), and the roots represent poles in the Green function $G(k, \omega)$ since $G(k, \omega) \propto 1/D(k, \omega)$. By inspection of equation (3.107), we can easily see that $g(k)e^{ikz} \rightarrow 0$ as $k \rightarrow i\infty$

for $z > a$, so it is possible to close the Fourier contour above and evaluate the response as a sum of the residues, each one representing one of the normal modes. In some cases, the poles may be replaced by singularities with a branch line, representing a continuum of modes, and methods of treating these are discussed by Briggs [22]. We can now express $F(z, \omega)$ in terms of a sum:

$$F(z, \omega) = \sum_{n_p} \frac{ig[k_{n_p}(\omega)]}{\left[\frac{\partial}{\partial k} G^{-1}(k, \omega) \right]_{k=k_{n_p}}} e^{ik_{n_p} z} \quad (3.116)$$

where the sum is over the roots of the dispersion relation which lie in the upper-half k -plane for some frequency ω which lies on the Laplace contour of [figure 3.5](#) ($\omega_i = \sigma$).

Analytic continuation. While the execution of the inverse Laplace integral along the path prescribed will give the response in detail, it will be advantageous to deform the contour since we only require *asymptotic* expressions. This may move the contour into a region where $F(z, \omega)$ is not defined, so we wish to define its analytic continuation. If we imagine the deformation of the Laplace contour to occur by letting the real part of ω stay fixed and varying only the imaginary part ω_i , then the poles of the dispersion relation will describe a trajectory in the k -plane. Providing these poles do not cross the real axis, then $F(z, \omega)$ is still the sum given in equation (3.116), with just slightly different values. When one of these poles does cross the real k -axis, however, then we must define the analytic continuation of $F(z, \omega)$ in terms of the integral

$$\tilde{F}(z, \omega) = \int_C G(k, \omega) g(k) e^{ikz} \frac{dk}{2\pi} \quad (3.117)$$

where now the contour C is deformed so that all poles which were originally below the contour remain below by deforming the contour over these poles, and all poles which were originally above the contour remain above the contour by deforming the contour to go under these poles. This means that the sum of equation (3.116) is over those roots which were *originally* above the real k -axis when $\omega_i = \sigma$, whether or not they remain above the axis when the Laplace contour is deformed.

Criteria for amplifying and evanescent waves. When the Laplace contour is deformed to just below the real axis, then we pick up the pole at ω_0 so the time asymptotic form of the response is

$$\lim_{t \rightarrow \infty} \psi(z, t) \rightarrow \tilde{F}(z, \omega_0) e^{-i\omega_0 t} \quad (3.118)$$

and the spatial behavior is determined by $\tilde{F}(z, \omega)$ for a real frequency. Since all of the k_{n_p} in the sum of equation (3.116) had a positive imaginary part ($k_i > 0$), these were evanescent, and providing they do not cross the real k -axis, they remain evanescent. If, however, one of the roots does move below the real k -axis, as root A does in [figure 3.6](#), then we have an amplifying wave in space. Any root which

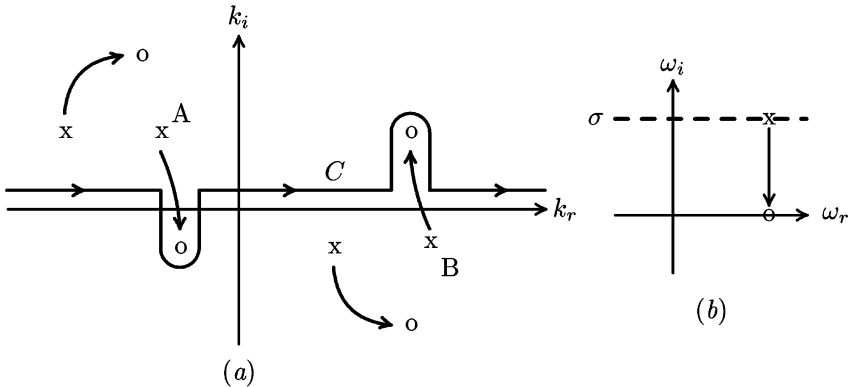


Figure 3.6. (a) Contour C for analytic continuation and motion of the poles of $G(k, \omega)$. (b) Movement of the Laplace contour which results in the motion of the poles of $G(k, \omega)$.

was originally below the axis was excluded from the sum for $z > a$ and hence does not lead to amplification. For the case when $z < -a$, however, the k -plane contour closes *below* to enclose evanescent roots, so only those roots which move *above* the real k -axis, such as root B in figure 3.6, are amplifying for $z < -a$. The criterion for amplifying roots is then that a root of the dispersion relation must cross the real k -axis as ω_i is reduced from σ to zero. If it crosses from above to below, it is amplifying for positive z , and if it crosses from below to above, it is amplifying for negative z .

Absolute instabilities. There is one case where this simple prescription necessarily fails, since if two poles merge, one coming from below and one coming from above, the C contour can no longer pass *between* the poles. This merging would, in general, occur with $\omega_i = \sigma_s > 0$, and corresponds to a saddle point of the dispersion relation so that $\partial\omega/\partial k = 0$ at $\omega = \omega_s$. Expanding about this saddle point, we may approximate

$$G^{-1}(k, \omega) \simeq \frac{\partial G^{-1}}{\partial \omega} \Bigg|_{\omega_s} (\omega - \omega_s) + \frac{1}{2} \frac{\partial^2 G^{-1}}{\partial k^2} \Bigg|_{k_s} (k - k_s)^2. \quad (3.119)$$

If we use this result in equation (3.115), near $\omega \sim \omega_s$ we obtain

$$\tilde{F}(z, \omega) = \frac{\pm i g(k_{\pm}) e^{ik_{\pm} z}}{q^2(k_{\pm} - k_{\mp})} \simeq \frac{g(k_s) e^{ik_s z}}{2pq\sqrt{\omega - \omega_s}} \quad (3.120)$$

where one choice is for $z > a$ and the other for $z < -a$ and where

$$k_{\pm} = k_s \pm \frac{ip}{q} \sqrt{\omega - \omega_s}$$

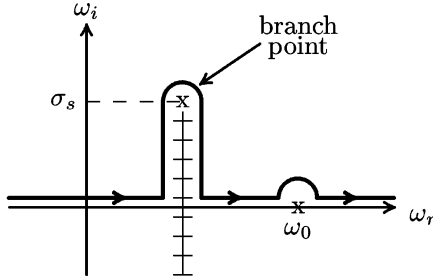


Figure 3.7. Laplace contour with absolute instability.

$$p^2 = \left. \frac{\partial G^{-1}}{\partial \omega} \right|_{\omega_s}$$

$$q^2 = \frac{1}{2} \left. \frac{\partial^2 G^{-1}}{\partial k^2} \right|_{k_s} .$$
(3.121)

Since the group velocity vanishes at the saddle point, the direction is immaterial. We now note from equation (3.120) that $\tilde{F}(z, \omega)$ has a branch point at $\omega = \omega_s$. This branch point is not due simply to the existence of a saddle point, but due to the convergence of the paths at the branch point from above and below, since if both the merging roots came either from above or below, the contour C would not include them.

This branch point must be carefully treated as we do the inverse Laplace transform, since the contour must remain *above* the branch point as we deform the contour down to the real ω -axis. The deformed contour thus goes over the branch point at ω_s and the pole at ω_0 as in figure 3.7.

We note that the entire upper-half ω -plane must be explored for the highest such singularity, since it is the fastest growing mode which will dominate. The time asymptotic response can now be evaluated as

$$\psi(z, t) \simeq \frac{g(k_s) f(\omega_s) e^{i(k_s z - \omega_s t)}}{pq} \int_{-\infty}^{\infty} \frac{e^{i(\omega_s - \omega)t}}{\sqrt{\omega - \omega_s}} \frac{d\omega}{2\pi}$$

$$\simeq \frac{g(k_s) f(\omega_s)}{2pq} \frac{e^{i(k_s z - \omega_s t)}}{\sqrt{\pi i t}}.$$
(3.122)

Although this expression has possible spatial growth or decay due to the fact that k_s is in general complex, the absolute instability is characterized by the positive imaginary part of ω_s which leads to growth everywhere in time.

Other kinds of unusual behavior, such as a triple pole at ω_s, k_s , or $p = 0$, or an essential singularity in the dispersion relation could occur, and have been considered by Briggs [22], but these pathological cases do not effectively change the criteria for stability or instability for reasonable plasma models.

The close connection between convective instabilities and amplifying waves has also been investigated by Sturrock [21] and Briggs [22] by considering the propagation of a pulse disturbance at a finite velocity and it has been shown that a system which supports convective but not absolute instabilities must have at least one amplifying root of the dispersion relation.

Problem 3.5.1. Absolute instability. Verify the steps leading to equation (3.122) when there is a saddle point in the dispersion relation.

3.5.1.4 Application of the criteria

Amplifying waves. The criteria established here for amplifying waves can be summarized as follows [22].

To decide whether a given wave with a complex $k = k_r + ik_i$ for some real ω is amplifying or evanescent, determine whether or not k_i has a different sign when the frequency takes on a large positive imaginary part.² If it does, then the wave is amplifying; otherwise, it is an evanescent wave.

The physical picture of the change in sign comes from considering a source which is localized in space, but growing exponentially in time. From causality, we expect waves to decay away from the source, so that the effective ‘growth rate’ must eventually change sign for sufficiently rapid growth in time.

Since a source is rarely monochromatic in wavenumber (a bounded source must have an infinite spectrum), it is generally necessary to find the *maximum* growth rate, since even though the source amplitude for this most rapidly growing component is small, it will eventually dominate. This phenomenon also modifies our concept of group velocity in an amplifying medium, for although the group velocity may be determined initially from the dominant wavenumber k in the source, it eventually will be determined by the wavenumber with maximum growth as it becomes the dominant component in the wave. In some cases, this maximum growth may be obtained analytically, but in general one needs to consider a mapping of a whole family of curves representing $\omega(k)$ where each member has constant ω_r and the imaginary part is reduced to zero, and the k -plane mapping then shows not only which members cross the axis, but which has the maximum growth rate, as in [figure 3.8](#). We also note that each root of the dispersion relation must be mapped separately, so that figure 3.8 represents only one sheet of the complex plane mapping if the dispersion relation is higher order than linear in ω and k .

Absolute instabilities. This same mapping procedure also indicates the presence of any absolute instabilities, except that the figure then appears as in [figure 3.9](#), and the criterion is summarized as [22]

² Negative imaginary part in Briggs, since he uses $j = -i$, (electrical engineering notation) everywhere.

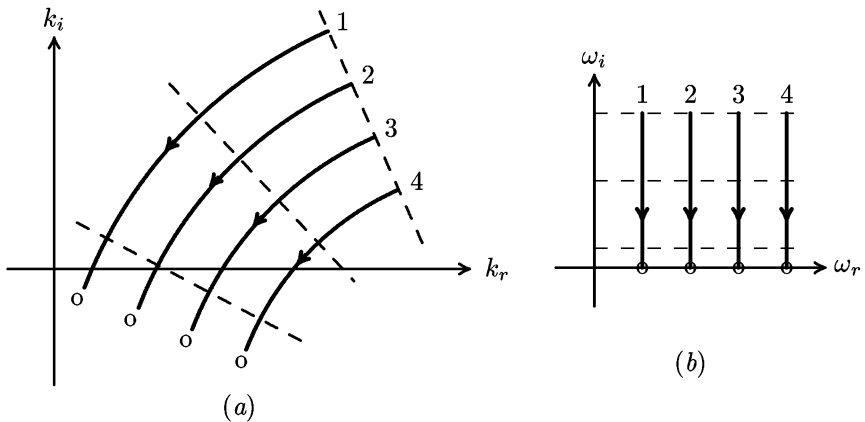


Figure 3.8. Mapping of $\omega(k)$ for an amplifying wave for paths in (a) the k -plane and (b) the ω -plane.

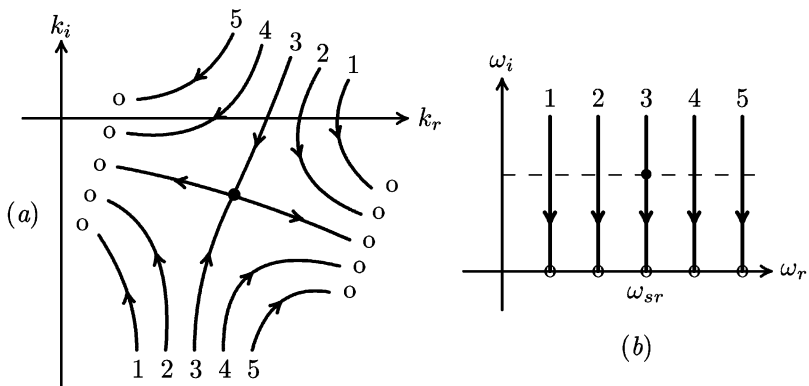


Figure 3.9. Mapping of $\omega(k)$ for an absolute instability for paths in (a) the k -plane and (b) the ω -plane with the saddle point located at the \bullet .

An absolute instability is obtained whenever there is a double root of k for some complex ω in the upper-half ω -plane³ for which the two merging roots come from different halves of the complex k -plane (upper and lower) when ω has a large positive imaginary part.

Since this criterion for merging roots is the same as for the existence of a saddle point, the saddle point should be apparent from the mapping.

A physical picture of the restriction that the merging roots come from *opposite* half-planes may be seen from considering a point source of a

³ Lower-half plane in Briggs, same reason as before.

disturbance. If we consider the source to be growing in time at some complex ω whose growth rate is sufficiently large that all waves must decay away from the source in space, as discussed earlier, then some of the roots will contribute to the waves for $z > 0$ (k_+) and some to the waves for $z < 0$ (k_-). For the point source, there will be some discontinuity at the origin in the wave amplitude in general, but if it should happen that $k_+ = k_-$, there would be no discontinuity, and no source required. Hence, if an ω exists where wavenumbers k_+ and k_- , each having come from different half-planes, should merge, then this is a natural mode of the system and needs no source, and the instability grows everywhere.

3.5.1.5 Cautions in using the criteria

These criteria are based on consideration of models of *infinite* systems, and some kinds of boundary reflections may affect the conclusions. Two warnings are in order:

- (i) It is not true that any system which supports an absolute instability is *always* unstable. It is usually required that the system exceed some minimum length (k_s may be excluded by boundary conditions), as is the case for the backward wave oscillator [23].
- (ii) It is also not true that a bounded system which supports only convective instabilities (amplifying waves) is stable. In the absence of reflections, this is true, but with sufficient reflections, for example, an amplifier may be turned into an oscillator, and grow everywhere.

3.5.2 Streaming instabilities

The simplest kind of plasma model which includes effects of zero-order particle velocities is to include a drift velocity v_0 , or a whole series of separate fluid components, each with its own drift velocity v_{0i} , which may approximate a zero-order velocity distribution. When we model the plasma by a cold plasma as the principal fluid and then add another component with a finite drift velocity, we generally refer to the drifting component as a streaming component or as a beam. In this section we shall consider several possibilities of streaming components interacting with a cold or fluid plasma, and examine their stability characteristics. In this chapter, we shall assume that both the plasma and beam are infinite in extent, and include either boundaries in [chapter 5](#) or inhomogeneous plasmas and drift waves in [chapter 6](#).

3.5.2.1 One-dimensional beam–plasma system

For our first example, we consider the cold electrostatic plasma wave with a beam component as the source of free energy and neglect ion inertia. Using equation (3.35) with a drift velocity v_0 for the beam component, the linearized

momentum equation with $\mathbf{B} = p = 0$ becomes

$$\rho_{0b} \left(\frac{\partial \mathbf{v}_{1b}}{\partial t} + \mathbf{v}_0 \cdot \nabla \mathbf{v}_{1b} \right) = -en_{0b} \mathbf{E} \quad (3.123)$$

or using the electrostatic potential $\mathbf{E} = -\nabla\varphi = -ik\varphi$ for harmonic dependence, equation (3.123) may be expressed as

$$\rho_{0b} v_{1b} = -\frac{en_{0b} k \varphi}{\omega - kv_0}. \quad (3.124)$$

Then using equation (3.34), the continuity equation,

$$\frac{\partial \rho_{1b}}{\partial t} + \nabla \cdot (\rho_{1b} \mathbf{v}_0 + \rho_{0b} \mathbf{v}_{1b}) = 0$$

becomes

$$\rho_{0b} v_{1b} = (\omega - kv_0) \rho_{1b} / k. \quad (3.125)$$

Using this result along with equation (3.124), we solve for ρ_{1b} as

$$\rho_{1b} = -\frac{en_{0b} k^2 \varphi}{(\omega - kv_0)^2}. \quad (3.126)$$

We combine this with a corresponding cold plasma background term (with $v_0 = 0$) through Poisson's equation,

$$\nabla^2 \varphi = -k^2 \varphi = \frac{e}{\epsilon_0} (n_{1p} + n_{1b})$$

where n_{1p} represents the first-order density perturbation for the cold plasma background. The resulting dispersion relation is

$$D(\omega, k) = 1 - \frac{\omega_p^2}{\omega^2} - \frac{\omega_{pb}^2}{(\omega - kv_0)^2} = 0 \quad (3.127)$$

where ω_p is the plasma frequency for the cold background plasma component, and ω_{pb} is the plasma frequency for the beam component.

This dispersion relation is quadratic in k , with roots

$$kv_0 = \omega \left(1 \pm \frac{\omega_{pb}}{\sqrt{\omega^2 - \omega_p^2}} \right) \quad (3.128)$$

so there are complex roots for $\omega < \omega_p$, one above the real k -axis and the other below for real ω . Letting ω have a large positive imaginary part ($|\omega| \rightarrow \infty$) leads to the roots

$$k \simeq (\omega \pm \omega_{pb})/v_0 \quad (3.129)$$

so both roots are in the upper half-plane. Thus one root must have crossed the axis and we have the condition for an amplifying wave. Both roots came from the ‘downstream’ side ($z \rightarrow +\infty$), so the wave grows in the direction the beam travels, as we might expect.

We note in passing that there is an essential singularity in $F(z, \omega)$ at $\omega = \omega_p$ since $\omega \rightarrow \omega_p$ as $k \rightarrow \infty$. This implies that there will be undamped oscillations at ω_p as well as at the driven frequency, but since the phase velocity approaches zero, the inadequacy of the cold plasma model and the fluid equations makes this result unreliable.

3.5.2.2 The two-stream instability

It is easy to generalize the dispersion relation of equation (3.127) to the case with two interpenetrating beams by adding another beam component, denoting the two beam velocities as v_1 and v_2 and the two beam plasma frequencies as ω_{p1} and ω_{p2} , with the result

$$D(\omega, k) = 1 - \frac{\omega_p^2}{\omega^2} - \frac{\omega_{p1}^2}{(\omega - kv_1)^2} - \frac{\omega_{p2}^2}{(\omega + kv_2)^2}. \quad (3.130)$$

One special case where we can get analytic results is to let $\omega_{p1} = \omega_{p2} = \omega_0$ and $v_1 = v_2 = v_0$. If we use the cold plasma notation that

$$P = 1 - \frac{\omega_p^2}{\omega^2}$$

then the solutions of equation (3.130) are

$$(k^\pm v_0)^2 = \omega^2 + \frac{\omega_0^2}{P} \pm \frac{\omega_0}{P} \sqrt{\omega_0^2 + 4P\omega^2} \quad (3.131)$$

so there is a double root or saddle point where $\omega_0^2 = -4P\omega^2$ or $\omega^2 = \omega_p^2 - \omega_0^2/4$. For $\omega_p < \omega_0/2$, this leads to complex roots and an absolute instability. If we plot the locus of k^2 for pure imaginary ω in the complex k^2 -plane with $\omega_p = 0$, the saddle point lies on the real k^2 -axis and branches off above and below the axis for large ω_i and branches out along the real k^2 -axis for small ω_i , ending with one root at the origin, and the other beyond the saddle point. In the k -plane, this means there are two symmetric saddle points, one with $k_r > 0$ and one with $k_r < 0$, and the branches for variable ω_i go either along the real k -axis or above and below the axis, which is the sufficient condition for the absolute instability. Examples of the trajectories for $\omega_p = 0.4\omega_0$ for both k^2 and k are shown in figure 3.10 where the two branches from above and below merge on the real axis at $k_r v_0/\omega_0 = 0.52$, indicating an absolute instability.

If, however, $\omega_p > \omega_0/2$, then there is no saddle point in the upper-half ω -plane, so there cannot be an absolute instability. There are generally complex

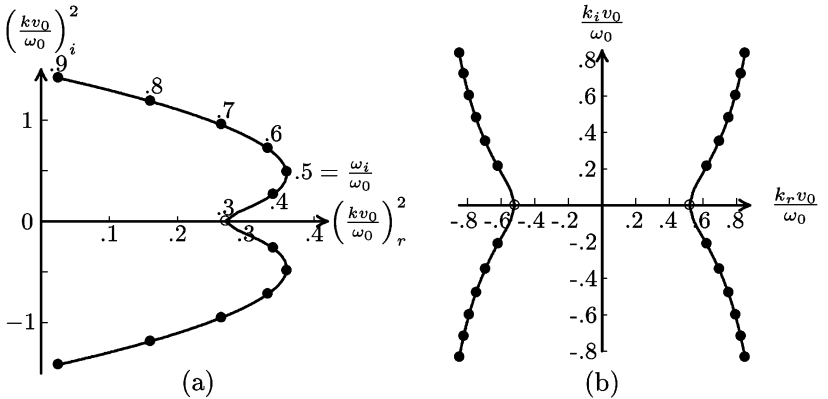


Figure 3.10. Locus of (a) $k^2(\omega_i)$ in the complex k^2 -plane and (b) $k(\omega_i)$ in the complex k -plane from equation (3.131) for $\omega_p = .4\omega_0$.

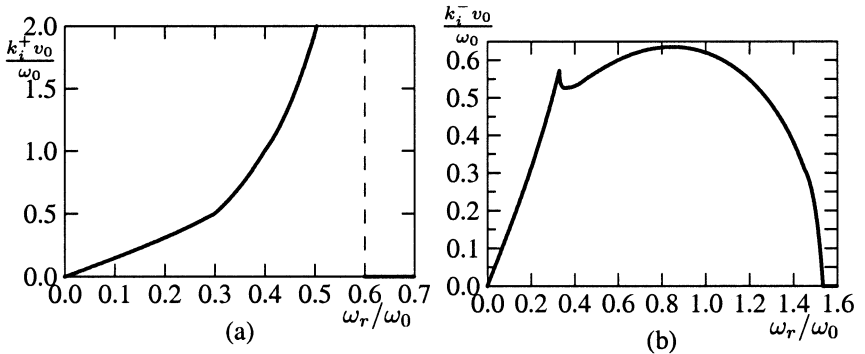


Figure 3.11. Absolute instability case with $\omega_p/\omega_0 = 0.6$: (a) $k_i^- v_0/\omega_0$ versus ω_r/ω_0 ; and (b) $k_i^+ v_0/\omega_0$ versus ω_r/ω_0 . There is a discontinuity in slope where the radical of equation (3.131) vanishes at $\omega_r = (\omega_p^2 - \omega_0^2/4)^{1/2}$. k_i^+ has a pole at $\omega_r = 0.6\omega_0$ and vanishes beyond, while k_i^- vanishes beyond $\omega_r = (2\omega_0^2 + \omega_p^2)^{1/2}$.

roots of k for real ω , however, from equation (3.130), so there is generally a convective instability as illustrated in figure 3.11. The two complex roots behave differently, since for k_i^+ in figure 3.11(a), there is a pole when $\omega_r = \omega_p$ ($P = 0$). The other root has no pole, but the imaginary part extends over the range $0 \leq \omega_r \leq (2\omega_0^2 + \omega_p^2)^{1/2}$. Although only positive imaginary parts are illustrated, the negative roots are also present and equivalent in magnitude.

Another special case where we can get analytic results is the case where

$\omega_p = 0$ so equation (3.130) simplifies to

$$1 = \frac{\omega_{p1}^2}{(\omega - kv_1)^2} + \frac{\omega_{p2}^2}{(\omega + kv_2)^2} \quad (3.132)$$

with the densities and velocities not equal but related by

$$\frac{\omega_{p1}^2}{v_1^2} = \frac{\omega_{p2}^2}{v_2^2} \equiv \frac{\omega_0^2}{v_0^2}. \quad (3.133)$$

Then we define a mean velocity given by

$$\frac{1}{v_0} \equiv \frac{1}{2} \left(\frac{1}{v_1} - \frac{1}{v_2} \right) \quad (3.134)$$

and introduce the normalized variables x and y such that

$$x = \frac{\omega}{\omega_0} \left(\frac{v_2 + v_1}{v_2 - v_1} \right) \quad k = \frac{\omega}{v_0} + y \frac{\omega_0}{v_0} \quad (3.135)$$

so that equation (3.132) reduces to

$$1 = \frac{1}{(x - y)^2} + \frac{1}{(x + y)^2}. \quad (3.136)$$

This equation is fourth order, but quadratic in either x^2 or y^2 , so that

$$y^2 = x^2 + 1 \pm \sqrt{1 + 4x^2}. \quad (3.137)$$

There is a double root at $x = \pm i/2$, and from the discussion of the previous case, this corresponds to an absolute instability. For $0 \leq x^2 \leq 2$, the lower branch has complex y for real x , so we have amplifying waves in this region. For the upper branch and for $x^2 > 2$, the system is stable.

The interpretation of this result may be made more evident by plotting the right-hand side of equation (3.132) versus k . In figure 3.12, the roots occur where the curves cross the line at unity and the curves are drawn for $v_2 = 2v_1$ so that $\omega = \omega_0 x/3$ and $kv_0/\omega_0 = x/3 + y$. For a low frequency case with $x = 1$, shown in figure 3.12(a), there are two real roots and two complex roots, one of which corresponds to an amplifying wave and one to a decaying wave. In figure 3.12(b), we have reached the critical frequency, $x = \sqrt{2}$, where the two inner roots have coalesced to form a double root, but *no instability* since this occurs for real ω and k , and the merging roots do not come from opposite sides of the real k -axis. For the high frequency case in figure 3.12(c), $x = 2$ and all four roots are real, the two outer roots corresponding to the upper branch of equation (3.137) and the two inner roots corresponding to the lower branch. This figure does not show the absolute instability at $x = i/2$ or $\omega_i = \omega_0/6$, since it is plotted for real ω . In

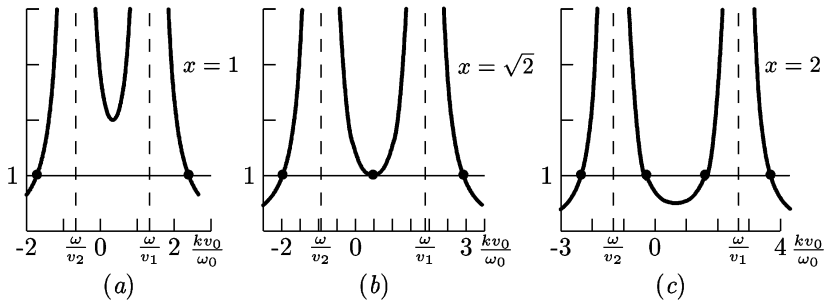


Figure 3.12. Plots of the right-hand side of equation (3.136) with $v_2 = 2v_1$ for (a) $x = 1$ (two real roots and two complex roots, one amplifying), (b) $x = \sqrt{2}$ (three stable roots), and (c) $x = 2$ (four stable roots).

figure 3.12(b), the double root corresponds to $\partial\omega_r/\partial k_r = 0$ and is at the bottom of a sloping valley in complex ω - k space, but the saddle point does not lie in the real ω - k plane.

The maximum growth rate for the amplifying wave occurs when y^2 is most negative, or when $x = \sqrt{3}/2$ and $y = -i/2$, so for the growing wave

$$k_{i,\max} = -\omega_0/2v_0. \quad (3.138)$$

Problem 3.5.2. Two-stream absolute instability.

- (i) For $\omega_p = 0$, sketch the locus of k^2 as a function of ω_i with $\omega_r = 0$, showing the end points where $\omega_i = 0$.
- (ii) For the same case, sketch the loci in the complex k -plane, and hence prove that this is an absolute instability.
- (iii) For $\omega_p = \omega_0/4$, draw similar sketches as a function of ω_i , and note any significant differences.

Problem 3.5.3. Two-stream amplifying wave growth rate. For $\omega_p = \omega_0$, find the maximum growth rate in terms of ω_0 and v_0 .

Problem 3.5.4. Unequal beams with $\omega_p = 0$. When equation (3.133) is satisfied, show that the transformations of equation (3.134) and equation (3.135) lead to equations (3.136) and (3.137).

Problem 3.5.5. Unequal beams with $\omega_p \neq 0$. The condition $\omega_p = 0$ is not necessary for the transformations of equations (3.134) and (3.135) when equation (3.133) is true.

- (i) If we define $\alpha = (\omega_p/\omega_0)(v_2 + v_1)/(v_2 - v_1)$, show that the dispersion relation is quadratic in y^2 with solution

$$y^2 = x^2 \left[1 + \left(1 \pm \sqrt{1 + 4x^2 - 4\alpha^2} \right) / (x^2 - \alpha^2) \right].$$

- (ii) Find the condition for an absolute instability.
- (iii) Plot the maximum growth rate as a function of α , and find the maximum value of α for which growth occurs (numerical problem).

3.6 Power and energy flow in fluid plasmas

When we have a warm plasma, the power and energy conservation theorems have temperature-dependent terms, so we must examine these expressions anew. We begin with the basic linearized fluid equations from section 3.2 and the Maxwell equations. If we now multiply equation (3.36) by p_1/ρ_0 and sum over species, take the scalar product of equation (3.37) with \mathbf{v}_1 and sum over species, the scalar product of equation (1.4) with \mathbf{H} , the scalar product of equation (1.5) with $-\mathbf{E}$ and then add all four, we obtain the result

$$\begin{aligned} \nabla \cdot \left(\mathbf{E} \times \mathbf{H} + \sum_j \kappa T_j n_{1j} \mathbf{v}_{1j} \right) \\ = -\frac{\partial}{\partial t} \left(\sum_j n_{0j} \frac{m_j v_{1j}^2}{2} + \sum_j \frac{\kappa T_j}{n_{0j}} \frac{n_{1j}^2}{2} + \frac{\mu_0 H^2}{2} + \frac{\epsilon_0 E^2}{2} \right). \end{aligned} \quad (3.139)$$

In this expression, we can interpret the terms on the left as energy flux and the terms on the right as stored energy. In each case, some of the energy and flux is in the fields and some in the particles. In this case the kinetic flux (or the acoustic power flow) is given by

$$\mathbf{T} = \sum_j \kappa T_j n_{1j} \mathbf{v}_{1j} \quad (3.140)$$

and represents the energy flux carried by the particles, and the Poynting flux represents the energy flux carried by the electromagnetic field. In longitudinal or electrostatic waves, the Poynting flux vanishes, so the energy is carried by the particle flux alone.

In equation (3.139) we have used the exact fields and fluid elements, whereas in waves, we generally use Fourier amplitudes to represent these quantities. In terms of the Fourier amplitudes (in time only, $\partial/\partial t \rightarrow -i\omega$), where each of the first order quantities is, in general, complex, the equations become

$$n_0 \nabla \cdot \mathbf{v}_1 = i\omega n_1 \quad (3.141)$$

$$\kappa T \nabla n_1 = i\omega m n_0 \mathbf{v}_1 + q n_0 \mathbf{E} + q n_0 \mathbf{v}_1 \times \mathbf{B}_0 \quad (3.142)$$

$$\nabla \times \mathbf{E} = i\omega \mu_0 \mathbf{H} \quad (3.143)$$

$$\nabla \times \mathbf{H} = \mathbf{j} - i\omega \epsilon_0 \mathbf{E}. \quad (3.144)$$

We wish now to examine the time-averaged power and energy flow, so we consider ω to be real. Then by taking the sum of the scalar product of equation (3.141) with \mathbf{v}_1^* summed over species, the product of $\kappa T n_1/n_0$ multiplied by the complex conjugate of equation (3.142) summed over species, the scalar product of \mathbf{H}^* with equation (3.143), less the scalar product of \mathbf{E} with the complex conjugate of equation (3.144), the result is

$$\begin{aligned} \nabla \cdot \left(\mathbf{E} \times \mathbf{H}^* + \sum_j p_{1j} \mathbf{v}_{1j}^* \right) \\ = i\omega \left(\sum_j n_{0j} m_j |v_{1j}|^2 - \sum_j \frac{|p_{1j}|^2}{p_{0j}} + \mu_0 |H|^2 - \epsilon_0 |E|^2 \right) \\ + \sum_j q_j n_{0j} (v_{1xj}^* v_{1yj} - v_{1yj}^* v_{1xj}) B_0. \end{aligned} \quad (3.145)$$

If we add equation (3.145) to its complex conjugate, the result may be expressed by

$$\nabla \cdot (\mathbf{P} + \mathbf{T}) = 0 \quad (3.146)$$

where

$$\mathbf{P} = \frac{1}{4}(\mathbf{E} \times \mathbf{H}^* + \mathbf{E}^* \times \mathbf{H}) \quad (3.147)$$

$$\mathbf{T} = \sum_j \frac{1}{4}(p_{1j} \mathbf{v}_j^* + p_{1j}^* \mathbf{v}_j) \quad (3.148)$$

and hence we have from Gauss' law that $\mathbf{P} = -\mathbf{T}$ when averaged over time if there are no losses (ω real).

When ω is complex, or full thermal corrections are included, the simple phasor analysis given here must be modified, and we treat these cases in section 4.6. These results, however, already demonstrate that both particles and fields contribute to the energy flux and the stored energy.

Chapter 4

Kinetic theory of plasma waves

4.1 The basic equations

Unfortunately, the detailed derivation of the basic equations of the kinetic theory of plasma waves is so complicated that it is beyond the scope of this book. For a more detailed account, one should consult a specialized text such as that by Montgomery and Tidman [24] or a more general plasma physics textbook. What follows is rather a description of the basic equations rather than a derivation. The point of the description is to indicate the content of the physics and mathematical methods so that the limits of the validity of the zero order theory may be grasped along with the directions one would go to include higher order terms and what physics is contained in those terms.

4.1.1 The Boltzmann equation

When including thermal effects and other motions of the particles in a plasma, it would seem that the usual Boltzmann equation,

$$\frac{df_j(\mathbf{r}, t)}{dt} = \frac{\partial f_j}{\partial t} + \mathbf{v} \cdot \nabla f_j = \left. \frac{df_j}{dt} \right|_c \quad (4.1)$$

where $f_j(\mathbf{r}, t)$ is the distribution function, would be a suitable starting point. This equation is just the conservation of particles or probability density, where the left-hand side gives the rate of change following the trajectory of a particle in space and the right-hand side represents the rate at which trajectories are terminated through collisions with corresponding new trajectories started so that particles are conserved. These collisions are generally understood to be binary collisions where particles make discontinuous jumps in velocity due to short-range molecular forces. While in one sense this is not incorrect for plasmas, it is not fruitful to use the Boltzmann equation in this form, since for long range forces such as gravity and electromagnetism, the leading term on the right due to long range forces needs to be separated out and treated differently. This was first

shown for a collection of massive objects (stars in a galaxy), where the cumulative effect of weak gravitational forces from a large number of distant masses is generally more important than the infrequent close encounter with an individual mass, providing the masses are dense enough. This same treatment extended to plasmas [25] also shows that the cumulative effect of weak electromagnetic forces due to many particles, represented by both the external electric and magnetic fields *and* the self-consistent internal electric and magnetic fields is more important than the occasional close collision resulting in a large deflection, providing there are many particles in a Debye sphere. In fact, for plasmas, the discussion of collisions leads to the conclusion that a 90° deflection is rarely due to a single encounter, but rather an accumulation of many small deflections, and a collision time must be interpreted not as the actual mean time between collisions, as in a gas, but as the mean time required to accumulate a specified deflection, usually defined to be 90° [26]. In view of these considerations, we rewrite the Boltzmann equation as

$$\frac{df_j(\mathbf{r}, \mathbf{v}, t)}{dt} = \frac{\partial f_j}{\partial t} + \mathbf{v} \cdot \nabla f_j + \frac{q_j}{m_j} (\mathbf{E} + \mathbf{v} \times \mathbf{B}) \cdot \nabla_{\mathbf{v}} f_j = \frac{df_j}{dt} \Big|_c \quad (4.2)$$

where now the term on the right is a nontrivial collision operator due to correlations between nearby particles and the conservation law follows particles in six-dimensional phase space. To this must be added the Maxwell equations, of course, since the particles are sources for the internal fields.

4.1.2 Collisions and the Fokker–Planck equation

Whenever a plasma deviates from equilibrium, there are generally relaxation processes which govern the return to equilibrium. The most common of these processes is binary collisions, and the relaxation rate of a test particle distribution toward the background distribution due to collisions with the various component species of a plasma is given by Krall and Trivelpiece [27] as

$$\frac{\partial f_T}{\partial t} \Big|_c = \sum_j n_j \gamma_j \left[-\nabla_{\mathbf{v}} \cdot (f_T \nabla_{\mathbf{v}} h_j) + \frac{1}{2} \nabla_{\mathbf{v}} \cdot \frac{\partial}{\partial v_i} \left(f_T \frac{\partial}{\partial v_i} \nabla_{\mathbf{v}} g_j \right) \right] \quad (4.3)$$

where the repeated subscript i is summed over v_x , v_y , and v_z , and

$$h_j = \frac{m_T}{\mu_j} \int \frac{f_j(\mathbf{v}')}{|\mathbf{v} - \mathbf{v}'|} d^3 v' \quad g_j = \int f_j(\mathbf{v}') |\mathbf{v} - \mathbf{v}'| d^3 v'$$

$$\gamma_j = \frac{q_T^2 q_j^2 \ln \Lambda}{4\pi \epsilon_0^2 m_T^2} \quad \mu_j = \frac{m_T m_j}{m_T + m_j}$$

and T refers to the test particles and $\Lambda = 9N_D$ where N_D is the number of particles in a Debye sphere. The first term primarily leads to a drag on a moving particle, tending to slow it down to the background mean velocity, and the second

describes velocity space diffusion, which spreads the velocities throughout the distribution. This form of the Fokker–Planck equation can be used to estimate thermalization times, slowing down times of streaming particles, spreading of a beam of particles, plasma conductivity, and diffusion rates. A more sophisticated form of this equation, such as the *Lenard–Balescu* [28] equation, also includes the dielectric properties of the plasma and shielding. The effects of collisions and velocity space diffusion on plasma transport is reviewed by Hinton [29], but these effects are beyond the scope of this book. Other versions of this basic equation describe the evolution of a distribution function in the presence of a driving radiofrequency field, whereby both resonant and nonresonant absorption of wave energy will cause the distribution to evolve away from an equilibrium distribution through quasilinear diffusion, discussed in [chapter 7](#), unless the drag forces are much stronger than the driving forces. It also describes the eventual relaxation of an unstable distribution, initially through quasilinear diffusion, and eventually through collisions, as in the bump-on-the-tail instability described in section 7.2.5.

We summarize here several important effects of the collisions that we will note again from time to time as the subject arises.

4.1.2.1 Relaxation

Clearly, collisions tend to relax a perturbed distribution function back toward equilibrium (the existence of an equilibrium is *assumed* here, although a true equilibrium is rare in a plasma) at some finite rate. In an anisotropic plasma, the relaxation rates parallel and perpendicular to an external magnetic field may differ.

4.1.2.2 Thermalization

This same process leads to thermalization of wave energy, or at least a tendency to thermalize, since a steady-state finite amplitude wave may maintain a nonthermal distribution indefinitely. Collisions add a dissipative term to the conductivity tensor so that in general $\langle \mathbf{j} \cdot \mathbf{E} \rangle$, averaged over a cycle, no longer vanishes as it did in the cold collisionless plasma of [chapter 3](#), with the dissipated wave energy going into thermal energy.

4.1.2.3 Validity of linear theory

The interactions between the particles and fields in a plasma are generally nonlinear, but linear descriptions have a bounded region of validity, usually governed by collision processes. In this chapter, we will describe collisionless damping processes, both Landau damping and cyclotron damping, the finite Larmor orbit (FLR) analog of Landau damping, and these will be analyzed with linear theory. Were it not for collisions, however, any finite amplitude

would produce deviations from the linear damping, since particles get trapped in traveling potential wells and eventually cease to exchange energy with the wave on the average, and the wave damping ceases. If collisions remove particles from these shallow potential wells before they ‘thermalize’ in the wells, then the linear analysis gives an accurate representation of the waves. This topic will be analyzed in more detail in [chapters 7 and 8](#) where we treat nonlinear processes, but except for these comments, collisions will be included explicitly for only one case in this chapter, but it is understood that they implicitly underlie the linear theory.

4.1.3 BBGKY theory

The most suitable way of treating the effects of correlations is to begin with an exact description and then proceed in a series of well defined steps to an approximate representation of the general form of equation (4.2). The details of this process are long and involved and beyond the scope of this book [30], but an outline of the process with an indication of the type of approximations and results is presented in order to give a clearer idea of the context in which the kinetic theory of plasma waves is developed.

4.1.3.1 Exact microscopic theory for a many-body system

A complete and exact description of a plasma must describe the coordinate and velocity of each particle of each species, where the total number of particles may exceed 10^{20} particles. Describing each of these particles individually is called a microscopic theory, and the function,

$$n_j(\mathbf{r}, \mathbf{v}, t) = \sum_{i=1}^{N_j} \delta[\mathbf{r} - \mathbf{r}_i(t)]\delta[\mathbf{v} - \mathbf{v}_i(t)] \quad (4.4)$$

is the microscopic distribution function for species j which has the property that

$$\lim_{\Delta\mathbf{r}\Delta\mathbf{v}\rightarrow 0} \int n_j(\mathbf{r}, \mathbf{v}, t) d\mathbf{r} d\mathbf{v}$$

is either equal to unity if a particle is located at the point \mathbf{r}, \mathbf{v} , at time t , or zero otherwise. These particles are sources for the microscopic electric and magnetic fields, given by the Maxwell equations,

$$\nabla \cdot \epsilon_0 \mathbf{E}_\mu = \sum_j q_j \int n_j(\mathbf{R}, t) d\mathbf{v} \quad (4.5)$$

$$\nabla \cdot \mathbf{B}_\mu = 0 \quad (4.6)$$

$$\nabla \times \mathbf{E}_\mu = - \frac{\partial \mathbf{B}_\mu}{\partial t} \quad (4.7)$$

$$\nabla \times \mathbf{B}_\mu = \mu_0 \sum_j q_j \int \mathbf{v} n_j(\mathbf{R}, t) d\mathbf{v} + \frac{1}{c^2} \frac{\partial \mathbf{E}_\mu}{\partial t} \quad (4.8)$$

where \mathbf{R} is the abbreviation for the six-dimensional variable $\mathbf{R} = (\mathbf{r}, \mathbf{v})$. The subscript μ reminds us that these are the microscopic fields.

To these equations describing the microscopic fields we add the equation of motion for the individual particles

$$\frac{d\mathbf{r}_i}{dt} = \mathbf{v}_i \quad \frac{d\mathbf{v}_i}{dt} = \frac{q_i}{m_i}(\mathbf{E}'_\mu + \mathbf{v}_i \times \mathbf{B}'_\mu) \quad (4.9)$$

where the prime denotes that the fields experienced by particle i are due to all the *other* particles so the sum in equation (4.4) is over all *except* particle i . Using these equations of motion, we can then obtain the time evolution equation for the microscopic distribution function as

$$\frac{\partial n_j(\mathbf{R}, t)}{\partial t} + \mathbf{v} \cdot \nabla n_j(\mathbf{R}, t) + \frac{q_j}{m_j}(\mathbf{E}'_\mu + \mathbf{v} \times \mathbf{B}'_\mu) \cdot \nabla_{\mathbf{v}} n_j(\mathbf{R}, t) = 0. \quad (4.10)$$

This expression is a statement of the conservation of particles in phase space, since it implies $d n_j(\mathbf{R}, t)/dt = 0$.

While these equations provide an exact description of the particle motions, they are impractical and serve only as a suitable starting point for the averaging process which leads us to the macroscopic distributions and fields.

Problem 4.1.1. The microscopic distribution function. Prove that the microscopic distribution function evolves according to equation (4.10) using only the equations of motion of equation (4.9) and the definitions.

4.1.3.2 Statistical theory for many-body systems—reduced distributions

Switching to the statistical approach, the system is described by a continuous distribution function which enables one to calculate the probability that a particle is to be found inside a specified volume of phase space, or within a specified volume in configuration space traveling at a velocity within a specified volume of velocity space, all at time t . This distribution function satisfies the Liouville equation for the probability density function in $6N$ dimensional phase space,

$$\frac{dF_N}{dt} = \frac{\partial F_N}{\partial t} + \sum_i v_i \frac{\partial F_N}{\partial x_i} + \sum_i a_i \frac{\partial F_N}{\partial v_i} = 0$$

which is a statement of the conservation of probability. Since F_N is a probability density, it can be normalized to unity as

$$\int F_N d\mathbf{r}_{j1} d\mathbf{r}_{j2} \dots d\mathbf{r}_{jN_j} d\mathbf{r}_{k1} d\mathbf{r}_{k2} \dots d\mathbf{r}_{kN_k} = \int F_N d\mathbf{r}_N = 1 \quad (4.11)$$

where all species j, k, \dots are included and $d\mathbf{r}_N$ represents the entire volume for all particles. This distribution contains essentially the same information and

complexity as the microscopic distribution function, except that it is generally regarded as a continuous function of the variables whereas the microscopic distribution is composed of delta functions.

Reduced functions, as the name implies, have less information and are correspondingly easier to manipulate. The general construction of reduced functions is implemented by integrating over the coordinates of all but one, two, or n particles to produce one-body, two-body, or n -body functions of the coordinates.

Clearly, a one-body distribution function, depending on only six coordinates plus time, is the simplest nontrivial description of the particles, giving the probability of finding a particle of species ℓ in a phase space volume of $d\mathbf{r}_\ell$ as $(1/V \int f_\ell(\mathbf{r}, \mathbf{v}, t) d\mathbf{r})$ where f_ℓ is obtained from

$$f_\ell(\mathbf{r}_{\ell 1}, \mathbf{v}_{\ell 1}, t) = V \int F_N d\mathbf{r}_{\ell 2} d\mathbf{r}_{\ell 3} \dots d\mathbf{r}_{\ell N_\ell} \prod_{j \neq \ell} d\mathbf{r}_{j 1} \dots d\mathbf{r}_{j N_j}. \quad (4.12)$$

It is also clear that this has a reduced amount of information because it gives the same probability of finding a particle of species ℓ at a particular point in phase space regardless of the distance and sign of the nearest neighbor. In other words, correlations between particles are completely ignored in the one-body functions. In order to include such correlations, we need at least a two-body function. A two-body function, where the two particles are of different species, would be defined by

$$f_{\ell m}(\mathbf{r}_{\ell 1}, \mathbf{r}_{m 1}, t) = V^2 \int F_N d\mathbf{r}_{\ell 2} d\mathbf{r}_{\ell 3} \dots d\mathbf{r}_{\ell N_\ell} d\mathbf{r}_{m 2} d\mathbf{r}_{m 3} \dots d\mathbf{r}_{m N_m} \prod_{j \neq \ell, m} d\mathbf{r}_{j 1} \dots d\mathbf{r}_{j N_j}. \quad (4.13)$$

With this two-body distribution function, we have the joint or conditional probability of finding one particle of species ℓ in one volume given that there is another particle of species m in another specific volume. It still ignores the specific locations of all the other particles, but does give a conditional probability and hence includes some correlations. If the correlations were ignored, then we would have $f_{\ell, m} = f_\ell f_m$. If higher order correlations were to be included, these could be treated with three-body or n -body distributions, which have increasingly more information, but become increasingly more complex.

The connection between the microscopic and the n -body distributions comes from recognizing that the trajectories for the microscopic distribution depend on initial conditions, and by taking an ensemble average, or by averaging over possible initial conditions, the bumpiness of the microscopic distribution function is smoothed out and we obtain the F_N probability distribution function. Integrating this over all but one, two, or n particles then leads to the reduced one-body, two-body, or n -body distributions above. This is still a formidable task, and were it not for the fact that there is a convenient smallness parameter due to

Debye shielding of individual particles, namely the reciprocal of the number of particles in a Debye sphere,

$$g \equiv \frac{1}{N_D} = \frac{3}{4\pi n \lambda_D^3} \quad (4.14)$$

there would be little hope of finding any tractable results. Indeed, when the opposite is true, namely when there are few particles in a Debye sphere, this is called a strongly coupled plasma, and relatively few properties of this type of plasma are known, especially the wave properties.

The method of solving for the distribution function when $g \ll 1$ invariably involves $f_{\ell m}$ in solving for f_{ℓ} , and involves $f_{\ell mn}$ in solving for $f_{\ell m}$, etc. The coupling may be written in terms of a correlation function which becomes more complicated at each step and involves the next higher-order reduced distribution function. This chain of equations is called the BBGKY hierarchy [30] of equations, and the smallness of g provides the basis for truncating this hierarchy since if the two-body correlation function is represented by the function $g_{\ell m}$ and the three-body correlation function by $g_{\ell mn}$, then the ordering in g is such that

$$\begin{aligned} f_{\ell} &= \mathcal{O}(1) \\ g_{\ell m} &= \mathcal{O}(g) \\ g_{\ell mn} &= \mathcal{O}(g^2) \end{aligned} \quad (4.15)$$

so that higher order correlations become smaller and smaller as g becomes small. If we neglect all correlations, we arrive at what is often called the collisionless Boltzmann equation, which is identical to equation (4.2) without the right-hand side. We recognize from this discussion that it should rather be called the *correlationless* Boltzmann equation, since it is correlations that are neglected, the collisionless nomenclature being more historical than functional.

One way to picture the difference between a collision and a deflection or correlation is to imagine a trajectory in phase space of a neutral particle when it encounters another neutral particle or a charged particle. Since it is not a Coulomb collision, we take the trajectory to be discontinuous so that it ends abruptly at one point in phase space (it is annihilated) and instantaneously appears at another point in phase space (it is created). Although it is continuous in ordinary space, it is discontinuous in velocity space and hence in phase space. A Coulomb collision, however, is always continuous, as a charged particle makes a multitude of distant encounters and a few close encounters as it is deflected. The trajectory may then have numerous small bends and a few relatively sharp bends, but it is continuous. The encounters between charged particles are accounted for by the *correlations* between the particle locations and no collisions (discontinuous trajectories) occur.

4.1.4 The Vlasov equations

The first and simplest approximation is to keep only the zero order terms in g by neglecting any effects due to correlations. This zero order equation, along

with the Maxwell equations, are called the Vlasov equations, although frequently this collisionless Boltzmann equation alone is referred to as the Vlasov equation. In the singular, we prefer to reference this fundamental equation either as the collisionless Boltzmann equation or as the kinetic equation, and refer to the system of equations as the Vlasov equations.

The Vlasov equations, then, are comprised of the set,

$$\frac{\partial f_j}{\partial t} + \mathbf{v} \cdot \nabla f_j + \frac{q_j}{m_j} (\mathbf{E} + \mathbf{v} \times \mathbf{B}) \cdot \nabla_{\mathbf{v}} f_j = 0 \quad (4.16)$$

for each species along with the Maxwell equations, with

$$\begin{aligned} \rho &= \sum_j q_j \int d^3 v f_j \\ \mathbf{j} &= \sum_j q_j \int d^3 v \mathbf{v} f_j \end{aligned} \quad (4.17)$$

as the sources. This set of equations is nonlinear and its solutions in the linear, quasilinear, and nonlinear approximation will comprise the majority of the remainder of this book. We note that the microscopic equations, equation (4.8) and equation (4.10), are linear but intractable because of the number of particles that must be considered separately. The averaging process has introduced the nonlinearity, but with suitable approximations, the reduced equations may be solved.

4.2 Waves in a thermal, unmagnetized plasma

Using the Vlasov–Maxwell equations, both the limitations of cold plasma (no finite temperature effects) and fluid plasma (phase velocity \gg thermal velocity) may finally be removed. In the unmagnetized plasma, the preferred direction is the \mathbf{k} direction, and motions of particles parallel and perpendicular to that direction will have different effects. We will examine first the general propagation problem in the unmagnetized plasma, but will focus particular attention on the classic problem that serves to illustrate the most important effects of thermal plasmas on waves. This classic case is the $K_{zz} = P = 0$ solution of cold plasma, or the Bohm–Gross solution of section 3.1.2 in the fluid plasma, namely an electrostatic wave near the plasma frequency.

In order to pave the way for more complicated cases later, we are first going to try a simple way to find the solution which will lead us to a dilemma because the method is not well posed. We will then back up and start again with a more carefully posed problem that will provide a recipe to be used with the simpler method so that it may be used subsequently.

4.2.1 Vlasov method

We first linearize the Vlasov equations by separating out zero and first order terms that are assumed to vary as

$$\begin{aligned} f_j &= f_{0j}(\mathbf{v}) + f_{1j}(\mathbf{v})e^{i(\mathbf{k} \cdot \mathbf{r} - \omega t)} \\ \mathbf{E} &= \quad \quad \quad + \mathbf{E}_1 e^{i(\mathbf{k} \cdot \mathbf{r} - \omega t)} \\ \mathbf{B} &= \quad \quad \quad + \mathbf{B}_1 e^{i(\mathbf{k} \cdot \mathbf{r} - \omega t)} \end{aligned} \quad (4.18)$$

and \mathbf{v} is now an independent variable so is not linearized. We choose the normalization of the velocity distribution function so that $\int d^3v f_j = n_j$. Using these results in equations (4.16) and (4.17) along with the Maxwell equations, and assuming only a single species of singly charged ions plus electrons so that charge neutrality requires $n_i = n_e = n_0$, the equations to be solved are

$$-i(\omega - \mathbf{k} \cdot \mathbf{v})f_{1j} + \frac{q_j}{m_j}(\mathbf{E}_1 + \mathbf{v} \times \mathbf{B}_1) \cdot \nabla_v f_{0j} = 0 \quad j = e, i \quad (4.19)$$

$$\begin{aligned} \rho &= e \int d^3v (f_{1i} - f_{1e}) \\ \mathbf{j} &= e \int d^3v \mathbf{v}(f_{1i} - f_{1e}) \end{aligned} \quad (4.20)$$

$$\begin{aligned} i\mathbf{k} \times \mathbf{E}_1 &= i\omega \mathbf{B}_1 \\ i\mathbf{k} \times \mathbf{B}_1 &= \mu_0 \mathbf{j} - \frac{i\omega}{c^2} \mathbf{E}_1. \end{aligned} \quad (4.21)$$

Solving equation (4.19) for $f_{1j}(\mathbf{v})$, the current is given by

$$\mathbf{j} = e^2 \int d^3v \mathbf{v} \frac{(\mathbf{E}_1 + \mathbf{v} \times \mathbf{B}_1) \cdot (\nabla_v f_{0i}/m_i + \nabla_v f_{0e}/m_e)}{i(\omega - \mathbf{k} \cdot \mathbf{v})}. \quad (4.22)$$

Assuming that the zero-order velocity distribution functions are isotropic (depending only on $(v_x^2 + v_y^2 + v_z^2)$), then $\nabla_v f_0$ is in the direction of \mathbf{v} so that $(\mathbf{v} \times \mathbf{B}_1) \cdot \nabla_v f_0 = 0$ and the current simplifies to

$$\mathbf{j} = (\boldsymbol{\sigma}_i + \boldsymbol{\sigma}_e) \cdot \mathbf{E}_1 \quad (4.23)$$

where $\boldsymbol{\sigma}_i$ and $\boldsymbol{\sigma}_e$ are diagonal for $\mathbf{k} = k\hat{e}_z$ and

$$\sigma_{jxx} = \sigma_{jyy} = \sigma_{jt} = \frac{e^2}{im_j} \int d^3v \frac{v_x \frac{\partial f_{0j}}{\partial v_x}}{\omega - kv_z} \quad (4.24)$$

$$\sigma_{jzz} = \sigma_{j\ell} = \frac{e^2}{im_j} \int d^3v \frac{v_z \frac{\partial f_{0j}}{\partial v_z}}{\omega - kv_z}. \quad (4.25)$$

Choosing $f_{0j}(\mathbf{v})$ to be Maxwellian, we find for σ_{et} after integrating over v_x and v_y ,

$$\sigma_{et} = -\frac{n_0 e^2}{im_e} \left(\frac{m_e}{2\pi\kappa T} \right)^{\frac{1}{2}} \int_{-\infty}^{\infty} \frac{e^{-m_e v_z^2/\kappa T}}{\omega - kv_z} dv_z. \quad (4.26)$$

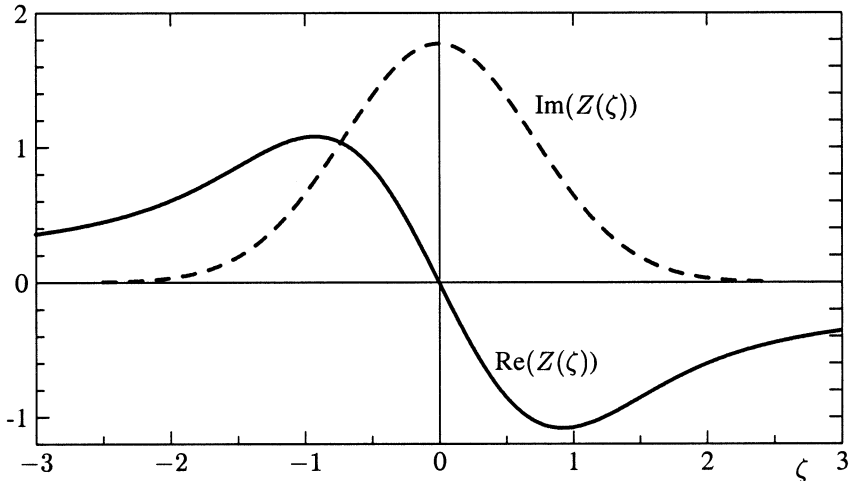


Figure 4.1. Real (full curve) and imaginary (dashed curve) parts of the plasma dispersion function for real ζ .

Now the difficulties begin. It is clear that the integral over v_z has a pole along the path of integration, at $v_z = \omega/k$, and is hence undefined unless we specify that the path should always go above or below the pole. At this point in the problem, Vlasov chose to take the principal part of the integral, or the average of the two paths above and below the pole [25]. This provides symmetry in time, but ignores some of the physics. We shall examine one of the two paths, and try to determine the implications of making one choice or the other after we see the effects of our choice. Let us assume that $\text{Im}(\omega) > 0$, so that ω has a small positive imaginary part which puts the pole just above the path of integration. This choice corresponds to ‘turning on’ the perturbation slowly from $t \rightarrow -\infty$, and happens to coincide with the definition of the plasma dispersion function (PDF) which is a tabulated function [31] defined by

$$Z(\zeta) \equiv \frac{1}{\sqrt{\pi}} \int_{-\infty}^{\infty} \frac{e^{-\xi^2}}{\xi - \zeta} d\xi \quad \text{Im}(\zeta) > 0 \quad (4.27)$$

and whose properties are listed in [appendix B](#). It is a complex analytic function even for real argument and its behavior for real argument is shown in figure 4.1. If we define $v_j^2 \equiv 2\kappa T/m_j$, then we find

$$\sigma_{jt} = \frac{n_0 e^2}{im_j k v_j} Z\left(\frac{\omega}{kv_j}\right). \quad (4.28)$$

For $\sigma_{j\ell}$, integrating by parts in the integral over v_z and comparing with the

derivative of the PDF (under the integral sign), leads to

$$\sigma_{j\ell} = -\frac{n_0 e^2 \omega}{i m_j k^2 v_j^2} Z' \left(\frac{\omega}{k v_j} \right). \quad (4.29)$$

From the conductivity tensor, we construct the dielectric tensor,

$$\mathbf{K} = \mathbf{I} - \frac{\boldsymbol{\sigma}}{i\omega\epsilon_0}$$

such that

$$K_t = 1 + \frac{\omega_{pi}^2}{\omega k v_i} Z \left(\frac{\omega}{k v_i} \right) + \frac{\omega_{pe}^2}{\omega k v_e} Z \left(\frac{\omega}{k v_e} \right) \quad (4.30)$$

$$K_\ell = 1 - \frac{\omega_{pi}^2}{k^2 v_i^2} Z' \left(\frac{\omega}{k v_i} \right) - \frac{\omega_{pe}^2}{k^2 v_e^2} Z' \left(\frac{\omega}{k v_e} \right). \quad (4.31)$$

Problem 4.2.1. Properties of the plasma dispersion function (PDF).

- (i) Prove from the definition of equation (4.27) that the PDF satisfies the differential equation

$$Z'(\zeta) = -2[1 + \zeta Z(\zeta)]. \quad (4.32)$$

- (ii) Expand the denominator of equation (4.27) to obtain the asymptotic expansion of the PDF ($\zeta \rightarrow \infty$). Compare with the result in [appendix B](#) and discuss why this simple expansion fails to get the imaginary part right.

- (iii) Derive the power series expansion for the PDF from its definition and its differential equation, and show that the series may be grouped into two series, one of which may be summed to get an analytic expression.

- (iv) If you were to make a numerical subroutine to evaluate the PDF for real argument, using only the power series and the asymptotic series:

- (a) show how to pick the crossover between the power series and asymptotic series for optimum accuracy; and
- (b) find the optimum crossover point for an eight-digit computer and for a 14-digit computer, and estimate the relative accuracy obtainable on the two machines.

Problem 4.2.2. Cold plasma limit. Show that in the cold plasma limit ($v_e, v_i \rightarrow 0$), both K_t and K_ℓ approach the same limit and that it is the cold plasma dielectric constant.

4.2.1.1 Electrostatic wave

The dispersion relation for longitudinal electrostatic oscillations is simply $P = K_{zz} = K_\ell = 0$. The cold plasma limit is for $v_i \rightarrow v_e \rightarrow 0$, in which case the

arguments of the Z -functions tend toward infinity. The asymptotic forms of the PDF, listed in [appendix B](#), vary for real argument as

$$\begin{aligned} Z(\zeta) &= i\sqrt{\pi}e^{-\zeta^2} - \frac{1}{\zeta} \left(1 + \frac{1}{2\zeta^2} + \frac{3}{4\zeta^4} + \dots \right) \\ Z'(\zeta) &= -2i\sqrt{\pi}\zeta e^{-\zeta^2} + \frac{1}{\zeta^2} \left(1 + \frac{3}{2\zeta^2} + \frac{15}{4\zeta^4} + \dots \right). \end{aligned} \quad (4.33)$$

Using the expansion for Z' for the electron term (the ion terms are of order m_e/m_i unless $T_e \gg T_i$, a case we will treat in section 4.2.5), the dispersion relation becomes

$$K_\ell \simeq 1 - \frac{\omega_{pe}^2}{\omega^2} \left[1 + \frac{3}{2} \left(\frac{v_e}{v_p} \right)^2 \right] + 2i\sqrt{\pi} \frac{\omega_{pe}^2}{k^2 v_e^2} \frac{v_p}{v_e} \exp \left[- \left(\frac{v_p}{v_e} \right)^2 \right] = 0 \quad (4.34)$$

or since $v_e/v_p \ll 1$,

$$\omega \simeq \omega_{pe} \left\{ 1 + \frac{3}{4} \left(\frac{v_e}{v_p} \right)^2 - i\sqrt{\pi} \left(\frac{v_p}{v_e} \right)^3 \exp \left[- \left(\frac{v_p}{v_e} \right)^2 \right] \right\} \quad (4.35)$$

where we see that $\omega \sim \omega_{pe}$ and $\text{Im}(\omega) < 0$! Unfortunately, our assumption about the imaginary part of ω being positive has led to the conclusion that the imaginary part is negative. It is not difficult to show that if we had chosen the imaginary part to be negative, then the analysis would have led to a positive imaginary part! There is no consistent solution, because the problem is ill-posed. While this seems to justify the approach of Vlasov in keeping only the principal part, so that there would be no imaginary part to ω , the question of whether there is or is not any damping of the wave was left unresolved. It did not stay unresolved for long, however, since the solution was provided within a year by Landau, although the result was disputed for over 20 years until unequivocally verified by experiment.

Although the relatively simple expressions for the real and imaginary parts of ω given by equation (4.35) are indicative of the behavior of the dispersion relation for the electrostatic plasma wave, they are not highly accurate, and even give the solution on the left in terms of $v_p = \omega/k$, so they are not complete. A procedure for making the solution more direct is to make successive approximations. Writing $\omega/\omega_{pe} \equiv w$ and $k\lambda_{De} \equiv \kappa$ (where $\lambda_{De}^2 = v_e^2/2\omega_{pe}^2$), we may write $v_e^2/2v_p^2 = \kappa^2/w^2$ so that for the real part of w , we have

$$w_n^2 = \sum_{\ell=0}^n (2\ell+1)!! \left(\frac{\kappa}{w_{n-1}} \right)^{2\ell} \quad (4.36)$$

where each denominator is expanded and each successive approximant is truncated to order $2n$. The first few are $w_0 = 1$, $w_1^2 = 1 + 3\kappa^2$ (the BGDR), etc, leading to the explicit dispersion relation for the real part of ω :

$$\omega_r = \omega_{pe} [1 + 3\kappa^2 + 6\kappa^4 + 24\kappa^6 + 180\kappa^8 + \mathcal{O}(\kappa^{10})]^{1/2}. \quad (4.37)$$

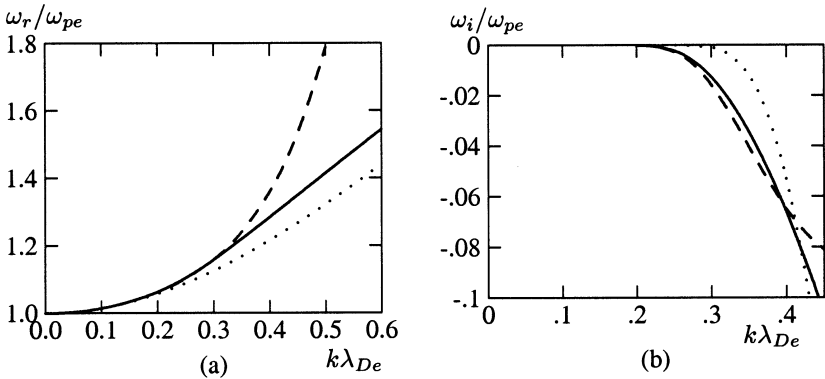


Figure 4.2. Real (a) and imaginary (b) parts of ω in the dispersion relation for the electrostatic plasma wave. In each case, the exact curve is the full curve, the dotted curve is the simplest approximation from equation (4.35), and the dashed curves are higher order approximations (see text).

Even this procedure is flawed, however, since the imaginary part of ω has been ignored. Even using the expression in equation (4.37) through eighth order, the error reaches 1% at $\kappa = 0.333$ and then rises rapidly. A comparison is shown in figure 4.2(a) between the exact expression for ω_r/ω_{pe} (full curve) and w_1 (the Bohm–Gross dispersion relation) (dotted curve) and w_4 from equation (4.37). An empirical formula for the real part of ω ,

$$\omega_r = \omega_{pe} \left[1 + \frac{1.37\kappa^2 + 10.4\kappa^4}{1 + 11.1\kappa^3} \right] \quad (4.38)$$

is accurate to 0.2% for $\kappa \leq 0.6$. This solution is not shown in figure 4.2(a) because it is within a linewidth of the accurate solution over the entire range.

More accurate expressions for the imaginary part of ω are more difficult to obtain. A much improved expression for ω_i is given by Stubbe and Sukhorukov [32]:

$$\omega_i = -\sqrt{\frac{\pi}{8}} \frac{\omega_{pe}}{\kappa^3(1+3\kappa^2)} \exp \left[-\frac{1+3\kappa^2}{2\kappa^2} \right]. \quad (4.39)$$

Figure 4.2(b) shows the exact behavior for ω_i (full curve), the simple expression from equation (4.35) with $v_p/v_e \rightarrow 1/\sqrt{2}\kappa$ (dotted curve) and the more accurate expression from equation (4.39) (dashed curve).

4.2.2 Landau solution

In 1946, Landau [33] recognized that the difficulty could be resolved by treating the problem as an initial value problem rather than using the Fourier transform

of Vlasov. Because of the importance of this and other related problems, we follow the Landau development closely, but restrict our attention to longitudinal plasma oscillations only and consider only the initial value problem in time rather than include the time harmonic antenna problem (which is treated, however, in Landau's original paper). We will also neglect ion motions, since they play little role (unless $T_e \gg T_i$ as noted earlier), and since the ion terms are so similar in form to the electron terms.

For the electrostatic case, $\mathbf{k} \parallel \mathbf{E}$, so $\mathbf{k} \times \mathbf{E} = 0$ and $\mathbf{E} = -\nabla\varphi$. The equations to be solved are then

$$\frac{\partial f_1}{\partial t} + \mathbf{v} \cdot \nabla f_1 - \frac{e}{m_e} \mathbf{E} \cdot \nabla_{\mathbf{v}} f_0 = 0 \quad (4.40)$$

$$\nabla \cdot \mathbf{E} = -\nabla^2\varphi = -\frac{e}{\epsilon_0} \int d^3v f_1 = -\frac{\rho}{\epsilon_0}. \quad (4.41)$$

Taking the Fourier transform in space,

$$f_1(\mathbf{r}, \mathbf{v}, t) = \tilde{f}(\mathbf{v}, t)e^{i\mathbf{k}\cdot\mathbf{r}}$$

$$\varphi(\mathbf{r}, t) = \tilde{\varphi}(t)e^{i\mathbf{k}\cdot\mathbf{r}}$$

the equations become, with $\mathbf{k} = k\hat{\mathbf{e}}_z$,

$$\frac{\partial \tilde{f}}{\partial t} + ikv_z \tilde{f} + \frac{e}{m_e} ik\tilde{\varphi} \frac{\partial f_0}{\partial v_z} = 0 \quad (4.42)$$

$$k^2 \tilde{\varphi} = -\frac{e}{\epsilon_0} \int d^3v \tilde{f} \quad (4.43)$$

where $f_0(\mathbf{v})$ is given and $\tilde{f}(\mathbf{v}, 0) \equiv g(\mathbf{v})$ is the given initial perturbation.

For the initial value problem in time, it is convenient to use the Laplace transform of the time variable,

$$X_p(\mathbf{v}, p) = \int_0^\infty e^{-pt} X(\mathbf{v}, t) dt \quad (4.44)$$

and its inverse

$$X(\mathbf{v}, t) = \int_{\sigma-i\infty}^{\sigma+i\infty} e^{pt} X_p(\mathbf{v}, p) \frac{dp}{2\pi i} \quad (4.45)$$

where σ ($\sigma > 0$) is to the right of all singularities of X_p . The Laplace transform of the time derivative is

$$\left(\frac{dX}{dt} \right)_p = pX_p + [X e^{-pt}]_{t=0}^{t \rightarrow \infty}.$$

The condition on σ comes from the assumption that $|\tilde{f}(\mathbf{v}, t)| < |M e^{\gamma t}|$, i.e. that the growth of \tilde{f} is bounded, and that $\text{Re}(p) > |\gamma|$. The Laplace transforms of

equations (4.42) and (4.43) are:

$$(p + ikv_z)\tilde{f}_p + \frac{e}{m_e}ik\tilde{\varphi}_p \frac{\partial f_0}{\partial v_z} = \tilde{f}(\mathbf{v}, 0) \equiv g(\mathbf{v}) \quad (4.46)$$

$$k^2\tilde{\varphi}_p = -\frac{e}{\epsilon_0} \int d^3v \tilde{f}_p \quad (4.47)$$

from which we deduce that

$$\tilde{f}_p(\mathbf{v}, k, p) = \frac{g(\mathbf{v}) - \frac{e}{m_e}ik\tilde{\varphi}_p \frac{\partial f_0}{\partial v_z}}{(p + ikv_z)} \quad (4.48)$$

$$\begin{aligned} \tilde{\varphi}_p &= -\frac{e}{\epsilon_0 k^2} \int d^3v \frac{g(\mathbf{v}) - \frac{e}{m_e}ik\tilde{\varphi}_p \frac{\partial f_0}{\partial v_z}}{(p + ikv_z)} \\ &= \frac{-\frac{e}{\epsilon_0} \int d^3v \frac{g(\mathbf{v})}{(p + ikv_z)}}{k^2 \left[1 + \frac{e^2}{m_e \epsilon_0 ik} \int d^3v \frac{\frac{\partial f_0}{\partial v_z}}{(p + ikv_z)} \right]}. \end{aligned} \quad (4.49)$$

We integrate first over v_x and v_y , using the notation,

$$\begin{aligned} g(u) &= \int_{-\infty}^{\infty} \int_{-\infty}^{\infty} g(\mathbf{v}) dv_x dv_y \\ \frac{d f_0(u)}{du} &= \int_{-\infty}^{\infty} \int_{-\infty}^{\infty} \frac{\partial f_0(\mathbf{v})}{\partial v_z} dv_x dv_y \end{aligned}$$

and we let $v_z \rightarrow u$. The remaining pair of equations is now one-dimensional,

$$\tilde{f}_p(u, k, p) = \frac{g(u) - \frac{e}{m_e}ik\tilde{\varphi}_p \frac{d f_0(u)}{du}}{(p + iku)} \quad (4.50)$$

$$\tilde{\varphi}_p(k, p) = \frac{-\frac{e}{\epsilon_0} \int_{-\infty}^{\infty} \frac{g(u) du}{(p + iku)}}{k^2 \left[1 + \frac{e^2}{m_e \epsilon_0 ik} \int_{-\infty}^{\infty} \frac{\frac{d f_0(u)}{du} du}{(p + iku)} \right]}. \quad (4.51)$$

The inverse transformation is

$$\varphi(z, t) = \int_{\sigma-i\infty}^{\sigma+i\infty} \frac{dp}{2\pi i} \int_{-\infty}^{\infty} \frac{dk}{2\pi} e^{ikz+pt} \tilde{\varphi}_p(k, p). \quad (4.52)$$

The normal path of integration as defined in the complex p -plane is to the right of all singularities as shown by the dashed line in figure 4.3. If, however, we deform the contour far enough to the left, the large negative real part of p eliminates the contribution from the vertical portion of the contour. Landau proposed moving the path to the left, but keeping to the right of all singularities and around all branch cuts as shown by the full path in figure 4.3. Since

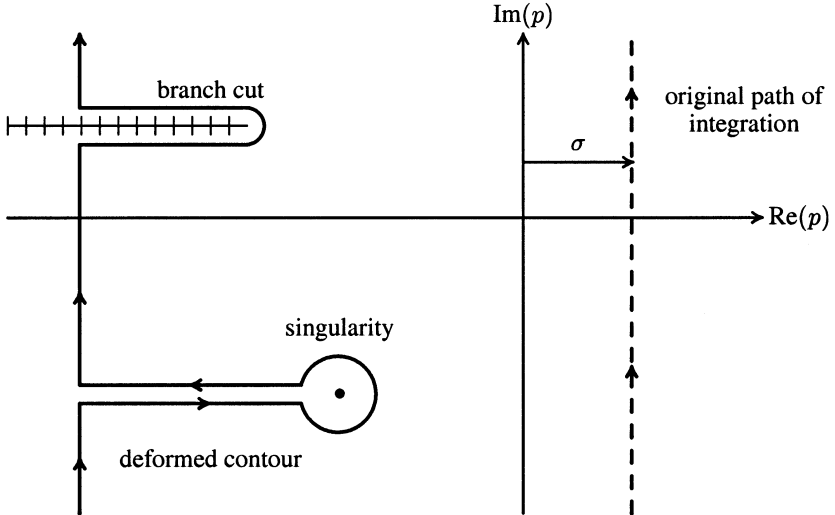


Figure 4.3. The Landau contour is moved to the left but remains to the right of all singularities and branch points.

the vertical portion of the contour no longer contributes, only the singularities (residues) and branch cuts need be evaluated. Consider the contribution from singularities, assuming there are no branch cuts. Then,

$$\begin{aligned}\tilde{\varphi}(k, t) &= \int_{\substack{\text{deformed} \\ \text{contour}}} \frac{dp}{2\pi i} e^{pt} \tilde{\varphi}_p(k, p) \\ &= \sum_n e^{p_n t} [(p - p_n) \tilde{\varphi}_p(k, p)]_{p=p_n}.\end{aligned}\quad (4.53)$$

Due to the $e^{p_n t}$ factor, after a short time only the rightmost pole in the p -plane will contribute to $\tilde{\varphi}(k, t)$, so the sum collapses to a single term.

In order to evaluate this remaining expression, we need to know $\tilde{\varphi}_p$ in a region where it was not defined, since it was defined for $\text{Re}(p) > |\gamma|$, and we need to know $\tilde{\varphi}_p$ for $\text{Re}(p) < |\gamma|$. It is this point which led to the difficulties in the Vlasov method. Here, however, we can study the analytic continuation (see [appendix A.2](#)) of $\tilde{\varphi}_p$ as we deform the contour. Since $\tilde{\varphi}_p$ is the ratio of two terms, we must investigate the numerator and denominator separately.

In the numerator of the expression for $\tilde{\varphi}_p$ in equation (4.51), we may take $g(u)$ to be an entire function of u (no poles in the complex u -plane), so that the integral,

$$G\left(\frac{ip}{k}\right) = -\frac{ie k}{\epsilon_0} \int_{-\infty}^{\infty} \frac{g(u) du}{u - ip/k} \quad (4.54)$$

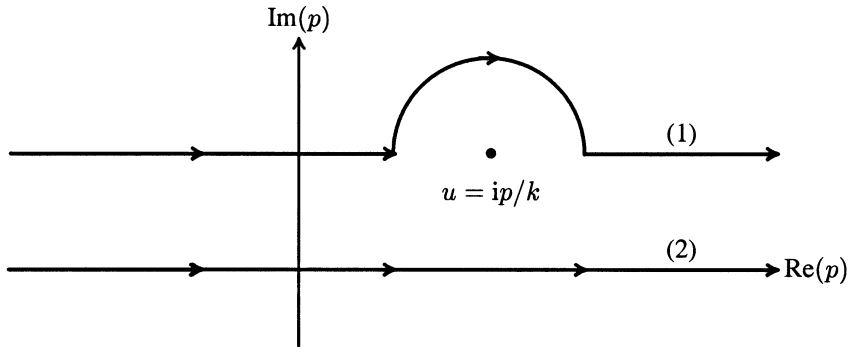


Figure 4.4. Paths above and below the singularity. Path (1) is the prescribed path.

can be evaluated by the residue theorem,

$$G\left(\frac{ip}{k}\right)_{(1)} = G\left(\frac{ip}{k}\right)_{(2)} + 2\pi i[g(u)]_{u=ip/k}$$

where the paths (1) and (2) are shown in figure 4.4.

The contour (1) is the prescribed contour, but note that it is equal to the contour (2) plus a contribution from the pole. As $\text{Re}(p)$ goes to negative values, contour (2) remains analytic, and since g was assumed analytic, $G(ip/k)_{(1)}$ is also always analytic provided we integrate *under* the pole (sometimes called the Nautilus convention) as in figure 4.5. With this convention, the numerator is always an entire function of p , or analytic everywhere.

Similar arguments apply to the denominator of $\tilde{\varphi}_p$ since $f(u)$ is also assumed to be an entire function of u , or analytic. Thus the only poles of $\tilde{\varphi}_p$ occur at the zeros of the denominator, and there are no branch cuts.

The value of p that makes the denominator vanish is the value such that

$$\begin{aligned} 1 + \frac{e^2}{m_e \epsilon_0 ik} \int_{-\infty}^{\infty} \frac{\frac{df_0(u)}{du}}{p + iku} du &= 0 \quad \text{Re}(p) > 0 \\ 1 + \frac{e^2}{m_e \epsilon_0 ik} \int_{-\infty}^{\infty} \frac{\frac{df_0(u)}{du}}{p + iku} du + \frac{e^2 2\pi i}{m_e \epsilon_0 (ik)^2} \left. \frac{df_0(u)}{du} \right|_{u=ip/k} &= 0 \quad \text{Re}(p) < 0 \end{aligned}$$

where both integrals are along the real axis.

The principal value of an integral through an isolated singular point is the average of the two integrals along paths just to either side of the point. We can use the concept to combine these two equations into one that is valid for all values of p :

$$1 + \frac{e^2}{m_e \epsilon_0 ik} \oint_{-\infty}^{\infty} \frac{\frac{df_0(u)}{du}}{p + iku} du - \frac{\pi i e^2}{m_e \epsilon_0 k^2} \left. \frac{df_0(u)}{du} \right|_{u=ip/k} = 0. \quad (4.55)$$

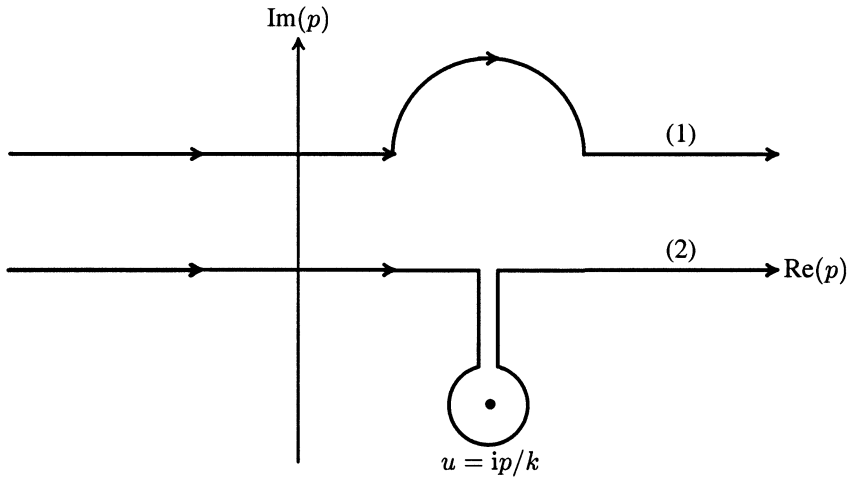


Figure 4.5. Analytic continuation by deforming the path to remain below the pole when $\text{Re}(p) < 0$.

If we now let $ip = \omega$ and use equation (4.34) to approximate the principal part, we may write this as

$$1 - \frac{\omega_{pe}^2}{\omega^2} \left[1 + \frac{3}{2} \left(\frac{v_e}{v_p} \right)^2 + \dots \right] - i\epsilon_i \simeq 0 \quad (4.56)$$

where

$$\epsilon_i = \frac{\pi \omega_{pe}^2}{k^2} \left. \frac{df_0(u)}{du} \right|_{u=\omega/k} = 0 \quad (4.57)$$

if we normalize $\int f_0 du = 1$ (instead of $\int f_0 du = n_0$). Then, breaking ω into real and imaginary parts, equation (4.56) becomes

$$(\omega_r + i\gamma)^2 \simeq \omega_{pe}^2 [1 + \mathcal{O}(v_e/v_p)^2] + i\omega^2 \epsilon_i$$

so if $\gamma \ll \omega_r$, then the imaginary part is given by

$$\gamma = \frac{1}{2} \omega_r \epsilon_i = \omega_r \frac{\pi \omega_{pe}^2}{2k^2} \left. \frac{df_0(u)}{du} \right|_{u=\omega_r/k} \quad (4.58)$$

and the sign of the imaginary part depends on the slope of the distribution function at the phase velocity.

If we take f_0 to be Maxwellian, then equation (4.55) becomes

$$1 + \frac{\omega_{pe}^2}{k^2 v_e} \wp \frac{1}{\sqrt{\pi}} \int_{-\infty}^{\infty} \frac{\frac{d}{du} [\exp(-u^2/v_e^2)] du}{\omega/k - u} + 2\sqrt{\pi} i \frac{\omega_{pe}^2 \omega}{k^3 v_e^3} e^{-(\omega/k v_e)^2} = 0. \quad (4.59)$$

Integrating by parts, this becomes

$$1 - \frac{\omega_{pe}^2}{k^2 v_e^2} \wp \frac{1}{\sqrt{\pi}} \int_{-\infty}^{\infty} \frac{\exp(-u^2/v_e^2) du}{(u - \omega/k)^2} + 2\sqrt{\pi} i \frac{\omega_{pe}^2 \omega}{k^3 v_e^3} e^{-(\omega/k v_e)^2} = 0. \quad (4.60)$$

For this case, the imaginary part of ω is given (to lowest order) by

$$\gamma = -\sqrt{\pi} \frac{\omega_{pe}^2 \omega_r^2}{k^3 v_e^3} e^{-(\omega_r/k v_e)^2} \quad (4.61)$$

and the dispersion relation is equivalent to

$$1 - \frac{\omega_{pe}^2}{k^2 v_e^2} Z' \left(\frac{\omega}{k v_e} \right) = 0 \quad (4.62)$$

which is the same result we got by the Vlasov method.

Throughout this discussion, we have assumed that $k > 0$. If this is not the case, then we must change our prescription. If $k < 0$, then the pole lies below the path of integration, so we must integrate *over* the pole (Byrd convention¹). Only the sign of the imaginary part changes, so that sometimes the PDF is written

$$Z \left(\frac{\omega}{k v_e} \right) = \frac{1}{\sqrt{\pi}} \wp \int_{-\infty}^{\infty} \frac{e^{-\xi^2} d\xi}{\left(\xi - \frac{\omega}{k v_e} \right)} + \left(\frac{k}{|k|} \right) i \sqrt{\pi} e^{-(\omega/k v_e)^2}. \quad (4.63)$$

It may seem surprising that the same result is obtained by both the Vlasov and Landau methods, but actually the Landau solution serves to justify the assumption we made that ω should have a small positive imaginary part in the Vlasov method. The initial value problem and the assumption that the perturbation was ‘turned on slowly’ from infinitely long ago both result in the recipe that the velocity integral should go under the pole. The fact that ω has a negative imaginary part is now seen as resulting from the initial value problem, guaranteeing that disturbances decay away if there are no sources of free energy, and is called Landau damping. Having done this problem both ways, we can now choose whichever is most convenient in the future as the meaning of the recipe is now clear. When magnetic field effects are included, it will be much simpler to use the Vlasov method with Fourier transforms in both time and space than to do the initial value problem.

Problem 4.2.3. Landau damping with a Lorentzian distribution.

- (i) Find the normalization constant A for the Lorentzian velocity distribution function $f_0(u) = A/(v_e^2 + u^2)$.

¹ Just as the Nautilus submarine first sailed under the North Pole, Admiral Byrd first flew over the pole!

- (ii) Find closed form expressions for both $\tilde{f}_p(u, k, p)$ and $\tilde{\varphi}_p(k, p)$ with $g(u) = f_0(u)\Delta u$ with Δ a constant.
- (iii) Do the inverse Laplace transform for both $\tilde{f}(u, k, t)$ and $\tilde{\varphi}(k, t)$ and show that the potential $\tilde{\varphi}$ decays in time but that \tilde{f} has a term that does not decay in time.

4.2.3 A Physical picture of Landau damping

The physical interpretation of Landau damping, where information seems to be lost without any collisions or other apparent randomizing interactions, requires careful analysis at more than one level. While the treatment has been strictly linear, it will become apparent that nonlinear effects must be brought in to fully understand the nature of Landau damping, but that linear calculations can be used to calculate the damping rate.

The history of this problem is long and surprising in many ways. Landau's 1946 calculation was followed by years of active debate about the correctness of the result. Although generally accepted, there were holdouts challenging the validity of the result until unequivocal experimental results settled the accuracy of Landau damping [34]. The acceptance of the mathematical result did not end discussions about the interpretation of the collisionless damping, however, as many physically appealing but technically incorrect explanations were given by many, including this author. The following sections explore a recent analysis by Stubbe and Sukhorukov [32] who give a critical look at the physics. The analysis begins with a variation on the usual method of taking moments that includes the kinetic effects.

4.2.3.1 Kinetic transport equations

The development of fluid-like moment equations that maintain the kinetic information has been implemented by Stubbe [35]. The development begins in the usual manner with the collisionless kinetic equation in one dimension,

$$\frac{\partial f}{\partial t} + u \frac{\partial f}{\partial z} + \frac{q}{m} E \frac{\partial f_0}{\partial u} = 0$$

where the zero-order velocity distribution is

$$f_0(u) = \frac{N_0}{\sqrt{\pi} v_t} e^{-(u-v_0)^2/v_t^2}.$$

Writing this in terms of the random component, $w = u - v_0$, this becomes

$$\left(\frac{\partial}{\partial t} + w \frac{\partial}{\partial z} + v_0 \frac{\partial}{\partial z} \right) f_1 = \frac{2q}{mv_t^2} E w f_0$$

where $f_1 = f - f_0$. Fourier transforming in space and time, so that $\partial/\partial t \rightarrow -i\omega$, $\partial/\partial z \rightarrow ik$, $f_1 \rightarrow \tilde{f}$, and $E \rightarrow \tilde{E}$, we find

$$\tilde{f} = \frac{2iqf_0}{mv_t^2} \frac{w\tilde{E}}{\omega' - kw}$$

where $\omega' = \omega - kv_0$.

We then take moments such that

$$\tilde{n} = \int \tilde{f} dw \quad (4.64)$$

$$\tilde{v} = \frac{1}{N_0} \int \tilde{f} w dw \quad (4.65)$$

and find

$$\frac{\tilde{n}}{N_0} = - \frac{2iq\tilde{E}}{mv_t^2 k} Z_1(\zeta') \quad (4.66)$$

$$\tilde{v} = - \frac{2iq\tilde{E}}{mkv_t} Z_2(\zeta') = \frac{iq\tilde{E}}{m\omega'} [1 - 2Z_3(\zeta')] \quad (4.67)$$

where $\zeta' = \omega'/kv_t$ and the $Z_n(\zeta)$ are generalized dispersion functions, defined by

$$Z_n(\zeta) = \frac{1}{\sqrt{\pi}} \mathcal{P} \int_C \frac{z^n e^{-z^2}}{z - \zeta} dz + i\sqrt{\pi} \frac{k}{|k|} \zeta^n e^{-\zeta^2} \quad (4.68)$$

so that $Z_0(\zeta) = Z(\zeta)$. The properties of the Z_n are described in [appendix B](#) where it is shown that $2Z_3(\zeta) = 2\zeta Z_2(\zeta) + 1$.

It is now desired to extend our idea of moment equations so that they have the information of fluid equations and reduce to them as $\zeta \rightarrow \infty$, but retain the kinetic information as well. To this end, we write the first two moment equations as

$$\frac{\partial N}{\partial t} + N \frac{\partial v}{\partial z} = R_1 \quad (4.69)$$

$$\frac{\partial v}{\partial t} - \frac{q}{m} E = R_2 \quad (4.70)$$

where $N = N(z, t)$, $v = v(z, t)$ and $E = E(z, t)$. Equation (4.69) is the continuity equation, and exact, so that $R_1 = 0$ (as may be shown from equations (4.66) and (4.67)). In order to determine R_2 , however, we must first write v from equation (4.67) as

$$v(z, t) = \frac{1}{(2\pi)^2} \int d\omega dk \tilde{v} e^{i(kz - \omega t)} \quad (4.71)$$

$$= \frac{iq}{m(2\pi)^2} \int d\omega dk \tilde{E} [1 - 2Z_3(\zeta')] e^{i(kz - \omega t)}. \quad (4.72)$$

Taking $z = v_0 t$, the exponent becomes $kz - \omega t \rightarrow (kv_0 - \omega)t = -\omega't$, so that we have

$$\frac{\partial v}{\partial t} = -\frac{i}{(2\pi)^2} \int d\omega dk \omega' \tilde{v} e^{-i\omega't} \quad (4.73)$$

$$= \frac{q}{m(2\pi)^2} \int d\omega dk \tilde{E} [1 - 2Z_3(\xi')] e^{-i\omega't} \quad (4.74)$$

so that

$$R_2 = \frac{\partial v}{\partial t} - \frac{q}{m} E = \frac{q}{m(2\pi)^2} \int d\omega dk e^{-i\omega't} [\tilde{E}(1 - 2Z_3) - \tilde{E}] \quad (4.75)$$

$$= -\frac{q}{2m\pi^2} \int d\omega dk e^{-i\omega't} Z_3(\xi') \tilde{E}. \quad (4.76)$$

Since all $Z_n(\xi) \rightarrow 0$ as $\xi \rightarrow \infty$, it is apparent that R_2 is a kinetic term that vanishes asymptotically in the cold plasma limit. We can also use equation (4.66) to eliminate \tilde{E} and write R_2 as

$$R_2 = -\frac{iv_t^2}{(2\pi)^2} \int d\omega dk e^{-i\omega't} \frac{k\tilde{n}}{N_0} \frac{Z_3(\xi')}{Z_1(\xi')}.$$

Noting that

$$\frac{1}{N_0} \frac{\partial N}{\partial z} = \frac{i}{(2\pi)^2} \int d\omega dk e^{-i\omega't} \frac{k\tilde{n}}{N_0}$$

the kinetic transport equations may be written in the form

$$\frac{\partial N}{\partial t} + N \frac{\partial v}{\partial z} = 0 \quad (4.77)$$

$$\frac{\partial v}{\partial t} - \frac{q}{m} E = \frac{\gamma v_t^2}{2} \frac{1}{N_0} \frac{\partial N}{\partial z} \quad (4.78)$$

where

$$\gamma = \frac{\int d\omega dk e^{-i\omega't} k\tilde{n} 2Z_3(\xi') / Z_1(\xi')}{\int d\omega dk e^{-i\omega't} k\tilde{n}}.$$

In this form, it is clear that all of the kinetic effects are contained in the factor γ which has the limit $\gamma \rightarrow 3$ as $\xi' \rightarrow \infty$ which is the fluid limit and in the opposite limit, $\gamma \rightarrow 1$ as $\xi' \rightarrow 0$, which is the subsonic limit. It is important to note that this set of equations is an *exact* moment representation of the kinetic equation. All of the kinetic effects are contained in the expression for γ .

If we move back into the Fourier-transformed variables, the kinetic transport equations become

$$-i\omega \frac{\tilde{n}}{\tilde{n}} + ik\tilde{v} = 0 \quad (4.79)$$

$$-i\omega \tilde{v} - \frac{q}{m} \tilde{E} = -\frac{ikv_t^2}{2} \frac{\tilde{p}}{p} = -\frac{ikv_t^2}{2} \gamma \frac{\tilde{n}}{\tilde{n}} \quad (4.80)$$

with $\gamma(\zeta) = 2G_3(\zeta)/G_1(\zeta)$ so that $\tilde{M}^{(2)} = v_t^2 \gamma \tilde{n}/2$ from section 3.1.2. This is now exact and includes both real and imaginary parts for the second moment term. The fact that kinetic effects occur exclusively in γ indicates that they are independent of charge, and indeed such collisionless damping has been observed in sound waves in a dilute gas (where collisions may be neglected) [36].

If we break up the frequency into real and imaginary parts so that $\omega = \omega_R + i\Gamma$ and the damping is weak, the damping rate may be written as

$$\frac{\Gamma}{\omega_R} = \sqrt{\pi} \zeta_R^3 \left(1 - \frac{3}{\zeta_R^2} + \mathcal{O}(\zeta_R^{-4}) \right) e^{-\zeta_R^2} \quad (4.81)$$

for large ζ_R . It is apparent that this expression is again independent of charge and only dependent on thermal effects. The fact that Landau damping does not depend on the existence of charge has also been noted by Hammett and Perkins [37]. Their treatment obtained the result when ζ is small but not the result when ζ is large.

4.2.3.2 Energy considerations for Landau damping

One point about the physics of Landau damping has already been made, namely that it does not depend on charge and therefore is *not* a purely plasma phenomenon. Since our most common explanations of the physics are in terms of charges and electric fields, they are evidently deficient. In our search for a proper description, we need to examine some of the energy balances involved. For this, we will use the first three moment equations written as

$$\frac{dN}{dt} + N \frac{\partial v}{\partial z} = 0 \quad (4.82)$$

$$\frac{\partial v}{\partial t} + \frac{1}{2} \frac{\partial v^2}{\partial z} - \frac{q}{m} E = - \frac{1}{mN} \frac{\partial p}{\partial z} \quad (4.83)$$

$$\frac{\partial p}{\partial t} + 2p \frac{\partial v}{\partial z} = - \frac{\partial}{\partial z} (vp + q) \quad (4.84)$$

where the pressure p and heat flow q are related to the moments $M^{(n)}$ of section 3.1.2 such that $p = mM^{(2)}$ and $q = M^{(3)}$. For this analysis, these equations are not fluid equations, but exact moments of the kinetic equation. Along with these moment equations, we have the energy densities

$$w_E = \frac{1}{2} \epsilon_0 E^2 \quad (4.85)$$

$$w_K = \frac{1}{2} \bar{n} m v^2 \quad (4.86)$$

where w_E is the electrostatic energy density and w_K is the kinetic energy density. We need to add a third energy density related to the compressional energy density, w_C . If we consider a gas with a constant number of particles

N_0 in a container of volume V , then reducing the volume in the z -direction requires work done *on* the gas $dw = -pdV$. Since $dV/V = -dN/N$, the work may also be expressed as $dW = -p(V/N)dN$. Doing this work on the gas increases its compressional energy by the amount $dE_C = dW$. The corresponding change in the compressional energy density, $w_C = E_C/V$, is $dw_C = (1/V)dE_C - w_C dV/V = (w_C + p)dN/N$. Then using the continuity equation of equation (4.82),

$$\frac{dw_C}{dt} = \frac{\partial w_C}{\partial t} + v \frac{\partial w_C}{\partial z} = -(p + w_C) \frac{\partial v}{\partial z}$$

we obtain

$$\frac{\partial w_C}{\partial t} = -p \frac{\partial v}{\partial z} - \frac{\partial}{\partial z}(vw_C). \quad (4.87)$$

For the electrostatic energy density, the Maxwell equations give

$$\frac{\partial w_E}{\partial t} = -jE \quad (4.88)$$

where $j = Nqv$. For the w_K term, we multiply equation (4.83) by Nmv to obtain

$$\frac{\partial w_K}{\partial t} = (p + w_K) \frac{\partial v}{\partial z} + jE - \frac{\partial}{\partial z} \left(pv + \frac{Nm v^3}{2} \right). \quad (4.89)$$

If we now average each of these terms over a wavelength, so that

$$\bar{w}(t) \equiv \frac{1}{\lambda} \int_z^{z+\lambda} w(z, t) dz$$

the last terms in equations (4.87) and (4.89) vanish and the sum of equations (4.87) through (4.89) is

$$\frac{d\bar{w}_K}{dt} + \frac{d\bar{w}_E}{dt} + \frac{d\bar{w}_C}{dt} = 0. \quad (4.90)$$

Extending now to second order, with

$$N = N_0 + N_1 + N_2 \quad (4.91)$$

$$v = v_1 + v_2 \quad (4.92)$$

$$E = E_1 + E_2 \quad (4.93)$$

$$p = p_0 + p_1 + p_2 \quad (4.94)$$

the rates of change of the energy densities are given by

$$\frac{d\bar{w}_K}{dt} = \frac{d\bar{w}_{K2}}{dt} = \frac{N_0 m}{2} \frac{dv_1^2}{dt} \quad (4.95)$$

$$\frac{d\bar{w}_E}{dt} = \frac{d\bar{w}_{E2}}{dt} = \frac{\epsilon_0}{2} \frac{dE_1^2}{dt} \quad (4.96)$$

$$\frac{d\bar{w}_C}{dt} = \frac{d\bar{w}_{C2}}{dt} = -p_1 \frac{\partial v_1}{\partial t} = \frac{1}{N_0} p_1 \frac{\partial N_1}{\partial t}. \quad (4.97)$$

Two important observations follow from these equations: (1) the spatially averaged energy densities contain no first-order contributions so that the *physics of Landau damping cannot be discovered from energy considerations*; and (2) the second-order energy terms are obtained from products of first order terms, so *the linear damping rate may be determined from a linear analysis*.

4.2.3.3 A special case

A surprising result may be obtained from a special case where we set

$$N_1(z, t) = N_0 n_1(t) \cos(kz - \omega_R t) \quad (4.98)$$

and assume weak damping, indicated by $(1/n_1)(dn_1/dt) \ll \omega_R$. We then proceed to calculate the various energy densities. First, from equations (4.85) and (4.96) and Poisson's equation given here by

$$\epsilon_0 \frac{\partial E}{\partial z} = q N_1$$

we find

$$\frac{d\overline{w_E}}{dt} = \frac{N_0 m \omega_p^2}{4k^2} \frac{dn_1^2}{dt^2}$$

which may also be written as

$$\frac{1}{\overline{w_E}} \frac{d\overline{w_E}}{dt} = \frac{1}{n_1^2} \frac{dn_1^2}{dt}. \quad (4.99)$$

Then, from equations (4.86), (4.95), and (4.82), written as

$$\frac{dN_1}{dt} = -N_0 \frac{dv}{dz}$$

we find (assuming weak damping as noted earlier)

$$\frac{d\overline{w_K}}{dt} = \frac{N_0 m \omega_R^2}{4k^2} \frac{dn_1^2}{dt^2}$$

or alternatively,

$$\frac{1}{\overline{w_K}} \frac{d\overline{w_K}}{dt} = \frac{1}{n_1^2} \frac{dn_1^2}{dt}. \quad (4.100)$$

Together, equations (4.99) and (4.100) show that both the electrostatic energy and the kinetic energy have the same relative damping rates, and therefore they decay together. A corresponding expression can be obtained from equations (4.97) and (4.83) where the latter is used to express p in terms of v and E , with the result

$$\frac{d\overline{w_C}}{dt} = -\frac{N_0 m}{4k^2} (\omega_p^2 + \omega_R^2) \frac{dn_1^2}{dt} \quad (4.101)$$

but the result could just as easily have been obtained from equations (4.99) and (4.100) along with equation (4.90), since it is not independent.

4.2.3.4 Polytropic and nonpolytropic gases

We now consider a case where p and N_1 are proportional and in phase (the previous example has both in phase and out-of-phase terms), which is called a polytropic gas. The polytropic coefficient, γ , is defined by

$$\frac{dp}{p} \equiv \gamma \frac{dN}{N} \quad (4.102)$$

where γ is complex in general, but may be real. For our first example, we choose the relation to be

$$p = \alpha m v_t^2 N_1$$

where α is real. Then equation (4.97) becomes

$$\frac{d\overline{w_C}}{dt} = \frac{m v_t^2}{N_0} \alpha N_1 \overline{\frac{\partial N_1}{\partial t}}.$$

Carrying on one step further with equation (4.98), we may write

$$\frac{d\overline{w_C}}{dt} = \frac{N_0 m v_t^2}{4} \alpha \frac{dn_1^2}{dt}.$$

This result may be combined with equation (4.101) to find

$$(\omega_R^2 + \omega_p^2 + \alpha k^2 v_t^2) \frac{dn_1^2}{dt} = 0.$$

The three wave energy terms represent the kinetic energy (ω_R^2), the electrostatic energy (ω_p^2), and the compressional energy ($\alpha k^2 v_t^2$), and the perhaps surprising result is that a (one constituent) polytropic gas is undamped.

If we generalize to a case where there is also an out-of-phase component, making the gas nonpolytropic, such as

$$p = m v_t^2 \left(\alpha N_1 + \beta \frac{\partial N_1}{\partial t} \right) \quad (4.103)$$

then the results go over to

$$\frac{d\overline{w_C}}{dt} = \frac{m v_t^2}{N_0} \left[\alpha \overline{N_1 \frac{\partial N_1}{\partial t}} + \beta \overline{\left(\frac{\partial N_1}{\partial t} \right)^2} \right] \quad (4.104)$$

$$= \frac{N_0 m}{4k^2} \left(\alpha k^2 v_t^2 \frac{dn_1^2}{dt} + 2\beta k^2 v_t^2 \omega_R^2 n_1^2 \right) \quad (4.105)$$

and

$$(\omega_R^2 + \omega_p^2 + \alpha k^2 v_t^2) \frac{dn_1^2}{dt} = -2\beta k^2 v_t^2 \omega_R^2 n_1^2. \quad (4.106)$$

We may identify the constants α and β from equation (4.80) as $\alpha = \text{Re}(Z_3/Z_1)$ and $\beta = -(1/\omega) \text{Im}(Z_3/Z_1)$. Assuming weak damping, where $\zeta \rightarrow \zeta_R$, we have

$$\alpha = \text{Re} \left(\frac{Z_3(\zeta_R)}{Z_1(\zeta_R)} \right) \quad \beta = \frac{1}{\omega_R} \text{Im} \left(\frac{Z_3(\zeta_R)}{Z_1(\zeta_R)} \right). \quad (4.107)$$

With our definitions of α and β , $\gamma = 2Z_3(\zeta_R)/Z_1(\zeta_R) = 2(\alpha + i\beta)$ is the polytropic coefficient (since $p = Nmv_t^2/2$). These relations lead us to the damping rate of

$$\frac{1}{n_1} \frac{dn_1}{dt} = -\omega_R \sqrt{\pi} \zeta_R^3 \left(1 - \frac{3}{\zeta_R^2} + \mathcal{O}(\zeta_R^{-4}) \right) e^{-\zeta_R^2} \quad (4.108)$$

which is the asymptotic form for Landau damping, but is equally valid for a gas as well as a plasma. This result shows that the energy lost through Landau damping goes into the nonpolytropic part of the compressional energy. In conventional discussions of Landau damping, compressional energy is traditionally ignored, and so these discussions are unable to properly describe the physics of Landau damping.

4.2.4 Conventional descriptions of Landau damping

The traditional description of the physics of Landau damping describes it as being due to a transfer of energy between the kinetic energy of particles and the electrostatic energy of the wave, making Landau damping a process unique to a plasma. To the first approximation, the resulting damping rate is the classical Landau rate, so this description has been propagated widely in textbooks. Since we have noted earlier in several places that the phenomenon also occurs in neutral gases and since we have concluded at the end of section 4.2.3.2 that second order terms are required for energy balance and these must include compressional energy as well as kinetic and electrostatic energy, we need to examine this matter more closely. This section will conclude with a more nearly accurate picture of the physics of Landau damping.

4.2.4.1 Electrostatic picture of Landau damping

The conventional analysis begins with a calculation of the kinetic energy of particles in the wave frame, where the electric field $E(x, t) = E_0 \sin(kx - \omega t)$ may be represented by

$$E = E_0 \sin kx.$$

We note already that the wave amplitude is taken to be constant even though the point of the calculation is to find the decay rate of the amplitude, so there is an

inconsistency already at the start. With this field, the rate of change of kinetic energy can then be expressed by

$$\frac{d\overline{w_K}}{dt} = n_0 \int_{-\lambda/2}^{\lambda/2} \frac{dx}{\lambda} \int_{-\infty}^{\infty} dv \frac{1}{2} m \left(v + \frac{\omega}{k} \right)^2 \frac{\partial f}{\partial t}. \quad (4.109)$$

The integration over space just gives the spatial average of the distribution function, so equation (4.109) becomes

$$\frac{d\overline{w_K}}{dt} = \frac{n_0 m}{2} \int_{-\infty}^{\infty} dv \left(v + \frac{\omega}{k} \right)^2 \frac{\partial \overline{f}}{\partial t}. \quad (4.110)$$

This time derivative of \overline{f} is obtained from the kinetic equation so that

$$\frac{\partial \overline{f}}{\partial t} = \frac{e}{m} E_0 \sin kx \frac{\partial \overline{f}}{\partial v}. \quad (4.111)$$

In order to solve this, we will linearize, taking $f = f_0 + f_1$ with f_0 being the unperturbed part of the distribution function that is uniform and hence makes no contribution to equation (4.111). The linearized kinetic equation is

$$\frac{\partial f_1}{\partial t} + v \frac{\partial f_1}{\partial x} = \frac{e}{m} E_0 \sin kx \frac{\partial f_0}{\partial v} \quad (4.112)$$

with solution

$$f_1(x, v, t) = f_1(v, 0) \cos(kx - kvt) - \frac{e E_0}{mkv} \frac{\partial f_0}{\partial v} [\cos kx - \cos(kx - kvt)] \quad (4.113)$$

for initial condition $f_1(x, v, 0) \equiv f_1(v, 0) \cos kx$. This result may be used in equation (4.111) to find

$$\frac{\partial \overline{f}}{\partial t} = \frac{\partial}{\partial v} \left[\frac{e E_0}{2m} f_1(v, 0) \sin kvt + \frac{1}{2} \left(\frac{e E_0}{m} \right)^2 \frac{\partial f_0}{\partial v} \frac{\sin kvt}{kv} \right]. \quad (4.114)$$

We now use equation (4.114) in equation (4.110), and integrate by parts to obtain the rate of change of the kinetic energy density as

$$\begin{aligned} \frac{d\overline{w_K}}{dt} &= -\frac{neE_0}{2} \int_{-\infty}^{\infty} dv f_1(v, 0) \left(v + \frac{\omega}{k} \right) \sin kvt \\ &\quad - \frac{ne^2 E_0^2}{2m} \int_{-\infty}^{\infty} dv \frac{\partial f_0}{\partial v} \left(v + \frac{\omega}{k} \right) \frac{\sin kvt}{kv}. \end{aligned} \quad (4.115)$$

After several cycles, the first integral phase mixes away, decaying exponentially in time (see problem 4.2.4), and the second integral is peaked about $v = 0$ (in the wave frame). We can see here that the initial perturbation is being carried away by streaming particles, dispersing the spatial coherence that

supported the electric field. The second integral of equation (4.115) approaches a delta function, of width $\Delta v \sim 1/kt$ so only those particles that are moving very slowly in the wave frame contribute to the change in energy density. If we let the peaked function $\sin kvt/kv \rightarrow \pi\delta(kv)$, then the integral becomes

$$\frac{d\overline{w_K}}{dt} = -\pi\omega \frac{\omega_p^2}{k^2} \frac{\partial f_0}{\partial v} \Big|_{v=0} \overline{w_E} \quad (4.116)$$

where $\overline{w_E} = \frac{1}{2}\epsilon_0 E_0^2$ is the wave energy density. By balancing the wave and particle energy by setting $d\overline{w_K}/dt = -\partial\overline{w_E}/\partial t = -2\Gamma\overline{w_E}$, we establish the linear damping rate as

$$\Gamma_L = \frac{\pi}{2}\omega \frac{\omega_p^2}{k^2} \frac{\partial f_0}{\partial v} \Big|_{v=\omega/k} \quad (4.117)$$

where now the distribution function is back in the laboratory frame so it is evaluated at the phase velocity. This is the Landau formula, and yet it is based on energy balance considerations that ignore the compressional energy and the analysis is fundamentally nonlinear. What this calculation does provide is an alternate insight into the process which includes an estimate of the *time* over which linear Landau damping is valid, since the nonlinear analysis limits the validity of the linear analysis. In the linear analysis, the particles are assumed to be undeflected by the wave, but it is clear that there will be some trapped particles for any finite E_0 , and when particles begin to bounce in the potential well, this analysis clearly fails. The bounce time, estimated from the small amplitude limit of the equation of motion,

$$m\ddot{x} = -eE_0 \sin kx \quad (4.118)$$

leads to a bounce time of $\tau_B = (m/eE_0k)^{1/2}$, so linear theory can only be valid for times $t \ll \tau_B$. For longer times and larger amplitudes, the analysis of the trapped particles must be followed carefully, and this is found in section 8.3.

Problem 4.2.4. The electrostatic picture of landau damping.

- (i) Show that equation (4.113) is a solution of equation (4.112).
- (ii) Fill in the steps leading to equation (4.115).
- (iii) Evaluate the first integral in equation (4.115) with $f_1(v, 0)$ a Maxwellian distribution, showing that it vanishes as $\exp(-\kappa t^2)$ (find κ).
- (iv) Evaluate the first integral in equation (4.115) with $f_1(v, 0)$ a Lorentzian distribution, $f_1(v, 0) = A/(v^2 + v_e^2)$, and show that it vanishes as $\exp(-kv_e t)$. (Use contour methods.)

Problem 4.2.5. The ordinary wave in a hot unmagnetized plasma. For the cold *O*-wave, problem 2.2.1, it was deduced that $v_p v_g = c^2$ so that the phase velocity always exceeds the velocity of light. In terms of the physical picture of Landau damping, what does this imply about the Landau damping of the *O*-wave from this electrostatic picture?

4.2.4.2 Electrostatic picture revisited

Looking at the problem in a slightly different way, we calculate the total kinetic energy density from

$$W_K = \frac{m}{2} \int u^2 f(u) du = w_K + \frac{1}{2} p$$

and we know from equation (4.90) that it obeys the energy relation

$$\frac{d\overline{W}_K}{dt} = \frac{d\overline{w}_K}{dt} + \frac{d\overline{w}_C}{dt} = -\frac{d\overline{w}_E}{dt}. \quad (4.119)$$

With a constant amplitude E_0 , this leads to the same result as in equation (4.116), which we may write as

$$\frac{d\overline{W}_K}{dt} = \frac{2\sqrt{\pi}\omega_p^2}{\omega_R} \zeta_R^3 e^{-\zeta_R^2 \overline{w}_E}. \quad (4.120)$$

We then postulate that the gain in total kinetic energy is balanced by a loss of total wave energy $\overline{w} = \overline{w}_K + \overline{w}_E + \overline{w}_C$, so that

$$\frac{d\overline{W}_K}{dt} = -\frac{d\overline{w}}{dt}. \quad (4.121)$$

Then, taking $\Gamma = -(1/\overline{w})d\overline{w}/dt$, we have

$$\frac{\Gamma}{\omega_R} \simeq F \sqrt{\pi} \zeta_R^3 e^{-\zeta_R^2} \quad (4.122)$$

where $F = (\omega_p^2/\omega_R^2)2\overline{w}_E/\overline{w}$. This gives the correct Landau rate in the limit $\zeta_R \gg 1$ and for simple plasma waves where we have $\overline{w} \simeq 2\overline{w}_E$ and $\omega_R \simeq \omega_p$. This answer is consistent with equation (4.117) for a thermal plasma.

Unfortunately, the derivation of equation (4.122) is based on two mistakes. The first, as noted previously, is based on the assumption that the amplitude is constant, whereas the result indicates it is not, so it is inconsistent. If we were to go back and let it vary slowly, so that $E_0 \rightarrow E_1(t)$, then equation (4.120) becomes

$$\frac{d\overline{W}_K}{dt} = \frac{2\sqrt{\pi}\omega_p^2}{\omega_R} \zeta_R^3 e^{-\zeta_R^2 \overline{w}_E} + 2(\overline{w}_K + \overline{w}_C) \frac{1}{E_1} \frac{dE_1}{dt} \quad (4.123)$$

where now $\overline{w}_E = \frac{1}{2}\epsilon_0 E_1^2$. The second mistake is that equation (4.121) was used instead of equation (4.119). Correcting this error, however, leads us back to equation (4.122). We thus have the unexpected result that we get the same answer whether we do it right or wrong. The interpretation of these two approaches is very different, however, since the incorrect equation (4.121) implies that the total wave energy \overline{w} has been converted into particle kinetic energy \overline{W}_K , while

the correct equation (4.119) gives a connection between the electrostatic energy density and the kinetic energy density, but not much insight.

Our focus on the electrostatic wave energy density has left us with a false impression that it is the principal element in the damping mechanism. In the case of longitudinal plasma waves, it is a substantial part, but this is not always true for related cases. Because the components of \bar{w} all decay together, a correct estimate of the decay rate of one component will always give a correct estimate of the overall rate. If, however, the electrostatic component were an insignificant part of the overall energy density, we would not imagine that a description of the physics of that small component gives us an accurate picture of the physics of the overall process.

Such a case occurs with ion acoustic waves described in the next section. This example always has $T_e/T_i \gg 1$ and the pertinent plasma frequency is ω_{pi} . The quasineutral limit requires $k^2\lambda_D^2 \ll 1$ and we have the relations (see equation (4.141))

$$\omega_R^2 = k^2 v_i^2 \frac{T_e}{2T_i} = \omega_{pi}^2 k^2 \lambda_D^2 \quad (4.124)$$

$$\frac{\overline{w}_E}{\overline{w}} = \frac{1}{2} k^2 \lambda_D^2. \quad (4.125)$$

We still have $F \simeq 1$ in this case, but now the electrostatic energy density is negligibly small in the energy balance. This means that the energy balance is principally between the kinetic energy density and the compressional energy density. If the electrostatic component is negligible in this case, then it cannot be the basis upon which our understanding of Landau damping rests. We must therefore look elsewhere for our explanation, and we must keep in mind that the correct description must be viable for gases as well as plasmas.

4.2.4.3 Thermal spreading picture of Landau damping

A term that is often used but rarely defined for the explanation of Landau damping is *phase mixing*. One use of the word appeared after equation (4.115). Problem 4.2.4 shows that for this kind of phase mixing, the decay is exponential as the square of the time, which is much faster than Landau damping and unrelated to it. For this reason, we eschew this term in our discussion. Another process deals with the free-streaming of particles after an initial perturbation. While the perturbation is remembered by the particles (until collisions eventually destroy that memory), the particles travel in all three directions at close to their original velocities, and in the process carry their information away so that the original coherence of the wave is lost. This process is described as *thermal spreading*.

In order to show that the thermal spreading description gives an adequate representation of the damping rate, we must embark on another lengthy analysis. Here again, we generally follow the development of Stubbe and Sukhorukov [32]. We start with a linear one-dimensional perturbation and consider the quantities

$n_1(z, t)$, $v_1(z, t)$, and $p_1(z, t)$, and choose a perturbed distribution function $f_1(z, u, t)$ that produces these quantities through moments of the distribution function, and let the density be perturbed by an undamped monochromatic plane wave. The key point is that we construct a distribution at time t by assuming that free-streaming of the particles began at time $t - \tau$ and average over τ . The resulting n'_1 and p'_1 will be used to define a polytropic coefficient through equation (4.102). The zero-order velocity distribution function is Maxwellian,

$$f_0(u) = \frac{n_0}{\sqrt{\pi} v_t} e^{-u^2/v_t^2}$$

and the first order distribution function is

$$\begin{aligned} f_1(z, u, t) &= f_0(u) \left[\frac{n_1(z, t)}{n_0} + \left(\frac{u^2}{v_t^2} - \frac{1}{2} \right) \right. \\ &\quad \times \left. \left(\frac{p_1(z, t)}{p_0} - \frac{n_1(z, t)}{n_0} \right) + \frac{2uv_1(z, t)}{v_t^2} \right]. \end{aligned} \quad (4.126)$$

It may be verified that integrating over u using the weight factors 1, u/n_0 , and mu^2 , reproduces the moments $n_1(z, t)$, $v_1(z, t)$, and $p_1(z, t)$. We introduce the plane wave by letting

$$n_1(z, t) = \bar{n} e^{i(kz - \omega t)}$$

where \bar{n} is a constant density. If the wave is to be undamped, we will need a real polytropic coefficient γ (see equation (4.102)). We also use the fact that v_1 and n_1 are connected by the continuity equation. With these last two assumptions, equation (4.126) becomes

$$f_1(z, u, t) = f_0(u) \frac{\bar{n}}{n_0} \left[1 + (\gamma - 1) \left(\frac{u^2}{v_t^2} - \frac{1}{2} \right) + \frac{2u\omega}{kv_t^2} \right] e^{i(kz - \omega t)}. \quad (4.127)$$

We now reinterpret equation (4.127) as the result of the free spreading that began at an earlier time $t - \tau$, so that

$$f'_1(z, u, t) = f_1(z - u\tau, u, t - \tau) \quad (4.128)$$

so that we have

$$f'_1(z, u, t) = f_0(u) \frac{\bar{n}}{n_0} \left[1 + (\gamma - 1) \left(\frac{u^2}{v_t^2} - \frac{1}{2} \right) + \frac{2u\omega}{kv_t^2} \right] e^{i(kz - \omega t)} e^{i(\omega - ku)\tau} \quad (4.129)$$

and we note that u now appears in the additional exponential term. Now we need to take the moments with this distribution function to find $n'_1(z, t)$ and $p'(z, t)$. The integrals are of the form

$$\begin{aligned} Q_n(\tau) &= \frac{1}{\sqrt{\pi} v_t} \int_{-\infty}^{\infty} u^n e^{-u^2/v_t^2 - iku\tau} du \\ &= \frac{v_t^n e^{-\tau'^2/4}}{\sqrt{\pi}} \int_{-\infty}^{\infty} \left(x - \frac{i\tau'}{2} \right)^n e^{-x^2} dx \end{aligned} \quad (4.130)$$

where $\tau' = kv_t \tau$. The two moments may then be written as

$$n'_1(z, t, \tau') = \bar{n} e^{i(kz - \omega t)} \left[1 - \frac{(\gamma - 1)}{4} \tau'^2 - i\zeta \tau' \right] e^{i\zeta \tau' - \tau'^2/4} \quad (4.131)$$

$$\begin{aligned} p'_1(z, t, \tau') = \bar{p} e^{i(kz - \omega t)} & \left[\gamma - \left(\frac{1}{2} + \frac{5}{4}(\gamma - 1) \right) \tau'^2 + \frac{\gamma - 1}{8} \tau'^4 \right. \\ & \left. - i\zeta \left(3\tau' - \frac{\tau'^3}{2} \right) \right] e^{i\zeta \tau' - \tau'^2/4}. \end{aligned} \quad (4.132)$$

We can now obtain a new polytropic coefficient $\gamma'(\tau')$ using $n'_1(z, t, \tau')$ and $p'_1(z, t, \tau')$, but we really want the average over all τ' , so we define γ' as

$$\gamma' = \frac{\int_0^\infty \left[\gamma - \frac{5\gamma-3}{4}\tau'^2 + \frac{\gamma-1}{8}\tau'^4 - i\zeta \left(3\tau' - \frac{\tau'^3}{2} \right) \right] e^{i\zeta \tau' - \tau'^2/4} d\tau'}{\int_0^\infty \left[1 - \frac{(\gamma-1)}{4}\tau'^2 - i\zeta \tau' \right] e^{i\zeta \tau' - \tau'^2/4} d\tau'} \quad (4.133)$$

which can be written in terms of generalized Gordeyev integrals as

$$\gamma' = \frac{\gamma i I_0(\zeta) - \frac{5\gamma-3}{4} i I_2(\zeta) + \frac{\gamma-1}{8} i I_4(\zeta) + \zeta \left(3I_1(\zeta) - \frac{I_3(\zeta)}{2} \right)}{i I_0(\zeta) - \frac{(\gamma-1)}{4} i I_2(\zeta) + \zeta I_1(\zeta)} \quad (4.134)$$

where

$$I_n(\zeta) \equiv -i \int_0^\infty \tau^n e^{i\zeta \tau - \tau^2/4} d\tau. \quad (4.135)$$

The Gordeyev integrals can in turn be written in terms of the generalized dispersion functions, $Z_n(\zeta)$ (see [appendix B.1.2](#)). Writing γ' in terms of the $Z_n(\zeta)$, we have the exact result

$$\gamma'(\zeta) = \frac{2(3-\gamma)Z_2(\zeta) + 4(\gamma-1)Z_4(\zeta) + 8\zeta Z_3(\zeta)}{2(\gamma-1)Z_2(\zeta) + 4\zeta Z_1(\zeta) + (3-\gamma)Z_0(\zeta)}.$$

Using the recursion relations $Z_4(\zeta) = \zeta Z_3(\zeta)$ and $Z_2(\zeta) = \zeta Z_1(\zeta)$ from [section B.1.2](#) to eliminate the Z_4 and Z_2 terms, this simplifies somewhat to

$$\gamma'(\zeta) = \frac{4(\gamma+1)\zeta Z_3(\zeta) + 2(3-\gamma)\zeta Z_1(\zeta)}{2(\gamma+1)\zeta Z_1(\zeta) + (3-\gamma)Z_0(\zeta)}. \quad (4.136)$$

For the final step, we are reminded that for $\zeta \gg 1$, $\gamma \rightarrow 3$, so in this limit, γ' takes the simple form

$$\gamma'(\zeta) \simeq \frac{2Z_3(\zeta)}{Z_1(\zeta)} \quad (4.137)$$

and this reproduces the damping of [equation \(4.81\)](#). We conclude this section by noting that the thermal spreading picture provides a conceptual picture for Landau damping for all ζ , is equally valid for both gases and plasmas, and for

large ζ , gives a quantitative value for the damping rate. The analysis is also manifestly linear, and thus must replace previous discussions for linear Landau damping. The electrostatic arguments are pertinent as the wave amplitude gets larger, however, and dominate the analysis for nonlinear Landau damping which is treated in section 8.3.1

Problem 4.2.6. Thermal spreading.

- (i) Verify that taking the first three moments of equation (4.126) with the weights indicated produces $n_1(z, t)$, $v_1(z, t)$, and $p_1(z, t)$ as claimed.
- (ii) Fill in the steps between equations (4.127) and (4.132).
- (iii) Use equations (4.131) and (4.132) and the Gordeyev integrals to obtain equation (4.136).

4.2.5 Ion acoustic waves and ion Landau damping

For the previous examples, the ion motions have been neglected, since they are usually unimportant. In the cold plasma limit this is due to the fact that $m_e/m_i \ll 1$. If we were to consider plasma oscillations near the electron plasma frequency, the ions again only appear to the same order. Near the ion plasma frequency, however, we must re-examine the case, since it is possible to consider a case where the ions are cold ($v_i \ll v_p$), but the electrons are hot ($v_e \gg v_p$). When the electron and ion temperatures are comparable, there is generally no oscillation, since when one moves some of the ions to form a slight charge imbalance which would induce the ions to oscillate, the period is so slow that electrons, being so much more mobile, rush in to fill the charge imbalance before the ions can respond. When the electron temperature is much higher than the ion temperature, however, the electrons have too much momentum to slow down and fill in the potential depressions, so some ion oscillations may occur.

4.2.5.1 Electron versus ion Landau damping

The dispersion relation for this case is the same as equation (4.62) except that we now include the ion term:

$$1 - \frac{\omega_{pi}^2}{k^2 v_i^2} Z' \left(\frac{\omega}{kv_i} \right) - \frac{\omega_{pe}^2}{k^2 v_e^2} Z' \left(\frac{\omega}{kv_e} \right) = 0. \quad (4.138)$$

The cold ion approximation means that we assume $\zeta_i = \omega/kv_i \gg 1$, so we use the large argument expansion for the $Z'(\zeta_i)$ term given by equation (4.33). For the electron term, we assume $\zeta_e = \omega/kv_e \ll 1$, so we need the power series expansion from [appendix B](#),

$$Z'(\zeta) = -2(1 - 2\zeta^2 + \dots) - 2i\sqrt{\pi}\zeta(1 - \zeta^2 + \dots). \quad (4.139)$$

Using these approximate expressions, the dispersion relation becomes

$$1 + \frac{\omega_{pe}^2}{k^2 v_e^2} (2 + 2i\sqrt{\pi} \zeta_e) - \frac{\omega_{pi}^2}{\omega^2} \left(1 + \frac{3}{2\zeta_i^2} - 2i\sqrt{\pi} \zeta_i^3 e^{-\zeta_i^2} \right) \simeq 0. \quad (4.140)$$

Setting the real and imaginary parts to zero separately and using $\lambda_{Dj}^2 = v_j^2/2\omega_{pj}^2$, we obtain

$$1 + k^2 \lambda_{De}^2 \frac{k^2 c_s^2}{\omega_r^2} \left(1 + \frac{3}{\zeta_i^2} \right)$$

or solving for ω_r ,

$$\omega_r^2 = \frac{k^2 c_s^2}{1 + k^2 \lambda_{De}^2} \left[1 + \frac{3T_i}{T_e} (1 + k^2 \lambda_{De}^2) \right] \quad (4.141)$$

and

$$\frac{\omega_i}{\omega_r} = -\frac{\sqrt{\pi} \zeta_{ir}^3}{1 + 3/\zeta_{ir}^2} \left(e^{-\zeta_{ir}^2} + \frac{T_i v_i}{T_e v_e} \right) \quad (4.142)$$

where $\omega = \omega_r + i\omega_i$ and $c_s = \sqrt{\kappa T_e/m_i}$ is the ion acoustic speed. We note that if $k\lambda_{De} \ll 1$, then the wave will travel at the ion acoustic speed, but then the correction term for ω_r allows us to redefine c_s so that

$$c_s^2 \rightarrow \frac{\gamma_e \kappa T_e + \gamma_i \kappa T_i}{m_i}$$

with $\gamma_e = 1$ and $\gamma_i = 3$ and $\omega_r = kc_s$. This limit agrees with the ion acoustic speed of equation (3.45) since $m_e \ll m_i$. A comparison of the exact real and imaginary parts of ω with the approximate formulas of equations (4.141) and (4.142) are shown in figure 4.6. It is evident that ω_r given by equation (4.141) is a good approximation, agreeing within 10% up to $k\lambda_{De} \sim 0.5$. It is also apparent that the imaginary part is much less accurate, deviating by a factor of two over the range illustrated. In this example, ion Landau damping is dominant. Doubling the electron temperature so that $T_e/T_i = 20$ increases the accuracy of both parts, the real part reaching 7% difference at $k\lambda_{De} \sim 0.5$ while the imaginary part ranges from a factor of 1.15 to 1.65 above the exact result over the range illustrated. For this temperature ratio, electron Landau damping dominates for $k\lambda_{De} < 0.4$ while ion Landau damping dominates for $k\lambda_{De} > 0.4$.

Now if we define weak damping as less than 10% decrease in amplitude per period, then this requires $|\omega_i| < \omega_r/60$. If we further look for ion Landau damping to be dominant, such that the electron term in equation (4.142) is less than 10% of the ion term, then $\zeta_i \geq 2.7$. These together require $T_e/T_i \geq 70A^{-1/3}$, where A is the atomic mass number, so generally ion acoustic waves require $T_e \gg T_i$.

Instability of the ion acoustic wave. As shown in section 3.5, electrostatic waves are subject to current driven instabilities. For the ion acoustic wave, we may add

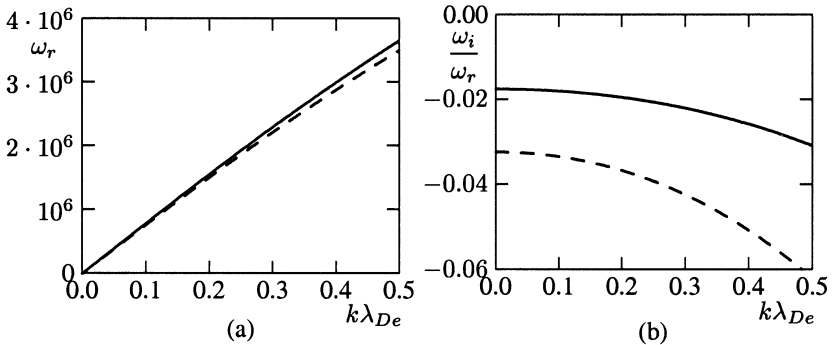


Figure 4.6. Real (*a*) and imaginary (*b*) parts of ω for the ion-acoustic wave. The full curves are exact solutions of equation (4.138) while the dashed curves are from equations (4.141) and (4.142) with $T_e/T_i = 10$, $n_0 = 10^{15} \text{ m}^{-3}$, $A = 39$, and $T_i = 300 \text{ K}$.

a small drift velocity to the electrons, so that $\zeta_e \rightarrow (\omega - kv_0)/kv_e$ and from equation (4.140), the imaginary part now may be solved as

$$\frac{\omega_i}{\omega_r} = -\frac{\sqrt{\pi}}{1 + 3/\zeta_{ir}^2} \left(\zeta_{ir}^3 e^{-\zeta_{ir}^2} + \frac{\zeta_e \omega_r^2}{2k^2 c_s^2} \right) \quad (4.143)$$

and if we set the right-hand side to zero for the instability threshold, we find

$$\frac{v_0}{v_e} = \frac{\omega_r}{kv_e} + \frac{T_e}{T_i} \frac{\omega_r}{kv_i} e^{-\zeta_{ir}^2} \quad (4.144)$$

$$= 2(1 + k^2 \lambda_{De}^2) \zeta_{ir}^3 e^{-\zeta_{ir}^2} + \left(\frac{m_e}{2m_i(1 + k^2 \lambda_{De}^2)} \right)^{1/2}. \quad (4.145)$$

For the case with $T_e/T_i = 20$, this result agrees with the exact results within 4% for $k\lambda_{De} \leq 0.2$ and the electron Landau damping term is comparable to the ion Landau damping term. The sensitivity to drifts is evident from the fact that $v_0/v_e \sim 0.0036$ with $k\lambda_{De} \leq 0.2$ for this case. For the case with $T_e/T_i = 10$, equation (4.144) agrees with the exact results within about 40% for $k\lambda_{De} \leq 0.2$. With this smaller temperature ratio, ion Landau damping dominates and $v_0/v_e \sim 0.034$ so the threshold is strongly dependent on the temperature ratio.

Problem 4.2.7. Current-driven instability. From the previous two examples, estimate the current density required to drive the ion acoustic wave unstable (in A/m^2) for both $T_e/T_i = 10$ and $T_e/T_i = 20$.

4.2.6 Effects of collisions on Landau damping

The analytic treatment of collisions in the context of Landau damping has been problematical because of the difficulty of representing the collision frequency in a kinetic treatment. Coulomb collisions have a significant range of velocities where the cross section varies as v^{-3} , and such behavior is generally intractable in solving the kinetic equation. If one considers electron-neutral collisions, however, an analytic collision operator can be formed, and even solved. For this analysis, we assume at the outset that we are looking for waves that have the dependence $\exp[i(kx - \omega t)]$, and our equations to be solved are the linearized kinetic equation and Poisson's equation,

$$\frac{\partial f}{\partial t} + v \frac{\partial f}{\partial x} - \frac{e}{m_e} \frac{\partial f_0}{\partial v} E = v \frac{\partial}{\partial v} \left(vf + \frac{\kappa T_e}{m_e} \frac{\partial f}{\partial v} \right) \quad (4.146)$$

$$\frac{\partial E}{\partial x} = - \frac{e}{\epsilon_0} \int_{-\infty}^{\infty} f \, dv. \quad (4.147)$$

The collision term comes from Lenard and Bernstein [38] and has the properties that it conserves particles and derives from a Fokker–Planck treatment of collisions. The development that follows is due to Short and Simon [39], but the notation is changed to be consistent with previous calculations.

We first change to dimensionless variables such that $u \equiv v/v_t$, $\zeta \equiv \omega/kv_t$, $g \equiv v_t f/n_0$, $g_0 \equiv \pi^{-1/2} e^{-u^2}$, $\eta \equiv \alpha(\partial g_0/\partial u)$, $\alpha \equiv \omega_{pe}^2/k^2 v_t^2$, and $\mu = v/kv_t$. With these changes of variable, equations (4.146) and (4.147) become

$$(u - \zeta)g(u) - \eta(u) \int_{-\infty}^{\infty} g(u') \, du' = -i\mu \frac{\partial}{\partial u} \left(ug + \frac{1}{2} \frac{\partial g}{\partial u} \right). \quad (4.148)$$

We next Fourier transform in velocity so that

$$G(w) = \frac{1}{\sqrt{2\pi}} \int_{-\infty}^{\infty} e^{iwu} g(u) \, du$$

so that equation (4.148) becomes

$$i(1 + \mu w) \frac{dG}{dw} + \left(\zeta + \frac{i\mu}{2} w^2 \right) G = \frac{i\alpha}{2} w e^{-w^2/4} G(0). \quad (4.149)$$

Changing variables so that $x \equiv 1 + \mu w$, equation (4.149) may be written (with $G(w) \rightarrow H(x)$) as

$$\begin{aligned} \frac{dH}{dx} + \left[\frac{1}{2x} \left(\frac{x-1}{\mu} \right)^2 - \frac{i\zeta}{\mu x} \right] H &= \frac{dH}{dx} + \left[b(\mu)(x-2) + \frac{a(\zeta, \mu)}{x} \right] H \\ &= ab(\mu) \left(1 - \frac{1}{x} \right) e^{-(x-1)^2/4\mu^2} H(1) \end{aligned} \quad (4.150)$$

where

$$b(\mu) = \frac{1}{2\mu^2} \quad \text{and} \quad a(\zeta, \mu) = \frac{1}{2\mu^2} - \frac{i\zeta}{\mu}.$$

Equation (4.150) is a first-order ordinary differential equation with solution

$$H(x) = e^{b(2x-x^2/2)} x^{-a} \left[C + \alpha b e^{-b/2} H(1) \int_0^x x'^a \left(1 - \frac{1}{x'} \right) e^{-bx'} dx' \right] \quad (4.151)$$

where C is a constant of integration. We find $g(u)$ from the inverse Fourier transformation,

$$g(u) = \frac{1}{\sqrt{2\pi}} \int_{-\infty}^{\infty} e^{-iwu} G(w) dw = \frac{1}{\sqrt{2\pi}\mu} e^{iu/\mu} \int_{-\infty}^{\infty} e^{-iux/\mu} H(x) dx.$$

Note that the first term in $H(x)$ blows up as $x \rightarrow 0$ as $1/x^b$ with $b > 0$. This means that for small μ (large b), the inverse Fourier transform will not converge, requiring that we set $C = 0$. Evaluating the remaining expression for $H(x)$ at $x = 1$ and dividing by $H(1)$, we have the consistency relation

$$1 = \alpha b e^b \int_0^1 (x^a - x^{a-1}) e^{-bx} dx \quad (4.152)$$

which is our dispersion relation. The integrals may be expressed in terms of the incomplete gamma function $\gamma(a, x) = \int_0^x e^{-t} t^{a-1} dt$, such that

$$\int_0^1 (x^a - x^{a-1}) e^{-bx} dx = [b^{-a}(a-b)\gamma(a, b) - e^{-b}]/b$$

where the recursion formula from [appendix B](#) has been used. The dispersion relation may then be written as

$$1 + \alpha \left[1 + \frac{i\zeta}{\mu} (2\mu^2)^{a(\zeta, \mu)} e^{b(\mu)} \gamma[a(\zeta, \mu), b(\mu)] \right] = 0 \quad (4.153)$$

where the dependence of a and b on ζ and μ are again displayed. A form more amenable to calculation may be obtained from the relation $\gamma(a, x) = \Gamma(a) - \Gamma(a, x)$, where $\Gamma(a, x) = \int_x^\infty e^{-t} t^{a-1} dt$ and may be evaluated by the continued fraction given in [appendix B](#).

For very weak collisions, μ is very small, and the numerical evaluation of the roots becomes more and more difficult. It is possible to expand the dispersion relation in a power series in μ of the form

$$1 + \alpha \left[1 + \sum_{n=0}^{\infty} \mu^n f_n(\zeta) \right] = 0 \quad (4.154)$$

Table 4.1. Roots of the dispersion relation as a function of μ , the collisions term. Both exact and approximate roots are shown for $\alpha = 9$, where the approximate roots keep only the first order term in μ . The bottom root is the Landau root.

μ	ζ (exact)	ζ (approx.)
0.1	$2.5177324 - 0.1270101i$	$2.5160641 - 0.1381947i$
0.01	$2.5428465 - 0.0622458i$	$2.5428231 - 0.0623408i$
0.001	$2.5455167 - 0.0556237i$	$2.5455164 - 0.0556246i$
0.0001	$2.5457849 - 0.0549602i$	$2.5457855 - 0.0549601i$
0.00001	$2.5458124 - 0.0548937i$	$2.5458124 - 0.0548937i$
0	$2.5458154 - 0.0548864i$	$2.5458154 - 0.0548864i$

where Short and Simon [39] find

$$f_0(\zeta) = \zeta Z(\zeta) \quad (4.155)$$

$$f_1(\zeta) = i\zeta[2(1 - \zeta^2) + i\zeta Z(\zeta)(3 - 2\zeta^2)]/3. \quad (4.156)$$

A table of roots for $\alpha = 9$ for several values of μ is given in table 4.1, where the last entry with $\mu = 0$ is the Landau result. It is apparent that the damping rate for the electric field increases as collisions increase. These values agree with those of Ng *et al* [40] who used a different numerical scheme, except for the real part of ζ for $\mu = 0.01$, which has a typographical error.

In problem 4.2.3, it was shown that the potential decays at the Landau rate but that the distribution function has a component that does not decay away. In the collisional environment, the perturbation to the distribution function will decay, but at a slower rate than the potential. The calculation of this rate is beyond the scope of this book, but an analysis of the decay rate in space away from a localized antenna has been investigated by Short and Simon [39]. The differential decay rates are crucial for the observation of plasma wave echoes where the potential of one antenna decays away and the potential from a second antenna at a different frequency and location also decays away, after which an echo is observed at yet another frequency. This phenomenon is nonlinear, and discussed in section 7.3.1.

Problem 4.2.8. Collisional dispersion relation.

- (i) Show that $H(x)$ in equation (4.151) represents a solution to equation (4.149).
- (ii) Fill in the steps leading from equation (4.151) to equation (4.153).

4.3 Waves in a magnetized hot plasma

The calculation of the response of a hot plasma in a magnetic field to a wave is considerably more formidable than the unmagnetized case. As was seen in

section 3.3.5, all nine of the dielectric tensor components are nonzero when thermal effects are included, and we shall find the symmetries of the tensor will be even more involved when the full kinetic effects are included. This difficulty relates to the additional effect that the zero order motions of electrons and ions in a uniform magnetic field are spirals, drifting uniformly parallel to the field while they execute circular motion at the cyclotron frequency with their individual Larmor radii around a field line.

The technique we shall use was introduced in 1958 by J E Drummond [41], R Z Sagdeev and V D Shafranov [42], and M N Rosenbluth and N Rostoker [43], but we will follow the development of Stix [6] most closely. The idea of the method is to find the perturbation of the distribution function due to the wave by integrating along the unperturbed orbits. This is called the method of characteristics, and we have effectively used it already, except in a trivial fashion, since up to this point the unperturbed orbits were straight lines.

4.3.1 The evolution of the distribution function

We begin by describing a zero order trajectory by

$$\mathbf{r}(t) = \mathbf{r}[\mathbf{r}(t), \mathbf{v}(t), t]$$

and calculate the rate of change of the distribution function along this trajectory by

$$\frac{df}{dt}\Big|_{\mathbf{R}} = \frac{\partial f}{\partial t} + \frac{\partial f}{\partial \mathbf{r}} \cdot \frac{d\mathbf{r}}{dt} + \frac{\partial f}{\partial \mathbf{v}} \cdot \frac{d\mathbf{v}}{dt} \quad (4.157)$$

where $d\mathbf{r}/dt = \mathbf{v}$ and $d\mathbf{v}/dt = \mathbf{a}$ where \mathbf{a} is the acceleration along the zero-order trajectory

$$\mathbf{a} = \frac{d\mathbf{v}}{dt} = \frac{q}{m} \mathbf{v} \times \mathbf{B}_0. \quad (4.158)$$

We then write equation (4.157) as

$$\frac{df}{dt}\Big|_{\mathbf{R}} = \frac{\partial f}{\partial t} + \mathbf{v} \cdot \nabla f + \frac{q}{m} \mathbf{v} \times \mathbf{B}_0 \cdot \nabla_v f. \quad (4.159)$$

The zero-order distribution function, f_0 , is, of course, independent of \mathbf{r} and t , so

$$\frac{df_0}{dt} = \frac{df_0}{dt}\Big|_{\mathbf{R}} = \frac{q}{m} \mathbf{v} \times \mathbf{B}_0 \cdot \nabla_v f_0 = 0. \quad (4.160)$$

The most general form of f_0 that satisfies equation (4.160) is

$$f_0(\mathbf{v}) = f_0(v_\perp, v_z) \quad (4.161)$$

where $v_{\perp}^2 = v_x^2 + v_y^2$. Adding and subtracting the wave field terms in equation (4.159) leads to

$$\begin{aligned}\frac{df}{dt}\Big|_{\mathbf{R}} &= \left\{ \frac{\partial f}{\partial t} + \mathbf{v} \cdot \nabla f + \frac{q}{m} [\mathbf{E}_1 + \mathbf{v} \times (\mathbf{B}_0 + \mathbf{B}_1)] \cdot \nabla_{\mathbf{v}} f \right\} \\ &\quad - \frac{q}{m} (\mathbf{E}_1 + \mathbf{v} \times \mathbf{B}_1) \cdot \nabla_{\mathbf{v}} f\end{aligned}\quad (4.162)$$

and the term in curly brackets vanishes due to the collisionless Boltzmann equation. If we now separate the distribution function into $f = f_0 + f_1$, then

$$\frac{df}{dt}\Big|_{\mathbf{R}} = \frac{df_0}{dt}\Big|_{\mathbf{R}} + \frac{df_1}{dt}\Big|_{\mathbf{R}} = -\frac{q}{m} (\mathbf{E}_1 + \mathbf{v} \times \mathbf{B}_1) \cdot \nabla_{\mathbf{v}} f \quad (4.163)$$

where the zero-order term vanishes by equation (4.160). This leaves us with a total derivative of f_1 , so if we integrate equation (4.163) along \mathbf{r} , we obtain

$$f_1(\mathbf{r}, \mathbf{v}, t) = -\frac{q}{m} \int_{t_0}^t [\mathbf{E}_1(\mathbf{r}', t') + \mathbf{v}' \times \mathbf{B}_1(\mathbf{r}', t')] \cdot \nabla_{\mathbf{v}'} f_0(\mathbf{v}') dt' + f_1(\mathbf{r}, \mathbf{v}, t_0). \quad (4.164)$$

The recipe we developed from the Vlasov–Landau analysis that ω should have a positive imaginary part corresponds to growing waves in time, but it guarantees that the waves vanish as $t_0 \rightarrow -\infty$, so if we change the lower limit in equation (4.164) to $-\infty$, we may neglect the effects of the initial conditions. This is effectively equivalent to the Landau prescription of the initial value problem, but will be easier to manipulate. The perturbed distribution function is then described by

$$f_1(\mathbf{r}, \mathbf{v}, t) = -\frac{q}{m} \int_{-\infty}^t [\mathbf{E}_1(\mathbf{r}', t') + \mathbf{v}' \times \mathbf{B}_1(\mathbf{r}', t')] \cdot \nabla_{\mathbf{v}'} f_0(\mathbf{v}') dt' \quad (4.165)$$

where we are to integrate along the trajectories, $\mathbf{r}(\mathbf{r}', \mathbf{v}', t')$, that end at $\mathbf{r}(\mathbf{r}, \mathbf{v}, t)$ when $t' \rightarrow t$.

Problem 4.3.1. Zero-order distribution function. Prove that any zero-order distribution function having the form of equation (4.161) will satisfy equation (4.160) as long as it is differentiable.

4.3.2 Integrating along the unperturbed orbits

In order to evaluate the integral of equation (4.165), we shall assume that the wave electric and magnetic fields are of the form

$$\mathbf{E}_1 = \mathbf{E} e^{i(k \cdot \mathbf{r}' - \omega t')} \quad (4.166)$$

$$\mathbf{B}_1 = \mathbf{B} e^{i(k \cdot \mathbf{r}' - \omega t')} \quad (4.167)$$

so we may use the Maxwell equations to obtain

$$\mathbf{B}_1 = \frac{\mathbf{k} \times \mathbf{E}_1}{\omega} = \frac{\mathbf{k} \times \mathbf{E}}{\omega} e^{i(\mathbf{k} \cdot \mathbf{r}' - \omega t')} \quad (4.168)$$

so that equation (4.165) may be written as

$$f_1(\mathbf{r}, \mathbf{v}, t) = -\frac{q}{m} \int_{-\infty}^t dt' \mathbf{E} \left(1 + \frac{\mathbf{v}' \cdot \mathbf{k} - \mathbf{v}' \cdot \mathbf{k}}{\omega} \right) \cdot \nabla_{\mathbf{v}'} f_0(\mathbf{v}') e^{i(\mathbf{k} \cdot \mathbf{r}' - \omega t')}. \quad (4.169)$$

The trajectory that reaches $\mathbf{r}' = \mathbf{r}$ when $t' = t$ is governed by the equation of motion from equation (4.158)

$$\frac{d\mathbf{v}'}{dt'} = \epsilon \mathbf{v}' \times \omega_c \hat{\mathbf{e}}_z \quad (4.170)$$

where $\epsilon = q/|q|$ and we suppress all other species-specific notation until we begin to combine each species' contribution to the total current. The solution of equation (4.170) that reaches $\mathbf{v}' = \mathbf{v}$ at $t' = t$ is

$$\begin{aligned} v'_x &= v_x \cos \omega_c \tau - \epsilon v_y \sin \omega_c \tau \\ v'_y &= \epsilon v_x \sin \omega_c \tau + v_y \cos \omega_c \tau \\ v'_z &= v_z \end{aligned} \quad (4.171)$$

where $\tau = t - t'$. Integrating these to find the zero order trajectory that ends at $\mathbf{r}' = \mathbf{r}$ at $t' = t$, we find that

$$\begin{aligned} x' &= x - \frac{v_x}{\omega_c} \sin \omega_c \tau + \frac{\epsilon v_y}{\omega_c} (1 - \cos \omega_c \tau) \\ y' &= y - \frac{\epsilon v_x}{\omega_c} (1 - \cos \omega_c \tau) - \frac{v_y}{\omega_c} \sin \omega_c \tau \\ z' &= z - v_z \tau. \end{aligned} \quad (4.172)$$

The phase factor in equation (4.169) becomes

$$\begin{aligned} i\mathbf{k} \cdot \mathbf{r}' - i\omega t' &= i\mathbf{k} \cdot \mathbf{r} - i\omega t + \frac{iv_x}{\omega_c} [-k_x \sin \omega_c \tau - \epsilon k_y (1 - \cos \omega_c \tau)] \\ &\quad + \frac{iv_y}{\omega_c} [-k_y \sin \omega_c \tau + \epsilon k_x (1 - \cos \omega_c \tau)] + i(\omega - k_z v_z) \tau. \end{aligned} \quad (4.173)$$

Because v_{\perp} and v_z are constants of the motion, we know that $f_0(v'_{\perp}, v'_z) = f_0(v_{\perp}, v_z)$. If we now define

$$\frac{\partial f_0}{\partial v_{\perp}} \equiv f_{0\perp} \quad (4.174)$$

$$\frac{\partial f_0}{\partial v_z} \equiv f_{0z} \quad (4.175)$$

then

$$\frac{\partial f_0}{\partial v_x} = \frac{v_x}{v_\perp} f_{0\perp} \quad \frac{\partial f_0}{\partial v_y} = \frac{v_y}{v_\perp} f_{0\perp}.$$

Using these definitions, the remaining factor in equation (4.169) may be written as

$$\begin{aligned} & \mathbf{E} \left(1 + \frac{\mathbf{v}' \cdot \mathbf{k} - \mathbf{v}' \cdot \mathbf{k}}{\omega} \right) \cdot \nabla_{\mathbf{v}'} f_0(\mathbf{v}') \\ &= (E_x v'_x + E_y v'_y) \left[\frac{f_{0\perp}}{v_\perp} + \frac{k_z}{\omega} \left(f_{0z} - \frac{v'_z}{v_\perp} f_{0\perp} \right) \right] \\ &+ E_z \left[f_{0z} - \frac{k_x v'_x + k_y v'_y}{\omega} \left(f_{0z} - \frac{v'_z}{v_\perp} f_{0\perp} \right) \right] \\ &= (v_x \cos \omega_c \tau - \epsilon v_y \sin \omega_c \tau) \left[\frac{E_x f_{0\perp}}{v_\perp} + \frac{E_x k_z - E_z k_x}{\omega} \left(f_{0z} - \frac{v_z}{v_\perp} f_{0\perp} \right) \right] \\ &+ (\epsilon v_x \sin \omega_c \tau + v_y \cos \omega_c \tau) \left[\frac{E_y f_{0\perp}}{v_\perp} + \frac{E_y k_z - E_z k_y}{\omega} \left(f_{0z} - \frac{v_z}{v_\perp} f_{0\perp} \right) \right] \\ &+ E_z f_{0z}. \end{aligned} \quad (4.176)$$

We complete the variable change by writing the integral in the form

$$f_1(\mathbf{r}, \mathbf{v}, t) = \int_{-\infty}^t dt' \dots = e^{i(\mathbf{k} \cdot \mathbf{r} - \omega t)} \int_0^\infty d\tau \dots$$

where we have factored out the leading terms of the phase factor and will subsequently suppress this factor, interpreting the remaining integral as the Fourier amplitude of the distribution function.

We conclude this section by noting that we need only integrate over τ and average the current density over velocity for some particular $f_0(v_\perp, v_z)$ to obtain the mean current density from

$$\mathbf{j} = q \int d^3v \ \mathbf{v} f_1. \quad (4.177)$$

From this current density, we can construct the effective dielectric tensor and obtain the dispersion relation as in previous chapters.

4.3.3 General $f_0(v_\perp, v_z)$

It is possible to execute the integral over τ without specifying the zero-order distribution function, $f_0(v_\perp, v_z)$. This is done most conveniently by using polar coordinates for the velocity and wavevector such that

$$\begin{aligned} v_x &= v_\perp \cos \phi & k_x &= k_\perp \cos \psi \\ v_y &= v_\perp \sin \phi & k_y &= k_\perp \sin \psi \end{aligned}$$

so that the phase factor of equation (4.173) may be written as

$$\begin{aligned} e^{i(k \cdot r' - \omega t')} &= e^{i(k \cdot r - \omega t)} e^{-ib[\sin(\phi - \psi + \epsilon \omega_c \tau) - \sin(\phi - \psi)] + ia\tau} \\ &= e^{i(k \cdot r - \omega t)} \sum_{m,n=-\infty}^{\infty} J_m(b) J_n(b) e^{i(m-n)(\phi - \psi)} e^{i(\omega - n\epsilon \omega_c - k_z v_z)\tau} \end{aligned} \quad (4.178)$$

where $a = (\omega - k_z v_z)$, $b = \epsilon k_{\perp} v_{\perp}/\omega_c$, and we have used the Bessel identity

$$e^{ib \sin \theta} = \sum_{n=-\infty}^{\infty} J_n(b) e^{in\theta}. \quad (4.179)$$

Assuming that ω has a positive imaginary part, the integral over τ can now be done immediately with the result (again suppressing the $e^{i(k \cdot r - \omega t)}$) so that the result is the Fourier amplitude)

$$\begin{aligned} f_1(\mathbf{k}, \mathbf{v}, \omega) &= -\frac{iq}{m} \sum_{m=-\infty}^{\infty} \sum_{n=-\infty}^{\infty} \frac{J_m(b) e^{i(m-n)(\phi - \psi)}}{(\omega - n\epsilon \omega_c - k_z v_z)} \\ &\times \left\{ \frac{n J_n(b)}{b} \left[f_{0\perp} + \frac{k_z}{\omega} (v_{\perp} f_{0z} - v_z f_{0\perp}) \right] (E_x \cos \psi + E_y \sin \psi) \right. \\ &+ i J'_n(b) \left[f_{0\perp} + \frac{k_z}{\omega} (v_{\perp} f_{0z} - v_z f_{0\perp}) \right] (-E_x \sin \psi + E_y \cos \psi) \\ &\left. + J_n(b) \left[f_{0z} - \frac{n\epsilon \omega_c}{\omega} \left(f_{0z} - \frac{v_z}{v_{\perp}} f_{0\perp} \right) \right] E_z \right\}. \end{aligned} \quad (4.180)$$

In obtaining equation (4.180), we have used the Bessel identities

$$\begin{aligned} J_{\ell-1}(b) + J_{\ell+1}(b) &= \frac{2\ell}{b} J_{\ell}(b) \\ J_{\ell-1}(b) - J_{\ell+1}(b) &= 2J'_{\ell}(b) \end{aligned}$$

and let $n \pm 1 \rightarrow \ell$ so that, for example, with $\psi = 0$,

$$\begin{aligned} \sum_{n=-\infty}^{\infty} J_n(b) e^{i(m-n)\phi - in\epsilon \omega_c \tau} \cos(\phi + \epsilon \omega_c \tau) \\ &= \sum_{n=-\infty}^{\infty} \frac{J_n(b)}{2} \left[e^{i(m+1-n)\phi - i(n-1)\epsilon \omega_c \tau} + e^{i(m-1-n)\phi - i(n+1)\epsilon \omega_c \tau} \right] \\ &= \sum_{\ell=-\infty}^{\infty} \left[\frac{J_{\ell+1}(b) + J_{\ell-1}(b)}{2} \right] e^{i(m-\ell)\phi - i\ell\epsilon \omega_c \tau} \\ &= \sum_{\ell=-\infty}^{\infty} \frac{\ell}{b} J_{\ell}(b) e^{i(m-\ell)\phi - i\ell\epsilon \omega_c \tau}. \end{aligned}$$

Then for $\psi \neq 0$,

$$\begin{aligned}\cos(\phi - \psi + \epsilon\omega_c\tau) &\rightarrow \frac{n}{b}J_n(b) \\ \cos(\phi + \epsilon\omega_c\tau) &\rightarrow \frac{n}{b}J_n(b)\cos\psi - iJ'_n(b)\sin\psi \\ \sin(\phi + \epsilon\omega_c\tau) &\rightarrow \frac{n}{b}J_n(b)\sin\psi + iJ'_n(b)\cos\psi.\end{aligned}\quad (4.181)$$

In order to complete the integrals over velocity to obtain the mean current density, we note that the volume element of the integral is

$$\int d^3v = \int_0^{2\pi} d\phi \int_0^\infty v_\perp dv_\perp \int_{-\infty}^\infty dv_z$$

and it is convenient to use the orthogonality integral over ϕ which takes the form (for $\langle v_x \rangle$, $\langle v_y \rangle$, and $\langle v_z \rangle$, respectively)

$$\begin{aligned}& \sum_{m=-\infty}^{\infty} J_m(b) \int_0^{2\pi} d\phi e^{i(m-n)(\phi-\psi)} \left\{ \begin{array}{c} \cos\phi \\ \sin\phi \\ 1 \end{array} \right\} \\ &= 2\pi \left\{ \begin{array}{c} \frac{nJ_n(b)}{b} \cos\psi + iJ'_n(b)\sin\psi \\ \frac{nJ_n(b)}{b} \sin\psi - iJ'_n(b)\cos\psi \\ J_n(b) \end{array} \right\}.\end{aligned}\quad (4.182)$$

Using these elements, the effective dielectric tensor may be expressed as

$$\mathbf{K} = \begin{pmatrix} K_1 + \sin^2\psi K_0 & K_2 - \cos\psi \sin\psi K_0 & \cos\psi K_4 + \sin\psi K_5 \\ -K_2 - \cos\psi \sin\psi K_0 & K_1 + \cos^2\psi K_0 & \sin\psi K_4 - \cos\psi K_5 \\ \cos\psi K_6 - \sin\psi K_7 & \sin\psi K_6 + \cos\psi K_7 & K_3 \end{pmatrix} \quad (4.183)$$

where

$$K_0 = \sum_j \frac{\omega_{pj}^2}{\omega} \sum_{n=-\infty}^{\infty} \int d^2v \frac{[b_j J'_n(b_j)]^2 - n^2 J_n^2(b_j)}{b_j^2(\omega - n\epsilon_j \omega_{cj} - k_z v_z)} F_\perp \quad (4.184)$$

$$K_1 = 1 + \sum_j \frac{\omega_{pj}^2}{\omega} \sum_{n=-\infty}^{\infty} \int d^2v \frac{n^2 J_n^2(b_j)}{b_j^2(\omega - n\epsilon_j \omega_{cj} - k_z v_z)} F_\perp \quad (4.185)$$

$$K_2 = i \sum_j \frac{\omega_{pj}^2}{\omega} \sum_{n=-\infty}^{\infty} \int d^2v \frac{n J_n(b_j) J'_n(b_j)}{b_j(\omega - n\epsilon_j \omega_{cj} - k_z v_z)} F_\perp \quad (4.186)$$

$$K_3 = 1 + \sum_j \frac{\omega_{pj}^2}{\omega} \sum_{n=-\infty}^{\infty} \int d^2v \frac{J_n^2(b_j)}{(\omega - n\epsilon_j \omega_{cj} - k_z v_z)} F_z \quad (4.187)$$

$$K_4 = \sum_j \frac{\omega_{pj}^2}{\omega} \sum_{n=-\infty}^{\infty} \int d^2v \frac{n J_n^2(b_j)}{b_j(\omega - n\epsilon_j \omega_{cj} - k_z v_z)} \frac{v_\perp}{v_z} F_z \quad (4.188)$$

$$K_5 = i \sum_j \frac{\omega_{pj}^2}{\omega} \sum_{n=-\infty}^{\infty} \int d^2v \frac{J_n(b_j) J'_n(b_j)}{(\omega - n\epsilon_j \omega_{cj} - k_z v_z)} \frac{v_{\perp}}{v_z} F_z \quad (4.189)$$

$$K_6 = \sum_j \frac{\omega_{pj}^2}{\omega} \sum_{n=-\infty}^{\infty} \int d^2v \frac{n J_n^2(b_j)}{b_j (\omega - n\epsilon_j \omega_{cj} - k_z v_z)} \frac{v_z}{v_{\perp}} F_{\perp} \quad (4.190)$$

$$K_7 = i \sum_j \frac{\omega_{pj}^2}{\omega} \sum_{n=-\infty}^{\infty} \int d^2v \frac{J_n(b_j) J'_n(b_j)}{(\omega - n\epsilon_j \omega_{cj} - k_z v_z)} \frac{v_z}{v_{\perp}} F_{\perp} \quad (4.191)$$

where $\int d^2v = 2\pi \int_{-\infty}^{\infty} dv_z \int_0^{\infty} v_{\perp} dv_{\perp}$ and

$$\begin{aligned} F_{\perp} &= v_{\perp} \left[\frac{\partial f_{0j}}{\partial v_{\perp}} \left(1 - \frac{k_z v_z}{\omega} \right) + \frac{k_z v_{\perp}}{\omega} \frac{\partial f_{0j}}{\partial v_z} \right] \\ F_z &= v_z \left[\frac{\partial f_{0j}}{\partial v_z} + \frac{n\epsilon_j \omega_{cj}}{\omega} \left(\frac{v_z}{v_{\perp}} \frac{\partial f_{0j}}{\partial v_{\perp}} - \frac{\partial f_{0j}}{\partial v_z} \right) \right]. \end{aligned}$$

When the distribution function is isotropic ($v_{\perp} \partial F / \partial v_z = v_z \partial F / \partial v_{\perp}$), then $K_6 = K_4$ and $K_7 = K_5$. Also, only the K_1 , K_2 , and K_3 components survive in the cold plasma limit, so all of the others are first order or higher in the temperature.

Problem 4.3.2. Polar coordinates in velocity space. Fill in the steps leading to equations (4.178) and (4.181).

Problem 4.3.3. General tensor elements. Fill in the steps leading to any (except $K_{zz} = K_3$) of the composite tensor elements K_{ij} in equation (4.183).

Problem 4.3.4. Sum rules.

(i) Using the Newberger sum rule [44],

$$\sum_{n=-\infty}^{\infty} \frac{J_n(z) J_{n-m}(z)}{a-n} = \frac{(-1)^m \pi}{\sin \pi a} J_{m-a}(z) J_a(z) \quad m \geq 0 \quad (4.192)$$

prove the identities

$$\sum_{n=-\infty}^{\infty} \frac{n^2 J_n^2(z)}{a-n} = \frac{\pi a^2}{\sin \pi a} J_a(z) J_{-a}(z) - a \quad (4.193)$$

$$\sum_{n=-\infty}^{\infty} \frac{[J'_n(z)]^2}{a-n} = \frac{\pi}{\sin \pi a} J'_a(z) J'_{-a}(z) + \frac{a}{z^2} \quad (4.194)$$

$$\sum_{n=-\infty}^{\infty} \frac{n J_n(z) J'_n(z)}{a-n} = \frac{\pi a}{\sin \pi a} J_a(z) J'_{-a}(z) + \frac{a}{z} \quad (4.195)$$

$$\sum_{n=-\infty}^{\infty} \frac{J_n(z) J'_n(z)}{a-n} = \frac{\pi}{\sin \pi a} J_a(z) J'_{-a}(z) + \frac{1}{z} \quad (4.196)$$

$$\sum_{n=-\infty}^{\infty} \frac{n J_n^2(z)}{a-n} = \frac{\pi a}{\sin \pi a} J_a(z) J_{-a}(z) - 1 \quad (4.197)$$

$$\sum_{n=-\infty}^{\infty} \frac{J_n^2(z)}{a-n} = \frac{\pi}{\sin \pi a} J_a(z) J_{-a}(z). \quad (4.198)$$

(ii) Show that the dielectric tensor elements of equations (4.184)–(4.191) can be written in terms of eight alternative integrals without any Bessel function sums by use of equations (4.193)–(4.198), the first four of which are:

$$A_0 = \sum_j \frac{\epsilon_j \omega_{pj}^2}{\omega \omega_{cj}} \int d^2v \frac{\pi J'_{aj}(b_j) J'_{-aj}(b_j)}{\sin \pi a_j} F_{\perp} \quad (4.199)$$

$$A_1 = \sum_j \frac{\epsilon_j \omega_{pj}^2}{\omega \omega_{cj}} \int d^2v \frac{\pi a_j^2 J_{aj}(b_j) J_{-aj}(b_j)}{b_j^2 \sin \pi a_j} F_{\perp} \quad (4.200)$$

$$A_2 = \sum_j \frac{\epsilon_j \omega_{pj}^2}{\omega \omega_{cj}} \int d^2v \frac{\pi a_j J_{aj}(b_j) J'_{-aj}(b_j)}{b_j \sin \pi a_j} F_{\perp} \quad (4.201)$$

$$A_{\perp} = \sum_j \frac{\epsilon_j \omega_{pj}^2}{\omega \omega_{cj}} \int d^2v \frac{a_j}{b_j^2} F_{\perp} \quad (4.202)$$

with $a_j = (\omega - k_z v_z)/\epsilon_j \omega_{cj}$.

(iii) Show that four of the dielectric tensor elements may be alternatively represented by

$$K_{xx} = 1 + A_0 \sin^2 \psi + A_1 \cos^2 \psi - A_{\perp} \cos 2\psi \quad (4.203)$$

$$K_{yy} = 1 + A_0 \cos^2 \psi + A_1 \sin^2 \psi + A_{\perp} \cos 2\psi \quad (4.204)$$

$$K_{xy} = i A_2 + \frac{1}{2} (A_1 - A_0) \sin 2\psi + A_{\perp} (i - \sin 2\psi) \quad (4.205)$$

$$K_{yx} = -i A_2 + \frac{1}{2} (A_1 - A_0) \sin 2\psi - A_{\perp} (i + \sin 2\psi). \quad (4.206)$$

Problem 4.3.5. Isotropic distribution function. Prove that $K_4 = K_6$ and $K_5 = K_7$ if the distribution function is isotropic.

4.3.4 Maxwellian distributions

When the distribution function is Maxwellian, the integrals over the perpendicular and parallel velocities can be done in closed form (although an infinite sum remains). We shall treat first only the perpendicular form of the distribution function, leaving the parallel distribution function until later, so that

$$f_0(v_{\perp}, v_z) = \frac{F(v_z)}{\pi v_t^2} e^{-v_{\perp}^2/v_t^2} \quad (4.207)$$

where $v_t^2 = 2\kappa T_\perp/m$ denotes the *transverse* thermal speed (we shall introduce v_ℓ , the *longitudinal* thermal speed later), and T_\perp is the perpendicular temperature. It is unlikely that a plasma will ever be truly Maxwellian with different perpendicular and parallel temperatures, but it is not so unlikely that the perpendicular and parallel distributions will differ, especially if a wave is preferentially heating one or the other, as is often the case. The deviation from equilibrium will occasionally lead to instabilities, as we shall show in a subsequent section.

4.3.4.1 Integrating over perpendicular velocities

It is possible to evaluate the integrals of equation (4.184) through equation (4.191), but the preferred method is to return to an earlier step and integrate over the perpendicular velocities *before* we integrate over τ . With the distribution function of equation (4.207), the Fourier amplitude of f_1 may be expressed as

$$f_1(\mathbf{k}, \mathbf{v}, \omega) = -\frac{q}{m\pi v_t^2} \int_0^\infty d\tau (A_x v_x + A_y v_y + \alpha_z) \times \exp \left[-ia_x v_x - \frac{v_x^2}{v_t^2} - ia_y v_y - \frac{v_y^2}{v_t^2} + i(\omega - k_z v_z)\tau \right] \quad (4.208)$$

where

$$\alpha_x = \frac{1}{\omega_c} [k_x \sin \omega_c \tau + \epsilon k_y (1 - \cos \omega_c \tau)] \quad (4.209)$$

$$\alpha_y = \frac{1}{\omega_c} [k_y \sin \omega_c \tau - \epsilon k_x (1 - \cos \omega_c \tau)] \quad (4.210)$$

$$A_x = \alpha_x \cos \omega_c \tau + \epsilon \alpha_y \sin \omega_c \tau \quad (4.211)$$

$$A_y = \alpha_y \cos \omega_c \tau - \epsilon \alpha_x \sin \omega_c \tau \quad (4.212)$$

$$\alpha_x = -\frac{2F}{v_t^2} E_x + \left(F' + \frac{2v_z}{v_t^2} F \right) \left(\frac{k_z E_x - k_x E_z}{\omega} \right) \quad (4.213)$$

$$\alpha_y = -\frac{2F}{v_t^2} E_y + \left(F' + \frac{2v_z}{v_t^2} F \right) \left(\frac{k_z E_y - k_y E_z}{\omega} \right) \quad (4.214)$$

$$\alpha_z = F' E_z. \quad (4.215)$$

Since we need to calculate the mean current density from equation (4.177), we will require integrals over the perpendicular velocities of the type

$$G_n(a) = \frac{1}{\sqrt{\pi} v_t} \int_{-\infty}^{\infty} v^n e^{-iav - v^2/v_t^2} dv \quad (4.216)$$

which by completing the square are

$$G_0(a) = e^{-a^2 v_t^2 / 4} \quad (4.217)$$

$$G_1(a) = e^{-a^2 v_t^2 / 4} \left(-\frac{ia v_t^2}{2} \right) \quad (4.218)$$

$$G_2(a) = e^{-a^2 v_t^2 / 4} \left(\frac{v_t^2}{2} - \frac{a^2 v_t^4}{4} \right). \quad (4.219)$$

Now each integral is of the form $G_n(a_x)G_m(a_y)$, so they all have the common exponential factor $\exp[-(a_x^2 + a_y^2)v_t^2/4]$, which may be written as

$$(a_x^2 + a_y^2) \frac{v_t^2}{4} = \lambda(1 - \cos \omega_c \tau) \quad (4.220)$$

where $\lambda = \frac{1}{2}k_{\perp}^2 \rho_L^2$ and $\rho_L = v_t/\omega_c$ is the Larmor radius.

The pertinent integrals then lead to

$$\langle f_1 \rangle_{\perp} = \frac{q}{m} \int_0^{\infty} d\tau e^{\phi} \left[\frac{iv_t^2}{2} (A_x a_x + A_y a_y) - \alpha_z \right] \quad (4.221)$$

$$\langle v_x f_1 \rangle_{\perp} = \frac{q}{m} \int_0^{\infty} d\tau e^{\phi} \left[\frac{v_t^4}{4} (A_x a_x + A_y a_y) a_x + \frac{v_t^2}{2} (ia_x \alpha_z - A_x) \right] \quad (4.222)$$

$$\langle v_y f_1 \rangle_{\perp} = \frac{q}{m} \int_0^{\infty} d\tau e^{\phi} \left[\frac{v_t^4}{4} (A_x a_x + A_y a_y) a_y + \frac{v_t^2}{2} (ia_y \alpha_z - A_y) \right] \quad (4.223)$$

where now, $\phi = i(\omega - k_z v_z)\tau - \lambda(1 - \cos \omega_c \tau)$, and

$$A_x a_x + A_y a_y = \frac{1}{\omega_c} [(\alpha_x k_x + \alpha_y k_y) \sin \omega_c \tau + \epsilon (\alpha_y k_x - \alpha_x k_y) (1 - \cos \omega_c \tau)].$$

Problem 4.3.6. Maxwellian distribution.

- (i) Fill in the steps leading to equation (4.208).
- (ii) Fill in the steps leading to equation (4.209) through equation (4.215).

Problem 4.3.7. Integrating over the perpendicular velocities.

- (i) Verify equation (4.217) through equation (4.219).
- (ii) Verify equation (4.220).

4.3.4.2 Integrating over time.

In order to integrate over τ , it will be convenient to introduce another Bessel identity,

$$e^{\lambda \cos \omega_c \tau} = \sum_{n=-\infty}^{\infty} I_n(\lambda) e^{in\omega_c \tau} \quad (4.224)$$

where $I_n(\lambda)$ is the modified Bessel function of the first kind. We may use this identity in a similar fashion to the other Bessel identity and its use in the orthogonality relation of equation (4.182) to obtain

$$\begin{aligned} & \sum_{n=-\infty}^{\infty} \int_0^{\infty} d\tau I_n(\lambda) e^{i(\omega+n\omega_c-k_z v_z)\tau} \left\{ \begin{array}{c} 1 \\ \cos \omega_c \tau \\ \sin \omega_c \tau \\ \sin \omega_c \tau \cos \omega_c \tau \\ \sin^2 \omega_c \tau \end{array} \right\} \\ &= \sum_{n=-\infty}^{\infty} \left\{ \begin{array}{c} iI_n(\lambda) \\ iI'_n(\lambda) \\ \frac{n}{\lambda} I_n(\lambda) \\ \frac{1}{\lambda^2} [\lambda I'_n(\lambda) - I_n(\lambda)] \\ \frac{1}{\lambda^2} [\lambda I'_n(\lambda) - n^2 I_n(\lambda)] \end{array} \right\} \frac{1}{(\omega + n\omega_c - k_z v_z)}. \end{aligned} \quad (4.225)$$

Using these relations in equation (4.221) through equation (4.223) accomplishes the integral over time, and the results may be summarized as follows.

$$\langle f_1 \rangle_{\perp} = \frac{iv_t^2 q e^{-\lambda}}{2\omega_c m} \sum_{n=-\infty}^{\infty} \frac{\kappa_+ n I_n / \lambda + i\epsilon\kappa_- (I_n - I'_n) - 2\alpha_z \omega_c I_n / v_t^2}{\omega + n\omega_c - k_z v_z} \quad (4.226)$$

$$\langle v_x f_1 \rangle_{\perp} = \frac{iv_t^2 q e^{-\lambda}}{2\omega_c m} \sum_{n=-\infty}^{\infty} \frac{\kappa_x n I_n + (i\epsilon\kappa_y - \kappa_- k_y v_t^2 / \omega_c) \lambda (I_n - I'_n)}{\lambda (\omega + n\omega_c - k_z v_z)} \quad (4.227)$$

$$\langle v_y f_1 \rangle_{\perp} = \frac{iv_t^2 q e^{-\lambda}}{2\omega_c m} \sum_{n=-\infty}^{\infty} \frac{\kappa_y n I_n - (i\epsilon\kappa_x - \kappa_- k_x v_t^2 / \omega_c) \lambda (I_n - I'_n)}{\lambda (\omega + n\omega_c - k_z v_z)} \quad (4.228)$$

where $\kappa_+ = \alpha_x k_x + \alpha_y k_y$, $\kappa_- = \alpha_y k_x - \alpha_x k_y$, $\kappa_x = \alpha_x n \omega_c - \alpha_z k_x$, and $\kappa_y = \alpha_y n \omega_c - \alpha_z k_y$.

4.3.4.3 Integrating over the parallel velocity

In order to integrate over the parallel velocity distribution, we must specify the form of the distribution, and we shall choose a shifted Maxwellian, or

equivalently, a Maxwellian with a drift velocity such that

$$F(v_z) = \frac{1}{\sqrt{\pi} v_\ell} \exp \left[-\frac{(v_z - v_0)^2}{v_\ell^2} \right] \quad (4.229)$$

where v_ℓ is the longitudinal thermal speed given by $v_\ell^2 \equiv 2\kappa T_{||}/m$. Since α_x, α_y and α_z may be expressed in terms of F and F' , and since

$$F'(v_z) = -\frac{2(v_z - v_0)}{v_\ell^2} F(v_z)$$

the required integrals are all of the form

$$F_m = \frac{1}{\sqrt{\pi} v_\ell} \int_{-\infty}^{\infty} dv_z \frac{v_z^m F(v_z)}{\omega + n\omega_c - k_z v_z} \quad m = 0, 1, 2. \quad (4.230)$$

Changing variables to $u = (v_z - v_0)/v_\ell$, these moments of F may be expressed as

$$F_m(\zeta_n) = -\frac{1}{k_z v_\ell \sqrt{\pi}} \int_{-\infty}^{\infty} \frac{(v_0 + u v_\ell)^m e^{-u^2} du}{u - \zeta_n} \quad (4.231)$$

where

$$\zeta_n = \frac{\omega + n\omega_c - k_z v_0}{k_z v_\ell}. \quad (4.232)$$

Using the definition of the plasma dispersion function of equation (4.27), the required moments are

$$F_0(\zeta_n) = -\frac{1}{k_z v_\ell} Z(\zeta_n) \quad (4.233)$$

$$F_1(\zeta_n) = \frac{1}{k_z} \left[\frac{1}{2} Z'(\zeta_n) - \frac{v_0}{v_\ell} Z(\zeta_n) \right] \quad (4.234)$$

$$F_2(\zeta_n) = \frac{v_\ell}{k_z} \left[\left(\frac{\zeta_n}{2} + \frac{v_0}{v_\ell} \right) Z'(\zeta_n) - \frac{v_0^2}{v_\ell^2} Z(\zeta_n) \right] \quad (4.235)$$

and using these, the integrals involving F' are

$$\int_{-\infty}^{\infty} dv_z \frac{F'(v_z)}{\omega + n\omega_c - k_z v_z} = -\frac{1}{k_z v_\ell^2} Z'(\zeta_n) \quad (4.236)$$

$$\int_{-\infty}^{\infty} dv_z \frac{v_z F'(v_z)}{\omega + n\omega_c - k_z v_z} = -\frac{1}{k_z v_\ell} \left(\zeta_n + \frac{v_0}{v_\ell} \right) Z'(\zeta_n). \quad (4.237)$$

The total current density is finally constructed from

$$\mathbf{j} = \sum_j n_j q_j \int_{-\infty}^{\infty} dv_z [\langle v_x f_{1j} \rangle_{\perp} \hat{e}_x + \langle v_y f_{1j} \rangle_{\perp} \hat{e}_y + v_z \langle f_{1j} \rangle_{\perp} \hat{e}_z]. \quad (4.238)$$

Problem 4.3.8. Parallel velocity integrals. Verify equations (4.234)–(4.237).

Problem 4.3.9. Lorentzian distribution. Evaluate the integrals corresponding to equations (4.233)–(4.237) for the Lorentzian distribution function:

$$F(v_z) = A / [(v_z - v_0)^2 + v_\ell^2].$$

4.3.5 The dielectric tensor

From the current density of equation (4.238), all of the dielectric tensor elements may be constructed from the mobility tensor, \mathbf{M} , where $\langle \mathbf{v}_j \rangle = \mathbf{M}_j \cdot \mathbf{E}$ by

$$\mathbf{K} = \mathbf{I} + \sum_j \frac{n_j q_j}{-i\omega\epsilon_0} \mathbf{M}_j. \quad (4.239)$$

The final forms are not unique, since

$$\sum_{n=-\infty}^{\infty} n I_n = \sum_{n=-\infty}^{\infty} (I_n - I'_n) = 0 \quad (4.240)$$

so certain terms can be added or subtracted. The general components may be expressed as

$$K_0 = 2 \sum_j \frac{\omega_{pj}^2 e^{-\lambda_j}}{\omega k_z v_{\ell j}} \sum_{n=-\infty}^{\infty} \lambda_j (I_n - I'_n) \left[\left(1 - \frac{k_z v_{0j}}{\omega} \right) Z(\zeta_{nj}) + \frac{k_z v_{\ell j}}{\omega} \left(1 - \frac{T_{\perp j}}{T_{\parallel j}} \right) \frac{Z'(\zeta_{nj})}{2} \right] \quad (4.241)$$

$$K_1 = 1 + \sum_j \frac{\omega_{pj}^2 e^{-\lambda_j}}{\omega k_z v_{\ell j}} \sum_{n=-\infty}^{\infty} \frac{n^2 I_n}{\lambda_j} \left[\left(1 - \frac{k_z v_{0j}}{\omega} \right) Z(\zeta_{nj}) + \frac{k_z v_{\ell j}}{\omega} \left(1 - \frac{T_{\perp j}}{T_{\parallel j}} \right) \frac{Z'(\zeta_{nj})}{2} \right] \quad (4.242)$$

$$K_2 = i \sum_j \frac{\epsilon_j \omega_{pj}^2 e^{-\lambda_j}}{\omega k_z v_{\ell j}} \sum_{n=-\infty}^{\infty} n (I_n - I'_n) \left[\left(1 - \frac{k_z v_{0j}}{\omega} \right) Z(\zeta_{nj}) + \frac{k_z v_{\ell j}}{\omega} \left(1 - \frac{T_{\perp j}}{T_{\parallel j}} \right) \frac{Z'(\zeta_{nj})}{2} \right] \quad (4.243)$$

$$K_3 = 1 - \sum_j \frac{\omega_{pj}^2 e^{-\lambda_j}}{\omega k_z v_{\ell j}} \sum_{n=-\infty}^{\infty} I_n \left(\frac{\omega + n\omega_{cj}}{k_z v_{\ell j}} \right) \times \left\{ \left[1 + \frac{n\omega_{cj}}{\omega} \left(1 - \frac{T_{\parallel j}}{T_{\perp j}} \right) \right] Z'(\zeta_{nj}) \right\}$$

$$+ \frac{2n\omega_{cj}T_{||j}v_{0j}}{\omega T_{\perp j}v_{\ell j}} \left[Z(\zeta_{nj}) + \frac{k_z v_{\ell j}}{\omega + n\omega_{cj}} \right] \} \quad (4.244)$$

$$K_4 = \sum_j \frac{k_{\perp} \omega_{pj}^2 e^{-\lambda_j}}{k_z \omega \omega_{cj}} \sum_{n=-\infty}^{\infty} \frac{n I_n}{\lambda_j} \left\{ \frac{n \omega_{cj} v_{0j}}{\omega v_{\ell j}} Z(\zeta_{nj}) \right. \\ \left. + \left[\frac{T_{\perp j}}{T_{||j}} - \frac{n \omega_{cj}}{\omega} \left(1 - \frac{T_{\perp j}}{T_{||j}} \right) \right] \frac{Z'(\zeta_{nj})}{2} \right\} \quad (4.245)$$

$$K_5 = i \sum_j \frac{k_{\perp} \epsilon_j \omega_{pj}^2 e^{-\lambda_j}}{k_z \omega \omega_{cj}} \sum_{n=-\infty}^{\infty} (I_n - I'_n) \left\{ \frac{n \omega_{cj} v_{0j}}{\omega v_{\ell j}} Z(\zeta_{nj}) \right. \\ \left. + \left[\frac{T_{\perp j}}{T_{||j}} - \frac{n \omega_{cj}}{\omega} \left(1 - \frac{T_{\perp j}}{T_{||j}} \right) \right] \frac{Z'(\zeta_{nj})}{2} \right\} \quad (4.246)$$

and $K_6 = K_4$ and $K_7 = K_5$, so the hot plasma dielectric tensor of equation (4.183) reduces to the form

$$\mathbf{K} = \begin{pmatrix} K_1 + \sin^2 \psi K_0 & K_2 - \cos \psi \sin \psi K_0 & \cos \psi K_4 + \sin \psi K_5 \\ -K_2 - \cos \psi \sin \psi K_0 & K_1 + \cos^2 \psi K_0 & \sin \psi K_4 - \cos \psi K_5 \\ \cos \psi K_4 - \sin \psi K_5 & \sin \psi K_4 + \cos \psi K_5 & K_3 \end{pmatrix} \quad (4.247)$$

where $k_x = k_{\perp} \cos \psi$ and $k_y = k_{\perp} \sin \psi$. The proof that $K_6 = K_4$ and $K_7 = K_5$, where K_6 and K_7 come from $\langle v_z \rangle$ and K_4 and K_5 come from either $\langle v_x \rangle$ or $\langle v_y \rangle$ is only apparent when the Bessel identities of equation (4.240) are used.

The dielectric tensor, which is *not*, in general, Hermitian, does have the symmetry property that $K_{ij}(B_0) = K_{ji}(-B_0)$ ($\omega_{cj} \rightarrow -\omega_{cj}$), since $K_2(-B_0) = -K_2(B_0)$ and $K_5(-B_0) = -K_5(B_0)$ while the other components are invariant, and this is a general result from the Onsager relations.

It is customary to set $\psi = 0$ so $k_x = k_{\perp}$ and $k_y = 0$, which can be accomplished by merely rotating the coordinate system, but the full symmetry is more apparent in this presentation.

Special Case: Isotropic Maxwellian without Drifts. When $v_{0j} = 0$ and $T_{\perp j} = T_{||j}$, then the tensor components simplify significantly, and may be represented by

$$K_0 = 2 \sum_j \frac{\omega_{pj}^2 e^{-\lambda_j}}{\omega k_z v_j} \sum_{n=-\infty}^{\infty} \lambda_j (I_n - I'_n) Z(\zeta_{nj}) \quad (4.248)$$

$$K_1 = 1 + \sum_j \frac{\omega_{pj}^2 e^{-\lambda_j}}{\omega k_z v_j} \sum_{n=-\infty}^{\infty} \frac{n^2 I_n}{\lambda_j} Z(\zeta_{nj}) \quad (4.249)$$

$$K_2 = i \sum_j \frac{\epsilon_j \omega_{pj}^2 e^{-\lambda_j}}{\omega k_z v_j} \sum_{n=-\infty}^{\infty} n (I_n - I'_n) Z(\zeta_{nj}) \quad (4.250)$$

$$K_3 = 1 - \sum_j \frac{\omega_{pj}^2 e^{-\lambda_j}}{\omega k_z v_j} \sum_{n=-\infty}^{\infty} I_n \zeta_{nj} Z'(\zeta_{nj}) \quad (4.251)$$

$$K_4 = \sum_j \frac{k_{\perp} \omega_{pj}^2 e^{-\lambda_j}}{2k_z \omega \omega_{cj}} \sum_{n=-\infty}^{\infty} \frac{n I_n}{\lambda_j} Z'(\zeta_{nj}) \quad (4.252)$$

$$K_5 = i \sum_j \frac{k_{\perp} \epsilon_j \omega_{pj}^2 e^{-\lambda_j}}{2k_z \omega \omega_{cj}} \sum_{n=-\infty}^{\infty} (I_n - I'_n) Z'(\zeta_{nj}). \quad (4.253)$$

Problem 4.3.10. Cold plasma limits. For $v_{0j} = 0$,

- (i) Calculate the six dielectric tensor elements as $T_{\perp} \rightarrow 0, T_{\parallel} \neq 0$.
- (ii) Calculate the six dielectric tensor elements as $T_{\parallel} \rightarrow 0, T_{\perp} \neq 0$.
- (iii) Calculate the six dielectric tensor elements as $T_{\parallel}, T_{\perp} \rightarrow 0$. Show that this reduces to the cold plasma dielectric tensor. Does the order in which these limits are taken matter?

4.3.6 The hot plasma dispersion relation

The vector wave equation of equation (2.18), when $k_y \neq 0$ takes the form

$$\begin{pmatrix} \kappa_{xx} - k_z^2 - k_y^2 & \kappa_{xy} + k_x k_y & \kappa_{xz} + k_x k_z \\ \kappa_{yx} + k_y k_x & \kappa_{yy} - k_z^2 - k_x^2 & \kappa_{yz} + k_y k_z \\ \kappa_{zx} + k_z k_x & \kappa_{zy} + k_z k_y & \kappa_{zz} - k_{\perp}^2 \end{pmatrix} \begin{pmatrix} E_x \\ E_y \\ E_z \end{pmatrix} = 0 \quad (4.254)$$

where the various tensor elements are given in equation (4.247) and we define $\kappa_j \equiv (\omega^2/c^2) K_j$. The dispersion relation is given by setting the determinant of coefficients to zero, and it may be written either in terms of K_{ij} , n_x , n_y , and n_z (dimensionless quantities), or in terms of κ_{ij} , k_x , k_y , and k_z as written here.

While it is apparent that the components of the wave equation depend on ψ , the hot plasma dispersion relation (HPDR) does not, and may be written as

$$\begin{aligned} & [\gamma(\gamma - \kappa_0 + k_{\perp}^2) + \kappa_2^2] \kappa_3 + k_{\perp}^2 [(\gamma - \kappa_0 + k_{\perp}^2) \kappa_1 - \kappa_2^2] \\ & + \kappa_4 (\gamma - \kappa_0 + k_{\perp}^2) (2k_{\perp} k_z + \kappa_4) - \kappa_5 [\gamma \kappa_5 + 2\kappa_2 (k_{\perp} k_z + \kappa_4)] = 0 \end{aligned} \quad (4.255)$$

where we have introduced $\gamma \equiv k_z^2 - \kappa_1$.

Problem 4.3.11. HPDR. Show that the determinant of coefficients of equation (4.254) results in the hot plasma dispersion relation given by equation (4.255).

4.3.7 Examples of hot plasma wave effects

4.3.7.1 Parallel propagation

For parallel propagation, $k_\perp = \lambda = 0$ and the tensor elements simplify since the infinite sums reduce to either one or two terms. In addition, we find $K_0 = K_4 = K_5 = 0$, so the dispersion relation reduces to

$$(\gamma^2 + \kappa_2^2)\kappa_3 = 0 \quad (4.256)$$

so the roots are $\kappa_3 = 0$, and $k_z^2 = \kappa_1 \pm i\kappa_2$. The first root is the plasma wave which is unaffected by the magnetic field, so it is the case treated in section 4.2.5 with the dispersion relation of equation (4.138). The other two roots are the R - and L -waves, whose dispersion relations reduce to

$$\begin{aligned} n_{R,L}^2 &= K_1 \pm iK_2 \\ &= 1 + \sum_j \frac{\omega_{pj}^2}{\omega k_z v_{\ell j}} \left[Z_{1j} \left(\frac{1 \pm \epsilon_j}{2} \right) + Z_{-1j} \left(\frac{1 \mp \epsilon_j}{2} \right) \right] \end{aligned} \quad (4.257)$$

where

$$Z_{\pm 1} = \left(1 - \frac{k_z v_0}{\omega} \right) Z(\zeta_{\pm 1}) + \frac{k_z v_\ell}{2\omega} \left(1 - \frac{T_\perp}{T_\parallel} \right) Z'(\zeta_{\pm 1}). \quad (4.258)$$

The structure of this dispersion relation confirms the general character we had observed with the cold plasma waves except that now resonance has a different meaning. The R -wave is here seen to be a function of $Z(\zeta_{1i})$ and $Z(\zeta_{-1e})$, and assuming that $\omega \gg k_z v_{\ell j}$, then there is virtually no ion damping associated with the R -wave since $|\zeta_{1i}| \gg 1$ and the ion damping is exponentially small. Near the electron cyclotron resonance, however, $|\zeta_{-1e}| \simeq 0$, and in this limit $Z(\zeta_{-1e}) \simeq i\sqrt{\pi}$ so there is no longer any resonance at the electron cyclotron frequency, but now there is strong damping. If we neglect drifts and anisotropic temperature effects, and assume that $|\zeta_{-1e}|$ is large, but not too large, then the R -wave dispersion relation reduces to

$$\frac{k_z^2 c^2}{\omega^2} = 1 - \frac{\omega_{pe}^2}{\omega(\omega - \omega_{ce})} + \frac{i\sqrt{\pi}\omega_{pe}^2}{\omega k_z v_e} \exp \left[- \left(\frac{\omega - \omega_{ce}}{k_z v_e} \right)^2 \right]. \quad (4.259)$$

Assuming weak damping such that $\omega_i \ll \omega_r$, the damping is approximately

$$\frac{\omega_i}{\omega_r} \sim - \frac{\sqrt{\pi}\omega_{pe}^2}{\omega_r k_z v_e [2 + \omega_{pe}^2 \omega_{ce}/\omega_r (\omega_r - \omega_{ce})^2]} \exp \left[- \left(\frac{\omega_r - \omega_{ce}}{k_z v_e} \right)^2 \right] \quad (4.260)$$

which indicates the damping is exponentially small far from resonance, but as resonance approaches, the exponential term grows but the denominator also

grows, suggesting a maximum value of the damping rate before resonance is reached. This is misleading, however, since the growing denominator depended on the weak damping assumption and this is no longer valid where this growing term dominates. In fact, it may be shown that for $\omega_r = \omega_{ce}$ that $\omega_i \gg \omega_r$. Except near this resonance, the damping is weak, so the cold plasma dispersion relation is relevant except near resonance.

The transition to an electron acoustic wave is much more questionable, however, since the transition does not occur until the influence of the resonance has slowed the phase velocity to the neighborhood of the thermal velocity. In order to see the difficulty more clearly, we write the dispersion relation including the next higher order term in the expansion of the PDF. This leads to

$$\frac{k_z^2 c^2}{\omega^2} = 1 - \frac{\omega_{pe}^2}{\omega(\omega - \omega_{ce})} \left[1 + \frac{k_z^2 v_e^2}{2(\omega - \omega_{ce})^2} \right] + \frac{i\sqrt{\pi}\omega_{pe}^2}{\omega k_z v_e} \exp \left[- \left(\frac{\omega - \omega_{ce}}{k_z v_e} \right)^2 \right] \quad (4.261)$$

where now we can see that for the thermal term to become important, which is a necessary condition for the acoustic branch, we require $k_z v_e / (\omega - \omega_{ce}) > 1$ and before this happens we have entered or passed through the strong cyclotron damping region. For waves dominated by the derivative of the PDF, $Z'(\zeta)$, rather than $Z(\zeta)$, as was the case for the ion acoustic wave in section 4.2.5, there is a weakly damped wave on the other side when $|\zeta| \ll 1$, but such is not the case for the R - or L -wave with $T_\perp = T_\parallel$.

Problem 4.3.12. Damping rate at resonance. Show that $\omega_i \gg \omega_r$ for the R -wave at $\omega_r = \omega_{ce}$.

4.3.7.2 Finite Larmor orbit effects

Considering the influence of a magnetic field on the hot plasma adds another effect that is entirely independent of the Landau or cyclotron damping we have discovered in the unmagnetized plasma or, in the case of parallel propagation, in a magnetized plasma. These effects are generally called finite Larmor orbit (FLR) effects and introduce two new general kinds of effects, one of which is the addition of higher cyclotron harmonic effects, indicated by the infinite sums in each of the dielectric tensor components, and the other a class of electrostatic waves that have no counterpart in the cold plasma, and differ dramatically from the warm plasma electrostatic waves we have already encountered. These latter waves, which are commonly called Bernstein modes after I Bernstein because of his analysis of the hot plasma electrostatic dispersion relation as $k_z \rightarrow 0$ [45], will be treated in the next section. In this section, we investigate the lowest-order FLR effects by treating $\lambda_j = \frac{1}{2}k_\perp^2 \rho_{Lj}^2$ as a small parameter.

Before expanding the tensor elements in λ_j , we first discuss the physics of this new phenomenon. When the wavelength perpendicular to the magnetic field

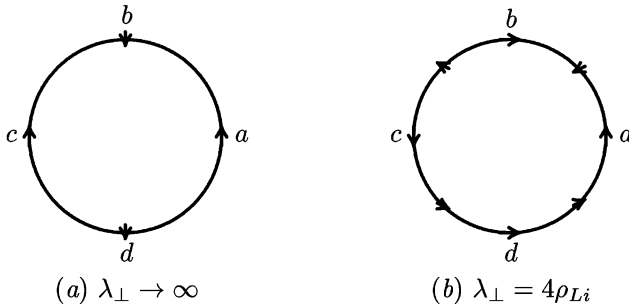


Figure 4.7. *L*-wave electric fields on an ion as it follows its orbit counterclockwise with $\omega = 2\omega_{ci}$: (a) with $k_\perp = 0$; (b) with $k_\perp \rho_{Li} = \pi/2$.

is infinite ($k_\perp = 0$), then as each particle executes its circular orbit, it maintains the same phase relation relative to the driving wave since the driving wave has no spatial dependence across the orbit. If we consider a case where $\omega = 2\omega_c$ and $k_\perp = 0$, and follow an ion making a counterclockwise orbit beginning at point *a* in figure 4.7(a) where the vectors indicate the direction of the wave's electric field at various points along the orbit, it is clear that the particle gains energy from the wave at *a* where the motion and the field are parallel. Following it around, it is moving perpendicular to the wave field at *b*, so it is neither accelerated nor decelerated there. It is moving antiparallel to the wave field at *c* so it is being slowed down there, and the point *d* is essentially equivalent to *b*, where there is no effect on the orbit. We can see that for this case, on the average, there is no net effect at this frequency, so the particles and wave show no special effects. If, however, we consider a case where the wavelength across the orbit is twice the orbit diameter, the situation is as shown in figure 4.7(b) (with the wave traveling to the right).

For this case, the phase is chosen so that the electric field is again parallel to the motion at *a*, but now it is antiparallel at *b*, and parallel again at both *c* and *d*. From the indicated directions for the wave field at the intermediate points, it may be seen that the interaction nearly cancels on the upper half of the orbit, while the ion is being accelerated continuously on the lower half of the orbit. This difference is due to the fact that in the upper half of the orbit, the particle is moving to the left and the wave is moving to the right, so the phase changes rapidly, while in the lower half, the particle is moving in the same direction as the wave and the particle nearly stays in phase with the wave field. For any finite k_\perp there is a nonvanishing contribution at *every* harmonic when averaged over the distribution, but for small $k_\perp \rho_L$, the interaction is progressively weaker as the harmonic number increases.

Keeping only first order terms in the expansion parameter λ_j (not to be confused with the perpendicular wavelength λ_\perp in figure 4.7), the isotropic

temperature tensor components of equation (4.248) through equation (4.253) are:

$$K_0 = \sum_j \frac{2\omega_{pj}^2 \lambda_j}{\omega k_z v_j} \{Z(\zeta_0) - \frac{1}{2}[Z(\zeta_1) + Z(\zeta_{-1})]\}_j \quad (4.262)$$

$$K_1 = 1 + \sum_j \frac{\omega_{pj}^2}{2\omega k_z v_j} \{[Z(\zeta_{-1}) + Z(\zeta_1)](1 - \lambda) + \lambda[Z(\zeta_{-2}) + Z(\zeta_2)]\}_j \quad (4.263)$$

$$K_2 = i \sum_j \frac{\epsilon_j \omega_{pj}^2}{2\omega k_z v_j} \{[Z(\zeta_{-1}) - Z(\zeta_1)](1 - 2\lambda) + \lambda[Z(\zeta_{-2}) - Z(\zeta_2)]\}_j \quad (4.264)$$

$$K_3 = 1 - \sum_j \frac{\omega_{pj}^2}{\omega k_z v_j} \{\xi_0 Z'(\zeta_0)(1 - \lambda) + \frac{\lambda}{2}[\xi_{-1} Z'(\zeta_{-1}) + \xi_1 Z'(\zeta_1)]\}_j \quad (4.265)$$

$$K_4 = \sum_j \frac{\omega_{pj}^2 \sqrt{\lambda_j}}{2\sqrt{2}\omega k_z v_j} [Z'(\zeta_1) - Z'(\zeta_{-1})]_j \quad (4.266)$$

$$K_5 = i \sum_j \frac{\epsilon_j \omega_{pj}^2 \sqrt{\lambda_j}}{\sqrt{2}\omega k_z v_j} \{Z'(\zeta_0) - \frac{1}{2}[Z'(\zeta_1) + Z'(\zeta_{-1})]\}_j. \quad (4.267)$$

From these expressions, several things are immediately evident. To zero order in λ_j , it is apparent that only K_1 , K_2 , and K_3 are nonzero, and they have no cyclotron interactions above the fundamental resonance (which we shall call the *first* harmonic so that $n = 1$ is the first harmonic, $n = 2$ is the second harmonic, etc. Other authors sometimes use $n = 1$ as the fundamental, $n = 2$ as the *first* harmonic, etc). From these it is easy to recover the cold plasma dielectric tensor by using the large argument expansion of the PDF. It is also apparent that through first order, only K_1 and K_2 have an interaction at the second harmonic ($n = \pm 2$). Thus if one wanted to examine effects near the second harmonic, it would be appropriate to neglect all other first-order terms in λ_j except the harmonic terms, because the harmonic resonant terms can be taken to be large near their resonance (a large term multiplied by a small term could be considered zero order, while all other first-order terms would be small by comparison). It follows that near these harmonics, we only need K_1 , K_2 , and K_3 .

Some comments about the order of K_4 and K_5 are in order since they appear to be of order $\sqrt{\lambda_j}$ in equations (4.266) and (4.267). That these are properly considered as first order in λ_j is evident first by noting from the HPDR, equation (4.255), that both K_4 and K_5 appear multiplied by $k_z k_\perp$ or one another, so their terms appear in the dispersion relation as first order in λ_j . If we use the large argument expansion for $Z(\zeta)$ in equation (4.266) for K_4 , for example, we

find

$$K_4 \simeq - \sum_j \frac{\omega_{pj}^2 k_z k_\perp v_j^2}{(\omega^2 - \omega_{cj}^2)^2}$$

and the expression for K_5 is similar. This means that multiplying either by $k_z k_\perp$ or by one another produces a term of the order of λ_j in the HPDR. Hence we have not included any higher-order terms for these components.

Problem 4.3.13. Third harmonic. Find the tensor elements corresponding to equations (4.262) through (4.267) near the third harmonic. (Neglect $n \pm 2$ terms, but go to order λ^2 for $n \pm 3$.)

4.4 Electrostatic waves

For hot plasmas, where the tensor elements are so formidable individually and the dispersion relation virtually defies any analytic analysis for any but the simplest cases, the simplifications of the electrostatic approximation make it even more attractive than it was in either the cold or warm plasma approximations. The general hot plasma electrostatic dispersion relation from equation (2.106) results in

$$k_\perp^2 \kappa_1 + 2k_\perp k_z \kappa_4 + k_z^2 \kappa_3 = 0. \quad (4.268)$$

While it is possible to combine the terms in the expressions for K_1 , K_3 , and K_4 to simplify this dispersion relation, it will be useful for a large k_\perp approximation to begin again with the integrals over the unperturbed orbits. We start with the electrostatic restriction that $\omega \mathbf{B}_1 = \mathbf{k} \times \mathbf{E}_1 = 0$ so the Fourier transform of the electric field may be represented by $\mathbf{E} = -i\mathbf{k}\varphi$. Then equation (4.221) reduces to

$$\langle f_1 \rangle_\perp = -\frac{q\varphi}{m} \int_0^\infty d\tau e^\phi \left(\frac{Fk_\perp^2}{\omega_c} \sin \omega_c \tau - ik_z F' \right). \quad (4.269)$$

Integrating over time, this becomes

$$\langle f_1 \rangle_\perp = -\frac{q\varphi e^{-\lambda}}{m} \sum_{n=-\infty}^{\infty} \left(\frac{nFk_\perp^2}{\lambda\omega_c} + k_z F' \right) \frac{I_n(\lambda)}{\omega + n\omega_c - k_z v_z} \quad (4.270)$$

and finally, integrating over the parallel velocity distribution, this becomes

$$\langle f_1 \rangle = \frac{2q\varphi e^{-\lambda}}{mv_\ell^2} \sum_{n=-\infty}^{\infty} \left[1 + \frac{\omega + n\omega_c(1 - T_{||}/T_\perp) - k_z v_0}{k_z v_\ell} Z(\zeta_n) \right] I_n(\lambda). \quad (4.271)$$

Then we use Poisson's equation,

$$\nabla^2 \varphi = -k^2 \varphi = -\frac{\rho}{\epsilon_0} = -\frac{1}{\epsilon_0} \sum_j n_0 j q_j \langle f_{1j} \rangle$$

to obtain the hot plasma electrostatic dispersion relation

$$k^2 + \sum_j \frac{2\omega_{pj}^2 e^{-\lambda_j}}{v_{\ell j}^2} \sum_{n=-\infty}^{\infty} \left[1 + \frac{\omega + n\omega_{cj}(1 - T_{\parallel j}/T_{\perp j}) - k_z v_{0j}}{k_z v_{\ell j}} Z(\zeta_{nj}) \right] \times I_n(\lambda_j) = 0. \quad (4.272)$$

Problem 4.4.1. The hot plasma electrostatic dispersion relation. Show that the hot plasma electrostatic dispersion relation of equation (4.272) (with $T_{\perp} = T_{\parallel}$ and $v_{0j} = 0$) can be obtained from the general hot plasma dielectric tensor elements. First show that $\mathbf{k} \cdot \mathbf{K} \cdot \mathbf{k} = 0$ leads to equation (4.268). Then use the tensor elements from equations (4.248) through (4.253) for $T_{\perp} = T_{\parallel}$ and $v_{0j} = 0$. (Hint: A Bessel identity is required.)

4.4.1 Perpendicular propagation–Bernstein modes

We have seen a variety of hot plasma effects due to Landau and cyclotron damping, but another important result has no damping associated with it at all, and this is the case for perpendicularly propagating electrostatic waves. As $k_z \rightarrow 0$, the dispersion relation reduces to

$$k_{\perp}^2 = \sum_j 2k_{Dj}^2 e^{-\lambda_j} \sum_{n=1}^{\infty} I_n \frac{n^2}{v_j^2 - n^2} \quad (4.273)$$

where again $k_{Dj}^2 = 2\omega_{pj}^2/v_j^2$ is the Debye wavenumber and $v_j = \omega/\omega_{cj}$. This dispersion relation has a resonance at every harmonic of both cyclotron frequencies but the ‘strength’ of the resonance indicated by $I_n(\lambda_j)$ becomes small for large n . We also note that there is no absorption here to damp out the wave at resonance. Within the framework of the collisionless theory outlined in this chapter, these resonances remain unresolved.

Examining equation (4.273) for small λ_i (which means $\lambda_e \ll 1$ since $\lambda_e/\lambda_i = T_e m_e / T_i m_i \ll 1$), we shall approximate $I_n(\lambda) \simeq (\lambda/2)^n/n!$ and consider cold electrons. In this case, the dispersion relation can be approximated by

$$\frac{V_A^2}{c^2} = \frac{1}{v^2 - 1} + \frac{\lambda_i}{v^2 - 4} + \frac{3\lambda_i^2}{8(v^2 - 9)} + \dots \quad (4.274)$$

where we have neglected m_e/m_i and taken $e^{-\lambda_i} = 1$. If we investigate the behavior near $v \simeq 2$, letting $v = 2$ in the nonresonant terms, then to lowest order,

$$v = 2 - \frac{3\lambda_i}{4(1 - 3V_A^2/c^2)} \quad (4.275)$$

so the wave propagates below the second harmonic, and for large λ_i , the dispersion relation approaches the fundamental. This is shown in figure 4.8(a)

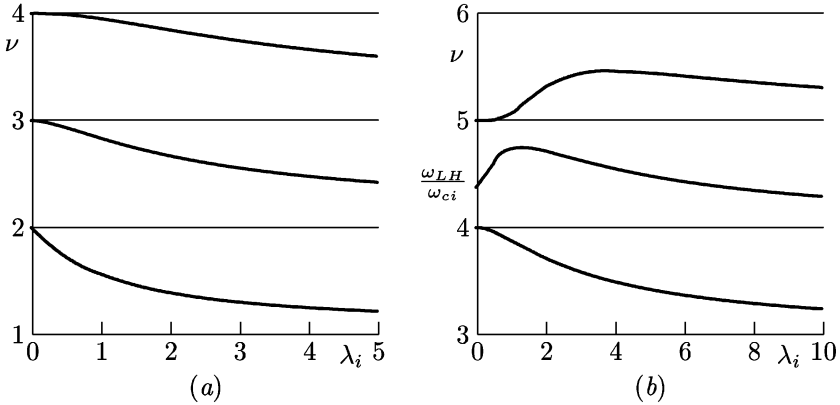


Figure 4.8. Ion Bernstein wave dispersion relations: (a) the first few modes with $\nu \ll \omega_{LH}$ ($\omega_{pe}^2/\omega_{ce}^2 = 10$); (b) higher order modes near ω_{LH} ($\omega_{pe}/\omega_{ce} = 0.1$).

where the dispersion relation falls away from $\nu = 2$ with linear slope for small λ_i .

Using the same technique near $\nu \simeq 3$, the result to lowest order is

$$\nu = 3 - \frac{\lambda_i^2}{2(1 - 8V_A^2/c^2)} \quad (4.276)$$

so this wave begins with zero slope in figure 4.8(a) and then falls toward $\nu = 2$ as λ_i gets large. We can generalize this analysis to

$$\nu = n - \frac{(n^2 - 1)\lambda_i^{n-1}}{2^n(n-1)![1 - (n^2 - 1)V_A^2/c^2]} \quad (4.277)$$

so for the higher harmonics, ν deviates less and less from the resonance for fixed λ_i , but eventually approaches the next lower harmonic.

For sufficiently high harmonics, or for sufficiently low density, however, the character of these dispersion curves changes, since for $\lambda_i = 0$, equation (4.273) reduces to

$$1 = \frac{\omega_{pe}^2}{\omega^2 - \omega_{ce}^2} + \frac{\omega_{pi}^2}{\omega^2 - \omega_{ci}^2} \quad (4.278)$$

which is the condition for the hybrid resonances. Hence one curve begins at $\nu = \omega_{LH}/\omega_{ci}$ for $\lambda_i = 0$ and then falls to the next lower harmonic as $\lambda_i \rightarrow \infty$. The wave whose dispersion curve starts at the next higher resonance then lies *above* the resonance, rising to a maximum at some finite λ_i (but below the next higher resonance) and then falls back to the same resonance as $\lambda_i \rightarrow \infty$. This behavior is illustrated in figure 4.8(b).

4.4.2 High-order Bernstein modes

Whenever the perpendicular wavelength gets very short (or k_{\perp} gets large), the Bessel function sum is a tedious representation since many terms are required for large λ . This situation occurs for lower hybrid waves, where the approach to the hybrid resonance leads to large values of λ_i . There are two ways of treating this case, and it is instructive to examine both.

4.4.2.1 Unmagnetized ions

First, if $k_{\perp}\rho_i \gg 1$, then an individual particle follows a nearly straight line over a single perpendicular wavelength, and during that portion of its orbit when it is traveling parallel to the wave, it may interact resonantly with the wave and one might expect Landau damping of the wave. This approximation is equivalent to ignoring the magnetic field entirely, but we still speak of the electrons as being magnetized with only the ions being unmagnetized. The electrostatic dispersion relation for this case, with cold electrons ($\lambda_e \ll 1, \omega/k_z v_e \gg 1$), becomes

$$k_z^2 \left(1 - \frac{\omega_{pe}^2}{\omega^2} \right) + k_{\perp}^2 \left(1 + \frac{\omega_{pe}^2}{\omega_{ce}^2} \right) - \frac{k_{Di}^2}{2} Z' \left(\frac{\omega}{kv_i} \right) = 0 \quad (4.279)$$

where we note that the electron terms distinguish between parallel and perpendicular directions, but the ion term does not. If we then take the limit as $k_z \rightarrow 0$, there is still Landau damping through the ion term, depending on the argument $\zeta_{\perp} = \omega/k_{\perp} v_i$. This conflicts with the general electrostatic dispersion relation, equation (4.272), where there were no imaginary parts with $k_z = 0$, and hence no damping of any kind. Obviously, there is some transition between these two cases, since if we let the magnetic field approach zero, Landau damping must eventually occur at any angle, but if we allow particles to execute their full Larmor orbits, the damping disappears. From the physical picture of Landau damping, where thermal spreading leads to the disappearance of the wave, this would imply that if the wave is completely damped before the particle orbit deviates significantly from a straight line, we would expect to observe Landau damping. However, it may be shown that as particles execute the remainder of their orbits, however slowly, the wave is reconstructed and there is no net damping. In order to observe this Landau damping, then, it is necessary that the usually neglected collisions be frequent enough that the particles lose their phase information before completing their Larmor orbits, or $\omega_{ci} \tau_i < 1$ where τ_i is the mean ion collision time (this limit is overly stringent, since phase information is generally lost before particles make 90° deflections, on the average).

Problem 4.4.2. The unmagnetized ion dispersion relation.

- (i) Show that in the cold ion limit of equation (4.279) that $\omega = \omega_{LH}$.

- (ii) Show that in keeping the first warm ion term in equation (4.279), there are two branches of the dispersion relation, and sketch them (ω versus k_{\perp} , k_z as a parameter).

4.4.2.2 The large- λ dispersion relation

The other way to understand this problem, without assuming the ions are unmagnetized, is to find another way to treat the Bessel sum so that some analytic function can guide us in this limit. For this analysis, we shall assume the electrons are again cold and separate out the cold electron terms with the result,

$$k_z^2 \left(1 - \frac{\omega_{pe}^2}{\omega^2} \right) + k_{\perp}^2 \left(1 + \frac{\omega_{pe}^2}{\omega_{ce}^2} \right) + k_{Di}^2 \sum_{m=-\infty}^{\infty} e^{-\lambda} I_m(\lambda) \left[1 + \frac{\omega}{k_z v_i} Z \left(\frac{\omega + m\omega_{ci}}{k_z v_i} \right) \right] = 0. \quad (4.280)$$

By adding and subtracting the leading asymptotic term for Z ($Z(\zeta) \rightarrow Z(\zeta) + 1/\zeta - 1/\zeta$) and regrouping the terms, the ion sum can be written exactly as

$$\sum_{m=-\infty}^{\infty} I_m \left[1 + \frac{\omega}{k_z v_i} Z(\zeta_m) \right] = -2 \sum_{m=1}^{\infty} \frac{m^2 I_m}{\nu^2 - m^2} - \sum_{m=-\infty}^{\infty} \frac{\nu I_m Z'(\zeta_m)}{2(\nu + m)}$$

where $\nu = \omega/\omega_{ci}$.

The single-ended sum has most of the dispersive information, and the sum involving the PDF is important only near each harmonic. We may thus make the approximation that the absorption is due to only a single resonant term and reduce that sum over m to the one term at $m = -n$ where n is the integer closest to ν . The other sum we define by

$$F(\nu, \lambda) \equiv -2e^{-\lambda} \sum_{m=1}^{\infty} I_m \frac{m^2}{\nu^2 - m^2} = 1 + i\nu \int_0^{\infty} e^{-\lambda(1-\cos z) + i\nu z} dz \quad (4.281)$$

where we have used the identity $\sum_{m=-\infty}^{\infty} e^{-\lambda} I_m(\lambda) = 1$ and equation (4.224) and $\text{Im}(\nu) > 0$ in establishing the second equality. At this point, we have simply backed up from the Bessel sum to the integral over time, but now we wish to evaluate $F(\nu, \lambda)$ by asymptotic methods instead of using the Bessel sums. To this end, we define our largeness parameter $\kappa = \sqrt{\nu^2 + \lambda^2}$ so that

$$F(\nu, \lambda) = 1 + i\nu e^{-\lambda} \int_0^{\infty} e^{\kappa h(z)} dz \quad (4.282)$$

where

$$h(z) = \frac{\lambda}{\kappa} \cos z + i\frac{\nu}{\kappa} z.$$

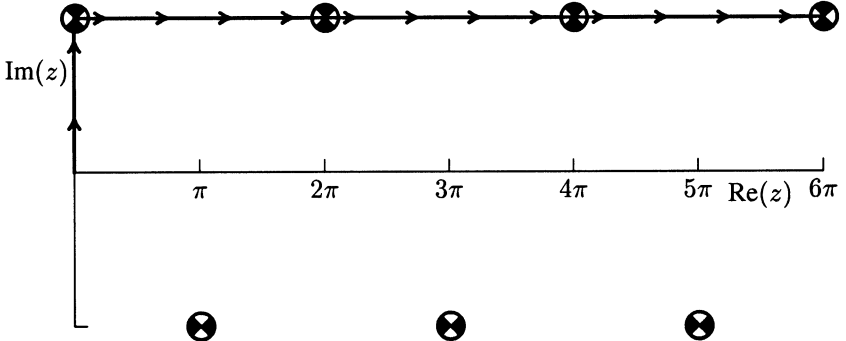


Figure 4.9. Saddle points and modified contour for evaluating $F(\nu, \lambda)$.

The saddle points occur where $h'(z) = 0$, or at

$$z_0 = n\pi + \begin{cases} i \log\left(\frac{\nu + \kappa}{\lambda}\right) & n \text{ even} \\ -i \log\left(\frac{\nu + \kappa}{\lambda}\right) & n \text{ odd} \end{cases}$$

so an infinite number of saddle points are located above and below the real z -axis as shown in figure 4.9 for real λ and ν .

The lower saddle points can be shown to be exponentially small for large real κ , so we will deform the path from along the real axis to go up along the imaginary axis to the first saddle point, and then turn and go to infinity, crossing *half* of the first saddle point and all of the remaining saddle points above the axis. Each saddle point of the integral of equation (4.282) contributes a term

$$T_n = \sqrt{\frac{2\pi}{\kappa}} \exp\left[\kappa - \nu \log\left(\frac{\nu + \kappa}{\lambda}\right)\right] e^{2\pi i n \nu} = 2\pi I_\nu(\lambda) e^{2\pi i n \nu} \quad (4.283)$$

where the latter equality comes from the large order expression for Bessel functions of fractional order. The total contribution from the saddle points is then

$$\sum T_n = 2\pi I_\nu(\lambda) \left(\frac{1}{2} + \sum_{n=1}^{\infty} e^{2\pi i n \nu} \right) = i\pi I_\nu(\lambda) \cot \pi \nu \quad (4.284)$$

where the geometric series has been summed. The factor of $1/2$ in the sum comes from crossing only the right-hand half of the first saddle point.

For the integral from the origin to the first saddle point along the imaginary axis, we note that at the end point $\eta \equiv \log[(\nu + \kappa)/\lambda] \simeq \nu/\lambda \ll 1$ since we take both ν and λ large but $\lambda \gg \nu$, but with $a^2 \equiv \nu^2/2\lambda$, we take a to be of order unity

($1 < a < 10$). Then we may approximate $\cos z \simeq 1 - z^2/2$ so that the integral becomes

$$\begin{aligned} i\nu \int_0^{i\eta} e^{\lambda(\cos z - 1) + i\nu z} dz &\simeq - \int_0^{v\eta} \exp\left(\frac{y^2}{4a^2} - y\right) dy \\ &= -2ae^{-a^2} \int_b^a e^{\xi^2} d\xi \\ &= a[\wp Z(a) - e^{b^2-a^2} \wp Z(b)] \end{aligned} \quad (4.285)$$

$$= a[Z(a) - e^{b^2-a^2} Z(b)] \quad (4.286)$$

where $vz = iy$, $\xi = a - y/2a$, and $b = a(1 - \lambda\eta/v) \simeq v^2/6\lambda^2 \ll 1$. The expressions in equation (4.285) came from equation (B.26), and we note that they represent the principal part of each Z -function, so there is no imaginary part (for real a and b). Each term in equation (4.286) has an imaginary part, but the sum does not. Since $b \ll 1$, it is convenient to discard that term and use the principal part notation, $\wp Z(a)$, for the remaining term.

We can finally combine the vertical segment with the saddle point contributions with the result

$$F(v, \lambda) = -\frac{1}{2}\wp Z'(a) - \pi\nu \cot \pi\nu e^{-\lambda} I_v(\lambda). \quad (4.287)$$

The dispersion relation then may be written without any sums as

$$\begin{aligned} k_z^2 \left(1 - \frac{\omega_{pe}^2}{\omega^2}\right) + k_\perp^2 \left(1 + \frac{\omega_{pe}^2}{\omega_{ce}^2}\right) - \frac{k_{Di}^2}{2} \wp Z' \left(\frac{\omega}{kv_i}\right) \\ = k_{Di}^2 \left[\pi\nu \cot \pi\nu e^{-\lambda} I_v(\lambda) + \frac{\nu e^{-\lambda} I_n(\lambda)}{2(v-n)} Z'(\zeta_{-n}) \right] \end{aligned} \quad (4.288)$$

since $a = \omega/k_\perp v_i$.

We note several things about this large- λ dispersion relation. First, if we neglect the resonant terms (the terms involving the Bessel functions), then there is no damping, but the dispersion relation is precisely the same as the unmagnetized dispersion relation except for the damping. This illustrates that there is no damping due to unmagnetized effects, although the dispersive behavior away from the resonances is well described by this simpler dispersion relation. Any damping comes only from the resonant term, and that only when $k_z \neq 0$. Second, there appears to be a singularity as $v \rightarrow n$, but both harmonic terms are resonant and the singularity cancels, so the dispersion relation is well behaved at the singularity. This may be seen by letting $v = n + \delta$ with δ small so that $\pi\nu \cot \pi\nu \sim 1 + n/\delta$ and expanding I_v about I_n so that the last two terms reduce to

$$-\pi\nu \cot \pi\nu e^{-\lambda} I_v(\lambda) - \frac{\nu e^{-\lambda} I_n(\lambda)}{2(v-n)} Z'(\zeta_{-n}) \simeq e^{-\lambda} I_n(\lambda) \zeta_0 Z(\zeta_{-n}) \quad (4.289)$$

which is nonsingular. Thirdly, numerical solutions of this dispersion relation show that the cold lower hybrid wave is uncoupled to these harmonic resonances, but the upper, warm branch, does couple to these ion Bernstein modes, with a region of nonpropagation at each harmonic resonance. Finally, if we were to imagine a wave propagating through a plasma with a very slowly varying magnetic field, so that the propagating wave passed through a series of these harmonic resonances, the warm wave would have to tunnel through a layer at each resonance, losing energy at each harmonic, and the net effect of this loss over a series of harmonics *is equivalent to unmagnetized ion Landau damping*. For this case, however, when $k_z \rightarrow 0$, there is no true damping, but the wave energy is mode converted out of the warm lower hybrid wave into the several ion Bernstein modes. The process of mode conversion is discussed in [chapter 6](#).

Problem 4.4.3. The large- λ dispersion relation.

- (i) Prove equation (4.281).
- (ii) Do the saddle point integrals to establish equation (4.283). (Fill in the steps from equation (4.282) to equation (4.283).)
- (iii) Do the integral along the imaginary axis to establish equation (4.286).
- (iv) For $v = 40$, $\lambda = 100$, evaluate a , b , η , $e^{b^2-a^2} Z(b)/Z(a)$ (principal part), and discuss the validity of the various approximations made earlier.

Problem 4.4.4. Extensions for $\lambda < 0$ or complex. Evaluate the contribution from the sum over the saddle points that lie below the axis, and show that these may be represented by the additional term in $F(v, \lambda)$:

$$F(v, \lambda) = \dots - i v \csc \pi v e^{-\lambda} K_v(\lambda).$$

With this additional term, the dispersion relation may be extended to complex and negative values of λ (where this term dominates).

Problem 4.4.5. Resonant damping term. Fill in the missing steps leading to equation (4.289).

4.5 Velocity space instabilities

4.5.1 Anisotropic temperature

While it is often difficult to do anything more than estimate the damping or growth rate when the imaginary part of ω is much smaller than the real part, there is one case where we can calculate exactly the threshold condition, or the marginal stability condition. For either the R - or L -wave, only one species contributes any damping or growth, and the condition that ω be exactly real is that Z_{-1} from equation (4.258) have no imaginary part. The imaginary part of Z_{-1} may be written as

$$\left[1 - \frac{k_z v_0}{\omega} - \left(1 - \frac{T_\perp}{T_\parallel} \right) \frac{\omega - k_z v_0 - \omega_c}{\omega} \right] i \sqrt{\pi} e^{-\zeta_{-1}^2} = 0. \quad (4.290)$$

With $v_0 = 0$, since we are considering only the anisotropic temperature effects here, this leads to the marginal stability condition

$$\omega_m = \left(1 - \frac{T_{\parallel}}{T_{\perp}}\right) \omega_c. \quad (4.291)$$

Instability occurs when $\text{Im}(Z_{-1}) < 0$ or whenever $\omega < \omega_m$, provided that k_z is real. To check this, we note that for $\omega = \omega_m$,

$$Z_{-1} = \frac{k_z v_{\ell}}{\omega_c} \frac{T_{\perp}}{T_{\parallel}} \quad (4.292)$$

which is purely real, and the dispersion relation for the *R*-wave, from equation (4.257) (neglecting the ion term), is

$$k_z^2 c^2 = \omega_{ce}^2 \left(1 - \frac{T_{\parallel}}{T_{\perp}}\right)^2 + \omega_{pe}^2 \left(\frac{T_{\perp}}{T_{\parallel}} - 1\right). \quad (4.293)$$

Thus, with $T_{\perp} > T_{\parallel}$, the wave is propagating and it does become unstable beyond the marginal condition. This implies that for any $T_{\perp} > T_{\parallel}$, the plasma is unstable, but unless $\omega \sim \omega_c$, the growth rate is very small as the exponent is very large. In practical terms, the anisotropy must be very large, in which case the marginal frequency may approach the cyclotron frequency closely enough to get significant effects.

Another way in which this effect of marginal stability may be perceived is the occurrence of a transition from strong absorption to transparency in plasma heating experiments using either electron or ion cyclotron waves. In this scenario, we imagine, for example, an *L*-wave propagating toward resonance in a very slowly decreasing magnetic field that is termed a ‘magnetic beach’ [46]. If we imagine that any wave energy absorbed leads to increasing T_{\perp} only, then the wave is absorbed very weakly far from resonance, but more strongly as resonance is approached. This stronger absorption increases T_{\perp} , raising ω_m to ω whereupon the plasma absorbs no further wave energy. Of course, as ω approaches ω_c , the transparency condition requires $T_{\perp} \rightarrow \infty$, so some absorption must always occur. It is clear from this example that this type of wave heating could never lead to an instability unless the plasma with higher T_{\perp} drifted back towards the source at higher magnetic field, a result that is unlikely due to the magnetic mirror effect which would confine the higher T_{\perp} plasma particles to the lower field region. In an interesting experiment on the Model C Stellarator, an *L*-wave was launched in a predominantly hydrogen plasma with a deuterium minority that was locally resonant in a narrow depression in the magnetic field ($\omega \simeq \omega_{cH}/2$ so no significant hydrogen absorption occurred). Since the mirror was only a few percent deep, it was possible to raise the $T_{D\perp}$ to nearly a hundred times the average temperature, trapping this small population in the mirror in the process [47].

Problem 4.5.1. Anisotropic temperature instability.

- (i) Fill in the steps leading to equations (4.291) and (4.293).
- (ii) Estimate the maximum k_{zi}/k_{zr} with $\omega_{ce}/k_{zr}v_e = 3$, $\omega_{pe}/\omega_{ce} = 2$, for $T_\perp/T_\parallel = 2$ and $T_\perp/T_\parallel = 10$.

4.6 Conservation of energy and power flow

In vacuum, we saw in [chapter 1](#) that energy conservation and power flow were related by the Maxwell equations, and that the energy was stored in the electromagnetic wave fields, and the power flow given by the Poynting vector was dependent only on the fields. Then in [chapter 3](#) we discovered that the plasma particles contributed both to the power flow and to the stored energy. In this section, we use a more general formalism to include the effects of the plasma and the effects of dissipation through an anti-Hermitian component of the dielectric tensor and/or the effects of a complex frequency. We treat first the temporal problem, where we obtain the stored energy density and the effects of dissipation. We then examine in more detail the concept of group velocity, and obtain the kinetic flux component of the power flow.

4.6.1 Poynting's theorem for kinetic waves

When the angular frequency ω is assumed to have an imaginary part, especially in the case where this imaginary part may vary slowly in time to represent the slow turning on of the wave, the steady-state results of chapter 1 are not the most fruitful for understanding energy density and power flow. Using the more general representation of a wave field amplitude by

$$\mathbf{A}(t) = \text{Re} \left[\hat{\mathbf{A}}(\omega) e^{-i\phi(t)} \right] \quad \phi(t) = \int_{-\infty}^t \omega(t') dt' \quad (4.294)$$

the general product of two vectors may be represented by

$$[\mathbf{A}][\mathbf{B}] = \frac{1}{4} \{ [\hat{\mathbf{A}}][\hat{\mathbf{B}}] e^{-2i\phi(t)} + ([\hat{\mathbf{A}}][\hat{\mathbf{B}}^*] + [\hat{\mathbf{A}}^*][\hat{\mathbf{B}}]) e^{2\phi_i(t)} + [\hat{\mathbf{A}}^*][\hat{\mathbf{B}}^*] e^{2i\phi^*(t)} \}. \quad (4.295)$$

If we now take $\omega_i \ll \omega_r$ and integrate over a period $T = 2\pi/\omega_r$, then

$$\frac{1}{T} \int_0^T \exp \left[-2i \int_{-\infty}^t \omega(t') dt' \right] dt \simeq \frac{-i\omega_i(0)}{\omega_r(0)} e^{-2i\phi(0)}.$$

This means both the first and last terms in equation (4.295) may be neglected so that a general product of this type reduces to

$$[\mathbf{A}][\mathbf{B}] = \frac{1}{4} ([\hat{\mathbf{A}}][\hat{\mathbf{B}}^*] + [\hat{\mathbf{A}}^*][\hat{\mathbf{B}}]) e^{2\phi_i(t)}. \quad (4.296)$$

Using these expressions, the complex Poynting vector is represented by

$$\mathbf{P} = \frac{1}{4}(\hat{\mathbf{E}} \times \hat{\mathbf{H}}^* + \hat{\mathbf{E}}^* \times \hat{\mathbf{H}})e^{2\phi_i(t)} \quad (4.297)$$

and the conservation law from the Maxwell equations,

$$\nabla \cdot (\mathbf{E} \times \mathbf{H}) = - \left(\mathbf{H} \cdot \frac{\partial \mathbf{B}}{\partial t} + \mathbf{E} \cdot \frac{\partial \mathbf{D}}{\partial t} \right)$$

becomes

$$\nabla \cdot \mathbf{P} = - \frac{\partial W}{\partial t} \quad (4.298)$$

where

$$\begin{aligned} \frac{\partial W}{\partial t} &= \frac{1}{4}[\hat{\mathbf{H}} \cdot (-i\omega \hat{\mathbf{B}})^* + \hat{\mathbf{H}}^* \cdot (-i\omega \hat{\mathbf{B}}) + \hat{\mathbf{E}} \cdot (-i\omega \epsilon_0 \mathbf{K} \cdot \hat{\mathbf{E}})^* \\ &\quad + \hat{\mathbf{E}}^* \cdot (-i\omega \epsilon_0 \mathbf{K} \cdot \hat{\mathbf{E}})]e^{2\phi_i(t)} \\ &= \frac{1}{4}[2\omega_i \mu_0 \hat{\mathbf{H}} \cdot \hat{\mathbf{H}}^* + \omega_i \epsilon_0 \hat{\mathbf{E}}^* \cdot (\mathbf{K} + \mathbf{K}^\dagger) \cdot \hat{\mathbf{E}} + \omega_r \epsilon_0 \hat{\mathbf{E}}^* \cdot (i\mathbf{K}^\dagger - i\mathbf{K}) \cdot \hat{\mathbf{E}}] \\ &\quad \times e^{2\phi_i(t)} \end{aligned} \quad (4.299)$$

where we have used $\hat{\mathbf{E}} \cdot (\mathbf{K} \cdot \hat{\mathbf{E}})^* = \hat{\mathbf{E}}^* \cdot \mathbf{K}^\dagger \cdot \hat{\mathbf{E}}$ and \mathbf{K}^\dagger is the Hermitian adjoint of \mathbf{K} given by $\mathbf{K}^\dagger = \tilde{\mathbf{K}}^*$. We define the Hermitian and anti-Hermitian portions of \mathbf{K} by

$$\mathbf{K}_h = \frac{1}{2}(\mathbf{K} + \mathbf{K}^\dagger) \quad \text{and} \quad \mathbf{K}_a = \frac{1}{2i}(\mathbf{K} - \mathbf{K}^\dagger).$$

It is apparent from equation (4.299) that if ω is real and \mathbf{K} is Hermitian, there is no loss, so any dissipation must arise from the anti-Hermitian portion of the dielectric tensor or the imaginary part of ω .

If we now expand the dielectric tensor about the real part of ω , we find that

$$\mathbf{K}(\omega) = \mathbf{K}(\omega_r) + \left. \frac{\partial \mathbf{K}}{\partial \omega} \right|_{\omega_r} i\omega_i + \dots$$

so that

$$\mathbf{K}_h(\omega) = \mathbf{K}_h(\omega_r) + \left. \frac{\partial \mathbf{K}_h}{\partial \omega} \right|_{\omega_r} i\omega_i + \dots \quad (4.300)$$

$$-i\mathbf{K}(\omega) + i\mathbf{K}^\dagger(\omega^*) = 2\mathbf{K}_a(\omega_r) + 2\omega_i \left. \frac{\partial \mathbf{K}_h}{\partial \omega} \right|_{\omega_r} + \dots \quad (4.301)$$

and the energy term of equation (4.299) becomes

$$\begin{aligned} \frac{\partial W}{\partial t} &= \frac{1}{4} \left[2\omega_i \left(\mu_0 \hat{\mathbf{H}} \cdot \hat{\mathbf{H}}^* + \epsilon_0 \hat{\mathbf{E}}^* \cdot \left. \frac{\partial}{\partial \omega} (\omega \mathbf{K}_h) \right|_{\omega_r} \cdot \hat{\mathbf{E}} \right) \right. \\ &\quad \left. + 2\omega_r \epsilon_0 \hat{\mathbf{E}}^* \cdot \mathbf{K}_a(\omega_r) \cdot \hat{\mathbf{E}} \right] e^{2\phi_i(t)} \end{aligned} \quad (4.302)$$

and we can identify the total energy as being comprised of the stored energy,

$$W_0 = \frac{1}{4} \left[\mu_0 \hat{\mathbf{H}} \cdot \hat{\mathbf{H}}^* + \epsilon_0 \hat{\mathbf{E}}^* \cdot \frac{\partial}{\partial \omega} (\omega \mathbf{K}_h) \Big|_{\omega_r} \cdot \hat{\mathbf{E}} \right] \quad (4.303)$$

and a dissipative term associated with the anti-Hermitian part of \mathbf{K} . We can also see that some of the stored energy is electromagnetic or electrostatic, and some is in the particle kinetic energy, even in the cold plasma.

It is often useful to relate these two terms through the quality factor, which is given by the ratio of the stored energy to the energy lost per cycle, or

$$Q = \frac{\omega_r W_0}{\partial W / \partial t \text{ (loss)}} = \frac{\mu_0 \hat{\mathbf{H}} \cdot \hat{\mathbf{H}}^* + \epsilon_0 \hat{\mathbf{E}}^* \cdot \partial(\omega \mathbf{K}_h) / \partial \omega|_{\omega_r} \cdot \hat{\mathbf{E}}}{2\epsilon_0 \hat{\mathbf{E}}^* \cdot \mathbf{K}_a(\omega_r) \cdot \hat{\mathbf{E}}} \quad (4.304)$$

so that a high Q indicates that the stored energy lasts many cycles and a low Q may mean that there is very little energy circulating, as if it were all absorbed on a single pass, or nearly so. Since in subsequent discussions, we deal nearly universally with the amplitudes, we will delete the hat from now on, but recall the recipe when questions about power or energy are desired.

Problem 4.6.1. Power and energy.

- (i) Fill in the steps leading to equation (4.296).
- (ii) Fill in the steps leading to equation (4.302) and justify equation (4.303).

Problem 4.6.2. Stored energy. Show that for simple cold plasma oscillations ($\omega = \omega_p$) that the electrostatic stored energy is equal to the particle kinetic energy.

4.6.2 Group velocity and kinetic flux

We have already discussed group velocity in the cold plasma in section 2.3, but now in the context of a hot plasma, we need to re-examine and extend the discussion to include the power flow due the particles, which we call the kinetic flux. For this discussion, we restrict ourselves to a lossfree plasma and introduce the Maxwell operator, \mathbf{M} , which represents the Maxwell wave equation, such that

$$\mathbf{M} \cdot \mathbf{E} = \frac{1}{4\mu_0\omega} \mathbf{k} \times (\mathbf{k} \times \mathbf{E}) + \frac{\omega\epsilon_0}{4} \mathbf{K}_h \cdot \mathbf{E} \quad (4.305)$$

and the wave equation is then simply

$$\mathbf{M} \cdot \mathbf{E} = 0. \quad (4.306)$$

The Hermitian adjoint of equation (4.306) is

$$\mathbf{E}^* \cdot \mathbf{M}^\dagger = \mathbf{E}^* \cdot \mathbf{M} = 0 \quad (4.307)$$

where the last equality holds for real ω and real \mathbf{k} in which case \mathbf{M} is Hermitian.

The idea at this point is to make small displacements in ω , \mathbf{k} , and in the plasma parameters, or what is essentially a variational calculation, and the extremum will yield the group velocity. The perturbed wave equation is

$$\mathbf{M}' \cdot \mathbf{E}' = 0 \quad (4.308)$$

but if the perturbations are small, then we can expand

$$\mathbf{M}' = \mathbf{M} + \delta\omega \frac{\partial \mathbf{M}}{\partial \omega} + \delta\mathbf{k} \cdot \frac{\partial \mathbf{M}}{\partial \mathbf{k}} + \delta\mathbf{M}.$$

We now take the scalar product of \mathbf{E}^* with equation (4.308) and use equation (4.307) to obtain

$$\mathbf{E}^* \cdot \left(\delta\omega \frac{\partial \mathbf{M}}{\partial \omega} + \delta\mathbf{k} \cdot \frac{\partial \mathbf{M}}{\partial \mathbf{k}} + \delta\mathbf{M} \right) \cdot \mathbf{E}' = 0$$

where $\partial/\partial\mathbf{k} = \nabla_k$. Since the perturbation is small, the differences between \mathbf{E} and \mathbf{E}' lead to second order corrections, so we may write, to first order,

$$\mathbf{E}^* \cdot \left(\delta\omega \frac{\partial \mathbf{M}}{\partial \omega} + \delta\mathbf{k} \cdot \frac{\partial \mathbf{M}}{\partial \mathbf{k}} + \delta\mathbf{M} \right) \cdot \mathbf{E} = 0. \quad (4.309)$$

Examining each of the terms in equation (4.309) separately, we find

$$\begin{aligned} \mathbf{E}^* \cdot \frac{\partial \mathbf{M}}{\partial \omega} \cdot \mathbf{E} &= \mathbf{E}^* \cdot \frac{-1}{4\omega^2\mu_0} \mathbf{k} \times (\mathbf{k} \times \mathbf{E}) + \frac{\epsilon_0}{4} \mathbf{E}^* \cdot \frac{\partial}{\partial \omega}(\omega \mathbf{K}_h) \cdot \mathbf{E} \\ &= \frac{1}{4} \left[\mu_0 \mathbf{H}^* \cdot \mathbf{H} + \epsilon_0 \mathbf{E}^* \cdot \frac{\partial}{\partial \omega}(\omega \mathbf{K}_h) \cdot \mathbf{E} \right] \\ &= W_0 \end{aligned} \quad (4.310)$$

$$\begin{aligned} \mathbf{E}^* \cdot \frac{\partial \mathbf{M}}{\partial \mathbf{k}} \cdot \mathbf{E} &= -\frac{1}{4} (\mathbf{E}^* \times \mathbf{H} + \mathbf{E} \times \mathbf{H}^*) + \mathbf{E}^* \cdot \frac{\omega\epsilon_0}{4} \frac{\partial}{\partial \mathbf{k}}(\mathbf{K}_h) \cdot \mathbf{E} \\ &= -\mathbf{P} - \mathbf{T} \end{aligned} \quad (4.311)$$

where

$$\mathbf{T} \equiv -\frac{\omega\epsilon_0}{4} \mathbf{E}^* \cdot \frac{\partial}{\partial \mathbf{k}}(\mathbf{K}_h) \cdot \mathbf{E}. \quad (4.312)$$

The vector \mathbf{T} is the kinetic flux for the hot plasma, and represents the generalization of the kinetic flux of equation (3.148). From the form of equation (4.312), it is apparent that $\mathbf{T} = 0$ in a cold plasma or any other case where \mathbf{K} does not depend on \mathbf{k} . In the thermal or streaming plasma, this term represents the power flow carried by the particles themselves, and is essential for the conservation of energy.

The final term in equation (4.309) is given by

$$\begin{aligned} \mathbf{E}^* \cdot \delta\mathbf{M} \cdot \mathbf{E} &= \mathbf{E}^* \cdot \frac{\omega}{4} \delta\mathbf{K}_h \cdot \mathbf{E} \\ &= \mathbf{E}^* \cdot \frac{\omega\epsilon_0}{8} [\delta\mathbf{K}_h - (\delta\mathbf{K}_h)^\dagger] \cdot \mathbf{E} + \mathbf{E}^* \cdot \frac{\omega\epsilon_0}{8} [\delta\mathbf{K}_h + (\delta\mathbf{K}_h)^\dagger] \cdot \mathbf{E} \end{aligned}$$

where we have broken the right-hand side into anti-Hermitian and Hermitian components. Referring back to equation (4.299), we have

$$\mathbf{E}^* \cdot \delta\mathbf{M} \cdot \mathbf{E} = \frac{i}{2} \delta \left(\frac{\partial W}{\partial t} \right)_{\text{loss}} + \text{Hermitian terms} \quad (4.313)$$

and for this term the changes are due only to variations in the plasma parameters. Since the Hermitian terms represent reactive or oscillating terms, and not energy flow, we will neglect them and write equation (4.309) as

$$W_0 \delta\omega - (\mathbf{P} + \mathbf{T}) \cdot \delta\mathbf{k} + \frac{i}{2} \delta \left(\frac{\partial W}{\partial t} \right)_{\text{loss}} = 0. \quad (4.314)$$

For the discussion of group velocity, we are not concerned with losses, provided they are small, in which case the last term in equation (4.314) may be ignored and the result written as

$$\mathbf{v}_g = \frac{\delta\omega}{\delta\mathbf{k}} = \frac{\mathbf{P} + \mathbf{T}}{W_0} = \frac{\text{energy flux}}{\text{energy density}}. \quad (4.315)$$

If, however, one wishes to consider losses, then another relationship can be derived from equation (4.314) for the temporal decay of the wave ($\delta\mathbf{k} = 0$) where

$$\delta\omega = -\frac{i}{2} \frac{1}{W_0} \delta \left(\frac{\partial W}{\partial t} \right)_{\text{loss}} \quad (4.316)$$

and for the spatial decay, we have the corresponding relationship ($\delta\omega = 0$)

$$(\mathbf{P} + \mathbf{T}) \cdot \delta\mathbf{k} = \frac{i}{2} \delta \left(\frac{\partial W}{\partial t} \right)_{\text{loss}}. \quad (4.317)$$

We find then from equation (4.314) the three basic components involved in energy conservation, namely the transport of energy in the direction of the group velocity, given in equation (4.315), and the temporal and spatial decay of wave energy through dissipation, indicated by equations (4.316) and (4.317). Together, these give a good picture of the transport of energy, and the expressions for W_0 , \mathbf{P} , and \mathbf{T} give the balance between electromagnetic stored energy and power flow and the kinetic components of each.

Problem 4.6.3. Ion-acoustic-wave energy balance. For the ion acoustic wave whose dispersion relation is given in equation (4.140),

- (i) find the electromagnetic and kinetic components of the energy density;
- (ii) find the electromagnetic and kinetic components of the power flow;
- (iii) find the temporal decay rate; and
- (iv) find the spatial decay rate.

4.7 Relativistic plasma effects

While some plasmas are relatively hot, in that thermal effects beyond those included through the pressure term are important, few plasmas are truly relativistic such that the mean thermal speed begins to approach the speed of light. However, some relativistic effects occur at relatively low temperatures when one encounters cyclotron fundamental and harmonic resonances and $k_{\parallel} \rightarrow 0$. In fact, the typical argument of the PDF, $\zeta_n = (\omega - n\omega_c)/k_{\parallel}v_{\parallel}$ is indeterminate as both the numerator and denominator may approach zero at cyclotron harmonics with $k_{\parallel} = 0$. Since the behavior of the PDF is dramatically different as $\zeta_n \rightarrow 0$ or $\zeta_n \rightarrow \infty$, we need to consider the physics more carefully, since the mathematics suggests some discontinuous behavior in this region of parameter space, and we suspect there is no such discontinuity in the physical world.

The fundamental weakness in our model is that we have taken the cyclotron frequency to be a simple constant, independent of velocity, whereas from special relativity, we know that this is not so, since we should write $\omega_c = qB_0/\gamma m$. In the integral over velocity, then, the singularity in the denominator is significantly changed, and the numerator of ζ_n effectively never vanishes. Thus the indeterminate nature of the appropriate limit to take as $k_{\parallel} \rightarrow 0$ is resolved, since it is possible to impose $k_{\parallel} = 0$ externally, but the cyclotron harmonic resonances are broadened to some finite (though frequently small) extent and prevent the argument of the PDF from vanishing.

It would seem from the previous discussion that since hot plasma theory has already indicated that $k_{\parallel} = 0$ implies no absorption, even at cyclotron harmonics, and the relativistic corrections appear to lead to large arguments for the PDF in this limit, that there is still no absorption. This, however, is not the case, and in fact the absorption at $k_{\parallel} = 0$ is considerably stronger than one might guess, since nontrivial absorption is encountered at the electron cyclotron fundamental and harmonics at temperatures of only a few keV. In order to see how this comes about, we will review the development of the relativistic dielectric tensor, including only electrons, and eventually pay particular attention to the $k_{\parallel} = 0$ case.

4.7.1 The relativistic dielectric tensor

In this section, we follow the development of Trubnikov [48] for the general development of the dielectric tensor, and present an outline of the derivation, noting the similarities to and differences from the hot plasma derivation.

We begin with the relativistic collisionless Boltzmann equation, and shall assume again that we may Fourier transform in both time and space, taking ω to have a small positive imaginary part when it becomes necessary to resolve the singularity in the momentum integrals and guarantee convergence. The kinetic equation is

$$\frac{\partial f}{\partial t} + \mathbf{v} \cdot \nabla f + q[\mathbf{E}_1 + \mathbf{v} \times (\mathbf{B}_0 + \mathbf{B}_1)] \cdot \nabla_p f = 0 \quad (4.318)$$

where the zero-order distribution is an equilibrium distribution given by

$$f_0 = A e^{-\mathcal{E}/\kappa T} \quad \int f_0(p) d^3 p = n_0 \quad \mathcal{E} = \sqrt{p^2 c^2 + m^2 c^4}. \quad (4.319)$$

We note that the Boltzmann equation is unchanged except that now the distribution function is a function of momentum rather than velocity. The distribution function is of the standard form, except that now the energy is the relativistic total energy (or relativistic kinetic energy by redefining the constant A).

At this point, we take the usual coordinate system, with $\mathbf{B}_0 = B_0 \hat{\mathbf{z}}$, and choose $k_\perp = k_x$ ($k_y = 0$) and use cylindrical coordinates in momentum space such that $p_x \equiv p_\perp \cos \phi$, $p_y \equiv p_\perp \sin \phi$. We then choose to write the first-order distribution function in terms of another function, defined by

$$f_1(\mathbf{r}, \mathbf{p}, t) \equiv e^{i(\mathbf{k} \cdot \mathbf{r} - \omega t)} f_0(p) \Phi(\mathbf{p}) \quad (4.320)$$

so that with $\mathbf{p} = \gamma m \mathbf{v}$, the first-order Boltzmann equation becomes

$$\begin{aligned} -i\omega f_1 + \frac{i(k_\parallel p_\parallel + k_\perp p_\perp \cos \phi)}{\gamma m} f_1 + q(\mathbf{E}_1 + \mathbf{v} \times \mathbf{B}_1) \cdot \nabla_p f_0 \\ + \frac{q}{\gamma m} (\mathbf{p} \times \mathbf{B}_0) \cdot \nabla_p f_1 = 0 \end{aligned} \quad (4.321)$$

since $(\mathbf{p} \times \mathbf{B}_0) \cdot \nabla_p f_0 = 0$ along the unperturbed orbit. Then we note that

$$\nabla_p f_0 = -\frac{f_0 c^2 \mathbf{p}}{\kappa T \mathcal{E}} \quad \text{so} \quad (\mathbf{v} \times \mathbf{B}_1) \cdot \nabla_p f_0 = 0$$

and

$$\nabla_p f_1 = -\frac{c^2 \mathbf{p}}{\kappa T \mathcal{E}} f_1 + \frac{f_1}{\Phi} \nabla_p \Phi$$

so

$$\frac{q}{\gamma m} (\mathbf{p} \times \mathbf{B}_0) \cdot \nabla_p f_1 = -\frac{\epsilon \omega_c}{\gamma} f_0 e^{i(\mathbf{k} \cdot \mathbf{r} - \omega t)} \frac{\partial \Phi}{\partial \phi}$$

(where $\epsilon = -1$ for electrons as before) and

$$q \mathbf{E}_1 \cdot \nabla_p f_0 = -\frac{f_0 q \mathbf{E} \cdot \mathbf{p}}{\gamma m \kappa T}$$

since $\mathcal{E} = \gamma m c^2$ (and we have dropped the subscript on \mathbf{E}). Using these relations, equation (4.321) may be written as

$$i \left(\frac{\gamma \omega}{\epsilon \omega_c} - \frac{k_\parallel p_\parallel + k_\perp p_\perp \cos \phi}{m \epsilon \omega_c} \right) \Phi + \frac{\partial \Phi}{\partial \phi} = -\frac{\mathbf{p} \cdot \mathbf{E}}{B_0 \kappa T}. \quad (4.322)$$

This is a first-order differential equation whose solution may be written as

$$\Phi(\mathbf{p}) = -\frac{1}{B_0 \kappa T} e^{i(a\phi - b \sin \phi)} \int_{\phi}^{\phi_0} e^{-i(a\psi - b \sin \psi)} (\mathbf{p} \cdot \mathbf{E})_{\psi} d\psi \quad (4.323)$$

with $a = \gamma\omega/\epsilon\omega_c - k_{\parallel}p_{\parallel}/m\epsilon\omega_c$, $b = k_{\perp}p_{\perp}/\epsilon m\omega_c$, and $(\mathbf{p} \cdot \mathbf{E})_{\psi} \equiv p_{\parallel}E_z + p_{\perp}(E_x \cos \psi + E_y \sin \psi)$. We may now let $\phi_0 \rightarrow -\infty$ and be guaranteed of convergence since we have assumed that ω has a positive imaginary part. Using the variable change $\psi = \phi - \xi$, this result may also be written as

$$\Phi(\mathbf{p}) = \frac{1}{B_0 \kappa T} \int_0^{\infty} e^{ia\xi - ib[\sin(\xi - \phi) + \sin \phi]} (\mathbf{p} \cdot \mathbf{E})_{\phi - \xi} d\xi. \quad (4.324)$$

The current is then given by

$$\mathbf{J}(\mathbf{k}, \omega) = \sum_j q_j \int \mathbf{v} f_{1j}(\mathbf{k}, \omega) d^3 p = \sum_j \frac{q_j}{m_j} \int \frac{f_0(p)\Phi_j(\mathbf{p})}{\gamma_j} \mathbf{p} d^3 p. \quad (4.325)$$

We may now proceed in either of the two directions we discussed in section 4.3.3, where we integrated over τ first, or in section 4.3.4 where we did some of the velocity integrals first. In this case we integrate over ξ first and find that $\Phi(\mathbf{p})$ may be written as

$$\Phi(\mathbf{p}) = \frac{1}{B_0 \kappa T} (p_{\perp} I_x(\phi) E_x + p_{\perp} I_y(\phi) E_y + p_{\parallel} I_z(\phi) E_z) \quad (4.326)$$

with

$$I_x(\phi) = \sum_{m,n=-\infty}^{\infty} \frac{i J_m(b) n J_n(b)}{b(a-n)} e^{i(n-m)\phi} \quad (4.327)$$

$$I_y(\phi) = \sum_{m,n=-\infty}^{\infty} \frac{J_m(b) J'_n(b)}{(a-n)} e^{i(n-m)\phi} \quad (4.328)$$

$$I_z(\phi) = \sum_{m,n=-\infty}^{\infty} \frac{i J_m(b) J_n(b)}{a-n} e^{i(n-m)\phi} \quad (4.329)$$

where $b = \bar{p}_{\perp} v_{\perp}$ and $\bar{p} = p/m_j c$ so that $\gamma_j = (1 + \bar{p}^2)^{1/2}$ and $v_{\perp} = n_{\perp}\omega/\epsilon\omega_c$. We next integrate over ϕ , but because of the complexity of the several dielectric tensor components, we will calculate only K_{xx} and then list the results for the complete tensor. From equation (1.19), this component is given by

$$\begin{aligned} K_{xx} &= 1 + \frac{i\sigma_{xx}}{\omega\epsilon_0} \\ &= 1 + \sum_j \frac{i q_j n_{0j}}{\epsilon_0 m_j \omega 4\pi m_j^2 c (\kappa T_j)^2 K_2(\mu_j) B_0} \int_{-\infty}^{\infty} dp_{\parallel} \int_0^{\infty} p_{\perp} dp_{\perp} \int_0^{2\pi} d\phi \end{aligned}$$

$$\begin{aligned}
& \times \sum_{m,n=-\infty}^{\infty} \frac{e^{-\mu_j \gamma_j}}{\gamma_j} p_{\perp}^2 \cos \phi \frac{i J_m(b) n J_n(b)}{b(a-n)} e^{i(m-n)\phi} \\
& = 1 + \sum_j \frac{\omega_{pj}^2}{\omega \epsilon_j \omega_{cj}} \frac{\mu_j^2}{4\pi K_2(\mu_j)} \int_{-\infty}^{\infty} d\bar{p}_{\parallel} \int_0^{\infty} \bar{p}_{\perp} d\bar{p}_{\perp} \frac{e^{-\mu_j \gamma_j}}{\gamma_j} \\
& \quad \times \sum_{n=-\infty}^{\infty} \frac{\bar{p}_{\perp}^2 n J_n(b)}{b(n-a)} \sum_{m=-\infty}^{\infty} J_m(b) \int_0^{2\pi} e^{i(m-n)\phi} \cos \phi d\phi \\
& = 1 + \sum_j \frac{\omega_{pj}^2}{\omega \epsilon_j \omega_{cj}} \frac{\mu_j^2}{2K_2(\mu_j)} \int_{-\infty}^{\infty} d\bar{p}_{\parallel} \int_0^{\infty} \bar{p}_{\perp} d\bar{p}_{\perp} \frac{e^{-\mu_j \gamma_j}}{\gamma_j} \\
& \quad \times \sum_{n=-\infty}^{\infty} \left(\frac{\bar{p}_{\perp} n J_n(b)}{b} \right)^2 \frac{1}{n-a} \tag{4.330}
\end{aligned}$$

where $\mu_j = m_j c^2 / \kappa T_j$ and we have used

$$\sum_{m=-\infty}^{\infty} J_m(b) \int_0^{2\pi} e^{i(m-n)\phi} \cos \phi d\phi = \pi [J_{n-1}(b) + J_{n+1}(b)] = \frac{2\pi n J_n(b)}{b}. \tag{4.331}$$

The remaining components may be obtained with the integrals

$$\sum_{m=-\infty}^{\infty} J_m(b) \int_0^{2\pi} e^{i(m-n)\phi} \sin \phi d\phi = -i\pi [J_{n-1}(b) - J_{n+1}(b)] = -2\pi i J'_n(b) \tag{4.332}$$

$$\sum_{m=-\infty}^{\infty} J_m(b) \int_0^{2\pi} e^{i(m-n)\phi} d\phi = 2\pi J_n(b) \tag{4.333}$$

so that including only the electron component of the dielectric tensor (only electrons are assumed to be relativistic), we may write

$$\begin{aligned}
K_{ij} &= \delta_{ij} - \frac{\omega_{pe}^2}{\omega^2} \frac{\mu_e^2}{2K_2(\mu_e)} \int_{-\infty}^{\infty} d\bar{p}_{\parallel} \int_0^{\infty} d\bar{p}_{\perp} \bar{p}_{\perp} \frac{e^{-\mu_e \gamma_e}}{\gamma_e} \\
&\quad \times \sum_{n=-\infty}^{\infty} \frac{P_{ij}^n}{\gamma_e - n_{\parallel} \bar{p}_{\parallel} + n \omega_{ce} / \omega} \tag{4.334}
\end{aligned}$$

where

$$P_{xx}^n = \frac{n^2}{v_{\perp}^2} J_n^2(v_{\perp} \bar{p}_{\perp}) \tag{4.335}$$

$$P_{xy}^n = -P_{yx}^n = \frac{i \bar{p}_{\perp} n}{v_{\perp}} J_n(v_{\perp} \bar{p}_{\perp}) J'_n(v_{\perp} \bar{p}_{\perp}) \tag{4.336}$$

$$P_{xz}^n = P_{zx}^n = -\frac{\bar{p}_\parallel n}{v_\perp} J_n^2(v_\perp \bar{p}_\perp) \quad (4.337)$$

$$P_{yy}^n = \bar{p}_\perp^2 J_n'^2(v_\perp \bar{p}_\perp) \quad (4.338)$$

$$P_{yz}^n = -P_{zy}^n = i\bar{p}_\parallel \bar{p}_\perp J_n(v_\perp \bar{p}_\perp) J_n'(v_\perp \bar{p}_\perp) \quad (4.339)$$

$$P_{zz}^n = \bar{p}_\parallel^2 J_n^2(v_\perp \bar{p}_\perp). \quad (4.340)$$

This representation is equivalent to that of Brambilla [49], except for notation such that his $\Omega_c = \epsilon\omega_c = -\omega_{ce}$ for electrons. If we change the definition of v_\perp to be positive so that $v_\perp = n_\perp \omega / \omega_{ce}$, then we must change the signs of P_{xz}^n and P_{yz}^n in equations (4.337) and (4.339), respectively.

Problem 4.7.1. Normalization constant. Find the normalization constant A for $f_0(p)$. (Answer. $A = n_0 \mu / 4\pi(mc)^3 K_2(\mu)$.)

Problem 4.7.2. Calculating $\Phi(\phi)$. Integrate equation (4.324) over ξ using the Bessel identity (4.179) and show that the result is given by equation (4.326) along with equations (4.327) through (4.329).

4.7.2 The relativistic dielectric tensor without sums

We may use the Newberger sum rules from equation (4.192) and equations (4.193) through (4.198) to eliminate the sums and cast the sums of the P_{ij}^n into the following form:

$$\sum_{n=-\infty}^{\infty} \frac{P_{xx}^n}{a+n} = \frac{1}{v_\perp^2} \left[\frac{\pi a^2}{\sin \pi a} J_a(v_\perp \bar{p}_\perp) J_{-a}(v_\perp \bar{p}_\perp) - a \right] \quad (4.341)$$

$$\sum_{n=-\infty}^{\infty} \frac{P_{xy}^n}{a+n} = -\frac{i\bar{p}_\perp}{v_\perp} \left[\frac{\pi a}{\sin \pi a} J_a(v_\perp \bar{p}_\perp) J'_{-a}(v_\perp \bar{p}_\perp) + \frac{a}{v_\perp \bar{p}_\perp} \right] \quad (4.342)$$

$$\sum_{n=-\infty}^{\infty} \frac{P_{xz}^n}{a+n} = \frac{\bar{p}_\parallel}{v_\perp} \left[\frac{\pi a}{\sin \pi a} J_a(v_\perp \bar{p}_\perp) J_{-a}(v_\perp \bar{p}_\perp) - 1 \right] \quad (4.343)$$

$$\sum_{n=-\infty}^{\infty} \frac{P_{yy}^n}{a+n} = \bar{p}_\perp^2 \left[\frac{\pi}{\sin \pi a} J'_a(v_\perp \bar{p}_\perp) J'_{-a}(v_\perp \bar{p}_\perp) + \frac{a}{v_\perp^2 \bar{p}_\perp^2} \right] \quad (4.344)$$

$$\sum_{n=-\infty}^{\infty} \frac{P_{yz}^n}{a+n} = i\bar{p}_\parallel \bar{p}_\perp \left[\frac{\pi}{\sin \pi a} J_a(v_\perp \bar{p}_\perp) J'_{-a}(v_\perp \bar{p}_\perp) + \frac{1}{v_\perp \bar{p}_\perp} \right] \quad (4.345)$$

$$\sum_{n=-\infty}^{\infty} \frac{P_{zz}^n}{a+n} = \bar{p}_\parallel^2 \frac{\pi}{\sin \pi a} J_a(v_\perp \bar{p}_\perp) J_{-a}(v_\perp \bar{p}_\perp) \quad (4.346)$$

where now $a = (\omega/\omega_{ce})(\gamma_e - n_\parallel \bar{p}_\parallel)$ and $v_\perp = n_\perp \omega/\omega_{ce}$. The dielectric tensor then assumes the form

$$K_{ij} = \delta_{ij} - \frac{\omega_{pe}^2}{\omega^2} \frac{\mu_e^2}{2K_2(\mu_e)} \int_{-\infty}^{\infty} d\bar{p}_\parallel \int_0^\infty d\bar{p}_\perp \bar{p}_\perp e^{-\mu_e \gamma_e} \Pi_{ij} + \text{ion term} \quad (4.347)$$

where

$$\Pi_{xx} = \frac{a}{n_\perp^2(a + n_\parallel \bar{p}_\parallel \omega/\omega_{ce})} \left[\frac{\pi a}{\sin \pi a} J_a(b) J_{-a}(b) - 1 \right] \quad (4.348)$$

$$\Pi_{xy} = -\Pi_{yx} = -\frac{ia}{n_\perp^2(a + n_\parallel \bar{p}_\parallel \omega/\omega_{ce})} \left[\frac{\pi b}{\sin \pi a} J_a(b) J'_{-a}(b) + 1 \right] \quad (4.349)$$

$$\Pi_{xz} = \Pi_{zx} = -\frac{\omega \bar{p}_\parallel}{\omega_{ce} n_\perp(a + n_\parallel \bar{p}_\parallel \omega/\omega_{ce})} \left[\frac{\pi a}{\sin \pi a} J_a(b) J_{-a}(b) - 1 \right] \quad (4.350)$$

$$\Pi_{yy} = \frac{1}{n_\perp^2(a + n_\parallel \bar{p}_\parallel \omega/\omega_{ce})} \left[\frac{\pi b^2}{\sin \pi a} J'_a(b) J'_{-a}(b) + a \right] \quad (4.351)$$

$$\Pi_{yz} = -\Pi_{zy} = -\frac{i\omega \bar{p}_\parallel}{\omega_{ce} n_\perp(a + n_\parallel \bar{p}_\parallel \omega/\omega_{ce})} \left[\frac{\pi b}{\sin \pi a} J_a(b) J'_{-a}(b) + 1 \right] \quad (4.352)$$

$$\Pi_{zz} = \frac{\omega^2 \bar{p}_\parallel^2}{\omega_{ce}^2(a + n_\parallel \bar{p}_\parallel \omega/\omega_{ce})} \frac{\pi}{\sin \pi a} J_a(b) J_{-a}(b) \quad (4.353)$$

where now $b = v_\perp \bar{p}_\perp$.

Problem 4.7.3. Off-diagonal tensor elements. Pick one of the off-diagonal dielectric tensor elements, and verify it is given by equation (4.347) along with either (4.349), (4.350), or (4.352), starting from equation (4.325).

4.7.3 The weakly relativistic dielectric tensor

In this section, we return to equation (4.325) and integrate over the momenta first instead of the phase. We can obtain another expression via the identity,

$$I(s, \mathbf{r}) = \frac{1}{4\pi} \int \frac{dp}{\sqrt{1+p^2}} e^{-s\sqrt{1+p^2}-i\mathbf{r}\cdot\mathbf{p}} = \frac{K_1(\sqrt{s^2+r^2})}{\sqrt{s^2+r^2}} \quad (4.354)$$

and its derivative where K_n is the modified Bessel function of the second kind of order n . The dielectric tensor is then given by

$$\mathbf{K} = \mathbf{I} + \sum_j \frac{i\omega_{pj}^2}{\epsilon_j \omega \omega_{cj}} \frac{\mu^2}{K_2(\mu)} \int_0^\infty d\xi \left[\frac{K_2(\sqrt{R})}{R} T_1 - \frac{K_3(\sqrt{R})}{R^{3/2}} T_2 \right] \quad (4.355)$$

where

$$R = \left(\mu - i\xi \frac{\omega}{\epsilon_j \omega_{cj}} \right)^2 + 2v_\perp^2(1 - \cos \xi) + v_\parallel^2 \xi^2$$

where $v_{\parallel} = n_{\parallel}\omega/\epsilon_j\omega_{cj}$, and

$$\mathbf{T}_1 = \begin{pmatrix} \cos \xi & -\sin \xi & 0 \\ \sin \xi & \cos \xi & 0 \\ 0 & 0 & 1 \end{pmatrix} \quad (4.356)$$

and

$$\mathbf{T}_2 = \begin{pmatrix} v_{\perp}^2 \sin^2 \xi & -v_{\perp}^2 \sin \xi (1 - \cos \xi) & v_{\perp} v_{\parallel} \xi \sin \xi \\ v_{\perp}^2 \sin \xi (1 - \cos \xi) & -v_{\perp}^2 (1 - \cos \xi)^2 & v_{\perp} v_{\parallel} \xi (1 - \cos \xi) \\ v_{\perp} v_{\parallel} \xi \sin \xi & -v_{\perp} v_{\parallel} \xi (1 - \cos \xi) & v_{\parallel}^2 \xi^2 \end{pmatrix}. \quad (4.357)$$

Up to this point, the analysis is exact, but it is valuable only for numerical integration of the tensor components. In the weakly relativistic limit, we follow the development of Shkarofsky [51] and take $\mu_e \gg 1$ (μ_i is generally so large that relativistic effects are negligible, so that the ion contributions will be ignored from this point on and we shall delete the subscript on μ). Since this quantity appears in the argument of the modified Bessel function, we can use the asymptotic limit so that $K_n(x) \simeq \sqrt{\pi/2x} e^{-x}$. If we also take the limit of small $\lambda = \frac{1}{2}k_{\perp}^2\rho_L^2 = v_{\perp}^2/\mu$, then we can simplify the expression for R such that

$$R^{\frac{1}{2}} = \mu \left[\left(1 + \frac{i\xi\omega}{\mu\omega_{ce}} \right)^2 + \left(\frac{v_{\parallel}}{\mu} \right)^2 \xi^2 \right]^{\frac{1}{2}} + \Lambda(1 - \cos \xi)$$

where

$$\Lambda \equiv \lambda \left[\left(1 + \frac{i\xi\omega}{\mu\omega_{ce}} \right)^2 + \left(\frac{v_{\parallel}}{\mu} \right)^2 \xi^2 \right]^{-\frac{1}{2}}.$$

Now we will need to keep the $\Lambda(1 - \cos \xi)$ term in the exponential of the K_n terms, because the oscillating phase in the exponent is important, but it is safe to neglect it otherwise since $\mu \gg \Lambda$. This approximation leads to $k_{\perp}^2 c^2 / R^{1/2} \omega_{ce}^2 = \Lambda$ except in the exponent. For the oscillating exponential term, we will use equation (4.224) to write

$$e^{\Lambda \cos \xi} = \sum_{n=-\infty}^{\infty} I_n(\Lambda) e^{-in\xi} \quad (4.358)$$

$$\cos \xi e^{\Lambda \cos \xi} = \sum_{n=-\infty}^{\infty} I'_n(\Lambda) e^{-in\xi} \quad (4.359)$$

and other similar results as in equation (4.225). Then by changing variables to $t = -\xi\omega/\mu\omega_{ce}$ so that \sqrt{R} becomes

$$\sqrt{R} = \mu[(1 - it)^2 + n_{\parallel}^2 t^2]^{\frac{1}{2}} + \Lambda(1 - \cos \xi)$$

and $\exp(-in\xi) \rightarrow \exp(iv_n t)$ with $v_n = n\mu\omega_{ce}/\omega$, then the weakly relativistic dielectric tensor may be written as

$$\mathbf{K} = \mathbf{I} + i \frac{\omega_p^2}{\omega^2} \mu \sum_{n=-\infty}^{\infty} \int_0^{\infty} \mathbf{T}_3 \frac{e^{-\Lambda} \exp\{\mu - \mu[(1-it)^2 + n_{\parallel}^2 t^2]^{\frac{1}{2}} + iv_n t\}}{[(1-it)^2 + n_{\parallel}^2 t^2]^{\frac{q}{4}}} dt \quad (4.360)$$

where

$$\mathbf{T}_3 = [(1-it)^2 + n_{\parallel}^2 t^2]^{\frac{1}{2}} \mathbf{T}_3^{(a)} + \frac{k_{\perp} k_{\parallel} c^2}{\omega \omega_c} \mathbf{T}_3^{(b)} \frac{\partial}{\partial v_n} \quad (4.361)$$

with

$$\mathbf{T}_3^{(a)} = \begin{pmatrix} \frac{n^2 I_n}{\Lambda} & -in(I'_n - I_n) & 0 \\ in(I'_n - I_n) & \frac{n^2 I_n}{\Lambda} + 2\Lambda(I_n - I'_n) & 0 \\ 0 & 0 & I_n \left(1 + k_{\parallel} \frac{\partial}{\partial k_{\parallel}}\right) \end{pmatrix} \quad (4.362)$$

$$\mathbf{T}_3^{(b)} = \begin{pmatrix} 0 & 0 & \frac{n I_n}{\Lambda} \\ 0 & 0 & i(I'_n - I_n) \\ \frac{n I_n}{\Lambda} & -i(I'_n - I_n) & 0 \end{pmatrix}. \quad (4.363)$$

For small Λ , we can write this in terms of the \mathcal{F}_q function that is defined by

$$\mathcal{F}_q(v_n, n_{\parallel}) \equiv -i \int_0^{\infty} dt \frac{\exp\{\mu - \mu[(1-it)^2 + n_{\parallel}^2 t^2]^{\frac{1}{2}} + iv_n t\}}{[(1-it)^2 + n_{\parallel}^2 t^2]^{\frac{q}{2}}} \quad (4.364)$$

although the most common definition is a further approximation in the smallness of n_{\parallel}^2 given by

$$\mathcal{F}_q(z_n, a) \equiv -i \int_0^{\infty} dt \frac{\exp[i z_n t - a t^2 / (1-it)]}{(1-it)^q} \quad (4.365)$$

where $z_n = \mu + v_n = \mu(\omega + n\omega_{ce})/\omega$ and $a = \frac{1}{2}\mu n_{\parallel}^2$. This generalized weakly relativistic dispersion function is real for $z_n \geq a$ and complex for $z_n < a$. Some of its characteristics are shown in figure 4.10 for $a = 1$ and in figure 4.11 for $a = 5$. Its mathematical properties are given in appendix B in section B.3.

Then for the case for small Λ , assuming the same dispersion function for each power of λ , the dielectric tensor elements are given by

$$K_{xx} \simeq 1 - \frac{\omega_p^2}{\omega^2} \mu e^{-\lambda} \sum_{n=1}^{\infty} \frac{n^2 I_n}{\lambda} [\mathcal{F}_{n+3/2}(z_n, a) + \mathcal{F}_{n+3/2}(z_{-n}, a)] \quad (4.366)$$

$$K_{xy} \simeq i \frac{\omega_p^2}{\omega^2} \mu e^{-\lambda} \sum_{n=1}^{\infty} n(I_n - I'_n) [\mathcal{F}_{n+3/2}(z_n, a) - \mathcal{F}_{n+3/2}(z_{-n}, a)] \quad (4.367)$$

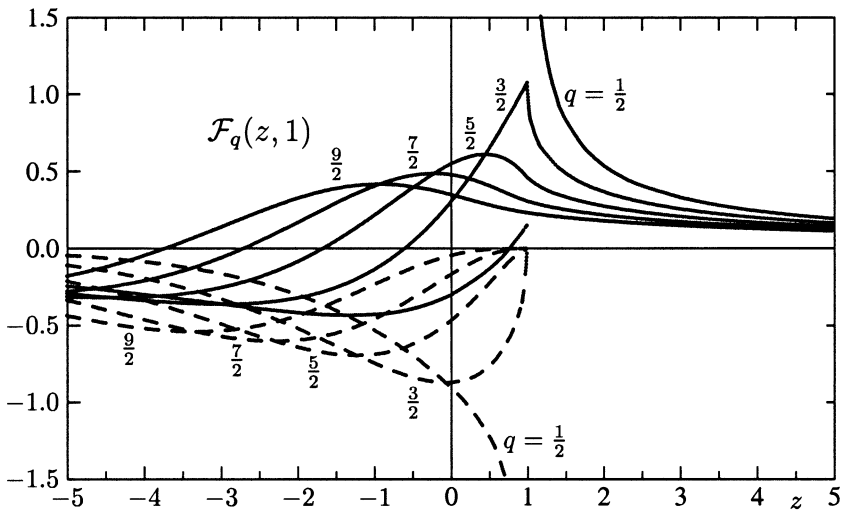


Figure 4.10. Generalized weakly relativistic dispersion function, $\mathcal{F}_q(z, a)$ for half-integral q and $a = 1$, showing both real (full curves) and imaginary (dashed curves) parts.

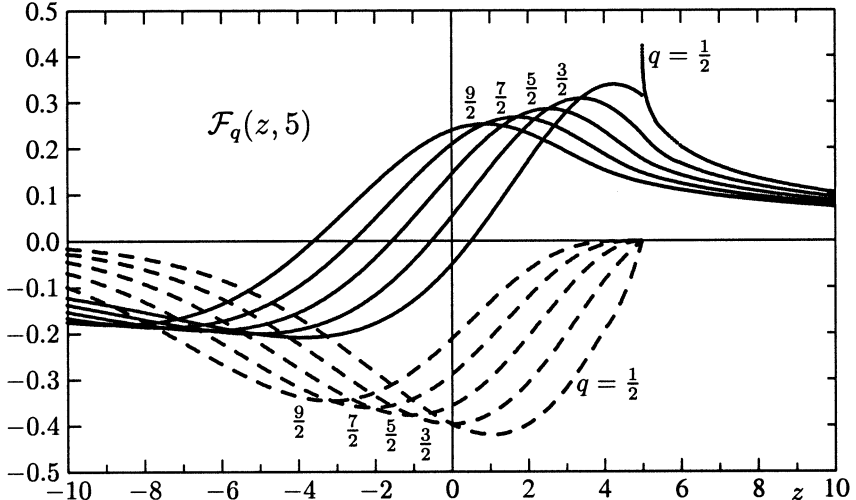


Figure 4.11. Generalized weakly relativistic dispersion function, $\mathcal{F}_q(z, a)$ for half-integral q and $a = 5$, showing both real (full curves) and imaginary (dashed curves) parts.

$$K_{zz} \simeq 1 - \frac{\omega_p^2}{\omega^2} \mu e^{-\lambda} \sum_{n=-\infty}^{\infty} I_n \left\{ (1 - 4a) \mathcal{F}_{n+5/2}(z_n, a) + 2a [\mathcal{F}_{n+3/2}(z_n, a) + \mathcal{F}_{n+7/2}(z_n, a)] \right\} \quad (4.368)$$

$$K_{yy} \simeq K_{xx} + \frac{\omega_p^2}{\omega^2} \mu e^{-\lambda} 2\lambda \left\{ (I_0 - I_1) \mathcal{F}_{5/2}(\mu, a) + \sum_{n=1}^{\infty} (I_n - I'_n) [\mathcal{F}_{n+5/2}(z_n, a) + \mathcal{F}_{n+5/2}(z_{-n}, a)] \right\} \quad (4.369)$$

$$K_{xz} \simeq - \frac{\omega_p^2}{\omega \omega_c} \mu e^{-\lambda} n_{\parallel} n_{\perp} \sum_{n=1}^{\infty} \frac{n I_n}{\lambda} [\mathcal{F}_{n+5/2}(z_n, a) - \mathcal{F}_{n+3/2}(z_n, a) - \mathcal{F}_{n+5/2}(z_{-n}, a) + \mathcal{F}_{n+3/2}(z_{-n}, a)] \quad (4.370)$$

$$K_{yz} \simeq -i \frac{\omega_p^2}{\omega \omega_c} \mu n_{\parallel} n_{\perp} e^{-\lambda} \left\{ (I_1 - I_0) \mathcal{F}_{7/2}(\mu, a) + \sum_{n=1}^{\infty} (I'_n - I_n) [\mathcal{F}_{n+5/2}(z_n, a) + \mathcal{F}_{n+5/2}(z_{-n}, a)] \right\} \quad (4.371)$$

where $K_{yx} = -K_{xy}$, $K_{zx} = K_{xz}$, $K_{zy} = -K_{yz}$, and $z_{\pm} = \mu(\omega \pm n\omega_{ce})/\omega$ and now the argument of I_n is λ (which is independent of t) instead of Λ (which is a function of t).

4.7.4 Moderately relativistic expressions

When one keeps higher order terms in the Bessel function expansions, higher-order dispersion functions should be used for those terms since Λ appeared *inside* the integral of equation (4.360). In fact, if we define the function of λ associated with K_{xx} as $f_{xx}(n, \lambda)$ such that

$$f_{xx}(n, \lambda) = \frac{n^2 e^{-\lambda} I_n(\lambda)}{\lambda} = \sum_{k=0}^{\infty} a_{xx,n}^{(k)} \lambda^k \quad (4.372)$$

then we could write a more nearly precise expression for K_{xx} as

$$K_{xx} = 1 - \frac{\omega_p^2}{\omega^2} \mu \sum_{n=1}^{\infty} \sum_{k=0}^{\infty} a_{xx,n}^{(k)} \lambda^k [\mathcal{F}_{k+5/2}(z_n, a) + \mathcal{F}_{k+5/2}(z_{-n}, a)]. \quad (4.373)$$

Although this is a doubly infinite sum, usually only an $n = 1$ and perhaps one other n needs to be included, and $k = 0$ through $k = 3$ will usually suffice unless λ is approaching unity, in which case an exact treatment is needed. Extending this same type of expansion to the other dielectric tensor terms leads to the *moderately relativistic* approximation.

As an example of the moderately relativistic expressions, the expression for K_{xx} through order λ^3 is given by

$$K_{xx} = 1 - \frac{\omega_p^2}{\omega^2} \mu \left\{ \frac{1}{2} [\mathcal{F}_{\frac{5}{2}}(z_1, a) + \mathcal{F}_{\frac{5}{2}}(z_{-1}, a)] - \frac{\lambda}{2} [\mathcal{F}_{\frac{7}{2}}(z_1, a) + \mathcal{F}_{\frac{7}{2}}(z_{-1}, a)] \right. \\ + \frac{5\lambda^2}{16} [\mathcal{F}_{\frac{9}{2}}(z_1, a) + \mathcal{F}_{\frac{9}{2}}(z_{-1}, a)] - \frac{7\lambda^3}{48} [\mathcal{F}_{\frac{11}{2}}(z_1, a) + \mathcal{F}_{\frac{11}{2}}(z_{-1}, a)] \\ + \frac{\lambda}{2} [\mathcal{F}_{\frac{7}{2}}(z_2, a) + \mathcal{F}_{\frac{7}{2}}(z_{-2}, a)] - \frac{\lambda^2}{2} [\mathcal{F}_{\frac{9}{2}}(z_2, a) + \mathcal{F}_{\frac{9}{2}}(z_{-2}, a)] \\ + \frac{7\lambda^3}{24} [\mathcal{F}_{\frac{11}{2}}(z_2, a) + \mathcal{F}_{\frac{11}{2}}(z_{-2}, a)] + \frac{3\lambda^2}{16} [\mathcal{F}_{\frac{9}{2}}(z_3, a) + \mathcal{F}_{\frac{9}{2}}(z_{-3}, a)] \\ \left. - \frac{3\lambda^3}{16} [\mathcal{F}_{\frac{11}{2}}(z_3, a) + \mathcal{F}_{\frac{11}{2}}(z_{-3}, a)] + \frac{\lambda^3}{24} [\mathcal{F}_{\frac{11}{2}}(z_4, a) + \mathcal{F}_{\frac{11}{2}}(z_{-4}, a)] \right\}. \quad (4.374)$$

This expression is better than the weakly relativistic approximation, but not exact. This approximation still uses the asymptotic form of $K_2(\mu)$ and is still based on the smallness of n_\parallel^2 for the $\mathcal{F}_q(z_n, a)$.

Problem 4.7.4. Moderately relativistic K_{xy} and K_{yy} . Work out the moderately relativistic expression for K_{xy} and K_{yy} corresponding to equation (4.374) (through order λ^3).

A further simplification we examine for both the weakly relativistic and the moderately relativistic approximations is the $n_\parallel \rightarrow 0$ limit (or the $a \rightarrow 0$ limit), where

$$\mathcal{F}_q(z, 0) = F_q(z) \equiv -i \int_0^\infty \frac{e^{izt}}{(1 - it)^q} dt \quad (4.375)$$

and for $q = \frac{1}{2}$, we have the relationship to the PDF (see equation (B.40))

$$iF_{\frac{1}{2}} = \int_0^\infty \frac{e^{izt}}{(1 - it)^{\frac{1}{2}}} dt = \frac{1}{\sqrt{z}} Z(i\sqrt{z}). \quad (4.376)$$

This weakly relativistic dispersion function, often referred to as the Dnestrakovskii function, is illustrated in figure 4.12. Other properties are listed in section B.2.

The higher order functions may be obtained from the recursion formula,

$$(q - 1)F_q(z) = 1 - zF_{q-1}(z) \quad (4.377)$$

and the analytic continuation for $\text{Im } \omega < 0$ is given by the properties of the PDF. Also, in this limit, $K_{xz} = K_{zx} = K_{yz} = K_{zy} = 0$, so the leading terms here are the only terms, not merely the dominant terms.

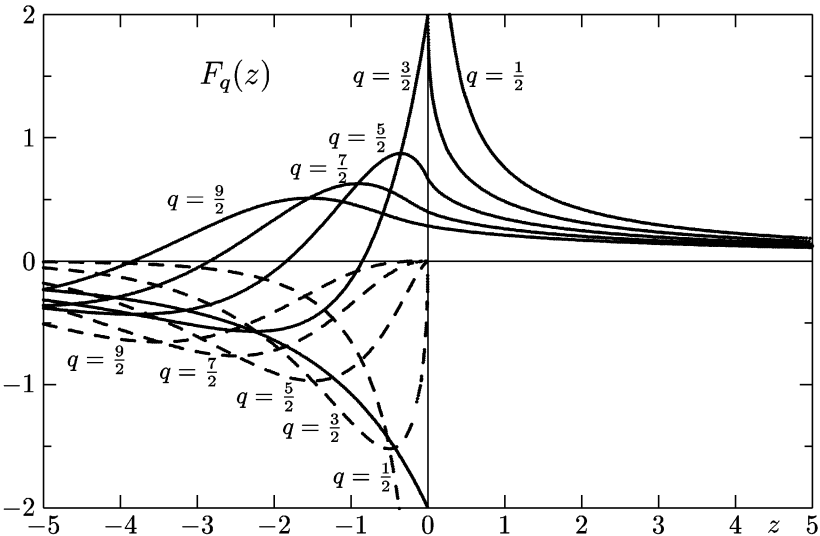


Figure 4.12. Weakly relativistic dispersion function, $F_q(z)$ for half-integral q , showing both real (full curves) and imaginary (dashed curves) parts.

4.7.5 Exact expressions with $n_{\parallel} = 0$

It is possible to obtain the exact dielectric tensor expressions in terms of a few relatively simple integrals when $n_{\parallel} = 0$. For this analysis, we return to the dielectric tensor elements without sums given in section 4.7.2. Although the dielectric tensor terms are complicated, since the order of the Bessel functions is not integral in the general case, by changing into polar coordinates in momentum space, the integrals over the angle can be done analytically, leaving us with either a single integral for each n or even with a single integral for the sum over n . The derivation for K_{xx} will be worked out in detail, while the others will be left as an exercise.

With $n_{\parallel} = 0$, we may write an exact expression for K_{xx} as

$$K_{xx} = 1 - \frac{\omega_p^2}{\omega^2} \sum_{n=1}^{\infty} F_{xx}^{(n)}$$

where each term in the sum is given by

$$F_{xx}^{(n)} = \frac{2\mu^2}{K_2(\mu)} \frac{n^2}{v_{\perp}^2} \int_0^{\pi} d\theta \sin \theta \int_0^{\infty} d\bar{p} \bar{p}^2 e^{-\mu\gamma} \frac{J_n^2(v_{\perp}\bar{p} \sin \theta)}{\gamma^2 - n^2 \omega_c^2/\omega^2}. \quad (4.378)$$

After integrating over the angle using equation (B.68), equation (4.378) may be

expressed as

$$F_{xx}^{(n)} = \frac{\mu^2}{K_2(\mu)} \frac{2n^2}{v_\perp^2 (2n+1)!} \int_0^\infty d\bar{p} \frac{\bar{p}^2 e^{-\mu\gamma}}{\bar{p}^2 - p_n^2} b^{2n} {}_1F_2(n + \frac{1}{2}; n + \frac{3}{2}, 2n+1; -b^2) \quad (4.379)$$

where $\gamma(\bar{p}) = \sqrt{1 + \bar{p}^2}$, $p_n^2 = n^2 \omega_c^2 / \omega^2 - 1$, and $b^2 = \mu\lambda\bar{p}^2$, since $v_\perp = n_\perp\omega/\omega_c = \sqrt{\mu\lambda}$. Alternatively, using the Newberger sum rule, we have a single expression for the sum as

$$F_{xx} = \frac{\mu^2}{2K_2(\mu)} \int_0^\pi d\theta \sin\theta \int_0^\infty d\bar{p} \bar{p}^2 \frac{e^{-\mu\gamma}}{\gamma} \frac{\omega a}{\omega_c v_\perp^2} \times \left[\frac{\pi a}{\sin \pi a} J_a(v_\perp \bar{p} \sin\theta) J_{-a}(v_\perp \bar{p} \sin\theta) - 1 \right] \quad (4.380)$$

where $a = \omega\gamma/\omega_c$. Integrating this expression over the angle (see equation (B.73) in [appendix B](#)), the result may be expressed as

$$K_{xx} = 1 - \frac{\omega_p^2}{\omega^2} \frac{\mu}{n_\perp^2} [I_1(z, \lambda, \mu) - 1] \quad (4.381)$$

where I_1 is the integral (*not* a Bessel function)

$$I_1(z, \lambda, \mu) = \frac{\mu}{K_2(\mu)} \int_0^\infty dp p^2 e^{-\mu\gamma} {}_2F_3(\frac{1}{2}, 1; \frac{3}{2}, 1-a, 1+a; -\lambda\mu p^2). \quad (4.382)$$

The dependence on $z = z_{-n} \equiv \mu(1 - n\omega_c/\omega)$ is through $a(z) = n\gamma/(1 - z/\mu)$. The integrands utilize the hypergeometric functions that are defined by equations (B.66) and (B.67).

Problem 4.7.5. Remaining exact tensor elements. Show that the remaining dielectric tensor elements with $n_{||} = 0$ may be written as

$$K_{xy} = i \frac{\omega_p^2}{\omega^2} \frac{\mu}{2n_\perp^2} [I_2(z, \lambda, \mu) - I_3(z, \lambda, \mu) + 1] \quad (4.383)$$

$$K_{zz} = 1 - \frac{\omega_p^2}{\omega^2} \mu I_4(z, \lambda, \mu) \quad (4.384)$$

$$K_{yy} = K_{xx} - \frac{\omega_p^2}{\omega^2} \frac{2\mu}{n_\perp^2} [1 + I_5(z, \lambda, \mu) - I_2(z, \lambda, \mu)] \quad (4.385)$$

where

$$I_2(z, \lambda, \mu) = \frac{\mu}{K_2(\mu)} \int_0^\infty dp p^2 e^{-\mu\gamma} {}_2F_3(\frac{1}{2}, 1; \frac{3}{2}, 1-a, a; -\lambda\mu p^2) \quad (4.386)$$

$$I_3(z, \lambda, \mu) = \frac{\mu}{K_2(\mu)} \int_0^\infty dp p^2 e^{-\mu\gamma} {}_2F_3(\frac{1}{2}, 1; \frac{3}{2}, -a, 1+a; -\lambda\mu p^2) \quad (4.387)$$

$$I_4(z, \lambda, \mu) = \frac{\mu}{K_2(\mu)} \int_0^\infty dp \frac{p^4 e^{-\mu\gamma}}{3(1+p^2)} {}_2F_3(\frac{1}{2}, 1; \frac{5}{2}, 1-a, 1+a; -\lambda\mu p^2) \quad (4.388)$$

$$I_5(z, \lambda, \mu) = \frac{\lambda\mu^2}{K_2(\mu)} \int_0^\infty dp \frac{p^4 e^{-\mu\gamma}}{3a(a-1)} {}_2F_3(\frac{1}{2}, 2; \frac{5}{2}, 2-a, a; -\lambda\mu p^2). \quad (4.389)$$

Problem 4.7.6. Hypergeometric function identity. Prove that $I_6 = I_2 - 1$ where

$$I_6(z, \lambda, \mu) = \frac{\lambda\mu^2}{K_2(\mu)} \int_0^\infty dp \frac{p^4 e^{-\mu\gamma}}{3a(a-1)} {}_2F_3(\frac{3}{2}, 1; \frac{5}{2}, 2-a, 1+a; -\lambda\mu p^2).$$

The imaginary parts of the tensor elements may be obtained rather directly by examining the poles of the integrands. In this section, we simplify the notation by dropping the electron subscript, and note that the pole in equation (4.379) is at $\bar{p} = \bar{p}_n$. Evaluating the integral at this pole yields

$$\text{Im}[F_{xx}^{(n)}] = -\frac{\mu^2}{K_2(\mu)} \frac{\pi n^2 e^{-\mu n \omega_c/\omega} b_n^{2n+1}}{(2n+1)!(\mu\lambda)^{3/2}} {}_1F_2(n+\frac{1}{2}; n+\frac{3}{2}, 2n+1; -b_n^2) \quad (4.390)$$

where $b_n^2 = \mu\lambda(n^2\omega_c^2/\omega^2 - 1)$. This expression is exact, but in order to compare it with the weakly relativistic approximation, we take $e^\mu K_2(\mu) \sim \sqrt{\pi/2\mu}$, so that the exponential term becomes e^{z_n} . If we write the corresponding weakly relativistic expression as $W_{xx}^{(n)}$, and examine the imaginary part, we find, using equation (B.48),

$$\text{Im}[W_{xx}^{(n)}] = -\frac{\mu n^2 e^{-\lambda} I_n(\lambda)}{\lambda} \frac{\pi(-z)^{q-1} e^z}{\Gamma(q)}$$

where $q = n + \frac{1}{2}$, then expanding both the Bessel function terms and the hypergeometric function, the ratio of the exact to the weakly relativistic expression may be written as

$$\frac{\text{Im}[F_{xx}^{(n)}]}{\text{Im}[W_{xx}^{(n)}]} = \frac{1 + \lambda z/q + \dots}{1 - \lambda + q\lambda^2/(2q-1) + \dots}. \quad (4.391)$$

From this ratio, we observe first that the exact expression is a function of the product, λz , not a function of λ multiplied by a function of z as the weakly relativistic expression indicates. Secondly, we see that the higher order terms in the Bessel function expansion do not improve the accuracy, so this justifies the truncation of the Bessel functions to the lowest order terms in equations (4.366) through (4.371). There is another interesting feature observable in comparing these imaginary parts in figure 4.13 for two different values of lambda. After factoring out some leading factors, it is apparent that the peak of the exact expressions always exceeds the peak of the weak expression, but for large negative

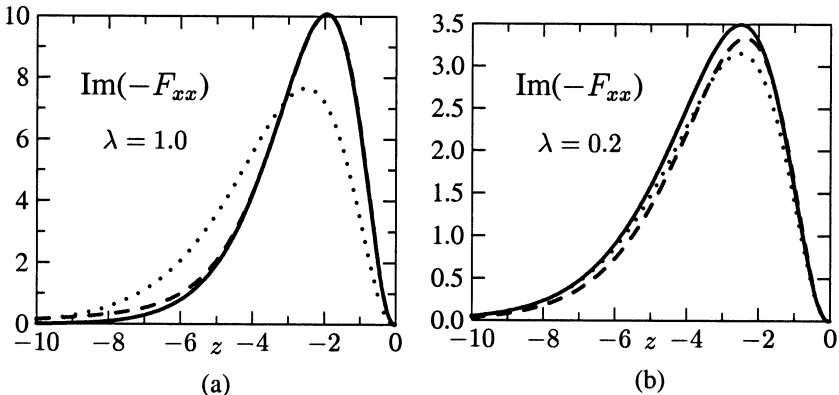


Figure 4.13. $\text{Im}(-F_{xx})$ versus z with $\mu = 50$ for the exact (full curves), moderately relativistic (dashed curves), and weakly relativistic case (dotted curves) with $n_{\parallel} = 0$ for (a) $\lambda = 1.0$ and (b) $\lambda = 0.2$.

z , the weak expression exceeds the exact expression. In fact, if one approximates $b_n^2 = -\lambda z(2 - z/\mu) \simeq -2\lambda z$, then the integral

$$\int_0^\infty dx e^{-x} x^{1/2} \int_0^\pi d\theta J_\nu^2(\sqrt{2\lambda x} \sin \theta) \sin \theta = \sqrt{\pi} e^{-\lambda} I_\nu(\lambda) \quad (4.392)$$

guarantees that each curve has equal area. Similar identities exist for the other dielectric terms. It is also apparent that the moderately relativistic approximation (with terms through λ^5) is much better than the weakly relativistic case with $\lambda = 1$, but the difference is small for small λ .

Problem 4.7.7. Weakly relativistic identities.

- (i) Use equation (4.392) to prove that the integrals over z for $\text{Im}[K_{xx}(z)]$ for the exact result and the weakly relativistic result are identical.
- (ii) Use the identity

$$2 \int_0^\infty dx e^{-x} x^{3/2} \int_0^\pi d\theta J_\nu^2(\sqrt{2\lambda x} \sin \theta) \cos^2 \theta \sin \theta = \sqrt{\pi} e^{-\lambda} I_\nu(\lambda) \quad (4.393)$$

to prove that the integrals over z for $\text{Im}[K_{zz}(z)]$ for the exact result and the weakly relativistic result are identical.

When μ is not so large and λ is of order unity or greater, the deviations from the weakly relativistic approximation are significant and the differences between K_{xx} and K_{xy} are no longer ignorable. A strongly relativistic case where $\mu = 20$ and $\lambda = 1$ is illustrated in figure 4.14(a) for F_{xx} in the exact and two approximations and in figure 4.14(b) for F_{xx} and F_{yy} for the exact case only. It is

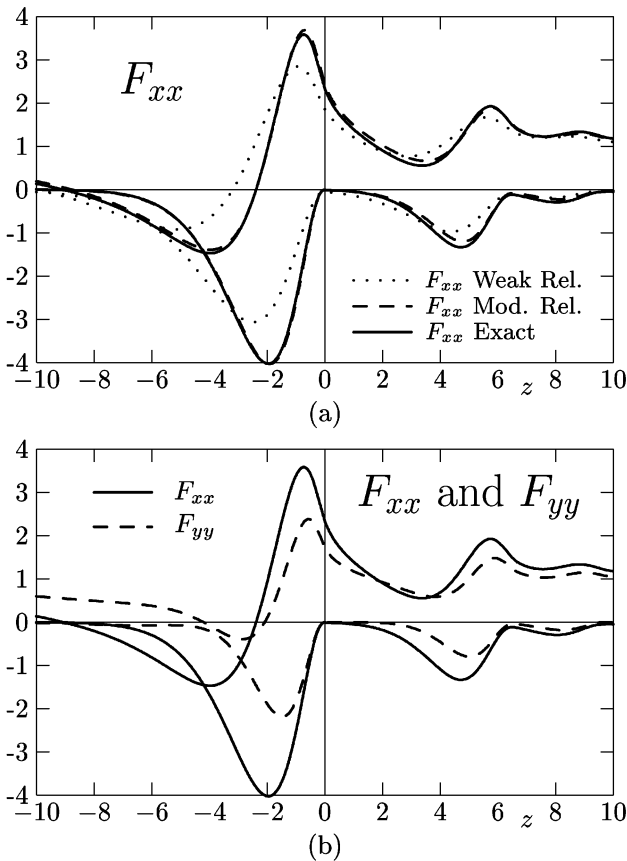


Figure 4.14. Plots of (a) the real and imaginary parts of F_{xx} for the exact, moderately relativistic, and weakly relativistic approximations for $\mu = 20$ and $\lambda = 1$ and (b) the exact real and imaginary parts of F_{xx} and F_{yy} .

apparent that the exact and moderately relativistic cases are still close, but that the weakly relativistic approximation is no longer reliable. Figure 4.14(a) also shows the effects from the third and fourth harmonics which occur at $z = \mu/3 = 6.67$ for $n = 3$ and at $z = \mu/2 = 10$ for $n = 4$.

4.7.6 The relativistic X-wave

The exact X-wave dispersion relation with $n_{\parallel} = 0$ is

$$n_{\perp}^2 = \frac{K_{xx} K_{yy} + K_{xy}^2}{K_{xx}}. \quad (4.394)$$

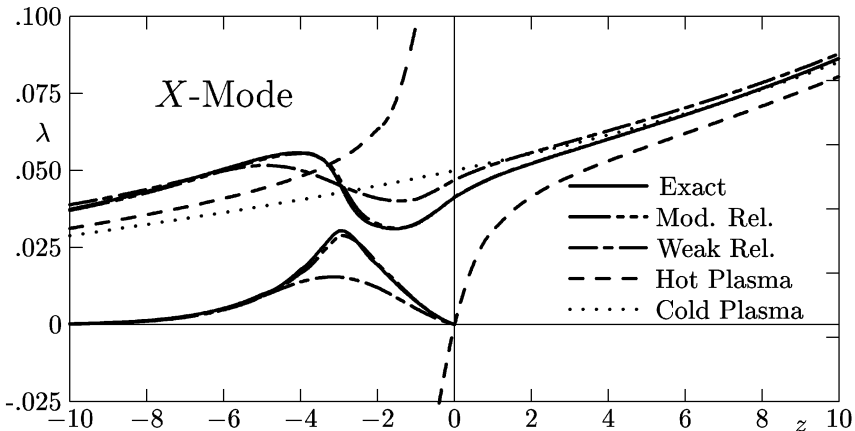


Figure 4.15. Variation of λ with z for the X -mode with $\mu = 50$ and $\omega^2/\omega_p^2 = 4$ (from [52]).

This case leads to no damping at all in the nonrelativistic theory, so the relativistic effects are especially apparent. Figure 4.15 shows an example dispersion relation with $\mu = 50$ ($T_e \sim 10$ keV) illustrating the differences between using the exact relativistic tensor components and the weakly and moderately relativistic expressions.

For this comparison, we let $\omega^2/\omega_p^2 = 4$ and solve for λ in the neighborhood of the second harmonic ($z = 0$ corresponds to $\omega = 2\omega_c$), assuming that the variation in z is due to changes in the magnetic field only. The dispersion is plotted for five separate cases. The cold plasma result is a simple curve showing no significant features near the second harmonic, while the nonrelativistic hot plasma case shows no absorption, but it does indicate a mode conversion region (see section 6.3.3). The exact result and the moderately relativistic cases nearly overlay one another while the weakly relativistic case shows that even with μ large and λ small, the differences are significant in the dispersion relation. The peak of the imaginary part of λ for the weakly relativistic case is approximately half the value for the exact case while the peak imaginary parts of F_{xx} , F_{yy} , and F_{xy} are about 3.7% low for $\lambda = 0.05$. For the moderately relativistic case, the peak imaginary part of λ is only 5.5% below the exact value while the individual component differences are less than 2.5% low for $\lambda = 0.05$.

Chapter 5

Bounded homogeneous plasmas

5.1 Introduction

The principal effect of boundaries on plasma waves is to restrict the spectrum of k to a discrete spectrum as in a waveguide problem instead of the continuous spectrum of the infinite, homogeneous plasma. Boundaries also introduce excitation or scattering resonances that are not present in the unbounded plasma. The oldest of these effects was described by Tonks [53] as he scattered electromagnetic waves from a plasma column, discovering a scattering resonance near the plasma frequency. Later studies were made of space charge waves and surface waves on plasma columns [54] and plasma-filled waveguides [55–57]. Numerous other examples have been described and demonstrated, but these examples will be used to demonstrate the method of approach and some of the fundamental characteristics of waves in bounded plasmas.

5.2 Boundary conditions

The usual boundary conditions we shall encounter are either a conducting wall or a boundary between the plasma and either vacuum or a dielectric (such as glass). These boundary conditions are generally taken as abrupt, and we use jump conditions to relate the fields on opposite sides of the discontinuity. This is never precise, since real plasmas do not have sharp boundaries. In general, as the plasma approaches either a conductor or a dielectric, the density falls either gradually, dominated by a variety of transport phenomena such as electron and ion diffusion, ionization, and recombination, or it falls off rather abruptly, so that a large change occurs in a few Debye lengths. Even in this latter case, the Debye length is ill-defined in this transition layer, since it is dependent on both density and temperature, both of which are changing rapidly. The use of any kind of refined model of the boundary generally requires either an arbitrary assumption about the profile and/or considerable numerical work. In this book, we shall treat only the sharp boundary cases because they illustrate the principal

effects of boundaries, offer analytic solutions, and generally agree well with most experiments, although we shall note one case where the inhomogeneity was crucial to the understanding of the phenomena. We thus restrict our attention to waves whose wavelength is long compared to the thickness of the boundary layer. Whenever the wavelength is short compared to the layer thickness, we treat these cases as an inhomogeneous plasma, and discuss them in the next chapter. For the in-between cases, the typical recourse is to solve the equations numerically.

5.2.1 Conducting boundary

The simplest case, by far, is the conducting boundary because the condition in a cold plasma is simply that the tangential electric field must vanish at a perfect conductor. This may be written as

$$E_t(a) = 0 \quad (5.1)$$

where the conducting wall is at a . This case is simplest because this condition is usually easy to apply and eliminates matching to any other fields beyond the boundary.

For hot plasmas, however, this is not so simple, because we must also prescribe boundary conditions on the velocity. The most straightforward condition for either a metallic or dielectric boundary is specular reflection, where the particle bounces off the wall with equal angles of incidence and reflection. One way to deal with this kind of boundary is to imagine a virtual plasma on the other side of the boundary such that for every particle crossing the boundary, one emerges from the virtual plasma as if the original particle had reflected, conserving particles and requiring $J_{pn}(a) = 0$ where J_{pn} is the particle current normal to the boundary. Then one needs only to imagine an infinite number of such slabs that are periodic in the slab width, and one has an infinite, uniform plasma which is simply periodic. The advantages of this kind of approach, however, are more than offset by their unreality, since specular reflection is probably an event of low likelihood, and nontrivial electric fields in the sheath region (a few Debye lengths wide) distort the particle motions, not to mention the fact that this assumes the temperature is uniform all the way to the wall. One other way to treat this problem is to assume that the magnetic field is parallel to the boundary and infinite in magnitude (or effectively so), in which case the particles move only parallel to the boundary, and only wave fields must be matched at the boundary. When the magnetic field is oblique to the boundary, there are no simple recipes.

5.2.2 Plasma–vacuum (or dielectric) interface

The boundary conditions used at the plasma–vacuum interface, or at an interface between a plasma and an isotropic, insulating dielectric (such as glass), are

derived from the integral form of the Maxwell equations, and using $\hat{\mathbf{E}}_n$ as a unit vector normal to the surface, pointing away from the plasma, are:

$$\hat{\mathbf{E}}_n \times (\mathbf{E}_v - \mathbf{E}_p) = 0 \quad (5.2)$$

$$\hat{\mathbf{E}}_n \cdot (\mathbf{B}_v - \mathbf{B}_p) = 0 \quad (5.3)$$

$$\hat{\mathbf{E}}_n \times (\mathbf{H}_v - \mathbf{H}_p) = \mathbf{j}_s \quad (5.4)$$

$$\hat{\mathbf{E}}_n \cdot (\mathbf{D}_v - \mathbf{D}_p) = \rho_s \quad (5.5)$$

where we denote either vacuum or an isotropic dielectric by the subscript v , and \mathbf{j}_s is the surface current density and ρ_s is the surface charge density. Now equation (5.3) is not independent of equation (5.2), as one may see from the component of the Maxwell equation,

$$\hat{\mathbf{E}}_n \cdot (\nabla \times \mathbf{E}) = i\omega \hat{\mathbf{E}}_n \cdot \mathbf{B}$$

which involves only the tangential components of \mathbf{E} . Usually neither the surface charge density nor the surface current density are specified, so neither equation (5.4) nor equation (5.5) are of much use alone, but the surface continuity equation,

$$\nabla_s \cdot \mathbf{j}_s + \frac{\partial \rho_s}{\partial t} = 0 \quad (5.6)$$

where ∇_s has only those components that lie in the surface, may be used to combine these two into an alternative condition,

$$\hat{\mathbf{E}}_n \cdot [\omega(\mathbf{D}_v - \mathbf{D}_p) + \mathbf{k} \times (\mathbf{H}_v - \mathbf{H}_p)] = 0. \quad (5.7)$$

This is an identity (the vacuum and the plasma terms vanish independently at any radius), so there is no condition at the boundary to apply.

One might try a *rigid wall* boundary condition, where the normal component of the velocity must vanish at the boundary, but for a cold plasma this requires the tangential component of \mathbf{E} that is perpendicular to the magnetic field to vanish, which we have already specified as continuous, and requiring it to vanish at the plasma–vacuum boundary again leads to an indeterminate expression (the plasma-dependent coefficients vanish, leaving the wave amplitudes unspecified).

In order to close the set of equations, the usual boundary condition added is the *ideal dielectric* boundary condition, which is to demand that both the surface currents and surface charge density vanish identically. We write this as

$$\hat{\mathbf{E}}_n \times (\mathbf{B}_v - \mathbf{B}_p) = 0. \quad (5.8)$$

Equations (5.2) and (5.8) then form the boundary conditions for the ideal dielectric model. This is not a trivial boundary condition, since for a single wave in the plasma (incident plus reflected, or standing wave normal to the surface, characterized by a single value of k_\perp), the condition of equation (5.2) requires

$\rho_s \neq 0$ (see problem 5.2.2). This condition thus implies that there must be two waves and that they are coupled. The second wave is characterized by the same wavenumber parallel to the surface, but distinct in k_{\perp} . The second value, which we shall denote $k_{\perp 2}$, is derived from the cold plasma dispersion relation, which is quadratic in k_{\perp}^2 , so choosing $k_{\perp 1}$ or k_z determines the value of $k_{\perp 2}$. If $k_{\perp 1}^2 > 0$ (propagating radially), the second root is frequently evanescent radially, so it is localized near the surface, in which case a surface wave is required to satisfy the ideal dielectric boundary condition.

For electrostatic waves, we take the potential to be continuous, and $\hat{\mathbf{E}}_n \cdot (\mathbf{D}_v - \mathbf{D}_p) = 0$. Equation (5.3) is not appropriate for electrostatic waves since they are assumed to have no wave magnetic field at all, and hence neither surface currents nor surface charges.

We note that in calculating the normal component of the displacement vector, the dielectric tensor elements are the ones given previously *only if the magnetic field is parallel to the interface and oriented in the z-direction*. When the magnetic field direction is oblique to the interface, then the usual dielectric tensor must be rotated, but this is rarely necessary, since plasma–vacuum interfaces are frequently magnetic surfaces.

Problem 5.2.1. Surfaces charges and currents. Show that equation (5.7) may be derived from equations (5.4)–(5.6).

Problem 5.2.2. Surface charge density at plasma–vacuum interface. Show that equation (5.2) leads to a discontinuity in \mathbf{D}_n and hence to a surface charge density for a single wave. Find an expression for ρ_s if $n_y = 0$ where the z -direction is the direction of the magnetic field and lies in the surface and the x -direction is normal to the surface. Express ρ_s in terms of E_z , n_x , n_z , and the cold plasma dielectric tensor elements.

Problem 5.2.3. Second value of k_{\perp} . Find an expression for $k_{\perp 2}^2$ in terms of $k_{\perp 1}^2$, the cold plasma dielectric tensor elements, and k_z^2 . (Hint: Look either for their sum or their product.) Assume the magnetic field is parallel to the boundary.

5.3 Unmagnetized plasmas

5.3.1 Scattering from a plasma column

When an electromagnetic wave scatters from a plasma column, it will generally excite plasma waves in the column, and whenever those plasma waves fit the plasma column so as to represent standing waves, the scattering amplitude exhibits a plasma column resonance. These resonances in the absence of a magnetic field are called the *Tonks–Dattner* resonances, and were first described by Tonks [53] and later described in more detail by Dattner [58] who showed they had a dipole character (dominantly linear rather than radial). In addition to verifying the general representation of a plasma by a dielectric constant, the

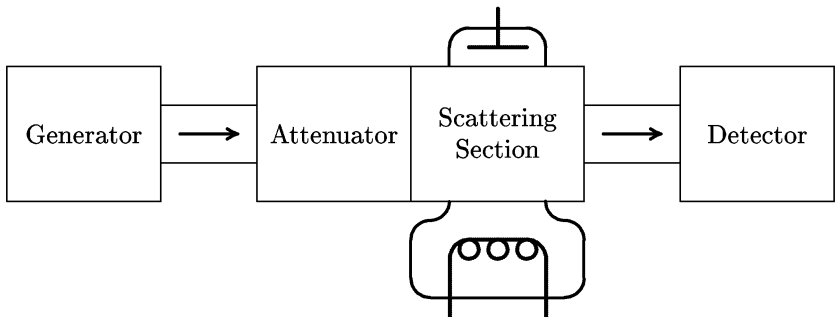


Figure 5.1. Schematic diagram of waveguide and mercury discharge plasma column used in the experiment to measure plasma column resonances.

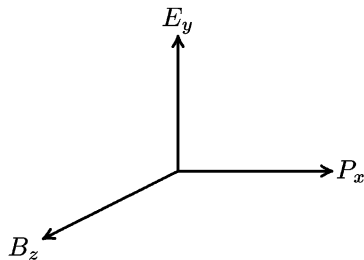


Figure 5.2. Wave fields for idealized experiment: $\lambda \gg a$.

rather widely separated series of resonances also led to the verification of the Bohm–Gross dispersion relation (BGDR) [15], which included the lowest-order thermal corrections to the cold unmagnetized plasma. The final understanding of these resonances required the inclusion of inhomogeneous plasma effects [59] and Landau damping [60].

The experimental arrangement is depicted in figure 5.1 where it is assumed that an electromagnetic wave is incident from the left and whose wavelength is large compared to the size of the plasma column. The wave coordinates for the idealized experiment are represented by figure 5.2 and the column coordinates by figure 5.3 where the glass envelope is ignored.

5.3.1.1 Cold plasma dielectric constant model

We use the electrostatic approximation, $\mathbf{E} = -\nabla\varphi$, where the potential must satisfy Poisson's equation,

$$\nabla \cdot \epsilon \nabla \varphi = -\rho_{\text{ext}}. \quad (5.9)$$

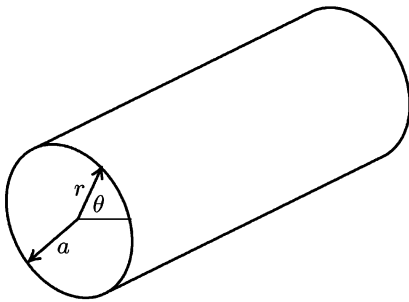


Figure 5.3. Coordinates for plasma column.

Here, ϵ is the uniform plasma dielectric constant and the plasma is assumed to have no *external* charge, so φ must satisfy Laplace's equation inside and outside the plasma column. Assuming no z -dependence, the solution in cylindrical coordinates is

$$\varphi = \sum_{m=0}^{\infty} (A_m r^m + B_m r^{-m}) (C_m \cos m\theta + D_m \sin m\theta).$$

The condition that the potential inside the plasma be regular at the origin demands that $B_m = 0$. Because the incident wave has only an E_y component, $\theta = 0$ must be equivalent to $\theta = \pi$ so $C_m = 0$. Thus inside the plasma, we have

$$\varphi_i = \sum_{m=1}^{\infty} A_m r^m \sin m\theta. \quad (5.10)$$

Outside the plasma, the potential must reduce to the potential of the incident and scattered waves as $r \rightarrow \infty$ so we require the outside potential to be of the form

$$\varphi_o = \sum_{m=1}^{\infty} B_m r^{-m} \sin m\theta + E_{\text{inc}} r \sin \theta. \quad (5.11)$$

The values of A_m and B_m must be obtained by matching boundary conditions at the plasma surface at $r = a$ where the boundary conditions are that the normal component of $\mathbf{D} = \epsilon \mathbf{E}$ and the tangential component of \mathbf{E} be continuous. These requirements at $r = a$ lead to the relations

$$K \left. \frac{\partial \varphi_i}{\partial r} \right|_a = \left. \frac{\partial \varphi_o}{\partial r} \right|_a \quad (5.12)$$

$$\varphi_i(a) = \varphi_o(a) \quad (5.13)$$

where $\epsilon = \epsilon_0 K$. Using the orthogonality of the trigonometric functions, these lead to the relations

$$A_1 = \frac{2E_{\text{inc}}}{1 + K} \quad (5.14)$$

$$(1 + K)A_m = 0 \quad m \geq 2$$

where $K = 1 - \omega_p^2/\omega^2$. The dominant mode (A_1) becomes large (resonant) as $1 + K \rightarrow 0$ so that the resonant frequency is given by

$$\omega = \frac{\omega_p}{\sqrt{2}}. \quad (5.15)$$

The fact that the resonance occurs at $\omega_p/\sqrt{2}$ rather than at the plasma frequency is a consequence of the finite geometry and the cylindrical coordinate system. For a spherical plasma, the resonance occurs at $\omega = \omega_p/\sqrt{3}$.

The existence of such a resonance in the column leads to several conclusions. First, near the resonance, the amplitude of the electric field in the plasma will be large and hence the motions of the plasma particles will be correspondingly large. Secondly, these moving charges will radiate, or scatter the incident radiation. Finally, this scattering of radiation will lead to reflection, so the reflection peak will correspond to the column resonance. It is generally the peak in the reflected power that is measured in the experiments.

While this simple analysis was sufficient to describe the main resonance, or that resonance which has the largest reflection coefficient, there appeared in the experiments a series of resonances that remained unexplained for many years. The multiplicity of resonances is evident in [figure 5.4](#) where as the current in the discharge tube was varied, varying the plasma frequency, the absorption spectrum (from transmission measurements) shows several resonances in addition to the main resonance.

Problem 5.3.1. Spherical Tonks–Dattner resonances. Show that in spherical coordinates, the cold plasma resonance occurs at $\omega = \omega_p/\sqrt{3}$.

Problem 5.3.2. Glass boundary effect. If the plasma column of radius a is surrounded by a glass tube of dielectric constant K_g from radius a to radius b and then there is a split conducting cylinder at radius c with potential $\pm V_0$ applied to the halves, show that the resonance occurs at $\omega = \omega_p/\sqrt{1 + K_{\text{eff}}}$ and find the expression for K_{eff} in terms of a , b , c , and K_g .

5.3.1.2 Warm plasma model

Efforts to explain the multiple resonances with a dielectric model with only a density profile were unsuccessful, generally leading to the conclusion that scattering would occur at all frequencies and no multiple resonances would occur. Gould [61] first suggested that finite temperature effects might lead to multiple resonances.

TOTAL ABSORPTION

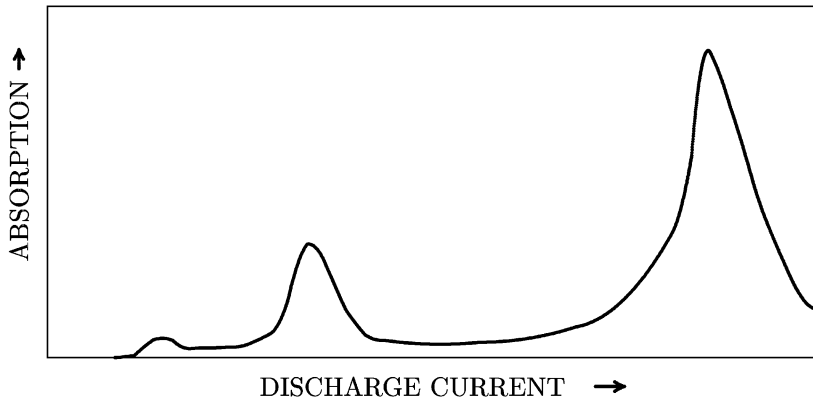


Figure 5.4. Typical absorption spectrum. The frequency is held constant and the electron density is varied by varying the discharge current. (From [59].)

For this analysis, we begin with the fluid equations from chapter 3, using equations (3.34) and (3.35) for electrons with a scalar pressure,

$$\frac{\partial n_e}{\partial t} + \nabla \cdot (n_e \mathbf{v}) = 0 \quad (5.16)$$

$$\frac{\partial \mathbf{v}}{\partial t} + (\mathbf{v} \cdot \nabla) \mathbf{v} = \frac{1}{m_e n_e} (-n_e e \mathbf{E} - \nabla p). \quad (5.17)$$

Then using Poisson's equation,

$$\nabla \cdot \mathbf{E} = \rho / \epsilon_0 \quad (5.18)$$

with $\mathbf{E} = -\nabla \varphi$, we proceed to separate out the zero and first order quantities with the assumption that the zero order density is constant. Thus

$$n_e = n_0 + n_1 e^{-i\omega t}$$

$$\mathbf{v} = \mathbf{v}_1 e^{-i\omega t}$$

$$\mathbf{E} = \mathbf{E}_0 + \mathbf{E}_1 e^{-i\omega t}$$

$$p = p_0 + p_1 e^{-i\omega t}$$

where $p_0 = n_0 \kappa T$ and $p_1 = \gamma n_1 \kappa T$ and we take $\gamma = 3$. The zero order equation gives

$$\nabla p_0 = -e n_0 \mathbf{E}_0$$

so $\mathbf{E}_0 = 0$. The first order equations are:

$$-i\omega n_1 + n_0 \nabla \cdot \mathbf{v}_1 = 0 \quad (5.19)$$

$$-i\omega m_e n_0 \mathbf{v}_1 = -n_0 e \mathbf{E}_1 - \nabla p_1 \quad (5.20)$$

$$\nabla \cdot \mathbf{E}_1 = -\frac{e}{\epsilon_0} n_1. \quad (5.21)$$

Taking the divergence of equation (5.20), eliminating $\nabla \cdot \mathbf{v}$ with equation (5.19) and using equation (5.21) and writing the result in terms of the potential φ_1 , the result may be expressed as

$$(\nabla^2 + k^2)\nabla^2\varphi_1 = 0 \quad (5.22)$$

where k^2 is given by

$$k^2 = \frac{1}{\gamma\lambda_D^2} \left(\frac{\omega^2}{\omega_p^2} - 1 \right). \quad (5.23)$$

Equation (5.23) is the usual BGDR, where λ_D is the Debye length.

Solutions to equation (5.22) are easily seen to be solutions of the second order equations

$$\nabla^2\varphi_1 = 0 \quad (5.24)$$

and

$$(\nabla^2 + k^2)\varphi_1 = 0. \quad (5.25)$$

Equation (5.24) describes the transverse waves (with infinite wavelength) while equation (5.25) describes the longitudinal (plasma) waves.

Two of the four solutions of these equations are singular at the origin and must be discarded. One of the arbitrary constants is simply an amplitude which we shall leave arbitrary. For the potential, then, we take

$$\varphi_1 = \sum_{m=1}^{\infty} \Phi_m(r) \sin m\theta \quad (5.26)$$

where

$$\Phi_m = A_m \left(\frac{r}{a} \right)^m + B_m \frac{J_m(kr)}{J_m(ka)}. \quad (5.27)$$

The boundary condition here is that the radial current must vanish at the edge of the plasma which, from equation (5.20), leads to

$$\nabla\Phi_m|_{r=a} = \gamma\lambda_D^2 \nabla\nabla^2\Phi_m|_{r=a}$$

which, in turn, leads to

$$mA_m = -\frac{\omega^2}{\omega_p^2} B_m ka \frac{J'_m(ka)}{J_m(ka)}.$$

For boundary conditions at the plasma edge, we require the normal displacement and the potential to be continuous (mode by mode), and to make the effect of a dielectric more apparent, we shall assume the region surrounding the plasma column to be entirely glass of dielectric constant K_{eff} (a glass wall of

finite thickness and constant K_g may be represented by an effective K_{eff} —see problem 5.3.2). The potential outside is given by equation (5.11), written as

$$\varphi_o = \sum_{m=1}^{\infty} C_m \left(\frac{a}{r}\right)^m \sin m\theta + E_{\text{inc}} r \sin \theta. \quad (5.28)$$

Then the boundary conditions require

$$\begin{aligned} \Phi'_m(a) &= \frac{mA_m}{a} + B_m k \frac{J'_m(ka)}{J_m(ka)} = \frac{B_m}{a} \frac{ka J'_m(ka)}{J_m(ka)} \left(1 - \frac{\omega^2}{\omega_p^2}\right) \\ &= K_{\text{eff}} \left(-\frac{m}{a} C_m + E_{\text{inc}} \delta_{1m}\right) \end{aligned} \quad (5.29)$$

where δ_{ij} is the Kronecker delta and

$$\begin{aligned} \Phi_m(a) &= A_m + B_m = B_m \left(1 - \frac{\omega^2}{\omega_p^2} \frac{ka J'_m(ka)}{m J_m(ka)}\right) \\ &= C_m + E_{\text{inc}} a \delta_{1m} \end{aligned} \quad (5.30)$$

so we may eliminate C_m and solve for B_m with the result

$$B_m = \frac{E_{\text{inc}} a \left(1 + \frac{1}{m}\right) \delta_{1m}}{\frac{ka}{K_{\text{eff}}} \frac{J'_m(ka)}{m J_m(ka)} \left(1 - \frac{\omega^2}{\omega_p^2}\right) + 1 - \frac{\omega^2}{\omega_p^2} \frac{ka J'_m(ka)}{m J_m(ka)}}. \quad (5.31)$$

The condition for resonance is, of course, that the denominator vanish, resulting in the resonance condition

$$\frac{m J_m(ka)}{ka J'_m(ka)} = \frac{\omega^2}{\omega_p^2} + \frac{1}{K_{\text{eff}}} \left(\frac{\omega^2}{\omega_p^2} - 1\right) \quad (5.32)$$

which must be solved simultaneously with the BGDR. To show the relationship to the cold plasma result, this may be rearranged as

$$\omega^2 = \frac{\omega_p^2}{1 + K_{\text{eff}}} \left[1 + \frac{K_{\text{eff}} m J_m(ka)}{ka J'_m(ka)}\right] \quad (5.33)$$

where $m = 1$ for the dipole resonances. It may be seen from this form of the dispersion relation that all resonances are higher than the cold plasma case. In fact, the lowest frequency solution is for $k \rightarrow 0$, which leads to $\omega = \omega_p$. All other solutions for $k > 0$ lead to $\omega > \omega_p$ so the main resonance needs a different analysis.

The Main resonance. For the main dipole resonance ($m = 1$), where we expect $\omega < \omega_p$, equation (5.23) indicates that $k^2 < 0$ so we define $\tau^2 = -k^2$ so that the potential in the plasma is described by

$$\Phi_1 = A_1 \frac{r}{a} + B_1 \frac{I_1(\tau r)}{I_1(\tau a)}. \quad (5.34)$$

Following the same procedures as before, this leads to a similar dispersion relation,

$$\omega^2 = \frac{\omega_p^2}{1 + K_{\text{eff}}} \left[1 + \frac{K_{\text{eff}} I_1(\tau a)}{\tau a I'_1(\tau a)} \right] \quad (5.35)$$

which must be solved simultaneously with

$$\omega^2 = \omega_p^2 \left[1 - 3 \frac{\lambda_D^2}{a^2} (\tau a)^2 \right]$$

so we expect τa to be large since λ_D/a is assumed to be very small. In the large argument limit, $I_1(x) \simeq I'_1(x)$, so the transcendental terms approximately cancel, leading to a cubic equation in τa . For some typical experimental parameters with $a^2/\lambda_D^2 = 10^3$, $K_{\text{eff}} = 2.1$, this leads to $\tau a \simeq 14.5$ and $\omega^2 = 0.37\omega_p^2$, which is only slightly above the cold plasma result of $\omega^2 = 0.32\omega_p^2$, and close to the experimental result of $\omega^2 = 0.42\langle\omega_p^2\rangle$.

The Higher resonances. The first root is $k \rightarrow 0$ with $\omega = \omega_p$. When $k \neq 0$, the resonance condition is transcendental, but approximate solutions may be found for larger values of $x = ka$ near the roots of $J'_1(x)$. If we take $x = x_0 - \epsilon$, with $J'_1(x_0) = 0$, then the BGDR may be written as

$$\omega^2 \simeq \omega_p^2 \left(1 + 3 \frac{\lambda_D^2}{a^2} x_0^2 \right)$$

and the resonance condition, using $J'_1(x_0 - \epsilon) \simeq \epsilon(1 - 1/x_0^2)J_1(x_0)$, is

$$\omega^2 \simeq \frac{\omega_p^2}{1 + K_{\text{eff}}} \left[1 + \frac{K_{\text{eff}}}{x_0 \epsilon (1 - 1/x_0^2)} \right]$$

so

$$\epsilon \simeq \frac{K_{\text{eff}}}{x_0 (1 - 1/x_0^2) [K_{\text{eff}} + (1 + K_{\text{eff}}) 3\lambda_D^2/a^2 x_0^2]}.$$

This leads to $x = 0, 5.2, 8.4, \dots$ and frequencies $\omega^2/\omega_p^2 = 1.0, 1.08, 1.21, \dots$, which are more closely spaced than experiment shows ($\omega^2/\langle\omega_p^2\rangle = 1.0, 1.5, \dots$). Combining these uniform warm plasma results, the estimated frequencies are $\omega^2/\omega_p^2 = 0.37, 1.00, 1.08, \dots$, while the experiment shows $\omega^2/\langle\omega_p^2\rangle = 0.42, 1.0, 1.5, \dots$, and the higher resonances are even more widely spread. Thus, although the finite temperature model does lead to the multiplicity of resonances, it does not give a quantitative result.

The discrepancy is resolved when one finally includes radial density gradients as well as the temperature effects. In order to understand this additional effect, we can examine the *local* wavenumber, given by

$$k^2(r) = [\omega^2 - \omega_p^2(r)]/(3\kappa T/m). \quad (5.36)$$

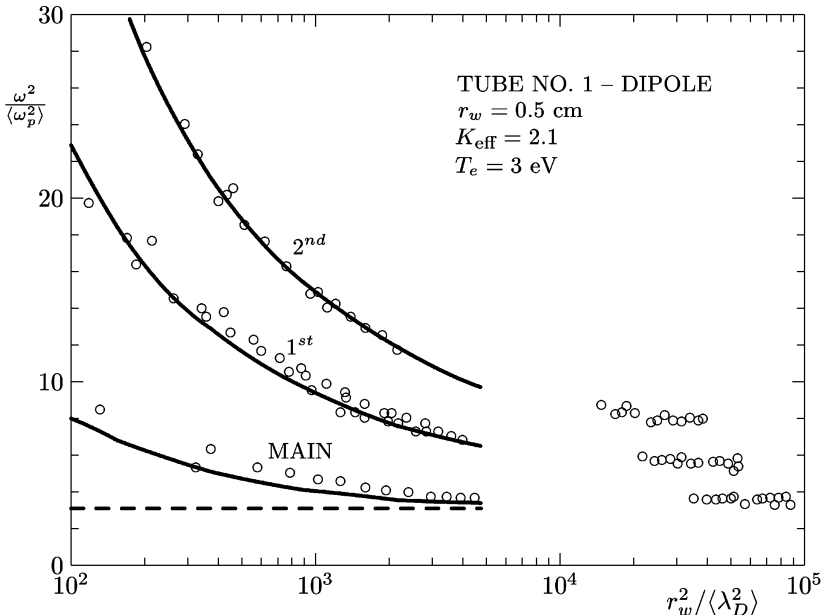


Figure 5.5. Comparison of theoretical and experimental results for dipole resonances on a plasma column. (From [59].)

In the low density regions, $\omega > \omega_p$ and the wave is propagating, but when $\omega < \omega_p$, the wave is nonpropagating, so the wave is confined to the outer portion of the plasma in a varying density profile, reflecting at the radius r_c where $\omega = \omega_p(r_c)$. An approximate way of expressing the new resonance condition is

$$\int_{r_c}^a k(r) dr = \theta_n \quad n = 1, 2, 3, \dots \quad (5.37)$$

where the θ_n differ by approximately π . This is closer to agreement with experiment and indicates that this is an important effect. Numerical calculations by Parker *et al* [59] achieved good agreement with experiment for both dipole and quadrupole resonances over a relatively wide range of a^2/λ_D^2 using the finite temperature and density variations with an analysis substantially the same as that given here except for the density variation. This agreement is shown in figure 5.5 for the main resonance and the first two thermal modes.

The final chapter was added by Baldwin [60] who showed another effect, namely that strong Landau damping of the wave would occur near the plasma boundary due to thermal effects, seeming to imply that the waves would be absorbed rather than resonate. This effect is due to the fact that the fluid equations require the phase velocity to greatly exceed the thermal speed, and while well satisfied near the turning point as $k \rightarrow 0$, the phase velocity approaches the

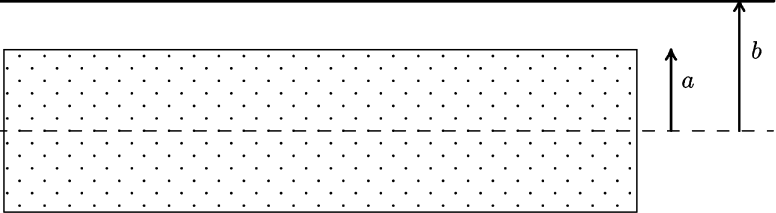


Figure 5.6. Schematic diagram of waveguide partially filled with cold plasma.

thermal speed at the plasma edge as the density approaches zero, and the wave damps through Landau damping. The fact that resonances still occur is due entirely to the fact that the wave energy is transferred to particles that reflect at the static potential barrier at the wall and *reconstruct* the wave as they re-enter the plasma. This effect was dramatically demonstrated in studies with a weak magnetic field where it was expected that the resonances would split by the gyrofrequency, but in fact by the time the two peaks could barely be resolved on the main resonance, the higher resonances were washed away and the main resonance was greatly broadened, as if strongly damped. This can easily be understood when one realizes that the small amount of curvature in the Larmor orbits of the electrons would dramatically affect the efficiency of the wave reconstruction due to the spread in phase. This interpretation also gives strong evidence that Landau damping is reversible (see chapters 4 and 7), indicating that even though the waves may completely damp out, the information remains in the particles until collisions or some other randomizing process is able to destroy it.

Problem 5.3.3. Estimates of the Tonks–Dattner Resonances. Estimate the frequencies of the three lowest resonances for $K_{\text{eff}} = 2.1$ and $a^2/\lambda_D^2 = 500$ and compare these with the data in figure 5.5.

5.3.2 Surface waves in a partially-filled plasma waveguide

For the case where $B_0 = 0$, the dielectric tensor reduces to a scalar and the electrostatic approximation is no longer necessary to simplify the problem. We consider a case where the plasma is cold and uniform out to radius a and vacuum from radius a to radius b where there is a conducting waveguide. This geometry is sketched in figure 5.6.

In this case, the wave equation with dielectric constant $1 - \omega_p^2/\omega^2$ in the plasma is the same for both B_{1z} and E_{1z} , and is given by

$$\left\{ \nabla_{\perp}^2 + \left[\frac{\omega^2}{c^2} \left(1 - \frac{\omega_p^2}{\omega^2} \right) - k^2 \right] \right\} \begin{pmatrix} E_{1z} \\ B_{1z} \end{pmatrix} = 0 \quad 0 < r < a \quad (5.38)$$

and in the vacuum region the wave equation is

$$\left[\nabla_{\perp}^2 + \left(\frac{\omega^2}{c^2} - k^2 \right) \right] \begin{pmatrix} E_{1z} \\ B_{1z} \end{pmatrix} = 0 \quad a < r < b. \quad (5.39)$$

Since the wave fields may be derived from either E_{1z} or B_{1z} , we refer to the corresponding wave fields as E -modes or B -modes, respectively. In the case of circular symmetry, they are uncoupled, but for the more general case, a linear combination of the two modes is necessary to satisfy boundary conditions. The two uncoupled solutions are distinct because the boundary conditions at the wall are different. We shall investigate only the cylindrically symmetric solutions in this example.

For waves with $v_p < c$ ($k > \omega/c$), the cylindrically symmetric solution for the E -mode that is regular at the origin may be written as

$$E_{1z} = \begin{cases} A \frac{I_0(\tau r)}{I_0(\tau a)} e^{i(kz - \omega t)} & 0 < r \leq a \\ (B I_0(\tau_0 r) + C K_0(\tau_0 r)) e^{i(kz - \omega t)} & a \leq r \leq b \end{cases} \quad (5.40)$$

where

$$\tau^2 = k^2 - \frac{\omega^2}{c^2} + \frac{\omega_p^2}{c^2} \quad (5.41)$$

$$\tau_0^2 = k^2 - \frac{\omega^2}{c^2} \quad (5.42)$$

and B and C may be obtained by the boundary conditions which require the tangential \mathbf{E} to be continuous at a and to vanish at b . This results in

$$E_{1z} = A \frac{I_0(\tau_0 r) K_0(\tau_0 b) - I_0(\tau_0 b) K_0(\tau_0 r)}{I_0(\tau_0 a) K_0(\tau_0 b) - I_0(\tau_0 b) K_0(\tau_0 a)} e^{i(kz - \omega t)} \quad a \leq r \leq b. \quad (5.43)$$

In these expressions, I_0 and K_0 are the modified Bessel functions of the first and second kind, and $K_0(x)$ is singular at the origin. Imposing the final boundary condition that tangential \mathbf{B} given by

$$B_{\theta} = \begin{cases} -\frac{i\omega(1 - \omega_p^2/\omega^2)}{\tau^2 c^2} \frac{dE_{1z}}{dr} & 0 \leq r \leq a \\ -\frac{i\omega}{\tau_0^2 c^2} \frac{dE_{1z}}{dr} & a \leq r \leq b \end{cases} \quad (5.44)$$

be continuous at the boundary leads to the dispersion relation

$$\left(1 - \frac{\omega_p^2}{\omega^2} \right) \frac{1}{\tau a} \frac{I_1(\tau a)}{I_0(\tau a)} = \frac{1}{\tau_0 a} \frac{I_1(\tau_0 a) K_0(\tau_0 b) + I_0(\tau_0 b) K_1(\tau_0 a)}{I_0(\tau_0 a) K_0(\tau_0 b) - I_0(\tau_0 b) K_0(\tau_0 a)}. \quad (5.45)$$

One approximate solution of equation (5.45) may be obtained by allowing $b/a \rightarrow \infty$. In this case, since $I_0(x) \propto e^x$ and $K_0(x) \propto e^{-x}$ as $x \rightarrow \infty$, we require $B = 0$ in equation (5.40), and the dispersion relation simplifies to

$$1 - \frac{\omega_p^2}{\omega^2} = -\frac{\tau a}{\tau_0 a} \frac{K_1(\tau_0 a)}{K_0(\tau_0 a)} \frac{I_0(\tau a)}{I_1(\tau a)} \quad (5.46)$$

and it is plotted in figure 5.7 for various values of $\omega_p a/c$. The saturation for large k may be obtained by assuming $\tau_0 a$ to be large in which case the dispersion relation may be simplified even further to

$$1 - \frac{\omega_p^2}{\omega^2} \simeq -\frac{\tau}{\tau_0}$$

which may be expressed as

$$k^2 = \frac{\omega^2}{c^2} \left[1 + \left(\frac{\omega_p^2}{\omega^2} - 2 \right)^{-1} \right]. \quad (5.47)$$

In this form, it may be seen that $k \rightarrow \infty$ as $\omega \rightarrow \omega_p/\sqrt{2}$ so that these surface waves represent traveling waves on the plasma column and the Tonks–Dattner resonances represent the $v_p = \omega/k \rightarrow 0$ limit. In the opposite limit, $v_p \rightarrow c$ as k becomes small. In the high density limit, as $\omega_p a/c$ becomes large, $v_p \rightarrow c$, but in this case it was shown by Trivelpiece and Gould [54] that the wave energy becomes highly localized near the plasma boundary and the plasma behaves much like a conductor. These surface waves are commonly referred to as Trivelpiece–Gould modes.

There are no corresponding B -modes with $v_p < c$, but there are B -modes with $v_p > c$ such that $\omega > \sqrt{k^2 c^2 + \omega_p^2}$. For this case,

$$B_{1z} = \begin{cases} A J_0(k_{\perp} r) e^{i(kz - \omega t)} & r \leq a \\ [B J_0(k_{\perp 0} r) + C Y_0(k_{\perp 0} r)] e^{i(kz - \omega t)} & a \leq r \leq b \end{cases} \quad (5.48)$$

$$E_{1\theta} = \begin{cases} \frac{i\omega A}{k_{\perp}} J_1(k_{\perp} r) e^{i(kz - \omega t)} & r \leq a \\ \frac{i\omega}{k_{\perp 0}} [B J_1(k_{\perp 0} r) + C Y_1(k_{\perp 0} r)] e^{i(kz - \omega t)} & a \leq r \leq b \end{cases} \quad (5.49)$$

where

$$k_{\perp}^2 = \frac{\omega^2 - \omega_p^2}{c^2} - k^2 > 0$$

$$k_{\perp 0}^2 = \frac{\omega^2}{c^2} - k^2 > 0.$$

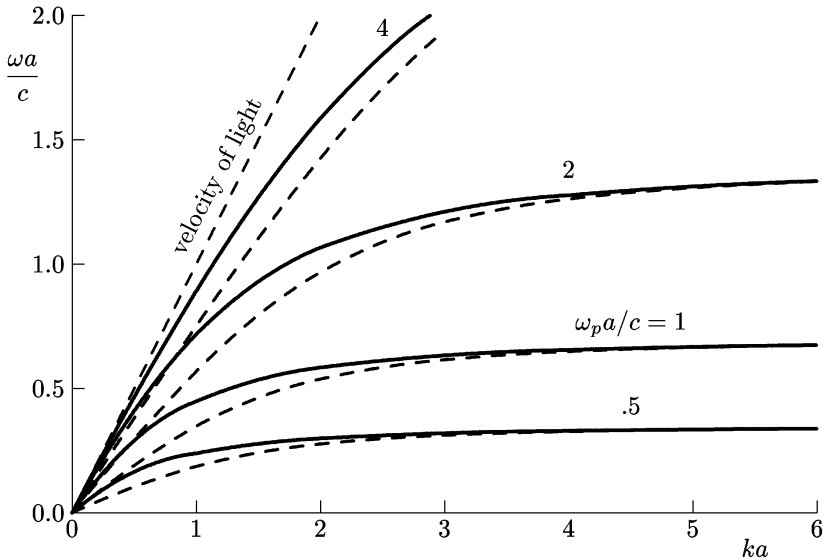


Figure 5.7. Dispersion relation for surface waves on an unmagnetized plasma column of radius a . Full curves are for $b/a \rightarrow \infty$ (from [54]), while dashed curves are for $b/a = 1.5$.

Problem 5.3.4. Wave equations in plasma and vacuum. Verify equations (5.38) and (5.39).

Problem 5.3.5. Surface wave dispersion relation. Fill in the steps leading to equation (5.47).

Problem 5.3.6. B-mode dispersion relation. Find the dispersion relation for the B -mode with $v_p > c$ starting with equations (5.48) and (5.49).

Problem 5.3.7. The unbounded finite column. For $\omega_p a / c = 1$ and $\tau_0 a = 2$, find ω/ω_p and ka and sketch $E_z(r)/E_z(0)$ as a function of r/a for the case $b/a \rightarrow \infty$.

5.4 Electrostatic waves on a plasma column in a magnetic field

Before launching into the general plasma-filled waveguide problem, we first consider electrostatic waves, also called slow waves because their phase velocity is low, or space charge waves since the charge density fluctuates. This simplification is unnecessary as $B \rightarrow \infty$ or $B \rightarrow 0$, but is useful for intermediate cases. Assuming charge neutrality in a cold plasma, Poisson's equation becomes

$$\nabla \cdot \epsilon_0 \mathbf{K} \cdot \nabla \varphi_1 = 0 \quad (5.50)$$

with a cold magnetized plasma dielectric tensor of the form of equation (2.10):

$$\mathbf{K} = \begin{pmatrix} K_1 & K_2 & 0 \\ -K_2 & K_1 & 0 \\ 0 & 0 & K_3 \end{pmatrix}. \quad (5.51)$$

Assuming a wavelike potential, i.e. $\varphi_1 = \varphi_1(\mathbf{r})e^{i(k_z z - \omega t)}$, then equation (5.50) becomes

$$(K_1 \nabla_{\perp}^2 - K_3 k_z^2) \varphi_1 = 0 \quad (5.52)$$

where $\nabla_{\perp}^2 = \nabla^2 - \partial^2 / \partial z^2$. Solutions in cylindrical coordinates are

$$\varphi_1 = \sum_{m=0}^{\infty} [A_m J_m(k_{\perp} r) + B_m Y_m(k_{\perp} r)] e^{i(k_z z + m\theta - \omega t)} \quad (5.53)$$

with

$$k_{\perp}^2 = -k_z^2 \frac{K_3}{K_1} \quad (5.54)$$

and since we wish to have regular solutions at $r = 0$, we must have $B_m = 0$. For a conducting waveguide, we require the tangential field to vanish at the wall at $r = a$, so we must have

$$J_m(k_{\perp} a) = 0 \quad \text{so} \quad k_{\perp} a = p_{mv} \quad (5.55)$$

where p_{mv} is the v th zero of the Bessel function of order m .

The electrostatic approximation is valid near the electron plasma frequency and the electron cyclotron frequency for sufficiently small a , so we will neglect the ion motion in K_1 and K_3 . The dispersion relation for the space charge waves is then given by

$$\left(\frac{p_{mv}}{k_z a} \right)^2 = -\frac{1 - \omega_p^2/\omega^2}{1 + \omega_{pe}^2/(\omega_{ce}^2 - \omega^2)}. \quad (5.56)$$

The dispersion relation for these electrostatic waves is shown in figure 5.8 for $\omega_p > \omega_{ce}$ and $\omega_p < \omega_{ce}$. It is apparent that the higher frequency branch begins at the upper hybrid resonance and ends at the higher of ω_p or ω_{ce} . This upper branch is a *backward* wave, since ω decreases with increasing k . The lower branch propagates down to zero frequency, but in that limit, the ion motion must be included.

It is interesting to note that as $B_0 \rightarrow 0$, the higher frequency branch reduces to the plasma resonance, $\omega = \omega_p$, and the lower branch collapses, so that no propagation can occur in an unmagnetized plasma column in a waveguide. With a vacuum layer between the plasma and the conducting wall, however, propagation again becomes possible in this limit. The waves in this case are called *surface waves* because they carry most of the wave energy in the vacuum region and may only penetrate a short distance into the plasma. The characteristics of these

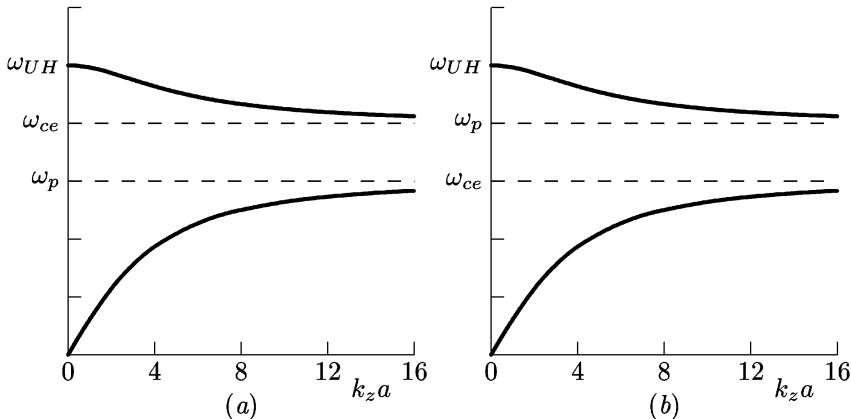


Figure 5.8. Dispersion relations for electrostatic waves for the cases (a) $\omega_{ce} > \omega_p$ and (b) $\omega_p > \omega_{ce}$ with $k_{\perp}a = 3.83$.

surface waves were demonstrated by Trivelpiece and Gould [54] on a plasma column similar to that used in the scattering resonance experiments.

Problem 5.4.1. The effects of ion motions. Derive and sketch the dispersion relation for low frequencies where ion motions are important. Label any new resonances or cutoffs on the sketch.

Problem 5.4.2. Effects of a vacuum layer. Consider a vacuum layer between the plasma radius a and the conducting wall radius b .

- (i) Derive the dispersion relation for this case.
- (ii) Show that propagation can occur for the case $B_0 \rightarrow 0$.
- (iii) Sketch the dispersion relations for $B_0 \neq 0$ and for $B_0 = 0$.
- (iv) Derive an expression for the power flow in this problem and sketch the power flow as a function of radius.
- (v) Note any cases where the electrostatic approximation fails.

5.5 Cold plasma-filled waveguide

5.5.1 The dispersion relation

For our most general example, the plasma model is a uniform cold magnetized plasma in a cylindrical conducting waveguide and the restrictions of the previous cases are removed. In this case, the plasma is represented by a dielectric tensor of

the form of equation (5.51),

$$\mathbf{K} = \begin{pmatrix} K_1 & K_2 & 0 \\ -K_2 & K_1 & 0 \\ 0 & 0 & K_3 \end{pmatrix} \quad (5.57)$$

and for convenience we again define the related tensor

$$\frac{\omega^2}{c^2} \mathbf{K} = \begin{pmatrix} \kappa_1 & \kappa_2 & 0 \\ -\kappa_2 & \kappa_1 & 0 \\ 0 & 0 & \kappa_3 \end{pmatrix}. \quad (5.58)$$

The electric fields are assumed to propagate down the waveguide in the z -direction, so the wave fields may be represented by the expression

$$\mathbf{E} = \mathbf{E}(r) e^{i(k_z z + m\theta - \omega t)}. \quad (5.59)$$

With this dependence, $\partial/\partial\theta \rightarrow im$, $\partial/\partial z \rightarrow ik_z$, and $\partial/\partial t \rightarrow -i\omega$ so that the components of the Maxwell equations

$$\begin{aligned} \nabla \times \mathbf{E} &= i\omega \mathbf{B} \\ \nabla \times \mathbf{B} &= -\frac{i\omega}{c^2} \mathbf{K} \cdot \mathbf{E} \end{aligned}$$

may be written as

$$(\nabla \times \mathbf{E})_r = \frac{im}{r} E_z - ik_z E_\theta = i\omega B_r \quad (5.60)$$

$$(\nabla \times \mathbf{E})_\theta = ik_z E_r - \frac{d}{dr} E_z = i\omega B_\theta \quad (5.61)$$

$$(\nabla \times \mathbf{E})_z = \frac{1}{r} \frac{d}{dr} (r E_\theta) - \frac{im}{r} E_r = i\omega B_z \quad (5.62)$$

$$(\nabla \times \mathbf{B})_r = \frac{im}{r} B_z - ik_z B_\theta = -\frac{i}{\omega} (\kappa_1 E_r + \kappa_2 E_\theta) \quad (5.63)$$

$$(\nabla \times \mathbf{B})_\theta = ik_z B_r - \frac{d}{dr} B_z = -\frac{i}{\omega} (-\kappa_2 E_r + \kappa_1 E_\theta) \quad (5.64)$$

$$(\nabla \times \mathbf{B})_z = \frac{1}{r} \frac{d}{dr} (r B_\theta) - \frac{im}{r} B_r = -\frac{i}{\omega} (\kappa_3 E_z). \quad (5.65)$$

We will solve this set of equations by solving first for the transverse components in terms of E_z and B_z . For example, solving equation (5.60) for iB_r and using this in equation (5.64) and rearranging, we obtain

$$\kappa_2 E_r + \gamma E_\theta = \frac{mk_z}{r} E_z + i\omega \frac{d}{dr} B_z \quad (5.66)$$

where $\gamma = k_z^2 - \kappa_1$. Similarly, solving equation (5.61) for iB_θ and using the result in equation (5.63), the result may be expressed as

$$\gamma E_r - \kappa_2 E_\theta = \frac{m\omega}{r} B_z - ik_z \frac{d}{dr} E_z. \quad (5.67)$$

These two equations may then be solved for E_r and E_θ with the result expressed as

$$\mathbf{E}_\perp = a\nabla_\perp E_z + b\nabla_\perp B_z + c\hat{e}_z \times \nabla_\perp E_z + d\hat{e}_z \times \nabla_\perp B_z \quad (5.68)$$

where $\nabla_\perp \equiv \nabla - \hat{e}_z \partial/\partial z$, $\mathbf{E}_\perp = \mathbf{E} - \hat{e}_z E_z$, and the coefficients are given by

$$a = -\frac{ik_z\gamma}{\gamma^2 + \kappa_2^2} \quad c = \frac{ik_z\kappa_2}{\gamma^2 + \kappa_2^2} \quad b = \frac{i\omega\kappa_2}{\gamma^2 + \kappa_2^2} \quad d = \frac{i\omega\gamma}{\gamma^2 + \kappa_2^2}. \quad (5.69)$$

Similar methods lead to the expression for the transverse \mathbf{B} :

$$\mathbf{B}_\perp = p\nabla_\perp E_z + a\nabla_\perp B_z + q\hat{e}_z \times \nabla_\perp E_z + c\hat{e}_z \times \nabla_\perp B_z \quad (5.70)$$

where

$$p = -\frac{ik_z^2\kappa_2}{\omega(\gamma^2 + \kappa_2^2)} \quad q = -\frac{i(\kappa_1\gamma - \kappa_2^2)}{\omega(\gamma^2 + \kappa_2^2)}. \quad (5.71)$$

These expressions for the transverse components may now be substituted into equation (5.62) with the result

$$c\nabla_\perp^2 E_z + d\nabla_\perp^2 B_z - i\omega B_z = 0 \quad (5.72)$$

and into equation (5.65) with the result

$$c\nabla_\perp^2 B_z + q\nabla_\perp^2 E_z + \frac{ik_3}{\omega} E_z = 0. \quad (5.73)$$

These two equations are coupled, and lead to a fourth order equation in either B_z or E_z . The fourth order equations are obtained by taking the ∇_\perp^2 of both equations (5.72) and (5.73), eliminating $\nabla_\perp^4 B_z$ between them (to find the equation for E_z) and eliminating $\nabla_\perp^2 B_z$ from the result from equation (5.73) so that the equation for E_z may be written as

$$(c^2 - qd)\nabla_\perp^4 E_z + \left(i\omega q - \frac{id\kappa_3}{\omega}\right)\nabla_\perp^2 E_z - \kappa_3 E_z = 0. \quad (5.74)$$

The equation for B_z is obtained similarly, with the result

$$(c^2 - qd)\nabla_\perp^4 B_z + \left(i\omega q - \frac{id\kappa_3}{\omega}\right)\nabla_\perp^2 B_z - \kappa_3 B_z = 0 \quad (5.75)$$

so the two equations are identical.

Because the coefficients are constants, the fourth order equations can also be written as

$$(\nabla_\perp^2 + k_{\perp 1}^2)(\nabla_\perp^2 + k_{\perp 2}^2) \begin{pmatrix} E_z \\ B_z \end{pmatrix} = 0 \quad (5.76)$$

where $k_{\perp 1}^2$ and $k_{\perp 2}^2$ are the two solutions of the quadratic equation

$$(c^2 - qd)k_\perp^4 - \left(i\omega q - \frac{id\kappa_3}{\omega}\right)k_\perp^2 - \kappa_3 = 0. \quad (5.77)$$

Since the two factors commute in a uniform plasma, it must be that each factor has solutions which are regular at the origin of the form

$$\Phi(r, \theta) = \sum_{m=-\infty}^{\infty} A_m J_m(k_{\perp} r) e^{im\theta}$$

so that B_z must be simply proportional to E_z such that $B_z = \Phi$ and $E_z = \alpha\Phi$ with α a constant. Then the general solutions are of the form

$$B_z(r, \theta, z, t) = \sum_{m=-\infty}^{\infty} A_m [J_m(k_{\perp 1} r) + \tau_m J_m(k_{\perp 2} r)] e^{i(k_z z + m\theta - \omega t)} \quad (5.78)$$

$$E_z(r, \theta, z, t) = \sum_{m=-\infty}^{\infty} A_m [\alpha_{1m} J_m(k_{\perp 1} r) + \alpha_{2m} \tau_m J_m(k_{\perp 2} r)] e^{i(k_z z + m\theta - \omega t)} \quad (5.79)$$

where α_1 and α_2 are the roots of the quadratic equation for α which may be obtained by using $B_z = \Phi$ and $E_z = \alpha\Phi$ in equation (5.72) and equation (5.73) and letting the determinant of coefficients of Φ and $\nabla_{\perp}^2 \Phi$ vanish. The relationship between α and k_{\perp} may be obtained from equation (5.72) by noting from equation (5.76) that $\nabla_{\perp}^2 \Phi = -k_{\perp}^2 \Phi$, with the result

$$k_{\perp j}^2 = -\frac{i\omega}{d + \alpha_j c} \quad j = 1, 2. \quad (5.80)$$

The quadratic is written most conveniently from equation (5.77) in terms of k_{\perp} as

$$(\gamma^2 + \kappa_2^2) \left[\gamma^2 + \kappa_2^2 + \gamma k_{\perp}^2 + \frac{\kappa_1 k_{\perp}^2}{\kappa_3} \left(\gamma - \frac{\kappa_2^2}{\kappa_1} + k_{\perp}^2 \right) \right] = 0 \quad (5.81)$$

which must be solved simultaneously with the boundary value problem.

The first factor in equation (5.81) does not vanish by assumption, since it was in the denominator of all the factors of equation (5.69) and equation (5.71). If it should vanish, then we must rederive the subsequent expressions, and it may be shown that it leads to a transverse electro magnetic (TEM) mode (no E_z or B_z) that requires a central conductor in order to satisfy the boundary conditions. These effectively represent the coaxial cable modes, and do not exist in a simply connected waveguide.

The remaining factor,

$$(\gamma^2 + \kappa_2^2 + \gamma k_{\perp}^2) \kappa_3 + k_{\perp}^2 [\kappa_1 (\gamma + k_{\perp}^2) - \kappa_2^2] = 0 \quad (5.82)$$

is the dispersion relation for a cold uniform plasma and is identical to the infinite cold plasma dispersion relation of equation (2.21) except that now k_{\perp} is subject to boundary conditions.

Problem 5.5.1. Derive the expressions for a , b , c , d , p , and q of equations (5.69) and (5.71) and prove that $pd - ac = 0$ and $ab + cd = 0$.

5.5.2 Wave fields and boundary conditions

The fully coupled electric and magnetic field components for the plasma-filled waveguide are given by

$$\mathbf{E} = \sum_m \sum_v \mathbf{E}_{mv}(r) e^{i(k_z z + m\theta - \omega t)} \quad (5.83)$$

$$\mathbf{B} = \sum_m \sum_v \mathbf{B}_{mv}(r) e^{i(k_z z + m\theta - \omega t)} \quad (5.84)$$

where the summation over v is over the various roots of the transcendental dispersion relation–boundary condition pair for fixed azimuthal mode number m . In the following expressions, the v subscript is suppressed, but it would normally appear with the quantities $k_{\perp 1}$ and $k_{\perp 2}$ and all quantities which involve these. The components of the fields then are given by

$$B_{zm} = A_m [J_m(k_{\perp 1}r) + \tau_m J_m(k_{\perp 2}r)] \quad (5.85)$$

$$\begin{aligned} B_{rm} = & i k_z A_m \left[\frac{J'_m(k_{\perp 1}r)}{k_{\perp 1}} + \tau_m \frac{J'_m(k_{\perp 2}r)}{k_{\perp 2}} \right] \\ & + \frac{m \kappa_1 A_m}{r k_z \kappa_2} \left[\beta_1 \frac{J_m(k_{\perp 1}r)}{k_{\perp 1}^2} + \tau_m \beta_2 \frac{J_m(k_{\perp 2}r)}{k_{\perp 2}^2} \right] \end{aligned} \quad (5.86)$$

$$\begin{aligned} B_{\theta m} = & \frac{i \kappa_1 A_m}{k_z \kappa_2} \left[\beta_1 \frac{J'_m(k_{\perp 1}r)}{k_{\perp 1}} + \tau_m \beta_2 \frac{J'_m(k_{\perp 2}r)}{k_{\perp 2}} \right] \\ & - \frac{m k_z A_m}{r} \left[\frac{J_m(k_{\perp 1}r)}{k_{\perp 1}^2} + \tau_m \frac{J_m(k_{\perp 2}r)}{k_{\perp 2}^2} \right] \end{aligned} \quad (5.87)$$

$$E_{zm} = \frac{\omega \kappa_1 A_m}{k_z \kappa_2 \kappa_3} [\beta_1 J_m(k_{\perp 1}r) + \tau_m \beta_2 J_m(k_{\perp 2}r)] \quad (5.88)$$

$$\begin{aligned} E_{rm} = & \frac{i \omega A_m}{\kappa_2} \left[\delta_1 \frac{J'_m(k_{\perp 1}r)}{k_{\perp 1}} + \tau_m \delta_2 \frac{J'_m(k_{\perp 2}r)}{k_{\perp 2}} \right] \\ & - \frac{m \omega A_m}{r} \left[\frac{J_m(k_{\perp 1}r)}{k_{\perp 1}^2} + \tau_m \frac{J_m(k_{\perp 2}r)}{k_{\perp 2}^2} \right] \end{aligned} \quad (5.89)$$

$$\begin{aligned} E_{\theta m} = & - \frac{m \omega A_m}{r \kappa_2} \left[\delta_1 \frac{J_m(k_{\perp 1}r)}{k_{\perp 1}^2} + \tau_m \delta_2 \frac{J_m(k_{\perp 2}r)}{k_{\perp 2}^2} \right] \\ & - i \omega A_m \left[\frac{J'_m(k_{\perp 1}r)}{k_{\perp 1}} + \tau_m \frac{J'_m(k_{\perp 2}r)}{k_{\perp 2}} \right] \end{aligned} \quad (5.90)$$

where

$$\beta_j = \gamma - \frac{\kappa_2^2}{\kappa_1} + k_{\perp j}^2 \quad \text{and} \quad \delta_j = \gamma + k_{\perp j}^2 \quad j = 1, 2,$$

and $\gamma = k_z^2 - \kappa_1$.

The boundary conditions in this case are very simple when the plasma completely fills the waveguide, since the tangential E must vanish at the wall at radius a . This leads to the two conditions

$$\beta_1 J_m(k_{\perp 1} a) + \tau_m \beta_2 J_m(k_{\perp 2} a) = 0 \quad (5.91)$$

$$\frac{J'_m(k_{\perp 1} a)}{k_{\perp 1}} + \tau_m \frac{J'_m(k_{\perp 2} a)}{k_{\perp 2}} = \frac{im}{a\kappa_2} \left[\delta_1 \frac{J_m(k_{\perp 1} a)}{k_{\perp 1}^2} + \tau_m \delta_2 \frac{J_m(k_{\perp 2} a)}{k_{\perp 2}^2} \right]. \quad (5.92)$$

Eliminating τ_m between these two conditions, the result may be written as

$$\frac{im\delta_1}{k_{\perp 1}^2 a\kappa_2 \beta_1} - \frac{1}{k_{\perp 1} \beta_1} \frac{J'_m(k_{\perp 1} a)}{J_m(k_{\perp 1} a)} = \frac{im\delta_2}{k_{\perp 2}^2 a\kappa_2 \beta_2} - \frac{1}{k_{\perp 2} \beta_2} \frac{J'_m(k_{\perp 2} a)}{J_m(k_{\perp 2} a)}. \quad (5.93)$$

Equations (5.93) and (5.82) represent a transcendental pair of equations which must be solved numerically where the values of $k_{\perp 1}$ and $k_{\perp 2}$ are determined from the quadratic roots of equation (5.82). Before examining some of the cases that exhibit the transcendental character, we will again look at some special cases.

Problem 5.5.2. Field components in cylindrical coordinates. Using the various definitions and the dispersion relation equation (5.82), show that the field components are of the form given in equations (5.85) through (5.90).

Problem 5.5.3. Waveguide cutoff frequencies. For the waveguide cutoff problem, the coupled modes simplify and there are two separate cutoff frequencies.

(i) Show that at cutoff, the dispersion relation can be factored as

$$(\kappa_1^2 + \kappa_2^2 - \kappa_1 k_{\perp}^2)(\kappa_3 - k_{\perp}^2) = 0.$$

(ii) Show that for the circularly symmetric modes, the fields are uncoupled, i.e. that the first factor (case 1) is associated with B_z , E_{θ} , and E_r and the second factor (case 2) is associated with E_z and B_{θ} .

(iii) Find the boundary condition and the values of k_{\perp} for each case ($m = 0$).

(iv) Find expressions for the cutoff frequency for each case and show that one is equivalent to the infinite magnetic field case. For case 1, find explicit expressions for the cutoff frequency for

(a) low frequency, $\omega \sim \omega_{ci}$, $c^2 \gg V_A^2$; and

(b) high frequency, $\omega \sim \omega_{ce} \sim \omega_{pe}$.

5.5.3 MHD approximation— $\omega \ll \omega_{ci}$

For frequencies well below the ion cyclotron frequency, K_1 and K_2 are approximately related as

$$K_2 \simeq \frac{\omega}{\omega_{ci}} K_1 \rightarrow 0 \quad \text{as} \quad \frac{\omega}{\omega_{ci}} \rightarrow 0$$

so we can neglect κ_2 . In this case, the dispersion relation can be factored into

$$(\gamma + k_\perp^2) \left(\gamma + \frac{k_\perp^2 \kappa_1}{\kappa_3} \right). \quad (5.94)$$

The fact that the dispersion relation may be factored is an indication that equations (5.72) and (5.73) are uncoupled. In this case it is due to the fact that $c \rightarrow 0$ as $\kappa_2 \rightarrow 0$, so they become

$$d \nabla_\perp^2 B_z - i\omega B_z = 0 \quad (5.95)$$

$$q \nabla_\perp^2 E_z + \frac{i\kappa_3}{\omega} E_z = 0. \quad (5.96)$$

The transverse wavenumber from equation (5.95) is

$$k_\perp^2 = -\frac{i\omega}{d} = -\gamma \quad (\text{with } \kappa_2 \rightarrow 0)$$

so that

$$\gamma + k_\perp^2 = 0 \quad (5.97)$$

is the dispersion relation for this case. The wave is a TE mode, since there is no E_z component. The boundary condition is only on E_θ , namely

$$E_\theta(a) \propto J'_m(k_\perp a) = 0 \quad \text{so} \quad k_\perp a = p'_{mv} \quad (5.98)$$

and the dispersion relation can then be written in the form

$$(k_z a)^2 = \left(\frac{\omega a}{V_A} \right)^2 - p'_{mv}^2 \quad (5.99)$$

where the approximation,

$$K_1 \simeq \frac{\omega_{pi}^2}{\omega_{ci}^2} = \frac{c^2}{V_A^2}$$

has been used. This dispersion relation is identical to that of electromagnetic waves in an empty cylindrical waveguide except that the effective dielectric constant is $K_{\text{eff}} = c^2/V_A^2$.

The cutoff frequencies are given by

$$\omega_{co} = k_\perp V_A = p'_{mv} V_A / a. \quad (5.100)$$

For circularly symmetric modes, $J'_0(x) = -J_1(x)$, so $p'_{0v} = p_{1v} = 3.83, 7.01, 10.17, \dots$, etc. For the lowest cutoff frequency, however, one must choose $m = \pm 1$, since the lowest root of $J'_1(x) = 0$ is $p'_{11} = 1.84$.

The second factor of equation (5.94) corresponds to equation (5.96) so the waves are transverse magnetic (TM) modes (no B_z component) and the boundary condition is on E_z which is given by

$$E_z(a) \propto J_m(k_\perp a) = 0 \quad \text{so} \quad k_\perp a = p_{mv} \quad (5.101)$$

and the dispersion relation is

$$\gamma = -\frac{\kappa_1}{\kappa_3} k_\perp^2 \quad \text{so} \quad k_z^2 \simeq \frac{\omega^2}{V_A^2} \left[1 + \left(\frac{p_{mv}c}{\omega_{pe}a} \right)^2 \right] \quad (5.102)$$

if $\omega_{pi} \gg \omega_{ci}$. The dispersion relation is the same as the electrostatic dispersion relation except that the electrostatic case demands $|k_\perp^2/\kappa_3| \gg 1$ which is always satisfied for sufficiently small a . The electrostatic case leads to $k_z^2 \simeq (\omega^2/\omega_{ce}\omega_{ci})k_\perp^2$ at low frequency. It should be noted that equation (5.102) has no cutoff, so TM modes propagate down to zero frequency. These waves are the slow Alfvén waves that exhibit the ion cyclotron resonance. Their absence of any waveguide cutoff is due to their torsional character and the fact that the group velocity is parallel to the waveguide, minimizing any wall interactions.

Problem 5.5.4. TE and TM modes in the MHD limit. Find expressions for all the field components for these two MHD cases, and show that the TE modes are compressional and the TM modes are torsional (i.e. that the static magnetic field is either compressed or twisted). Sketch the field patterns for the lowest $m = 1$ mode for each case.

5.5.4 Intermediate frequency case— $\omega \simeq \omega_{ci} \ll \omega_p$

When $\omega \simeq \omega_{ci}$, another approximation can be made by assuming that $|k_\perp^2/\kappa_3| \ll 1$. We also note that in this frequency range, $\kappa_3 \simeq -\omega_p^2/c^2$ and $\kappa_1 \simeq \kappa_2 \simeq \omega^2/V_A^2$ unless ω is too close to ω_{ci} . Then $\kappa_1/\kappa_3 \simeq m_e/m_i$ so the approximation is called the neglect of electron inertia and we take $\kappa_3 \rightarrow \infty$. In this case the dispersion relation simplifies to

$$\gamma^2 + \kappa_2^2 + \gamma k_\perp^2 = 0 \quad (5.103)$$

or writing this another way,

$$k_z^2 = \kappa_1 - \frac{1}{2}k_\perp^2 \pm [(\frac{1}{2}k_\perp^2)^2 - \kappa_2^2]^{1/2} \quad (5.104)$$

so there are two branches for the same k_\perp . From equation (5.88), $\kappa_3 \rightarrow \infty$ means $E_z \rightarrow 0$, so the boundary condition is only on E_θ and both solutions are TE modes. For circularly symmetric modes, we have

$$E_\theta(a) \propto J_1(k_\perp a) = 0 \quad \text{so} \quad k_\perp = p_{1v}/a. \quad (5.105)$$

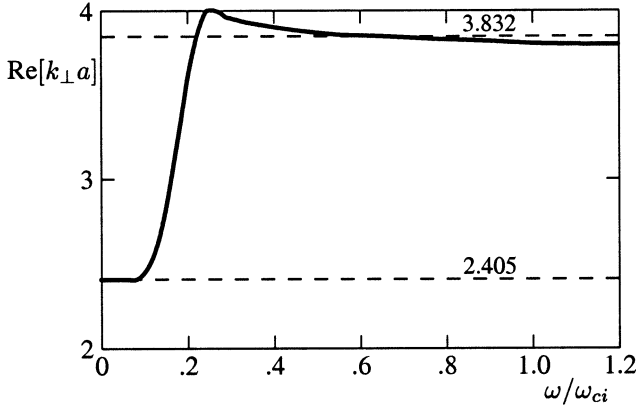


Figure 5.9. The transition from TM to TE for the torsional Alfvén wave in a conducting waveguide. (From [55].)

When we compare the results with the MHD approximation $\omega/\omega_{ci} \rightarrow 0$, we get disagreement as both here are TE modes and the MHD approximation yielded one TE mode and one TM mode, and one of the values of k_\perp appears to change from $3.83/a$ to $2.405/a$ as $\omega/\omega_{ci} \rightarrow 0$. This can be understood by observing that

$$\left| \frac{E_z}{E_\theta} \right| \sim \frac{\kappa_1 \beta_1 k_\perp}{\kappa_2 \kappa_3 k_z} \simeq \frac{\omega_{ci}}{\omega} \frac{k_\perp V_A}{\omega} \left(\frac{k_\perp c}{\omega_{pe}} \right)^2 \quad (5.106)$$

so for sufficiently low frequency, $E_z \gg E_\theta$, so that the boundary condition is dominated by E_z . However, for $k_\perp c / \omega_{pe} \ll 1$, there is a range of frequencies below the ion cyclotron frequency where $E_\theta \gg E_z$, so the E_θ component dominates the boundary condition. Thus the transition does occur at some intermediate (but low) frequency, and the full transcendental set of equations must be solved to find the crossover. An example of the transition is shown in figure 5.9. In order to get a better picture of the dispersion characteristics in this frequency range, we first let $\omega \rightarrow \omega_{ci}$ so that κ_1 and κ_2 become large. Since $\kappa_1 \rightarrow \omega^2/V_A^2(1-\omega^2/\omega_{ci}^2)$ and $\kappa_2 \rightarrow i(\omega/\omega_{ci})\kappa_1$, $\kappa_1^2 + \kappa_2^2 \rightarrow \omega^4/V_A^4(1-\omega^2/\omega_{ci}^2)$ so the dominant terms in the dispersion relation all have the same resonant denominator, and the approximate solutions are

$$k_z^2 \rightarrow \frac{1}{2} \left(\frac{\omega^2}{V_A^2} - k_\perp^2 \right) \quad \text{fast wave} \quad (5.107)$$

$$k_z^2 \rightarrow \frac{\omega^2}{V_A^2(1 - \omega/\omega_{ci})} \quad \text{slow wave.} \quad (5.108)$$

These dispersion relations are plotted in figure 5.10, and show the resonance for the slow Alfvén wave and the breaking away of the fast Alfvén wave from the

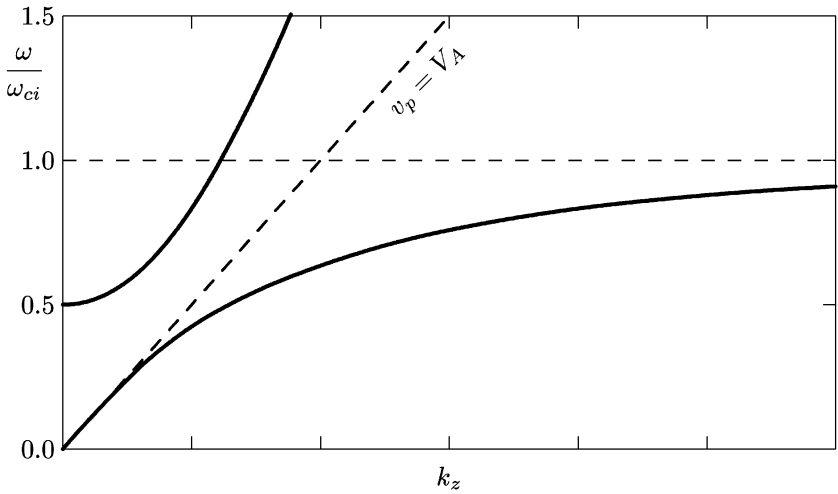


Figure 5.10. The dispersion relation for the fast and slow Alfvén waves in a conducting waveguide.

Alfvén distribution function speed at higher frequency. In this approximation, the cutoff frequency is still given by equation (5.100) if $c^2/V_A^2 \gg 1$.

5.5.5 Mode orthogonality and power flow

In this section, the plasma is assumed to be cold as before, but it may be lossy, so that the dielectric tensor may not be Hermitian. We then choose to solve the Maxwell equations for \mathbf{E} , \mathbf{B} , $\tilde{\mathbf{E}}$ and $\tilde{\mathbf{B}}$ where the tilde fields satisfy the Maxwell equations with $\tilde{\mathbf{K}}$, the transpose of \mathbf{K} (for the lossless case, $(\tilde{\mathbf{K}})_{ij} = (\mathbf{K})_{ji}^*$). Then for each individual mode that satisfies the appropriate dispersion relation and boundary conditions, we have

$$\begin{aligned}\nabla \times \mathbf{E}_\mu &= i\omega \mathbf{B}_\mu & \nabla \times \tilde{\mathbf{E}}_\nu &= i\omega \tilde{\mathbf{B}}_\nu \\ \nabla \times \mathbf{B}_\mu &= -\frac{i\omega}{c^2} \mathbf{K} \cdot \mathbf{E}_\mu & \nabla \times \tilde{\mathbf{B}}_\nu &= -\frac{i\omega}{c^2} \tilde{\mathbf{K}} \cdot \tilde{\mathbf{E}}_\nu\end{aligned}\quad (5.109)$$

where the subscripts μ and ν each indicate the combination of a radial and an azimuthal mode. We now examine the vector identity,

$$\begin{aligned}\nabla \cdot (\mathbf{E}_\mu \times \tilde{\mathbf{B}}_\nu) &= \tilde{\mathbf{B}}_\nu \cdot \nabla \times \mathbf{E}_\mu - \mathbf{E}_\mu \cdot \nabla \times \tilde{\mathbf{B}}_\nu \\ &= i\omega \tilde{\mathbf{B}}_\nu \cdot \mathbf{B}_\mu + \frac{i\omega}{c^2} \mathbf{E}_\mu \cdot \tilde{\mathbf{K}} \cdot \tilde{\mathbf{E}}_\nu.\end{aligned}\quad (5.110)$$

Similarly,

$$\nabla \cdot (\tilde{\mathbf{E}}_\nu \times \mathbf{B}_\mu) = \mathbf{B}_\mu \cdot \nabla \times \tilde{\mathbf{E}}_\nu - \tilde{\mathbf{E}}_\nu \cdot \nabla \times \mathbf{B}_\mu$$

$$= i\omega \mathbf{B}_\mu \cdot \tilde{\mathbf{B}}_\nu + \frac{i\omega}{c^2} \tilde{\mathbf{E}}_\nu \cdot \mathbf{K} \cdot \mathbf{E}_\mu \quad (5.111)$$

and subtracting equation (5.111) from equation (5.110), we obtain

$$\nabla \cdot (\mathbf{E}_\mu \times \tilde{\mathbf{B}}_\nu - \tilde{\mathbf{E}}_\nu \times \mathbf{B}_\mu) = \frac{i\omega}{c^2} (\mathbf{E}_\mu \cdot \tilde{\mathbf{K}} \cdot \tilde{\mathbf{E}}_\nu - \tilde{\mathbf{E}}_\nu \cdot \mathbf{K} \cdot \mathbf{E}_\mu) \equiv 0. \quad (5.112)$$

The quantity in the last parentheses is identically zero for any two vectors and any tensor, so it is a tensor identity. Now from Gauss' theorem,

$$\int_{Vol} \nabla \cdot (\mathbf{E}_\mu \times \tilde{\mathbf{B}}_\nu - \tilde{\mathbf{E}}_\nu \times \mathbf{B}_\mu) dV = \oint_{Surf} (\mathbf{E}_\mu \times \tilde{\mathbf{B}}_\nu - \tilde{\mathbf{E}}_\nu \times \mathbf{B}_\mu) \cdot d\mathbf{S} = 0 \quad (5.113)$$

where we choose the surface of the volume as the cylindrical waveguide boundary and two circular ends, one at z_1 and one at z_2 . We note that $(\mathbf{E} \times \mathbf{B}) \cdot \hat{e}_r$ involves either $E_z B_\theta$ or $E_\theta B_z$, but since both E_θ and E_z vanish at the conducting boundary, the waveguide surface contribution to the integral vanishes. The contribution at each end involves $(\mathbf{E} \times \mathbf{B}) \cdot \hat{e}_z$ which has $E_\theta B_r$ and $E_r B_\theta$ or only transverse (\perp) components of the fields. Factoring the z -dependence out of the integral, we have

$$\left[e^{i(k_{z\mu} + \tilde{k}_{z\nu})z_1} - e^{i(k_{z\mu} + \tilde{k}_{z\nu})z_2} \right] \int_{Area} (\mathbf{E}_{\perp\mu} \times \tilde{\mathbf{B}}_{\perp\nu} - \tilde{\mathbf{E}}_{\perp\nu} \times \mathbf{B}_{\perp\mu}) \cdot \hat{e}_z dS = 0. \quad (5.114)$$

Assuming $z_1 \neq z_2$, we find that the integral over a cross section is zero unless $k_{z\mu} = -\tilde{k}_{z\nu}$, so

$$\int_{Area} (\mathbf{E}_{\perp\mu} \times \tilde{\mathbf{B}}_{\perp\nu} - \tilde{\mathbf{E}}_{\perp\nu} \times \mathbf{B}_{\perp\mu}) \cdot \hat{e}_z dS = P_\ell \delta_{k_{z\mu}, -\tilde{k}_{z\nu}} \quad (5.115)$$

which is the basic orthogonality integral.

Now the Maxwell equations are invariant under a reflection ($k_z \rightarrow -k_z$) if

$$\begin{aligned} \mathbf{E}_\perp(-k_z) &= -\mathbf{E}_\perp(k_z) \\ \mathbf{B}_\perp(-k_z) &= \mathbf{B}_\perp(k_z) \\ E_z(-k_z) &= E_z(k_z) \\ B_z(-k_z) &= -B_z(k_z) \\ K_{zx}(-k_z) &= -K_{zx}(k_z) \quad (= 0 \text{ in the cold plasma}) \end{aligned}$$

and we can use these reflection symmetries to write the orthogonality integral in a different way, letting $\tilde{k}_{z\nu} \rightarrow -\tilde{k}_{z\nu}$, so that

$$\int_{Area} (\mathbf{E}_{\perp\mu} \times \tilde{\mathbf{B}}_{\perp\nu} - (-\tilde{\mathbf{E}}_{\perp\nu}) \times \mathbf{B}_{\perp\mu}) \cdot \hat{e}_z dS = Q_\mu \delta_{k_{z\mu}, \tilde{k}_{z\nu}}. \quad (5.116)$$

Adding the two integrals leads to the simpler result

$$2 \int_{Area} (\mathbf{E}_{\perp\mu} \times \tilde{\mathbf{B}}_{\perp\nu}) \cdot \hat{e}_z dS = P_\mu \delta_{k_{z\mu}, -\tilde{k}_{z\nu}} + Q_\mu \delta_{k_{z\mu}, \tilde{k}_{z\nu}}. \quad (5.117)$$

We note at this point that \tilde{K} can be obtained from K by changing the sign of the static magnetic field ($B_0 \rightarrow -B_0$), which in a cold plasma changes $K_2 \rightarrow -K_2$. Therefore the dispersion relation, which is a function of K_2^2 only, is unchanged for $K \rightarrow \tilde{K}$, and its solutions must be unchanged, so $k_{zv} = \tilde{k}_{zv}$. Thus we can again simplify equation (5.117) as

$$2 \int_{\text{Area}} (\mathbf{E}_{\perp\mu} \times \tilde{\mathbf{B}}_{\perp\nu}) \cdot \hat{e}_z \, dS = P_\mu \delta_{k_{z\mu}, -k_{z\nu}} + Q_\mu \delta_{k_{z\mu}, k_{z\nu}}. \quad (5.118)$$

Then we note from equations (5.86) and (5.87) that (using double subscripts to denote both the azimuthal mode number m and the radial mode numbers μ and ν)

$$\tilde{B}_{rmv} = B_{r(-m)\nu} \quad \text{and} \quad \tilde{B}_{\theta mv} = -B_{\theta(-m)\nu} \quad (5.119)$$

so the orthogonality integral,

$$2 \int_0^{2\pi} \int_0^a (E_{rm\mu} \tilde{B}_{\theta mv} - E_{\theta m\mu} \tilde{B}_{rmv}) r \, dr \, d\theta = P_\mu \delta_{k_{z\mu}, -k_{z\nu}} + Q_\mu \delta_{k_{z\mu}, k_{z\nu}}$$

using equation (5.119), becomes

$$4\pi \int_0^a (E_{rm\mu} B_{\theta(-m)\nu} + E_{\theta m\mu} B_{r(-m)\nu}) r \, dr = -(P_\mu \delta_{k_{z\mu}, -k_{z\nu}} + Q_\mu \delta_{k_{z\mu}, k_{z\nu}}). \quad (5.120)$$

When $\mu = \nu$, the orthogonality relation yields the power flow down the waveguide. When the plasma is lossless, then $\tilde{K} = K^*$, and the tilde is replaced everywhere by the complex conjugate operator.

5.5.6 Antenna problems

5.5.6.1 Excitation coefficient for a current loop

Here we consider a loop of radius b inside a waveguide of radius a , with $b < a$, carrying a current I in the $z = 0$ plane. See figure 5.11 for the geometry of the loop and figure 5.12 for the field it produces in its immediate vicinity.

If the loop is circularly symmetric, it will excite only circularly symmetric modes, and we will treat only this case although the extension to arbitrary θ -dependence is not greatly different.

If we now examine the symmetries as $z \rightarrow 0$, then any field component of the form $F(k, z) = A(k)e^{ikz}$ has the symmetries represented by

$$F(k, -z) = A(k)e^{-ikz} = A(-k)e^{ikz} = F(-k, z) \quad (5.121)$$

and since we will be letting $z \rightarrow 0$, we will denote the fields by $F(\pm k)$ instead of $F(\pm z)$. We now define the jump condition which is defined by

$$[\tilde{\mathbf{B}}_\perp] \equiv \lim_{z \rightarrow 0} [\tilde{\mathbf{B}}_\perp(z) - \mathbf{B}_\perp(-z)] \quad (5.122)$$

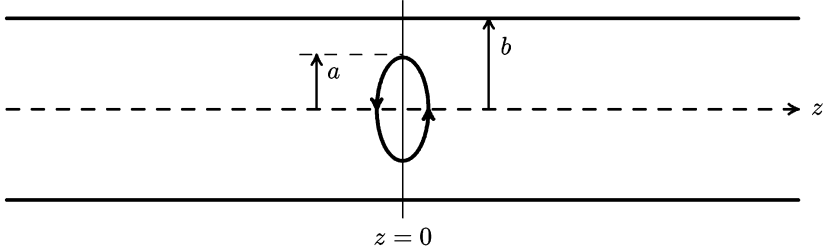


Figure 5.11. Geometry of a loop in cylindrical waveguide.

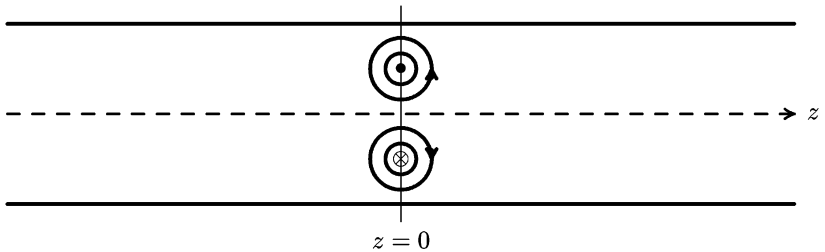


Figure 5.12. Magnetic fields produced by a current loop.

so that using equation (5.121) this may be written as

$$\begin{aligned} [\tilde{\mathbf{B}}_{\perp}] &= [\tilde{B}_r(k) - B_r(-k)]\hat{e}_r + [\tilde{B}_\theta(k) - B_\theta(-k)]\hat{e}_\theta \\ &= [B_r(k) - B_r(-k)]\hat{e}_r + [-B_\theta(k) + B_\theta(k)]\hat{e}_\theta \\ &= \mu_0 I \delta(r - b)\hat{e}_r \end{aligned} \quad (5.123)$$

where we have used $\tilde{B}_r = B_r$, $\tilde{B}_\theta = -B_\theta$, and $\mathbf{B}_{\perp}(-k) = -\mathbf{B}_{\perp}(k)$ in the second line and Ampère's law in the third line. We also examine the quantity

$$\begin{aligned} \tilde{\mathbf{B}}_{\perp}(k) + \mathbf{B}_{\perp}(-k) &= [\tilde{B}_r(k) + B_r(-k)]\hat{e}_r + [\tilde{B}_\theta(k) + B_\theta(-k)]\hat{e}_\theta \\ &= [B_r(k) - B_r(k)]\hat{e}_r - [B_\theta(k) - B_\theta(-k)]\hat{e}_\theta \\ &= 0 \end{aligned} \quad (5.124)$$

where we have used the same symmetries as before for the vanishing of the B_r component, and again used Ampère's law for the vanishing of the B_θ component. It is presumed here that each field component is a sum over all the radial modes in order to completely describe the fields of the loop.

Now we can construct the products needed for the orthogonality integral:

$$\begin{aligned} (\mathbf{E}_{\perp\mu} + \tilde{\mathbf{E}}_{\perp\mu}) \times [\tilde{\mathbf{B}}_{\perp}(k) - \mathbf{B}_{\perp}(-k)] &= (\mathbf{E}_{\perp\mu} + \tilde{\mathbf{E}}_{\perp\mu}) \times \mu_0 I \delta(r - b)\hat{e}_r \\ (\mathbf{E}_{\perp\mu} - \tilde{\mathbf{E}}_{\perp\mu}) \times [\tilde{\mathbf{B}}_{\perp}(k) + \mathbf{B}_{\perp}(-k)] &= 0 \end{aligned}$$

and adding these we obtain

$$\begin{aligned} (\mathbf{E}_{\perp\mu} + \tilde{\mathbf{E}}_{\perp\mu}) \times [\tilde{\mathbf{B}}_{\perp}(k) - \mathbf{B}_{\perp}(-k)] + (\mathbf{E}_{\perp\mu} - \tilde{\mathbf{E}}_{\perp\mu}) \times [\tilde{\mathbf{B}}_{\perp}(k) + \mathbf{B}_{\perp}(-k)] \\ = 2(\mathbf{E}_{\perp\mu} \times \tilde{\mathbf{B}}_{\perp} + \tilde{\mathbf{E}}_{\perp\mu} \times \mathbf{B}_{\perp}) = -2\mu_0 I E_{\theta\mu} \delta(r - b) \hat{e}_z \end{aligned} \quad (5.125)$$

providing $\tilde{A}_{\mu} = A_{\mu}$. Integrating over the cross section, then, we obtain

$$\int_{\text{Area}} (\mathbf{E}_{\perp\mu} \times \tilde{\mathbf{B}}_{\perp} + \tilde{\mathbf{E}}_{\perp\mu} \times \mathbf{B}_{\perp}) \cdot \hat{e}_z \, dS = - \int_{\text{Area}} \mu_0 I E_{\theta\mu} \delta(r - b) \, dS \quad (5.126)$$

and using the orthogonality relation and the delta function, this reduces to

$$-4\pi \int_0^a (E_{r\mu} B_{\theta\mu} + E_{\theta\mu} B_{r\mu}) r \, dr = -\mu_0 b E_{\theta\mu}(b) \int_0^{2\pi} I(\theta) \, d\theta. \quad (5.127)$$

If the loop current is independent of θ , then the integral on the right is $\int_0^{2\pi} I \, d\theta = 2\pi b E_{\theta\mu}(b)$ and only circularly symmetric modes are excited. Introducing the notation that $E_{r\mu} = A_{\mu} \mathcal{E}_{r\mu}$ and $B_{r\mu} = A_{\mu} \mathcal{B}_{r\mu}$, equation (5.127) allows us to find the amplitude for each mode A_{μ} as

$$A_{\mu} = \frac{\mu_0 I b \mathcal{E}_{\theta\mu}(b)}{2 \int_0^a (\mathcal{E}_{r\mu} \mathcal{B}_{\theta\mu} + \mathcal{E}_{\theta\mu} \mathcal{B}_{r\mu}) r \, dr}. \quad (5.128)$$

The impedance of the loop antenna is then directly obtained from $V_{\theta} = 2\pi b E_{\theta} = I \mathcal{Z}$ where the resistance $R = \text{Re}(\mathcal{Z})$ and the inductance $L = \text{Im}(\mathcal{Z})$. This leads to the expression

$$\mathcal{Z} = \sum_{\mu} \frac{\mu_0 \pi b^2 \mathcal{E}_{\theta\mu}^2}{\int_0^a (\mathcal{E}_{r\mu} \mathcal{B}_{\theta\mu} + \mathcal{E}_{\theta\mu} \mathcal{B}_{r\mu}) r \, dr}. \quad (5.129)$$

Problem 5.5.5. Excitation coefficient symmetry. Show that if $\tilde{A}_{\mu} \neq A_{\mu}$ the integral in equation (5.128) is equal to $2A_{\mu}\tilde{A}_{\mu}/(A_{\mu} + \tilde{A}_{\mu})$. Then show that in fact, $\tilde{A}_{\mu} = A_{\mu}$.

5.5.6.2 Low frequency, compressional mode excitation

In order to avoid the complexity of the coupled mode expressions, we assume $\omega \ll \omega_{ci}$ (the MHD approximation) so that the simpler orthogonality relations of Bessel functions can be used. In this case, for the compressional mode, $B_{\theta} \rightarrow 0$, so $[B_{\theta}]$ is not needed. We still have

$$[B_r] = \mu_0 I \delta(r - b)$$

from the general treatment. The dispersion relation from equations (5.97) and (5.99) may be written as

$$k_{zv}^2 = \frac{\omega^2}{V_A^2} - k_{\perp v}^2$$

with the boundary condition from equation (5.98) for circularly symmetric modes being given by

$$k_{\perp v}a = 3.83, 7, 01, \dots$$

The principal fields are B_r , B_z , and E_θ . In particular,

$$B_{rv} = -\frac{ik_{zv}}{k_{\perp v}} A_v J_1(k_{\perp v}r)$$

so

$$B_r(\pm z) = \mp \sum_v \frac{ik_{zv} A_v}{k_{\perp v}} J_1(k_{\perp v}r) e^{ik_{zv}|z|}$$

for $k_{zv} > 0$. Then the jump condition gives

$$[B_r] = -2 \sum_v \frac{ik_{zv} A_v}{k_{\perp v}} J_1(k_{\perp v}r) = \mu_0 I \delta(r - b).$$

In order to use the orthogonality properties of $J_1(k_{\perp v}r)$, we multiply by $J_1(k_{\perp \mu}r)$ and integrate:

$$\mu_0 I \int_0^a J_1(k_{\perp \mu}r) \delta(r - b) r dr = -2 \sum_v \int_0^a \frac{ik_{zv} A_v}{k_{\perp v}} J_1(k_{\perp \mu}r) J_1(k_{\perp v}r) r dr$$

which reduces to

$$\mu_0 I J_1(k_{\perp \mu}b) b = -\frac{ik_{z\mu} A_\mu a^2}{k_{\perp \mu}} J_0^2(k_{\perp \mu}a)$$

due to the Bessel function orthogonality relations,

$$\int_0^a J_m(k_{\perp \mu}r) J_m(k_{\perp v}r) r dr = \begin{cases} \frac{a^2}{2} [J'_m(k_{\perp \mu}a)]^2 & \mu = v \\ 0 & \mu \neq v \end{cases}$$

if $J_m(k_{\perp \mu}a) = J_m(k_{\perp v}a) = 0$. The excitation coefficient is then given by

$$A_\mu = \frac{i\mu_0 I b k_{\perp \mu}}{k_{z\mu} a^2} \frac{J_1(k_{\perp \mu}b)}{J_0^2(k_{\perp \mu}a)}. \quad (5.130)$$

The B_z component of the field can then be written as

$$B_z(r, z, \omega) = \frac{i\mu_0 I b}{a^2} \sum_v \frac{k_{\perp v} J_1(k_{\perp v}b)}{k_{zv} J_0^2(k_{\perp v}a)} J_0(k_{\perp v}r) e^{i(k_{zv}z - \omega t)} \quad (5.131)$$

where $k_{zv}^2 = (\omega^2 - \omega_v^2)/V_A^2$ where $\omega_v = k_{\perp v} V_A$ is the cutoff frequency for radial mode v . It is possible to adjust b to eliminate one radial mode, but in general there are an infinite number of modes.

Problem 5.5.6. Compressional mode excitation coefficients. Find the ratio b/a which will eliminate the second radial mode, and then calculate the relative amplitudes of the next three radial modes ($v = 3, 4, 5$) relative to the lowest mode. Assume $\omega = 6\omega_1$.

5.5.6.3 Impulse response

For this same MHD case, it is instructive to examine the time dependence of the response for a given input instead of looking only at the steady state response of equation (5.131). Since k_{zv} depends on ω , a nonsinusoidal disturbance will be distorted as it propagates down the waveguide. For a specific example, we consider the response to an impulse so that we assume the current has the time dependence

$$I(t) = I\delta(t) = \int_{-\infty}^{\infty} I e^{-i\omega t} \frac{d\omega}{2\pi}.$$

We then construct $B_z(r, z, t)$ by superposition and do the inverse Fourier transform,

$$B_z(r, z, t) = \frac{\mu_0 Ib}{a^2} \sum_v \frac{k_{\perp v} J_1(k_{\perp v} b)}{J_0^2(k_{\perp v} a)} J_0(k_{\perp v} r) \int_{-\infty}^{\infty} \frac{e^{i(k_{zv} z - \omega t)}}{-ik_{zv}} \frac{d\omega}{2\pi}$$

and using the dispersion relation for $k_{zv}(\omega)$, the integral is tabulated with the result

$$\int_{-\infty}^{\infty} \frac{e^{i(k_{zv} z - \omega t)}}{-ik_{zv}} \frac{d\omega}{2\pi} = \begin{cases} J_0(\omega_v \sqrt{t^2 - z^2/V_A^2}) & t > z/V_A \\ 0 & t < z/V_A. \end{cases} \quad (5.132)$$

Each radial mode has a similar time dependence, each of which is of the form shown in figure 5.13, and the total B_z is the sum of such terms. We can understand the response by noting first that $v_g \leq V_A$ always, so nothing can appear before the Alfvén transit time $t = z/V_A$. Then the high frequencies appear first and give the sharp initial rise, and then, since $v_g \rightarrow 0$ as the frequency nears the cutoff frequency, the long time behavior exhibits an oscillation which approaches the cutoff frequency since for large arguments,

$$J_0(\omega_v t) \sim e^{i(\omega_v t + \phi)} / \omega_v t.$$

For realistic waveguides where there is some loss going down the guide, the higher modes damp more quickly and round off the sharp rise, and the long time behavior is dominated by the cutoff frequency of the lowest mode.

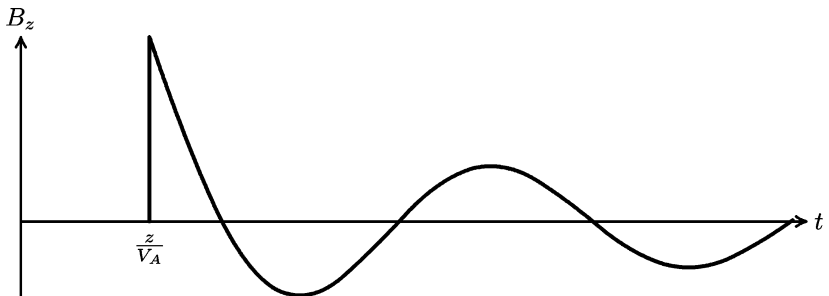


Figure 5.13. Impulse response for a single radial mode for the compressional Alfvén wave (MHD approximation).

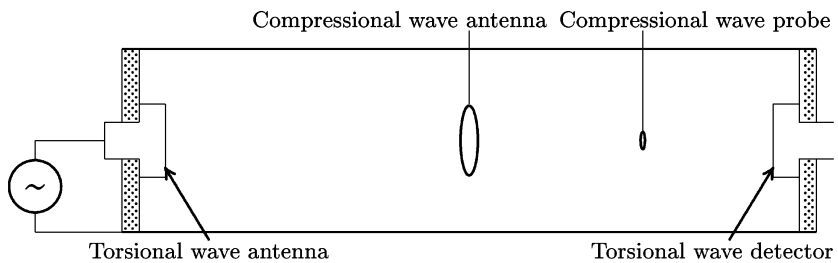


Figure 5.14. Schematic diagram of an experiment for Alfvén wave measurements. The electrodes at each end launch and detect the $m = 0$ torsional Alfvén wave since E_r is dominant while the loop antenna and B_z probe launch and detect the $m = 0$ compressional Alfvén wave where B_z is dominant.

5.5.7 Experiments in plasma-filled waveguides

5.5.7.1 Torsional wave experiments

Although some early measurements of the Alfvén wave were made by Lehnert in liquid sodium [62], the damping was so strong that the results were marginal at best in demonstrating the wave characteristics. Definitive measurements were made by Wilcox *et al* [63], who measured the propagation in a copper tube filled with cold ($\simeq 1$ eV) plasma immersed in a magnetic field. The configuration was similar to the one shown in figure 5.14 where the wave was launched by applying a voltage between the central electrode and the wall, producing an E_r and a B_θ . Wilcox *et al* measured the propagation speed and observed reflections from the far end of the tube, which in their case had a matching electrode at both ends.

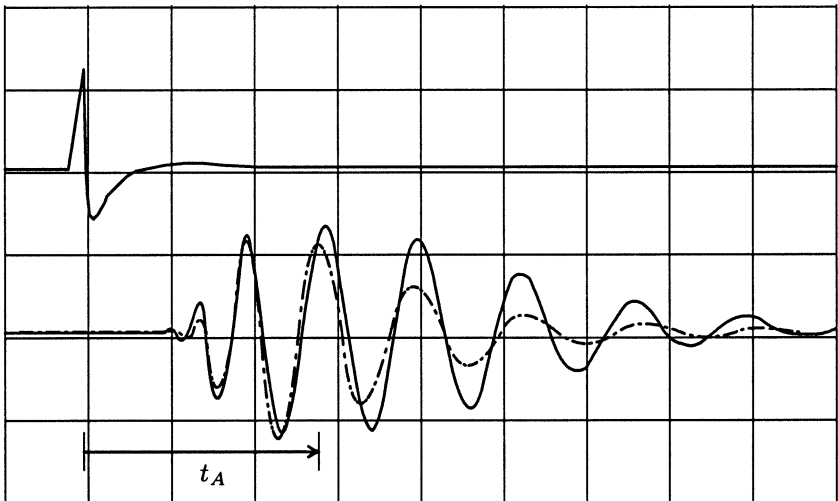


Figure 5.15. Impulse response for the fast wave in a plasma-filled waveguide; full curve, experimental results (from photograph, where the upper trace is the driving signal); dot-dashed curve, theoretical response (from ‘best fit’ parameters). The horizontal scale is $0.2 \mu\text{s}/\text{division}$. (From [55].)

5.5.7.2 Compressional wave experiments

Using a similar device to the one used by Wilcox *et al*, the more dramatic effects of the waveguide on fast wave propagation was observed by Swanson *et al* [55], and Jephcott and Malein [56]. In these experiments, the source was either a near impulse (a critically damped sine wave) [55] or a pulsed oscillator [56]. Because these measurements were done near the ion cyclotron frequency, the impulse response deviated from figure 5.13 because the higher frequencies arrived faster than V_A (see figure 5.10), and because the damping was strong enough that the long time amplitude was exponentially decaying rather than varying as $t^{-1/2}$. This is evident in equation (5.15) where the peak amplitude arrived near the Alfvén transit time ($t_A = z/V_A$) and the final observed frequency was very nearly the waveguide cutoff frequency.

One great advantage of finding the impulse response is that the Fourier transform of the impulse response is the dispersion relation. The Fourier transform of figure 5.15 is shown in figure 5.16 where both the phase (ω versus k_z) and amplitude are shown. The dispersion relation is shown compared with an analytical model including electron-ion collisions and ion-neutral collisions and the full transcendental boundary conditions. The collisions prevent a sharp cutoff, but there is general agreement with the theoretical model which is based on ‘best fit’ parameters for the percentage ionization, electron temperature, and the ion-neutral cross section. Using these parameters, an expected impulse response

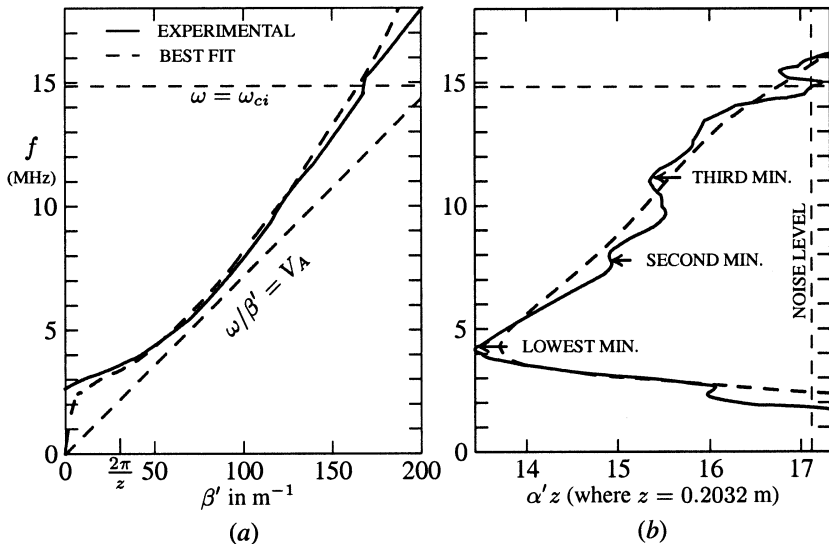


Figure 5.16. Fourier transform of the measured impulse response where $k_z = \beta' + i\alpha'$: (a) dispersion relation for the fast wave; (b) attenuation factor versus frequency. (From [55].)

was calculated and is shown in the dot-dash pattern of figure 5.15. The amplitude plot (figure 5.16(b)) shows that the largest amplitude was observed near the cutoff frequency, as can be seen in the excitation coefficient in equation (5.131) which is inversely proportional to k_z so that the amplitude peaks at cutoff. The radius of the antenna loop in the experiment was designed to eliminate the second radial mode, but due to plasma nonuniformities, the amplitude measurements show a small amount of the second mode and a significant amount of the third radial mode as evidenced by the absorption minima at each cutoff frequency.

5.5.7.3 Cavity modes

When the length of the waveguide is bounded, then boundary conditions on k_z also exist, and restrict the solutions to eigenfrequencies where the waves are standing waves in all directions. While all plasma-filled waveguides have finite dimensions, most linear devices have sufficiently strong damping that cavity modes are not observed. In a tokamak, however, the wave damping may be very low, and cavity modes have been observed [64]. In this case, the waveguide is bent around to close on itself, and though this requires a nonuniform B_0 and nonuniform density, the cylindrical waveguide analysis is quite pertinent to these experiments, except that the antennas are invariably outside the plasma in a vacuum sheath region, and the excitation coefficients are more difficult to calculate. Both high order azimuthal modes (toroidal direction, so $2\pi R_0 k_z = \ell$,

$\ell = 0, 1, 2, \dots$) and radial modes have been observed, many with very high Q (very low loss).

5.6 Conducting wall with vacuum layer, $m = 0, \pm 1$

For this case, we need to match the fields in the plasma to the vacuum fields, which are derived from an equation like equation (5.76) except that now there is only one factor, and the dispersion relation is simple. Thus we have

$$(\nabla_{\perp}^2 + k_{\perp}^2) \begin{pmatrix} E_z \\ B_z \end{pmatrix} = 0 \quad (5.133)$$

and

$$k_{\perp}^2 + k_z^2 = \frac{\omega^2}{c^2}. \quad (5.134)$$

Since k_z is the same inside and outside the plasma, then unless $k_z \rightarrow 0$, we usually will have $k_{\perp}^2 < 0$ in the vacuum region. Thus we define

$$T^2 = -k_{\perp}^2 = k_z^2 - \frac{\omega^2}{c^2} \quad (5.135)$$

so that solutions of equation (5.133) will be of the form

$$E_z(r, z, t) = \sum_{m=-\infty}^{\infty} [B_m I_m(Tr) + C_m K_m(Tr)] e^{ik_z z + im\theta - i\omega t} \quad (5.136)$$

$$B_z(r, z, t) = \sum_{m=-\infty}^{\infty} [D_m I_m(Tr) + F_m K_m(Tr)] e^{ik_z z + im\theta - i\omega t} \quad (5.137)$$

where $I_m(Tr)$ and $K_m(Tr)$ are the modified Bessel functions of the first and second kind, respectively, of order m . The TE modes, whose transverse fields are derived from equation (5.137), are independent of the TM modes, whose transverse fields are derived from equation (5.136), except when they are coupled through the boundary conditions to the plasma modes. The transverse fields are given by (suppressing the common phase factor)

$$\begin{aligned} E_{\theta} &= \frac{mk_z}{T^2 r} [B_m I_m(Tr) + C_m K_m(Tr)] + \frac{i\omega}{T} [D_m I'_m(Tr) + F_m K'_m(Tr)] \\ B_{\theta} &= -\frac{i\omega}{T c^2} [B_m I'_m(Tr) + C_m K'_m(Tr)] + \frac{mk_z}{T^2 r} [D_m I_m(Tr) + F_m K_m(Tr)]. \end{aligned}$$

If we set the plasma radius at a , where we require E_{θ} , B_{θ} , E_z , and B_z to be continuous ($\mathbf{B} = \mu_0 \mathbf{H}$, so \mathbf{H}_t is continuous in the ideal dielectric model), and the conducting wall to be at radius b , where E_z and E_{θ} must vanish, then we have six

conditions with six unknowns (A_m , τ_m , B_m , C_m , D_m , and F_m). Although we can immediately obtain

$$C_m = -B_m \frac{I_m(Tb)}{K_m(Tb)} \quad F_m = -D_m \frac{I'_m(Tb)}{K'_m(Tb)}$$

from the condition at the conducting wall, this is still a formidable set, and effectively requires numerical analysis to investigate the implications of adding the vacuum layer.

Because of the complexity of the results possible for this case, we only summarize the findings of Paoloni [65], who first investigated the character of the $m = +1, 0, -1$ modes in the intermediate frequency range, i.e. in the vicinity of the ion cyclotron frequency and below. If we define the cutoff frequency for the fast wave to be

$$\omega_{co} \equiv k_{\perp} V_A \quad k_{\perp} \equiv \frac{q_m v}{a} \quad (5.138)$$

then for the lowest radial mode, he found that

$$p_{01} < q_{01} < p_{11} \quad (5.139)$$

$$p_{11} < q_{-11} < p_{02} \quad (5.140)$$

but $q_{11} \rightarrow 0$ for relatively small vacuum layers. This means that the $m = +1$ fast wave has no cutoff frequency when the vacuum layer exceeds a few centimeters. The other azimuthal modes behave as one might expect, with only slight effects due to the vacuum layer, but this one mode is very different. He also found that the slow wave was essentially insensitive to boundary conditions, with the dispersion relation being indistinguishable for the three cases $m = 0, \pm 1$.

Generally, radial dependences of the $m = 0$ transverse fields for the fast waves are the same as for the slow waves, but the fast wave is everywhere right-handed and the slow wave is everywhere left-handed. For the slow wave, the $m = -1$ wave is left-hand polarized at low frequencies, while the $m = +1$ wave is right-hand polarized on axis, switching polarization about midway to the outer radius, but both cases become totally left-handed as $\omega \rightarrow \omega_{ci}$. At resonance, the $m = -1$ slow wave peaks on the axis, while the $m = +1$ slow wave has a null on the axis.

Problem 5.6.1. Boundary condition for vacuum layer in a conducting waveguide. Find the boundary condition for the case with a uniform plasma out to radius a and vacuum from a to b where there is a conducting waveguide. This may be accomplished by first eliminating the vacuum field coefficients from the conditions on $B_{\theta}(a)$ and $E_{\theta}(a)$, then writing each of these expressions with A_m factored out as $B(k_{\perp 1}) = \tau_m B(k_{\perp 2})$ and $E(k_{\perp 1}) = \tau_m E(k_{\perp 2})$, then eliminating τ_m to find an expression of the form $U(k_{\perp 1}) - U(k_{\perp 2}) = 0$. The problem then is to find a suitable form for $U(k_{\perp})$. The actual numerical solution then can be found by finding a root of this transcendental function of $k_{\perp 1}$, since the choice of $k_{\perp 1} \rightarrow k_z \rightarrow k_{\perp 2}$ through equation (5.82). (Nontrivial problem.)

5.7 Infinite magnetic field approximation

5.7.1 Cold plasma-filled waveguide in an infinite magnetic field

The approximation of an infinite magnetic field simplifies the problem of wave propagation to essentially a one-dimensional problem and allows the application of simple boundary conditions. Experimentally, Landau damping has been measured in magnetized plasmas because the desired plasma properties were easier to obtain, but with $\omega_{ce} \gg \omega_{pe}$, which we approximate by considering the field to be infinite. In this case the Maxwell equations for the wave fields are

$$\nabla \times \mathbf{E}_1 = i\omega \mathbf{B}_1 \quad (5.141)$$

$$\nabla \times \mathbf{B}_1 = -\frac{i\omega}{c^2} \mathbf{K} \cdot \mathbf{E}_1 \quad (5.142)$$

$$\nabla \cdot \mathbf{B}_1 = 0 \quad (5.143)$$

$$\nabla \cdot \epsilon_0 \mathbf{K} \cdot \mathbf{E}_1 = 0. \quad (5.144)$$

In this special case, as $B_0 \rightarrow \infty$, the dielectric tensor is especially simple,

$$\mathbf{K} = \begin{pmatrix} 1 & 0 & 0 \\ 0 & 1 & 0 \\ 0 & 0 & 1 - \frac{\omega_p^2}{\omega^2} \end{pmatrix} \quad (5.145)$$

since there are no transverse motions across the field. Taking the curl of equation (5.141) and substituting in equation (5.142), we obtain

$$\nabla(\nabla \cdot \mathbf{E}_1) - \nabla^2 \mathbf{E}_1 = \frac{\omega^2}{c^2} \mathbf{K} \cdot \mathbf{E}_1. \quad (5.146)$$

Using equation (5.145) in equation (5.144), we find

$$\begin{aligned} \nabla \cdot \mathbf{K} \cdot \mathbf{E}_1 &= \nabla \cdot \left[\hat{e}_r E_r + \hat{e}_\theta E_\theta + \hat{e}_z E_z \left(1 - \frac{\omega_p^2}{\omega^2} \right) \right] \\ &= \nabla \cdot \mathbf{E}_1 - \frac{\omega_p^2}{\omega^2} \frac{\partial E_z}{\partial z} = 0 \end{aligned} \quad (5.147)$$

so that the z -component of equation (5.146) is

$$\nabla^2 E_z + \frac{\omega^2}{c^2} \left(1 - \frac{\omega_p^2}{\omega^2} \right) E_z - \frac{\omega_p^2}{\omega^2} \frac{\partial^2 E_z}{\partial z^2} = 0. \quad (5.148)$$

Assuming now a wave field of the form

$$E_z(r, \theta, z, t) = E_z(r, \theta, k_z, \omega) e^{i(k_z z - \omega t)} \quad (5.149)$$

equation (5.148) becomes

$$\left[\nabla_{\perp}^2 + \left(\frac{\omega^2}{c^2} - k_z^2 \right) \left(1 - \frac{\omega_p^2}{\omega^2} \right) \right] E_z = 0 \quad (5.150)$$

with solutions that are regular at the origin given by

$$E_z = \sum_{m=0}^{\infty} A_m J_m(k_{\perp}r) e^{i(k_z z + m\theta - \omega t)} \quad (5.151)$$

where

$$k_{\perp}^2 = \left(\frac{\omega^2}{c^2} - k_z^2 \right) \left(1 - \frac{\omega_p^2}{\omega^2} \right). \quad (5.152)$$

The boundary condition at the vacuum wall, which is taken to be a perfectly conducting waveguide, is that the tangential electric field vanish at $r = a$, so the boundary condition requires

$$J_m(k_{\perp}a) = 0 \quad \text{so} \quad k_{\perp}a = p_{mv}. \quad (5.153)$$

Using this result, the dispersion relation may be conveniently written as

$$(k_z a)^2 = \frac{\omega^2 a^2}{c^2} - \frac{p_{mv}^2}{1 - \omega_p^2/\omega^2}. \quad (5.154)$$

The dispersion relation of equation (5.154) is plotted in figure 5.17 where a number of things should be noted. The upper propagating branch of the dispersion relation represents ordinary waveguide modes which are altered only slightly by the presence of the plasma by raising the waveguide cutoff frequency for each mode from the empty waveguide cutoff frequency $\omega_0 = p_{mv}c/a$ to $\omega = (\omega_0^2 + \omega_p^2)^{1/2}$. The lower propagating branch represents plasma waves in the finite waveguide. The cold plasma dispersion relation for plasma waves in an infinite medium is nondispersive with $\omega = \omega_p$, but the boundaries have introduced the dispersive effects.

Problem 5.7.1. The Poynting vector profile. Find an expression for the Poynting vector in this problem, and sketch the power flow as a function of radius for $m = 0, v = 1, 2$.

Problem 5.7.2. Thermal corrections. Find the dispersion relation corresponding to equation (5.154) for a warm fluid plasma where $p_1 = \gamma n_1 \mathcal{K}T$ with $\gamma = 3$. Sketch this dispersion relation for $a \gg \lambda_D$.

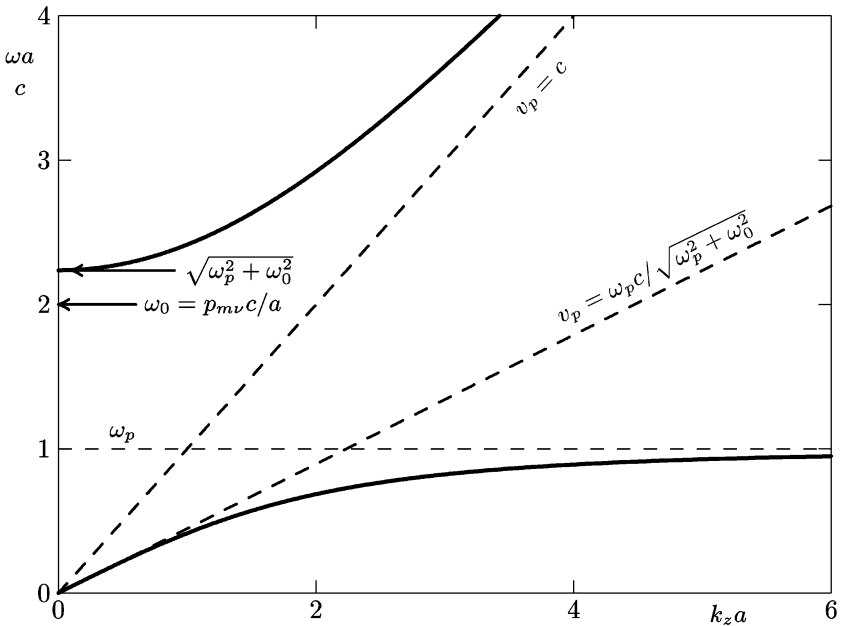


Figure 5.17. Dispersion relation for a cylindrical waveguide as $B_0 \rightarrow \infty$.

5.7.2 Hot plasma-filled waveguide

Our last example of bounded plasmas adds the effects of a hot plasma, but in the limit of an infinite magnetic field. This reduces the problem to one dimension in velocity space, since only parallel particle motions are possible, while remaining three-dimensional in configuration space subject to boundary conditions. Because the boundary puts no restriction on the parallel motion, only electromagnetic boundary conditions are appropriate, and considering only a plasma-filled waveguide, we will require the tangential \mathbf{E} fields to vanish at the wall radius.

We shall consider the Landau-type problem with an initial value problem in time. We shall ignore the initial conditions at the beginning, matching the normal mode fields to an actual perturbation later. While the electric field may have other components, only the E_z component will be of interest since the motion of the particles is one-dimensional. We will follow the general development of Kuehl [66], but use the notation of chapter 4. Taking the Fourier transforms in space, such that

$$f_1(\mathbf{r}, \mathbf{v}, t) \Rightarrow \tilde{f}(r, \theta, k, \mathbf{v}, t) e^{ikz}$$

$$\mathbf{E}(\mathbf{r}, t) \Rightarrow \tilde{\mathbf{E}}(r, \theta, k, t) e^{ikz}$$

the kinetic equation becomes

$$\frac{\partial \tilde{f}}{\partial t} + ikv_z \tilde{f} - \frac{e}{m_e} \tilde{E}_z \frac{\partial f_0}{\partial v_z} = 0. \quad (5.155)$$

The Maxwell wave equation,

$$\nabla(\nabla \cdot \mathbf{E}) - \nabla^2 \mathbf{E} = -\mu_0 \frac{\partial \mathbf{j}}{\partial t} - \frac{1}{c^2} \frac{\partial^2 \mathbf{E}}{\partial t^2}$$

along with

$$\epsilon_0 \nabla \cdot \mathbf{E} = \rho \quad \text{and} \quad \nabla \cdot \mathbf{j} + \frac{\partial \rho}{\partial t} = 0$$

can be used to write a relation in terms of \mathbf{E} and \mathbf{j} only. After taking the Laplace transform in time as in equation (4.44), the z -component of the wave equation becomes

$$\left(\nabla_{\perp}^2 - k^2 - \frac{p^2}{c^2} \right) \tilde{E}_p = \left(k^2 + \frac{p^2}{c^2} \right) \frac{\tilde{J}_p}{p\epsilon_0} \quad (5.156)$$

where \tilde{E}_p is the Laplace transform of \tilde{E}_z and \tilde{J}_p is the corresponding transform of the z -component of the current density. The transformed kinetic equation becomes

$$(p + ikv_z) \tilde{f}_p - \frac{e}{m} \tilde{E}_p \frac{\partial f_0}{\partial v_z} = 0. \quad (5.157)$$

From equation (5.157), the transformed current density is given by

$$\begin{aligned} \tilde{J}_p &= -en_0 \int_{-\infty}^{\infty} v_z \tilde{f}_p \, dv_z \\ &= -\epsilon_0 \omega_p^2 \tilde{E}_p \int_{-\infty}^{\infty} \frac{v_z \frac{\partial f_0}{\partial v_z}}{p + ikv_z} \, dv_z \end{aligned} \quad (5.158)$$

which may be written in the form

$$\frac{\tilde{J}_p}{p\epsilon_0} = -\tilde{E}_p \frac{\omega_p^2}{k^2} \int_{-\infty}^{\infty} \frac{\frac{\partial f_0}{\partial v_z}}{v_z - ip/k} \, dv_z. \quad (5.159)$$

Using this result in equation (5.156), we may write the resulting equation as

$$\left[\nabla_{\perp}^2 - \left(k^2 + \frac{p^2}{c^2} \right) K \right] \tilde{E}_p = 0 \quad (5.160)$$

where

$$K = 1 - \frac{\omega_p^2}{k^2} \int_{-\infty}^{\infty} \frac{\frac{\partial f_0}{\partial v_z}}{v_z - ip/k} \, dv_z. \quad (5.161)$$

The solution of equation (5.160) that is regular at the origin is

$$\tilde{E}_p = \sum_m A_m J_m(k_{\perp m} r) e^{im\theta} \quad (5.162)$$

where $k_{\perp m}$ is related to K , k , and p by the dispersion relation

$$k_{\perp m}^2 + \left(k^2 + \frac{p^2}{c^2} \right) K = 0. \quad (5.163)$$

We now take for an initial condition a z -directed azimuthally symmetric electric field that is localized in the vicinity of $z = 0$ and is impressed on the plasma at the waveguide wall radius $r = b$. It is turned on at $t = 0$ and is harmonic in time subsequently with angular frequency ω so that the perturbation can be represented by

$$E_z(r, \theta, z, t) = E_0(z) \delta(r - b) e^{-i\omega t} \quad t \geq 0. \quad (5.164)$$

Then the transformed initial condition is

$$\tilde{E}_p(b, k, p) = \frac{E_0(k)}{p + i\omega}. \quad (5.165)$$

Since there is no θ dependence, we know already that only the $m = 0$ term, $J_0(k_{\perp}r)$, will contribute, so we drop the subscript on k_{\perp} . Then matching the field at $r = b$ determines the constant so that

$$\tilde{E}_p(r, k, p) = \frac{E_0(k) J_0(k_{\perp}r)}{(p + i\omega) J_0(k_{\perp}b)}. \quad (5.166)$$

At long times after the perturbation is turned on, the Laplace transform is easily done, since only the contribution near the pole at $p = -i\omega$ will survive as the other contributions will damp away in time, leaving

$$\tilde{E}_p(r, k, t) = \frac{E_0(k) J_0(k_{\perp}r)}{J_0(k_{\perp}b)} e^{-i\omega t} \quad (5.167)$$

where now K and k are determined at $p = -i\omega$. The inverse Fourier transform is much more difficult now, however, since with ω having a positive imaginary part (since p had a positive real part), the pole in the velocity integral of equation (5.159) is either above the v_z axis for $k > 0$ or below the axis for $k < 0$. Hence we must break the inverse Fourier transform into two pieces, such that

$$\begin{aligned} E_z(r, z, t) = & \frac{e^{-i\omega t}}{\sqrt{2\pi}} \left[\int_{-\infty}^0 E_0(k) \frac{J_0(k_{\perp}^- r)}{J_0(k_{\perp}^- b)} e^{ikz} dk \right. \\ & \left. + \int_0^{\infty} E_0(k) \frac{J_0(k_{\perp}^+ r)}{J_0(k_{\perp}^+ b)} e^{ikz} dk \right] \end{aligned} \quad (5.168)$$

where k_{\perp}^{\pm} represents the cases where the pole lies above or below the v_z axis. The dispersion relation then becomes

$$k_{\perp}^{\pm 2} + \left(k^2 - \frac{\omega^2}{c^2} \right) K^{\pm} = 0 \quad (5.169)$$

where

$$K^+ = 1 - \frac{\omega_{pe}^2}{k^2 v_e^2} Z' \left(\frac{\omega}{kv_e} \right) \quad (5.170)$$

$$K^- = 1 - \frac{\omega_{pe}^2}{k^2 v_e^2} \tilde{Z}' \left(\frac{\omega}{kv_e} \right). \quad (5.171)$$

Since both Z' and \tilde{Z}' are entire functions, we can now let ω be purely real, and it will be taken as such in the remaining discussion.

For large z , the principal contributions to the response will come from the poles of the integrands, or where $k_{\perp}^{\pm} b = p_{0v}$ and p_{0v} is the v th root of the zero-order Bessel function. An additional contribution comes from a saddle point of the integrals, and was included in the discussion by Landau [33], but is generally not the dominant term. We also note that in this case, the root of equation (5.169) with K^- is just the negative of the root with K^+ , so we will not need to investigate the two cases separately. Thus equation (5.169) becomes

$$\left(\frac{p_{0v}}{b} \right)^2 + \left(k^2 - \frac{\omega^2}{c^2} \right) \left[1 - \frac{\omega_{pe}^2}{k^2 v_e^2} Z' \left(\frac{\omega}{kv_e} \right) \right] = 0. \quad (5.172)$$

There are two general classes of solutions for equation (5.172); those with $\omega/kv_e \gg 1$, where $K \simeq 1 - \omega_p^2/\omega^2$ and we have the cold plasma result of equation (5.154), and the case with $(\omega/kv_e) \ll 1$, where we can neglect $(\omega/c)^2$ compared to k^2 . For this latter case, there are no weakly damped solutions. The only simple root is for $\omega = 0$ where from equation (5.172),

$$\left(\frac{p_{0v}}{b} \right)^2 + k^2 + \frac{2\omega_{pe}^2}{v_e^2} = 0$$

with a purely imaginary solution

$$(k_i/k_D) = [1 + (p_{0v}/k_D b)^2]^{1/2}. \quad (5.173)$$

Problem 5.7.3. Lorentzian plasma in an infinite field waveguide. Find the roots of equation (5.172) for the Lorentzian distribution, $f_0(v) = v_e/\pi(v_z^2 + v_e^2)$.

Problem 5.7.4. Approximate solution. For $k_{\perp}/k_D = 0.1$ and $k_{\perp}/k_D = 0.3$, estimate k/k_D at $\omega = \omega_p$ (real and imaginary parts) and compare these with the cold plasma result.

Chapter 6

Waves in inhomogeneous plasmas

6.1 Introduction

The uniform plasmas of the previous chapters are idealizations which are rarely realized, although in some bounded regions, the approximation may be very good. We can generally assume a plasma is uniform if the plasma parameters vary little over a wavelength. In most laboratory plasmas, however, and over the vast regions of space, densities and magnetic fields vary to such an extent that it is sometimes difficult to estimate from uniform plasma theory where the wave energy will go and whether it will reach specified regions. It is very common to cross boundaries in the CMA diagram in inhomogeneous plasmas, either traveling up or down due to changes in the magnetic field, or laterally due to changes in density, or both. The questions to be addressed in this chapter relate to where the wave energy goes in a slowly varying medium, and what happens in those regions where geometric optics or WKB theory breaks down. The analysis of these special regions includes the effects of reflection at cutoffs, and absorption and mode conversion at resonances. Finite density gradients also give rise to electric fields and drift waves, along with new drift and gradient-driven instabilities. In many instances, these various effects can be separated and dealt with one at a time, but there are important cases where a combination of effects occur, several of which are simultaneously important, and each individual technique breaks down. We will generally discuss these effects in isolation, although the analysis of a cutoff resonance pair usually includes both mode conversion and absorption and will be treated as a single problem.

6.2 WKB method for one-dimensional inhomogeneities

As an illustration of the method used in treating one-dimensional inhomogeneities, we consider an unmagnetized plasma with only a density variation.

The wave equation,

$$\nabla(\nabla \cdot \mathbf{E}) - \nabla^2 \mathbf{E} + \frac{1}{c^2} \frac{\partial^2 \mathbf{E}}{\partial t^2} = -\mu_0 \frac{\partial \mathbf{J}}{\partial t} \quad (6.1)$$

depends only on variations in the plasma density through the plasma current, so we let $n_0 = n_0(x)$. Since all equilibrium quantities are independent of y and z , we can Fourier transform in those directions and assume harmonic time dependence. Then

$$\nabla \rightarrow \hat{e}_x \frac{d}{dx} + \hat{e}_y i k_y + \hat{e}_z i k_z \quad \text{and} \quad \frac{\partial}{\partial t} \rightarrow -i\omega$$

but another simplification is possible since the plasma is isotropic, since then one can rotate the coordinate system about the x -axis until the wave has no k_z component. Then the current may be derived from the equations of motion for ions and electrons

$$m_j \frac{\partial \mathbf{v}_j}{\partial t} = q_j \mathbf{E} \quad j = i, e$$

and

$$\mathbf{j} = e n_0(x) (\mathbf{v}_i - \mathbf{v}_e)$$

with the result that

$$\mathbf{j} \simeq \frac{i n_0(x) e^2}{\omega m_e} \mathbf{E} = \frac{i \epsilon_0}{\omega} \omega_{pe}^2(x) \mathbf{E}$$

where $\omega_{pe}^2(x) \equiv n_0(x) e^2 / (m_e \epsilon_0)$. Then the z -component of equation (6.1), which is not coupled to the other components, is

$$-\left(\frac{d^2}{dx^2} - k_y^2 \right) E_z + \left[\frac{\omega_{pe}^2(x)}{c^2} - \frac{\omega^2}{c^2} \right] E_z = 0.$$

This can then be cast into the WKB form of equation (1.54):

$$\frac{d^2 y}{dx^2} + k^2(x) y = 0 \quad (6.2)$$

where $y(x) = E_z(x)$ and

$$k^2(x) \equiv \frac{\omega^2 - \omega_{pe}^2(x)}{c^2} - k_y^2. \quad (6.3)$$

If it is assumed that $k^2(x)$ is slowly varying, then the eikonal or WKB method (see section 1.3.5) allows us to find good approximations to the exact solutions in rather general form.

For $k(x) = \text{constant}$, the solution is trivial and of the form

$$y = A_1 e^{ikx} + A_2 e^{-ikx}$$

and represents waves traveling to the left and to the right. Looking for solutions which are similar to the uniform result, we assume an eikonal solution of the form

$$y(x) = A(x)e^{i\psi(x)} \quad (6.4)$$

where $A(x)$ is assumed to be a slowly varying amplitude and $\psi(x)$ is the eikonal, a rapidly varying phase such that $\psi'(x) = \pm k(x)$. In order to determine the limits of validity of this method, we choose the upper sign and insert equation (6.4) into equation (6.2), first noting the derivatives

$$\begin{aligned} y' &= ikAe^{i\psi} + A'e^{i\psi} \\ y'' &= -k^2Ae^{i\psi} + 2ikA'e^{i\psi} + ik'Ae^{i\psi} + A''e^{i\psi} \end{aligned}$$

so that equation (6.2) becomes

$$A'' + 2ikA' + ik'A = 0. \quad (6.5)$$

If A'' is assumed small, then to lowest order, $A(x) = 1/\sqrt{k(x)}$, and the complete solution is written (for either sign) as

$$y(x) = \frac{A_0}{\sqrt{k(x)}} \exp \left[\pm i \int^x k(x') dx' \right]. \quad (6.6)$$

Taking this as the zero order result, we assume the solution is modified by the correction term,

$$A(x) = [1 + \eta(x)]/\sqrt{k(x)}$$

where again we assume that η is slowly varying so that we neglect η'' when this is inserted into equation (6.5). The result may be expressed as

$$\frac{\eta'}{1 + \eta} = \frac{1}{4i} \frac{\frac{k''}{k^2} - \frac{3}{2} \frac{k'^2}{k^3}}{1 + \frac{1}{2i} \frac{k'}{k^2}}$$

so that

$$\eta \simeq \frac{1}{4i} \frac{k'}{k^2}. \quad (6.7)$$

The condition for validity may thus be written as $|\eta| \ll 1$ or as

$$\left| \frac{1}{k} \frac{dk}{dx} \right| \ll k \quad (6.8)$$

which means that the change of wavelength over a wavelength should be small. This approximation fails when $k \rightarrow 0$ or when $k' \rightarrow \infty$, or whenever the wave approaches either a cutoff or a resonance.

Problem 6.2.1. WKB approximation. Show what approximations must be made to establish equation (6.7) and show that equation (6.8) is equivalent to saying the amplitude must vary little over a wavelength.

6.2.1 Behavior near a cutoff

The behavior near a cutoff is important enough to justify further analysis, and was analyzed so long ago that it is considered by many to be part of the WKB formalism rather than restricted to the condition of equation (6.8). In the neighborhood of the cutoff, we expand $k^2(x)$ about the cutoff,

$$k^2(x) = k^2(x_0) + \frac{d}{dx} k^2(x) \Big|_{x_0} (x - x_0) + \mathcal{O}(x - x_0)^2$$

where $k^2(x_0) = 0$ defines x_0 and we define the coefficient such that $k^2(x) = \beta^2(x - x_0)$. Then the result of equation (6.6) is valid whenever $|x - x_0| \gg \beta^{-2/3}$. The behavior near the cutoff must come from the solution of the differential equation, however, since the approximations always fail sufficiently close to cutoff. The differential equation may be written as

$$\frac{d^2y}{dx^2} + \beta^2(x - x_0)y = 0$$

which by means of the variable change $z \equiv -\beta^{2/3}(x - x_0)$ can be written

$$y'' - zy = 0 \quad (6.9)$$

which is the Airy equation.

The solutions of the Airy equation are well known [67] and may be represented by the two independent solutions

$$y(z) = C_1 \text{Ai}(z) + C_2 \text{Bi}(z)$$

which have the asymptotic forms

$$\text{Ai}(z) = \frac{1}{2\sqrt{\pi}z^{1/4}} e^{-\zeta} \quad (6.10)$$

$$\text{Ai}(-z) = \frac{1}{\sqrt{\pi}z^{1/4}} \left[\sin\left(\zeta + \frac{\pi}{4}\right) - \cos\left(\zeta + \frac{\pi}{4}\right) \right] \quad (6.11)$$

$$\text{Bi}(z) = \frac{1}{\sqrt{\pi}z^{1/4}} e^\zeta \quad (6.12)$$

$$\text{Bi}(-z) = \frac{1}{\sqrt{\pi}z^{1/4}} \left[\sin\left(\zeta + \frac{\pi}{4}\right) + \cos\left(\zeta + \frac{\pi}{4}\right) \right] \quad (6.13)$$

where $\zeta = \frac{2}{3}z^{3/2}$. These asymptotic solutions must be matched to the approximate eikonal solutions which represent incoming and outgoing waves, which are given by equation (6.6) as

$$y(x) = \frac{A_1}{(x - x_0)^{1/4}} e^{i\frac{2}{3}\beta(x-x_0)^{3/2}} + \frac{A_2}{(x - x_0)^{1/4}} e^{-i\frac{2}{3}\beta(x-x_0)^{3/2}} \quad x > x_0 \quad (6.14)$$

$$y(x) = \frac{B_1}{|x - x_0|^{1/4}} e^{\frac{2}{3}\beta|x-x_0|^{3/2}} + \frac{B_2}{|x - x_0|^{1/4}} e^{-\frac{2}{3}\beta|x-x_0|^{3/2}} \quad x < x_0. \quad (6.15)$$

Now as $z \rightarrow \infty$ ($x \rightarrow -\infty$), $\text{Bi}(z) \rightarrow \infty$, so in an unbounded plasma, we must require $C_2 = 0$. Then simplifying the expression for $\text{Ai}(-z)$ and writing the result in terms of x , using $\zeta = -\frac{2}{3}\beta(x - x_0)^{3/2}$,

$$\text{Ai}(-z) \simeq \left(\frac{2}{\pi\sqrt{z}} \right)^{1/2} \sin \zeta = -\frac{\sqrt{2/\pi} e^{-i\pi/4}}{(x - x_0)^{1/4} \beta^{3/8}} \sin \left[\frac{2}{3}\beta(x - x_0)^{3/2} \right] \quad (6.16)$$

so we require $A_2 = -A_1$. This principal result indicates that there is total reflection, since the amplitudes of the incoming and outgoing waves are the same. The asymptotic expressions, once far from the cutoff, can be matched onto more realistic expressions for $k(x)$ than the linear ones, and the phase of the reflected wave at a distant point estimated.

The matching implied here between the asymptotic forms of the Airy function solutions and the WKB solutions requires that there be a finite region of overlap where both approximations are simultaneously valid. The conditions for validity are shown in [figure 6.1](#). When the exact expression for $k^2(x)$ is linear, the overlapping region is unbounded, of course, but for any other variation, there is some limit when the linear approximation fails. If the real variation of $k^2(x)$ deviates substantially from linear before the WKB expressions are valid, then there may be no overlap, so that accurate matching may not always be possible.

Whenever the plasma is bounded, either due to the fact that there is a definite plasma edge, or due to the density or field not changing monotonically so that another cutoff is nearby, both the $\text{Ai}(z)$ and $\text{Bi}(z)$ functions must be used to satisfy the boundary conditions or connection formulas. The back-to-back cutoff problem, where two cutoffs occur a finite distance apart and the wave is not propagating between the cutoffs, is treated in the following section. This situation leads to tunneling and only partial reflection.

Problem 6.2.2. Validity of linear matching to WKB solutions. Suppose the density variation in equation (6.3) is such that

$$k^2(x) = k_0^2 \left(\frac{1}{1 + e^{-\alpha x}} - \frac{1}{2} \right).$$

- (i) Find the linear form of $k^2(x)$ near the cutoff and find the value of $u = \alpha x/2$ where the linear expression deviates from the exact expression by 10%.
- (ii) Assuming $|\zeta| = 3$ is large enough for the asymptotic forms of the Airy function to be valid, find an expression for u at this point.

(iii) Show that

$$\frac{1}{k^2} \frac{dk}{dx} = \frac{\alpha}{2k_0(2 \cosh u)^{1/2} (\sinh u)^{3/2}}.$$

- (iv) If this last quantity must be less than 0.1 for the validity of the WKB approximation, show that for sufficiently small α/k_0 , valid matching may always be obtained (i.e. that $|\zeta| \geq 3$, that the linear expression is within 10% and $|k'/k^2| \leq 0.1$, all for the same u).

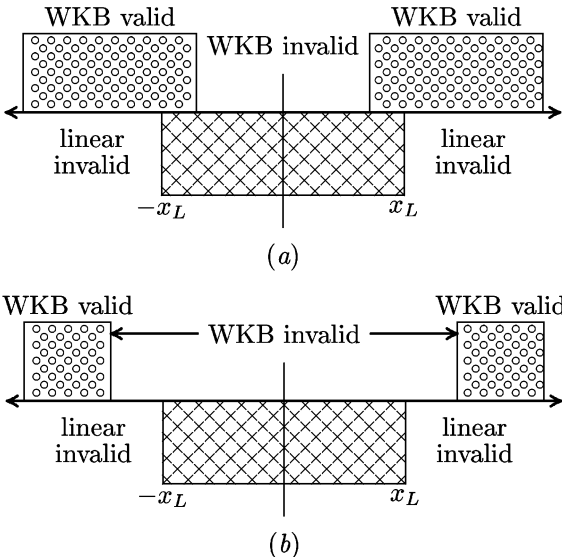


Figure 6.1. Validity conditions for matching the asymptotic forms of the inner functions and the outer WKB approximants. The cross-hatched regions indicate the range of validity of the linear approximation (between $-x_L$ and x_L) and the circles indicate the region of validity of WKB. (a) Finite overlap case, so the matching is valid. (b) No overlap case, so the matching is inaccurate.

- (v) As α/k_0 decreases, the accuracy of the matching increases. Using the value of u from part (i) where the linear expression is within 10%, find the value of α/k_0 where both $\zeta \geq 3$ and $|k'/k^2| \leq 0.1$. Repeat for the linear variation within 5% and $|k'/k^2| \leq 0.05$.

6.2.2 Tunneling between back-to-back cutoffs

For our first example of tunneling, we consider a case where a cold electromagnetic wave in an unmagnetized plasma is propagating in the low density portions of a plasma column where $\omega > \omega_p$ but near the center of the column, the density rises so that $\omega_p > \omega$ in the center. A schematic diagram of the situation is shown in figure 6.2 where cutoff occurs at both a and b .

In order to analyze this situation, we need the coupling formulas for the Airy functions where $k(x) = k_1(x)$ in the propagating region where $k^2(x) > 0$ and $k(x) = ik_2(x)$ in the nonpropagating region where $k^2(x) < 0$. For large x , these are given by the two following cases.

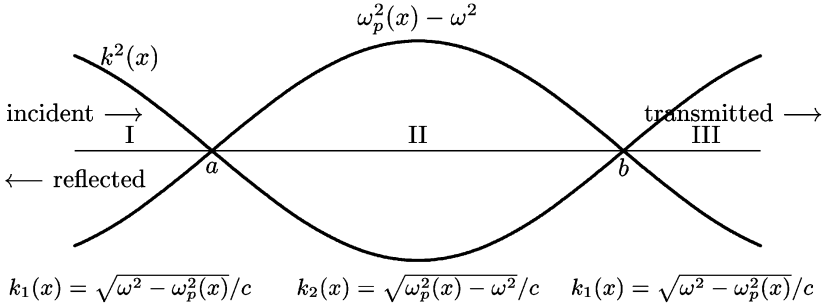


Figure 6.2. Plots of density variation and $k^2(x)$ showing where the wave propagates ($k(x) = k_1(x)$ for $x \leq a$ and $x \geq b$) and where it is evanescent ($\text{Im}[k(x)] = k_2(x)$ for $a < x < b$).

Case I, barrier on the right:

$$\frac{2}{\sqrt{k_1(x)}} \cos \left(\int_x^a k_1(x') dx' - \frac{\pi}{4} \right) \longleftrightarrow \frac{1}{\sqrt{k_2(x)}} \exp \left(- \int_a^x k_2(x') dx' \right)$$

$$\frac{1}{\sqrt{k_1(x)}} \sin \left(\int_x^a k_1(x') dx' - \frac{\pi}{4} \right) \longleftrightarrow - \frac{1}{\sqrt{k_2(x)}} \exp \left(- \int_a^x k_2(x') dx' \right).$$

Case II, barrier on the left:

$$\frac{1}{\sqrt{k_2(x)}} \exp \left(- \int_x^b k_2(x') dx' \right) \longleftrightarrow \frac{2}{\sqrt{k_1(x)}} \cos \left(\int_b^x k_1(x') dx' - \frac{\pi}{4} \right)$$

$$\frac{1}{\sqrt{k_2(x)}} \exp \left(\int_x^b k_2(x') dx' \right) \longleftrightarrow - \frac{1}{\sqrt{k_1(x)}} \sin \left(\int_b^x k_1(x') dx' - \frac{\pi}{4} \right).$$

We then use these connection formulas to construct a solution that represents an incoming wave from the left, such that

$$\begin{aligned}
y_I &= \frac{A}{\sqrt{k_1}} \cos \left(\int_x^a k_1(x') dx' - \frac{\pi}{4} \right) + \frac{B}{\sqrt{k_1}} \sin \left(\int_x^a k_1(x') dx' - \frac{\pi}{4} \right) \\
y_{II} &= \frac{A}{2\sqrt{k_2}} \exp \left(- \int_a^x k_2(x') dx' \right) - \frac{B}{\sqrt{k_2}} \exp \left(\int_a^x k_2(x') dx' \right) \\
&= \frac{A}{2\sqrt{k_2}} \exp \left(- \int_a^b k_2(x') dx' + \int_x^b k_2(x') dx' \right) \\
&\quad - \frac{B}{\sqrt{k_2}} \exp \left(\int_a^b k_2(x') dx' - \int_x^b k_2(x') dx' \right) \\
y_{III} &= - \frac{A e^{- \int_a^b k_2(x') dx'}}{2\sqrt{k_1}} \sin \left(\int_b^x k_1(x') dx' - \frac{\pi}{4} \right)
\end{aligned}$$

$$-\frac{2Be^{\int_a^b k_2(x') dx'}}{\sqrt{k_1}} \cos\left(\int_b^x k_1(x') dx' - \frac{\pi}{4}\right) \\ = i\left(\frac{Ae^{-\eta}}{4} + iBe^\eta\right) \frac{e^{i\phi}}{\sqrt{k_1}} - i\left(\frac{Ae^{-\eta}}{4} - iBe^\eta\right) \frac{e^{-i\phi}}{\sqrt{k_1}}$$

where $\phi(x) = \int_b^x k_1(x') dx' - \pi/4$, $\eta \equiv \int_a^b k_2(x) dx$, and $\int_a^x = \int_a^b - \int_x^b$. For an outgoing wave only in region III, we require $Ae^{-\eta} = 4iBe^\eta$ to eliminate the $e^{-i\phi}$ term. The result in region III is therefore

$$y_{III} = \frac{iAe^{-\eta}}{2\sqrt{k_1}} e^{i\phi}. \quad (6.17)$$

In order to relate the solution in region III to the solution in region I, we note that $\phi(x)$ increases with increasing x , while $\int_x^a k(x') dx'$ decreases with increasing x . This means that $\int_x^a k(x') dx' \sim -\phi + \Delta\phi$ (although there is no phase shift between a and b , $k(-x)$ may differ from $k(x)$ so there may be an accumulated phase shift for large x). Then eliminating B in region I leads to

$$y_I = \frac{A}{2\sqrt{k_1}}(e^{-i\phi+i\Delta\phi} + e^{i\phi-i\Delta\phi}) + \frac{B}{2i\sqrt{k_1}}(e^{-i\phi+i\Delta\phi} - e^{i\phi-i\Delta\phi}) \\ = \frac{A+iB}{2\sqrt{k_1}}e^{i\phi-i\Delta\phi} + \frac{A-iB}{2\sqrt{k_1}}e^{-i\phi+i\Delta\phi} \\ = \frac{Ae^{-i\Delta\phi}}{2\sqrt{k_1}} \left(1 + \frac{e^{-2\eta}}{4}\right) e^{i\phi} + \frac{Ae^{i\Delta\phi}}{2\sqrt{k_1}} \left(1 - \frac{e^{-2\eta}}{4}\right) e^{-i\phi} \quad (6.18)$$

so the transmission and reflection coefficients may be written as

$$T = \frac{1}{(e^\eta + \frac{1}{4}e^{-\eta})^2} \quad (6.19)$$

$$R = \frac{(e^\eta - \frac{1}{4}e^{-\eta})^2}{(e^\eta + \frac{1}{4}e^{-\eta})^2}. \quad (6.20)$$

This leads to $R = 1 - T$, and for thick enough barriers that $e^{-2\eta} \ll 1$, T simplifies to $T = e^{-2\eta}$.

Problem 6.2.3. Transmission and reflection coefficients.

- (i) Show that equations (6.17) and (6.18) lead to equations (6.19) and (6.20).
- (ii) Show that $R + T = 1$ for any η .

6.2.3 Behavior near an isolated resonance

The analysis of resonances is intrinsically more difficult than the analysis of cutoffs, because the physics of what resolves the resonance must be included

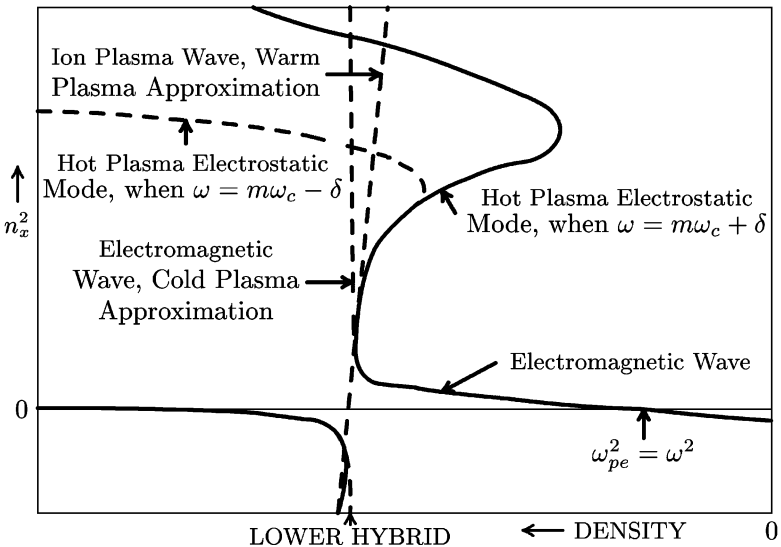


Figure 6.3. Dispersion relation for a wave approaching the lower hybrid resonance in a finite temperature plasma. (From [68].)

in order to obtain physically meaningful results. While effects of losses are invariably important near resonances, the effects of collisions in high temperature plasmas frequently are so weak as to be insignificant if any other effects are involved. While collisions may be the only effect in cold plasmas which could resolve resonances, thermal effects are frequently more important than collisions. This was demonstrated by Stix [68] when he investigated the nature of the lower hybrid resonance in a finite temperature plasma. He discovered that rather than approach a true pole as the wave approached the resonance, the $k^2(x)$ for the wave doubled back and continued on a warm backward wave branch, illustrated in figure 6.3, leading to the phenomenon of *mode conversion* where a wave of one type (mode) is linearly coupled to a wave of another type (mode). The example shown actually has a second mode-conversion point where it mode converts into a forward wave once again. The phenomenon can be understood in terms of Huygen's principle, where the wave can be thought of as shaking the plasma at a particular frequency and wavenumber at each point. If there are two waves that have the same wavenumber and matching phase velocity at that point, the excited plasma will excite both waves and transfer some energy between the waves. It is even possible for oppositely directed group velocities to be coupled, provided the phase velocities are in the same direction, and for all of the wave energy to be transferred from one mode to the other so that the wave energy flow turns around *without reflecting* where we define reflection as being due to wave energy coming back *on the incident branch* or mode.

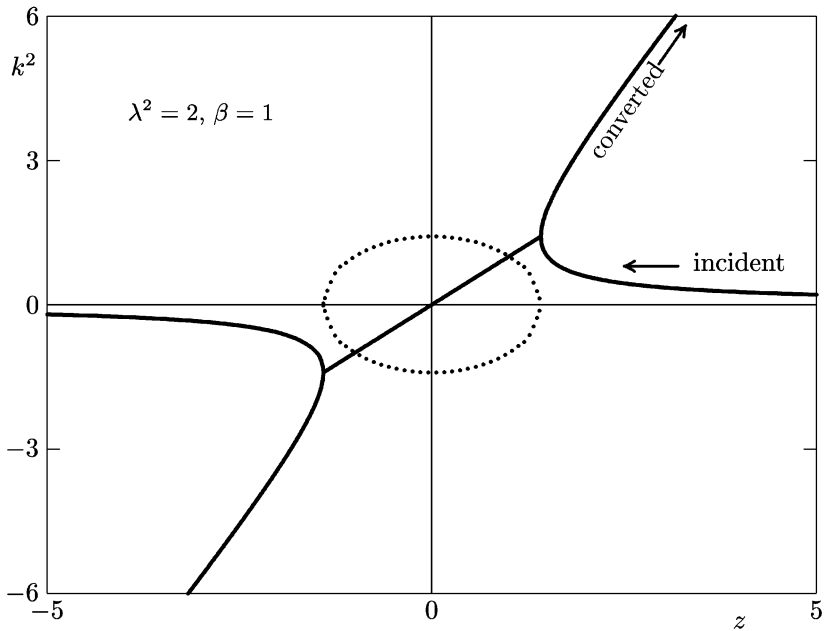


Figure 6.4. Dispersion relation for the Wasow equation when $\lambda^2 > 0$.

The simplest model which can represent two types of coupled waves traveling in either direction is a fourth-order wave equation (since there are *two kinds* of waves with each having two components traveling in opposite directions), and the isolated resonance may be modeled by the Wasow equation,

$$y^{iv} + \lambda^2(z y'' + \beta y) = 0 \quad (6.21)$$

which was first analyzed by Wasow [69] and generalized by Rabenstein [70] to include a first derivative term and complex coefficients. The eikonal analysis of this equation yields a quadratic for $k^2(z)$,

$$k^4 - \lambda^2 z k^2 + \lambda^2 \beta = 0 \quad (6.22)$$

with asymptotic solutions $k^2(z) \simeq \lambda^2 z, \beta/z$. This approximate dispersion relation is shown in figure 6.4 where the same general features of the turning point connecting the incoming and outgoing solutions are evident as in the numerical dispersion relation, but the linear asymptotes allow analytic solutions. The WKB type of analysis leads to asymptotic expressions of the form $z^{1/4} \exp(\pm 2i\sqrt{\beta}z)$ and $z^{-5/4} \exp(\pm 2i\lambda z^{3/2}/3)$. The difficulty is that the connections between these is not obvious until the differential equation has been solved exactly and the coupling established by the asymptotic forms of the exact solutions.

The solutions for this problem are tabulated [71], and the pertinent connection formula is

$$-(\beta z)^{1/4} e^{-2\sqrt{-\beta z}} \longleftrightarrow \frac{\beta}{\lambda^{3/2} z^{5/4}} e^{-i(\frac{2}{3}\lambda z^{3/2} + \frac{\pi}{4})} + i\sqrt{\pi\beta z} H_1^{(2)}(2\sqrt{\beta z}) \quad (6.23)$$

where the Hankel function term varies as $\exp(-2i\sqrt{\beta z})$. The general techniques for solving this kind of problem are developed in section 6.3.2. The conclusion from this connection formula is that the incident cold wave, represented by the Hankel function term, is coupled to the warm wave, represented by the $\exp(-2i\lambda z^{3/2}/3)$ term, both on the right-hand side, and that there is no reflection. The fact that both phase terms are negative is indicative of the fact that the phase velocities match at the turning point, but in this case, the group velocities do not as they travel in opposite directions. The scenario is that the wave energy on the cold branch is totally mode converted to the warm branch which propagates back away from the hybrid resonance layer. The exponentially decaying term for $x < 0$ carries no energy on that side unless a boundary is nearby.

6.2.4 Behavior near a resonance–cutoff pair

The nonuniform plasma medium allows a wide variety of possibilities for cutoffs, resonances, back-to-back cutoffs, and resonance–cutoff pairs. The tunneling through the nonpropagating region between back-to-back cutoffs can be estimated by connecting solutions of the Airy type, but the tunneling through the region between a cutoff and a resonance requires considerably more analysis. The simplest model for $k^2(x)$ of such a cutoff–resonance pair is shown in figure 6.5 along with the amplitude reflection and tunneling coefficients from the analysis of Budden [72] who analyzed the wave equation, equation (6.2), with

$$k^2(x) = k_0^2 \left(1 + \frac{a}{x}\right) \quad (6.24)$$

where $\eta = \pi k_0 a / 2$. This is commonly called the Budden equation. The arrows in the figure indicate the direction of an incident wave with its corresponding amplitude transmission and reflection coefficients.

The results by Budden established that there was no reflection when the wave approached the tunneling layer from the resonance side, but that there was reflection when the cutoff was encountered first. It also established that the tunneling coefficient was symmetric, i.e. the same from both sides. The difficulties with the Budden results are evident when one tries to establish power balance, since in both cases, $R^2 + T^2 < 1$. This indicates that not all the energy is accounted for in the outgoing waves, and since there is no physical absorption mechanism, the failure to conserve energy is problematical.

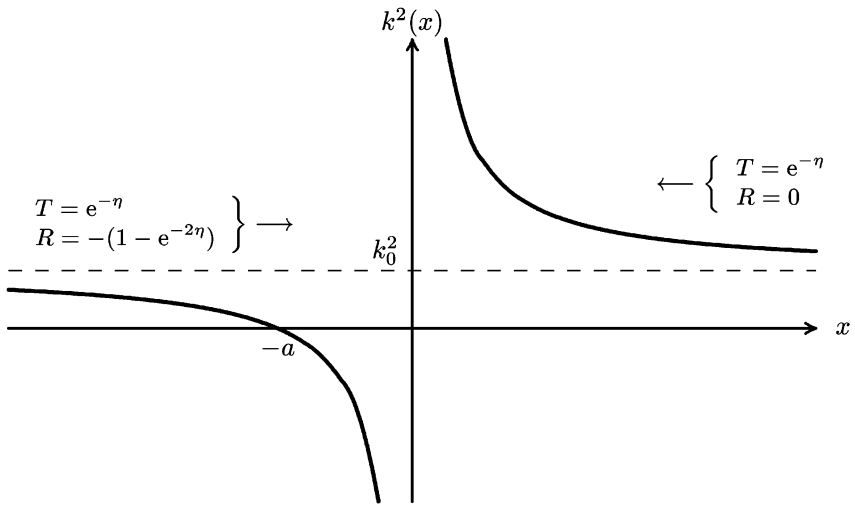


Figure 6.5. Spatial variation of $k^2(x)$ for a tunneling problem with a resonance at $x = 0$ and a cutoff at $x = -a$.

6.3 Mode conversion theory

Mode conversion theory was developed to deal with resonances in inhomogeneous plasmas, taking into account the influence of the merging of two different types of wave modes along with tunneling, reflection, conversion, and absorption. The method is nontrivial in its mathematical sophistication, but it incorporates a substantial amount of physics and is involved in virtually every type of plasma wave energy absorption except Landau damping and collisional damping.

6.3.1 The mode conversion theorem

It may appear that the necessity of using these mode conversion equations is relatively rare, and that simpler models might be able to adequately represent the physics of resonances, but except for certain order-reduction schemes, it is easily proved this is not so in the Mode Conversion Theorem [73].

Theorem 1. In an inhomogeneous plasma, linear mode conversion is always involved to some extent in resolving every plasma resonance.

Proof. Consider a general dispersion relation of the form $D(k, z) = 0$. Expand this about k_c , the turning point, and obtain the result

$$D(k, z) = D[k_c(z), z] + \frac{\partial D}{\partial k} \Big|_{k_c} (k - k_c) + \frac{1}{2} \frac{\partial^2 D}{\partial k^2} \Big|_{k_c} (k - k_c)^2 + \mathcal{O}(k - k_c)^3. \quad (6.25)$$

The turning point is where the group velocity vanishes, or where $v_g = \partial\omega/\partial k = (\partial D/\partial k)/(\partial D/\partial\omega) = 0$, so the first order term vanishes because of the choice of k_c . Then if we neglect the higher order terms, the result can be written in the form

$$D(k, z) = P(z) + Q(z)(k - k_c)^2 = 0$$

so by defining a shifted k by $k - k_c = k_s$, the dispersion relation is

$$k_s^2 = -P(z)/Q(z)$$

and $P(z_0) = 0$ is a cutoff and $Q(z_R) = 0$ is a resonance. In the event that $Q(z)$ vanishes, however, it does not represent a true resonance since then the neglected higher order terms in equation (6.25) dominate the expression for k_s . Even if z_R is not on the real axis, implying that $Q(z)$ never truly vanishes for any real z , the magnitude of the second order term must still be compared with the higher order terms before the relative importance of the various terms can be established. The next higher order term is commonly a fourth order term (since all the odd order terms may vanish if the first order term vanishes), and any such equation with a higher order term is a mode conversion equation. \square

An important qualifier in the theorem is the statement ‘to some extent’, since absorption may decrease the coupling to the mode converted wave. Essentially, if z_R is close to the real axis, then mode conversion is significant, while just the opposite is true as z_R moves far from the real axis.

6.3.2 Solution of the tunneling equation

The additional physics which is required to resolve this problem is to be found in mode conversion, the same general kind of process which occurred in the isolated resonance. The appropriate wave equation in this case is also a fourth order equation similar to equation (6.21) with the addition of only one term

$$y^{iv} + \lambda^2 z y'' + (\lambda^2 z + \gamma) y = 0 \quad (6.26)$$

which we call the *tunneling equation*. This equation was first analyzed by Erokhin [74] and later by Ngan and Swanson [75] in applying it to the tunneling problem at the ion cyclotron harmonic, both for the case $\gamma > -1$. The solution for $\gamma < -1$ was analyzed by Faulconer [76]. This is a very general equation, since every fourth order equation with only constant and linear coefficients of the form,

$$y^{iv} + (a_2 + b_2 x) y'' + (a_0 + b_0 x) y = 0 \quad (6.27)$$

can be cast into the form of equation (6.26) if $b_0 \neq 0$ or into the form of equation (6.21) if $b_0 = 0$.

Equations of the form of equation (6.26) or equation (6.27) along with equation (6.21) are special cases of a class of n th-order differential equations that

have constant and linear coefficients and which represent coupled waves. The general analysis of these equations is tedious [77], but relatively straightforward. The following example demonstrates the various arguments and calculations in the process and allows one to see the interaction back and forth between the mathematics and the physics in solving the problem.

Problem 6.3.1. Changing to dimensionless variables. Assume $x = \alpha(z - z_0)$ in the previous equation and find expressions for α , z_0 , λ , and γ for the case $b_0 \neq 0$. If $b_0 = 0$, find the corresponding expressions for equation (6.21) (find β instead of γ).

Problem 6.3.2. The case for $\lambda^2 < 0$.

- (i) Plot the dispersion curve corresponding to figure 6.4 for $\lambda^2 = -\lambda_0^2$ where $\lambda_0^2 > 0$ in equation (6.22).
- (ii) Plot the dispersion curve for the tunneling equation when $\lambda^2 < 0$ and $\gamma < -1$ in equation (6.34) by also letting $z \rightarrow -x$ so that $\lambda^2 z \rightarrow \lambda_0^2 x$. Sketch on the curves which are incoming and outgoing waves (i.e. is e^{ix} incoming or outgoing on the left, etc). Is this slow wave a backward or a forward wave?

6.3.2.1 The exact solution

Equation (6.26) can be solved exactly by using Laplace's method, namely assuming the solution can be written as a Laplace integral of the form,

$$y(z) = \int_C e^{-ikz} f(k) dk \quad (6.28)$$

where C represents some contour in the complex k -plane. Inserting this into equation (6.26) and integrating by parts, the result may be written as

$$\begin{aligned} \int_C [(k^4 + 2ik\lambda^2 + \gamma)f(k) + i\lambda^2(k^2 - 1)f'(k)]e^{-ikz} dk \\ + i\lambda^2(1 - k^2)f(k)e^{-ikz}|_C = 0 \end{aligned} \quad (6.29)$$

so if the integrand vanishes everywhere and the quantity $(1 - k^2)f(k)e^{-ikz}$ vanishes at the end points of the contour, then this satisfies the original equation. This demands that $f(k)$ be a solution of the first order differential equation,

$$\frac{f'(k)}{f(k)} = \frac{i(k^4 + 2ik\lambda^2 + \gamma)}{\lambda^2(k^2 - 1)}$$

so the solution for $y(z)$ is given by

$$\begin{aligned} y(z) = \int_C \exp \left[-ikz + \frac{ik^3}{3\lambda^2} + \frac{ik}{\lambda^2} \right. \\ \left. - \left(1 + \frac{i\eta}{\pi} \right) \ln(k+1) - \left(1 - \frac{i\eta}{\pi} \right) \ln(k-1) \right] dk \end{aligned} \quad (6.30)$$

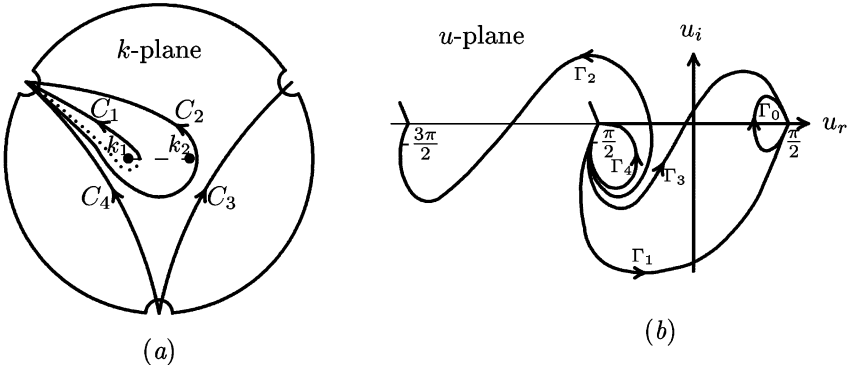


Figure 6.6. General contours for the tunneling equation: (a) k -plane contours; (b) u -plane contours.

where

$$\eta = \frac{\pi(1 + \gamma)}{2\lambda^2} \quad (6.31)$$

and η is called the *tunneling factor*. Using $f(k)$ in the end point expression, it is clear that the k^3 term dominates and that the end points must approach infinity along the directions $\pi/6$, $5\pi/6$, and $-\pi/2$. It is also apparent that there are branch points at $k = \pm 1$, so we draw a branch cut between these branch points as indicated in figure 6.6(a). Since this is a fourth order equation, there must be four linearly independent solutions represented by four independent contours and a possible basis set is also shown in figure 6.6(a). This technique has been extended to n th order equations where the highest order coefficient is constant and all subsequent coefficients are constant plus linear by Gambier *et al* [77] and is sometimes referred to as the GSS theory.

In order to eliminate the difficulties of dealing with the branch points and the branch cut, it is possible to make a variable change from $k \rightarrow i \tan u$. The exact solution in this case is

$$y(z) = \int_C \exp \left[\left(z - \frac{1}{\lambda^2} \right) \tan u + \frac{\tan^3 u}{3\lambda^2} + \frac{1 + \gamma}{\lambda^2} u \right] du \quad (6.32)$$

so the end points in this case are located where $\tan^3 u \rightarrow -\infty$ which places them at $u = (2n + 1)\pi/2$, $n = 0, \pm 1, \pm 2, \dots$ and these points must be approached along the angles $0, \pm 2\pi/3$. A set of possible contours for this case is illustrated in figure 6.6(b), where not all the contours are independent (e.g. $C_1 + C_0 = C_3$). It is worth noting that since $\tan u$ is periodic with period π that the effect of shifting from u to $u \pm \pi$ is equivalent to simply multiplying the integral by $e^{\pm 2\eta}$ so that the various Riemannian sheets in the complex k -plane have been laid out along the real axis of the u -plane. The amplitude transmission coefficient will turn out

to be simply $e^{-\eta}$, so the connection from one sheet to another in the k -plane, or from one node to another in the u -plane, is the dominant feature in establishing the various transmission, reflection, and conversion coefficients.

6.3.2.2 Saddle point approximations

The task at this point is to establish the asymptotic forms of the solutions for the various contours, and this is done by using the method of steepest descents or the saddle point method. For this analysis, it is convenient to cast the integral into the form,

$$y(z) = \int e^{zh(u)} du \quad (6.33)$$

where z is the asymptotic parameter, and expand $h(u) = (1 - 1/\lambda^2 z) \tan u + \tan^3 u / 3\lambda^2 z + (2\eta/\pi z)u$ about the various saddle points. These are located wherever $h'(u_0) = 0$. Writing this condition in terms of $k^2 = -\tan^2 u_0$ we obtain the familiar result,

$$k^4 - \lambda^2 z k^2 + \lambda^2 z + \gamma = 0 \quad (6.34)$$

which is the same result as that which would be obtained from WKB analysis. This dispersion curve, shown in figure 6.7, should be compared with figure 6.5, where the cutoff is still apparent, but the resonance is now evidently a turning point where mode conversion takes place. Evaluating this for large $|z|$, the asymptotic roots are located where

$$\begin{aligned} k_s &\simeq \pm(\lambda^2 z - 1)^{1/2} & u_s &\simeq (2n + 1)\frac{\pi}{2} \pm \begin{cases} i/\lambda\sqrt{z} & z > 0 \\ \tan^{-1}(\lambda\sqrt{-z}) & z < 0 \end{cases} \\ k_f &\simeq \pm \left(1 + \frac{1 + \gamma}{\lambda^2 z}\right)^{1/2} & u_f &\simeq \begin{cases} (2n + 1)\frac{\pi}{2} \pm \frac{i}{2} \ln \left(\frac{4\lambda^2 z}{1 + \gamma}\right) & z > 0 \\ n\pi \pm \frac{i}{2} \ln \left|\frac{4\lambda^2 z}{1 + \gamma}\right| & z < 0 \end{cases} \end{aligned}$$

with $n = 0, \pm 1, \pm 2, \dots$, and where k_s and u_s refer to the slow wave solutions and k_f and u_f refer to the fast wave solutions. In this context, fast and slow are purely relative to one another, such that $k_s > k_f$, as it could be that the fast wave here could be an electrostatic wave that is a slow wave in some other context.

The individual saddle-point contributions are calculated by factoring out the leading constant factor $\exp[zh(u_0)]$ from the integral, keeping only the second order term, and integrating over the saddle point in such a direction that $zh''(u_0)u^2 < 0$ and the resulting integral yields

$$y_i = \left[\frac{2\pi}{|zh''(u_i)|} \right]^{1/2} e^{zh(u_i) + i\phi} \quad i = f, s \quad (6.35)$$

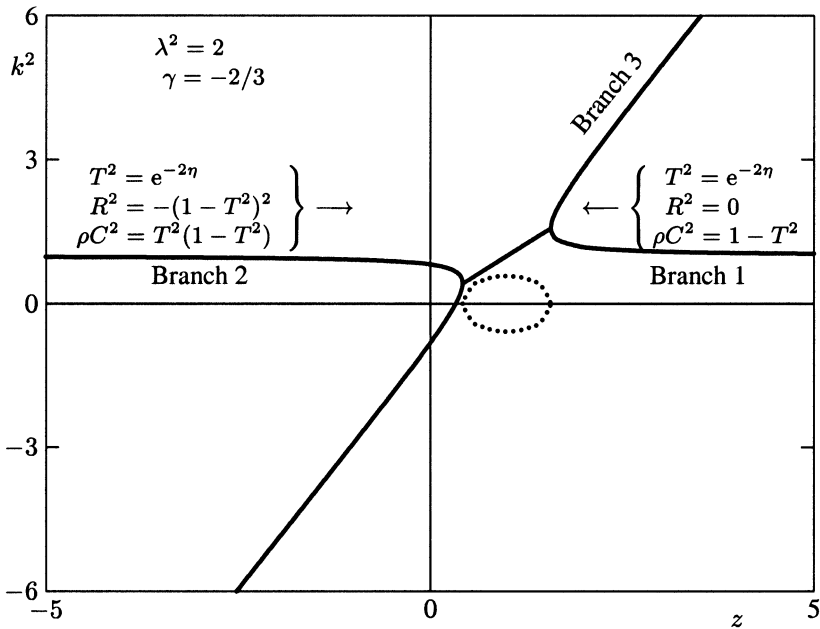


Figure 6.7. Dispersion relation for tunneling equation when $\gamma > -1$.

where ϕ is the crossing angle. This method gives a good approximation for the slow wave, where the contribution comes only from the immediate neighborhood of the saddle point as $|z| \rightarrow \infty$, with the result

$$s_{\pm} = \frac{\sqrt{\pi}}{\lambda^{3/2} z^{5/4}} \exp \left[\pm i \left(\frac{2}{3} \lambda z^{3/2} + \frac{\pi}{4} \right) \right] \quad z \rightarrow \infty \quad (6.36)$$

where s_{\pm} is multiplied by $e^{\pm\eta}$ if the real part of u_s is $\pm\pi/2$. For $z \rightarrow -\infty$, the results are

$$\left. \begin{aligned} \sigma_+ &= \frac{\sqrt{\pi}}{\lambda^{3/2} |z|^{5/4}} \exp \left(\frac{2}{3} \lambda |z|^{3/2} \right) \\ \sigma_- &= \frac{i\sqrt{\pi}}{\lambda^{3/2} |z|^{5/4}} \exp \left(-\frac{2}{3} \lambda |z|^{3/2} \right) \end{aligned} \right\} \quad z \rightarrow -\infty. \quad (6.37)$$

6.3.2.3 The fast-wave approximate solution

For the fast-wave saddle point, the use of equation (6.35) is inaccurate because even as $|z| \rightarrow \infty$, the contribution to this integral is spread and many higher order terms are necessary to represent the integral. For this integral, it is better to go back into the k representation and expand about the singular points. Letting

$k + 1 = \alpha t$ in equation (6.30) and expanding about $t = 0$, keeping zero and first order terms, the solution can be cast into the form

$$y(z) = \exp\left[iz - \frac{4i}{3\lambda^2} - \left(1 - \frac{i\eta}{\pi}\right)\ln(-2)\right] \\ \times \int_C (\alpha t)^{(1+i\eta/\pi)} \exp\left[\alpha t\left(-iz + \frac{2i}{\lambda^2} + \frac{1}{2} - \frac{i\eta}{2\pi}\right)\right] \alpha dt \quad (6.38)$$

where the contour starts where $z \rightarrow -i\infty$, circles the origin counterclockwise, and returns (on a different Riemannian sheet). This is equivalent to the Hankel integral (see [appendix B](#)),

$$\frac{1}{\Gamma(\zeta)} = \frac{i}{2\pi} \int_C (-t)^{-\zeta} e^{-t} dt \quad (6.39)$$

where the contour begins as $t \rightarrow \infty + i\epsilon$, circles the origin counterclockwise and ends as $t \rightarrow \infty - i\epsilon$. By letting

$$\alpha = \left[iz - \frac{2i}{\lambda^2} - \frac{1}{2} + \frac{i\eta}{2\pi}\right]^{-1}$$

and $\zeta = 1 + i\eta/\pi$, this leads to the result

$$f_+ = \frac{\pi ie^{-\eta/2}}{\Gamma(1 + i\eta/\pi)} \exp\left[iz + \frac{i\eta}{\pi} \ln\left|2z - \frac{4}{\lambda^2} + \frac{\eta}{\pi} + i\right| - \frac{4i}{3\lambda^2}\right] \quad (6.40)$$

and $f_- = f_+^*$ and each must be multiplied by the same $e^{\pm\eta}$ if the real part of u_f is $\pm\pi/2$.

Except for the constants associated with these solutions, we could obtain the same asymptotic forms from the WKB formulas, but now we are in a position to find all the coupling coefficients, because all of the relative amplitudes can be determined exactly by using the appropriate contours and picking up the relevant saddle point contributions from each saddle we cross. This is facilitated by examining the location, orientation, and labeling of all the saddle points for both positive and negative z . These are shown in [figure 6.8\(a\)](#) for $z \rightarrow \infty$ and in [figure 6.8\(b\)](#) for $z \rightarrow -\infty$.

6.3.2.4 Incoming and outgoing wave identification

The final step before constructing the solutions is to establish which waves are traveling in which direction. The fast waves are simple enough, with the $f_+ \simeq e^{iz}$ so that it represents a wave traveling in the positive z direction, or from left to right in [figure 6.7](#). Similarly, the f_- solution represents a wave traveling from right to left, or in the negative z direction. The slow wave solutions are less obvious, and, in general, one must return to the physical model and introduce a small amount of damping to establish the direction of energy flow, or do an analysis

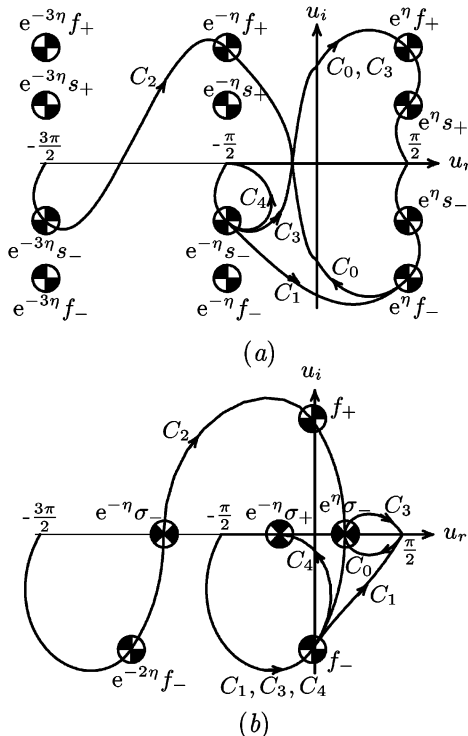


Figure 6.8. Saddle points and contours in the u -plane: (a) for $z \rightarrow \infty$ and (b) for $z \rightarrow -\infty$.

of the relative directions of the phase and group velocities. For this example, it may be established that the slow wave is a backward wave, in that its phase and group velocities are in opposite directions. Thus, the s_- solution has a phase velocity from right to left, but the group velocity is from left to right, so it is an outgoing wave in the sense of energy flow. Similarly, s_+ is an incoming wave. For negative z , σ_- is exponentially decaying away from the tunneling layer, while σ_+ is exponentially growing, and must be avoided for any physically meaningful solution in an unbounded medium.

6.3.2.5 Solution y_1 , fast wave incident from the right

With these numerous preliminaries out of the way, we now can construct the contours for a physically relevant problem. We consider first a fast wave incident from the right, so the incident wave is an f_- term. This means the solution must cross an f_- saddle point and we choose one at $+\pi/2$ so the contribution is $e^\eta f_-$. Now we must terminate the contour at either $\pm\pi/2$ on the real axis,

and the steepest descent paths require that terminating at angles $\pm\pi/3$ demands a crossing of the s_{\pm} saddle points, respectively. We must avoid the s_+ crossing since that is an incoming wave, so we choose an s_- crossing. It might be imagined from looking only at figure 6.8(a) that one could also choose to terminate along the real axis, but the contour must have the same topology for negative z and the contour terminating along the real axis must cross the σ_+ in figure 6.8(b). Thus we are restricted to the $-\pi/3$ approach angle, and the contour then terminates at both $-\pi/2$ and at $\pi/2$, crossing two slow wave saddle points along the way, the one on the left multiplied by $e^{-\eta}$ and the one on the right by e^{η} . This contour is labeled C_1 in figure 6.8(a) and must have the same topology (start and end at the same points and same number of axis crossings) in figure 6.8(b). This requires the simple C_1 contour with only an f_- crossing for negative z , so we can immediately establish the connection formula

$$f_- \leftarrow y_1 \rightarrow e^{\eta} f_- - e^{\eta}(1 - e^{-2\eta})s_- . \quad (6.41)$$

The f_- term on the left is clearly the transmitted wave and hence the transmission coefficient is given by $T = e^{-\eta}$. We label the coefficient of the s_- term as the conversion coefficient relative to the incident term having unit amplitude (e.g. multiplying equation (6.41) by $e^{-\eta}$ so the incident term is simply f_-) so $C_1 = -(1 - e^{-2\eta})$. Because the contour never crossed an f_+ saddle in either figure, the reflection coefficient is identically zero.

Except for the addition of the conversion coefficient, we recognize that this result is identical with the Budden result except that the Budden tunneling factor was $\eta_B = \pi\gamma/2\lambda^2$ so the tunneling factors agree only if $\gamma \gg 1$. The relationship to the Budden equation may be noted by observing that if one drops the fourth derivative term in equation (6.26) and divides by $\lambda^2 z$, we obtain the Budden equation except that we have let $z = k_0 x$.

An approximation which reduces the problem to a second order equation that still successfully obtains the proper tunneling factor has been found [78], but the wave solutions fail to exhibit the proper asymptotic form for the slow wave and it is not easily generalized to include absorption.

6.3.2.6 Solution y_2 , fast wave incident from the left

The second solution, representing a fast wave incident from the left, is more complicated because the contour must cross an incident wave f_+ saddle in figure 6.8(b) but still end at angle $-\pi/3$ in order to avoid an incoming slow wave or a growing wave. The crossing points are the σ_- saddle points, but it is ambiguous from figure 6.8(b) which way to turn after crossing the axis. If we were to terminate the contour which crosses the real axis between $-\pi/2$ and $\pi/2$ by turning immediately to the right into the nearest end point in figure 6.8(b), the implication of this termination in figure 6.8(a) is that the contour must first cross the $e^{\eta} f_-$ saddle point which represents an incoming wave on that side. Thus this contour must rather turn to the left and cross the f_- saddle point before

terminating at $-\pi/2$. The other end of the contour, which must cross the real axis to the left of $-\pi/2$ in figure 6.8(b), must also bear to the left after crossing the axis and cross the $e^{-2\eta} f_-$ saddle point before terminating at $-3\pi/2$ for the same reasons. The contour C_2 , then, with the starting point chosen at $-\pi/2$, crosses the f_- saddle point in figure 6.8(b) in the positive sense, then the $e^\eta \sigma_-$ saddle in the positive sense, the f_+ saddle in the negative sense (the positive directions are all taken to lie in the first or fourth quadrants), the $e^{-\eta} \sigma_-$ saddle in the negative sense and finally the $e^{-2\eta} f_-$ saddle in the negative sense. Starting from the same point in figure 6.8(a), we first cross the $e^{-\eta} s_-$ saddle in the positive sense, then the real axis (the steepest descent path would end at $-\pi/2$ along the real axis, but we immediately reverse direction and head back out and up, thus avoiding any difficulty with the exponentially growing solutions), then the $e^{-\eta} f_+$ saddle in the negative sense, then the real axis again between $-\pi/2$ and $-3\pi/2$ and finally cross the $e^{-3\eta} s_-$ saddle in the negative sense before terminating at $-3\pi/2$. Collecting these components, the connection formula is given by

$$-f_+ + (1 - e^{-2\eta})(f_- + e^\eta \sigma_-) \leftarrow y_2 \rightarrow -e^{-\eta} f_+ + e^{-\eta}(1 - e^{-2\eta})s_- \quad (6.42)$$

Comparing the incident f_+ term on the left with the transmitted f_+ term on the right, the transmission coefficient is again $T = e^{-\eta}$. The f_- term on the left is the reflected term, so $R_2 = -(1 - e^{-2\eta})$, and the s_- term on the right is the converted term, so $C_2 = -e^{-\eta}(1 - e^{-2\eta})$. Except for the conversion term again, this result is the same as the result from the Budden equation. The important difference between the Budden result and the results of the tunneling equation is that now it is possible to conserve energy since the energy neither reflected nor transmitted is converted.

To demonstrate this, we note that the tunneling equation has the conserved quantity

$$P = \psi''' \psi''^* + \psi''' \psi^* - \psi'' \psi'^* + \gamma \psi' \psi^* - \text{c.c.} \quad (6.43)$$

from which can be obtained the asymptotic expressions for each wave type,

$$\frac{P(s_\pm)}{2\pi i \lambda^2} = \pm 1 \quad \frac{P(f_\pm)}{2\pi i \lambda^2} = \mp(1 - e^{-2\eta})$$

so that the connection formula for solution y_2 ,

$$f_+ + R_2 f_- \leftarrow -y_2 \rightarrow T_2 f_+ + C_2 s_-$$

becomes

$$P(f_+) + R_2^2 P(f_-) = T_2^2 P(f_+) + C_2^2 P(s_-).$$

Using the asymptotic expressions and dividing by $P(f_+)$, this becomes the power conservation law,

$$R^2 + T^2 + \rho C^2 = 1 \quad (6.44)$$

with $\rho = (1 - e^{-2\eta})^{-1}$, and this expression is valid for either solution. This conservation law is a property of the tunneling equation, and its relevance to

Table 6.1. Tunneling equation connection formulas between asymptotic forms for large $|z|$ with $1 + \gamma > 0$.

$z \rightarrow -\infty$	y_n	$z \rightarrow \infty$
$e^\eta \sigma_-$	y_0	$e^\eta (f_+ - s_+ - f_- + s_-)$
f_-	y_1	$e^\eta f_- - e^\eta (1 - e^{-2\eta}) s_-$
$(1 - e^{-2\eta})(f_- + e^\eta \sigma_-) - f_+$	y_2	$-e^{-\eta} f_+ + e^{-\eta} (1 - e^{-2\eta}) s_-$
$f_- + e^\eta \sigma_-$	y_3	$e^\eta f_+ - e^\eta s_+ + e^{-\eta} s_-$
$f_- - e^{-\eta} \sigma_+$	y_4	$e^{-\eta} s_-$

power conservation must be independently shown by relating ψ and its derivatives to \mathbf{P} (fast wave) and \mathbf{T} (slow wave). Within the limits of the approximations made that led to the tunneling equation, it does correspond to power conservation.

A similar conserved quantity exists for equation (6.21) of the form

$$P = \psi''' \psi''^* - \lambda^2 \beta \psi' \psi^* - \text{c.c.} \quad (6.45)$$

but without any reflection or transmission, the results are trivial, indicating total mode conversion.

Problem 6.3.3. Conservation laws.

- (i) Prove that the quantities P in equations (6.43) and (6.45) are conserved (i.e. show that $P' = 0$ for each case).
- (ii) Evaluate the asymptotic forms of $P(f_\pm)$ and $P(s_\pm)$ from the expressions given by equations (6.40) and (6.36).
- (iii) Prove ρ is the same for solution y_1 .

6.3.2.7 Tunneling equation summary

Using similar methods, a third solution, y_3 , that represents an incident slow wave can be constructed which has a reflected slow-wave component and converted fast-wave components on both sides. The fourth solution, y_4 , includes an exponentially growing term to form a complete set of solutions. The connection formulas are summarized in table 6.1 and the reflection, transmission, and conversion coefficients for both amplitude and power are summarized in [table 6.2](#). A fifth solution that is not independent, since it is given by $y_0 = y_3 - y_1$, is added for convenience.

Problem 6.3.4. Connection formulas for the case $\gamma < -1$. Find the tables corresponding to tables 6.1 and 6.2 for the case with $\gamma < -1$. Note for this case that it generally occurs from the case where $\lambda^2 = -\lambda_0^2$ so that $z \rightarrow -z$

Table 6.2. Amplitude and energy coefficients for the tunneling equation with $1 + \gamma > 0$. For this case, $\rho = (1 - e^{-2\eta})^{-1}$.

Transmission	Reflection	Conversion
$T_1 = e^{-\eta}$ $ T_1 ^2 = e^{-2\eta}$	$R_1 = 0$ $ R_1 ^2 = 0$	$C_1 = -(1 - e^{-2\eta})$ $\rho C_1 ^2 = 1 - e^{-2\eta}$
$T_2 = e^{-\eta}$ $ T_2 ^2 = e^{-2\eta}$	$R_2 = -(1 - e^{-2\eta})$ $ R_2 ^2 = (1 - e^{-2\eta})^2$	$C_2 = -e^{-\eta}(1 - e^{-2\eta})$ $\rho C_2 ^2 = e^{-2\eta}(1 - e^{-2\eta})$
$T_3 = 0$ $ T_3 ^2 = 0$	$R_3 = -e^{-2\eta}$ $ R_3 ^2 = e^{-4\eta}$	$C_3^+ = -1$ $C_3^- = -e^{-\eta}$ $ C_3^+ ^2/\rho = 1 - e^{-2\eta}$ $ C_3^- ^2/\rho = e^{-2\eta}(1 - e^{-2\eta})$

brings us back to the basic form but now the phase and group velocities of the fast waves are in opposite directions.

Problem 6.3.5. The Wasow equation, equation (6.21) for $\lambda^2 > 0$.

- (i) Find the exact integral solution corresponding to equation (6.30).
- (ii) Find the end points in the k -plane and sketch four independent contours.
- (iii) Find the saddle points as $z \rightarrow \infty$ and as $z \rightarrow -\infty$.
- (iv) Find the saddle point contribution for each saddle point, then locate and label each saddle point on the k -planes for large positive z and large negative z , and indicate the crossing angles.
- (v) Determine which are incoming, outgoing, fast, slow, growing, decaying, etc.
- (vi) Find the contour that leads to equation (6.23).

6.3.3 Mode conversion examples

6.3.3.1 The second harmonic of the ion cyclotron frequency

In cold plasma theory, there is no interaction at the various cyclotron harmonics above the fundamental, and for $k_\perp = 0$ this interaction vanishes even in a hot plasma, but FLR effects do lead to interactions at each of the harmonics when $k_\perp \neq 0$. From chapter 4, the relevant dielectric tensor components are:

$$K_1 = 1 + \frac{\omega_{pi}^2 e^{-\lambda_i}}{\omega k_z v_i} \sum_{n=-\infty}^{\infty} \frac{n^2 I_n(\lambda_i)}{\lambda_i} Z(\zeta_n) \quad (6.46)$$

$$K_2 = \frac{i\omega_{pi}^2 e^{-\lambda_i}}{\omega k_z v_i} \sum_{n=-\infty}^{\infty} n [I_n(\lambda_i) - I'_n(\lambda_i)] Z(\zeta_n) - \frac{i\omega_{pi}^2}{\omega \omega_{ci}} \quad (6.47)$$

$$K_0 = \frac{\omega_i^2 e^{-\lambda_i}}{\omega k_z v_i} \sum_{n=-\infty}^{\infty} \lambda_i [I_n(\lambda_i) - I'_n(\lambda_i)] Z(\zeta_n) \quad (6.48)$$

where we have taken $\omega_{ce} \gg 2\omega_{ci} \sim \omega$, $\lambda_e \ll \lambda_i \ll 1$ so the electrons are taken to be cold, $\lambda_i = \frac{1}{2}k_{\perp}^2 \rho_{Li}^2$, and $\zeta_n = (\omega + n\omega_{ci})/k_z v_i$. To simplify the dispersion relation, we neglect electron inertia (and neglect electron Landau damping in the process), assuming $\kappa_3 \rightarrow \infty$, so the dispersion relation for the hot plasma from equation (4.255) is

$$(k_z^2 - \kappa_1)(k_z^2 - \kappa_1 - 2\kappa_0 + k_{\perp}^2) + \kappa_2^2 = 0. \quad (6.49)$$

Expanding about $\omega = 2\omega_{ci0}$, assuming that $|\zeta_n| \gg 1$ for all n except $n = -2$, and keeping only first order terms in λ_i , these tensor elements simplify to

$$\kappa_1 \simeq \frac{\omega^2}{V_A^2} \left[\frac{1}{1 - \omega^2/\omega_{ci}^2} + \frac{\lambda_i}{8} \frac{\omega}{k_z v_i} Z(\zeta_{-2}) \right] \quad (6.50)$$

$$\kappa_2 \simeq i \frac{\omega^2}{V_A^2} \left[\frac{\omega}{\omega_{ci}(1 - \omega^2/\omega_{ci}^2)} + \frac{\lambda_i}{8} \frac{\omega}{k_z v_i} Z(\zeta_{-2}) \right] \quad (6.51)$$

$$\kappa_0 \simeq - \frac{\omega^2}{V_A^2} \lambda_i \left[\frac{\omega^2}{\omega_{ci}^2} + \frac{1}{1 - \omega^2/\omega_{ci}^2} \right]. \quad (6.52)$$

We now let the magnetic field vary with x so that the resonance is localized and can be approached in space. Assuming that $\omega_{ci} = \omega_{ci0}(1 + x/L)$ where L is the scale length for the variation ($L=R_0$ in a toroidal field), then $\zeta_{-2} = -2(\omega/k_z v_i)x/L$. We keep only zero order terms, but assume that $\lambda_i L/x$ is of zero order as the ratio of two small terms. Making the further definition that $F \equiv -\zeta Z(\zeta)$, so that asymptotically $F \rightarrow 1$, the dispersion relation can be put into the form,

$$\left(p^2 + \frac{1}{3} - \frac{\beta_i L F}{4x} D^2 \right) \left(p^2 + \frac{1}{3} - \frac{\beta_i L F}{4x} D^2 + D^2 \right) - \left(\frac{2}{3} - \frac{\beta_i L F}{4x} D^2 \right)^2 = 0 \quad (6.53)$$

where $\beta_i = v_i^2/V_A^2$ is the ratio of the ion thermal pressure to the magnetic pressure and we have defined the wavenumbers normalized to the Alfvén speed by the relations $p = k_z V_A/\omega$ and $D = k_{\perp} V_A/\omega$. Rearranging equation (6.53) as a quadratic in D^2 , we find

$$D^4 - \left[2 \left(\frac{1}{3} - p^2 \right) + \left(\frac{1}{3} + p^2 \right) \frac{4x}{\beta_i L F} \right] D^2 + \left(\frac{1}{3} - p^2 \right) (1 + p^2) \frac{4x}{\beta_i L F} = 0. \quad (6.54)$$

At this point we identify the algebraic equation in k_{\perp} with a differential equation in x , the inverse of the previous analyses where we have identified an algebraic expression as resulting from a differential equation using the WKB

method. This introduces ambiguities, of course, since it is not immediately apparent (nor is it in fact true) that the differential operator associated with D operates only the field quantity E_y (if the magnetic field is taken to be in the z direction) since here D commutes with everything but a differential operator does not. Ignoring this detail for the moment, however, we let $k_\perp \rightarrow -i d/dx$ along with the variable change into dimensionless variables $z - z_0 = \mu x \omega / V_A$, so

$$y^{iv} + \left[\frac{2(\frac{1}{3} - p^2)}{\mu^2} + \frac{(\frac{1}{3} + p^2)4(z - z_0)V_A}{\beta_i L F \omega \mu^3} \right] y'' + \frac{(\frac{1}{3} - p^2)(1 + p^2)4(z - z_0)V_A}{\beta_i L F \omega \mu^5} y = 0 \quad (6.55)$$

and this is identical to equation (6.26) if we assume $F = 1$ and define

$$\begin{aligned} \lambda^2 &= \frac{2c(\frac{1}{3} + p^2)}{\omega_{pi} L \beta_i \mu^3} & \mu^2 &= \frac{(\frac{1}{3} - p^2)(1 + p^2)}{\frac{1}{3} + p^2} \\ \gamma &= -\lambda^2 z_0 = -2(\frac{1}{3} + p^2)/(1 + p^2) & \zeta_{-2} &= (z_0 - z)/\kappa \end{aligned} \quad (6.56)$$

where $\kappa = \mu \sqrt{\beta_i} k_z L$. The tunneling factor is

$$\eta = \frac{\pi}{4} \frac{\omega_{pi} L}{c} \frac{\mu^5}{(1 + p^2)^2} \beta_i \rightarrow \frac{\pi}{4} \frac{\omega_{pi} L}{c} \beta_i \quad \text{as } p \rightarrow 0. \quad (6.57)$$

Strictly speaking, this analysis is valid only in the limit $p \rightarrow 0$ since then $F \rightarrow 1$ and the ambiguities disappear. When $p \neq 0$, however, the tunneling equation with absorption may be written as

$$\psi^{iv} + \lambda^2 z \psi'' + (\lambda^2 z + \gamma) \psi = \lambda^2 (z - z_0) (1 - 1/F) (\psi'' + \psi) \quad (6.58)$$

and although the right-hand side does vanish as z^{-1} asymptotically, it vanishes identically only for $p = 0$. The localized absorption term on the right is thus connected to cyclotron absorption and gives a prescription for the modified coupling. This equation is only tractable numerically, but it has been proved analytically [79, 80] that the transmission is unaffected by absorption, so that equation (6.57) is valid for all p such that $\mu^2 > 0$, and that the reflection coefficient $R_1 = 0$ still and that $R_2 = -(1 - e^{-2\eta})e^{-\kappa^2}$ to high accuracy for the pure second harmonic case [73]. No analytic forms are apparent for C_1 and C_2 with absorption, but both approach zero exponentially as κ gets large.

Whenever mode conversion occurs, it is useful to identify the converted wave, and in this case it is the ion Bernstein wave described in section 4.4. There are Bernstein modes between all harmonics of both the electron and ion cyclotron frequencies, but these are typically heavily Landau damped unless k_z is small, meaning the wave must propagate nearly perpendicular to the direction of the magnetic field. Although the phase velocity is nearly across the field, the group

velocity for these waves is nearly parallel to the magnetic field. In most realistic plasmas, even the small deviations from the one-dimensional approximation made here are sufficient to couple k_z and k_{\perp} so that as k_{\perp} grows on the mode converted branch, the wave is typically electron Landau damped.

Problem 6.3.6. Tunneling equation with absorption. Beginning with the expressions in chapter 4, fill in the missing steps leading to equation (6.58).

6.3.3.2 The two-ion hybrid resonance

Since the concept of a pure single-ion species plasma is only an idealization of the real world, and since many interesting plasmas have more than one ion species, it is important to examine the effects of multiple ion species. The two-ion hybrid resonance (where in cold plasma, $S = 0$ between the two ion cyclotron frequencies) is the principal new effect, in addition of course to the new cyclotron resonance for each new species and its harmonics.

Since the inclusion of absorption effects prevents any analytical results anyway, we will ignore the effects of absorption by assuming $k_z = 0$. This is, in fact, consistent with the definition of the hybrid resonance, but there is still a resonance with $k_z \neq 0$ except that it is slightly shifted. This assumption allows us to always take the asymptotic forms of the plasma dispersion function, so that the plasma is effectively cold in the direction parallel to the magnetic field. We include FLR effects, however, through the inclusion of terms in λ_i and let $\lambda_e \rightarrow 0$. We also neglect electron inertia, so $\kappa_3 \rightarrow \infty$.

With these assumptions and approximations, and assuming that neither fundamental is at the harmonic of the other ion species (nondegenerate case), the relevant dielectric tensor elements may be written to first order in λ_i , $i = 1, 2$,

$$\kappa_1 = \frac{\omega^2}{c^2} \left[1 + \frac{\omega_{p1}^2(1 - \lambda_1)}{\omega_{c1}^2 - \omega^2} + \frac{\omega_{p2}^2(1 - \lambda_2)}{\omega_{c2}^2 - \omega^2} + \frac{\omega_{p1}^2 \lambda_1}{4\omega_{c1}^2 - \omega^2} + \frac{\omega_{p2}^2 \lambda_2}{4\omega_{c2}^2 - \omega^2} \right] \quad (6.59)$$

$$\kappa_2 = i \frac{\omega^2}{c^2} \left[\frac{\omega \omega_{p1}^2}{\omega_{c1}(\omega_{c1}^2 - \omega^2)} + \frac{\omega \omega_{p2}^2}{\omega_{c2}(\omega_{c2}^2 - \omega^2)} \right] \quad (6.60)$$

where the electron term has been incorporated into the expression for κ_2 and neglected in κ_1 . The majority species is species 1, and the minority species is species 2 such that $\alpha \equiv \omega_{p2}^2/\omega_{p1}^2 < 1$ which is effectively the density ratio. We choose $x = 0$ at the minority fundamental, so that $\omega = \omega_{c20}$, and the hybrid resonance occurs where $\kappa_1(x_R) = 0$. The variation of the magnetic field is given by $\omega_{ci} = \omega_{ci0}/(1+x/L)$ with the gradient normal to the field direction. The FLR terms are required to resolve the resonance since κ_1 is already a first order quantity in λ_i . For κ_2 , however, the first order terms in λ_i are unimportant, but the first order terms in x/L determine the cutoff, so they will be kept. Since the location of the two-ion hybrid resonance depends on both the concentration of each ion

species and on their charge-to-mass ratio, we define $\mu = \omega_{c2}/\omega_{c1} = q_2 m_1/q_1 m_2$ for the mass ratio. Defining the temperature ratio by $\theta = T_2/T_1$, the dielectric tensor elements may be approximated by

$$\kappa_1 \simeq \frac{\omega_{p1}^2}{c^2} \left[\frac{(1 - \lambda_1)}{1/\mu^2(1 + x/L)^2 - 1} + \frac{\alpha(1 - \lambda_2)}{1/(1 + x/L)^2 - 1} + \frac{\lambda_1}{4/\mu^2(1 + x/L)^2 - 1} + \frac{\alpha\lambda_2}{4/(1 + x/L)^2 - 1} \right] \quad (6.61)$$

$$i\kappa_2 = \frac{\omega_{p1}^2}{c^2} \left[\frac{\mu(1 + x/L)}{1/\mu^2(1 + x/L)^2 - 1} + \frac{\alpha(1 + x/L)}{1/(1 + x/L)^2 - 1} \right] \quad (6.62)$$

where $\lambda_1 = k_\perp^2 \kappa T_1/m_1 \omega_{c2}^2$ and $\lambda_2 = (q_1 \theta / q_2 \mu) \lambda_1$. The two-ion hybrid resonance occurs at $x = x_R$ where $\kappa_1 = 0$ with $\lambda_1 = \lambda_2 = 0$ (cold plasma), so we find first that

$$\left(1 + \frac{x_R}{L}\right)^2 = \frac{1 + \alpha/\mu^2}{1 + \alpha} \equiv \epsilon$$

with the result that the resonance is located at

$$x_R/L = \sqrt{\epsilon} - 1. \quad (6.63)$$

It follows from equation (6.63) that if $\mu > 1$ so that $\epsilon < 1$ that $x_R < 0$, while for $\mu < 1$ so that $\epsilon > 1$, $x_R > 0$ so that the resonance may occur on either side of the minority fundamental, and switches sides if the minority and majority are interchanged.

If we now linearize in x/L , expanding about the resonance location so that

$$(1 + x/L)^2 \sim \epsilon(1 + \delta)$$

then $\delta = 2(x - x_R)/\sqrt{\epsilon}L$. The linearized dielectric tensor elements may then be expressed as

$$\kappa_1 = \frac{\omega_{p1}^2}{c^2} \left[A\delta - \frac{k_\perp^2 c^2}{\omega_{p1}^2} B \right] \quad (6.64)$$

$$i\kappa_2 = \frac{\omega_{p1}^2}{c^2} (C + D\delta) \quad (6.65)$$

where

$$A = \chi_1 + \alpha\chi_2$$

$$B = \frac{3\beta_1 \mu^2 \epsilon^2}{2(1 - \mu^2 \epsilon)(4 - \mu^2 \epsilon)} + \frac{3\beta_2 \epsilon^2}{2(1 - \epsilon)(4 - \epsilon)}$$

$$C = \epsilon^{3/2} \left[\frac{\mu^3}{1 - \mu^2 \epsilon} + \frac{\alpha}{1 - \epsilon} \right]$$

$$\begin{aligned} D &= \mu\chi_1 + \alpha\chi_2 + C/2 \\ \chi_1 &= \mu^2\epsilon/(1 - \mu^2\epsilon)^2 \\ \chi_2 &= \epsilon/(1 - \epsilon)^2 \end{aligned}$$

where $\beta_i = 2\mu_0 n_i k T_i / B_0^2$ are the ratios of the plasma pressures to the magnetic pressure.

The dispersion relation with $\kappa_3 \rightarrow \infty$ and $k_z = 0$ is

$$\kappa_1(\kappa_1 - k_{\perp}^2) + \kappa_2^2 = 0$$

which leads to a quadratic in $k_p^2 \equiv k_{\perp}^2 c^2 / \omega_{p1}^2$,

$$B k_p^4 - \delta A k_p^2 - C(C + 2D\delta) = 0 \quad (6.66)$$

where only the dominant terms have been kept. The character of the solutions of this quadratic equation changes dramatically when $B = 0$, which occurs when $\theta = \theta_c \equiv m_2(4 - \epsilon)/m_1(4/\mu^2 - \epsilon)$. Whenever θ is in the vicinity of θ_c , some of the previous approximations become suspect. An example is given in figure 6.9 where the first two cases have minority ${}^3\text{He}$ in D with $\theta < \theta_c$ in figure 6.9(a) and $\theta > \theta_c$ in figure 6.9(b). In each case, the majority density is $n_1 = 10^{20}/\text{m}^3$, $n_2/n_1 = 0.1$, the magnetic field is 1.0 T, and $T_1 = 1.0 \text{ keV}$. The last two cases reverse minority and majority, with $\theta < \theta_c$ in figure 6.9(c) and $\theta > \theta_c$ in figure 6.9(d). Along with the solutions of equation (6.66), which are dashed, solutions with exact Bessel function expressions through $n = 3$ without linearization are shown by the full curves. It is evident that in addition to the shift of the resonance by reversing the minority/majority ratio and the change of topology from the change in θ , there are significant deviations between the linearized and nearly exact expressions, especially when θ is close to θ_c . For example, with $\theta = 4$ ($\theta/\theta_c = 1.16$), the upper branch of figure 6.9(b) still curves back in the nearly exact case, as in figure 6.9(a), while the lower branch does not. It is interesting to note that if one were to use minority rf heating, where most of the wave energy goes to the minority species, the increasing minority temperature may change the topology of the mode conversion process as θ ranges from below θ_c to above θ_c in the $\mu > 1$ case (figures 6.9(a) and (b)), but not for the $\mu < 1$ case since $\theta_c < 1$.

Equation (6.66) is transformed into a differential equation by letting $k_{\perp} \rightarrow -i(d/dx)$, becoming the tunneling equation with the substitution $z - z_0 = \kappa x/L$ (where κ has the same sign as B which is positive for $(\mu - 1)(\theta/\theta_c - 1) > 0$ and negative for $(\mu - 1)(\theta/\theta_c - 1) < 0$) and

$$\lambda^2 = \frac{c}{\omega_{p1} L} \frac{A^{5/2}}{\sqrt{2\epsilon}|B|(CD)^{3/2}} \quad (6.67)$$

$$\gamma = -A^2/4BD^2 \quad (6.68)$$

$$\kappa^2 = -\frac{\omega_{p1}^2 L^2}{c^2} \frac{2CD}{A} > 0. \quad (6.69)$$

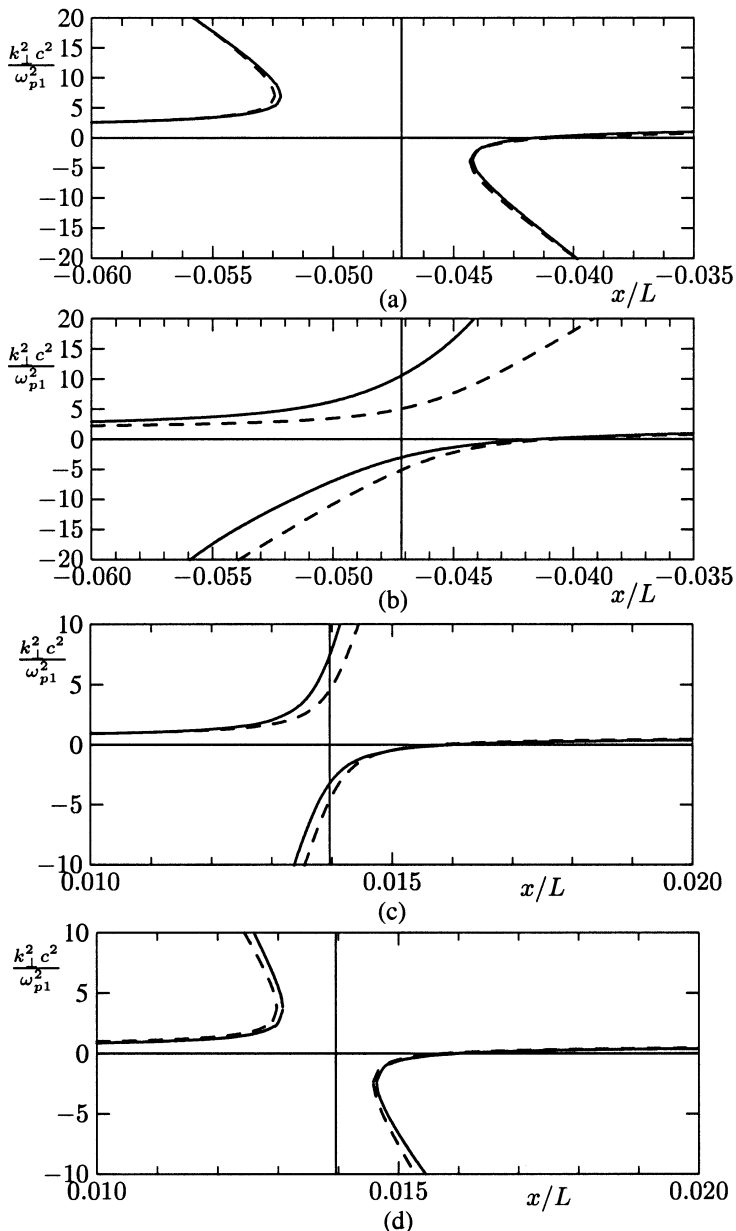


Figure 6.9. Two-ion hybrid, with (a) minority ${}^3\text{He}$ in D with $\theta = 2$, (b) minority ${}^3\text{He}$ in D with $\theta = 5$, (c) minority D in ${}^3\text{He}$ with $\theta = 0.25$, (d) minority D in ${}^3\text{He}$ with $\theta = 0.5$. The full curves include higher order terms in x and λ_i while the dashed curves are linear in x and first order in λ_i . (From [81].)

Since typically $|\gamma| \gg 1$ for the two-ion hybrid resonance, the tunneling factor is given by

$$\eta = \frac{\pi\gamma}{2\lambda^2} \simeq \frac{\pi\omega_{p1}L}{4c} \left[\frac{(-C)^3\epsilon}{2AD} \right]^{1/2}. \quad (6.70)$$

We note that the transmission coefficient is independent of the temperature ratio, θ , so the topological change does not affect the transmission. With γ large in this problem, varying as $1/\beta_1$, the Budden tunneling factor is accurate in this example, while it failed badly in the previous example where $\gamma < 0$.

Whereas the tunneling factor for the second harmonic of the ion cyclotron is frequently small, being proportional to β_i , so that little energy is absorbed or converted for low to moderate temperature plasmas, the two-ion hybrid resonance tunneling factor is typically large. Furthermore, except for the minority species case where the resonance is close to the fundamental of the minority species, there is little absorption, so the mode-converted wave is strongly excited. Because of the difficulty of detecting the mode converted wave in high temperature plasmas, the experimental verification of this aspect of mode conversion theory went unresolved for many years, but wave scattering experiments eventually detected the slow wave and from the measured dispersion relation were even able to determine the ion temperature [82].

Problem 6.3.7. Two-ion hybrid resonance tunneling—budden equation. Since the Budden equation is appropriate for the two-ion hybrid tunneling problem, one may use cold plasma equations in a general form to estimate the tunneling. Show that the tunneling factor from the Budden equation may be represented by $\eta = \pi k_0 a / 2$ where the mean wavenumber k_0 and layer width a are given by

$$k_0^2 = \frac{\omega^2 \frac{d}{dx}[(L - n_{||}^2)(R - n_{||}^2)]|_0}{c^2 \frac{d}{dx}(S - n_{||}^2)|_0}$$

$$a = \frac{-(L - n_{||}^2)(R - n_{||}^2)|_0}{\frac{d}{dx}[(L - n_{||}^2)(R - n_{||}^2)]|_0}$$

where the resonance is defined to occur at $x = 0$. (See [83] for applications.)

6.3.3.3 The electron cyclotron fundamental and harmonic

For the cold plasma, the ordinary wave does not have any dependence on the magnetic field and the extraordinary wave experiences the upper hybrid resonance but no cyclotron resonances. For the hot plasma, however, the ordinary wave does experience a resonance at the cyclotron fundamental and the extraordinary wave experiences a resonance at the electron cyclotron harmonic through the finite Larmor orbit terms of equations (4.184)–(4.187). We shall examine these two

examples of mode conversion and tunneling separately, but both originate from the hot plasma dispersion relation with $k_z = 0$ which may be factored as

$$(k_{\perp}^2 - \kappa_3)(\kappa_1^2 + \kappa_2^2 + 2\kappa_0\kappa_1 - \kappa_1 k_{\perp}^2) = 0. \quad (6.71)$$

The first factor is the O -mode dispersion relation and the second factor gives the X -mode dispersion relation.

6.3.3.4 The ordinary mode at the electron cyclotron fundamental

For this case, we assume $\omega \simeq \omega_{ce} > \omega_{pe}$ with a variation in magnetic field characterized by $\omega_{ce} = \omega(1 + x/L)$. With $k_z = 0$, then the quantity $\zeta_n Z'(\zeta_n)/k_z v_e = 1/(\omega + n\omega_{ce})$. The x -variation leads to $\omega - \omega_{ce} = -\omega x/L$ so through second order in λ_e , the dispersion relation $\kappa_3 = k_{\perp}^2$ is given by

$$\begin{aligned} \kappa_3 &\simeq \frac{\omega^2}{c^2} - \frac{\omega_{pe}^2}{c^2} e^{-\lambda_e} \left[I_0(\lambda_e) + I_1(\lambda_e) \left(\frac{1}{2} - \frac{L}{x} \right) - \frac{2}{3} I_2(\lambda_e) \right] \\ &\simeq \frac{\omega^2 - \omega_{pe}^2}{c^2} + \frac{\omega_{pe}^2}{c^2} \left(\frac{\lambda_e L}{2x} - \frac{\lambda_e^2 L}{2x} \right) = k_{\perp}^2 \end{aligned}$$

where the ions are neglected, $\lambda_e \ll 1$ and $L/x \gg 1$. If we multiply by x/L and use $\lambda_e = \frac{1}{2}k_{\perp}^2\rho_{Le}^2$, this becomes a quadratic in k_{\perp}^2 , namely,

$$\frac{\omega_{pe}^2 \rho_{Le}^4}{8c^2} k_{\perp}^4 + \left(\frac{x}{L} - \frac{\omega_{pe}^2 \rho_{Le}^2}{4c^2} \right) k_{\perp}^2 - \left(\frac{\omega^2 - \omega_{pe}^2}{c^2} \right) \frac{x}{L} = 0$$

which we convert to a differential equation by letting $k_{\perp} \rightarrow -i(d/dx)$,

$$y^{iv} + \left(\frac{2}{\rho_{Le}^2} - \frac{8c^2}{\omega_{pe}^2 \rho_{Le}^4} \frac{x}{L} \right) y'' - \frac{8(\omega^2 - \omega_{pe}^2)}{\omega_{pe}^2 \rho_{Le}^4} \frac{x}{L} y = 0. \quad (6.72)$$

If we make the usual variable change here to cast this into the form of the tunneling equation, then we find $\lambda^2 < 0$, so we instead let $k_0 x = z_0 - z$ so the positive and negative axes are reversed. Then we obtain the usual tunneling equation with

$$\lambda^2 = \frac{8c^2}{\omega_{pe}^2 \rho_{Le}^4 L k_0^3} = \frac{8(\omega^2 - \omega_{pe}^2)}{\omega_{pe}^2 \rho_{Le}^4 L k_0^5} \quad \text{so} \quad k_0^2 = \frac{\omega^2 - \omega_{pe}^2}{c^2} \quad (6.73)$$

$$\gamma = -\lambda^2 z_0 = -\frac{2}{k_0^2 \rho_{Le}^2} \quad (6.74)$$

and thus the tunneling factor is given by

$$\eta = \frac{\pi}{2} \left| \frac{1 + \gamma}{\lambda^2} \right| \simeq \frac{\pi}{8} \frac{\omega_{pe}^2 \rho_{Le}^2}{c^2} k_0 L \quad (6.75)$$

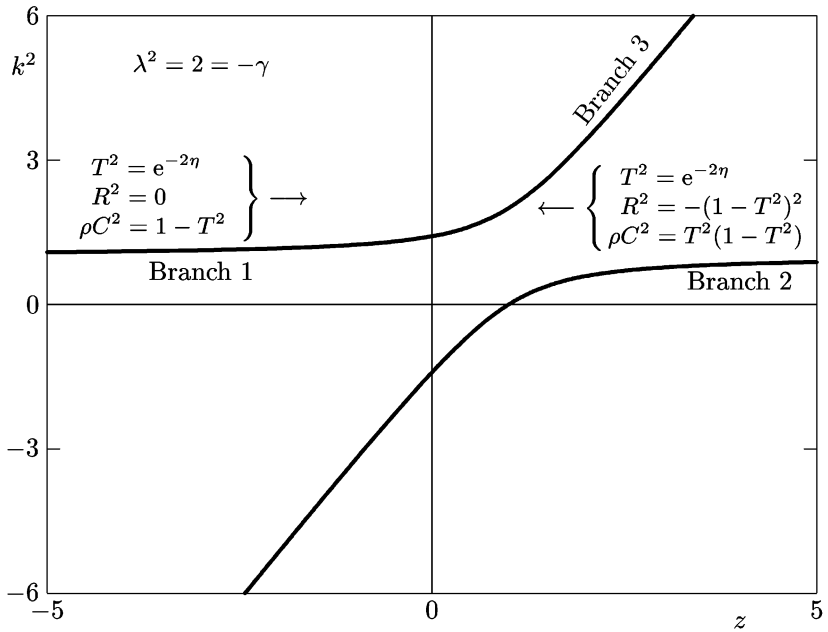


Figure 6.10. Dispersion relation for tunneling equation when $1 + \gamma < 0$.

since $1 + \gamma < 0$ as $\gamma \sim -1/\lambda_e$. In this case, the converted wave propagates through the resonance layer rather than back from it. The dispersion curve is illustrated in figure 6.10 and the connection formulas are given in [table 6.3](#) (where $y_0 = e^{-2\eta}y_3 - y_2$ in this case) and the coupling coefficients in [table 6.4](#). For this case, we note that there is still no reflection from the resonance side, and that the group velocity directions have changed since $x \propto -z$. It may appear that there is no turning point in this problem since the group velocity does not appear to vanish anywhere, but mathematically the turning point is off the real axis and all the same couplings still occur.

6.3.3.5 The extraordinary mode at the electron cyclotron harmonic

In the hot plasma dispersion relation for the X -mode, we need expressions for κ_0 , κ_1 and κ_2 , but the first order terms in λ_e are not resonant at $\omega = 2\omega_{ce}$ in κ_0 so we will examine only the two dominant components. Again using $k_z = 0$ so that $Z(\zeta_n)/k_z v_e = -1/(\omega + n\omega_{ce})$, and letting $2\omega_{ce} = \omega(1 + x/L)$ so that $\omega - 2\omega_{ce} = -\omega x/L$, the tensor components may be represented by

$$\kappa_1 \simeq \frac{\omega^2}{c^2} \left[1 - \alpha \left(\frac{4}{3} - \frac{\lambda_e L}{2x} \right) \right] \quad (6.76)$$

Table 6.3. Tunneling equation connection formulas between asymptotic forms for large $|z|$ and $1 + \gamma < 0$.

$z \rightarrow -\infty$	y_n	$z \rightarrow \infty$
$e^{-\eta}\sigma_-$	y_0	$f_+ - f_- + e^{-\eta}(s_- - s_+)$
$e^\eta f_+$	y_1	$f_+ + e^\eta(1 - e^{-2\eta})s_+$
$e^{-\eta}f_- - e^{-\eta}(1 - e^{-2\eta})\sigma_-$	y_2	$f_- - (1 - e^{-2\eta})(f_+ - e^{-\eta}s_+)$
$e^\eta f_- + e^{-\eta}\sigma_-$	y_3	$f_+ + e^\eta s_- - e^{-\eta}s_+$
$e^\eta(f_+ - \sigma_+)$	y_4	$e^\eta s_+$

Table 6.4. Amplitude and energy coefficients for the tunneling equation with $1 + \gamma < 0$. For this case, $\rho = (1 - e^{-2\eta})^{-1}$.

Transmission	Reflection	Conversion
$T_1 = e^{-\eta}$	$R_1 = 0$	$C_1 = 1 - e^{-2\eta}$
$ T_1 ^2 = e^{-2\eta}$	$ R_1 ^2 = 0$	$\rho C_1 ^2 = 1 - e^{-2\eta}$
$T_2 = e^{-\eta}$	$R_2 = -(1 - e^{-2\eta})$	$C_2 = e^{-\eta}(1 - e^{-2\eta})$
$ T_2 ^2 = e^{-2\eta}$	$ R_2 ^2 = (1 - e^{-2\eta})^2$	$\rho C_2 ^2 = e^{-2\eta}(1 - e^{-2\eta})$
$T_3 = 0$	$R_3 = -e^{-2\eta}$	$C_3^+ = e^{-\eta}$
$ T_3 ^2 = 0$	$ R_3 ^2 = e^{-4\eta}$	$C_3^- = 1$
		$ C_3^+ ^2/\rho = e^{-2\eta}(1 - e^{-2\eta})$
		$ C_3^- ^2/\rho = 1 - e^{-2\eta}$

$$\kappa_2 = i\alpha \frac{\omega^2}{c^2} \left(\frac{2}{3} - \frac{\lambda_e L}{2x} \right) \quad (6.77)$$

where $\alpha = \omega_{pe}^2/\omega^2$ and $\omega_{ce} = \omega/2$ except in the resonant second harmonic term. The dispersion relation is then

$$k_\perp^2 = \frac{\omega^2}{c^2} \frac{RL}{S} = \frac{\omega^2}{c^2} \frac{[1 - \alpha(2 - \lambda_e L/x)](1 - 2\alpha/3)}{1 - \alpha(\frac{4}{3} - \lambda_e L/2x)} \quad (6.78)$$

which can be rearranged into a quadratic in k_\perp^2 as

$$\begin{aligned} k_\perp^4 - & \left[2\frac{\omega^2}{c^2} \left(1 - \frac{2\alpha}{3} \right) - \left(\frac{4\alpha}{3} \right) \frac{4x}{\alpha \rho_{Le}^2 L} \right] k_\perp^2 \\ & - (1 - 2\alpha) \left(1 - \frac{2\alpha}{3} \right) \frac{4\omega^2 x}{\alpha \rho_{Le}^2 c^2 L} = 0. \end{aligned} \quad (6.79)$$

This can be converted into a fourth-order differential equation in the usual way and with variable change $k_0x = z_0 - z$, into the tunneling equation with

$$\lambda^2 = \frac{4(3 - 4\alpha)}{3\alpha\rho_{Le}^2 L k_0^3} = \frac{(1 - 2\alpha)(3 - 2\alpha)4\omega^2}{3\alpha\rho_{Le}^2 c^2 L k_0^5}$$

so

$$\begin{aligned} k_0^2 &= \frac{\omega^2(1 - 2\alpha)(3 - 2\alpha)}{c^2(3 - 4\alpha)} \\ \lambda^2 z_0 &= \frac{2(3 - 4\alpha)}{3(1 - 2\alpha)} = -\gamma \end{aligned} \quad (6.80)$$

where $1 + \gamma < 0$ for $\alpha < 1/2$ ($\alpha = 1/2$ is the $R = 0$ cutoff), so that the tunneling factor is given by

$$\eta = \frac{\pi}{2} \left| \frac{1 + \gamma}{\lambda^2} \right| = \frac{\pi}{2} \left[\frac{(3 - 2\alpha)\omega_{pe}\rho_{Le}}{(3 - 4\alpha)2c} \right]^2 k_0 L. \quad (6.81)$$

This dispersion relation is qualitatively the same as for the O -mode at fundamental resonance, since the converted wave again converts through the layer rather than convert back from the resonance layer.

Problem 6.3.8. X-mode tunneling. When $3/4 < \alpha < 3/2$ between the $S = 0$ upper hybrid resonance and the $L = 0$ cutoff, show that this corresponds to the $\gamma > -1$ case for the X-mode at the harmonic resonance.

6.3.4 Conservation of energy

The conservation of energy in inhomogeneous plasmas is much more difficult to establish than it is for uniform plasmas. While the various mode conversion equations suggest that energy is conserved and that all incident wave energy which is neither transmitted nor reflected is converted, it cannot be proved for any of the previous examples since the conserved quantities of equations (6.43) and (6.45) are not identical to the conservation of energy. This is due to the fact that for the slow waves, their primary energy content is in their kinetic flux rather than their Poynting flux, although the fast-wave energy flux terms can be related to Poynting's vector.

In order to get the kinetic flux correct for the slow wave, Kuehl [84] demonstrated that the relevant fourth order equation had to include the odd order derivatives in the coupled wave equation which was derived directly from the Vlasov equations without first taking the Fourier transform. This method eliminates the problem we identified earlier where the inverse Fourier transform left ambiguous whether the derivatives acted only on the field variables or also on the equilibrium variables. In order to get the energy content correct, it was demonstrated that the derivatives of the equilibrium quantities are crucial. We

will show first a specific example where the correct form of the coupled wave equation is derived for tunneling at the ion cyclotron harmonic [85], and then calculate the appropriate expression for the kinetic and electromagnetic flux as a special case of a more general method due to Colestock and Kashuba [86].

6.3.4.1 Direct integration of the Vlasov equations

For this problem, we break the distribution function into zero and first order quantities, assuming the zero order distribution function is isotropic (which means we neglect drift velocities), and we assume all equilibrium quantities are uniform in the z -direction, which is the direction of \mathbf{B}_0 , and in the y -direction which is perpendicular both to the magnetic field and its gradient, which is in the x -direction. In this case, the zero order equation,

$$v_x \frac{\partial f_0}{\partial x} + \omega_{ci} \mathbf{v} \times \hat{\mathbf{e}}_z \cdot \nabla_v f_0 = 0$$

is satisfied identically. The first order equation, assuming $\exp(ikz - \omega t)$ dependence, is given by

$$-i(\omega - kv_z) f_1 + v_x \frac{\partial f_1}{\partial x} + \omega_{ci} \left(v_y \frac{\partial f_1}{\partial v_x} - v_x \frac{\partial f_1}{\partial v_y} \right) = \frac{2qf_0}{m_i v_i^2} (v_x E_x + v_y E_y) \quad (6.82)$$

where $v_i^2 = 2\kappa T_i / m_i$ and f_0 is Maxwellian. Changing variables to $v_x = v_\perp \cos \phi$ and $v_y = v_\perp \sin \phi$, equation (6.82) becomes

$$\frac{\partial f_1}{\partial \phi} + i \left(\frac{\omega - kv_z}{\omega_{ci}} \right) f_1 - \frac{v_\perp \cos \phi}{\omega_{ci}} \frac{\partial f_1}{\partial x} = -\frac{2v_\perp f_0}{v_i^2} \left(\frac{\cos \phi E_x + \sin \phi E_y}{B_0} \right) \quad (6.83)$$

which may be integrated at once to

$$f_1 = e^{-i\Omega\phi} \int^\phi e^{i\Omega\phi'} \left[\frac{v_\perp \cos \phi'}{\omega_{ci}} \frac{\partial f_1}{\partial x} - \frac{2v_\perp f_0}{v_i^2} \left(\frac{\cos \phi' E_x + \sin \phi' E_y}{B_0} \right) \right] d\phi' \quad (6.84)$$

with $\Omega = (\omega - kv_z)/\omega_{ci}$. This is an integral equation, and we will solve it by successive approximation, expanding f_1 in the series,

$$f_1 = f_1^{(0)} + \frac{v_\perp}{\omega_{ci}} f_1^{(1)} + \left(\frac{v_\perp}{\omega_{ci}} \right)^2 f_1^{(2)} + \dots$$

and we will keep only through second order. Formally, the expansion appears divergent, since v_\perp is an unbounded variable of integration, but we shall only consider integrals over a Maxwellian velocity distribution as in section 4.3.4, so the real expansion parameter is the mean Larmor radius, $\langle v_\perp \rangle / \omega_{ci}$, which is presumed to be small.

Inside the integrand, the $\partial f_1 / \partial x$ term is already first order, so this term is represented adequately by zero and first order terms as

$$\frac{\partial f_1}{\partial x} \simeq \frac{\partial f_1^{(0)}}{\partial x} + v_{\perp} \frac{\partial}{\partial x} \left(\frac{f_1^{(1)}}{\omega_{ci}} \right).$$

Doing the various integrals, the results are:

$$f_1^{(0)} = \frac{i q v_{\perp} f_0}{m_i v_i^2} \left[\frac{(E_x - i E_y) e^{i\phi}}{\omega + \omega_{ci} - k v_z} + \frac{(E_x + i E_y) e^{-i\phi}}{\omega - \omega_{ci} - k v_z} \right] \quad (6.85)$$

$$f_1^{(1)} = \frac{\omega_{ci} q v_{\perp} f_0}{2 m_i v_i^2} \left[\left(\frac{e^{2i\phi}}{\omega + 2\omega_{ci} - k v_z} + \frac{1}{\omega - k v_z} \right) \frac{\partial}{\partial x} \left(\frac{E_x - i E_y}{\omega + \omega_{ci} - k v_z} \right) + \left(\frac{e^{-2i\phi}}{\omega - 2\omega_{ci} - k v_z} + \frac{1}{\omega - k v_z} \right) \frac{\partial}{\partial x} \left(\frac{E_x + i E_y}{\omega - \omega_{ci} - k v_z} \right) \right] \quad (6.86)$$

$$f_1^{(2)} = \frac{\omega_{ci}^3 q v_{\perp} f_0}{4 i m_i v_i^2} \left(\frac{e^{-i\phi}}{\omega - \omega_{ci} - k v_z} + \frac{e^{-3i\phi}}{\omega - 3\omega_{ci} - k v_z} \right) \times \frac{\partial}{\partial x} \left[\frac{1}{\omega_{ci}(\omega - 2\omega_{ci} - k v_z)} \frac{\partial}{\partial x} \left(\frac{E_x + i E_y}{\omega - \omega_{ci} - k v_z} \right) \right] \quad (6.87)$$

where only the resonant terms ($\omega \simeq 2\omega_{ci}$) are kept in $f_1^{(1)}$ in going to second order.

The average velocities are obtained by integrating over ϕ , v_{\perp} , and v_z according to

$$\begin{Bmatrix} \langle v_x \rangle \\ \langle v_y \rangle \end{Bmatrix} = \int_0^{2\pi} d\phi \int_0^\infty v_{\perp} dv_{\perp} \int_{-\infty}^\infty dv_z f_1 \begin{Bmatrix} \cos \phi \\ \sin \phi \end{Bmatrix}.$$

The velocity expansion is similar to the expansion of f_1 , namely

$$\langle v \rangle = \langle v^{(0)} \rangle + \rho_L \langle v^{(1)} \rangle + \rho_L^2 \langle v^{(2)} \rangle + \dots$$

with $\rho_L = v_i / \omega_{ci}$, so that to zero order,

$$\begin{Bmatrix} i \langle v_x^{(0)} \rangle \\ \langle v_y^{(0)} \rangle \end{Bmatrix} = \frac{nq}{2mkv_i} \left[Z(\zeta_1)(E_x - i E_y) + \begin{Bmatrix} 1 \\ -1 \end{Bmatrix} Z(\zeta_{-1})(E_x + i E_y) \right] \quad (6.88)$$

where $\zeta_n = (\omega + n\omega_{ci})/kv_i$ and $Z(\zeta_n)$ is the plasma dispersion function. The first order terms do not contribute to the final result, and for the second order terms, only the resonant terms are kept and the kv_z terms will be dropped except for the $\omega - 2\omega_{ci} - kv_z$ term, since only harmonic damping will be significant. With these restrictions, the second order term in equation (6.87) can be integrated over

velocities to obtain

$$-\text{i}\langle v_x^{(2)} \rangle = \langle v_y^{(2)} \rangle = \frac{nq}{4mkv_i} \left(\frac{\omega_{ci}^2}{\omega - \omega_{ci}} \right) \frac{\partial}{\partial x} \left[\frac{Z(\zeta)}{\omega_{ci}} \frac{\partial}{\partial x} \left(\frac{E_x + \text{i}E_y}{\omega - \omega_{ci}} \right) \right]$$

where now we have replaced $\zeta_{-2} \rightarrow \zeta$ since it is the only remaining argument of the plasma dispersion function. Using the magnetic field variation $2\omega_{ci} = \omega(1 + x/L)$, then $\zeta = -\omega x/Lkv_i$ and the second order average becomes

$$\begin{aligned} -\text{i}\langle v_x^{(2)} \rangle = \langle v_y^{(2)} \rangle &= \frac{nq}{4mkv_i} \\ &\times \left[Z(\zeta)(E_x'' + \text{i}E_y'') - \frac{\omega}{kv_i} Z'(\zeta) \left(\frac{E'_x + \text{i}E'_y}{L} + \frac{E_x + \text{i}E_y}{L^2} \right) \right] \end{aligned}$$

where at this final stage, terms of order x/L have been neglected after the derivatives were taken.

The results of this expansion can be represented either as a current or as an equivalent dielectric tensor. Writing the result as dielectric tensor components, the result is

$$K_1 = 1 + \frac{\omega_{pi}^2}{\omega_{ci}^2 - \omega^2} + \frac{\omega_{pi}^2}{4\omega_{ci}^2} \frac{Z'(\zeta)}{k^2 L^2} - \frac{\omega_{pi}^2 \rho_L^2}{4\omega k v_i} \frac{d}{dx} Z(\zeta) \frac{d}{dx} \quad (6.89)$$

$$K_2 = \frac{\text{i}\omega \omega_{pi}^2}{\omega_{ci}(\omega_{ci}^2 - \omega^2)} + \frac{\text{i}\omega_{pi}^2}{4\omega_{ci}^2} \frac{Z'(\zeta)}{k^2 L^2} - \frac{\text{i}\omega_{pi}^2 \rho_L^2}{4\omega k v_i} \frac{d}{dx} Z(\zeta) \frac{d}{dx} \quad (6.90)$$

where now the dielectric tensor elements are operators due to the nonlocal nature of the dielectric tensor. The wave equation then may be written as

$$\left(K_1 - \frac{k^2 c^2}{\omega^2} \right) E_x + K_2 E_y = 0 \quad (6.91)$$

$$-K_2 E_x + \left(K_1 - \frac{k^2 c^2}{\omega^2} + \frac{c^2}{\omega^2} \frac{d^2}{dx^2} \right) E_y = 0. \quad (6.92)$$

If K_1 and K_2 commute, then this may be written as an equation in E_y only as

$$\left(K_1 - \frac{k^2 c^2}{\omega^2} \right) \left(K_1 - \frac{k^2 c^2}{\omega^2} + \frac{c^2}{\omega^2} \frac{d^2}{dx^2} \right) E_y + K_2^2 E_y = 0. \quad (6.93)$$

Since the commutator is proportional to the quantity $(d/dx)(K_2 - \text{i}K_1)$ which involves taking only the cold plasma terms to be constant, we assume equation (6.93) to be the relevant equation. Using the previous definitions, the

energy-conserving tunneling equation becomes

$$\frac{d}{dx} \left[Z(\zeta) \frac{d^3 E_y}{dx^3} \right] + \left[\frac{16(\frac{1}{3} + p^2)}{\rho_L^2} \frac{k v_i}{\omega} + \frac{1}{L} \frac{dZ(\zeta)}{dx} \right] \frac{d^2 E_y}{dx^2} + \frac{2\omega^2(\frac{1}{3} - p^2)}{V_A^2} \times \left\{ \frac{d}{dx} \left[Z(\zeta) \frac{dE_y}{dx} \right] + \left[\frac{8(1 + p^2)}{\rho_L^2} \frac{k v_i}{\omega} + \frac{1}{L} \frac{dZ(\zeta)}{dx} \right] E_y \right\} = 0 \quad (6.94)$$

where $p = k V_A / \omega$ as before. This equation now has odd order terms, and it is clear that even as $k \rightarrow 0$ it does not reduce to the standard tunneling equation. The fields associated with this equation, however, can be shown to conserve energy, as shown in the next section. If $Z(\zeta)$ were treated as a constant, as is effectively assumed in the Fourier transforms which led to the tunneling equation with only even order terms, this would reduce to that case and the standard tunneling equation as $k \rightarrow 0$. This more complicated equation can only be treated numerically, however, even as $k \rightarrow 0$, with the conclusion that the results are substantially identical to those obtained from the corresponding equation with only even order terms in the transmission, reflection, and conversion coefficients, but that the asymptotic electric fields are significantly different for the slow wave and the total wave fields and absorption profiles change in the coupling region.

Problem 6.3.9. The energy-conserving tunneling equation. Let $k \rightarrow 0$ in equation (6.94) and then:

- (i) Show that the odd order terms persist.
- (ii) Change to the dimensionless variables of equation (6.56) and use the normalized scale length $\ell = \mu\omega L / V_A$.
- (iii) Eliminate the third derivative term by letting $E_y = u\Phi$ and choosing u so that the third derivative term vanishes.
- (iv) Find the asymptotic form of the equation for Φ (neglect terms now with coefficients that vanish asymptotically), and show that one odd order term persists.
- (v) Find the asymptotic forms of E_y for both the fast and the slow wave solutions. (Hint: Reference [71] may be useful for this generalized tunneling equation for Φ .)

6.3.4.2 Energy flux and energy conservation

In this section, we develop the expressions for the Poynting flux, the kinetic flux, and the loss terms by using Poynting's theorem. We begin by writing down the Maxwell equations for harmonic time dependence,

$$\begin{aligned} \nabla \times \mathbf{E} &= i\omega \mathbf{B} & \nabla \times \mathbf{E}^* &= -i\omega \mathbf{B}^* \\ \nabla \times \mathbf{B} &= \mu_0 (\mathbf{j} - i\omega\epsilon_0 \mathbf{E}) & \nabla \times \mathbf{B}^* &= \mu_0 (\mathbf{j}^* + i\omega\epsilon_0 \mathbf{E}^*). \end{aligned} \quad (6.95)$$

We then examine the divergence of the complex Poynting vector,

$$\begin{aligned}\nabla \cdot \left(\frac{\mathbf{E} \times \mathbf{B}^*}{\mu_0} \right) &= \frac{1}{\mu_0} \mathbf{B}^* \cdot \nabla \times \mathbf{E} - \mathbf{E} \cdot \left(\frac{\nabla \times \mathbf{B}^*}{\mu_0} \right) \\ &= \frac{i\omega}{\mu_0} \mathbf{B}^* \cdot \mathbf{B} - \mathbf{E} \cdot \mathbf{j}^* - i\omega\epsilon_0 \mathbf{E} \cdot \mathbf{E}^*\end{aligned}$$

and since the time average over a cycle of the real part of the Poynting vector is given by

$$\mathbf{S} = \frac{1}{2} \operatorname{Re} \left(\frac{\mathbf{E} \times \mathbf{B}^*}{\mu_0} \right) \quad (6.96)$$

then it follows that

$$\nabla \cdot \mathbf{S} = -\frac{1}{2} \operatorname{Re}(\mathbf{E} \cdot \mathbf{j}^*) \quad (6.97)$$

with $\mathbf{j} = \sigma \cdot \mathbf{E}$ and $\sigma^* = i\omega\epsilon_0(\mathbf{K}^* - \mathbf{I})$ is the conductivity tensor. Then if we define

$$Q \equiv \frac{1}{2} \operatorname{Re}(\mathbf{E} \cdot \mathbf{j}^*) = P(x) + \nabla \cdot \mathbf{T}(x)$$

we may write our conservation law in the form

$$\nabla \cdot (\mathbf{S} + \mathbf{T}) = -P.$$

From the form of this expression, it is clear that since \mathbf{S} is the electromagnetic flux, then \mathbf{T} is also a flux which we designate the kinetic flux and represents the power carried by the coherent motions of the particles in the plasma. From Poynting's theorem, P represents the loss term.

In order to evaluate these expressions, we write out

$$Q = \frac{\omega\epsilon_0}{2} \operatorname{Re}[i\mathbf{E} \cdot (\mathbf{K}^* - \mathbf{I}) \cdot \mathbf{E}^*] = \frac{i\omega\epsilon_0}{4} (\mathbf{E} \cdot \mathbf{K}^* \cdot \mathbf{E}^* - \text{c.c.})$$

where c.c. stands for the complex conjugate of the preceding function. Now the dielectric tensor of equation (6.90) can be represented by

$$\mathbf{K} = \mathbf{K}_0 + \frac{1}{L} \mathbf{K}'_H + \frac{d}{dx} \mathbf{K}_H \frac{d}{dx} \quad (6.98)$$

where \mathbf{K}_0 is the cold plasma dielectric tensor and \mathbf{K}_H is the hot plasma correction given by

$$\mathbf{K}_H = \begin{pmatrix} 1 & i \\ -i & 1 \end{pmatrix} K_H$$

where $K_H = -\omega_{pi}^2 \rho_L^2 Z(\zeta)/4\omega k v_i$ and $\mathbf{K}'_H = d\mathbf{K}_H/dx$. Then $\mathbf{E} \cdot \mathbf{K}_0 \cdot \mathbf{E}^* - \text{c.c.} = 0$, and since

$$\begin{pmatrix} E_x^* & E_y^* \end{pmatrix} \begin{pmatrix} 1 & i \\ -i & 1 \end{pmatrix} \begin{pmatrix} E_x \\ E_y \end{pmatrix} = E_+^* E_+$$

then we may write

$$\begin{aligned}\mathbf{E} \cdot \mathbf{K}^* \cdot \mathbf{E}^* - \text{c.c.} &= \frac{(K_{H'}^* - K_H')}{L} |E_+|^2 + (K_H - K_H^*) |E'_+|^2 \\ &\quad + \frac{d}{dx} (E_+ K_H^* E'_+{}^* - \text{c.c.})\end{aligned}$$

so that finally we can identify terms and obtain

$$\begin{aligned}T_x &= \frac{i\omega\epsilon_0}{4} (E_+ K_H^* E'_+{}^* - \text{c.c.}) \\ &= \frac{\omega\epsilon}{2} \operatorname{Im}(E_+^* K_H E'_+)\end{aligned}\tag{6.99}$$

$$\begin{aligned}P &= \frac{i\omega\epsilon_0}{4} \left[\frac{1}{L} (K_{H'}^* - K_H') |E_+|^2 + (K_H - K_H^*) |E'_+|^2 \right] \\ &= \frac{\omega\epsilon}{2} \operatorname{Im}(K_H' |E_+|^2 - K_H |E'_+|^2)\end{aligned}\tag{6.100}$$

$$\begin{aligned}\mathbf{S} &= \frac{1}{2\mu_0} \operatorname{Re}(\mathbf{E} \times \mathbf{B}^*) \\ &= \frac{1}{2\mu_0\omega} \operatorname{Im}(E_y^* E'_y \hat{e}_x - E_x^* E'_y \hat{e}_y) + \frac{k}{2\mu_0\omega} (|E_x|^2 + |E_y|^2) \hat{e}_z\end{aligned}\tag{6.101}$$

where the last result was obtained by expanding equation (6.95).

From these results, it is evident that the principal electromagnetic flux is due to the E_y component while the kinetic flux due to the E_+ component. Since $K_H \sim 1/z$ as $z \rightarrow \infty$, the fast wave kinetic flux vanishes asymptotically since it is dominated by E_y whose amplitude is asymptotically constant. Thus we have shown that the fast wave is an electromagnetic wave, dominated by the electromagnetic flux. The slow wave solutions of equation (6.94) vary as $E_+ \sim z^{1/4} \exp(-2i\lambda z^{3/2}/3)$ so that for the slow wave solutions the kinetic flux is asymptotically constant while the electromagnetic flux vanishes. The slow wave solutions of equation (6.26), however, do satisfy the conservation law of equation (6.43) without the odd order terms, but fail to conserve the kinetic flux which falls off as $1/z$ in that case. Thus we have shown that the existence of a conservation law is not equivalent to the conservation of energy unless a direct connection between the two can be established. From numerical solutions of both equation (6.55), which is the generalization of the tunneling equation to include absorption but not the odd order terms, and equation (6.94) which includes both, the reflection coefficients are found to be equivalent and the conversion coefficients are close but not exactly the same.

Problem 6.3.10. Kinetic flux and power conservation.

- (i) Derive an exact expression for E_+ in terms of E_y and its derivatives from equation (6.92).

- (ii) From the results of problem 6.3.9 for E_y , show that the slow wave kinetic flux is asymptotically constant.
- (iii) If the solution of equation (6.26) is used for E_y , show that the kinetic flux vanishes asymptotically.

6.4 Absorption and emission

Radiation from a plasma, by which we mean electromagnetic radiation, is necessarily from an inhomogeneous (or at least bounded) plasma since in the uniform plasma, there is nowhere for the radiation to go which is ‘outside’. The most important reasons for examining radiation or emission theory is to either measure the radiation for diagnostic purposes or to estimate the energy loss rate for power balance purposes. There are sources of radiation in many plasmas from atomic processes, especially from highly stripped atoms, but in this section we will deal only with the emission due to the thermal character of the plasma, and since the plasma is inhomogeneous, the source will be localized into a layer within which the plasma is assumed to be slowly varying. The fundamental approach is to calculate the absorption and then extract the emission from an application of Kirchhoff’s law. Although this topic is not new, and textbooks exist on this topic (e.g. see Bekefi [87]), the proper treatment of Kirchhoff’s law as it relates to emission from cyclotron resonance layers is relatively recent [80, 88]. This is because the mode conversion phenomenon changes our picture of the absorption process such that absorption affects only the reflected and converted branches while the transmission coefficient is independent of absorption. It is surprising that traditional estimates of emission have been based exclusively on calculations of the transmission coefficient, the only parameter that is *independent* of absorption.

6.4.1 Generalized Kirchhoff’s law

Emission and absorption are intimately related through the fluctuation–dissipation theorem. Therefore, it is to be expected that the emission along any of the principal branches will be related to the absorption along the corresponding branch.

For an example problem, we choose an ion harmonic resonance where $1 + \gamma > 0$. From the dispersion relation illustrated in figure 6.7, we let power densities I_1 , I_2 , and I_3 be incident along the corresponding branches (incidence on branch 1 is from the right, incidence on branch 2 is from the left and incidence on branch 3 is from above) and let the power emitted along each branch be E_1 , E_2 , and E_3 , respectively. Then an assumption of equilibrium requires that the incoming and outgoing power must balance branch by branch (asymptotic independence), such that

$$I_1 = E_1 + |R_1|^2 I_1 + |T_2|^2 I_2 + \varepsilon |C_{31}|^2 I_3 \quad (6.102)$$

$$I_2 = E_2 + |T_1|^2 I_1 + |R_2|^2 I_2 + \varepsilon |C_{32}|^2 I_3 \quad (6.103)$$

$$I_3 = E_3 + |R_3|^2 I_3 + |C_{13}|^2 I_1 / \varepsilon + |C_{23}|^2 I_2 / \varepsilon \quad (6.104)$$

where $\varepsilon \equiv 1 - e^{-2\eta}$.

If it is further assumed that the system is in thermal equilibrium with perfectly absorbing walls, where both the plasma and walls are at the same temperature, then it is required by equipartition that

$$I_1 = I_2 = I_3 = I_{BB} \quad (6.105)$$

where I_{BB} is the blackbody radiation intensity. We may solve for the emitted power on each branch to obtain

$$E_1 = (1 - |T_1|^2 - |R_1|^2 - \varepsilon |C_{31}|^2) I_{BB} \quad (6.106)$$

$$E_2 = (1 - |T_2|^2 - |R_2|^2 - \varepsilon |C_{32}|^2) I_{BB} \quad (6.107)$$

$$E_3 = (1 - |R_3|^2 - |C_{13}|^2 / \varepsilon - |C_{23}|^2 / \varepsilon) I_{BB}. \quad (6.108)$$

Using the reciprocity relations that state that the fractional power between any two branches is the same in either direction, these equations reduce to the general result

$$E_k = A_k I_{BB} \quad (6.109)$$

where the absorption is given by

$$A_1 = 1 - |T_1|^2 - |R_1|^2 - |C_{13}|^2 / \varepsilon$$

$$A_2 = 1 - |T_2|^2 - |R_2|^2 - |C_{23}|^2 / \varepsilon$$

$$A_3 = 1 - |R_3|^2 - \varepsilon |C_{31}|^2 - \varepsilon |C_{32}|^2.$$

Equation (6.109) is called the *generalized Kirchhoff's law* (GKL) since it relates emission and absorption on each branch.

The proof may be extended from a local proof, requiring walls of the same temperature as the plasma, to a global proof by removing the walls to infinity so that there are only outgoing waves. In this case, the emission must be unchanged provided there is some nonradiative source of energy to maintain equilibrium, such as collisions, because the individual solutions representing incoming waves and the solution representing the radiation are linearly independent.

6.4.2 Absorption and mode conversion

In order to evaluate the emission from equation (6.109), it is necessary to know the effects of absorption on the scattering coefficients which up to this point are known only without absorption. Generally speaking, these coefficients can only be obtained numerically, but a few are known analytically. In this section we outline the procedures that have proven effective in determining these coefficients, but the details are found elsewhere [80].

6.4.2.1 Green's function method

While the GKL applies to all cases where there is both mode conversion and tunneling, there are subtle differences in the methods with $1 + \gamma > 0$ and with $1 + \gamma < 0$, so the development that follows is for a pure ion second harmonic case. The objective then is to solve equation (6.58) by using a Green function such that

$$\psi(z) = \int_{-\infty}^z G_-(z, x)g(x, \psi) dx + \int_z^\infty G_+(z, x)g(x, \psi) dx \quad (6.110)$$

where the $G_\pm(z, x)$ form the Green function that is constructed from the adjoint solutions of the tunneling equation which satisfy $Y = y'' + y$ and the sink term is

$$g(x, \psi) = \lambda^2(x - x_0)[1 - 1/F(x)](\psi'' + \psi). \quad (6.111)$$

The adjoint functions satisfy the adjoint tunneling equation,

$$Y^{iv} + \lambda^2 z Y'' + 2\lambda^2 Y' + (\lambda^2 z + \gamma)Y = 0 \quad (6.112)$$

which was obtained by integrating equation (6.110) by parts. $G_+(z, x)$ and $G_-(z, x)$ are linear functions of $Y_k(x)$ of the form

$$G_\pm(z, x) = A_\pm(z)Y_1(x) + B_\pm(z)Y_2(x) + C_\pm(z)Y_3(x) + D_\pm(z)Y_4(x)$$

where the z -dependent coefficients may be determined from boundary conditions. The resulting solutions may be written as

$$\psi_k(z) = y_k(z) + y_2(z)I_{1k}^-/\varepsilon + y_4(z)I_{0k}^- + y_1(z)I_{2k}^+/\varepsilon + y_0(z)I_{4k}^+ \quad (6.113)$$

where $y_0 = y_3 - y_1$ has been introduced for convenience, and the integrals are over a semi-infinite range defined by

$$I_{jk}^-(z) = \frac{1}{2\pi i \lambda^2} \int_{-\infty}^z Y_j(x)g(x, \psi_k) dx \quad (6.114)$$

$$I_{jk}^+(z) = \frac{1}{2\pi i \lambda^2} \int_z^\infty Y_j(x)g(x, \psi_k) dx. \quad (6.115)$$

6.4.2.2 Scattering coefficients with absorption

The scattering coefficients may be expressed in terms of the I_{jk} integrals over the infinite range and are given in [table 6.5](#).

While in general, the I_{jk} integrals must be calculated numerically, it has been proved that $I_{11} = I_{12} = I_{21} = 0$ identically [79], so that $T_1 = T_2 = e^{-\eta}$ always and $R_1 = 0$. For the coefficients that do depend on damping, the typical behavior is for the reflection and conversion coefficients to decrease exponentially as $|R_2|^2 = R_{20}^2 e^{-2\alpha_R \kappa^2}$ where $R_{20} = 1 - e^{-2\eta}$ is the value without absorption, κ is

Table 6.5. Scattering coefficients with absorption for the tunneling equation with $1 + \gamma > 0$.

Transmission	Reflection	Conversion
$T_1 = e^{-\eta}(1 + I_{21}/\varepsilon)$	$R_1 = -e^{-2\eta}I_{11}/\varepsilon$	$C_{13} = -\varepsilon + e^{-2\eta}I_{31}$
$T_2 = e^{-\eta}(1 + I_{12}/\varepsilon)$	$R_2 = -(\varepsilon + I_{22}/\varepsilon)$	$C_{23} = -e^{-\eta}(\varepsilon + I_{32})$
$T_3 = 0$	$R_3 = -e^{-2\eta}(1 + I_{33})$	$C_{31} = -(1 - e^{-2\eta}I_{13}/\varepsilon)$ $C_{32} = -e^{-\eta}(1 + I_{23}/\varepsilon)$

the normalized parallel wavenumber, and α_R is dependent on plasma parameters. The conversion coefficients have a similar character. For a single-ion component plasma, $\alpha_R = 1$ within 1%, but for multiple-ion species, there is no simple approximation.

The results are similar for absorption/emission at the electron cyclotron harmonic for the X -mode, but some interesting auxiliary effects influence the emission. First, the electrons are weakly relativistic at even modest temperatures, so the sink term in equation (6.111) must be replaced by the appropriate relativistic expression. Second, the mode-converted branch is typically absorbed very close to the resonance layer because the Bernstein mode turns around and returns to the resonance layer where it is completely absorbed. The consequence is that since a perfect absorber is a blackbody emitter, we must consider the *emitted* blackbody radiation which traces the same path to the mode conversion layer as an incident slow wave which then mode converts some of its power to an electromagnetic wave, and though incoherent with the direct emission, it adds to the overall radiation. The total emission on branches 1 or 2 is therefore given by

$$E_1 = (1 - e^{-2\eta} - |C_{13}|^2)I_{BB}(T) + |C_{31}|^2I_{BB}(T') \quad (6.116)$$

$$E_2 = (1 - e^{-2\eta} - |R_2|^2 - |C_{23}|^2)I_{BB}(T) + |C_{32}|^2I_{BB}(T') \quad (6.117)$$

where the original layer is at temperature T and the other blackbody layer is at temperature T' . These expressions are also simplified so that the $|C_{ij}|^2$ represents the *power* converted from branch i to branch j . It is evident that if the temperatures are equal (or very nearly equal), the conversion terms cancel, and the results simplify to

$$E_1 = (1 - e^{-2\eta})I_{BB} \quad (6.118)$$

$$E_2 = (1 - e^{-2\eta} - |R_2|^2)I_{BB} \quad (6.119)$$

where the first result is completely independent of the strength of absorption, depending *only* on the asymptotic parameter η which depends *only on cold plasma parameters*. Equation (6.118) is exactly the same result commonly used for electron cyclotron emission where mode conversion is ignored and

the finite transmission is *presumed to be due to absorption processes*. In the simpler analysis that neglects mode conversion, however, the emission is always symmetric, but we see from equation (6.119) that the symmetry between the high magnetic field side emission and the low magnetic field side emission is broken if $R_2 \neq 0$. It has been shown that if the parameter, $\ell T_e \geq 1000$ where ℓ is the dimensionless length $\ell = \omega L/c$ with L the scale length of the magnetic field variation, and the temperature is in keV, then R_2 is small enough that neglecting it produces less than 1% error [80]. If, however, $\ell T_e \leq 500$ and $X = \omega_p^2/\omega^2$ is not small, the error in estimating the temperature can exceed a factor of two.

Problem 6.4.1. Green's function.

- (i) Show that by using equation (6.58) in equation (6.110) and integrating by parts that the Green function must satisfy the adjoint equation.
- (ii) Show that the $G_+(z, x)$ and $G_-(z, x)$ and their derivatives must satisfy certain *jump conditions* of the form $G_+^{(n)}(z, z_+) - G_-^{(n)}(z, z_-) = g_n$ and find g_n for $n = 0$ through $n = 3$.

6.5 WKB Method for three-dimensional inhomogeneous plasmas—ray tracing

6.5.1 The ray equations

When the variation in the equilibrium parameters is no longer restricted to one dimension, then there are no longer any simple invariants, and the direction of the group velocity, or of the wave packet, is less obvious. There is a generalization of the WKB method, however, which will answer this question and give a prescription for following a wave packet and its energy density [89, 90].

We begin with the Maxwell equations

$$\nabla \times \mathbf{B} = \mu_0 \mathbf{j} + \frac{1}{c^2} \frac{\partial \mathbf{E}}{\partial t} \quad (6.120)$$

$$\nabla \times \mathbf{E} = - \frac{\partial \mathbf{B}}{\partial t} \quad (6.121)$$

where we define

$$\mathbf{E} = \mathbf{a} e^{i\psi} \quad (6.122)$$

$$\mathbf{B} = \mathbf{b} e^{i\psi} \quad (6.123)$$

$$\nabla \psi = \mathbf{k}(\mathbf{r}, t) \quad (6.124)$$

$$\frac{\partial \psi}{\partial t} = -\omega(\mathbf{r}, t) \quad (6.125)$$

and we assume that \mathbf{k} , ω , \mathbf{a} , and \mathbf{b} are slowly varying in space and time. At this point, we recognize that ψ is just the eikonal of WKB theory generalized to three

dimensions. Then expanding the space and time derivatives,

$$\nabla \times \mathbf{B} = e^{i\psi} (\nabla \times \mathbf{b} + ik \times \mathbf{b}) \quad (6.126)$$

$$\nabla \times \mathbf{E} = e^{i\psi} (\nabla \times \mathbf{a} + ik \times \mathbf{a}) \quad (6.127)$$

$$\frac{\partial \mathbf{B}}{\partial t} = e^{i\psi} \left(\frac{\partial \mathbf{b}}{\partial t} - i\omega \mathbf{b} \right) \quad (6.128)$$

$$\frac{\partial \mathbf{E}}{\partial t} = e^{i\psi} \left(\frac{\partial \mathbf{a}}{\partial t} - i\omega \mathbf{a} \right) \quad (6.129)$$

$$\mathbf{j} = e^{i\psi} (\sigma^A \cdot \mathbf{a} + K\{\mathbf{a}\}) \quad (6.130)$$

where σ^A is the anti-Hermitian component of the conductivity tensor and $K\{\mathbf{a}\}$ is related to the anti-Hermitian component of the dielectric tensor which is a function of the loss terms in the plasma and to the nonlocal terms in the dielectric tensor. If we assume the loss terms and nonlocal terms are of order δ compared to the dominant terms, then $K\{\mathbf{a}\}$ is of order δ compared to σ^A (since the anti-Hermitian terms in σ correspond to the Hermitian terms in K and vice versa). Expanding in order δ for the remaining quantities so that

$$\begin{aligned} \mathbf{a} &= \mathbf{a}_0 + \delta \mathbf{a}_1 + \delta^2 \mathbf{a}_2 \dots \\ \mathbf{b} &= \mathbf{b}_0 + \delta \mathbf{b}_1 + \delta^2 \mathbf{b}_2 \dots \end{aligned}$$

then the ordering is such that

$$K\{\mathbf{a}\} \text{ is of order } \delta \text{ compared to } \sigma^A$$

$$\nabla \times \mathbf{a} \text{ is of order } \delta \text{ compared to } ik \times \mathbf{a}$$

$$\nabla \times \mathbf{b} \text{ is of order } \delta \text{ compared to } ik \times \mathbf{b}$$

$$\frac{\partial \mathbf{a}}{\partial t} \text{ is of order } \delta \text{ compared to } -i\omega \mathbf{a}$$

$$\frac{\partial \mathbf{b}}{\partial t} \text{ is of order } \delta \text{ compared to } -i\omega \mathbf{b}$$

where the first relation is due to weak damping and the others are due to the slow variation of \mathbf{a} and \mathbf{b} . Then the zero order equations from equation (6.121) are

$$i \left[\mathbf{k} \times \mathbf{b}_0 + \frac{\omega}{c^2} \mathbf{a}_0 + \mu_0 i \sigma^A \cdot \mathbf{a}_0 \right] = 0 \quad (6.131)$$

$$i[\mathbf{k} \times \mathbf{a}_0 - \omega \mathbf{b}_0] = 0 \quad (6.132)$$

and the first order equations are

$$i\delta \left[\mathbf{k} \times \mathbf{b}_1 + \frac{\omega}{c^2} \mathbf{a}_1 + \mu_0 i \sigma^A \cdot \mathbf{a}_1 \right] = \delta \left[\mu_0 K\{\mathbf{a}\} - \nabla \times \mathbf{b}_0 + \frac{1}{c^2} \frac{\partial \mathbf{a}_0}{\partial t} \right] \quad (6.133)$$

$$i\delta[\mathbf{k} \times \mathbf{a}_1 - \omega \mathbf{b}_1] = -\delta \left[\nabla \times \mathbf{a}_0 + \frac{\partial \mathbf{b}_0}{\partial t} \right]. \quad (6.134)$$

Now equation (6.132) gives $\mathbf{b}_0 = \mathbf{k} \times \mathbf{a}/\omega$ and this result in equation (6.131) gives

$$\frac{\mathbf{k} \times (\mathbf{k} \times \mathbf{a}_0)}{\omega} + \frac{\omega \mathbf{a}_0}{c^2} + \mu_0 i \sigma^A \cdot \mathbf{a}_0 = 0$$

which may also be written as

$$\boldsymbol{\epsilon} \cdot \mathbf{a}_0 \equiv \left[i \left(1 - \frac{k^2 c^2}{\omega^2} \right) + \frac{c^2}{\omega^2} \mathbf{k} \mathbf{k} + \frac{i \sigma^A}{\omega \epsilon_0} \right] \mathbf{a}_0 = 0 \quad (6.135)$$

and $\det |\boldsymbol{\epsilon}| = 0$ is the dispersion relation with no losses (σ^A only). We may denote this dispersion relation in many ways, such as

$$\det |\boldsymbol{\epsilon}| = D(\mathbf{k}, \omega, \mathbf{r}, t) = 0 \quad (6.136)$$

or as

$$\omega = \Omega(\mathbf{k}, \mathbf{r}, t). \quad (6.137)$$

Now from the definitions of equation (6.125), we may establish that

$$\frac{\partial}{\partial t} (\nabla \psi) = \frac{\partial \mathbf{k}}{\partial t} = \nabla \left(\frac{\partial \psi}{\partial t} \right) = -\nabla \omega$$

which leads to

$$\nabla \omega + \frac{\partial \mathbf{k}}{\partial t} = 0. \quad (6.138)$$

We may also establish that

$$\nabla \omega = \Omega_{\mathbf{r}} + (\nabla \mathbf{k}) \cdot \Omega_{\mathbf{k}}$$

where the last term is the dyadic

$$(\nabla \mathbf{k}) \cdot \Omega_{\mathbf{k}} = \frac{\partial \Omega}{\partial k_x} \nabla k_x + \frac{\partial \Omega}{\partial k_y} \nabla k_y + \frac{\partial \Omega}{\partial k_z} \nabla k_z$$

and the subscript means the derivative holding the other variables fixed so that

$$\Omega_{\mathbf{r}} + (\nabla \mathbf{k}) \cdot \Omega_{\mathbf{k}} + \frac{\partial \mathbf{k}}{\partial t} = 0. \quad (6.139)$$

Now taking \mathbf{k} , \mathbf{r} , and t as the independent variables, we may write equation (6.136) as

$$D(\mathbf{k}, \omega(\mathbf{k}, \mathbf{r}, t), \mathbf{r}, t) = 0$$

and then it follows that

$$\begin{aligned} \frac{\partial D}{\partial \mathbf{k}} + \frac{\partial D}{\partial \omega} \frac{\partial \omega}{\partial \mathbf{k}} &= 0 & \text{or} & & D_{\mathbf{k}} + D_{\omega} \Omega_{\mathbf{k}} &= 0 \\ \frac{\partial D}{\partial \mathbf{r}} + \frac{\partial D}{\partial \omega} \frac{\partial \omega}{\partial \mathbf{r}} &= 0 & \text{or} & & D_{\mathbf{r}} + D_{\omega} \Omega_{\mathbf{r}} &= 0 \\ \frac{\partial D}{\partial t} + \frac{\partial D}{\partial \omega} \frac{\partial \omega}{\partial t} &= 0 & \text{or} & & D_t + D_{\omega} \Omega_t &= 0. \end{aligned} \quad (6.140)$$

Using these, then equation (6.139) may be written as

$$(\nabla \mathbf{k}) \cdot \Omega_{\mathbf{k}} + \frac{\partial \mathbf{k}}{\partial t} = -\Omega_{\mathbf{r}} = \frac{D_{\mathbf{r}}}{D_{\omega}}. \quad (6.141)$$

Now at this point we introduce the concept of rays or trajectories defined by the group velocity $\mathbf{v}_g = \partial \omega / \partial \mathbf{k} = \Omega_{\mathbf{k}}$ such that

$$\frac{d\mathbf{r}}{dt} = \Omega_{\mathbf{k}} = -\frac{D_{\mathbf{k}}}{D_{\omega}}. \quad (6.142)$$

Since these rays follow the direction of the group velocity, they represent the trajectory of a wave packet in the inhomogeneous medium. Using equation (6.142), equation (6.141) can be written as

$$\frac{\partial \mathbf{k}}{\partial t} + \frac{d\mathbf{r}}{dt} \cdot \frac{d\mathbf{k}}{d\mathbf{r}} = -\Omega_{\mathbf{r}} = \frac{D_{\mathbf{r}}}{D_{\omega}} = \frac{d\mathbf{k}}{dt} \quad (6.143)$$

where we have used the symmetry of the dyadic so that $(\nabla \mathbf{k}) \cdot \Omega_{\mathbf{k}} = \Omega_{\mathbf{k}} \cdot (\nabla \mathbf{k})$. If we then consider the evolution of D along the ray by examining

$$\frac{dD}{dt} = D_{\mathbf{k}} \frac{d\mathbf{k}}{dt} + D_{\mathbf{r}} \frac{d\mathbf{r}}{dt} + D_{\omega} \frac{d\omega}{dt} + D_t = 0$$

then the first two terms cancel so

$$\frac{d\omega}{dt} = -\frac{D_t}{D_{\omega}} \quad \text{or} \quad \frac{d\Omega}{dt} = \Omega_t. \quad (6.144)$$

This set of equations represents a set of Hamiltonian equations with Ω playing the role of the Hamiltonian. By rescaling the variable along the trajectory to τ , such that $D_{\omega} = dt/d\tau$, then these three equations may be written in the compact form,

$$\frac{d\mathbf{k}}{d\tau} = D_{\mathbf{r}} \quad (6.145)$$

$$\frac{d\mathbf{r}}{d\tau} = -D_{\mathbf{k}} \quad (6.146)$$

$$\frac{d\omega}{d\tau} = -D_t. \quad (6.147)$$

The trajectories so defined are the characteristics of the wave equation and are used to follow the power flow.

Problem 6.5.1. Analytic two-dimensional ray tracing. Consider the dispersion relation,

$$D = (k_x^2 + k_y^2)^2 - axk_x^2 + bk_y^2 + c + dx + ey = 0.$$

- (i) Solve the ray equations to find $x(\tau)$ and $y(\tau)$ with $k_x^2 > d/a$.
- (ii) Sketch k_x^2 versus x for $d = 0$ and at least two values of y_0 as a parameter.

6.5.2 The inhomogeneous plasma dispersion relation

The numerous dispersion relations for cold plasmas, warm plasmas, hot plasmas, etc, have all had one common feature, namely that the z -axis has been in the direction of the magnetic field (if any). In the inhomogeneous plasma, the magnetic field may vary in direction so that except at a point, the magnetic field points in an arbitrary direction. If the magnetic field is curved, it may still be possible to keep the dispersion relation simple if the field always follows one of the coordinates, such as in a simple toroidal field (with no shear) where the field is in the ϕ -direction. In general, however, with a fixed coordinate system, the dielectric tensor has all nine components nonzero and the dispersion relation is somewhat more complicated than our previous examples.

To find the weakly inhomogeneous dispersion relation, we consider only the cold plasma case, where the equations of motion may be written as

$$\begin{pmatrix} -i\omega & -\omega_{cjz} & \omega_{cjy} \\ \omega_{cjz} & -i\omega & -\omega_{cjx} \\ \omega_{cjy} & \omega_{cjx} & -i\omega \end{pmatrix} \begin{pmatrix} v_{jx} \\ v_{jy} \\ v_{jz} \end{pmatrix} = \frac{q_j}{m_j} \begin{pmatrix} E_x \\ E_y \\ E_z \end{pmatrix} \quad (6.148)$$

where $\omega_{cjz} = q_j B_z / m_j$, $\omega_{cjy} = q_j B_y / m_j$, $\omega_{cjx} = q_j B_z / m_j$, and $\omega_{cj}^2 = \omega_{cjx}^2 + \omega_{cjy}^2 + \omega_{cjz}^2$. Solving for the velocity components, we find for the mobility tensor,

$$v_j = \frac{i q_j}{m_j \omega} \mathbf{T}_j \cdot \mathbf{E} \quad (6.149)$$

where

$$\mathbf{T}_j = \begin{pmatrix} \frac{\omega^2 - \omega_{cjx}^2}{\omega^2 - \omega_{cj}^2} & \frac{i\omega\omega_{cjz} - \omega_{cjx}\omega_{cjy}}{\omega^2 - \omega_{cj}^2} & \frac{-\omega_{cjx}\omega_{cjz} + i\omega\omega_{cjy}}{\omega^2 - \omega_{cj}^2} \\ \frac{-i\omega\omega_{cjz} + \omega_{cjx}\omega_{cjy}}{\omega^2 - \omega_{cj}^2} & \frac{\omega^2 - \omega_{cjy}^2}{\omega^2 - \omega_{cj}^2} & \frac{i\omega\omega_{cjx} - \omega_{cjy}\omega_{cjz}}{\omega^2 - \omega_{cj}^2} \\ \frac{i\omega\omega_{cjy} - \omega_{cjx}\omega_{cjz}}{\omega^2 - \omega_{cj}^2} & \frac{-i\omega\omega_{cjx} + \omega_{cjy}\omega_{cjz}}{\omega^2 - \omega_{cj}^2} & \frac{\omega^2 - \omega_{cjz}^2}{\omega^2 - \omega_{cj}^2} \end{pmatrix}$$

and using the usual transformation to the dielectric tensor from the mobility tensor, we have

$$\sum_j n_j q_j \mathbf{v}_j - i\omega\epsilon_0 \mathbf{E} = -i\omega\epsilon_0 \mathbf{K} \cdot \mathbf{E}$$

so the general form for \mathbf{K} is

$$\mathbf{K} = \mathbf{I} - \sum_j \frac{\omega_{pj}^2}{\omega^2} \mathbf{T}_j. \quad (6.150)$$

The dielectric tensor components may then be written as

$$K_{xx} = 1 - \frac{\omega_{pi}^2 [\omega^2 - \omega_{ci}^2]}{\omega^2 [\omega^2 - \omega_{ci}^2]} - \frac{\omega_{pe}^2 (\omega^2 - \omega_{ce}^2)}{\omega^2 (\omega^2 - \omega_{ce}^2)} \quad (6.151)$$

$$K_{yy} = 1 - \frac{\omega_{pi}^2 [\omega^2 - \omega_{ciy}^2]}{\omega^2 [\omega^2 - \omega_{ci}^2]} - \frac{\omega_{pe}^2 (\omega^2 - \omega_{cey}^2)}{\omega^2 (\omega^2 - \omega_{ce}^2)} \quad (6.152)$$

$$K_{zz} = 1 - \frac{\omega_{pi}^2 [\omega^2 - \omega_{ciz}^2]}{\omega^2 [\omega^2 - \omega_{ci}^2]} - \frac{\omega_{pe}^2 (\omega^2 - \omega_{cez}^2)}{\omega^2 (\omega^2 - \omega_{ce}^2)} \quad (6.153)$$

$$K_{xy} = K_{yx}^* = \frac{\omega_{pi}^2 [\omega_{ci} \omega_{cy} - i\omega \omega_{ciz}]}{\omega^2 [\omega^2 - \omega_{ci}^2]} + \frac{\omega_{pe}^2 (\omega_{ce} \omega_{cey} + i\omega \omega_{cez})}{\omega^2 (\omega^2 - \omega_{ce}^2)} \quad (6.154)$$

$$K_{xz} = K_{zx}^* = \frac{\omega_{pi}^2 [\omega_{ci} \omega_{cz} + i\omega \omega_{ciz}]}{\omega^2 [\omega^2 - \omega_{ci}^2]} + \frac{\omega_{pe}^2 (\omega_{ce} \omega_{cez} - i\omega \omega_{cey})}{\omega^2 (\omega^2 - \omega_{ce}^2)} \quad (6.155)$$

$$K_{yz} = K_{zy}^* = \frac{\omega_{pi}^2 [\omega_{cy} \omega_{ciz} - i\omega \omega_{cix}]}{\omega^2 [\omega^2 - \omega_{ci}^2]} + \frac{\omega_{pe}^2 (\omega_{cey} \omega_{cez} + i\omega \omega_{cex})}{\omega^2 (\omega^2 - \omega_{ce}^2)} \quad (6.156)$$

and where now we have taken $\omega_{cjk} = |q_j|B_k/m_j$, $k = x, y, z$, so that all of the cyclotron frequencies are taken to be positive if the corresponding magnetic field component is positive. Without collisions, the tensor is Hermitian, but with collisions, all nine components are distinct.

Because of the inhomogeneity, we cannot rotate the coordinate system about the field direction, so the dispersion relation becomes

$$\begin{aligned} & \{[K_{xx} - (n_x^2 + n_z^2)][K_{yy} - (n_x^2 + n_z^2)] - |K_{xy} + n_x n_y|^2\}[K_{zz} - (n_x^2 + n_y^2)] \\ & \quad - [K_{xx} - (n_y^2 + n_z^2)]|K_{yz} + n_y n_z|^2 \\ & \quad - [K_{yy} - (n_x^2 + n_z^2)]|K_{xz} + n_x n_z|^2 \\ & \quad + 2 \operatorname{Re}[(K_{xy} + n_x n_y)(K_{yz} + n_y n_z)(K_{xz}^* + n_x n_z)] = 0. \end{aligned} \quad (6.157)$$

If collisions or collisionless damping are included, then the dielectric tensor is no longer Hermitian, and the dispersion relation is even longer, since no longer can we use $K_{ij} = K_{ji}^*$ to simplify the expression.

6.5.3 The amplitude equations

From the first order terms, after considerable vector manipulation given in appendix C, an expression for the amplitude may be obtained of the form

$$\frac{dU}{dt} = -U \nabla \cdot \omega_k - \frac{1}{2} \mathbf{a}_0^* \cdot \sigma^H \cdot \mathbf{a}_0 \quad (6.158)$$

where U is the energy density in the wave from the Hermitian portion of the dielectric tensor (*anti-Hermitian* part of the conductivity tensor). Clearly, the $\nabla \cdot \omega_k$ term represents the effects of convergence or divergence of a ray bundle, or focusing. When this term becomes large, the WKB formalism eventually breaks down. When the divergence term is small or vanishes, then the σ^H term, which represents losses due to dissipation, dominates the changes in energy density.

Another limit to the validity of the ray tracing equations has to do with the fact that the rays are presumed to be single rays. The determinant of the dielectric tensor generally has two roots for a cold plasma and more for a hot plasma, and if two of the roots begin to coalesce, then the ray tracing theory breaks down. While the ray tracing will continue as long as the two roots do not exactly coincide, the energy flow is split between two nearby roots, and hence both the rays and the amplitudes are invalid near such a coalescence. The greater problem is with the amplitudes, since the divergence of the group velocity is effectively sampling the vicinity near the ray, while the ray equations effectively sample only along the ray. Thus, even though a ray may experience a mode conversion at a coalescence of two roots, entering the region on one root and leaving on another, following a valid ray after the encounter, it is possible that most of the energy may have transferred to the other ray. Such problems are outside the suitable domain for geometric optics, and fall in the mode conversion domain where full wave solutions in the coalescence region are found and then matched to WKB solutions where ray tracing and geometric optics are once again valid.

6.6 Drift waves and instabilities

6.6.1 Introduction—drift waves

Whenever there is a gradient in one of the equilibrium parameters, it generally leads to crossed electric and magnetic fields that allow the propagation of drift waves. The literature is extensive in the kinds of instabilities that may arise from these gradients [91, 92], and it is beyond the scope of this book to investigate all of them, so again we will examine some of the basic principles and illustrate with a few examples. The literature is difficult to survey because there are examples of collisionless drift instabilities from a kinetic equation, there are collisional or dissipative drift instabilities from the fluid equations, and some use a mixture of both. There is no unified theory of drift instabilities, and hence there is also no unified nomenclature for the various instabilities, and while the various approximations are commonly very specific, they may not always be consistent, and the results are sometimes abstract in the sense that a consistent set of plasma parameters is not always invoked. For example, one case in which simplifications and approximations were made in order to get an analytic result for the instability growth rate was subsequently found to be stable when a more nearly complete model was analyzed. Because the literature is so vast and complicated, we shall only show a few examples of the various types of analysis and a small set of the

known drift instabilities.

In order to see some of the nature of the problem without extensive analysis, we first begin with a case of electrons and ions in the long wavelength limit ($k^2 \ll k_D^2$ so that $n_e = n_i$) using the fluid equations and examine low-frequency electrostatic waves. If we neglect electron inertia ($m_e \rightarrow 0$) in the momentum equation, then we have the balance between the pressure gradient and the electric field as

$$e \frac{\partial \varphi}{\partial x} = \frac{\kappa T_e}{n_e} \frac{\partial n_e}{\partial x}$$

whose solution is $n_e = \exp(e\varphi/\kappa T_e)$. We shall assume the potential varies as $\varphi \sim e^{ik_y y - i\omega t}$, and that the density perturbations are given by

$$n_i = n_e = n_0 \exp(e\varphi/\kappa T_e) = n_0 + n_{1e} = n_0 + n_0 e\varphi/\kappa T_e.$$

The equation of motion for ions is

$$-i\omega m_i v_i = e(\mathbf{E} + \mathbf{v}_i \times \mathbf{B}_0) \simeq 0$$

since $\omega \ll \omega_{ci}$. Hence, $v_{ix} \simeq E_y/B_0 = -ik_y\varphi/B_0$. The ion continuity equation gives

$$-i\omega n_{1i} + v_{ix} \frac{dn_0}{dx} = 0$$

and using the expressions for n_{1i} and v_{ix} , this may be solved for ω as

$$\omega = -\frac{k_y \kappa T_e}{e B_0} \frac{1}{n_0} \frac{dn_0}{dx} \equiv \omega_e^*. \quad (6.159)$$

Usually $n_0(x)$ decreases with increasing x , so normally $\omega_e^* > 0$. The wave travels in the direction of $\nabla n_0 \times \mathbf{B}_0$ with phase velocity $c_s \rho_s / L_n$ where c_s is the ion acoustic speed, $\rho_s = c_s / \omega_{ci}$ is like an ion Larmor radius, except it depends on T_e rather than T_i , and L_n is the scale length of the density variation.

One way of thinking about the source of free energy for this instability is to realize that the density gradient tends to establish a radial electric field to balance the diffusion rates, and this radial field sets the plasma into rotation due to the $\mathbf{E} \times \mathbf{B}_0$ drift. As we saw in chapter 3, drifting plasmas are frequently unstable. In this case, a cylindrical plasma leads to waves rotating with an azimuthal mode number $k_y \simeq 2\pi m/r$, so the waves may be localized about a radius where m is an integer. These drifting low-frequency waves are susceptible to a variety of instabilities.

6.6.2 The drift resistive instability

For this example we shall generalize somewhat the previous elementary analysis, but still use the long wavelength approximation and the electrostatic approximation, but with $\mathbf{E} = \mathbf{E}(x) \exp[i(k_y y + k_z z - \omega t)]$. This allows the wave

to propagate parallel to the magnetic field in addition to its drift perpendicular to both the field and the gradient. Then using the fluid equation for electrons with collisions,

$$m_e n_0 \frac{\partial \mathbf{v}_e}{\partial t} = -n_0 e (\mathbf{E} + \mathbf{v}_e \times \mathbf{B}_0) - \nabla p_e - m_e n_0 v_{ei} \mathbf{v}_e$$

we find from the z -component (with $\omega \ll v_{ei} \ll \omega_{ce}$) that

$$v_{ez} = \frac{i n_0 e k_z \varphi - i k_z n_e \kappa T_e}{m_e n_0 v_{ei}}. \quad (6.160)$$

The electron continuity equation is

$$-i\omega n_e + v_{ex} \frac{dn_0}{dx} + i n_0 (k_x v_{ex} + k_y v_{ey} + k_z v_{ez}) = 0$$

and we have taken a WKB form for $\mathbf{E}(x)$ so that k_x is a slowly varying function of x . Then for $\omega \ll \omega_{ce}$, $v_{ex} \simeq E_y/B_0$ and $v_{ey} \simeq -E_x/B_0$, we may solve the continuity equation for v_{ez} and equate it to the expression in equation (6.160) and write the result in the form

$$\left(\frac{\omega}{k_z} + \frac{i k_z \kappa T_e}{m_e v_{ei}} \right) \frac{n_e}{n_0} = e \varphi \left(\frac{i k_z}{m_e v_{ei}} - \frac{k_y}{k_z e B_0} \frac{1}{n_0} \frac{dn_0}{dx} \right).$$

Then this may be written as

$$\frac{n_e}{n_0} = \frac{e \varphi}{\kappa T_e} \frac{(1 - i \omega_e^* m_e v_{ei} / k_z^2 \kappa T_e)}{(1 - i \omega m_e v_{ei} / k_z^2 \kappa T_e)}. \quad (6.161)$$

For the ions, we assume $\omega \ll \omega_{ci}$ but keep first order terms, so that

$$\begin{aligned} v_{ix} &= \frac{E_y}{B_0} - \frac{i \omega}{\omega_{ci}} \frac{E_x}{B_0} \\ v_{iy} &= -\frac{E_x}{B_0} - \frac{i \omega}{\omega_{ci}} \frac{E_y}{B_0} \\ v_{iz} &= \frac{i e E_z}{m_i \omega}. \end{aligned}$$

Then the ion continuity equation,

$$-i\omega n_i + v_{ix} \frac{dn_0}{dx} + i n_0 \mathbf{k} \cdot \mathbf{v}_i = 0$$

leads to

$$\frac{n_i}{n_0} = \frac{e \varphi}{\kappa T_e} \left(\frac{\omega_e^*}{\omega} + \frac{k_z^2 c_s^2}{\omega^2} - k_\perp^2 \rho_s^2 \right) \quad (6.162)$$

where we neglected a term of order $i\omega_e^* k_x / \omega_{ci} k_y$ compared to unity. Equating equation (6.161) to equation (6.162) leads to the dispersion relation,

$$1 - \frac{\omega_e^*}{\omega} + \left(k_\perp^2 \rho_s^2 - \frac{k_z^2 c_s^2}{\omega^2} \right) \left(1 - \frac{i\omega m_e v_{ei}}{k_z^2 \mathcal{K} T_e} \right) = 0. \quad (6.163)$$

This dispersion relation may be written as a quadratic equation,

$$\omega^2 + i\omega_s \left(1 + k_\perp^2 \rho_s^2 - \frac{k_z^2 c_s^2}{\omega^2} \right) \omega - i\omega_e^* \omega_s = 0 \quad (6.164)$$

where

$$\omega_s = \frac{\omega_{ce} \omega_{ci}}{v_{ei}} \left(\frac{k_\perp^2}{k_z^2} - \frac{\omega_{ci}^2}{\omega^2} \right)^{-1}.$$

The unstable root is given by

$$\omega = -\frac{i\omega_s}{2} \left(1 + k_\perp^2 \rho_s^2 - \frac{k_z^2 c_s^2}{\omega^2} \right) \left\{ 1 - \left[1 - \frac{4i\omega_e^*}{\omega_s (1 + k_\perp^2 \rho_s^2 - k_z^2 c_s^2 / \omega^2)^2} \right]^{1/2} \right\} \quad (6.165)$$

and its maximum growth rate occurs when $\omega_e^* \simeq \omega_s \left(1 + k_\perp^2 \rho_s^2 - \frac{k_z^2 c_s^2}{\omega^2} \right)^2$ at which point

$$\omega = \frac{\omega_e^* (0.618 + 0.300i)}{1 + k_\perp^2 \rho_s^2 - k_z^2 c_s^2 / \omega^2}.$$

Problem 6.6.1. Drift instability growth rate. We define

$$\alpha \equiv \frac{4\omega_e^*}{\omega_s (1 + k_\perp^2 \rho_s^2 - k_z^2 c_s^2 / \omega^2)^2}.$$

- (i) Show that with ω_e^* fixed that $\text{Im}(\omega)$ has a maximum as a function of α .
- (ii) Show that for $\alpha \ll 1$,

$$\omega \sim \omega_e^* (1 + i\alpha/4) (1 + k_\perp^2 \rho_s^2 - k_z^2 c_s^2 / \omega^2)^{-1}$$

and for $\alpha \gg 1$,

$$\omega \sim \omega_e^* (1 + i) \sqrt{\frac{2}{\alpha}} (1 + k_\perp^2 \rho_s^2 - k_z^2 c_s^2 / \omega^2)^{-1}.$$

- (iii) Find α_m for maximum growth rate.

6.6.3 Kinetic theory of drift waves

In order to include collisionless plasmas and the effects of resonant particles along with nonuniform distribution functions, we need to use extensions of the kinetic theory of [chapter 4](#). In this expanded formalism, we will include gradients in temperature, magnetic field, density, and curvature of the magnetic field. Because of the additional complexity which these additional effects add to the problem, we will restrict ourselves to electrostatic waves, but electromagnetic drift waves also occur. In this list, we have distinguished between magnetic field gradients, which we take to come from currents inside the plasma, such as that caused by finite β effects where $\nabla \times \mathbf{H} = \mathbf{j}$ and the magnetic field gradient is related to a density gradient such that $(1/B)dB/dx \simeq \beta(1/n)dn/dx$. Curvature effects are taken to be due to external currents, so that inside the plasma $\nabla \times \mathbf{B} = 0$, and we represent the inertial response to these curvature effects in terms of a ‘gravitational’ potential where $g = (\frac{1}{2}v_{\perp}^2 + v_z^2)/R_c$ wherein R_c is the radius of curvature of the magnetic field. When a combination of these gradients occur, they could, in principle, act in different directions, but because most gradients occur normal to the flux surfaces, we shall assume they all occur in the x -direction with the magnetic field in the usual z -direction, so drifts commonly are in the y -direction. In this section, we shall generally follow the review by Krall [92], but use the conventions and notation of our earlier chapters.

6.6.3.1 The equilibrium distribution function

Our basic set of equations are the familiar Vlasov equations, except that with the electrostatic approximation, these are

$$\frac{\partial f_j}{\partial t} + \mathbf{v} \cdot \nabla f_j + \left[\mathbf{g} + \frac{q_j}{m_j}(\mathbf{E} + \mathbf{v} \times \mathbf{B}) \right] \cdot \nabla_{\mathbf{v}} f_j = 0 \quad (6.166)$$

$\mathbf{g} = -g\hat{\mathbf{e}}_x$, and Poisson’s equation

$$\epsilon_0 \nabla \cdot \mathbf{E} = \sum_j q_j \int d^3v f_j. \quad (6.167)$$

Our zero-order distribution function, $f_0(\mathbf{v}, x)$, must satisfy

$$v_x \frac{\partial f_{0j}}{\partial x} + \left(\mathbf{g} + \frac{q_j}{m_j} \mathbf{v} \times \mathbf{B}_0 \right) \cdot \nabla_{\mathbf{v}} f_{0j} = 0. \quad (6.168)$$

In order to guarantee this, we must construct f_{0j} from the constants of the motion,

$$\begin{aligned} \mathcal{E} &= \frac{1}{2}m_j v^2 + m_j g x \\ p_y &= m_j v_y + q_j A_y \simeq m_j (v_y + \epsilon_j \omega_{cj} x) \\ p_z &= m_j v_z \end{aligned}$$

which are the energy and the two components of the momentum perpendicular to the gradients, and we have assumed weak gradients in estimating the vector potential A_y . The weak gradients may then be used again to write the zero-order distribution function in the form

$$f_{0j} = \frac{n_0 e^{-(v_{\perp}^2 + 2gx)/v_{ij}^2 - v_z^2/v_{\ell j}^2}}{\pi^{3/2} v_{ij}^2 v_{\ell j}} \left[1 + \left(x + \frac{v_y \epsilon_j}{\omega_{cj}} \right) \left(\epsilon' + \delta_{\perp} \frac{v_{\perp}^2}{v_j^2} + \delta_z \frac{v_z^2}{v_j^2} \right) \right] \quad (6.169)$$

where $v_{ij}^2 = 2\kappa T_{\perp j}/m_j$ and $v_{\ell j}^2 = 2\kappa T_{\parallel j}/m_j$. We identify the various constants by evaluating

$$\begin{aligned} n_j &= \int d^3v f_{0j} = n_0 e^{-2gx/v_{ij}^2} [1 + x(\epsilon' + \delta_{\perp} + \frac{1}{2}\delta_z)] \\ n_j \kappa T_{\perp j} &= \int d^3v (\frac{1}{2}mv_{\perp}^2) f_{0j} = n_0 \kappa T_{\perp j} e^{-2gx/v_{ij}^2} [1 + x(\epsilon' + 2\delta_{\perp} + \frac{1}{2}\delta_z)] \\ n_j \kappa T_{\parallel j} &= \int d^3v (\frac{1}{2}mv_z^2) f_{0j} = \frac{1}{2} n_0 \kappa T_j e^{-2gx/v_{ij}^2} [1 + x(\epsilon' + \delta_{\perp} + \frac{3}{2}\delta_z)] \end{aligned}$$

so that we may find

$$\begin{aligned} T_{\perp j} &\simeq T_{\perp j}(1 + \delta_{\perp}x) \Rightarrow \delta_{\perp} = \frac{1}{T_{\perp}} \frac{dT_{\perp}}{dx} \\ T_{\parallel j} &\simeq \frac{T_{\parallel j}}{2}(1 + \delta_z x) \Rightarrow \delta_z = \frac{1}{T_{\parallel}} \frac{dT_{\parallel}}{dx} \\ \frac{1}{n_j} \frac{dn_j}{dx} &= \epsilon' + \delta_{\perp} + \frac{1}{2}\delta_z \Rightarrow \epsilon' = \frac{1}{n_j} \frac{dn_j}{dx} - \delta_{\perp} - \frac{1}{2}\delta_z. \end{aligned}$$

Problem 6.6.2. Constants of the motion. Verify that any function of the constants of the motion, $f_0(\mathcal{E}, p_y, p_z)$, satisfies equation (6.168).

6.6.3.2 Integrating over the unperturbed orbits

If we now examine the evolution of the perturbed distribution function in a fashion similar to section 4.3.2, then we may write for the first order terms

$$\frac{df_1}{dt} = \frac{\partial f_1}{\partial t} + \mathbf{v} \cdot \nabla f_1 + \left(\mathbf{g} + \frac{q}{m} \mathbf{v} \times \mathbf{B}_0 \right) \cdot \nabla_{\mathbf{v}} f_1 = -\frac{q}{m} (\mathbf{E}_1 + \mathbf{v} \times \mathbf{B}_1) \cdot \nabla_{\mathbf{v}} f_0 \quad (6.170)$$

where we have used equations (6.166) and (6.168). Then, assuming the perturbation vanishes for sufficiently long times in the past, we may integrate directly to obtain

$$f_1(\mathbf{r}, \mathbf{v}, t) = -\frac{q}{m} \int_{-\infty}^t dt' [\mathbf{E}_1(\mathbf{r}', t') + \mathbf{v}' \times \mathbf{B}_1(\mathbf{r}', t')] \cdot \nabla_{\mathbf{v}'} f_0(\mathcal{E}, p_y, p_z) \quad (6.171)$$

where we integrate along the unperturbed orbit defined by

$$\mathbf{v}' = \frac{d\mathbf{r}'}{dt'} \quad \frac{d\mathbf{v}'}{dt'} = \mathbf{g} + \frac{q}{m} \mathbf{v}' \times \mathbf{B}_0$$

with $\mathbf{v}'(t' = t) = \mathbf{v}$ and $\mathbf{r}'(t' = t) = \mathbf{r}$ and where now $B_0 = B_0(1 + x/L_B)$ and $\mathbf{B}_1 = 0$ in the electrostatic approximation.

The unperturbed orbit equations are similar to the case without drifts except for the drift terms, such that

$$\begin{aligned} v'_x &= v_x \cos \omega_c \tau - \epsilon v_y \sin \omega_c \tau \\ v'_y &= \epsilon v_x \sin \omega_c \tau + v_y \cos \omega_c \tau - \epsilon g/\omega_c + \epsilon v_\perp^2/2\omega_c L_B \\ v'_z &= v_z \end{aligned} \quad (6.172)$$

for the velocities and the displacements are given by

$$x' = x + \frac{\epsilon v_y}{\omega_c} (1 - \cos \omega_c \tau) - \frac{v_x}{\omega_c} \sin \omega_c \tau \quad (6.173)$$

$$y' = y - \frac{\epsilon v_x}{\omega_c} (1 - \cos \omega_c \tau) - \frac{v_y}{\omega_c} \sin \omega_c \tau + \epsilon g \tau / \omega_c - \epsilon v_\perp^2 \tau / 2\omega_c L_B \quad (6.174)$$

$$z' = z - v_z \tau \quad (6.175)$$

and $\tau = t - t'$ as before. We have neglected some oscillating terms of the order of the drift speed varying as $\sin(2\omega_c \tau + \phi)$ in these expressions. Since the plasma is not uniform in the x -direction, we shall not Fourier analyze in that direction, and in fact we shall restrict our case to $E_{1x} = 0$, which is a low- β limit. Then the phase term becomes

$$\begin{aligned} i\mathbf{k} \cdot \mathbf{r}' - i\omega t' &= i\mathbf{k} \cdot \mathbf{r} - i\omega t - \frac{i\epsilon v_x k_y}{\omega_c} (1 - \cos \omega_c \tau) - \frac{iv_y k_y}{\omega_c} \sin \omega_c \tau \\ &\quad + i \left(\omega - k_z v_z + \frac{\epsilon k_y g}{\omega_c} + \omega^* \frac{v_\perp^2}{v_j^2} \right) \tau. \end{aligned} \quad (6.176)$$

Now the drift velocities are proportional to the velocity squared, so that, for example, the drift frequency from g is not a constant, but given by

$$\frac{\epsilon k_y g}{\omega_c} = \omega_g \left(\frac{v_\perp^2}{2v_j^2} + \frac{v_z^2}{v_j^2} \right) \quad (6.177)$$

where $\omega_g \equiv \epsilon k_y v_j^2 / \omega_c R_c$. Also, the gradient B drift is velocity dependent, being proportional to v_\perp^2 , so for the integrals over perpendicular velocities, we shall introduce the combined drift frequency,

$$\omega_d \equiv \omega^* + \frac{1}{2} \omega_g.$$

The integrals over the perpendicular velocities are then all of the form

$$\begin{aligned} G(a_q, n) &= \frac{1}{v_j \sqrt{\pi}} \int_{-\infty}^{\infty} v^n \exp \left(-\frac{v^2}{v_j^2} - i a_q v + i \omega_d \tau \frac{v^2}{v_j^2} \right) dv \\ &= e^{-\lambda_q/2} f(a_q, n) / \sqrt{\alpha_d} \end{aligned} \quad (6.178)$$

where $q = x, y$, $\lambda_q = a_q^2 v_j^2 / 2\alpha_d$, $\alpha_d = 1 - i\omega_d \tau$, and $a_x = (\epsilon k_y / \omega_c)(1 - \cos \omega_c \tau)$, $a_y = (k_y / \omega_c) \sin \omega_c \tau$, so $\lambda_x + \lambda_y = 2\lambda(1 - \cos \omega_c \tau) / \alpha_d$, and $f(a_q, 0) = 1$. This time we need through $n = 4$, so we list the results as

$$\begin{aligned} f(a_q, 1) &= -\frac{i a_q v_j^2}{2\alpha_d} & f(a_q, 2) &= \frac{v_j^2}{2\alpha_d}(1 - \lambda_q) \\ f(a_q, 3) &= \frac{i a_q v_j^4}{4\alpha_d^2}(-3 + \lambda_q) & f(a_q, 4) &= \frac{v_j^4}{4\alpha_d^2}(3 - 6\lambda_q + \lambda_q^2) \end{aligned}$$

so that the products are of the form

$$G(a_x, n)G(a_y, m) = \frac{f(a_x, n)f(a_y, m)}{1 - i\omega_d \tau} \exp \left[-\frac{\lambda(1 - \cos \omega_c \tau)}{1 - i\omega_d \tau} \right].$$

The form of these results with $\omega_d \neq 0$ prevents any further exact analysis, so we will make an approximation based on the smallness of ω_d . Since τ is unbounded, it would appear that $\omega_d \tau$ cannot be treated as a perturbation, but by examining the integral over the parallel velocities *first*, we will demonstrate that it is effectively small. For this demonstration, the parallel velocity integrals are of the form

$$\begin{aligned} &\frac{1}{v_j \sqrt{\pi}} \int_{-\infty}^{\infty} v_z^n \exp \left[-\frac{v_z^2}{v_j^2} + i \left(\omega - k_z v_z + \omega_g \frac{v_z^2}{v_j^2} \right) \tau \right] dv_z \\ &= \frac{v_j^n e^{i\omega\tau - (k_z v_j \tau)^2 / 4\alpha_g}}{\sqrt{\pi} \alpha_g^{(n+1)/2}} \int_{-\infty}^{\infty} e^{-x^2} \left(x - \frac{i k_z v_j \tau}{2\sqrt{\alpha_g}} \right)^n dx \end{aligned} \quad (6.179)$$

where $\alpha_g = 1 - i\omega_g \tau$. From this expression, it is clear that the integrand of the integral over τ will be exponentially small for $k_z v_j \tau \gg 1$. If we imagine then that the τ integral is ‘cut off’ at τ_0 where, say, $k_z v_j \tau_0 = 4$, then $\omega_d \tau_0 = 4\omega_d / k_z v_j$. Hence, if we take $\omega_d / k_z v_j \ll 1$ (this guarantees also that $\omega_g / k_z v_j \ll 1$), then we may treat $\omega_d \tau$ as a perturbation. This approximation thus assumes that before $\omega_d \tau$ reaches order unity, the other terms in the integrand have made the contribution from the range $1/\omega_d < \tau < \infty$ of no consequence. Treating $\omega_d \tau$ now as a small quantity, we will back up and do the τ integral first before doing the average over parallel velocities.

Using the electrostatic approximation in equation (6.171), the average over perpendicular velocities of the Fourier amplitude of f_{1j} may be written as

$$\begin{aligned}\langle f_1(\mathbf{k}, \mathbf{v}, \omega) \rangle_{\perp} &= \frac{\mathrm{i}q}{m} e^{-\lambda} \int_0^{\infty} d\tau e^{\phi} \varphi \langle \mathbf{k} \cdot \nabla_{\mathbf{v}'} f_0(x', \mathbf{v}') \rangle_{\perp} \\ &\simeq -\frac{qf_0(x, v_z)}{m} e^{-\lambda} \int_0^{\infty} d\tau e^{\phi} \varphi (\langle h_0 \rangle_{\perp} + \epsilon' \langle h_n \rangle_{\perp} \\ &\quad + \delta_{\perp} \langle h_{\perp} \rangle_{\perp} + \delta_z \langle h_z \rangle_{\perp}) (1 + i\omega_d \tau)\end{aligned}\quad (6.180)$$

where now $f_0(x, v_z) = (n_0 / \sqrt{\pi} v_j) e^{-(2gx + v_z^2/v_j^2)}$, and

$$\begin{aligned}\phi &= \mathrm{i} \left(\omega + \omega_g \frac{v_z^2}{v_j^2} - k_z v_z \right) \tau + \frac{\lambda \cos \omega_c \tau}{1 - i\omega_d \tau} \\ &\simeq \mathrm{i} \left(\omega + \omega_g \frac{v_z^2}{v_j^2} - k_z v_z \right) \tau + \lambda \cos \omega_c \tau (1 + i\omega_d \tau)\end{aligned}$$

and

$$\begin{aligned}\langle h_0 \rangle_{\perp} &= \frac{k_y^2}{\omega_c \alpha_d^2} \sin \omega_c \tau + \frac{2\mathrm{i}}{\alpha_d v_j^2} \left[k_z v_z - \omega_g \frac{v_z^2}{v_j^2} - \frac{\omega_d}{\alpha_d} (1 - f_d) \right] \\ \langle h_n \rangle_{\perp} &= x \langle h_0 \rangle_{\perp} - \frac{\mathrm{i}\epsilon k_y}{\omega_c \alpha_d^2} (\alpha_d - \cos \omega_c \tau + \lambda \sin^2 \omega_c \tau) \\ &\quad + \frac{\epsilon k_y}{\omega_c^2 \alpha_d} \sin \omega_c \tau \left[k_z v_z - \omega_g \frac{v_z^2}{v_j^2} - \omega_d (2 - f_d) \right] \\ \langle h_{\perp} \rangle_{\perp} &= \frac{k_y}{\omega_c \alpha_d^3} \left\{ k_y x \sin \omega_c \tau (2 - \alpha_d - f_d) + \mathrm{i}\epsilon [2 - \alpha_d (1 + \cos \omega_c \tau) \right. \\ &\quad \left. + \alpha_d f_d \left(2 + \cos \omega_c \tau + \frac{3 + 4 \cos \omega_c \tau}{\alpha_d} + \frac{\lambda}{\alpha_d} \sin^2 \omega_c \tau \right)] \right\} \\ &\quad + \frac{(k_z v_z + \omega_d - \omega_g v_z^2/v_j^2)}{\alpha_d^2 v_j^2} \left[2\mathrm{i}x(1 - f_d) + \frac{\epsilon k_y v_j^2}{\alpha_d \omega_c^2} \sin \omega_c \tau (2 - f_d) \right] \\ &\quad - \frac{2\omega_d}{\alpha_d^3 v_j^2} \left[\mathrm{i}x(2 - 4f_d + f_d^2) + \frac{\epsilon k_y v_j^2}{\alpha_d \omega_c^2} (3 - 3f_d + f_d^2) \right] \\ &\quad + \frac{\omega_g v_z^2}{\alpha_d v_j^4} \left(2\mathrm{i}x + \frac{\epsilon k_y v_j^2}{\alpha_d \omega_c^2} \sin \omega_c \tau \right) \\ \langle h_z \rangle_{\perp} &= \frac{v_z^2}{v_j^2} \langle h_n \rangle_{\perp} - \frac{2k_z v_z}{\alpha_d v_j^2} \left(\mathrm{i}x + \frac{\epsilon k_y v_j^2}{\alpha_d \omega_c^2} \sin \omega_c \tau \right)\end{aligned}$$

where $f_d = \lambda(1 - \cos \omega_c \tau) / \alpha_d$.

The next step is to integrate over τ , where each component integral may be written in the form

$$I_{f\ell} = \int_0^\infty d\tau \exp[i(\omega + \omega_g v_z^2/v_j^2 - k_z v_z)\tau - \lambda(1 - \cos \omega_c \tau)(1 + i\omega_d \tau)] \frac{f(\omega_c \tau)}{\alpha_d^\ell}. \quad (6.181)$$

Expanding $\alpha_d^{-\ell} = (1 - i\omega_d \tau)^{-\ell} \simeq 1 + i\ell \omega_d \tau$, then the integral can be represented, using the Bessel function identity equation (4.224), by

$$\begin{aligned} I_{f\ell} &= e^{-\lambda} \sum_{n=-\infty}^{\infty} I_n(\lambda) \int_0^\infty d\tau e^{i(\omega + n\omega_c + \omega_g v_z^2/v_j^2 - k_z v_z - \lambda \omega_d)\tau} \\ &\quad \times \sum_{m=-\infty}^{\infty} i^m J_m(\lambda \omega_d \tau) e^{im\omega_c \tau} f(\omega_c \tau)(1 + i\ell \omega_d \tau). \end{aligned} \quad (6.182)$$

For small λ and small $\omega_d \tau$, we need only keep $m = 0, \pm 1$, so for the second sum

$$\sum_{m=-1}^1 i^m J_m(\lambda \omega_d \tau) e^{im\omega_c \tau} \simeq 1 - \lambda \omega_d \tau \sin \omega_c \tau.$$

The integrals of equation (6.181) are then of the form

$$\begin{aligned} I_{f\ell} &= \sum_{n=-\infty}^{\infty} I_n(\lambda) \int_0^\infty d\tau e^{i\omega_n \tau} (1 + i\ell \omega_d \tau - \lambda \omega_d \tau \sin \omega_c \tau) f(\omega_c \tau) \\ &= \sum_{n=-\infty}^{\infty} \frac{f_{n\ell}}{\omega_n} \end{aligned} \quad (6.183)$$

with $\omega_n = \omega + n\omega_c + \omega_g v_z^2/v_j^2 - k_z v_z$, and these integrals may be performed with the pertinent terms given in [table 6.6](#).

The final step is to average over the parallel velocities, where each integral may be written as

$$H_{rm} = \frac{1}{\sqrt{\pi} v_j} \int_{-\infty}^{\infty} \frac{v_z^r e^{-v_z^2/v_j^2}}{(\omega + n\omega_c + \omega_g v_z^2/v_j^2 - k_z v_z)^{m+1}} dv_z. \quad (6.184)$$

Here again, the exponential guarantees that there is little contribution from large values of v_z , so again we can treat ω_g as a small parameter and expand the denominator. Then with $\zeta_n = (\omega + n\omega_c)/k_z v_j$, the integrals are all of the form

$$H_{rm} = \frac{(-1)^m}{(k_z v_j)^m m!} \frac{d^m}{d\zeta_n^m} \left[F_r + \frac{\omega_g}{k_z v_j^3} \frac{d}{d\zeta_n} F_{r+2} \right] + \mathcal{O}\left(\frac{\omega_g}{k_z v_j}\right)^2 \quad (6.185)$$

Table 6.6. Representation of trigonometric functions by corresponding Bessel functions as defined by equation (6.183) with $g_{n\ell} = 1 - (n + \ell)\omega_d/\omega_n$.

$f(\omega_c \tau)$	$f_{n\ell}$
1	$iI_n g_{n\ell}$
$\cos \omega_c \tau$	$iI'_n g_{n\ell} + i\omega_d n I_n / \omega_n \lambda$
$\cos^2 \omega_c \tau$	$iI''_n g_{n\ell} + \frac{2i\omega_d n}{\omega_n \lambda} \left(I'_n - \frac{I_n}{\lambda} \right)$
$\cos^3 \omega_c \tau$	$iI'''_n g_{n\ell} + \frac{i\omega_d}{2\omega_n} \left\{ \frac{\lambda I_n}{2} + n \left[\left(I'_n - \frac{I_n}{\lambda} \right) \left(1 - \frac{12}{\lambda^2} \right) + \frac{6I''_n}{\lambda} \right] \right\}$
$\sin \omega_c \tau$	$\frac{n}{\lambda} I_n g_{n\ell} + \frac{\omega_d}{\omega_n} I'_n$
$\cos \omega_c \tau \sin \omega_c \tau$	$\frac{n}{\lambda} \left(I'_n - \frac{I_n}{\lambda} \right) g_{n\ell} + \frac{\omega_d}{\omega_n} (2I''_n - I'_n)$

where

$$F_r = \frac{1}{\sqrt{\pi} v_j} \int_{-\infty}^{\infty} \frac{v_z^r e^{-v_z^2/v_j^2}}{\omega + n\omega_c - k_z v_z} dv_z \quad (6.186)$$

$$= \frac{(-v_z)^{r-1} r!}{k_z 2^r} \sum_{k=0}^{r/2} \frac{1}{(r-2k)! k!} \frac{d^{(r-2k)}}{d\zeta_n^{r-2k}} Z(\zeta_n) \quad (6.187)$$

whose first few terms may be written as

$$\begin{aligned} F_0 &= -\frac{1}{k_z v_j} Z(\zeta_n) & F_1 &= \frac{1}{2k_z} Z'(\zeta_n) \\ F_2 &= \frac{v_j}{2k_z} \zeta_n Z'(\zeta_n) & F_3 &= -\frac{v_j^2}{2k_z} [1 - \zeta_n^2 Z'(\zeta_n)]. \end{aligned}$$

6.6.3.3 The dispersion relation

At this point, after developing terms consistently through first order in $\omega_d/k_z v_j$, the inclusion of these terms in general formulas is too cumbersome, so from this point on, we will neglect these terms. For problems with curvature ($g \neq 0$) these terms must be kept in $\langle h_0 \rangle$, but one frequently neglects the other corrections in δ_\perp or δ_z for these problems. The corrections for $\langle h_0 \rangle$ are included as a problem.

Assembling now the pieces, the averages over velocities of the several terms are:

$$\langle h_0 \rangle = \frac{2e^{-\lambda}}{v_j^2} \sum_{n=-\infty}^{\infty} I_n [1 + \zeta_0 Z(\zeta_n)]$$

$$\begin{aligned}
\langle h_n \rangle &= x \langle h_0 \rangle - e^{-\lambda} \sum_{n=-\infty}^{\infty} \frac{\epsilon k_y}{\omega_c} \left[\frac{I_n - I'_n + \lambda(I_n - I''_n)}{k_z v_j} Z(\zeta_n) - \frac{n I_n}{2\omega_c \lambda} Z'(\zeta_n) \right] \\
\langle h_{\perp} \rangle &= - \frac{e^{-\lambda}}{v_j^2} \sum_{n=-\infty}^{\infty} 2x\lambda(I_n - I'_n)[1 + \zeta_0 Z(\zeta_n)] + x I_n Z'(\zeta_n) \\
&\quad - \frac{n}{\epsilon k_y} [n I_n - n\lambda(I_n - I'_n)] Z'(\zeta_n) \\
&\quad - \frac{\epsilon k_y v_j}{k_z \omega_c} \left[1 + 5\lambda + \lambda^2 + 5\lambda \frac{d}{d\lambda} - \lambda^2 \frac{d^2}{d\lambda^2} \right] (I_n - I'_n) Z(\zeta_n) \\
\langle h_z \rangle &= e^{-\lambda} \sum_{n=-\infty}^{\infty} x I_n [1 - \zeta_0 \zeta_n Z'(\zeta_n)] \\
&\quad + \frac{1}{\epsilon k_y} \left\{ \frac{\lambda \omega_c}{k_z v_j} [I_n - I'_n + \lambda(I_n - I''_n)] \zeta_n Z'(\zeta_n) - n I_n [1 - \zeta_n^2 Z'(\zeta_n)] \right\}
\end{aligned}$$

With these expressions, the dispersion relation can finally be written as

$$\begin{aligned}
k^2 + \sum_j \frac{2\omega_{pj}^2}{v_j^2} e^{-\lambda} \sum_{n=-\infty}^{\infty} I_n(\lambda) \left[1 + \frac{\omega}{k_z v_j} Z(\zeta_n) \right] \\
= - \sum_j \omega_{pj}^2 (\epsilon' \langle h_n \rangle_j + \delta_{\perp} \langle h_{\perp} \rangle_j + \delta_z \langle h_z \rangle_j). \quad (6.188)
\end{aligned}$$

Problem 6.6.3. Gravitational corrections for $\langle h_0 \rangle$. Work out the first order terms in ω_g and ω_d in $\langle h_0 \rangle$.

6.6.3.4 The universal instability

A very important special case of drift instabilities is that due to the density gradient alone in the range where $|\omega/k_z v_e| \ll 1$ and $|\omega/k_z v_i| \gg 1$. For this case we will keep first order terms in λ_i and let $\lambda_e \rightarrow 0$, set $\delta_{\perp} = \delta_z = x = 0$ and use $\omega_{ci} \gg \omega$. With these restrictions and approximations, equation (6.188) reduces to

$$\begin{aligned}
k^2 + \frac{2\omega_{pe}^2}{v_e^2} [1 + \zeta_e Z(\zeta_e)] + \frac{2\omega_{pi}^2}{v_i^2} (1 - \lambda_i) [1 + \zeta_i Z(\zeta_i)] + \frac{2\omega_{pi}^2}{v_i^2} \lambda_i \\
= - \frac{k_y \epsilon' \omega_{pe}^2}{\omega_{ce} k_z v_e} Z(\zeta_e) + \frac{k_y \epsilon' \omega_{pi}^2}{\omega_{ci} k_z v_i} (1 - \lambda_i) Z(\zeta_i)
\end{aligned}$$

where $\zeta_j = \omega/k_z v_j$. If we now multiply by $\omega^2 \lambda_{De}^2$ and neglect $k^2 \lambda_{De}^2$ compared to 1, the result may be written as

$$\omega^2 (1 + k_{\perp}^2 \rho_s^2) + \omega(\omega - \omega_e^*) \zeta_e Z(\zeta_e) - (1 - \lambda_i) (k_z^2 c_s^2 + \omega \omega_e^*) = 0 \quad (6.189)$$

where c_s is the ion acoustic speed and $\rho_s = c_s/\omega_{ci}$. With ζ_e small, $Z(\zeta_e) \sim i\sqrt{\pi} - 2\zeta_e$, so if we let $\omega = \omega_r + i\gamma$ with $\omega_r \sim \omega_e^*$ so that $k_z c_s \ll \omega_r$ and $\gamma \ll \omega_r$, then

$$\omega_r \simeq \omega_e^* \frac{(1 - \lambda_i)}{(1 + k_\perp^2 \rho_s^2)} \quad (6.190)$$

$$\gamma \simeq \sqrt{\pi} \omega_e^* \left(\frac{k_\perp \rho_s}{1 + k_\perp^2 \rho_s^2} \right)^2 (1 + 2T_i/T_e). \quad (6.191)$$

This instability is called the universal drift instability because it requires only a density gradient, a finite Larmor radius, and electron Landau damping, all of which are universally present in magnetized plasmas.

Problem 6.6.4. The universal drift instability. Fill in the steps leading to equations (6.189)–(6.191).

Chapter 7

Quasilinear theory

7.1 Introduction

In the preceding chapters, we have considered a variety of plasma wave phenomena where waves are treated linearly, so that particles and waves have a self-consistent motion, but the effects of the finite wave amplitudes has been neglected. For some externally excited waves, where the wave amplitude can be maintained low, this is often adequate, but for unstable waves, where the linear theory indicates wave amplitude growth, the amplitude will eventually become large enough to affect the zero-order distribution function and couple the primary wave to other waves. When this leads to a large number of finite amplitude waves, or a broad spectrum of waves, the plasma has become turbulent and nonlinear effects may dominate.

In hydrodynamic theory, the turbulent state is particularly difficult because the various nonlinear couplings are characteristically strong, so it is difficult to isolate the various nonlinear couplings. In a plasma, however, this is frequently not the case, since the nonlinearly induced waves are frequently excited with small amplitudes, and unless these waves are also unstable, we may have a case of *weak turbulence*. As a first approximation, then, we may consider the different modes to be independent, and then add the coupling at various levels and focus our attention on one phenomenon at a time.

In the first approximation, the nonlinear coupling coefficients between various linear modes change slowly in time, and this is the domain of weak turbulence theory. The fundamental smallness parameter in this expansion is the ratio of the wave energy density to the plasma energy density. This theory began with the work of Drummond and Pines [93] and Vedenov *et al* [94], and was developed further by Kadomtsev [95] and Kennel and Engelmann [96], while more complete treatments are given by Davidson [97] and Galeev and Sagdeev [98].

Weak turbulence theory is generally broken into three types of interactions:

- (i) *Quasilinear wave-particle interactions.* This is generally a resonant wave-particle process where $\omega = \mathbf{k} \cdot \mathbf{v}$ without any magnetic field, or where $\omega - n\omega_c = k_z v_z$ in a magnetic field. This interaction is due to a group of particles that remain in phase with the wave over many cycles and have time to exchange energy with the wave, resulting in slow changes in the distribution function which may be attributed to a diffusion process called quasilinear diffusion. Because of the resonance nature of the interaction, this is a kinetic process, and gives rise to phenomena such as plateau formation on the distribution function, and general distortions of the distribution function such as tail formation.
- (ii) *Nonlinear wave-wave interactions.* Sometimes also called wave-wave scattering, this process is resonant among the waves such that

$$\sum_i \omega_i = 0 \quad \sum_i \mathbf{k}_i = 0$$

where ω_i and \mathbf{k}_i are the frequencies and wavevectors of the participating waves. For this case, there are no particle resonances involved, so a fluid approach may suffice. One of the most important examples of this kind of interaction is the class of parametric instabilities where two waves beat together to interact with a third, and above a certain threshold, the interaction goes unstable. We leave this class of nonlinear interactions to the final chapter in section 8.4.

- (iii) *Nonlinear wave-particle-wave interactions.* This process is also resonant, but here the particles keep constant phase relative to the beat frequency of two waves, so that the resonance condition is $\omega_1 - \omega_2 = (\mathbf{k}_1 - \mathbf{k}_2) \cdot \mathbf{v}$. This process is also a kinetic process, and gives rise to phenomena such as plasma wave echoes.

All of these resonance conditions can be viewed as arising from the conservation of energy and momentum, so it will not be surprising when we find these conservation laws built into the various nonlinear formalisms. There are also quantum analogs to each of these three processes, but the quantum approach is generally much more complicated than a direct perturbation expansion.

7.2 Quasilinear theory

7.2.1 Basic equations

Quasilinear theory was developed to treat weak turbulence observed in nonequilibrium plasmas. Due to the non-Maxwellian nature of a turbulent plasma, a spectrum of electromagnetic waves is generated from local charge separations or particle currents. This spectrum of waves, known as fluctuations, can then interact with the plasma through Landau processes described in [chapter 4](#). On a short enough time scale, such that $t \ll \tau_B = \sqrt{m/ek^2\varphi_0}$, where τ_B is the bounce

time for a particle in the electrostatic potential well of the wave, the linear Landau theory is adequate. However, as illustrated in section 4.2.3, the kinetic energy gain of the particles is proportional to the slope of the zero-order distribution function, $\partial f_0 / \partial v|_{v=v_p}$. This implies that the damping or growth rate of the wave is independent of time even on the longer time scale over which the first-order distribution function changes since the zero-order distribution is unaffected by the growth of the first-order distribution function. At some time, this clearly fails to describe the physics of wave–particle interaction if the first order distribution function grows to be a non-negligible perturbation on the zero order distribution.

It is the purpose of quasilinear theory to address the time evolution of the zero-order distribution function f_0 . Moreover, we will show that this theory conserves energy and momentum between the wave and the particle distribution function. Another useful aspect of quasilinear theory is the interaction of the particles with an externally imposed wave such as in wave heating of a plasma or driving a macroscopic current in a plasma with waves. We should be cautious in applying these results, since these wave damping or wave growth processes are collisionless, so the final state of the distribution function will not be Maxwellian. The treatment of only one nonlinear effect at a time for a non-Maxwellian distribution may occasionally lead to a serious error, especially as the amplitude grows, since somewhere one crosses the boundary from weak turbulence to strong turbulence. One rather surprising experimental observation is that the quasilinear description of the wave–particle interaction is quite good even for fairly large amplitude waves.

For simplicity, we shall first restrict our discussion to the case of an unmagnetized plasma and develop the more general case later. This will enable us to bring out the physical processes more clearly without the mathematical complexity added by the magnetic field. Furthermore, the one-dimensional problem will be applicable to wave–particle interactions along a magnetic field where the Lorentz force is negligible.

The basic procedure of developing the one-dimensional quasilinear equations is the same as the treatment of the linear Landau case given in chapter 4. Here, however, the quasilinear approximation implies that the distribution function is allowed to evolve nonlinearly while the wave is calculated using the linear method of chapter 4. The distribution function is assumed to be locally uniform in space, but approach zero as one tends toward infinity, or $f(x \rightarrow \pm\infty, v, t) = 0$. We again assume there are no zero order electric or magnetic fields and use the Vlasov equations for electrons only (assuming a uniform, stationary ion background to cancel all zero-order electric fields). Thus we have

$$\frac{\partial f}{\partial t} + v \frac{\partial f}{\partial x} - \frac{e}{m_e} E \frac{\partial f}{\partial v} = 0 \quad (7.1)$$

where the distribution function is assumed to have the properties

$$f(x, v, t) = f_0(v, t) + f_1(x, v, t) \quad (7.2)$$

$$f_1(x, v, t) = \int_{-\infty}^{\infty} \frac{dk}{2\pi} \tilde{f}_k(k, v, t) e^{ikx} \quad (7.3)$$

$$E(x, t) = \int_{-\infty}^{\infty} \frac{dq}{2\pi} \tilde{E}_q(q, t) e^{iqx} \quad (7.4)$$

where now the zero-order distribution function depends on time and the tilde denotes the Fourier-transformed quantity. We will denote the average over space by

$$\langle f \rangle = \lim_{L \rightarrow \infty} \frac{1}{L} \int_{-L/2}^{L/2} dx f \quad (7.5)$$

so the first order perturbations average to zero so that

$$\langle f \rangle = f_0(v, t) \quad (7.6)$$

$$\langle E \rangle = 0. \quad (7.7)$$

We note that the zero-order distribution function is a function of time, and the average of the second term of equation (7.1) is eliminated by the boundary condition

$$\left\langle \frac{\partial f}{\partial x} \right\rangle = \lim_{L \rightarrow \infty} \frac{1}{L} \int_{-L/2}^{L/2} dx \frac{\partial f}{\partial x} = 0 \quad (7.8)$$

since $f(x \rightarrow \pm\infty) = 0$ so we have a nonlinear equation for the time evolution of the zero-order distribution function from averaging equation (7.1),

$$\frac{\partial}{\partial t} f_0(v, t) = \frac{e}{m_e} \frac{\partial}{\partial v} \langle Ef_1 \rangle \quad (7.9)$$

where

$$\langle Ef_1 \rangle = \lim_{L \rightarrow \infty} \frac{1}{L} \int_{-L/2}^{L/2} dx \int_{-\infty}^{\infty} \frac{dk}{2\pi} \int_{-\infty}^{\infty} \frac{dq}{2\pi} \tilde{f}_k \tilde{E}_q e^{i(k+q)x}. \quad (7.10)$$

We will integrate over the space coordinates first and use the identity

$$\int_{-\infty}^{\infty} e^{i(k+q)x} dx = 2\pi \delta(k + q)$$

so

$$\langle Ef_1 \rangle = \lim_{L \rightarrow \infty} \frac{1}{L} \int_{-\infty}^{\infty} \frac{dk}{2\pi} \int_{-\infty}^{\infty} dq \tilde{f}_k \tilde{E}_q \delta(k + q) \quad (7.11)$$

and then integrating over q , we have nothing unless $q = -k$ so

$$\langle Ef_1 \rangle = \frac{1}{L_\infty} \int_{-\infty}^{\infty} \frac{dk}{2\pi} \tilde{f}_k(t) \tilde{E}_{-k}(t) \quad (7.12)$$

where we have introduced the abbreviated notation $\lim_{L \rightarrow \infty} 1/L \equiv 1/L_\infty$.

As we have seen in [chapter 4](#), the linear solution for \tilde{f}_k is

$$\tilde{f}_k(v, t) = \frac{e\tilde{E}_k}{m_e(p + ikv)} \frac{\partial f_0}{\partial v} \quad (7.13)$$

so we have the time evolution of $f_0(v, t)$ in terms of \tilde{E}_k as

$$\frac{\partial f_0}{\partial t} = \left(\frac{e}{m_e} \right)^2 \frac{\partial}{\partial v} \frac{1}{L_\infty} \int_{-\infty}^{\infty} \frac{dk}{2\pi} \frac{\tilde{E}_k \tilde{E}_{-k}}{(p + ikv)} \frac{\partial f_0}{\partial v}. \quad (7.14)$$

The form of equation (7.14) is that of a diffusion equation with the spatial coordinate replaced by the velocity, or

$$\frac{\partial f_0}{\partial t} = \frac{\partial}{\partial v} D \frac{\partial}{\partial v} f_0 \quad (7.15)$$

where

$$D = \frac{e^2}{m_e^2 L_\infty} \int_{-\infty}^{\infty} \frac{dk}{2\pi} \frac{\tilde{E}_k \tilde{E}_{-k}}{p + ikv}. \quad (7.16)$$

If we separate the integral of equation (7.16) into the principal part and a pole term as was done in equation (4.55), where

$$\lim_{b \rightarrow 0} \frac{1}{a + ib} = \frac{\wp}{a} - i\pi\delta(a)$$

then equation (7.16) becomes two parts: a principal part and a resonant term. If we let $p = \gamma - i\omega$, we have

$$\frac{\partial f_0}{\partial t} = \frac{\partial}{\partial v} \frac{e^2}{m_e^2 L_\infty} \int_{-\infty}^{\infty} \frac{dk}{2\pi} \left[i\wp \left(\frac{\tilde{E}_k \tilde{E}_{-k}}{\omega - kv} \right) + \pi\delta(\omega - kv) \tilde{E}_k \tilde{E}_{-k} \right] \frac{\partial f_0}{\partial v}. \quad (7.17)$$

The two terms in equation (7.17) contribute differently to the wave-particle interaction. Since the principal part does not involve the particle with velocity $v = \omega/k$, it is nonresonant and has only a weak effect.

7.2.2 Conservation laws

The basic conservation laws in weak turbulence theory are direct consequences of the kinetic equation, but we wish to show that even in the multicomponent environment of weak turbulence that the conservation of momentum and energy are explicitly conserved. We first note the trivial case, where the normalization of the velocity distribution function is invariant, since

$$\frac{d}{dt} \int dv f_{0j} = \int dv \frac{\partial f_{0j}}{\partial t} = 0 \quad (7.18)$$

from equation (7.15) for the one-dimensional case we are treating here, and j denotes the species.

Momentum conservation is less trivial, since it requires a sum over wave momentum and particle species. For electrostatic waves, this is relatively simple, since the waves carry no momentum, and the rate of change of particle momentum density is given by

$$\begin{aligned}\frac{d}{dt} \sum_j P_j(t) &= \sum_j \bar{n}_j m_j \int dv v \frac{\partial f_{0j}}{\partial t} \\ &= - \sum_j \bar{n}_j m_j \int dv D_j \frac{\partial f_{0j}}{\partial v} \\ &= - \sum_\alpha \sum_j \frac{\bar{n}_j q_j^2}{m_j L_\infty} \int_{-\infty}^\infty \frac{dk}{2\pi} \int dv \frac{\tilde{E}_k^\alpha \tilde{E}_{-k}^\alpha}{(p^\alpha + ikv)} \frac{\partial f_0}{\partial v} \quad (7.19)\end{aligned}$$

where the middle result was obtained by integrating by parts and the last expression from equation (7.16), and the sum \sum_α is over the spectrum of unstable waves, with $p^\alpha = \gamma_k^\alpha - i\omega_k^\alpha$ and $\gamma_k^\alpha > 0$. From Poisson's equation and equation (7.13), however, the dispersion relation for electrostatic waves (see also equation (4.55)) is

$$1 = \sum_j \frac{i\omega_{pj}^2}{k} \int \frac{\frac{\partial f_{0j}}{\partial v}}{p + ikv} dv \quad (7.20)$$

so equation (7.19) becomes

$$\frac{d}{dt} \sum_j P_j(t) = 2i \sum_\alpha \int_{-\infty}^\infty \frac{dk}{2\pi} \mathcal{W}_k^\alpha k \quad (7.21)$$

where $\mathcal{W}_k^\alpha = \epsilon_0 |E_k^\alpha|^2 / 2L_\infty$ is the wave energy density since $E_{-k}^\alpha = E_k^{\alpha*}$. Then, since \mathcal{W}_k^α is even in k and k is odd, the integral vanishes and momentum density is conserved.

For the conservation of energy density, we examine

$$\begin{aligned}\frac{d}{dt} \sum_j \frac{1}{2} \bar{n}_j m_j \int dv v^2 f_j &= - \sum_j \bar{n}_j m_j \int dv v D_j \frac{\partial f_{0j}}{\partial v} \\ &= 2 \sum_\alpha \int \frac{dk}{2\pi} \mathcal{W}_k^\alpha \sum_j \frac{\omega_{pj}^2}{k^2} \int dv \frac{(ikv)ik \frac{\partial f_{0j}}{\partial v}}{p^\alpha + ikv}.\end{aligned}$$

Then we let $ikv \rightarrow (ikv + p^\alpha) - p^\alpha$ in the numerator, and use equation (7.20) to obtain

$$\frac{d}{dt} \sum_j \frac{1}{2} \bar{n}_j m_j \int dv v^2 f_j = -2 \sum_\alpha \int \frac{dk}{2\pi} \mathcal{W}_k^\alpha \gamma_k^\alpha \quad (7.22)$$

since $p_{-k}^\alpha = p_k^{\alpha*}$. We then use the fact that the energy density varies in time as

$$\frac{\partial \mathcal{W}_k^\alpha}{\partial t} = 2\gamma_k^\alpha \mathcal{W}_k^\alpha \quad (7.23)$$

so that we may write equation (7.22) in the form

$$\frac{d}{dt} \left[\sum_j \frac{1}{2} \bar{n}_j m_j \int dv v^2 f_j + \sum_\alpha \int \frac{dk}{2\pi} \mathcal{W}_k^\alpha \right] = 0 \quad (7.24)$$

which demonstrates that the sum of the particle energy and wave energy is conserved.

For the more general problem of electromagnetic waves in the presence of a static magnetic field, the demonstration is much more involved, since the waves carry both momentum and energy in general, and the dispersion relation is much more formidable, so it will not be given here, but the conservation laws still follow from the kinetic equation.

Problem 7.2.1. Conservation of momentum density.

- (i) Fill in the steps between the first part of equation (7.19) and equation (7.21).
- (ii) Fill in the steps leading to equation (7.24).

7.2.3 Velocity space diffusion in a magnetic field

While the simplified theory given here outlined the methods of quasilinear theory, it can only be applied to the case with no magnetic field or the case with an infinite magnetic field. In order to examine the more interesting problems associated with wave heating or current drive, it is necessary to include the effects of magnetic fields, since wave heating usually uses either electron or ion cyclotron fundamental or harmonic resonances, and current drive (the generation of unidirectional currents by transferring wave momentum to selected particles) usually employs waves that only propagate in magnetized plasmas.

When the effects of a magnetic field are included, the problem is no longer one-dimensional, so we now need for the Fourier transforms of the basic variables,

$$f(\mathbf{r}, \mathbf{v}, t) = f_0(\mathbf{v}, t) + f_1(\mathbf{r}, \mathbf{v}, t) \quad (7.25)$$

$$f_1(\mathbf{r}, \mathbf{v}, t) = \int_{-\infty}^{\infty} \frac{d^3 k}{(2\pi)^3} \tilde{f}_k(\mathbf{v}, t) e^{ik \cdot r} \quad (7.26)$$

$$\mathbf{E}(x, t) = \int_{-\infty}^{\infty} \frac{d^3 q}{(2\pi)^3} \mathbf{E}_{\mathbf{q}}(t) e^{i\mathbf{q} \cdot \mathbf{r}} \quad (7.27)$$

$$\mathbf{B}(x, t) = \int_{-\infty}^{\infty} \frac{d^3 q}{(2\pi)^3} \tilde{\mathbf{B}}_{\mathbf{q}}(t) e^{i\mathbf{q} \cdot \mathbf{r}} \quad (7.28)$$

and again $\langle f \rangle = f_0(\mathbf{v}, t)$ where now the average is over the volume V .

We begin the analysis looking for the fast (wave) time scale, and then use the quasilinear diffusion equation to analyze the slow time scale evolution of f_0 . Following the development of Kennel and Engelmann [96] we choose to analyze this problem in cylindrical coordinates in velocity space and wavevector space, establishing \mathbf{B}_0 to be in the z -direction, so that

$$\begin{aligned} v_x &= v_\perp \cos \phi & v_y &= v_\perp \sin \phi \\ k_x &= k_\perp \cos \psi & k_y &= k_\perp \sin \psi. \end{aligned}$$

It is clear that the dispersion properties do not depend on ψ , since there are only two directions specified, that of the magnetic field and of the wavevector \mathbf{k} . Due to asymmetric initial or boundary conditions, however, a physical problem may have such dependence. Hence, if there were no asymmetries in the physical problem, we could let $\psi = 0$ with no loss of generality.

It is also convenient to use rotating coordinates for the wave field components in the form

$$\begin{aligned} \tilde{E}^\pm &= \tilde{E}_x \pm i\tilde{E}_y \\ \tilde{B}^\pm &= \tilde{B}_x \pm i\tilde{B}_y. \end{aligned}$$

In this representation, \tilde{E}^+ and \tilde{E}^- represent left- and right-handed waves, respectively, for $\text{Re } \omega > 0$. If $\text{Re } \omega < 0$, the polarizations are reversed. In these rotating coordinates, the additional phase shift ψ can be included by rotating an additional angle, so that the electric field vector for a specific \mathbf{k} can be represented by $\tilde{\mathbf{E}}_{\mathbf{k}} = (\tilde{E}_{\mathbf{k}}^+ e^{-i\psi}, \tilde{E}_{\mathbf{k}}^- e^{i\psi}, \tilde{E}_{\mathbf{k}}^\parallel)$.

Using these in the Fourier-transformed kinetic equation, the result may be written as

$$\hat{L}_{\mathbf{k}} \tilde{f}_{\mathbf{k}} = \hat{P}_{\mathbf{k}} f_0 + \frac{1}{2} \int_{-\infty}^{\infty} \frac{d^3 k'}{(2\pi)^3} (\hat{P}_{\mathbf{k}-\mathbf{k}'} \tilde{f}_{\mathbf{k}'} + \hat{P}_{\mathbf{k}} \tilde{f}_{\mathbf{k}-\mathbf{k}'}) \quad (7.29)$$

where we have introduced the operators

$$\hat{L}_{\mathbf{k}} = \frac{\partial}{\partial t} + i[k_z v_z + k_\perp v_\perp \cos(\phi - \psi)] - \epsilon \omega_c \frac{\partial}{\partial \phi} \quad (7.30)$$

$$\hat{P}_{\mathbf{k}} = -\frac{\epsilon e}{m} (\tilde{\mathbf{E}}_{\mathbf{k}} + \mathbf{v} \times \tilde{\mathbf{B}}_{\mathbf{k}}) \cdot \frac{\partial}{\partial \mathbf{v}}. \quad (7.31)$$

We note that the convolution term in equation (7.29) has been explicitly symmetrized. This term is second order in the amplitude (hence the convolution form), and represents wave-wave or mode-mode coupling which will be neglected in this quasilinear treatment since we are primarily interested in the slow development of $f_0(t)$ from quasilinear diffusion. We now need to solve the linear wave problem on the fast time scale, where the relation between \mathbf{k} and ω_k

is determined from the dispersion relation of equation (4.255) with the dielectric tensor elements of section 4.3.3 for an arbitrary distribution function.

If we now let $\partial/\partial t \rightarrow -i\omega_k$ where ω_k is the complex wave frequency, then equation (7.29) is a first-order differential equation in ϕ if we neglect the second-order convolution terms, with solution

$$\begin{aligned}\tilde{f}_k &= (\hat{L}_{k,\omega_k})^{-1} \hat{P}_k f_0 \\ &= \exp \left\{ \frac{-i[(\omega_k - k_z v_z)\phi - k_\perp v_\perp \sin(\phi - \psi)]}{\epsilon \omega_c} \right\} \\ &\quad \times \int^\phi d\phi' \exp \left\{ \frac{i[(\omega_k - k_z v_z)\phi' - k_\perp v_\perp \sin(\phi' - \psi)]}{\epsilon \omega_c} \right\} \hat{P}_k f_0.\end{aligned}\tag{7.32}$$

It is assumed that ω_k has a positive imaginary part so that the integral converges. This appears to limit the discussion to unstable modes since $\text{Im } \omega_k > 0$, but it can be extended to damped modes by analytic continuation.

In order to express \hat{P}_k more explicitly, we use the Bessel function identity of equation (4.179) in order to express the operator $(\hat{L}_{k,\omega_k})^{-1}$ as

$$\begin{aligned}(\hat{L}_{k,\omega_k})^{-1} &= - \sum_{n,m=-\infty}^{\infty} \frac{J_m J_n}{\epsilon \omega_c} \exp \left[i(n-m)\psi \frac{-i(\omega_k - m\epsilon \omega_c - k_z v_z)\phi}{\epsilon \omega_c} \right] \\ &\quad \times \int^\phi d\phi' \exp \left[\frac{i(\omega_k - n\epsilon \omega_c - k_z v_z)\phi'}{\epsilon \omega_c} \right]\end{aligned}\tag{7.33}$$

where the argument of the Bessel function is $k_\perp v_\perp / \epsilon \omega_c$, and we use the Maxwell equations to eliminate the wave magnetic fields from \hat{P}_k , with the result

$$\begin{aligned}\hat{P}_k &= - \frac{q}{m} \left[\frac{e^{i(\phi-\psi)}}{2} \left(\tilde{E}_k^- e^{i\psi} \hat{G}_k^+ + \frac{k_\perp \tilde{E}_k^\parallel}{\omega_k} \hat{H}^+ \right) \right. \\ &\quad + \frac{e^{-i(\phi-\psi)}}{2} \left(\tilde{E}_k^+ e^{-i\psi} \hat{G}_k^- + \frac{k_\perp \tilde{E}_k^\parallel}{\omega_k} \hat{H}^- \right) \\ &\quad \left. + \frac{ik_\perp}{2\omega_k} (\tilde{E}_k^+ e^{-i\psi} - \tilde{E}_k^- e^{i\psi}) \frac{\partial}{\partial \phi} + \tilde{E}_k^\parallel \frac{\partial}{\partial v_z} \right]\end{aligned}\tag{7.34}$$

where

$$\begin{aligned}\hat{G}_k^\pm &= \frac{\partial}{\partial v_\perp} \pm \frac{i}{v_\perp} \frac{\partial}{\partial \phi} - \frac{k_z}{\omega_k} \hat{H}^\pm \\ \hat{H}^\pm &= v_z \frac{\partial}{\partial v_\perp} - v_\perp \frac{\partial}{\partial v_z} \pm \frac{iv_z}{v_\perp} \frac{\partial}{\partial \phi}.\end{aligned}\tag{7.35}$$

This completes the problem of solving for \tilde{f}_k in terms of f_0 and the wave fields and polarizations.

For the evolution of $f_0(t)$, we use the space-averaged kinetic equation, which, after Fourier transformation and again symmetrizing the convolution terms, is

$$\begin{aligned}\frac{\partial f_0}{\partial t} - \epsilon \omega_c \frac{\partial f_0}{\partial \phi} &= \frac{1}{2V_\infty} \int \frac{d^3 k}{(2\pi)^3} [\hat{P}_{-k} (\hat{L}_{k,\omega_k})^{-1} \hat{P}_k + \hat{P}_k (\hat{L}_{-k,\omega_{-k}})^{-1} \hat{P}_{-k}] f_0 \\ &= \frac{1}{2} \int \frac{d^3 k}{(2\pi)^3} (\hat{D}_k + \hat{D}_{-k}) f_0\end{aligned}\quad (7.36)$$

where the linear expression for \tilde{f}_k has been substituted into the convolution terms, and we again use the abbreviated form $\lim_{V \rightarrow \infty} 1/V \equiv 1/V_\infty$. This formally completes the derivation of the evolution of the zero-order distribution function from quasilinear theory and the quasilinear diffusion operators, \hat{D}_k and \hat{D}_{-k} , are explicit, but very complicated.

Problem 7.2.2. Solving the linearized kinetic equation.

- (i) Show that equation (7.32) is the solution of the linearized Vlasov equation.
- (ii) Show that \hat{P}_k has the form given by equation (7.34).
- (iii) Show that \hat{H}^\pm vanishes for isotropic distributions.

7.2.3.1 Gyroperiod expansion

It is fruitful to introduce a small parameter in order to simplify some of the complications in our treatment. If we limit ourselves to time scales that are long compared to the gyroperiod, and length scales that are long compared to the Larmor radius, then many simplifications occur. We note that this also limits us to instabilities whose growth over a gyroperiod is small. This approximation immediately smooths out any inhomogeneities in the ϕ distribution, since all particles make so many orbits on the macroscopic time scales. It is possible that the first order distribution, \tilde{f}_k , may have rapid variations due to the waves, but the space-averaged $f_0(t)$ must vary slowly. We make the dependence explicit by defining

$$f_0 = f_0^{(0)} + \frac{\epsilon}{\omega_c} f_0^{(1)} + \mathcal{O}\left(\frac{1}{\omega_c^2}\right). \quad (7.37)$$

Substituting equation (7.37) into equation (7.36), and keeping only the lowest order terms, we find simply

$$\frac{\partial f_0^{(0)}}{\partial \phi} = 0 \quad (7.38)$$

since we assume the wave background produces only a slow variation in time.

This result already tells us several things about the ϕ -dependence of the diffusion process. It says that the lowest-order spatially averaged distribution function is independent of the phase ϕ because it has to make many gyro-orbits before it can diffuse enough to be significant. The corresponding diffusion in

velocity space is therefore two-dimensional, since $\partial f_0^{(0)}/\partial\phi$ always vanishes. A corollary of this is that if the excited wave spectrum is axially symmetric in k -space, the diffusion is intrinsically two-dimensional, and the initial axial symmetry is preserved for all times.

The zero order equation (7.38) still leaves the time dependence of $f_0^{(0)}$ undetermined, so we must go to the next order to find

$$\frac{\partial f_0^{(0)}}{\partial t} - \frac{\partial f_0^{(1)}}{\partial\phi} = \frac{1}{2} \int \frac{d^3k}{(2\pi)^3} (\hat{D}_k + \hat{D}_{-k}) f_0^{(0)}. \quad (7.39)$$

If we now demand that all $f_0^{(n)}$ be exactly periodic in ϕ , so that averaging over the period $[0, 2\pi]$ in ϕ eliminates all of the higher order terms, then we can obtain a Larmor phase-averaged equation of the form

$$\frac{\partial f_0^{(0)}}{\partial t} = \frac{1}{4\pi} \int_0^{2\pi} d\phi \int \frac{d^3k}{(2\pi)^3} (\hat{D}_k + \hat{D}_{-k}) f_0^{(0)}. \quad (7.40)$$

Since now only the ϕ -independent term is left, we can delete the superscript notation. This also greatly simplifies the linear portion of the problem, so that now we may write (with $\partial/\partial\phi \rightarrow 0$ from equation (7.38) in equations (7.34) and (7.35) so that the \pm terms and notation disappear for \hat{G}_k and \hat{H})

$$\tilde{f}_k = \frac{iq}{m} \sum_{m,n=-\infty}^{\infty} \frac{J_m e^{i(m-n)(\phi-\psi)}}{\omega_k - n\epsilon\omega_c - k_z v_z} (\mathcal{E}_{n,k} \hat{G}_k + J_n \tilde{E}_k^\parallel \hat{K}_{n,k}) f_0 \quad (7.41)$$

where $\mathcal{E}_{n,k}$ is defined by

$$\mathcal{E}_{n,k} \equiv \frac{1}{2} (\tilde{E}_k^- e^{i\psi} J_{n+1} + \tilde{E}_k^+ e^{-i\psi} J_{n-1}) \quad (7.42)$$

and $\hat{K}_{n,k}$ is the operator

$$\hat{K}_{n,k} \equiv \frac{\partial}{\partial v_z} + \frac{\epsilon n \omega_c}{\omega_k v_\perp} \hat{H}. \quad (7.43)$$

Equation (7.41) is equivalent to equation (4.180), and can be used to generate the linear dielectric tensor and dispersion relation through equation (4.177).

In order to evaluate those terms involving the $-k$ subscript, we note the symmetry relations for the variable ψ , where $-k = (k_\perp, -k_z, \psi + \pi)$ so that $E_{-k} = E_k^*$ and $B_{-k} = B_k^*$, so that

$$\begin{aligned} \tilde{E}_{-k}^+ e^{-i(\psi+\pi)} &= -(\tilde{E}_k^- e^{i\psi})^* \\ \tilde{E}_{-k}^- e^{i(\psi+\pi)} &= -(\tilde{E}_k^+ e^{-i\psi})^* \\ \tilde{E}_{-k}^\parallel &= (\tilde{E}_k^\parallel)^*. \end{aligned}$$

These relations, along with $\omega_{-\mathbf{k}} = -\omega_{\mathbf{k}}^*$, lead to $\hat{P}_{-\mathbf{k}} = (\hat{P}_{\mathbf{k}})^*$, $\tilde{f}_{-\mathbf{k}} = (\tilde{f}_{\mathbf{k}})^*$, and $\hat{D}_{-\mathbf{k}} = (\hat{D}_{\mathbf{k}})^*$. Hence the quasilinear term in equation (7.40) is pure real.

Averaging over ϕ at this point, we note that $\partial/\partial\phi$ from equations (7.34) and (7.35) in the *first* operator of $\hat{D}_{\pm\mathbf{k}}$ operates not only on f_0 , but that we can replace $e^{\pm i\phi} i\partial/\partial\phi \rightarrow \pm e^{\pm i\phi}$ and $i\partial/\partial\phi \rightarrow 0$. Using these relations and the earlier symmetry relations, we may write the averaged *first* operator $\hat{P}_{-\mathbf{k}}$ of $\hat{D}_{\mathbf{k}}$ (operating on $\tilde{f}_{\mathbf{k}}$ of equation (7.41)) as

$$\begin{aligned}\hat{P}_{-\mathbf{k}} = & -\frac{q}{m} \left[\frac{e^{i(\phi-\psi)}}{2} \left(\tilde{E}_{\mathbf{k}}^+ e^{-i\psi} \hat{G}_{\mathbf{k}}^+ + \frac{k_{\perp} \tilde{E}_{\mathbf{k}}^{\parallel}}{\omega_{\mathbf{k}}} \hat{H}^+ \right)^* \right. \\ & \left. + \frac{e^{-i(\phi-\psi)}}{2} \left(\tilde{E}_{\mathbf{k}}^- e^{i\psi} \hat{G}_{\mathbf{k}}^+ + \frac{k_{\perp} \tilde{E}_{\mathbf{k}}^{\parallel}}{\omega_{\mathbf{k}}} \hat{H}^+ \right)^* + (\tilde{E}_{\mathbf{k}}^{\parallel})^* \frac{\partial}{\partial v_z} \right] \quad (7.44)\end{aligned}$$

where now

$$\begin{aligned}\hat{G}_{\mathbf{k}}^+ &= \hat{G}_{\mathbf{k}} + \frac{\omega_{\mathbf{k}} - k_z v_z}{\omega_{\mathbf{k}} v_{\perp}} \\ \hat{H}^+ &= \hat{H} + \frac{v_z}{v_{\perp}}.\end{aligned}$$

Noting now that the only remaining ϕ -dependence is the simple exponential phase which leads to a Kronecker delta function, collapsing the double sum to a single sum, we may write equation (7.40) in the form

$$\frac{\partial f_0}{\partial t} = \frac{\partial}{\partial \mathbf{v}} \cdot \left(\mathbf{D} \cdot \frac{\partial f_0}{\partial \mathbf{v}} \right) \quad (7.45)$$

where the quasilinear diffusion tensor is given by the dyadic

$$\mathbf{D} = \frac{q^2}{m^2} \sum_{n=-\infty}^{\infty} \frac{1}{V_{\infty}} \int \frac{d^3k}{(2\pi)^3} \frac{i}{\omega_{\mathbf{k}} - n\epsilon\omega_c - k_z v_z} (\mathbf{a}_{n,\mathbf{k}})^* (\mathbf{a}_{n,\mathbf{k}}) \quad (7.46)$$

with

$$\begin{aligned}\mathbf{a}_{n,\mathbf{k}} = & \mathcal{E}_{n,\mathbf{k}} \frac{k_z}{\omega_{\mathbf{k}}} \left[\left(\frac{\omega_{\mathbf{k}}}{k_z} - v_z \right) \hat{E}_{v_{\perp}} + v_{\perp} \hat{E}_z \right] \\ & + \tilde{E}_{\mathbf{k}}^{\parallel} J_n \left[\hat{E}_z + \frac{n\epsilon\omega_c}{\omega_{\mathbf{k}} v_{\perp}} (v_z \hat{E}_{v_{\perp}} - v_{\perp} \hat{E}_z) \right]. \quad (7.47)\end{aligned}$$

Again, as in [chapter 4](#), we could eliminate the Bessel function sum by use of the Newberger sum rule.

Since all of these expressions depend on the relation between $\omega_{\mathbf{k}}$ and \mathbf{k} , any actual solutions for the quasilinear diffusion must include the solution of the linear dispersion relation for the given f_0 which relates them. This is a difficult problem,

since in these cases, the Maxwellian distribution is suitable only for a zero-order trial solution, if that, so that generally each component of the dielectric tensor is a combination of formidable integrals and transcendental functions. In some specific cases, the solution may simplify because either the specific wave branches are given along with their polarization, or because the problem is one-dimensional and many terms vanish. For example, with waves propagating exactly parallel to the magnetic field, we have $k_{\perp} = 0$ and the waves are either right-handed, as in the fast Alfvén wave (the whistler wave at higher frequencies), or left-handed, as in the slow or torsional Alfvén wave, or electrostatic wave. Each of these cases reduces the complexity substantially, but represents a severely restricted problem which may not be representative of the physics of quasilinear diffusion.

Problem 7.2.3. Zero order equation. Justify equation (7.38).

Problem 7.2.4. Averaging over ϕ . Show that in the average over ϕ , integrating the terms involving $\partial/\partial\phi$ by parts in the first operator of $\hat{D}_{\pm k}$ leads to the recipes $e^{\pm i\phi} i\partial/\partial\phi \rightarrow \pm e^{\pm i\phi}$ and $i\partial/\partial\phi \rightarrow 0$ in obtaining equation (7.44).

7.2.3.2 Electrostatic case

When all the waves in the weak turbulence spectrum are slow waves such that we may use the electrostatic approximation, $\tilde{\mathbf{E}} = -ik\tilde{\varphi}$, then

$$\frac{1}{2\pi} \int_0^{2\pi} \tilde{f}_k d\phi = \frac{q}{m} k_z \tilde{\varphi}_k \sum_{n=-\infty}^{\infty} \frac{J_n^2}{\omega_k - \epsilon\omega_c - k_z v_z} \left(\frac{\partial}{\partial v_z} + \frac{n\epsilon\omega_c}{k_z v_{\perp}} \frac{\partial}{\partial v_{\perp}} \right) f_0. \quad (7.48)$$

Using this expression, the diffusion tensor may be described by

$$D = \frac{q^2}{m^2} \sum_{n=-\infty}^{\infty} \frac{1}{V_{\infty}} \int \frac{d^3 k}{(2\pi)^3} \frac{i J_n^2 |\tilde{\varphi}_k|^2}{\omega_k - n\epsilon\omega_c - k_z v_z} \mathbf{b}_{n,k} \mathbf{b}_{n,k} \quad (7.49)$$

since $\mathbf{a}_{n,k} = -i\tilde{\varphi}_k J_n \mathbf{b}_{n,k}$ with

$$\mathbf{b}_{n,k} = \frac{n\epsilon\omega_c}{v_{\perp}} \hat{\mathbf{E}}_{v_{\perp}} + k_z \hat{\mathbf{E}}_z. \quad (7.50)$$

If we define $\omega_k \equiv \omega_{rk} + i\gamma_k$, then we may write equation (7.49) in terms of its real part only as

$$D = \frac{q^2}{m^2} \sum_{n=-\infty}^{\infty} \frac{1}{V_{\infty}} \int \frac{d^3 k}{(2\pi)^3} \frac{\gamma_k J_n^2 |\tilde{\varphi}_k|^2}{(\omega_{rk} - n\epsilon\omega_c - k_z v_z)^2 + \gamma_k^2} \mathbf{b}_{n,k} \mathbf{b}_{n,k} \quad (7.51)$$

since the imaginary contribution vanishes.

Problem 7.2.5. Electrostatic quasilinear diffusion tensor. Show that equation (7.46) reduces to equation (7.49) if $\tilde{\mathbf{E}} = -ik\tilde{\varphi}$.

7.2.4 H-theorem for quasilinear theory

One of the purposes of quasilinear theory is to study the effects of saturation of growing waves by the modification of the distribution function by the waves themselves. One way of addressing this problem is to examine the positive definite functional H ,

$$H = \frac{1}{2} \sum_j \int d^3 v (f_{0j})^2 \quad (7.52)$$

where the sum is over the species j . Integrating by parts, we find that dH/dt may be written

$$\begin{aligned} \frac{dH}{dt} &= - \sum_j \int d^3 v \frac{\partial f_{0j}}{\partial \mathbf{v}} \cdot \mathbf{D} \cdot \frac{\partial f_{0j}}{\partial \mathbf{v}} \\ &= - \sum_j \frac{q_j^2}{m_j^2} \sum_{n=-\infty}^{\infty} \int d^3 v \frac{1}{V_\infty} \int \frac{d^3 k}{(2\pi)^3} \\ &\quad \times \left| \frac{\partial f_0}{\partial \mathbf{v}} \cdot \mathbf{a}_{n,k} \right|^2 \frac{\gamma_k}{(\omega_{rk} - n\epsilon_j \omega_c - k_z v_{zj})^2 + \gamma_k^2} \leq 0. \end{aligned} \quad (7.53)$$

Then, since H is positive definite, and dH/dt is negative definite, it follows that H must decrease monotonically with time until it reaches some time asymptotic limit. This limit corresponds to a zero in dH/dt , which implies a marginally stable state, since there is neither growth nor decay.

As an alternative to marginal stability, we consider the possibility of a domain in \mathbf{k} -space where γ_k is positive and we have $dH/dt = 0$. Then, since each term in dH/dt is positive definite, it follows that

$$\mathbf{a}_{n,k} \cdot \frac{\partial f_0}{\partial \mathbf{v}} = (\mathcal{E}_{n,k} \hat{G}_k + J_n \tilde{E}_k^\parallel \hat{K}_{n,k}) f_0 \equiv 0 \quad (7.54)$$

for all \mathbf{v} and n in the domain of \mathbf{k} , which from equation (7.41) implies that $\tilde{f}_k \equiv 0$ so that there are no waves at all in that region, which is contradictory. Hence, the asymptotic state implies marginal stability for all waves.

7.2.4.1 Plateau formation and resonant diffusion

In developing this argument, we avoided taking $\gamma_k \rightarrow 0^+$, first, so that we did not distinguish between resonant ($\omega_k - n\epsilon\omega_c - k_z v_z = 0$) and nonresonant diffusion. If, however, we consider the limit $\gamma_k \rightarrow 0^+$ first, then we may discuss the formation of the quasilinear plateau, at which point the wave growth ceases. In this limit, equation (7.46) becomes

$$\mathbf{D} = \frac{\pi q^2}{m^2} \sum_{n=-\infty}^{\infty} \frac{1}{V_\infty} \int \frac{d^3 k}{(2\pi)^3} \delta(\omega_k - n\epsilon\omega_c - k_z v_z) (\mathbf{a}_{n,k})^* (\mathbf{a}_{n,k}) \quad (7.55)$$

where now

$$\mathbf{a}_{n,\mathbf{k}} = \left(\mathcal{E}_{n,\mathbf{k}} + \frac{v_z}{v_\perp} \tilde{\mathbf{E}}_{\mathbf{k}}^\parallel J_n \right) \left(\frac{n\epsilon\omega_c}{\omega_{\mathbf{k}}} \hat{\mathbf{E}}_{v_\perp} + \frac{k_z v_\perp}{\omega_{\mathbf{k}}} \hat{\mathbf{E}}_z \right). \quad (7.56)$$

A sufficient condition for the steady state case, which leads both to $dH/dt = 0$ and $\partial f_0/\partial t = 0$ is that

$$\mathbf{a}_{n,\mathbf{k}} \cdot \frac{\partial f_0}{\partial \mathbf{v}} = \left(\mathcal{E}_{n,\mathbf{k}} + \frac{v_z}{v_\perp} \tilde{\mathbf{E}}_{\mathbf{k}}^\parallel J_n \right) \hat{\mathbf{G}}_{\mathbf{k}} f_0 = 0.$$

or more simply,

$$\hat{\mathbf{G}}_{\mathbf{k}} f_0 = \frac{k_z}{\omega_{\mathbf{k}}} \left[\left(\frac{\omega_{\mathbf{k}}}{k_z} - v_z \right) \frac{\partial f_0}{\partial v_\perp} + v_\perp \frac{\partial f_0}{\partial v_z} \right] = 0 \quad (7.57)$$

and this condition is required everywhere in velocity space where the diffusion tensor is nonzero. For one particular value of \mathbf{k} (or of k_z), this is satisfied by the characteristics of $\hat{\mathbf{G}}_{\mathbf{k}}$, such that

$$(v_z - \omega_{\mathbf{k}}/k_z)^2 + v_\perp^2 = \text{constant} \quad (7.58)$$

or if $f_0 = f_0[(v_z - \omega_{\mathbf{k}}/k_z)^2 + v_\perp^2]$ in that region of velocity space. This represents curves of constant particle energy in the wave frame moving at the parallel phase velocity.

If only one value of \mathbf{k} were excited, then the single wave characteristics would be a set of concentric circles in velocity space, with the origin displaced by the parallel phase velocity of the wave. Once this distribution was established, there would be no further diffusion, and particles would have bounded energies. When multiple waves are excited, however, and this is the general case considered by quasilinear theory, these characteristics intersect, and for a broad spectrum of waves, the single wave condition cannot be satisfied except for the trivial solution that f_0 be constant. The intersection of the characteristics allows individual particles to move from one set to another, and may lead to unbounded energies.

If we restrict our attention to either the zero magnetic field case, or the infinite magnetic field case, then the Landau resonance at $v_z = \omega_{\mathbf{k}}/k_z$ restricts the parallel motion, so the surfaces are restricted to constant v_\perp . Then if the spectrum of \mathbf{k} is bounded, so that we can define a v_{\max} and a corresponding v_{\min} , where these are the maximum and minimum parallel phase velocities of the excited spectrum of waves, then we only require the distribution function to be flat over that range of v_z . This flat region in figure 7.1 is called a plateau region, and is the limit condition of quasilinear diffusion. On longer, collisional time scales, this plateau will be changed back towards an equilibrium distribution, but quasilinear theory by itself does not evolve toward equilibrium, since it ends in a state with finite amplitude, steady state waves.

When the magnetic field is finite, the problem is much more complicated unless we restrict our attention to $k_\perp = 0$ modes, where the waves are purely

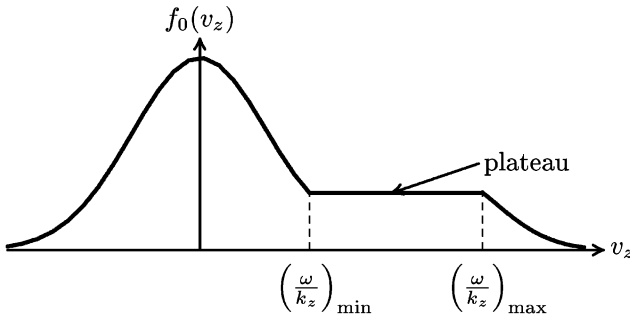


Figure 7.1. Quasilinear plateau between the end points of the k_z spectrum.

right-handed or left-handed, and the characteristics may not intersect. In general, however, more general k -vectors are excited, and true plateaus do not exist, but quasi-plateaus, through the coupling of quasilinear diffusion with a Fokker-Planck analysis including collisions, are possible, but do not admit analytic solutions.

7.2.5 Weak bump-on-the-tail instability

One of the simplest instabilities that leads to quasilinear diffusion and to plateau formation is the weak beam-plasma instability, or since in this case the weak beam is taken to be spread out in velocity and hence adds a gentle bump on the tail of the distribution function, it is also called the bump-on-the-tail instability. We require both that the magnitude of the bump be small and that it be spread out in order to use quasilinear theory. Otherwise, the bump leads to strong turbulence, and the approximations we have used fail long before the plateau is reached. For simplicity, we shall consider an unmagnetized plasma (we could also use the infinite magnetic field limit) in order to make the problem one-dimensional. The initial distribution is illustrated in figure 7.2 where the two velocities v_1 and v_2 denote the limits where unstable waves occur.

We can see from figure 7.2 some of the quasilinear processes that must evolve as waves grow in the unstable region between v_1 and v_2 , since from equation (4.58), γ_k is proportional to the slope of the distribution function, and hence positive in this range. The first step is for the waves to grow to sufficient amplitude that quasilinear diffusion begins to change the distribution function, tending to flatten the distribution in the positive slope (resonant) region due to resonant diffusion. Lowering the level at the upper end and raising the level at the lower end, however, extends the region of instability unless the regions for $v > v_2$ and $v < v_1$ are simultaneously lowered and raised, respectively, but these are initially in the nonresonant diffusion region. Resonant diffusion alone, then, would tend to broaden the resonant region until the plateau indicated was

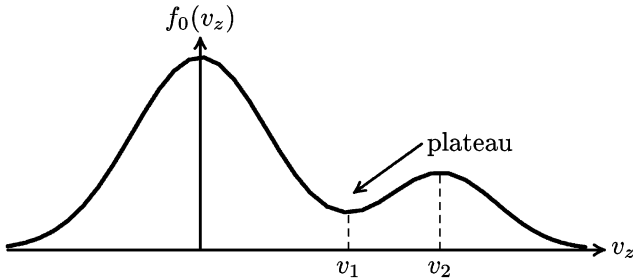


Figure 7.2. Bump-on-tail distribution showing initial unstable region and eventual plateau.

reached, at which point resonant diffusion ceases. The indicated plateau is only suggestive, however, since it was drawn to conserve energy, but fails to conserve momentum. In order to conserve both, the entire distribution must be shifted by various amounts, and this requires nonresonant diffusion processes.

7.2.5.1 Resonant diffusion

Looking more carefully at these processes, we have, from equation (4.58), that the growth rate, for $\omega \simeq \omega_{pe}$, may be represented by

$$\gamma_k = \frac{\pi}{2} \omega_k \frac{\omega_{pe}^2}{|k|^3} k \left. \frac{\partial f_0}{\partial v} \right|_{v=\omega_k}. \quad (7.59)$$

Thus, for the velocity range $v_1 < v < v_2$, since $\omega_{pe}/k_1 \simeq v_1$ and $\omega_{pe}/k_2 \simeq v_2$, there is a range of k , $k_2 < k < k_1$ (or $-k_1 < k < -k_2$ since $\omega_{-k} = -\omega_k^*$) where waves grow in time. At time 0^+ , this leads to a growth spectrum illustrated in figure 7.3(a) and a low wave energy spectrum shown in figure 7.3(b). As the wave energy density grows according to equation (7.23), the resonant diffusion coefficient builds as shown in figure 7.3(c), since

$$D^r = \frac{2e^2}{\epsilon_0 m_e^2} \int_{-\infty}^{\infty} \frac{dk}{2\pi} \pi \delta(\omega_k - kv) \mathcal{W}_k \simeq \frac{e^2}{\epsilon_0 m_e^2 v} \mathcal{W}_{\omega_{pe}/v}(t) \quad (7.60)$$

leading to changes in the distribution function which will tend to reduce γ_k . As the plateau develops, eventually $\gamma_k < 0$ everywhere as in the lower curve of figure 7.3(a).

7.2.5.2 Nonresonant diffusion

Generally speaking, nonresonant diffusion is much weaker than resonant diffusion, but it acts on many more particles, so the net effects may be of the

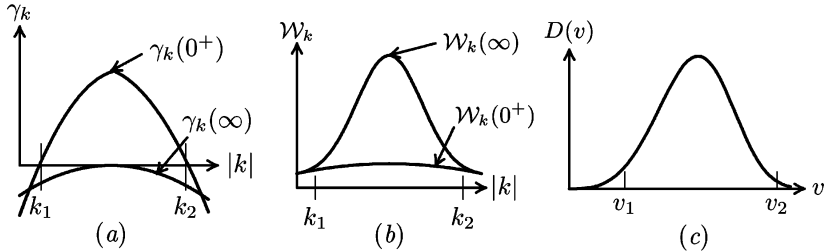


Figure 7.3. (a) Initial and asymptotic growth rate spectrum; (b) wave energy density spectrum; and (c) quasilinear diffusion coefficient at general time t .

same order of magnitude. The nonresonant diffusion coefficient for our one-dimensional example is given by the principal part of equation (7.17) as

$$\begin{aligned} D^{nr} &= \frac{2e^2}{\epsilon_0 m_e^2} \int_{-\infty}^{\infty} \frac{dk}{2\pi} \mathcal{W}_k \frac{\gamma_k}{(\omega_r - kv)^2} \\ &\simeq \frac{2}{\bar{n}m_e} \int_{-\infty}^{\infty} \frac{dk}{2\pi} \gamma_k \mathcal{W}_k \\ &\simeq \frac{1}{\bar{n}m_e} \frac{\partial}{\partial t} \int_{-\infty}^{\infty} \frac{dk}{2\pi} \mathcal{W}_k \end{aligned} \quad (7.61)$$

where the first approximation is valid for speeds much less than the phase velocity and $k^2 \lambda_D^2 \ll 1$, and the second uses equation (7.23). That $D^{nr} \ll D^r$ is apparent from the fact that $D^{nr} \sim \gamma_k \mathcal{W}_k$ while $D^r \sim \mathcal{W}_k$.

Now since from equation (7.61), D^{nr} is independent of v , then the velocity diffusion equation becomes

$$\frac{\partial f_0(v, t)}{\partial t} = D^{nr} \frac{\partial^2}{\partial v^2} f_0(v, t) \quad (7.62)$$

which may also be written as

$$\frac{\partial f_0(v, \tau)}{\partial \tau} = \frac{1}{2m_e} \frac{\partial^2}{\partial v^2} f_0(v, \tau) \quad (7.63)$$

by changing variables to $\tau(t) = (1/\bar{n}\pi) \int_{-\infty}^{\infty} \mathcal{W}_k(t) dk$. This is the standard form of the diffusion equation, whose solution may be written for an arbitrary initial distribution $f_0(v, \tau(0))$ in terms of the Green function as

$$f_0(v, \tau(t)) = \int dv' f_0(v', \tau(0)) G(v', v, \tau(t)) \quad (7.64)$$

$$G(v', v, \tau(t)) = \left\{ \frac{m_e}{2\pi[\tau(t) - \tau(0)]} \right\}^{1/2} \exp \left\{ -\frac{m_e(v' - v)^2}{2[\tau(t) - \tau(0)]} \right\}. \quad (7.65)$$

If the zero order distribution is Maxwellian (in the nonresonant region), the solution of equation (7.64) is especially simple, and takes the form

$$f_0(v, t) = \left\{ \frac{m_e}{2\pi[\kappa T_e + \tau(t) - \tau(0)]} \right\}^{1/2} \exp \left\{ -\frac{m_e v^2}{2[\kappa T_e + \tau(t) - \tau(0)]} \right\}. \quad (7.66)$$

From the form of the solution of equation (7.66) and from the general character of diffusion equations, the evolution of the distribution function in the nonresonant region takes the form of a broadening of the distribution function, as one might expect from the conversion of wave energy to particle energy. The energy gain per particle is

$$\frac{1}{2}\kappa T_e \rightarrow \frac{1}{2}\kappa T_e + \frac{1}{n} \int_{-\infty}^{\infty} \frac{dk}{2\pi} [\mathcal{W}_k(\infty) - \mathcal{W}_k(0)].$$

The additional energy is due to the change in $\tau(t)$, such that if we define the quantity $\Delta\mathcal{W} \equiv \int_{-\infty}^{\infty} [\mathcal{W}_k(\infty) - \mathcal{W}_k(0)] dk / 2\pi$, the change in energy for the resonant particles may be found from equation (7.15) with equation (7.60) and the change for the nonresonant particles from equation (7.62) with equation (7.61), so that the results may be summarized as

$$\Delta \left(\bar{n} \int dv \frac{1}{2} m_e v^2 f_0 \right)^r = -2\Delta\mathcal{W} \quad (7.67)$$

$$\Delta \left(\bar{n} \int dv \frac{1}{2} m_e v^2 f_0 \right)^{nr} = +\Delta\mathcal{W}. \quad (7.68)$$

These results lead to the interpretation that the resonant electrons lose two units of energy for every unit of energy the nonresonant electrons gain, the extra unit of energy going to the waves, so the resonant particles have both heated the main bulk of the plasma and increased the energy density of the wave fluctuations.

At this point, we cannot calculate in detail the form of the distribution function as it evolves without doing a numerical calculation. We can, however, indicate the basic form of the evolved distribution as the plateau forms and the distribution broadens by also noting that the conservation of momentum requires that as the resonant electrons lose momentum (they fall back on the average in order to fill in the depression in $f(v)$), the bulk electrons must gain momentum, shifting the main distribution slightly to the right in [figure 7.2](#). Assuming the distribution will remain relatively smooth (since diffusion processes always tend to smooth transition regions), we sketch the general form of the asymptotic distribution function in [figure 7.4](#) where the broadening and shifts are exaggerated.

We conclude this section by noting that although the distribution eventually is modified so that it is everywhere stable or marginally stable, it is not an equilibrium distribution and there remain finite amplitude waves in the marginally stable regions of the wave spectrum as a remnant of the originally unstable

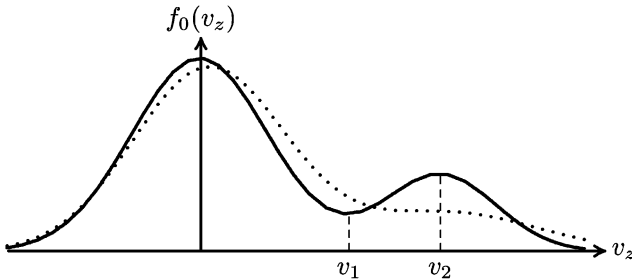


Figure 7.4. Original bump-on-tail distribution (full curve) and time asymptotic form of $f_0(v, \infty)$ (dotted curve).

distribution. It remains for collisional effects to finally relax the distribution towards an equilibrium. We also note that while only quasilinear effects have been considered in this section, there are inevitably other nonlinear wave–wave interactions also which will modify these conclusions somewhat.

Problem 7.2.6. The nonresonant diffusion equation. Show that the general solution of equation (7.64) and the specific solution of equation (7.66) are both solutions of equation (7.63).

Problem 7.2.7. Energy gain and loss. Verify equation (7.67) for the resonant electrons and equation (7.68) for the nonresonant electrons.

7.2.6 Effects of collisions

In the restricted domain of quasilinear theory outlined in the previous sections, it has been assumed that the plasma is collisionless. In cases where the growth rates of the instabilities are large enough that quasilinear diffusion modifies the distribution on a time scale which is short compared to the collision time scale, this neglect is reasonable. In the latter phases of the plateau formation, however, there always comes a stage where collisions become important because the growth rates decrease monotonically. When collisions are included, the evolution equation becomes the Fokker–Planck equation,

$$\frac{df_i}{dt} = \sum_j C(f_i, f_j) + \frac{\partial}{\partial \mathbf{v}} \cdot \left(\mathbf{D} \cdot \frac{\partial f_i}{\partial \mathbf{v}} \right) \quad (7.69)$$

where $C(f_i, f_j)$ denotes the collision operator between species i and j , and is taken to be of the form given by Landau [99]:

$$C(f_i, f_j) = - \frac{\partial}{\partial \mathbf{v}} \cdot \mathbf{S}_i^j \quad (7.70)$$

$$\begin{aligned} \mathbf{S}_i^j = & \frac{q_i^2 q_j^2}{8\pi\epsilon_0 m_i} \ln \Lambda \int d^3 v' \frac{(\mathbf{v} - \mathbf{v}')^2 \mathbf{l} - (\mathbf{v} - \mathbf{v}')(\mathbf{v} - \mathbf{v}')}{|\mathbf{v} - \mathbf{v}'|^3} \\ & \times \left[\frac{f_i(\mathbf{v})}{m_j} \frac{\partial}{\partial \mathbf{v}'} f_j(\mathbf{v}') - \frac{f_j(\mathbf{v}')}{m_i} \frac{\partial}{\partial \mathbf{v}} f_i(\mathbf{v}) \right]. \end{aligned} \quad (7.71)$$

In general, the sum over species includes collisions between particles of the same species (electron-electron or ion-ion) as well as collisions between different species (electron-ion).

We can get an idea of the possible domain where collisions become important if we treat a particularly simple case, where we use equation (7.60) for the quasilinear diffusion coefficient and represent the electron-electron collisions only through the approximate operator in the resonant region as

$$C(f_0, f_0) \sim \nu v_t^2 \frac{d^2}{dv^2} (f_M - f_0)$$

where f_M is a Maxwellian distribution and ν is the collision frequency, while v_t is not the true mean velocity, but is of that order. The important feature to notice is that the collision term depends on the second derivative of the deviation of the distribution function from equilibrium. If we assume that the quasilinear term approximately balances the collision term, then

$$D \frac{\partial f_0}{\partial v} + \nu v_t^2 \frac{\partial}{\partial v} (f_0 - f_M) \simeq 0$$

so that

$$\frac{\partial f_0}{\partial v} \simeq \left[1 + \frac{\omega_{pe}^2 \mathcal{W}_{\omega_{pe}/v}}{\nu v \bar{n} m_e v_t^2} \right]^{-1} \frac{\partial f_M}{\partial v}. \quad (7.72)$$

Using this expression in the Landau damping formula equation (7.59) indicates that the damping rate is roughly

$$\gamma_k \simeq \gamma_L \left[1 + \frac{\omega_{pe}}{\nu} \frac{k \mathcal{W}_k}{\bar{n} m_e v_t^2} \right]^{-1} \quad (7.73)$$

so that both the ratio of the wave frequency ($\omega \sim \omega_{pe}$) to the collision frequency and the ratio of the wave energy density to the particle energy density influence the deviation of the growth rate from the Landau rate. It is apparent from equation (7.73) that either a low wave energy density or a large (relatively speaking) collision frequency reduces the quasilinear effects.

7.3 Nonlinear wave-particle-wave applications

7.3.1 Plasma wave echoes

Plasma wave echoes, described by Gould *et al* [100], are fundamentally a nonlinear response to two different impulses separated in time by an interval

τ . The analysis is based on weak turbulence theory which couples wave modes through weak nonlinear interactions. Before calculating the echo response, we discuss the problem in its simplest terms in order to understand the fundamental physics involved.

The echo phenomenon is a classic example which demonstrates the ‘memory’ of the plasma. We are familiar with the fact that an impulse in time (or space) will lead to Landau damping of the plasma wave potential, but there remains an undamped perturbation of the distribution function. The echo is a means of adding another perturbation to this undecayed perturbation (making it a second order perturbation) so that the stored information can be momentarily (or locally) recovered. This can be understood by imagining an undamped first-order perturbation varying as $\exp[i\omega_1(-t + x/v)]$ that was produced at $x = 0$ at frequency ω_1 . Downstream, after the potential perturbation has Landau damped away, another perturbation varying as $\exp[i\omega_2(t - (x - \ell/v))]$ is introduced a distance ℓ from the first, so the second order perturbation varies as $\exp[i((\omega_2 - \omega_1) + \omega_2\ell/v + (\omega_1 - \omega_2)x/v)]$. Now at the position given by $\ell' = \ell\omega_2/(\omega_2 - \omega_1)$, the integral over velocity will not phase mix as the exponential has no v -dependence there. Hence, at this position, a second order potential will be generated at frequency $\omega_3 = \omega_2 - \omega_1$. For a distribution over velocities, this echo will have finite extent in space. For the temporal echo, the echo occurs at $\tau' = k_2\tau/k_3$ where τ is the delay between two impulses with wavenumbers k_1 and k_2 and $k_3 = k_2 - k_1$. We will calculate the temporal echo case, but the fundamental phenomenon is the same in either time or space.

This phenomenon is not unique to plasmas, as spin echoes and numerous other examples have been found in other fields. The ability to generate an echo is dependent, of course, on the retention of the original information, and if collisions, though weak enough to be ignored in the Landau damping of the potentials, are sufficiently frequent to damp the perturbation before the echo can form, then the echo will not be observed. When collisions are ignorable, however, the echo provides a dramatic demonstration that Landau damping does not represent a loss of information, since long after the potential has died away, the information is recoverable. Landau damping is then seen rather as carrying the initial perturbation in velocity space, where it is undamped until collisions randomize the information, and the velocity spread distributes the perturbation in configuration space so that the potential dies away.

7.3.1.1 Basic equations

We begin the analysis with the kinetic equation, equation (7.1), for electrons, assuming a uniform, stationary background of ions. For this case, we assume a zero order distribution that is time independent, or

$$f = f_0(v) + f_1(x, v, t)$$

with the initial condition $f_1(x, v, 0) = 0$. We then expand f_1 in a Fourier series in space and examine the k th component, such that

$$\frac{\partial f_k}{\partial t} + ikv f_k = \frac{e}{m} E_k \frac{\partial f_0}{\partial v} + \frac{e}{m} \sum_q E_{k-q} \frac{\partial f_q}{\partial v} \quad (7.74)$$

where the nonlinear term is the discrete sum analog of the convolution integral of equation (7.12). The Laplace transform in time then leads to

$$(p + ikv) \tilde{f}_k(p) = \frac{e}{m_e} \tilde{E}_k(p) \frac{\partial f_0}{\partial v} + \frac{e}{m_e} \sum_q \int_{\sigma'-i\infty}^{\sigma'+i\infty} \frac{dp'}{2\pi i} E_{k-q}(p - p') \frac{\partial \tilde{f}_q(p')}{\partial v} \quad (7.75)$$

where now we have a convolution integral from the product term. Assuming the field is electrostatic, we also have $\tilde{E}_k(p) = -ik\tilde{\varphi}_k(p)$ so equation (7.75) becomes

$$\begin{aligned} \tilde{f}_k(p) = & -ik \frac{e}{m_e} \frac{\tilde{\varphi}_k(p)}{(p + ikv)} \frac{\partial f_0}{\partial v} \\ & - \frac{ie}{m_e} \sum_q \int_{\sigma'-i\infty}^{\sigma'+i\infty} \frac{dp'}{2\pi i} \frac{(k - q)\tilde{\varphi}_{k-q}(p - p')}{p + ikv} \frac{\partial \tilde{f}_q(p')}{\partial v}. \end{aligned} \quad (7.76)$$

7.3.1.2 The source potential

The sources for the echo are assumed to be impulses at time 0 and time τ with wavenumbers k_1 and k_2 , respectively, so that the source potential is

$$\varphi_{\text{ext}} = \varphi_1 \cos(k_1 x) \delta(\omega_{pe} t) + \varphi_2 \cos(k_2 x) \delta[\omega_{pe}(t - \tau)]. \quad (7.77)$$

The sources of the potential in the plasma are due to the external field and the density fluctuations, so from Poisson's equation, we have

$$\nabla^2 \varphi = -\frac{\rho}{\epsilon_0} + \nabla^2 \varphi_{\text{ext}}$$

and taking Fourier and Laplace transforms of this, we find

$$\tilde{\varphi}_k(p) = -\frac{ne}{k^2 \epsilon_0} \int_{-\infty}^{\infty} dv \tilde{f}_k(p) + \frac{\varphi_1}{2\omega_{pe}} (\delta_{k,k_1} + \delta_{k,-k_1}) + \frac{\varphi_2}{2\omega_{pe}} (\delta_{k,k_2} + \delta_{k,-k_2}) e^{-p\tau} \quad (7.78)$$

where the sum of the Kronecker delta functions comes from transforming $\cos(k_{1,2}x)$ and the $1/\omega_{pe}$ and $e^{-p\tau}/\omega_{pe}$ terms come from the Laplace transforms.

7.3.1.3 The echo potential

Now the echo will, in general, occur at a wavenumber different from either k_1 or k_2 , so we are looking for a potential of the form $\varphi_{k_3}(t)$. Using equation (7.78), we

have the simple result

$$\tilde{\varphi}_{k_3}(p) = -\frac{ne}{k_3^2 \epsilon_0} \int_{-\infty}^{\infty} dv \tilde{f}_{k_3}(p) \quad (7.79)$$

and from equation (7.76) we find

$$\begin{aligned} \tilde{f}_{k_3}(p) &= \frac{-ik_3 e \tilde{\varphi}_{k_3}(p)}{m_e(p + ik_3 v)} \frac{\partial f_0}{\partial v} \\ &+ \frac{ie}{m_e} \sum_q \int_{\sigma'-i\infty}^{\sigma'+i\infty} \frac{dp'}{2\pi i} \frac{k_3 - q}{p + ik_3 v} \tilde{\varphi}_{k_3-q}(p - p') \frac{\partial \tilde{f}_q(p')}{\partial v}. \end{aligned}$$

Inserting this result into equation (7.79) and solving for $\tilde{\varphi}_{k_3}(p)$, we can write the result as

$$\tilde{\varphi}_{k_3}(p) = \frac{\omega_{pe}^2}{k_3^2 \epsilon(k_3, p)} \sum_q \int_{\sigma'-i\infty}^{\sigma'+i\infty} \frac{dp'}{2\pi i} \int_{-\infty}^{\infty} dv \frac{i(k_3 - q)}{(p + ik_3 v)} \tilde{\varphi}_{k_3-q}(p - p') \frac{\partial \tilde{f}_q(p')}{\partial v} \quad (7.80)$$

where

$$\epsilon(k, p) = 1 - \frac{\omega_{pe}^2}{k^2} \int_{-\infty}^{\infty} dv \frac{\frac{\partial f_0}{\partial v}}{\frac{p}{ik} + v}. \quad (7.81)$$

Now to obtain a response, $\tilde{\varphi}_{k_3}$ must couple to either $\tilde{\varphi}_{k_1}$ or $\tilde{\varphi}_{k_2}$ or both, so in the sum over q , $k_3 - q$ must be either $\pm k_1$ or $\pm k_2$ for a nonvanishing response (to lowest order). Let us examine $k_3 = k_2 - k_1$ and include the lowest order terms. These terms will occur when $q = k_2$ and $q = -k_1$. These will be the only second order terms that couple to $\tilde{\varphi}_{\pm k_1}$ or $\tilde{\varphi}_{\pm k_2}$. Since the terms in equation (7.81) are already second order for lowest order in $\tilde{\varphi}_{k_3-q}$ and \tilde{f}_q , we need these latter terms only to first order. For $q = k_2$, $k_3 - q = -k_1$, so we need $\tilde{\varphi}_{-k_1}(p - p')$ and $\tilde{f}_{k_2}(p')$. From equations (7.78) and (7.76) (to first order), these are

$$\tilde{\varphi}_{-k_1}(p - p') = -\frac{ne}{k_1^2 \epsilon_0} \int_{-\infty}^{\infty} dv \tilde{f}_{-k_1}(p - p') + \frac{\varphi_1}{2\omega_{pe}} \quad (7.82)$$

$$\tilde{f}_{-k_1}(p - p') = \frac{ik_1 e}{m_e} \frac{\tilde{\varphi}_{-k_1}(p - p')}{(p - p' - ik_1 v)} \frac{\partial f_0}{\partial v}. \quad (7.83)$$

Solving this pair for $\tilde{\varphi}_{-k_1}(p - p')$, we obtain

$$\tilde{\varphi}_{-k_1}(p - p') = \frac{\varphi_1}{2\omega_p \epsilon(-k_1, p - p')}. \quad (7.84)$$

For $\tilde{f}_{k_2}(p')$, we use equations (7.76) and (7.78) again to obtain the result

$$\tilde{f}_{k_2}(p') = \frac{-ik_2 e \varphi_2 e^{-p'^\tau}}{2m_e \omega_{pe} \epsilon(k_2, p')(p' + ik_2 v)} \frac{\partial f_0}{\partial v}. \quad (7.85)$$

When $q = -k_1$, then $k_3 - q = k_2$, and we find by similar methods

$$\tilde{\varphi}_{k_2}(p - p') = \frac{\varphi_2 e^{-(p-p')\tau}}{2\omega_{pe}\epsilon(k_2, p - p')} \quad (7.86)$$

and

$$\tilde{f}_{-k_1}(p') = \frac{i k_1 e \varphi_1}{2 m_e \omega_{pe} \epsilon(-k_1, p')(p' - i k_1 v)} \frac{\partial f_0}{\partial v}. \quad (7.87)$$

Inserting equations (7.84)–(7.87) into equation (7.80), we find

$$\begin{aligned} \tilde{\varphi}_{k_3}(p) &= \frac{-e k_1 k_2 \varphi_1 \varphi_2}{4 m_e k_3^2} \int_{\sigma'-i\infty}^{\sigma'+i\infty} \frac{dp'}{2\pi i} \int_{-\infty}^{\infty} dv \\ &\times \left[\frac{e^{-p'\tau}}{(p + i k_3 v) \epsilon(-k_1, p - p') \epsilon(k_2, p')} \frac{\partial}{\partial v} \left(\frac{\frac{\partial f_0}{\partial v}}{(p' + i k_2 v)} \right) \right. \\ &\left. + \frac{e^{-(p-p')\tau}}{(p + i k_3 v) \epsilon(k_2, p - p') \epsilon(-k_1, p')} \frac{\partial}{\partial v} \left(\frac{\frac{\partial f_0}{\partial v}}{(p' - i k_1 v)} \right) \right] \end{aligned}$$

so to find $\varphi_{k_3}(t)$, we do the inverse Laplace transform with the result

$$\begin{aligned} \varphi_{k_3}(t) &= -\frac{e k_1 k_2 \varphi_1 \varphi_2}{4 m_e k_3^2} \int_{-\infty}^{\infty} dv \int_{\sigma'-i\infty}^{\sigma'+i\infty} \frac{dp'}{2\pi i} \int_{\sigma-i\infty}^{\sigma+i\infty} \frac{dp}{2\pi i} \frac{1}{\epsilon(k_3, p)(p + i k_3 v)} \\ &\times \left[\frac{e^{pt-p'\tau}}{\epsilon(-k_1, p - p') \epsilon(k_2, p')} \frac{\partial}{\partial v} \left(\frac{\frac{\partial f_0}{\partial v}}{(p' + i k_2 v)} \right) \right. \\ &\left. + \frac{e^{p(t-\tau)+p'\tau}}{\epsilon(k_2, p - p') \epsilon(-k_1, p')} \frac{\partial}{\partial v} \left(\frac{\frac{\partial f_0}{\partial v}}{(p' - i k_1 v)} \right) \right]. \end{aligned}$$

Integrating by parts in the velocity integrals, this becomes

$$\begin{aligned} \varphi_{k_3}(t) &= -\frac{e k_1 k_2 \varphi_1 \varphi_2}{4 m_e k_3^2} \int_{-\infty}^{\infty} dv \int_{\sigma'-i\infty}^{\sigma'+i\infty} \frac{dp'}{2\pi i} \int_{\sigma-i\infty}^{\sigma+i\infty} \frac{dp}{2\pi i} \frac{\partial f_0}{\partial v} \\ &\times \frac{i k_3}{\epsilon(k_3, p)(p + i k_3 v)^2} \left[\frac{e^{pt-p'\tau}}{\epsilon(-k_1, p - p') \epsilon(k_2, p')(p' + i k_2 v)} \right. \\ &\left. + \frac{e^{p(t-\tau)+p'\tau}}{\epsilon(k_2, p - p') \epsilon(-k_1, p')(p' - i k_1 v)} \right]. \quad (7.88) \end{aligned}$$

7.3.1.4 Evaluating the inverse Laplace integrals

We first do the p' integral by closing the contour in figure 7.5 on the side that will produce a vanishingly small exponential. For the first term in equation (7.88),

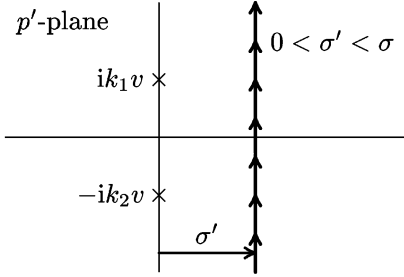


Figure 7.5. Path in the p' -plane.

which varies as $e^{-p'\tau}$, we must close to the right, so we enclose no pole (since we assume τ to be larger than the Landau decay time of either of the initial waves, only the poles at $ik_1 v_1$ and $-ik_2 v_2$ will contribute at a later time). For the second term which varies as $e^{p'\tau}$, we must close to the left and hence enclose the pole at $ik_1 v_1$ with the result

$$\begin{aligned} \varphi_{k_3}(t) = & -\frac{e k_1 k_2 \varphi_1 \varphi_2}{4 m_e k_3^2} \int_{-\infty}^{\infty} dv \int_{\sigma-i\infty}^{\sigma+i\infty} \frac{dp}{2\pi i} \frac{\partial f_0}{\partial v} \\ & \times \frac{i k_3 e^{p(t-\tau)+ik_1 v \tau}}{\epsilon(k_3, p)(p+ik_3 v)^2 \epsilon(k_2, p-ik_1 v) \epsilon(-k_1, ik_1 v)}. \end{aligned} \quad (7.89)$$

For the p integral, we must examine two cases. If $t < \tau$, then we must close to the right and include no pole, hence $\varphi_{k_3}(t) \sim 0$ for $t < \tau$. For $t > \tau$, we close to the left and pick up the double pole of $-ik_3 v$ to obtain

$$\begin{aligned} \varphi_{k_3}(t) = & -\frac{e k_1 k_2 \varphi_1 \varphi_2}{4 m_e k_3^2} \int_{-\infty}^{\infty} dv \frac{i k_3 e^{ik_1 v \tau}}{\epsilon(-k_1, ik_1 v)} \frac{\partial f_0}{\partial v} \\ & \times \frac{\partial}{\partial p} \left[\frac{e^{p(t-\tau)}}{\epsilon(k_3, p) \epsilon(k_2, p-ik_1 v)} \right]_{p=-ik_3 v}. \end{aligned} \quad (7.90)$$

Now all three terms in the expanded partial derivative have the same exponent so the total exponent is $-ik_3 v(t - \tau - k_1 \tau / k_3)$ or $-ik_3 v(t - \tau')$ where $\tau' = k_2 \tau / k_3$. In general, the integral over velocity will phase mix to zero except where $t \simeq \tau'$. At this point in time, the largest of the terms in the derivative is the derivative of the exponential, since the other terms still relate to Landau decay times and those terms are presumably small at this time, so neglecting the other terms, we have

$$\varphi_{k_3}(t) \simeq -\frac{i e k_1^2 k_2 \varphi_1 \varphi_2 \tau}{4 m_e k_3^2} \int_{-\infty}^{\infty} dv \frac{e^{-ik_3 v(t-\tau')}}{\epsilon(-k_1, ik_1 v) \epsilon(k_3, -ik_3 v) \epsilon(k_2, -ik_2 v)} \frac{\partial f_0}{\partial v}. \quad (7.91)$$

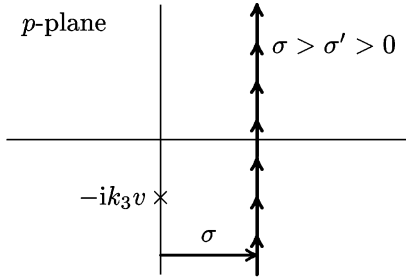


Figure 7.6. Path in the p -plane.

7.3.1.5 Doing the velocity integral

We now need to know where the poles of the integrand are, so we note that

$$\epsilon(k_3, -ik_3v) = 1 - \frac{\omega_{pe}^2}{k_3^2} \int_{-\infty}^{\infty} \frac{dv'}{v' - v} \frac{\partial f_0(v')}{\partial v'} \quad \text{Im}(v) > 0$$

where the condition on the imaginary part of v comes from figure 7.6 where the contour specified that the path went to the right (positive real part) of $-ik_3v$. If we choose a Maxwellian, $f_0 = (1/\sqrt{\pi}v_e) \exp(-v^2/v_e^2)$, then

$$\epsilon(k_3, -ik_3v) = 1 - \frac{\omega_{pe}^2}{k_3^2 v_e^2} Z' \left(\frac{v}{v_e} \right) \quad (7.92)$$

$$\epsilon(k_2, -ik_2v) = 1 - \frac{\omega_{pe}^2}{k_2^2 v_e^2} Z' \left(\frac{v}{v_e} \right) \quad (7.93)$$

$$\epsilon(-k_1, ik_1v) = 1 - \frac{\omega_{pe}^2}{k_1^2 v_e^2} \tilde{Z}' \left(\frac{v}{v_e} \right) \quad (7.94)$$

where the path for \tilde{Z}' is defined to go *over* the pole while the path for Z goes *under* the pole since the sign of the real part is determined by the sign of k . If we now assume that the zeros of the dielectric functions are where $v \gg v_e$, then expanding the plasma dispersion function in equation (7.92) with $v = v_3 \simeq \omega_{pe}/k_3$, we find

$$k_3 v_3 \simeq \omega_{pe} \left[1 + \frac{3}{2} k_3^2 \lambda_D^2 - \frac{i\sqrt{\pi}}{2\sqrt{2}k_3^3 \lambda_D^3} \exp \left(-\frac{1}{2k_3^2 \lambda_D^2} \right) \right] \quad (7.95)$$

where $v_e^2/\omega_{pe}^2 = 2\lambda_D^2$ and λ_D is the Debye length, and we obtain a similar result for k_2 . For k_1 , the result is similar except that kv_1 has a positive imaginary part. Hence we have established that the poles associated with k_2 and k_3 are in the lower half-plane and that the pole associated with k_1 is in the upper half-plane as shown in figure 7.7.

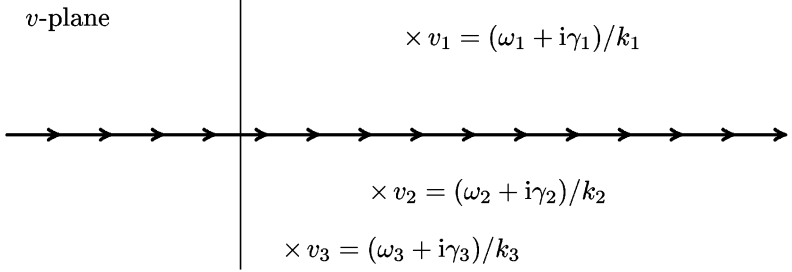


Figure 7.7. Poles and specified path in the v -plane.

We now wish to perform the integral of equation (7.91) by the residue method and close the contour where the exponential will give a vanishing component for finite $(t - \tau')$. We first note that $\partial f_0 / \partial v$ will generally diverge for either positive or negative imaginary part of v , but the divergent factor is canceled either by a similar factor in $\epsilon(-k_1, ik_1 v)$ when closing above and from either $\epsilon(k_3, -ik_3 v)$ or $\epsilon(k_2, -ik_2 v)$ when closing below. Hence for the case $t - \tau' < 0$, we must close above and thus pick up the pole from the zero of $\epsilon(-k_1, ik_1 v)$ which we designate v_1 . Thus for the case for $t < \tau'$, equation (7.91) gives

$$\varphi_{k_3}(t) = \frac{ek_1^2 k_2 \varphi_1 \varphi_2 2\pi \tau}{4m_e k_3^2} \frac{\frac{\partial f_0}{\partial v} \Big|_{v_1} e^{-ik_3 v_1(t-\tau')}}{\epsilon(k_2, -ik_2 v_1) \epsilon(k_3, -ik_3 v_1) [\frac{\partial}{\partial v} \epsilon(-k_1, ik_1 v)]_{v=v_1}}.$$

For $t > \tau'$, we close below and pick up poles at both v_2 and v_3 :

$$\begin{aligned} \varphi_{k_3}(t) = & \frac{\pi ek_1^2 k_2 \varphi_1 \varphi_2 \tau}{2m_e k_3^2} \left\{ \frac{\frac{\partial f_0}{\partial v} \Big|_{v_1} e^{-ik_3 v_1(t-\tau')}}{\epsilon(-k_1, ik_1 v_2) \epsilon(k_3, -ik_3 v_2) [\frac{\partial}{\partial v} \epsilon(k_2, -ik_2 v)]_{v=v_2}} \right. \\ & \left. + \frac{\frac{\partial f_0}{\partial v} \Big|_{v_3} e^{-ik_3 v_3(t-\tau')}}{\epsilon(-k_1, ik_1 v_3) \epsilon(k_2, -ik_2 v_3) [\frac{\partial}{\partial v} \epsilon(k_3, -ik_3 v)]_{v=v_3}} \right\}. \end{aligned} \quad (7.96)$$

We now take the case where the echo is largest, namely where $k_3 \simeq k_1$ so that $k_2 \simeq 2k_3$. Now if we define $k_i v_i = \omega_i - i\gamma_i$, so that γ_i represents the damping rate for the k_i root, then $\gamma_2 \gg \gamma_3$ so the only important term in equation (7.96) is the $v = v_3$ root. From equation (7.95), we have

$$\omega_3 \simeq \omega_{pe} \left(1 + \frac{3}{2} k_3^2 \lambda_D^2\right) \quad \gamma_3 \simeq \frac{\sqrt{\pi} \omega_{pe}}{2^{3/2} k_3^3 \lambda_D^3} \exp(-1/2k_3^2 \lambda_D^2). \quad (7.97)$$

Problem 7.3.1. Plasma wave echo damping. Show that $\gamma_2 \gg \gamma_3$.

7.3.1.6 Putting the pieces together

Assembling the components, we find using equation (7.97) that

$$\left. \frac{\partial f_0}{\partial v} \right|_{v=v_3} = \frac{-2\gamma_3 k_3^2}{\pi \omega_3 \omega_{pe}^2}. \quad (7.98)$$

Then evaluating $\epsilon(k_2, -ik_2 v_3)$ and $\epsilon(-k_1, ik_1 v_3)$, noting that v_3 is defined by $k_3^2 v_e^2 = \omega_{pe}^2 Z'(v_3/v_e)$, we find that

$$\epsilon(k_2, -ik_2 v_3) = 1 - \frac{\omega_{pe}^2}{k_2^2 v_e^2} Z' \left(\frac{v_3}{v_e} \right) = k_1(k_2 + k_3)/k_2^2 \quad (7.99)$$

$$\epsilon(-k_1, ik_1 v_3) \simeq 1 - \frac{k_3^2}{k_1^2} \left(1 + 4i \frac{\gamma_3}{\omega_3} \right) = \frac{1}{k_1^2} \left(k_1^2 - k_3^2 - 4i \frac{k_3^2 \gamma_3}{\omega_3} \right) \quad (7.100)$$

$$= \frac{k_2}{k_1^2} \left(k_1 - k_3 - 4i \frac{k_3^2 \gamma_3}{k_2 \omega_3} \right). \quad (7.101)$$

where we may not neglect the imaginary part compared to the real part in equation (7.100), since $k_1 \sim k_3$ and the real part may be very small. In this case the echo is nearly resonant. The final result was obtained using $k_1^2 - k_3^2 = k_2(k_1 - k_3)$. Finally, we note that

$$\frac{\partial}{\partial v} \epsilon(k_3, -ik_3 v) = -\frac{\omega_{pe}^2}{k_3^2 v_e^3} Z'' \left(\frac{v}{v_e} \right) \quad (7.102)$$

which leads to

$$\left. \frac{\partial}{\partial v} \epsilon(k_3, -ik_3 v) \right|_{v=v_3} = \frac{2k_3}{\omega_3} \left(1 - \frac{i\gamma_3 \omega_3}{k_3^2 \lambda_D^2 \omega_{pe}^2} \right) \quad (7.103)$$

where we have used equation (7.97). Neglecting the imaginary part at this step, we can now combine these several expressions to obtain the result

$$\varphi_{k_3}(t) = \frac{e\varphi_1\varphi_2}{m_e v_e^2} \frac{k_3^3 k_2^2 v_e^2 (\gamma_3 \tau) e^{-\gamma_3(t-\tau') - i\omega_3(t-\tau')}}{2k_3 \omega_{pe}^2 (k_2 + k_3) \left(k_1 - k_3 - 4i \frac{k_3^2 \gamma_3}{k_2 \omega_3} \right)}. \quad (7.104)$$

Now we should write $k_3 v_3 = \pm \omega_3 - i\gamma_3$, since both yield poles when $\epsilon(k_3, -ik_3 v_3) = 0$. If we sum over these two solutions, then we obtain the final results for $t > \tau'$:

$$\varphi_{k_3}(t) = \frac{2e\varphi_1\varphi_2}{m_e v_e^2} \frac{\gamma_3 \tau k_1^3 k_2^2 \lambda_D^2 e^{-\gamma_3(t-\tau')} \cos[\omega_3(t-\tau') + \delta']}{k_3(k_2 + k_3) \left[(k_1 - k_3)^2 + \left(\frac{4k_3^2 \gamma_3}{k_2 \omega_3} \right)^2 \right]^{1/2}} \quad (7.105)$$

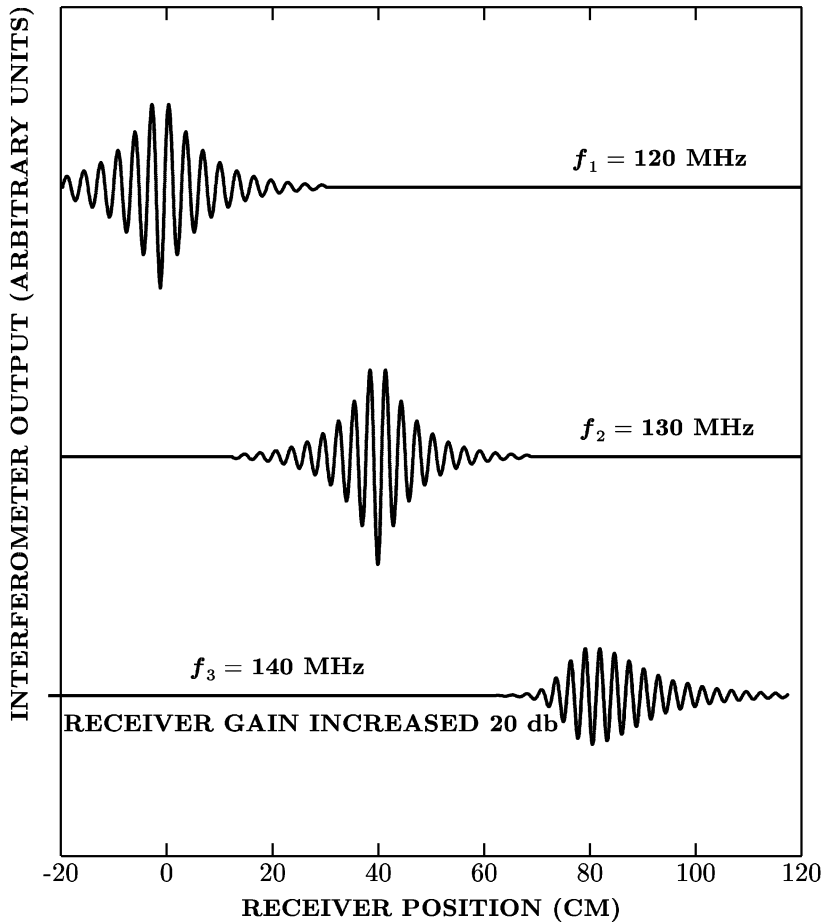


Figure 7.8. Third order echo. The transmitter probes were separated by 40 cm and the receivers were tuned to the indicated frequencies. (From [101].)

with $\tan \delta' = -4k_3^2\gamma_3/k_2(k_1 - k_3)\omega_3$, and for $t < \tau'$,

$$\varphi_{k_3}(t) = \frac{2e\varphi_1\varphi_2}{m_e v_e^2} \frac{\gamma_1 \tau k_1^3 k_2^2 \lambda_D^2 e^{-(\gamma_1 k_3/k_1)(\tau'-t)} \cos[(\omega_1 k_3/k_1)(\tau' - t) + \delta']}{k_3(k_2 + k_1) \left[(k_1 - k_3)^2 + \left(\frac{4k_1^2\gamma_1}{k_2\omega_1} \right)^2 \right]^{1/2}} \quad (7.106)$$

where $\tan \delta' = -4k_1^2\gamma_1/k_2(k_1 - k_3)\omega_1$.

From equation (7.105), it is apparent that the growth rate of the echo is given by $\gamma_1 k_3/k_1$ while the decay rate is given by γ_3 . The growth of the echo is dependent on both k_1 and k_2 , but once created at time τ' , it decays with a decay

rate determined by its own characteristic wavenumber k_3 .

In a classic experiment where these results were adapted to spatial decay with a finite spacing between launching antennas, each driven at a different frequency, rather than temporal decay with a time interval between sources, the principal features of the echo were verified [101]. As seen in [figure 7.8](#), the individual sources had decayed away and subsequently the third order echo was reconstructed with appropriate growth and decay lengths. The experiments detected both second and third order echoes, where higher order echoes occur at a distance $\ell' = (n\omega_1/\omega_3)\ell$ with $\omega_3 = m\omega_2 - n\omega_1$, where m and n relate to the order in perturbation theory that each term appears. The basic frequency and position relationships were verified over a wide range of frequencies (110–280 MHz) and separations (10–60 cm).

Problem 7.3.2. Plasma wave echo.

- (i) Fill in the steps leading to equations (7.98), (7.99), (7.101), and (7.103).
- (ii) Show that equation (7.105) and equation (7.106) follow from equation (7.104) when summed over $\pm\omega_3$.

Chapter 8

Finite amplitude plasma waves

8.1 Nonlinear mechanisms in plasmas

Beyond the weakly nonlinear effects described by quasilinear diffusion and weak turbulence, there are several well-documented nonlinear effects that lead to very different types of behavior. In the strongly nonlinear limit, shock waves may occur when the wave energy density is comparable to or exceeds the plasma energy density. Some of these can be described by solitary waves, and in the lower but significant amplitude limit, some of these solitary waves relax to solitons which have unique particle-like and stability properties.

Another area where nonlinear effects exhibit new features is due to trapped particles. In section 4.2.3, we outlined a weakly nonlinear picture of trapped particles to help us to understand Landau damping, but when the amplitude gets large, the trapped particles begin to bounce on short time scales relative to the Landau damping rate, and these particles will severely modify the energy balance between particles and waves and hence the damping rate. In the large amplitude limit, the damping eventually ceases, and the distribution function is modified in the vicinity of the phase velocity to support these stationary waves.

The final nonlinear effect we consider is the class of parametric instabilities where a driven pump wave, above a certain threshold, will interact with other normal modes in the plasma through the beating of the pump wave with a normal mode to produce a third wave, typically at a much lower frequency. The number of such instabilities in plasmas is legion, since nearly every linear wave type we have considered can beat with another of the same type or with every other wave type, and the third wave does not even have to be resonant if the pump amplitude is high enough.

Before considering these three topics, we examine another nonlinear effect that plays a role in several of them.

8.1.1 Ponderomotive effects

When waves travel in a plasma, particularly when the plasma or the wave amplitude is not homogeneous, the wave amplitude itself can effectively modify the plasma density profile through the *ponderomotive force*. One of the consequences of this ponderomotive force is that a localized wave can effectively expel plasma from the vicinity of the wave amplitude maximum, and this may tend to make the wave even more localized, leading to a trough in the plasma that is called a *caviton*. We give here a brief derivation of the ponderomotive force and its associated potential. Applications in both solitons and parametric instabilities follow in subsequent sections.

In an inhomogeneous, high frequency field, the motion of an electron may be divided into two parts which describe the high frequency oscillation about an effective center of oscillation, and the relatively slow motion of this oscillation center. If we take the electric field to be given by $E(x, t) = E_0(x) \cos \omega t$, and imagine that the amplitude is increasing in the positive x -direction, then as the electron moves into the stronger field, it will be accelerated more strongly back toward the oscillation center. However, as it moves toward the weaker field as x goes negative, it receives a weaker restoring force. On the average, then, it will experience a slow drift toward the weaker field as if under the influence of a steady or slowly varying force, while at the same time experiencing the rapid oscillation at the high frequency.

In order to make this more nearly quantitative, we examine the equation of motion for a charged particle in an inhomogeneous electric field:

$$m\ddot{\mathbf{r}} = q\mathbf{E}_0(\mathbf{r}) \cos \omega t. \quad (8.1)$$

We will separate the motion into a slow motion and a fast motion such that $\mathbf{r} = \mathbf{r}_0 + \mathbf{r}_1$ where $\langle \mathbf{r} \rangle = \mathbf{r}_0$ is the average over the fast time scale, or over the period, $T = 2\pi/\omega$. \mathbf{r}_0 hence describes the *oscillation center*. \mathbf{r}_1 describes the rapidly oscillating motion, and is determined by

$$m\ddot{\mathbf{r}}_1 = q\mathbf{E}_0 \cos \omega t \quad (8.2)$$

where $\mathbf{E}_0 = \mathbf{E}_0(\mathbf{r}_0)$. The solution is simply

$$\mathbf{r}_1 = -(q\mathbf{E}_0/m\omega^2) \cos \omega t. \quad (8.3)$$

For the slow variation, we will expand $\mathbf{E}_0(\mathbf{r})$ about \mathbf{r}_0 such that the equation of motion becomes

$$m(\ddot{\mathbf{r}}_0 + \ddot{\mathbf{r}}_1) = q[\mathbf{E}_0 + (\mathbf{r}_1 \cdot \nabla)\mathbf{E}_0] \cos \omega t \quad (8.4)$$

and we wish to average this over a period such that

$$m\ddot{\mathbf{r}}_0 = q \langle \mathbf{r}_1 \cos \omega t \rangle \cdot \nabla \mathbf{E}_0. \quad (8.5)$$

Using equation (8.3) for \mathbf{r}_1 , the average is simply $\langle \mathbf{r}_1 \cos \omega t \rangle = -q \mathbf{E}_0 / 2m\omega^2$, so equation (8.5) becomes

$$m\ddot{\mathbf{r}}_0 = -\frac{q^2}{2m\omega^2} \mathbf{E}_0 \cdot \nabla \mathbf{E}_0 = -\frac{q^2}{4m\omega^2} \nabla(E_0^2). \quad (8.6)$$

The ponderomotive force and its associated ponderomotive potential, then, are given by

$$\mathbf{F}_p = -\frac{q^2}{4m\omega^2} \nabla(E_0^2) = -\nabla\psi_p \quad (8.7)$$

$$\psi_p = \frac{q^2}{4m\omega^2} E_0^2. \quad (8.8)$$

If inhomogeneous magnetic fields are included, there is a drift of the guiding center in addition to the motion from the ponderomotive force, but the ponderomotive force is unchanged.

8.2 Solitary waves and solitons

When the amplitude of a wave is not small, there are a variety of effects that may result due to the finite amplitude effects, several of which are important in laboratory and astrophysical plasmas. Considering only the dispersive effects and neglecting possible coupling to other waves, we begin with a simple model for solitary waves in a one-dimensional, field-free plasma.

8.2.1 Ion-acoustic solitary wave

We shall assume the ions to be cold, but the electrons will have a finite temperature. We begin with the fluid equations of continuity, equation (3.34), and momentum, equation (3.35),

$$\begin{aligned} \frac{\partial n}{\partial t} + \frac{\partial}{\partial z} nv &= 0 \\ \frac{\partial v}{\partial t} + v \frac{\partial v}{\partial z} &= -\frac{q}{m} \frac{\partial \varphi}{\partial z} - \frac{1}{nm} \frac{\partial p}{\partial z} \end{aligned}$$

and Poisson's equation,

$$\frac{\partial^2 \varphi}{\partial z^2} = -\frac{e}{\epsilon_0}(n_i - n_e).$$

For electrons, m_e is taken to be so small that we can neglect the left-hand side of the momentum equation, and then letting $p_e = n_e \kappa T_e$ (assumed isothermal because of the high electron mobility), we obtain

$$\frac{e}{\kappa T_e} \frac{\partial \varphi}{\partial z} = \frac{1}{n_e} \frac{\partial n_e}{\partial z} \quad (8.9)$$

with solution

$$n_e = n_0 e^{e\varphi/\kappa T_e}. \quad (8.10)$$

Assuming now a wavelike solution so that all functions may be written as a function of $\xi = z - Ut$, then $\partial/\partial t \rightarrow -U\partial/\partial\xi$ and $\partial/\partial z \rightarrow \partial/\partial\xi$, so the continuity equation for ions becomes

$$-Un'_i + n_i v' + vn'_i = 0 \text{ and integrating, } n_i(v - U) = \text{constant}$$

where the prime denotes the derivative with respect to the argument, and the momentum equation becomes

$$-Uv' + vv' = -\frac{e}{m_i}\varphi' \text{ and integrating, } -Uv + \frac{1}{2}v^2 = -\frac{e}{m_i}\varphi + \text{constant}$$

which is the conservation of energy, and we set this last constant to zero. Solving for v , we find

$$v = U \pm \left[U^2 - \frac{2e}{m_i}\varphi \right]^{1/2}$$

so that the ion density is given by

$$n_i = \frac{n_0}{\sqrt{1 - \frac{2e\varphi}{m_i U^2}}}$$

and Poisson's equation gives

$$\frac{d^2\varphi}{d\xi^2} = -\frac{n_0 e}{\epsilon_0} \left[\frac{1}{\sqrt{1 - \frac{2e\varphi}{m_i U^2}}} - e^{e\varphi/\kappa T_e} \right]. \quad (8.11)$$

Then using the change of variable, $\eta = d\varphi/d\xi$, we may write

$$\frac{d^2\varphi}{d\xi^2} = \eta \frac{d}{d\varphi} \eta = \frac{d}{d\varphi} \left(\frac{\eta^2}{2} \right) \quad (8.12)$$

where now we can separate variables and integrate, with the result

$$\frac{\eta^2}{2} = \frac{n_0}{\epsilon_0} \left[m_i U^2 \left(\sqrt{1 - \frac{2e\varphi}{m_i U^2}} - 1 \right) + \kappa T_e (e^{e\varphi/\kappa T_e} - 1) \right] \quad (8.13)$$

where the constant terms are chosen so that $\eta \rightarrow 0$ as $\varphi \rightarrow 0$. Now solitary wave solutions do not exist for all values of φ and U . It is clear from equation (8.13) that $e\varphi \leq m_i U^2/2$ for a meaningful solution.

If we consider $v(\varphi) = -\eta^2/2$ to be a 'pseudopotential' with φ the 'coordinate' and ξ the 'time', then equation (8.12) has the form of an equation of motion for a particle moving in a 'pseudopotential well',

$$\frac{d^2\varphi}{d\xi^2} = -\frac{dv(\varphi)}{d\varphi}$$

and we need a potential well for $v(\varphi)$ with two zero crossings for a ‘bound’ (localized) solution. From equation (8.12), $v' = 0$ at $\varphi = 0$ and from equation (8.13) we have $v(\varphi) = 0$ at $\varphi = 0$, so we require another zero crossing for a solitary wave. Using the parameter $\alpha \equiv U^2/c_s^2$ with $c_s^2 = \kappa T/m_i$, then for $\alpha < 1$, v increases monotonically with φ , so there is no second zero crossing. For $\alpha_c > \alpha > 1$ with $\alpha_c \simeq 2.5$, there is a well with two zero crossings, while for $\alpha > \alpha_c$ there is a well but without a second zero. Thus there exist solitary wave solutions of this type only for Mach numbers $1 < \mathcal{M} < \sqrt{\alpha_c}$ where the Mach number is defined as $\mathcal{M} = U/c_s$ and c_s is the ion acoustic speed.

Problem 8.2.1. The solitary wave ‘pseudopotential’. Sketch $v(\varphi)$ versus φ for values of $\alpha < 1$, $1 < \alpha < \alpha_c$, and $\alpha > \alpha_c$ and determine α_c to show the features described earlier.

Problem 8.2.2. Small (but finite) amplitude solitary wave solution.

- (i) Show that if one expands equation (8.11) or equation (8.13) for small φ that there is a solution of the form $\varphi = \varphi_m \operatorname{sech}^\ell(\xi/\Delta)$.
- (ii) Find ℓ , Δ and U in terms of φ_m .

The ion-acoustic solitary wave described earlier is only one example among many for solitary waves which include shocks and other nonlinear waves. A special subset of these cases are solitons where two (or n) solitary waves can collide and maintain their identity. Because of their unusual stability and other properties (infinite number of conservation laws, solvable by linear methods via the inverse scattering technique [102, 103], etc) this subset is of sufficient interest to examine a systematic derivation of the relevant nonlinear wave equation for the same basic case given earlier, but without the assumption of solitary waves until the basic nonlinear partial differential equation is established.

8.2.2 The Korteweg–de Vries (KdV) equation

Although there are many different nonlinear partial differential equations that give rise to solitons, there is one soliton equation which is generic to many different kinds of waves. The Korteweg–de Vries equation, which was shown in 1896 to describe shallow water waves, has turned out to be the key to understanding many types of waves and the key to solving these nonlinear PDEs by the method of inverse scattering. The general form of the KdV equation is

$$u_\tau + auu_\xi + bu_{\xi\xi\xi} = 0 \quad (8.14)$$

where a and b are constants (the classical form has $a = 6$ and $b = 1$), and the subscripts denote partial derivatives (e.g. $u_\tau = \partial u / \partial \tau$). The nonlinearity is evident from the middle term. We may note that the first two terms typically come from the first two terms of the momentum equation, equation (3.8), so that τ and ξ usually represent normalized time and space variables, respectively. The third

term of equation (8.14) is a dispersive term, and we elucidate its form and indicate its generality by examining the form of a very simple dispersion relation.

Neglecting damping, the simple dispersion relation for the ion acoustic wave is given by equation (4.141) which we may write as

$$\omega = \pm k c_s (1 - k^2 \lambda_{De}^2 / 2 + \dots) \quad (8.15)$$

which to the order indicated is representative in form of the dispersion relations of a great many waves that are characterized by a constant phase velocity in the long wavelength limit and some dispersion. Neglecting the higher order terms, we can identify the term on the left as coming from $\partial/\partial t$, and the first term on the right as coming from $\partial/\partial x$ (with the characteristic speed being amplitude dependent if we compare term by term with equation (8.14)). The second term on the right is proportional to k^3 , so it represents a third-order spatial derivative as we find in the KdV equation. The importance of this dispersive term must not be underestimated, since if it were neglected in equation (8.14), then the peak amplitude would grow and speed up, eventually leading to wave breaking where the peak overtakes the trough, and the wave becomes multiple valued. The dispersive term limits this growth and the tradeoff between the tendency to peak from the nonlinear term and the tendency to spread due to the dispersive term leads to the stable character of solitons.

The single soliton solution of equation (8.14) may be simply found by assuming that a stationary solution exists in some rest frame moving at velocity U . Assuming then that $u = u(\xi - U\tau)$ leads to an ordinary differential equation, and the boundary conditions that $\lim_{|\xi| \rightarrow \infty} u = 0$ along with all its derivatives allows the solution to be found.

Problem 8.2.3. Soliton solution of the KdV equation.

- (i) Assuming $u = u(\eta)$ with $\eta = \xi - U\tau$, write the ordinary differential equation representing the soliton solution of equation (8.14).
- (ii) Integrate this equation once and evaluate the integration constant if $\lim_{|\eta| \rightarrow \infty} u = 0$.
- (iii) Make a variable change as in equation (8.12) and integrate to find the one soliton solution of the KdV equation.

8.2.3 Ion acoustic solitons

The proof that ion acoustic waves are KdV solitons follows the development of Washimi and Taniuti [104] where we begin with the same equations as in the previous section. We then normalize the variables, defining $n = n_i/n_0$, $u = v_i/c_s$, $x = z/\lambda_D$, $\tau = c_s t/\lambda_D$, and $\Phi = e\varphi/\kappa T_e$. Then the ion fluid equations become

$$\frac{\partial n}{\partial \tau} + \frac{\partial}{\partial x}(nu) = 0 \quad (8.16)$$

$$\frac{\partial u}{\partial \tau} + u \frac{\partial u}{\partial x} = - \frac{\partial \Phi}{\partial x}. \quad (8.17)$$

The normalized electron density from equation (8.10) is $n_e = \exp(\Phi)$, so Poisson's equation becomes

$$\frac{\partial^2 \Phi}{\partial x^2} = e^\Phi - n. \quad (8.18)$$

We now linearize these equations to see the general behavior of the solutions, which leads to the ion acoustic waves of section 4.2.5 with $\omega \simeq kc_s \ll \omega_{pi}$ (unnormalized), but will return to the nonlinear set. To this end, we let $\partial/\partial\tau \rightarrow -i\omega$, $\partial/\partial x \rightarrow ik$, $n = 1 + \tilde{n}$, and $n_e = 1 + \tilde{n}_e$. These lead to

$$\begin{aligned} -i\omega\tilde{n} + iku &= 0 \Rightarrow u = \omega k\tilde{n} \\ -i\omega u &= -ik\Phi \Rightarrow \Phi = \frac{\omega}{k}u = \frac{\omega^2}{k^2}\tilde{n} \\ k^2\Phi &= \tilde{n} - \Phi \Rightarrow k^2 = \frac{\omega^2}{1 - \omega^2} \simeq \omega^2(1 + \omega^2 + \omega^4 + \dots) \end{aligned}$$

since $\omega^2 \ll 1$ (ω is normalized to ω_{pi}) and $\omega/k \simeq 1$ (normalized). Thus

$$kx - \omega\tau \simeq \omega x + \frac{1}{2}\omega^3 x - \omega\tau = \omega(x - \tau) + \frac{1}{2}\omega^3 x$$

so it is advantageous to introduce new variables $\eta = \omega(x - \tau)$, $\xi = \omega^3 x$, and a smallness parameter $\epsilon = \omega^2$ so that

$$kx - \omega\tau \sim \epsilon^{1/2}(x - \tau) + \frac{1}{2}\epsilon^{3/2}x = \eta + \frac{1}{2}\xi. \quad (8.19)$$

These variable changes lead to

$$\begin{aligned} \frac{\partial}{\partial x} &= \frac{\partial \eta}{\partial x} \frac{\partial}{\partial \eta} + \frac{\partial \xi}{\partial x} \frac{\partial}{\partial \xi} = \epsilon^{1/2} \frac{\partial}{\partial \eta} + \epsilon^{3/2} \frac{\partial}{\partial \xi} \\ \frac{\partial}{\partial \tau} &= \frac{\partial \eta}{\partial \tau} \frac{\partial}{\partial \eta} + \frac{\partial \xi}{\partial \tau} \frac{\partial}{\partial \xi} = -\epsilon^{1/2} \frac{\partial}{\partial \eta}. \end{aligned}$$

Using these in equations (8.16) through (8.18) and expanding to second order in ϵ ,

$$\begin{aligned} n &= 1 + \epsilon n^{(1)} + \epsilon^2 n^{(2)} + \dots \\ u &= \epsilon u^{(1)} + \epsilon^2 u^{(2)} + \dots \\ \Phi &= \epsilon \Phi^{(1)} + \epsilon^2 \Phi^{(2)} + \dots \end{aligned}$$

then one obtains to first order,

$$\frac{\partial n^{(1)}}{\partial \eta} = \frac{\partial u^{(1)}}{\partial \eta} = \frac{\partial \Phi^{(1)}}{\partial \eta} \quad (8.20)$$

which leads to $n^{(1)} = u^{(1)} = \Phi^{(1)} \equiv \phi$. Then to second order,

$$\begin{aligned}\frac{\partial n^{(2)}}{\partial \eta} - \frac{\partial u^{(2)}}{\partial \eta} &= \frac{\partial u^{(1)}}{\partial \xi} + \frac{\partial}{\partial \eta}(n^{(1)}u^{(1)}) = \phi_\xi + (\phi^2)_\eta \\ \frac{\partial u^{(2)}}{\partial \eta} - \frac{\partial \Phi^{(2)}}{\partial \eta} &= \frac{\partial u^{(1)}}{\partial \xi} + u^{(1)}\frac{\partial u^{(1)}}{\partial \eta} = \phi_\xi + \phi\phi_\eta \\ \Phi^{(2)} - n^{(2)} &= \frac{\partial^2 \Phi^{(1)}}{\partial \eta^2} - \frac{(\Phi^{(1)})^2}{2} = \phi_{\eta\eta} - \frac{1}{2}\phi^2\end{aligned}$$

and we can eliminate the second order quantities if we differentiate the last equation with respect to η , and then add all three equations, with the result

$$\phi_\xi + \phi\phi_\eta + \frac{1}{2}\phi_{\eta\eta\eta} = 0 \quad (8.21)$$

which is the KdV equation with $a = 1$ and $b = \frac{1}{2}$.

The KdV equation is more than an ordinary solitary-wave equation since it has been proved that individual solitary waves survive collisions and hence these are called solitons to indicate their particle-like behavior. The KdV equation and other soliton equations may be solved by the method of inverse scattering which is a method of solving the nonlinear partial differential equations for *arbitrary initial conditions* by *linear* methods. The solution via inverse scattering for the KdV equation is discussed by Davidson [97], but for a more complete discussion of this method and its application to other soliton equations, Ablowitz and Segur [102] and Lamb [103] are useful references. Through this formalism, it has been possible to show that the solitary waves are indeed *normal modes* and that arbitrary perturbations invariably relax to these solitary waves and the remainder ‘radiates’ away. Analytic N -soliton solutions are also known and there are an infinite number of conservation laws associated with the KdV equation and other soliton equations.

Problem 8.2.4. Ion acoustic solitons.

- (i) Show by direct substitution that equation (8.21) has solutions of the form

$$\phi = A \operatorname{sech}^2[k(\eta - U\xi)].$$

- (ii) Find expressions for $k(A)$ and $U(A)$.

- (iii) Find the corresponding equation for the potential ϕ in terms of the original variables z and t and the amplitude ϕ_m .

8.2.4 Alfvén wave solitons

In addition to ion acoustic solitons, which have been experimentally observed to survive collisions, nonlinear Alfvén waves also are characterized by the KdV equation. This is due to the fact that they propagate near the Alfvén speed at

low frequency and long wavelength, and, especially begin to show dispersion at higher frequencies and one begins to have finite ω/ω_{ci} . The fast Alfvén waves were shown to satisfy the KdV equation by Gardner and Morikawa [105] and the slow waves by Morton [106].

Problem 8.2.5. Alfvén wave soliton solutions. In [106], Alfvén waves are shown to be governed by the KdV equation in the weak nonlinear limit. Fill in the missing steps in that paper leading to equation (4.5). Then find a solution for $B_2^{(1)}$ in unnormalized form.

8.2.5 Nonlinear Schrödinger equation

The nonlinear Schrödinger equation describes a nonlinear wave where the wave amplitude is large enough to modify the dispersion relation by changing the parameters of the medium. Also called the Zakharov–Shabat equation after the authors who showed it to be a soliton and found the inverse scattering solution [107], its solution is an envelope soliton where the wave packet envelope has the soliton character where the medium is modified, and the complex phase term propagates at the wave phase velocity.

We begin with the assumption of a plane wave of the form

$$A e^{i(\mathbf{k} \cdot \mathbf{r} - \omega t)} + A^* e^{-i(\mathbf{k} \cdot \mathbf{r} - \omega t)} \quad (8.22)$$

and a nonlinear dispersion relation

$$D(\omega, \mathbf{k}, |A|^2) = 0 \quad (8.23)$$

where it has been assumed that the nonlinearity depends on the amplitude of the wave and not on the phase. This kind of nonlinearity is quite typical of the ponderomotive force (see section 8.1.1). We also presume the medium is homogeneous and isotropic in the absence of the wave, so D and A are scalar quantities. We assume the nonlinear effects will result in a slow modulation of the wave amplitude about an average amplitude A_0 , so we expand ω and \mathbf{k} , which represent the time and space differential operators, about the fast variation values, so that equation (8.23) becomes a differential equation for the slowly varying amplitude:

$$D \left[\omega + i \frac{\partial}{\partial t}, \mathbf{k} - i \nabla, |A(\mathbf{r}, t)|^2 \right] A = 0. \quad (8.24)$$

Assuming that the differential operators are small ($\omega \gg \partial/\partial t$, $\mathbf{k} \gg \nabla$) and $|A^2| - |A_0|^2 \ll |A_0|^2$, this may be expanded to obtain

$$\left[i \frac{\partial D}{\partial \omega} \frac{\partial}{\partial t} - i \frac{\partial D}{\partial \mathbf{k}} \cdot \nabla - \frac{1}{2} \frac{\partial^2 D}{\partial \mathbf{k} \partial \mathbf{k}} : \nabla^2 + (|A|^2 - |A_0|^2) \frac{\partial D}{\partial |A_0|^2} + \dots \right] A = 0.$$

Dividing by $\partial D / \partial \omega$, this may be written as

$$i \left(\frac{\partial}{\partial t} + \mathbf{v}_g \cdot \nabla \right) A - \mathbf{P} : \nabla^2 A + Q(|A|^2 - |A_0|^2)A = 0 \quad (8.25)$$

where $\mathbf{v}_g = -(\partial D / \partial \mathbf{k}) / (\partial D / \partial \omega) = \partial \omega / \partial \mathbf{k}$ is the group velocity and

$$\begin{aligned} \mathbf{P} &= \frac{1}{2} \frac{\partial \mathbf{v}_g}{\partial \mathbf{k}} = \frac{1}{2} \frac{\partial^2 \omega}{\partial \mathbf{k} \partial \mathbf{k}} \\ Q &= \frac{\partial D}{\partial |A_0|^2} \left(\frac{\partial D}{\partial \omega} \right)^{-1} = -\frac{\partial \omega}{\partial |A_0|^2}. \end{aligned}$$

We can see that Q represents the nonlinear frequency shift due to the finite wave amplitude. If we now shift to the wave frame moving with the group velocity, so that $\xi = \mathbf{r} - \mathbf{v}_g t$, we then obtain the three-dimensional nonlinear Schrödinger equation

$$i \frac{\partial A}{\partial t} + \mathbf{P} : \nabla_\xi^2 A + Q(|A|^2 - |A_0|^2)A = 0. \quad (8.26)$$

We note a difficulty with names at this point, since the one-dimensional version of equation (8.26),

$$i \frac{\partial A}{\partial t} + P \frac{\partial^2 A}{\partial \xi^2} + Q(|A|^2 - |A_0|^2)A = 0 \quad (8.27)$$

is commonly called the nonlinear Schrödinger equation. The Zakharov–Shabat equation, however, whose solutions are solitons, has $A_0 = 0$, and is also called the nonlinear Schrödinger equation, although the character of the solutions is quite different.

8.2.5.1 Linear stability of the nonlinear Schrödinger equation

We first consider the linear stability of equation (8.27) by considering a small perturbation of the form $A - A_0 = x + iy$ and linearize, separating the real and imaginary parts so that we have

$$-\frac{\partial y}{\partial t} + P \frac{\partial^2 x}{\partial \xi^2} + 2Q|A_0|^2 x = 0 \quad (8.28)$$

$$\frac{\partial x}{\partial t} + P \frac{\partial^2 y}{\partial \xi^2} = 0 \quad (8.29)$$

and with

$$x = x_0 \sin(\kappa \xi - \Omega t) \quad y = y_0 \cos(\kappa \xi - \Omega t)$$

the dispersion relation is

$$\Omega^2 = P^2 \kappa^4 - 2PQ\kappa^2 |A_0|^2. \quad (8.30)$$

In order for an instability to occur, ($\text{Im } \Omega \neq 0$), it is clear that we must have $PQ > 0$ and the wavenumber must satisfy $0 < \kappa^2 < 2Q|A_0|^2/P$, with the maximum growth rate occurring for $\kappa = \sqrt{Q|A_0|^2/P}$ where the growth rate is

$$(\text{Im } \Omega)_{\max} = Q|A_0|^2. \quad (8.31)$$

The implication of this linear instability is that provided $PQ > 0$, there exists a range of κ where the wave amplitude will grow. This leads to a collapse where the amplitude will grow until all of the plasma has been expelled due to the ponderomotive force, resulting in a density cavity, or *caviton*. For a driven wave, then, it is expected that the wave will collapse, but the severe modification of the plasma may decouple the driven pump wave, so that effectively $A_0 \rightarrow 0$ in which case the equation becomes the soliton equation that is stable. These general characteristics are borne out in numerical simulations and experiments.

Problem 8.2.6. Nonlinear Schrödinger equation.

- (i) Fill in the steps leading to equations (8.30) and (8.31).
- (ii) Show that equations (8.28) and (8.29) require $\text{Re } A_0 \gg \text{Im } A_0$.

8.2.5.2 Soliton solutions of the Zakharov–Shabat equation

Here we wish to establish the form of the solitons from the Zakharov–Shabat equation

$$iu_t + Pu_{\xi\xi} + Q|u|^2u = 0 \quad (8.32)$$

where the subscript indicates a partial derivative. We assume a wave packet solution of the form

$$u = e^{ik(\xi - v_p t)} \Phi[K(\xi - v'_g t)]. \quad (8.33)$$

We note from $\xi - v'_g t = x - (v_g + v'_g)t$ that v'_g represents the *excess velocity* of the wave packet over the linear group velocity. Inserting equation (8.33) into equation (8.32) and separating the real and imaginary parts results in

$$kv_p \Phi + P(\kappa^2 \Phi'' - k^2 \Phi) + Q\Phi^3 = 0 \quad (8.34)$$

$$-iK\Phi'(v'_g - 2Pk) = 0 \quad (8.35)$$

where Φ' represents the derivative of Φ with respect to its argument, so the wavenumber is $k = v'_g/2P$. We may write equation (8.34) as

$$\frac{1}{2} \frac{d}{d\Phi} (\Phi')^2 = a\Phi - b\Phi^3 \quad (8.36)$$

where

$$a = (k^2 - kv_p)/PK^2 \quad b = Q/2PK^2.$$

Separating variables and doing the first integral, a localized solution leads to

$$K(\xi - v'_g t) = \int \frac{d\phi}{\Phi \sqrt{a - b\Phi^2}} = -\frac{1}{\sqrt{a}} \operatorname{sech}^{-1} \left(\frac{\sqrt{b}\Phi}{\sqrt{a}} \right)$$

with solution

$$\begin{aligned} \Phi(\xi, t) &= \sqrt{a/b} \operatorname{sech}[\sqrt{a} K(\xi - v'_g t)] \\ &= \Phi_m \operatorname{sech}[K(\xi - v'_g t)] \end{aligned} \quad (8.37)$$

so $a = 1$ and $b = 1/\Phi_m^2$, resulting in $K = \Phi_m \sqrt{Q/2P}$ and $v_p = (v'_g/2) - \Phi_m^2 Q P / v'_g$. We note again that v_p represents the phase velocity *relative to the linear group velocity*. The normal form for the Zakharov–Shabat equation has $P = 1$ and $Q = 2$ so that $K = \Phi_m$, $k = v'_g/2$, and $v_p = (v'_g/2) - 2\Phi_m^2/v'_g$.

8.2.5.3 Nonlinear plasma wave instability

In this section, we consider a driven plasma wave with $\omega \simeq \omega_{pe}$, where the amplitude is large enough that the ponderomotive force causes a nonlinear frequency shift. Beginning with the fluid equations (through the third moment) for the electrons along with Poisson's equation, we obtain

$$\tilde{n}_e(\omega^2 - \omega_{pe}^2 - \frac{3}{2}k^2 v_e^2) + \tilde{n}_i \omega_{pe}^2. \quad (8.38)$$

This was obtained on the fast time scale of the driven frequency. The ponderomotive effects occur on a longer time scale, and on this slow time scale, the momentum equations lead to

$$\begin{aligned} eE &\simeq -\frac{\kappa T_e}{m_e} \frac{\partial}{\partial x} \left(\frac{\tilde{n}_e}{n_0} \right) \\ 0 &\simeq \frac{e}{m_i} E - \frac{1}{m_i} \frac{\partial \psi}{\partial x} - \frac{\kappa T_i}{m_i} \frac{\partial}{\partial x} \left(\frac{\tilde{n}_i}{n_0} \right) \\ &\simeq -\frac{1}{m_i} \frac{\partial \psi}{\partial x} - c_s^2 \frac{\partial}{\partial x} \left(\frac{\tilde{n}_i}{n_0} \right) \end{aligned}$$

where on the slow time scale $\tilde{n}_e \simeq \tilde{n}_i$, $c_s^2 = \mathcal{K}(T_e + T_i)/m_i$, and ψ is the ponderomotive potential from the high-frequency electron motion. This leads to

$$\tilde{n}_i = -\frac{n_0}{m_i c_s^2} \psi \quad (8.39)$$

which, in turn, leads to the nonlinear dispersion relation

$$\omega^2 - \omega_{pe}^2 - \frac{3}{2}k^2 v_e^2 - \frac{e^2}{4m_e m_i c_s^2} |E + E_0|^2 = 0 \quad (8.40)$$

where E_0 represents the uniform amplitude of the high-frequency driven wave and E represents the slowly varying wave amplitude, and we have taken $\omega_0 \simeq \omega_{pe}$. This dispersion relation is of the form of equation (8.23) so we may immediately write

$$i \frac{\partial E}{\partial t} + \frac{3v_e^2}{4\omega_0} \frac{\partial^2 E}{\partial x^2} + \frac{e^2}{8\omega_0 m_e m_i c_s^2} (|E+E_0|^2 - |E+E_0|_{k=0}^2) (E+E_0) = S(t) \quad (8.41)$$

where $S(t)$ represents the coupling between the source antenna and the plasma, since if the instability is strong enough, the source may be decoupled from the plasma wave and $S(t) \rightarrow 0$. The $k = 0$ component of $|E + E_0|$ is subtracted out because it represents the spatially homogeneous part of the electric field and hence does not contribute to the ponderomotive force. This equation was first derived by Morales *et al* [108] who demonstrated in numerical simulations that the driven wave collapses into cavitons. The instability is called the oscillating two-stream instability (OTSI), and is a parametric instability (see section 8.4.2) which couples two plasma waves and an ion-acoustic wave, hence the appearance of c_s . Once the plasma is decoupled from the source, the nonlinear Schrödinger equation may relax to the Zakharov–Shabat equation, so the final state of the caviton is a soliton. In fact, it has been shown that yet another nonlinear soliton equation describes both the collapse and the decoupling, so that one can be assured that cavitons are solitons [109].

Problem 8.2.7. Nonlinear Schrödinger equation example. Calculate P and Q from the dispersion relation (8.40) and estimate the maximum growth rate of the instability.

8.3 Trapped particle effects

8.3.1 Nonlinear Landau damping

A celebrated example of the effects of trapped particles is the calculation of nonlinear Landau damping. In the linear treatment of section 4.2.2, the effects of resonant particles were already apparent in the limit of vanishing amplitude, giving rise to either growth or damping depending on the slope of the distribution function at the phase velocity of the wave. When one considers the finite amplitude of the wave, as in section 4.2.3, it is clear that some of the particles traveling near the phase velocity will be trapped and oscillate in the quasistationary potential well of the wave. Others will be nearly trapped, but will also exchange energy with the wave. To make matters even more complicated, as the wave amplitude initially falls at the linear rate, some of the initially trapped particles will become untrapped. As will be shown, the amplitude will actually oscillate some if the initial amplitude is sufficiently large, so there is both trapping and untrapping going on as the amplitude evolves and the energy sloshes back and forth between wave field energy and particle energy. For a sufficiently large initial

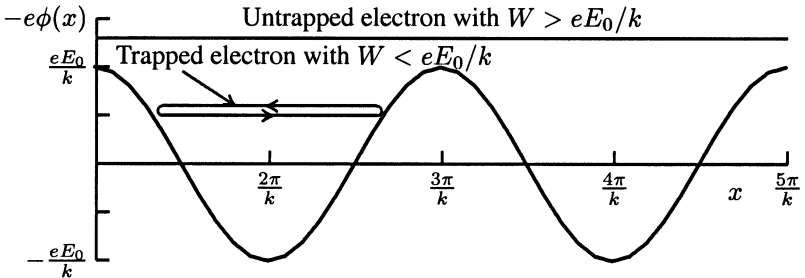


Figure 8.1. Potential well and particle motions in the wave frame.

amplitude, the wave finally settles down to a steady but finite amplitude where the zero-order distribution function is modified.

8.3.1.1 Particle motions in a constant wave field

In order to grasp first some of the physical principles and important parameters, we begin with the assumption of a driven sinusoidal electrostatic traveling wave field of infinite extent imposed on a plasma. In the wave frame, however, the field is a stationary potential well, so we represent the traveling wave field $E(x, t) = E_0 \sin(kx - \omega t)$ by its wave frame counterpart

$$E(x) = E_0 \sin kx \quad (8.42)$$

where E_0 is constant, and examine particles whose velocity is nearly $v_p = \omega/k$, or $v \sim 0$ in the wave frame. If we describe the trajectory of an electron by $x_e(t)$, then its equation of motion is that given in equation (4.118):

$$\frac{d^2}{dt^2} x_e(t) = -\frac{e}{m_e} E_0 \sin[kx_e(t)]. \quad (8.43)$$

The solution for $E_0 \rightarrow 0$ is, of course, trivial, leading to free-streaming solutions of the form $x_e(t) = x + vt$ where x and v are the initial position and velocity respectively.

Equation (8.43) is identical in form to the equation of motion for a finite amplitude pendulum, whose solutions lead to an expression for the period in terms of an elliptic integral, but for small amplitudes about the bottom of the potential well, it is clear that the ‘bounce’ period is given by

$$\tau_B \equiv \omega_B^{-1} = \sqrt{m_e/e k E_0}. \quad (8.44)$$

Particles traveling sufficiently close to the phase velocity that their kinetic energy, as measured in the wave frame, is less than eE_0/k will be unable to climb out of the potential well, illustrated in figure 8.1, and so will make periodic orbits.

Particles with wave frame energy greater than eE_0/k will be slowed down and speeded up by the wave, but will continue to pass over each successive potential hill, as shown above the well in figure 8.1. If, however, the amplitude is not steady, but varies slowly, then as long as the amplitude varies little over a bounce period, the motions of the trapped and untrapped particles will be affected little unless they are very close to the boundary (where the bounce time approaches infinity so any variation is relatively fast). The slowly varying condition, which limits the validity of the following analysis, is

$$\left| \frac{1}{E_0} \frac{dE_0}{dt} \right| \ll \omega_B. \quad (8.45)$$

This condition limits the number of particles that change from trapped to untrapped, and vice versa, to a small fraction of the affected particles.

The slowly varying condition is related to the Landau damping rate, which from equation (4.61) may be approximated by

$$\gamma_L \simeq -\sqrt{\frac{\pi}{8}} \frac{\omega_{pe}}{k^3 \lambda_{De}^3} \exp\left(-\frac{1}{2k^2 \lambda_{De}^2} - \frac{3}{2}\right) \quad (8.46)$$

where we use the long wavelength limit for plasma waves such that $\omega_k^2 \sim \omega_{pe}^2(1 + 3k^2 \lambda_{De}^2)$. It is convenient to define $\tau_L \equiv |\gamma_L|^{-1}$, and the plasma period $\tau_p \equiv \omega_{pe}^{-1}$ so that the weak damping condition is $\tau_p \ll \tau_L$ and the slowly varying condition is $\tau_B \ll \tau_L$. We combine these, requiring that the wave period be short compared to the bounce period, so that the general validity condition is

$$\tau_p \ll \tau_B \ll \tau_L. \quad (8.47)$$

If $k\lambda_{De}$ is not small, then there is no environment where the slowly varying condition is valid. If the bounce period approaches the wave period, then the assumption of a sinusoidal variation is very restrictive, since in general nonlinear effects will distort the wave for a general distribution function. Although there exists a distribution function that is consistent with a large amplitude sinusoidal wave, the distribution is not Maxwellian. We will return to this case in section 8.3.2, but it is not typical. These conditions imply both a minimum and a maximum amplitude for nonlinear Landau damping. We will examine some of the qualitative effects of violating these conditions at the end of this section.

Problem 8.3.1. Exact bounce time. Solve equation (8.43) exactly for the bounce period without making x_e small.

- (i) Using the variable change of equation (8.12), with $dx_e/dt \equiv v_e$, separate variables to do the first integral with the integration constant representing the amplitude x_m where $v_e = 0$ (the turning point), showing that the critical energy for periodic motion is eE_0/k .

- (ii) Using the definition of v_e , separate variables again to solve for the bounce period in terms of a definite integral over $[0, x_m]$.
- (iii) Using trigonometric identities, cast the integral into the form of an elliptic integral and show that as the amplitude is small, the full period is $2\pi/\omega_B$.

Problem 8.3.2. Limits of validity.

- (i) Show that equation (8.47) fails if $k\lambda_{De}$ approaches unity.
- (ii) Find $k\lambda_{De}$ where $100\tau_p = 10\tau_B = \tau_L$.
- (iii) Find $k\lambda_{De}$ where $9\tau_p = 3\tau_B = \tau_L$.
- (iv) Find eE_0/k in terms of κT_e for cases (ii) and (iii) where $E_{\max} = E_{\min}$.

8.3.1.2 Exact trajectories of trapped and nearly trapped electrons

When the linear theory fails, as it inevitably does for any finite amplitude wave, we need to treat the trapped and nearly trapped particles carefully. In this section, we follow O’Neil [110] and Davidson [97] where we solve

- (i) equation (8.43) exactly for both trapped and untrapped particles for constant E_0 ; and then
- (ii) solve for the slow variation of E_0 from the conservation of energy (particle energy plus wave energy).

We wish to solve for the distribution in the wave frame variables where the evolution of $f_e(x, v, t)$ is obtained from

$$\frac{\partial}{\partial t} f_e(x, v, t) + v \frac{\partial}{\partial x} f_e(x, v, t) - \frac{e}{m_e} E_0 \sin kx \frac{\partial}{\partial v} f_e(x, v, t) = 0. \quad (8.48)$$

Using the method of characteristics, we write this from the Liouville theorem as

$$\frac{d}{d\tau} f_e[x_e(\tau), v_e(\tau), \tau] = 0 \quad (8.49)$$

where $x_e(\tau)$ and $v_e(\tau)$ are the particle orbits in the wave field $E_0 \sin kx$ and are solutions of

$$\frac{d^2 x_e(\tau)}{d\tau^2} = -\frac{eE_0}{m_e} \sin[kx_e(\tau)]. \quad (8.50)$$

The solutions we need are the orbits that satisfy the end point conditions

$$x_e(\tau = t) = x \quad v_e(\tau = t) = v.$$

From equation (8.49), we have

$$f_e[x_e(\tau), v_e(\tau), \tau] = \text{constant (independent of } \tau) \quad (8.51)$$

and by evaluating equation (8.51) at $\tau = t$ and $\tau = 0$, we have

$$f_e(x, v, t) = f_e[x_e(0), v_e(0), 0] \quad (8.52)$$

which expresses $f_e(x, v, t)$ in terms of the initial distribution.

Following the first step of problem 8.3.1, the first integral gives

$$\frac{m_e}{2} \left[\frac{d}{d\tau} x_e(\tau) \right]^2 - \frac{eE_0}{k} \cos[kx_e(\tau)] = W = \text{constant}. \quad (8.53)$$

Changing variables to $\xi(\tau) \equiv kx_e(\tau)/2$ and $\kappa^2 \equiv 2eE_0/(kW + eE_0)$ where we take $k > 0$ and $E_0 > 0$ without loss of generality, then equation (8.53) becomes

$$\left[\frac{d}{d\tau} \xi(\tau) \right]^2 = \frac{1}{\kappa^2 \tau_B^2} [1 - \kappa^2 \sin^2 \xi(\tau)]. \quad (8.54)$$

The solution of equation (8.54) may be written in terms of the incomplete elliptic integral of the first kind, $F(\kappa, z)$, where

$$F(\kappa, z) \equiv \int_0^z \frac{dz'}{\sqrt{1 - \kappa^2 \sin^2 z'}}. \quad (8.55)$$

The case $\kappa^2 < 1$ —untrapped particles. When $W > eE_0/k$, then $\kappa^2 < 1$ and the particles are untrapped. In this case, the solution of equation (8.54) may be written as

$$F[\kappa, \xi(\tau)] - F[\kappa, \xi(t)] = (\tau - t)/\kappa \tau_B. \quad (8.56)$$

At $\tau = 0$, this reduces to

$$F[\kappa, kx_0/2] - F[\kappa, kx/2] = -t/\kappa \tau_B \quad (8.57)$$

and this determines $x_0 = x_e(0)$ implicitly. This can be inverted to give the explicit dependence

$$\sin kx_0 = 2\text{sn}[F(\kappa, \xi) - t/\kappa \tau_B, \kappa] \text{cn}[F(\kappa, \xi) - t/\kappa \tau_B, \kappa] \quad (8.58)$$

where sn and cn are Jacobi elliptic functions. Using this result in equation (8.54), we may then solve for $v_e(0)$ with the result

$$v_e(0) = \frac{2}{k \kappa \tau_B} \sqrt{1 - \kappa^2 \sin^2 [kx_e(0)/2]}. \quad (8.59)$$

These expressions may then be used in equation (8.52) to express $f_e(x, v, t)$ in terms of the initial conditions. The phase space trajectories of these particles are shown in figure 8.2 where they lie outside the shaded area.

The case $\kappa^2 > 1$ —trapped particles. When $-eE_0/k < W < eE_0/k$, then $\kappa^2 > 1$ and the particles are trapped. In this case, it is convenient to introduce the variable

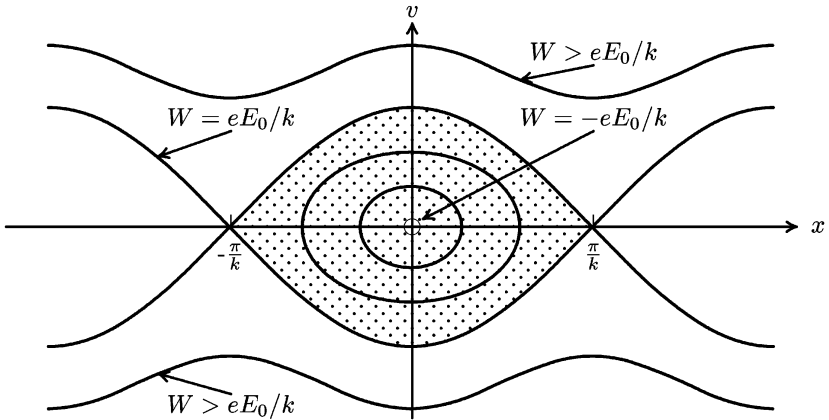


Figure 8.2. Constant energy surfaces in phase space (x, v) for the electrons.

$\zeta(\tau)$ such that $\sin[\zeta(\tau)] = \kappa \sin[\xi(\tau)]$. With this variable change, equation (8.54) becomes

$$\left[\frac{d}{d\tau} \zeta(\tau) \right]^2 = \frac{1}{\kappa^2 \tau_B^2} [\kappa^2 - \sin^2 \zeta(\tau)] \quad (8.60)$$

with solution

$$F[1/\kappa, \zeta(\tau)] - F[1/\kappa, \zeta(t)] = (\tau - t)/\tau_B. \quad (8.61)$$

At $\tau = 0$, this reduces to

$$F[1/\kappa, \zeta_0] - F[1/\kappa, \zeta(t)] = -t/\tau_B \quad (8.62)$$

which again implicitly determines $x_e(0) = (k/2) \sin^{-1} [\kappa^{-1} \sin \zeta_0]$ for the trapped electrons. Again inverting,

$$\sin kx_0 = (2/\kappa) \operatorname{sn}[F(1/\kappa, \zeta) - t/\tau_B, 1/\kappa] \operatorname{dn}[F(1/\kappa, \zeta) - t/\tau_B, 1/\kappa] \quad (8.63)$$

where dn is another Jacobi elliptic function. We can again use equation (8.59) for $v_e(0)$ in terms of $x_e(0)$. The trajectories for the trapped particles are illustrated by the closed loops in the shaded area of figure 8.2, where each closed contour represents the motion of a particle characterized by a particular total energy $W = \frac{1}{2}m_e v^2 - (eE_0/k) \cos kx$.

Problem 8.3.3. Solving the equations of motion. Fill in the steps leading to equations (8.58) and (8.63).

8.3.1.3 Conservation of energy

In order to estimate the slow variation of the amplitude, we look at the exact energy conservation expression which follows from the Vlasov–Maxwell

equations, so that we have

$$\frac{d}{dt} \left[\int_{-\pi/k}^{\pi/k} dx \frac{\epsilon_0 E^2(x, t)}{2} + \int_{-\pi/k}^{\pi/k} dx \int_{-\infty}^{\infty} dv \frac{1}{2} m_e v^2 f_e(x, v, t) \right] = 0. \quad (8.64)$$

If we assume the wave field varies as $E(x, t) = E_0(t) \sin(kx - \omega t)$, this conservation law expressed in the wave frame becomes

$$\begin{aligned} & \frac{d}{dt} \int_{-\pi/k}^{\pi/k} dx \frac{\epsilon_0 E_0^2(t)}{2} \sin^2 kx \\ &= - \int_{-\pi/k}^{\pi/k} dx \int_{-\infty}^{\infty} dv \frac{1}{2} m_e \left(v + \frac{\omega}{k} \right)^2 \frac{\partial}{\partial t} f_e(x, v, t). \end{aligned}$$

Averaging first over space, this reduces further to

$$\frac{d\mathcal{E}(t)}{dt} = - \int_{-\infty}^{\infty} dv \frac{1}{2} m_e \left(v + \frac{\omega}{k} \right)^2 \frac{\partial}{\partial t} \langle f_e \rangle(v, t) \quad (8.65)$$

where $\mathcal{E}(t) = \epsilon_0 E_0^2(t)/4$ is the spatially averaged electrostatic energy density, and $\langle f_e \rangle(v, t)$ is the spatially averaged distribution, defined by

$$\langle f_e \rangle(v, t) = \frac{k}{\pi} \int_{-\pi/k}^{\pi/k} dx f_e(x, v, t). \quad (8.66)$$

We now need an expression for $\partial f_e / \partial t$ which, from equation (8.52), is related to an initial condition that we take to be of the form

$$f_e(x, v, 0) = f_0(v) + f_1(v, 0) \cos kx \quad (8.67)$$

which is consistent at least with the linear problem. Then using $\partial x_e / \partial t = -\partial x_e / \partial \tau = -v_e$ and $\partial v_e / \partial t = (e/m_e) E_0 \sin kx_e$ at $\tau = 0$, we obtain

$$\begin{aligned} \frac{\partial}{\partial t} f_e(x, v, t) &= \left\{ \frac{e}{m_e} E_0 \sin kx' \frac{\partial}{\partial v'} [f_0(v') + f_1(v', 0) \cos kx'] \right. \\ &\quad \left. + kv' f_1(v', 0) \sin kx' \right\}_{x'=x_e(0), v'=v_e(0)}. \end{aligned} \quad (8.68)$$

We expect the principal contribution to equation (8.65) to come from the neighborhood of $v = 0$, since these are the trapped or nearly trapped particles. In the other limit, when $W \gg eE_0/k$, the orbits are nearly straight lines in phase space, and $x_e(0) \sim x - vt$ and $v_e(0) \sim v$ in which case the only variation with x in equation (8.68) is simple sinusoidal, and when averaged over a period these terms vanish. If we do an ordering of the various terms in the smallness of v and τ_p/τ_B , then it can be shown that the dominant term in equation (8.68) is [110]

$$\frac{\partial}{\partial t} f_e(x, v, t) \simeq \frac{\partial f_0(v)}{\partial v} \Big|_{v=0} \frac{eE_0}{m_e} \sin[kx_e(0)] \left[1 + \mathcal{O}\left(\frac{\tau_p}{\tau_B}\right) \right]. \quad (8.69)$$

At this point, the expressions for $\sin[kx_e(0)]$ from equation (8.58) for the untrapped particles and equation (8.63) for the trapped particles, and the subsequent integration of equation (8.65) with equation (8.69) for the time derivative of the distribution function leads to

$$\frac{d}{dt}\mathcal{E}(t) = 2\gamma(t)\mathcal{E}(t) \quad (8.70)$$

where

$$\begin{aligned} \gamma(t) \equiv \gamma_L \sum_{n=0}^{\infty} \frac{64}{\pi} \int_0^1 dk & \left\{ \frac{2n\pi^2 \sin(\pi nt/\kappa F \tau_B)}{\kappa^5 F^2 (1+q^{2n})(1+q^{-2n})} \right. \\ & \left. + \frac{(2n+1)\pi^2 \kappa \sin[(2n+1)\pi t/2F\tau_B]}{F^2 (1+q^{2n+1})(1+q^{-2n-1})} \right\} \end{aligned} \quad (8.71)$$

and

$$q \equiv e^{\pi F'/F} \quad F \equiv F(\kappa, \pi/2) \quad F' \equiv F\left(\sqrt{1-\kappa^2}, \pi/2\right).$$

The details of this calculation [110] are long and tedious, but the results allow us to get some insights into the nature of the nonlinear effects.

First, we note that the first term in the curly brackets of equation (8.71) is due to the untrapped electrons and that the second term is due to the trapped electrons. At short times, $t \ll \tau_B$, the untrapped electrons dominate and lead to $\gamma(t) \sim \gamma_L$ so initially the amplitude follows the linear decay (or growth if the distribution is initially unstable) rate. This is to be expected, since the bounce effects require roughly a bounce period to become important. When they do become important, the wave energy density ceases to decay as the bouncing particles begin to reconstruct the wave. This is illustrated in figure 8.3 where the energy density is seen to oscillate several times before finally settling down to a finite amplitude that is lower than the original amplitude. Since it may be shown that

$$\left| \int_0^\infty dt \gamma(t) \right| = \gamma_L \tau_B \frac{64}{\pi} \int_0^1 dk \left\{ \frac{1}{\kappa^4} \left[\frac{E}{\pi} - \frac{\pi}{4F} \right] + \frac{\kappa}{\pi} [E + (\kappa^2 - 1)F] \right\} \simeq \mathcal{O}(\tau_B/\tau_L) \quad (8.72)$$

where $E = E(\kappa, \frac{1}{2}\pi)$ is the complete elliptic integral of the first kind and the final amplitude is given approximately by $E_0(\infty) \sim E_0(0)[1 - (\tau_B/\tau_L)]$ (in figure 8.3, with $\tau_B/\tau_L = 0.1$, $\int_0^\infty \gamma(t) dt \simeq -0.2$). In the fully saturated wave, the trapped particles with differing bounce periods have completely lost their original coherence with the wave and as many are giving energy to the wave as taking energy from the wave. The distribution function is now distinctly different from the original distribution, and was known long before the nonlinear decay problem was solved as the self-consistent distribution associated with BGK waves, which we describe in the next section.

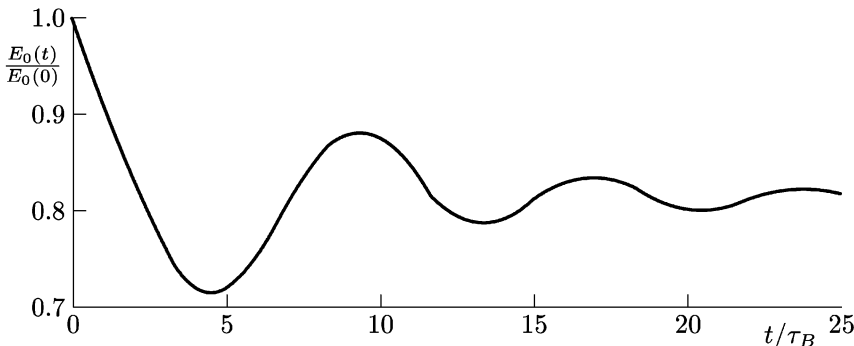


Figure 8.3. Amplitude variation of the electric field with $\tau_L/\tau_B = 10$. Note the suppressed zero.

Problem 8.3.4. Approximate damping rates. Following O’Neil [110], use the expressions of equations (8.71) and (8.72) to prove

- (i) $\gamma(t) \sim \gamma_L$ for $t \ll \tau_B$ and
- (ii) $\int_0^\infty dt \gamma(t) \sim \mathcal{O}(\gamma_L \tau_B)$.

8.3.1.4 Other nonlinear effects

Although finite amplitude damping appears to be due only to the modification of Landau damping by the trapped particles, cyclotron damping is also akin to Landau damping, except that it occurs in a rotating reference frame. Indeed, large-amplitude cyclotron damping also occurs and is similar to that previously sketched out, although the analysis is somewhat more formidable [111].

Because we have considered only one nonlinear effect, the energy oscillation and decay pattern of figure 8.3 is never precisely observed. One of the observed nonlinearities that interfere with this picture is due to wave–particle–wave interactions when the bounce period is an integral multiple of the wave period. Particles with this period will, after a fixed number of oscillations in the well, come back in phase with the wave and have a resonant interaction. This group of particles can also lead to sidebands or daughter waves at frequencies that are submultiples of the wave frequency. These exchanges modify the energy content of the primary wave, and hence the evolution will differ from that pictured.

If one considered lowering the amplitude to avoid these other nonlinearities, then the validity conditions begin to fail, and it is worthwhile to note the behavior when this begins to happen. We could begin to get an idea of the changes when the amplitude is lowered by considering that the bounce period, previously considered to be constant, is now taken as $\tau_B = \tau_B(t)$, where $\tau_B(t)$ is calculated from the instantaneous value of $E_0(t)$. This is only a first step, since it still completely ignores the transitions from trapped to untrapped and vice versa. This case can be

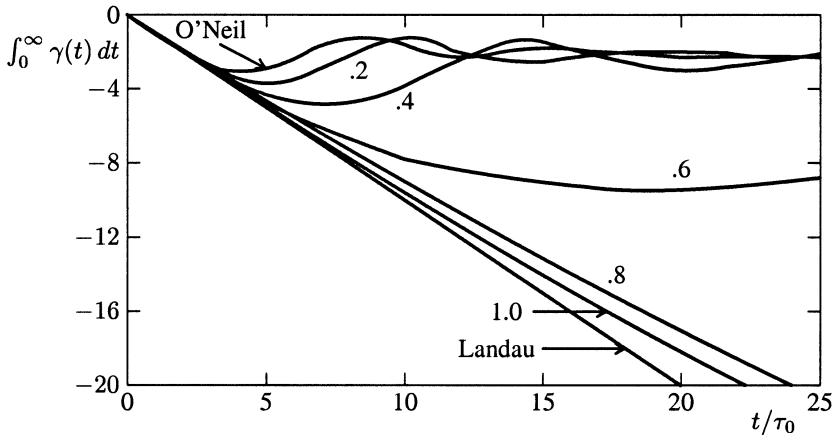


Figure 8.4. Integral of the damping coefficient with $\gamma_L \tau_0$ as a parameter.

solved as an integral equation [112] where

$$\tau_B(t) = \sqrt{m_e} \left[e k E_0(0) \exp \left(\int_0^t \gamma(t') dt' \right) \right]^{-1/2} \quad (8.73)$$

so $\gamma(t)$ appears both inside and outside the integral. When this expression is solved for various values of $E_0(0)$, as the initial amplitude is lowered, it takes longer (of course the nominal bounce time is longer) to oscillate and oscillates fewer times before settling down to a BGK mode at a much lower amplitude. Eventually a critical amplitude is reached where there are no oscillations at all and the decay is smooth until the saturation is reached. Below this amplitude, the wave continues to decay forever, but the rate is slower than for the linear case. This behavior is illustrated in figure 8.4 where we show the integral of the damping coefficient as a function of time, where the time is normalized to the initial bounce period $\tau_0 = \tau_B(0)$, and the parameter is $\gamma_L \tau_0$. It is apparent the critical level in this simplified case is near $\gamma_L \tau_0 = 0.6$.

The neglect of the effects of the trapping–untrapping transitions becomes a larger and larger error as the initial amplitude decreases. Clearly, as the amplitude is lowered, more trapped particles are dumped out of the well, and become untrapped. The inclusion of these effects must involve numerical codes, and these show the same qualitative features as the previous integral equation method, but the separatrix between the oscillatory and steady decay cases occurs for somewhat higher initial amplitudes. For example, more detailed numerical calculations by Canosa and Gazdag [113] indicate the transition from oscillatory to monotonic decay is closer to $\gamma_L \tau_0 = 0.5$.

Another effect that accompanies nonlinear damping is the nonlinear frequency shift. Because of the conservation of both energy and momentum, the

change of energy of the trapped particles must be balanced by the change of the total wave energy, and in the wave frame, this energy must be proportional to the frequency shift. This effect is found to oscillate as the amplitude does, saturating asymptotically to [114]

$$\delta\Omega(\infty) = -1.63\Omega_0 \quad (8.74)$$

$$\Omega_0 \equiv \left(\frac{eE_0}{mk} \right)^{1/2} \left(\frac{\omega_p}{k} \right)^2 \left(\frac{\partial^2 f_0}{\partial v^2} \right)_{v_p} \left(\frac{\partial \epsilon}{\partial \omega} \right)^{-1}_{\omega_L} \quad (8.75)$$

where ϵ is the dielectric constant for linear plasma oscillations.

8.3.2 Bernstein–Greene–Kruskal (BGK) modes

We have alluded to the fact that there exist exact solutions for finite amplitude sinusoidal waves, where the distribution function is modified from an equilibrium distribution to support these waves. In fact, any wave profile, periodic or not, can be established by a suitable modification of the distribution function. For example, a single Gaussian pulse could be established as well as a periodic square wave. These large amplitude waves are stationary in the wave frame, and referred to as Bernstein–Greene–Kruskal (BGK) waves [115].

We are looking for nonlinear electrostatic waves that are stationary in the wave frame, so the basic equations to be solved are

$$v \frac{\partial}{\partial x} f_j(x, v) + \frac{q_j}{m_j} E(x) \frac{\partial}{\partial v} f_j(x, v) = 0 \quad (8.76)$$

$$\frac{\partial}{\partial x} E(x) = \sum_j \frac{q_j}{\epsilon_0} \int_{-\infty}^{\infty} dv f_j(x, v) \quad (8.77)$$

where the wave frame variables are related to the laboratory frame variables through $x = x' - v_0 t'$ and $v = v' - v_0$ where v_0 is the phase velocity of the wave. The coordinate and velocity variables are related through the conservation of energy

$$W_j = \frac{1}{2} m_j v^2 + q_j \phi(x) \quad (8.78)$$

where $\phi(x)$ is the electrostatic potential from $E(x) = -\partial\phi(x)/\partial x$, so the distribution function can be written in terms of W_j and v as

$$f_j = H(v) f_j^+(W_j) + H(-v) f_j^-(W_j) \quad (8.79)$$

where $H(x)$ is the Heaviside step function, defined such that $H(x) = 1$ for $x \geq 0$ and $H(x) = 0$ for $x < 0$. Equation (8.79) satisfies equation (8.76) if

$$f_j^+(W_j) = f_j^-(W_j) \quad q_j \phi_{\min} < W_j < q_j \phi_{\max}. \quad (8.80)$$

Equation (8.80) simply states that for the trapped particles, lying between the absolute minimum and maximum potential energies, there cannot be any net

momentum in the wave frame, so the distributions must match. For the untrapped particles, there is no such limitation.

If we now take Poisson's equation, equation (8.77), and use equation (8.78) to express dv in terms of W_j , such that

$$dv = \frac{dW_j}{\sqrt{2m_j(W_j - q_j\phi)}}$$

then we obtain

$$\frac{\partial^2 \phi}{\partial x^2} = - \sum_j \frac{q_j}{\epsilon_0} \int_{q_j\phi}^{\infty} dW_j \frac{f_j^+(W_j) + f_j^-(W_j)}{\sqrt{2m_j(W_j - q_j\phi)}}. \quad (8.81)$$

This equation relates the potential to the distribution function, but it can be regarded either as determining the potential function for a given distribution function, or the other way around, determining the distribution function for a given potential function.

8.3.2.1 Solving for the potential

We make a first step by introducing a pseudopotential, multiplying equation (8.81) by $\partial\phi/\partial x$ and integrating once to

$$\frac{1}{2} \left(\frac{\partial \phi}{\partial x} \right)^2 + V(\phi) = \text{constant} \quad (8.82)$$

where the pseudopotential $V(\phi)$ is given by

$$V(\phi) \equiv - \sum_j \frac{1}{\epsilon_0} \int_{q_j\phi}^{\infty} dW_j [f_j^+(W_j) + f_j^-(W_j)] \sqrt{2(W_j - q_j\phi)/m_j}. \quad (8.83)$$

We may then solve equation (8.82) in terms of the quadrature

$$x - x_0 = \pm \frac{1}{\sqrt{2}} \int_{\phi_0}^{\phi} \frac{d\phi}{\sqrt{V(\phi) - V(\phi_0)}} \quad (8.84)$$

where $\phi_0 = \phi(x_0)$ and x_0 is a point where $d\phi/dx = 0$. This gives the implicit relationship of the potential to the coordinate for a specific distribution function.

Problem 8.3.5. BGK distributions.

- (i) Show that equation (8.80) is a solution of equation (8.76).
- (ii) Fill in the steps leading to equation (8.84).

8.3.2.2 Solving for the distribution function

If we suppose that the distribution functions for the ions and the untrapped electrons are specified, along with a specific potential that may or may not be periodic, then we can solve for the trapped-electron distribution function. If we define the trapped electron term from equation (8.81) to be

$$g(e\phi) \equiv \int_{-e\phi}^{-e\phi_{\min}} dW_e \frac{f_e^T(W_e)}{\sqrt{2m_e(W_e + e\phi)}} \quad (8.85)$$

then Poisson's equation may be written as

$$\begin{aligned} g(e\phi) = & \frac{\epsilon_0}{e} \frac{\partial^2 \phi}{\partial x^2} + \int_{-e\phi}^{\infty} dW_i \frac{[f_i^+(W_i) + f_i^-(W_i)]}{\sqrt{2m_i(W_i - e\phi)}} \\ & - \int_{-e\phi_{\min}}^{\infty} dW_e \frac{[f_e^+(W_e) + f_e^-(W_e)]}{\sqrt{2m_e(W_e + e\phi)}} \end{aligned} \quad (8.86)$$

where f_e^T is the trapped-electron distribution function. From equation (8.80), f_e^T for $W_e < -e\phi_{\min}$ is related to f_e by $f_e^T(W_e) = f_e^+(W_e) + f_e^-(W_e) = 2f_e^+(W_e)$. The solution to this integral equation is

$$f_e^T(W_e) = \frac{\sqrt{2m_e}}{\pi} \int_{e\phi_{\min}}^{-W_e} \frac{dW}{\sqrt{-W - W_e}} \frac{dg(W)}{dW} \quad W_e < -e\phi_{\min} \quad (8.87)$$

with the condition that $g(e\phi_{\min}) = 0$, and that f_e^T be nonnegative.

Problem 8.3.6. Trapped particle solution. Prove by direct substitution that equation (8.87) is a solution of equation (8.86).

8.3.2.3 BGK example—sinusoidal wave

If we assume the electrostatic potential is a simple sinusoidal wave, described by

$$\phi(x) = \phi_0 \sin kx \quad (8.88)$$

and then assume that both the ions and untrapped electrons are monoenergetic beams of particles moving to the left (in the wave frame) with sufficient energy that neither are trapped by the potential such that

$$f_i^+(W_i) = 0 \quad (8.89)$$

$$f_i^-(W_i) = n_{i0} \sqrt{2m_i(W_{i0} + e\phi_0)} \delta(W_i - W_{i0}) \quad W_{i0} > e\phi_0 \quad (8.90)$$

$$f_e^+(W_e) = 0 \quad (8.91)$$

$$f_e^-(W_e) = n_{e0} \sqrt{2m_e(W_{e0} - e\phi_0)} \delta(W_e - W_{e0}) \quad W_{e0} > e\phi_0 \quad (8.92)$$

where n_{i0} , n_{e0} , W_{i0} , and W_{e0} are constants. From their respective contributions to equation (8.81), the corresponding charge densities are

$$n_i(x) = n_{i0} \left[\frac{W_{i0} + e\phi_0}{W_{i0} - e\phi(x)} \right]^{1/2} \quad (8.93)$$

$$n_e^U(x) = n_{e0} \left[\frac{W_{e0} - e\phi_0}{W_{e0} + e\phi(x)} \right]^{1/2}. \quad (8.94)$$

From the form of equation (8.93), we note that n_{i0} is the *minimum* value of n_i , whereas from equation (8.94), n_{e0} is the *maximum* value of n_e^U , and these maxima and minima occur at $kx = \pm\pi/2, \pm 3\pi/2, \dots$. Using these expressions, $g(e\phi)$ from equation (8.86) becomes

$$g(e\phi) = -\frac{\epsilon_0 k^2}{e^2} e\phi + n_{i0} \left[\frac{W_{i0} + e\phi_0}{W_{i0} - e\phi(x)} \right]^{1/2} - n_{e0} \left[\frac{W_{e0} - e\phi_0}{W_{e0} + e\phi(x)} \right]^{1/2}. \quad (8.95)$$

From this result we can obtain dg/dW and insert this into equation (8.87) to obtain the trapped-electron distribution function,

$$f_e^T(W_e) \simeq \frac{\sqrt{2m_e}}{\pi} \sqrt{e\phi_0 - W_e} \left(-\frac{2\epsilon_0 k^2}{e^2} + \frac{n_{i0}}{W_{i0} + W_e} + \frac{n_{e0}}{W_{e0} - W_e} \right) \quad (8.96)$$

for all $W_e < e\phi_0$. The auxiliary conditions put some constraints on the various constants, since $g(-e\phi_0) = \epsilon_0 k^2 \phi_0 / e + n_{i0} - n_{e0} = 0$ and the condition that $f_e^T(W_e)$ be nonnegative leads to

$$-\frac{2\epsilon_0 k^2}{e^2} + \frac{n_{i0}}{W_{i0} + W_e} + \frac{n_{e0}}{W_{e0} - W_e} > 0 \quad (8.97)$$

and the two combined lead to

$$\frac{n_{i0}(W_{i0} + W_e + \frac{1}{2}e\phi_0)}{W_{i0} + W_e} - \frac{n_{e0}(W_{e0} - W_e - \frac{1}{2}e\phi_0)}{W_{e0} - W_e} > 0. \quad (8.98)$$

Problem 8.3.7. BGK example.

- (i) Fill in the missing steps for this example.
- (ii) Show that $n_{i0} \geq n_{e0}$ is a sufficient condition for equation (8.98).
- (iii) Sketch $n_i(x)$, $n_e^U(x)$, and $g(e\phi)$ as a function of x over a full period.

8.4 Parametric instabilities

Parametric instabilities are not unique to plasmas, as they relate to any oscillatory system where one of the parameters (hence parametric) is modulated at an appropriate frequency. A simple system is that of a child's swing, whose period

depends on the length of the swing from its support, and the parametric instability occurs when the child lengthens or shortens the effective length twice each period. This modulation at twice the natural frequency leads to growth of the fundamental oscillation, through what is commonly called ‘pumping’. A similar situation was described by Lord Rayleigh in 1883 [116] where a tuning fork was attached to one end of a stretched string and tuned to twice the natural frequency of the string. The modulation of the tension at twice the natural frequency led to an increased amplitude in the string’s oscillation through the parametric instability.

A rather extensive review of parametric instabilities in plasmas, including magnetized and unmagnetized plasmas, inhomogeneous and uniform plasmas, for linear and nonlinear electrostatic and electromagnetic waves, is given by Kaw *et al* [117]. This section is intended to be an introduction to some of these topics in order to establish the fundamentals of parametric instabilities with a few examples, and as such abstracts some of the topics from this review.

Quite generally, parametric excitations require a minimal set of common characteristics:

- (i) *Matching condition*: The modulation and the natural oscillation should satisfy a phase matching condition, such as $\omega T = n\pi$, $n = 1, 2, \dots$ where ω is the natural frequency and T is the period of the modulation. The previous examples have $n = 1$.
- (ii) *Threshold*: Instability or amplification occurs only when the amplitude of the modulation exceeds a critical value.
- (iii) *Frequency locking*: The frequencies of the amplified oscillations are determined by the modulation frequency rather than the natural frequency. For the previous examples for $n = 1$, amplification is at frequency π/T (the natural frequency), but for $n = 2$, amplification occurs at $2\pi/T$ (the natural frequency again) *and* at zero frequency.

The matching and frequency locking conditions follow from the intrinsic nonlinearity of the multiple frequency system, and can be viewed either as coming from conservation of energy and momentum or as coming from the resonance conditions of the weak turbulence analysis such that

$$\omega_0 = \omega_i + \omega_s \quad (8.99)$$

$$\mathbf{k}_0 = \mathbf{k}_i + \mathbf{k}_s \quad (8.100)$$

where the subscripts 0, i , s stand for pump, idler and signal, respectively. The instability occurs when the pump exceeds a certain threshold and the idler and signal waves grow. In general, we assume that the idler and signal represent waves that satisfy a dispersion relation in a plasma and are weakly damped modes, but this is not a strict requirement. When one of the waves is highly damped, we call it a quasimode, and numerous important applications involve quasimodes. From the nonlinear nature of the coupling, it is apparent that energy can be drawn from the pump wave and diverted to the idler and signal waves, or daughter waves.

This process can become so efficient that as a pump wave propagates, it loses energy to the daughter waves until it is depleted to the extent that it falls below threshold. Among the various effects which limit this efficiency of coupling are: finite wavelength effects, where the phase matching conditions cannot be satisfied everywhere; finite pump extent, where the daughter waves grow only to a finite value because they propagate beyond the extent of the pump; and nonlinear effects, where saturation may occur due to quasilinear effects changing the decay and amplification rates, or to nonlinear frequency shifts that modify the matching condition.

In order to sort out this somewhat bewildering array of possible effects, we will examine a few basic models that illustrate the fundamental phenomena, and then apply the principles thus discovered to a few specific plasma problems.

8.4.1 The modulated harmonic oscillator model

We consider first a damped oscillator described by

$$\frac{d^2x}{dt^2} + 2\gamma_0 \frac{dx}{dt} + (\Omega^2 + \gamma_0^2)x = 0 \quad (8.101)$$

which has the simple solution $x = A \exp(-i\Omega t - \gamma_0 t)$ if Ω and γ_0 are constants and represent the frequency and damping rate of the oscillator. If, however, we take the frequency to be modulated at frequency ω_0 , such that

$$\Omega^2 = \Omega_0^2(1 - 2\epsilon \cos \omega_0 t) \quad (8.102)$$

where Ω_0 is the natural frequency and ω_0 and ϵ the pump frequency and amplitude of the modulation, respectively, then the transformation $x(t) = e^{-\gamma_0 t} y(t)$ brings equation (8.101) into the form

$$\frac{d^2y}{dt^2} + \Omega_0^2(1 - 2\epsilon \cos \omega_0 t)y = 0 \quad (8.103)$$

which is the Mathieu equation. All of the characteristics of the parametric instability are contained in the properties of Mathieu functions, but since these are neither trivial nor commonly known, it is more instructive to examine the properties of equation (8.103) by a perturbational analysis assuming that the damping decrement, γ_0/Ω_0 , and modulation amplitude, ϵ , are both small.

Taking the Fourier transform of equation (8.103) leads to

$$D(\omega)\tilde{x}(\omega) = \epsilon\Omega_0^2[\tilde{x}(\omega + \omega_0) + \tilde{x}(\omega - \omega_0)] \quad (8.104)$$

where

$$D(\omega) \equiv -\omega^2 - 2i\omega\gamma_0 + \Omega_0^2 + \gamma_0^2.$$

The convolution integral has led to a function of ω being coupled to the response at frequencies $\omega \pm \omega_0$. We examine two special cases.

8.4.1.1 Case I: $\omega_0 \simeq 2\Omega_0$

If we choose $\omega \simeq \Omega_0$, then the first term on the right-hand side of equation (8.104) represents the response at $\sim 3\Omega_0$, so is far from resonant. The second term on the right gives a response at frequency $\omega - \omega_0 \simeq -\Omega_0$, so this term is nearly resonant. Keeping only the resonant term, we need $\tilde{x}(\omega - \omega_0)$ which we obtain from equation (8.104) to be

$$D(\omega - \omega_0)\tilde{x}(\omega - \omega_0) \simeq \epsilon\Omega_0^2\tilde{x}(\omega) \quad (8.105)$$

then the dispersion relation becomes

$$D(\omega)D(\omega - \omega_0) = \epsilon^2\Omega_0^4. \quad (8.106)$$

Making simple resonant approximations for the $D(\omega)$,

$$\begin{aligned} D(\omega) &= -(\omega + \Omega_0 + i\gamma_0)(\omega - \Omega_0 + i\gamma_0) \\ &\simeq -2\Omega_0(\omega - \Omega_0 + i\gamma_0) \\ D(\omega - \omega_0) &\simeq 2\Omega_0(\omega - \omega_0 + \Omega_0 + i\gamma_0) \end{aligned}$$

the dispersion relation may be written as

$$(\omega - \Omega_0 + i\gamma_0)(\omega - \Omega_0 - \Delta + i\gamma_0) + \frac{1}{4}\epsilon\Omega_0^2 = 0 \quad (8.107)$$

where $\Delta \equiv \omega_0 - 2\Omega_0$ is the frequency mismatch. Then using the definition $\omega \equiv \Omega_0 + \delta + i\gamma$, where δ is the real frequency shift and γ is the growth rate, separating the real and imaginary parts of equation (8.107) results in

$$\delta(\delta - \Delta) - (\gamma + \gamma_0)^2 + \frac{1}{4}\epsilon\Omega_0^2 = 0 \quad (8.108)$$

$$(2\delta - \Delta)(\gamma + \gamma_0) = 0 \quad (8.109)$$

so there are two types of solutions from equation (8.109):

- (i) *Damped zolution:* $\gamma = -\gamma_0$. This describes damped oscillations with frequencies given by

$$\delta = \frac{1}{2} \left(\Delta \pm \sqrt{\Delta^2 - \epsilon^2\Omega_0^2} \right)$$

which requires $\Delta^2 \geq \epsilon^2\Omega_0^2$, or that the frequency mismatch be sufficiently large or the modulation amplitude be sufficiently small.

- (ii) *Locked solution:* $\delta = \Delta/2$. This describes frequency locked oscillations since $\text{Re } \omega = \delta + \Omega_0 = \omega_0/2$ so that the frequency is independent of the natural frequency. Then from equation (8.108), this root gives

$$\gamma = -\gamma_0 \pm \frac{1}{2}\sqrt{\epsilon^2\Omega_0^2 - \Delta^2} \quad (8.110)$$

which is complementary to the other case in the sense that this case requires $\Delta^2 \leq \epsilon^2 \Omega_0^2$. The more weakly damped root of equation (8.110) becomes unstable when

$$\epsilon^2 > (\Delta^2 + 4\gamma_0^2)/\Omega_0^2 \quad (8.111)$$

so this is the parametric instability and equation (8.111) gives the threshold as a function of the mismatch. The maximum growth rate occurs when $\Delta = 0$, where the minimum threshold and maximum growth rate are given by

$$\epsilon_{\min} = 2\gamma_0/\Omega_0 \quad (8.112)$$

$$\gamma_{\max} = -\gamma_0 + \epsilon\Omega_0/2. \quad (8.113)$$

We note that in the limit as $\gamma_0 \rightarrow 0$, there is no threshold, so an infinitesimal excitation can drive the instability.

8.4.1.2 Case II: $\omega_0 \simeq \Omega_0$

For this case, we expect the coupling near $\omega \sim 0$ which is the difference frequency. The coupling from the symmetric forms of equation (8.105),

$$D(\omega \pm \omega_0)\tilde{x}(\omega \pm \omega_0) \simeq \epsilon\Omega_0^2\tilde{x}(\omega)$$

leads to the dispersion relation,

$$1 = \frac{\epsilon^2\Omega_0^4}{D(\omega)} \left[\frac{1}{D(\omega + \omega_0)} + \frac{1}{D(\omega - \omega_0)} \right]. \quad (8.114)$$

Using the approximation $D(\omega \pm \omega_0) \simeq \mp 2\Omega_0(\omega \pm \Delta + i\gamma_0)$, where the frequency mismatch is given in this case by $\Delta = \omega_0 - \Omega_0$, and approximating $D(\omega)$ by $D(0)$, equation (8.114) simplifies to

$$1 = \frac{\epsilon^2\Omega_0}{2} \left[\frac{1}{\omega - \Delta + i\gamma_0} - \frac{1}{\omega + \Delta + i\gamma_0} \right]. \quad (8.115)$$

Separating this into real and imaginary parts, with $\omega \equiv \omega_r + i\gamma$,

$$\omega_r^2 - \Delta^2 - (\gamma + \gamma_0)^2 = \epsilon^2\Omega_0\Delta \quad (8.116)$$

$$\omega_r(\gamma + \gamma_0) = 0. \quad (8.117)$$

Again there are two types of solution:

- (i) *Damped solution:* $\gamma = -\gamma_0$, $\omega_r = \pm\sqrt{\Delta(\Delta + \epsilon^2\Omega_0)}$. This solution requires either $\Delta > 0$ or $\Delta \leq -\epsilon^2\Omega_0$.
- (ii) *Locked solution.* For this case,

$$\omega_r = 0 \quad \gamma = -\gamma_0 \pm \sqrt{-\Delta(\Delta + \epsilon^2\Omega_0)} \quad (8.118)$$

so $-\epsilon^2\Omega_0 \leq \Delta \leq 0$. For this case, a growing solution occurs whenever the threshold is exceeded, given by

$$\epsilon^2 \geq -(\gamma_0^2 + \Delta^2)/\Delta\Omega_0. \quad (8.119)$$

The minimum threshold occurs when $\Delta = -\gamma_0$ and is given by

$$\epsilon_{\min} = \sqrt{2\gamma_0/\Omega_0}. \quad (8.120)$$

The maximum growth rate occurs when $\Delta = -\epsilon^2\Omega_0/2$ and is given by

$$\gamma_{\max} = -\gamma_0 + \epsilon^2\Omega_0/2. \quad (8.121)$$

Comparing these several results, each case has a damped solution and a locked solution, and there is a threshold for the instability. In case I, the threshold is lower and the growth rate is higher than the corresponding case II solution. In case I, the minimum threshold and the maximum growth rate occur for the same mismatch, while the maximum growth rate for case II is amplitude dependent. Examples of both these cases are to be found in plasmas.

Problem 8.4.1. Growth rates and thresholds. Fill in the missing steps leading to equations (8.112), (8.113), (8.120), and (8.121).

8.4.2 Excitation of coupled mode oscillations

The previous simple example had only one natural frequency, but plasmas are characterized by numerous natural frequencies. We shall choose as an example a case where the two natural frequencies are far apart, with the pump frequency close to the higher frequency. When the sum of the two natural frequencies nearly equals the pump frequency, then both kinds of instabilities, cases I and II, may be excited.

For the special case of a uniform pump, the natural oscillations are described by

$$\mathcal{L}_s x_s = \frac{d^2 x_s}{dt^2} + 2\gamma_s \frac{dx_s}{dt} + (\omega_s^2 + \gamma_s^2) x_s = 0 \quad s = 1, 2. \quad (8.122)$$

We assume the frequencies ω_s and damping rates γ_s are both constant. We choose to denote the lower frequency as ω_1 . The pump field is described by

$$Z(t) = 2\epsilon \cos \omega_0 t \quad (8.123)$$

with ϵ constant. This pump field couples $x_1(t)$ and $x_2(t)$ through the nonlinear interaction. We assume the coupling is of the form

$$\mathcal{L}_1 x_1(t) = \lambda_1 Z(t) x_2(t) \quad (8.124)$$

$$\mathcal{L}_2 x_2(t) = \lambda_2 Z(t) x_1(t) \quad (8.125)$$

where the λ_s are constants. We can imagine the pump and the high frequency producing a modulation at their beat frequency, and if this forced oscillation resonates with the low frequency, then we expect a resonant energy transfer when

$$\omega_0 \simeq \omega_1 + \omega_2. \quad (8.126)$$

Taking the Fourier transforms of equations (8.124) and (8.125), we find

$$D_1(\omega)\tilde{x}_1(\omega) = \lambda_1\epsilon[\tilde{x}_2(\omega + \omega_0) + \tilde{x}_2(\omega - \omega_0)] \quad (8.127)$$

$$D_2(\omega \pm \omega_0)\tilde{x}_2(\omega \pm \omega_0) = \lambda_2\epsilon[\tilde{x}_1(\omega) + \tilde{x}_1(\omega \pm 2\omega_0)] \quad (8.128)$$

where $D_s(\omega) = -\omega^2 - 2i\omega\gamma_s + \omega_s^2 + \gamma_s^2$. From equation (8.127) we see that $\tilde{x}_1(\omega)$ couples with $\tilde{x}_2(\omega \pm \omega_0)$, which through equation (8.128) couples with $\tilde{x}_1(\omega)$ and $\tilde{x}(\omega \pm 2\omega_0)$, the latter of which is nonresonant and can be neglected. We need to keep both $\tilde{x}_2(\omega \pm \omega_0)$, however, since for $\omega \sim \omega_1 \ll \omega_0$, both may be near $\pm\omega_2$. The dispersion relation is then given by

$$1 = \frac{\lambda_1\lambda_2\epsilon^2}{D_1(\omega)} \left[\frac{1}{D_2(\omega + \omega_0)} + \frac{1}{D_2(\omega - \omega_0)} \right] \quad (8.129)$$

which is similar to equation (8.114). For weak coupling, ($|\lambda_1\lambda_2\epsilon^2| \ll 1$), one or more of the denominators must be nearly resonant, or

$$D_1(\omega) \simeq 0 \quad \text{or} \quad D_2(\omega + \omega_0) \simeq 0 \quad \text{or} \quad D_2(\omega - \omega_0) \simeq 0. \quad (8.130)$$

From comparison with equation (8.114), two of the denominators must be resonant for the instability, so the two possible cases are:

- (i) $D_1(\omega) \simeq 0$ and $D_2(\omega + \omega_0) \simeq 0$ or $D_2(\omega - \omega_0) \simeq 0$.
- (ii) $D_2(\omega + \omega_0) \simeq 0$ and $D_2(\omega - \omega_0) \simeq 0$.

The first case corresponds to case I in the previous section by comparison with equation (8.106) (in the limit as $\omega_1 \rightarrow \omega_2 \rightarrow \omega_0/2$). The second case corresponds to case II by comparing equation (8.129) to equation (8.114) (in the limit as $\omega_2 \rightarrow \omega_0$). Making resonant approximations for $D_2(\omega \pm \omega_0)$ with $\Delta = \omega_0 - \omega_2$, but not approximating $D_1(\omega)$ since ω may differ significantly from $\pm\omega_1$, equation (8.129) reduces to

$$\omega^2 + 2i\omega\gamma_1 - \omega_1^2 - \gamma_1^2 = \frac{\lambda_1\lambda_2\epsilon^2}{\omega_2} \left(\frac{1}{\omega + \Delta + i\gamma_2} - \frac{1}{\omega - \Delta + i\gamma_2} \right). \quad (8.131)$$

Again defining $\omega \equiv \omega_r + i\gamma$ and separating the real and imaginary parts, we obtain

$$\omega_r^2 - \omega_1^2 - (\gamma + \gamma_1)^2 + [\omega_r^2 - \Delta^2 - (\gamma + \gamma_2)^2]/F(\gamma, \omega_r) = 0 \quad (8.132)$$

$$\omega_r[\gamma + \gamma_1 - (\gamma + \gamma_2)/F(\gamma, \omega_r)] = 0 \quad (8.133)$$

where

$$F(\omega_r, \gamma) = \frac{\omega_2}{\Delta\lambda_1\lambda_2\epsilon^2}[(\omega_r + \Delta)^2 + (\gamma + \gamma_2)^2][(\omega_r - \Delta)^2 + (\gamma + \gamma_2)^2]. \quad (8.134)$$

From this there are two solutions:

- (1) $\omega_r = 0$ is the *purely growing mode instability* since ω is purely imaginary. The oscillating two-stream instability (OTSI) is the best known example that occurs when a plasma is driven by a uniform pump close to the electron plasma frequency.
- (2) $\omega_r \neq 0$ and $\gamma + \gamma_1 = (\gamma + \gamma_2)/F(\omega_r, \gamma)$ which corresponds to the *decay instability*. This describes the decay of the pump wave into two lower frequency waves (idler and signal). This is the most common case, and has numerous examples in plasma physics.

Problem 8.4.2. Thresholds and growth rates:

- (i) The purely growing instability (case (1) above)
 - (a) Show that the threshold condition may be written as

$$|\lambda_1\lambda_2|\epsilon_{\min}^2 = 2\omega_1^2\omega_2\gamma_2. \quad (8.135)$$

- (b) Show that the maximum growth rate condition is

$$\omega_0 = \omega_2 - (\gamma_{\max} + \gamma_2). \quad (8.136)$$

- (c) Show that near threshold,

$$\gamma_{\max} = \frac{|\lambda_1\lambda_2|(\epsilon^2 - \epsilon_{\min}^2)}{2\omega_2(\omega_1^2 + 2\gamma_1\gamma_2)}. \quad (8.137)$$

- (ii) The decay instability (case (2) above)

- (a) Show that the threshold ϵ_{\min} as a function of the offset Δ , is given by

$$\epsilon_{\min}^2 = \frac{\gamma_1\gamma_2\omega_2}{\Delta\lambda_1\lambda_2} \left[4\Delta^2 + \frac{(\gamma_2^2 + 2\gamma_1\gamma_2 + \omega_1^2 + \gamma_1^2 - \Delta^2)^2}{(\gamma_1 + \gamma_2)^2} \right] \quad (8.138)$$

and hence vanishes when either γ_1 or γ_2 is zero.

- (b) Show that $\omega_c(\Delta)$, the real part of the frequency at threshold, is given by

$$\omega_c(\Delta) = \pm \sqrt{\frac{\gamma_2\omega_1^2 + \gamma_1\Delta^2 + \gamma_1^2\gamma_2 + \gamma_2^2\gamma_1}{\gamma_1 + \gamma_2}}. \quad (8.139)$$

- (c) Find Δ , ϵ_{\min} , and ω_c for the limiting cases $\omega_1 \gg \gamma_2$ and $\omega_1 \ll \gamma_2$.

8.4.3 Effects of finite pump wavelength

For this case we replace equation (8.123) by

$$Z(\mathbf{r}, t) = 2\epsilon \cos(\mathbf{k}_0 \cdot \mathbf{r} - \omega_0 t) \quad (8.140)$$

and must now Fourier transform in both space and time, so that equations (8.127) and (8.128) become

$$D_1(\omega, \mathbf{k})\tilde{x}_1(\omega, \mathbf{k}) = \epsilon[\lambda_1^+\tilde{x}_2(\omega + \omega_0, \mathbf{k} + \mathbf{k}_0) + \lambda_1^-\tilde{x}_2(\omega - \omega_0, \mathbf{k} - \mathbf{k}_0)] \quad (8.141)$$

$$D_2(\omega \pm \omega_0, \mathbf{k} \pm \mathbf{k}_0)\tilde{x}_2(\omega \pm \omega_0, \mathbf{k} \pm \mathbf{k}_0) = \epsilon\lambda_2^\pm\tilde{x}_1(\omega, \mathbf{k}) \quad (8.142)$$

where now ω_s and γ_s are the frequency and damping rate for a wave with wavevector \mathbf{k} for an uncoupled wave. The dispersion relation corresponding to equation (8.129) is then

$$1 = \frac{\epsilon^2}{D_1(\omega, \mathbf{k})} \left[\frac{\lambda_1^+\lambda_2^+}{D_2(\omega + \omega_0, \mathbf{k} + \mathbf{k}_0)} + \frac{\lambda_1^-\lambda_2^-}{D_2(\omega - \omega_0, \mathbf{k} - \mathbf{k}_0)} \right]. \quad (8.143)$$

We solve equation (8.143) in the same way in which we solved equation (8.129), but now it is more complicated. In order to keep the arguments clear, we take $\lambda_1^+\lambda_2^+ = \lambda_1^-\lambda_2^- > 0$. Separating the real and imaginary parts as before, we now find that

$$\omega_r^2 - \omega_1^2 - (\gamma + \gamma_1)^2 = [\Delta^2 - (\omega_r - \mu)^2 + (\gamma + \gamma_2)^2]/F(\gamma, \omega_r - \mu) \quad (8.144)$$

$$\omega_r(\gamma + \gamma_1) = (\omega_r - \mu)(\gamma + \gamma_2)/F(\gamma, \omega_r - \mu) \quad (8.145)$$

where now

$$\mu = \frac{1}{2}[\omega_2(\mathbf{k} + \mathbf{k}_0) - \omega_2(\mathbf{k} - \mathbf{k}_0)] \quad (8.146)$$

$$\Delta = \omega_0 - \langle \omega_2 \rangle \quad (8.147)$$

$$\langle \omega_2 \rangle = \frac{1}{2}[\omega_2(\mathbf{k} + \mathbf{k}_0) + \omega_2(\mathbf{k} - \mathbf{k}_0)] \quad (8.148)$$

and we have used the approximation that $|\mu| \ll \langle \omega_2 \rangle$. It is convenient to recast equations (8.144) and (8.145) by eliminating $F(\gamma, \omega_r - \mu)$ between them to obtain

$$\omega_r(\gamma + \gamma_1)[\Delta^2 - (\omega_r - \mu)^2 + (\gamma + \gamma_2)^2] = (\omega_r - \mu)(\gamma + \gamma_2)[\omega_r^2 - \omega_1^2 - (\gamma + \gamma_1)^2] \quad (8.149)$$

and eliminating the Δ^2 terms from $F(\gamma, \omega_r - \mu)$ leads to

$$\frac{\Delta\kappa}{\langle \omega_2 \rangle} = \omega_r(\omega_r - \mu)(\gamma + \gamma_1)(\gamma + \gamma_2) \left\{ 4 + \frac{[\omega_r^2 - \omega_1^2 - (\gamma + \gamma_1)^2]^2}{\omega_r^2(\gamma + \gamma_1)^2} \right\} \quad (8.150)$$

where $\kappa \equiv \epsilon^2\lambda_1^+\lambda_2^+ = \epsilon^2\lambda_1^-\lambda_2^-$. Equation (8.149) has three roots for ω_r , where for $\mu > 0$,

$$(I) \quad \omega_r > \mu \quad (II) \quad \mu > \omega_r > 0 \quad (III) \quad \omega_r < 0 \quad (8.151)$$

where each root is labeled. Since $\kappa > 0$, equation (8.150) indicates that modes I and III both occur when $\Delta > 0$, and mode II corresponds to $\Delta < 0$. The uniform pump case ($\mu = 0$) shows that mode II is the purely growing mode and the other two are decay type modes. For this case with $\mu \neq 0$, however, there is no longer any purely growing mode. When $\mu > \omega_1$, then the frequency of mode I becomes nonresonant and we have a quasimode. For $\mu \neq 0$, the threshold can be substantially reduced for $\omega_r \sim \omega_1$, and the growth rate well above threshold can be significantly increased.

Problem 8.4.3. Coupled equations. Show that equations (8.149) and (8.150) follow from equations (8.144) and (8.145). (Hint: writing (8.144) and (8.145) as $A = B/F$ and $C = D/F$, with $F = (\langle \omega_2 \rangle / \Delta \kappa) E^+ E^-$, and using $\Delta^2 = B + ?$, show that $E^+ E^- = B^2 + 4D^2$.)

Problem 8.4.4. Resonant decay. When ω_r is resonant ($D_1(\omega, k) \simeq 0$), show that the growth rate and threshold are given by

$$\gamma = \frac{1}{2} \left[-(\gamma_1 + \gamma_2) + \sqrt{(\gamma_1 - \gamma_2)^2 + \frac{\kappa}{\omega_r \langle \omega_2 \rangle}} \right] \quad (8.152)$$

and

$$\kappa_0 = 4\omega_r \langle \omega_2 \rangle \gamma_1 \gamma_2. \quad (8.153)$$

(Hint: Show that equation (8.149) leads to $\Delta \sim \omega_r - \mu$.)

8.4.4 Unmagnetized plasma examples

In the unmagnetized plasma, the principal wave is the ordinary wave from equation (2.37), where the dispersion relation may be written as

$$D(\omega, k) = \omega_{pe}^2 + k^2 c^2 - (\omega - i\nu_e)^2 \quad (\text{photons}) \quad (8.154)$$

where ν_e is due to collisional damping since there is no Landau damping. The plasma wave dispersion relation may be obtained from equation (3.32) or equation (4.56) and may be written as

$$D(\omega, k) = \omega_{pe}^2 + \frac{3}{2} k^2 v_e^2 - (\omega - i\gamma_p)^2 \quad (\text{plasmons}) \quad (8.155)$$

where

$$\gamma_p = \sqrt{\frac{\pi}{8}} \frac{\omega_{pe}}{k^3 \lambda_{De}^3} \exp \left[-\frac{1}{2k^2 \lambda_{De}^2} - \frac{3}{2} \right] \quad (8.156)$$

from equation (4.61). The ion-acoustic wave dispersion relation comes from equation (4.141), written as

$$D(\omega, k) = \frac{k^2 c_s^2}{1 + k^2 \lambda_{De}^2} - (\omega - i\gamma_a)^2 \quad (\text{phonons}) \quad (8.157)$$

where $k\lambda_{De} \ll 1$ and

$$\gamma_a = \sqrt{\frac{\pi}{8}} \left[\sqrt{\frac{m_e}{m_i}} + \left(\frac{T_e}{T_i} \right)^{3/2} e^{-T_e/2T_i} \right] + v_i \quad (8.158)$$

from equation (4.142) plus a collisional term. In each case, the name for the quantized excitation is given as a convenient label to designate the appropriate wave type.

8.4.4.1 Case 1—The pump is a plasma wave

For this case, ω_0 satisfies equation (8.155) with wavevector \mathbf{k}_0 . If $\mathbf{k} \parallel \mathbf{k}_0$, (otherwise $\lambda_1^+ \lambda_2^+ \neq \lambda_1^- \lambda_2^-$), then

$$\mu \simeq \frac{3k k_0 v_e^2}{2\omega_0} \quad \Delta \simeq -\frac{3k^2 v_e^2}{4\omega_0}.$$

With $\Delta < 0$, this is mode II where $\mu > \omega_r > 0$. We note two special cases:

- (a) When $\mu \gg \omega_1 \simeq \omega_r$, then equation (8.149) requires that $\Delta^2 \sim \mu^2$ so that $k \sim 2k_0 \sim 2(k - k_0)$. In this case, a plasmon has decayed into another plasmon (ω_2 from equation (8.155)) and a phonon (ω_1 from equation (8.157)). This is an example where an electron plasma wave is *backscattered* by an ion wave since $k_0 - k \sim -k_0$.
- (b) Another limiting case is when $\mu \simeq \omega_1 \simeq \omega_r$, in which case equation (8.149) leads to $\Delta^2 \sim 0$, so k^2 must be small. In this limit, $k_0 \pm k \sim k_0$, so this case represents *forward scattering*.

8.4.4.2 Case 2—The pump is an electromagnetic wave

Here we note four special cases:

- (a) When the pump frequency is just above the plasma frequency, it may decay into a plasmon (ω_2) and a phonon ($\omega_1 = \omega_0 - \omega_2 \ll \omega_0$). Since all three waves are different, (photon → plasmon+phonon), this is just a decay process that damps the pump.
- (b) Instead of decaying into a plasmon and a phonon when the pump frequency is just above the plasma frequency, it can also decay into another photon (a scattered electromagnetic wave) and a phonon. This type of scattering is called *Brillouin scattering*.
- (c) When the pump frequency is higher such that $\omega_0 > 2\omega_p$, then it may decay into another photon (a scattered electromagnetic wave) and a plasmon. This type of scattering is called *Raman scattering*.
- (d) For the special case of $\omega_0 = 2\omega_p$, the photon may decay into two plasmons.

In order to examine any of these cases in more detail, we must first examine some of the physics that goes into the amplitude (ϵ) and coupling coefficients (λ_1

and λ_2). For an electromagnetic wave pump, we take the electric field amplitude to be

$$\mathbf{E}_0(\mathbf{r}, t) = 2E_0\hat{\mathbf{e}}_0 \cos(\mathbf{k}_0 \cdot \mathbf{r} - \omega_0 t) \quad (8.159)$$

from which we find the electron velocity to be

$$\mathbf{v}_0 = \mathbf{v}_0^+ + \mathbf{v}_0^-$$

where $\mathbf{v}_0^\pm = \mp ie\mathbf{E}_0^\pm/m_e\omega_0$ and

$$\mathbf{E}_0^\pm = E_0\hat{\mathbf{e}}_0 \exp[\pm i(\mathbf{k}_0 \cdot \mathbf{r} - \omega_0 t)]. \quad (8.160)$$

This driven velocity of the electrons multiplied by the density fluctuation of a daughter wave generates a current density which drives waves at the sum and difference frequencies of the velocity and density fluctuations. From the wave equation, driven waves satisfy

$$\left[k^2 I - \frac{\omega^2}{c^2} K - \mathbf{k}\mathbf{k} \right] \cdot \mathbf{E} = i\omega\mu_0 j_{\text{pump}}$$

or casting this result into the form of equation (8.142), we have

$$\mathbf{D}_2(\omega_\pm, \mathbf{k}_\pm) \cdot \mathbf{E}^\pm(\omega_\pm, \mathbf{k}_\pm) = -\omega_p^2 \frac{\tilde{n}_e(\omega, \mathbf{k})}{n_0} \mathbf{E}_0^\pm \quad (8.161)$$

where $\omega_\pm = \omega \pm \omega_0$ and $\mathbf{k}_\pm = \mathbf{k} \pm \mathbf{k}_0$, and we have assumed $\omega_0 \gg \omega_1$. Because \mathbf{D}_2 is a tensor, the inversion of equation (8.161) is nontrivial, but one form of the inversion may be written as

$$\mathbf{E}^\pm \cdot \mathbf{E}_0^\mp = \frac{\omega_{pe}^2 \tilde{n}_e(\omega, \mathbf{k})}{k_\pm^2 n_0} \left[\frac{(\mathbf{k}_\pm \times \mathbf{E}_0^\mp)^2}{D_{2t}^\pm} - \frac{(\mathbf{k}_\pm \cdot \mathbf{E}_0^\mp)^2}{D_{2\ell}^\pm} \right] \quad (8.162)$$

where D_{2t} and $D_{2\ell}$ are the transverse and longitudinal dispersion functions given by

$$D_{2t}^\pm = k_\pm^2 c^2 - \omega_\pm K_t(\omega_\pm, \mathbf{k}_\pm) \quad (\text{photons})$$

$$D_{2\ell}^\pm = -\omega_\pm K_\ell(\omega_\pm, \mathbf{k}_\pm) \quad (\text{plasmons})$$

and K_t and K_ℓ are given by equation (4.31).

The low-frequency density fluctuations, $\tilde{n}_e(\omega, \mathbf{k})$, result from the beating of the high and low frequency waves, forming a nonuniform wave field. This inhomogeneous field in turn drives a low frequency perturbation through the ponderomotive force. The ponderomotive potential from equation (8.8) uses the low-frequency beat component of the electric fields, such that

$$\psi = \frac{e^2}{4m_e} \left| \frac{\mathbf{E}_0}{\omega_0} + \frac{\mathbf{E}^+}{\omega_+} + \frac{\mathbf{E}^-}{\omega_-} \right|^2. \quad (8.163)$$

The low frequency components, with $\omega \ll \omega_0$, then lead to

$$\psi = \frac{e^2}{m_e \omega_0^2} (\mathbf{E}_0^+ \cdot \mathbf{E}^- + \mathbf{E}_0^- \cdot \mathbf{E}^+). \quad (8.164)$$

In order to calculate the electron density fluctuations due to the ponderomotive potential, the linearized kinetic equation for electrons gives

$$\frac{\partial f_1}{\partial t} + \mathbf{v} \cdot \nabla f_1 + \frac{1}{m_e} (e \nabla \varphi - \nabla \psi) \cdot \nabla_{\mathbf{v}} f_0 = 0 \quad (8.165)$$

and taking Fourier and Laplace transforms, we have

$$\tilde{n}_e = \int_{-\infty}^{\infty} \tilde{f}_1 d^3 v = -\frac{n_0 e}{2 \kappa T_e} (\tilde{\varphi} - \tilde{\psi}/e) Z'(\zeta_e). \quad (8.166)$$

The ions do not respond to the ponderomotive potential, so the ion density and Poisson's equation become

$$\begin{aligned} \tilde{n}_i &= \frac{n_0 e}{2 \kappa T_i} \tilde{\varphi} Z'(\zeta_i) \\ k^2 \tilde{\varphi} &= \frac{e}{\epsilon_0} (\tilde{n}_i - \tilde{n}_e). \end{aligned}$$

If we represent the dielectric constant from equation (4.138) in terms of the electron and ion susceptibilities as

$$K = 1 + \chi_e + \chi_i$$

where

$$\chi_e = -\frac{\omega_{pe}^2}{k^2 v_e^2} Z'(\zeta_e) \quad \chi_i = -\frac{\omega_{pi}^2}{k^2 v_i^2} Z'(\zeta_i)$$

we finally obtain for the perturbed electron density,

$$\tilde{n}_e = -\frac{k^2 \epsilon_0 \chi_e (1 + \chi_i)}{K e^2} \tilde{\psi}. \quad (8.167)$$

It is convenient to rearrange this, using equation (8.164), so that

$$\left(\frac{1}{\chi_e} + \frac{1}{1 + \chi_i} \right) \tilde{n}_e = -\frac{k^2 \epsilon_0}{m_e \omega_0^2} (\mathbf{E}_0^+ \cdot \mathbf{E}^- + \mathbf{E}_0^- \cdot \mathbf{E}^+)$$

which can be put into the form of equation (8.141) where D_1 represents either a plasmon or a phonon, such that

$$D_1(\omega, \mathbf{k}) \tilde{n}_e(\omega, \mathbf{k}) = -\frac{\omega_{pe}^2 k^2 \epsilon_0}{m_e \omega_0^2} (\mathbf{E}_0^+ \cdot \mathbf{E}^- + \mathbf{E}_0^- \cdot \mathbf{E}^+) \quad (\text{plasmon})$$

$$D_1(\omega, \mathbf{k}) \tilde{n}_e(\omega, \mathbf{k}) = -\frac{\omega_{pi}^2 k^2 \epsilon_0}{m_e \omega_0^2 (1 + k^2 \lambda_{De}^2)} (\mathbf{E}_0^+ \cdot \mathbf{E}^- + \mathbf{E}_0^- \cdot \mathbf{E}^+) \quad (\text{phonon}).$$

Table 8.1. Threshold parameter κ for several combinations of daughter waves for an electromagnetic pump wave.

Case	D_1	D_2	κ
(c) Raman	plasmon	photon	$k^2 \omega_{pe}^2 (\mathbf{k}_\pm \times \mathbf{v}_0)^2 / k_\pm^2$
(b) Brillouin	phonon	photon	$k^2 \omega_{pi}^2 (\mathbf{k}_\pm \times \mathbf{v}_0)^2 / (1 + k^2 \lambda_{De}^2) k_\pm^2$
(d) decay	plasmon	plasmon	$k^2 \omega_{pe}^2 (\mathbf{k}_\pm \cdot \mathbf{v}_0)^2 / k_\pm^2$
(a) decay	phonon	plasmon	$k^2 \omega_{pi}^2 (\mathbf{k}_\pm \cdot \mathbf{v}_0)^2 / (1 + k^2 \lambda_{De}^2) k_\pm^2$

From these results and equation (8.161) along with equation (8.162), we find that the threshold parameters for several cases may be expressed in terms of $\mathbf{v}_0 = e\mathbf{E}_0/m_e\omega_0$ as in table 8.1.

Problem 8.4.5. The threshold parameter. Find $\lambda_1^\pm, \lambda_2^\pm$ and fill in the missing steps from equation (8.165) to fill in the values of table 8.1.

8.4.4.3 Brillouin scattering

For this case, D_2 is a photon dispersion function and D_1 is a phonon dispersion function, so $\kappa = (k/k_\pm)^2 \omega_{pi}^2 (\mathbf{k}^- \times \mathbf{v}_0)^2 / (1 + k^2 \lambda_{De}^2)$, since $\mathbf{k} \sim 2\mathbf{k}_0$ making \mathbf{k}^- the resonant mode. For the photon case, with $\omega_0 \sim \omega_2 \sim \omega_{pe}$, we have $\mu \simeq kk_0c^2/\omega_0$, $\Delta \simeq -k^2c^2/\omega_0$ (so case II again from equation (8.151)), and with $\omega_1 = \omega_2 - \omega_2^-$, $\mu - \omega_1 \simeq k^2c^2/\omega_0$. In the resonant scattering case, $\omega \simeq \omega_1$, so the threshold condition from equation (8.150) or equation (8.153) with $\gamma = 0$ is

$$k^2 v_0^2 \sin^2 \theta \simeq 4\gamma_a \gamma_2 \omega_1 \omega_0 (1 + k^2 \lambda_{De}^2) / \omega_{pi}^2 \quad (8.168)$$

where θ is related to the angle between \mathbf{k}_- and \mathbf{v}_0 ($\sin \theta = 1$ if $\mathbf{k}_- \perp \mathbf{v}_0$). The corresponding growth rate just above threshold (from equation (8.152)) is

$$\gamma = -\gamma_2 + \frac{\omega_{pi}^2 k^2 v_0^2 \sin^2 \theta}{4\omega_1 \omega_0 \gamma_a (1 + k^2 \lambda_{De}^2)} \quad (8.169)$$

for $\gamma \gg \gamma_2 \sim \nu_e$.

Problem 8.4.6. Maximum growth rate. Show that the maximum growth rate for Brillouin scattering is given by

$$\gamma_{\max} \simeq \frac{\omega_{pi} k v_0 \sin \theta}{\sqrt{\omega_1 \omega_0 (1 + k^2 \lambda_{De}^2)}}.$$

This is maximized when $k \simeq 2k_0$ (backscattering). For $k_0 \lambda_{De} \ll 1$, show that this maximum growth rate is given by $\gamma_{\max} = \omega_{pi} v_0 / \sqrt{c_s \omega_0 / 2k_0}$.

8.4.4.4 Resonant raman scattering

In this example, a photon is scattered off a plasmon rather than a phonon. Hence, D_1 represents a plasma wave from equation (8.155), and D_2 an electromagnetic wave from equation (8.154). Again for this case, $k - k_0$ is the resonant root, so $\kappa = (k/k_-)^2 \omega_{pe}^2 (\mathbf{k}_- \times \mathbf{v}_0)^2 = k^2 v_0^2 \omega_{pe}^2 \sin^2 \theta'$ from [table 8.1](#) where θ' again represents an angle between \mathbf{k} and \mathbf{v}_0 . Also for this case, $\omega - \mu \simeq \Delta$ (from $\omega_0 = \omega_1 + \omega_2^-$). The threshold is then given by equation (8.153) as

$$k^2 v_0^2 \sin^2 \theta' = 4\gamma_p \gamma_2 \langle \omega_2 \rangle / \omega_{pe} \quad (8.170)$$

and the minimum threshold is for $k \sim 2k_0$ (backscattering) and $\theta' = \pi/2$, when $k_0^2 v_0^2 = \gamma_p \gamma_2 \langle \omega_2 \rangle / \omega_{pe}$. The gain just above threshold from equation (8.152) (resonant case) is

$$\gamma = -\gamma_2 + \frac{\omega_{pe} k^2 v_0^2 \sin^2 \theta'}{4 \langle \omega_2 \rangle \gamma_p}. \quad (8.171)$$

Problem 8.4.7. Raman example. With $\omega_0 = 3\omega_{pe}$, $v_e/\omega_{pe} = 0.01$, and $v_e/c = 0.05$, find the daughter wave frequencies, the threshold for Raman scattering (v_0/c)_{min}, and maximum growth rate ($\gamma_{\max}/\omega_{pe}$). (Hint: Let $k = \alpha k_0$ and find α from $\omega_0 = \omega_2^- + \omega_1$.)

Appendix A

Complex variables

It is not the intention of this discussion of complex variables to give a full treatise on the subject, as this is covered in numerous textbooks. What follows is rather an indication of how the theorems and properties of analytic functions can be used to solve the kinds of problems which appear in the body of the text. In each case, we give some of the general principles, and then illustrate the technique with an example.

A.1 Contour integrals

Many of the integrals in this book are conveniently evaluated by the use of contour integrals, which are based on the Cauchy integral theorem. In its simplest form, this theorem states that

$$\oint_C \frac{f(z)}{z - z_0} dz = 2\pi i f(z_0) \quad (\text{A.1})$$

if $f(z)$ is an analytic function everywhere inside the closed contour C (which is traversed in the counterclockwise direction). Since the path integral of an analytic function is independent of the path, we are free to deform paths to suit ourselves unless they encounter a pole, whereupon the Cauchy integral theorem tells us what the contribution is from circumnavigating the pole. More generally, for a function which may have a series of poles, we may write the result in terms of the residues at the poles:¹

$$\oint_C F(z) dz = 2\pi i \sum_k \text{res}_k \quad (\text{A.2})$$

where for simple poles the residues are given by

$$\text{res}_k = \lim_{z \rightarrow z_k} (z - z_k) F(z).$$

¹ These are rumored to be due to Cauchy's dog, who went around leaving residues at every pole.

By simple poles, we mean that $F(z)$ may be written as

$$F(z) = f(z) \left[\prod_{k=1}^N (z - z_k) \right]^{-1}$$

where $f(z)$ is analytic and all of the z_k are distinct (no higher order poles). If there are higher order poles, then the residue from a pole of order N is given by

$$\text{res}_k = \frac{1}{(N-1)!} \lim_{z \rightarrow z_k} \frac{d^{N-1}}{dz^{N-1}} [(z - z_k)^N F(z)].$$

We illustrate some of the methods by evaluating a nontrivial integral by contour methods. We wish to evaluate

$$\begin{aligned} I &= \int_{-\infty}^{\infty} \frac{\cos \alpha z}{a^4 + z^4} dz = I_1 + I_2 \\ I_1 &= \frac{1}{2} \int_{-\infty}^{\infty} \frac{e^{i\alpha z}}{a^4 + z^4} dz \\ I_2 &= \frac{1}{2} \int_{-\infty}^{\infty} \frac{e^{-i\alpha z}}{a^4 + z^4} dz \end{aligned}$$

where α is real and positive. In order to use the contour method, we must close the contour, and we do this on a semicircle above or below the real axis, and let the radius of this semicircle approach infinity. We choose whether to close above or below depending upon which will give us a vanishing contribution in the limit as the radius gets large. For this case, we have broken the $\cos \alpha z$ term into two exponentials because the original expression blows up both above and below (as $z \rightarrow \pm i\infty$), while the first exponential vanishes as $z \rightarrow i\infty$ so that we may close above, and the second vanishes as $z \rightarrow -i\infty$ so we may close below. These two cases are shown in figure A.1 along with the location of the poles located at $z = x + iy = a\sqrt[4]{-1}$.

The contour of I_1 clearly encloses z_1 and z_2 , and the contour of I_2 clearly encloses z_3 and z_4 , so

$$\begin{aligned} I_1 &= \oint \frac{e^{i\alpha z} dz}{(z - z_1)(z - z_2)(z - z_3)(z - z_4)} \\ &= 2\pi i \left[\frac{e^{i\alpha z_1}}{(z_1 - z_2)(z_1 - z_3)(z_1 - z_4)} + \frac{e^{i\alpha z_2}}{(z_2 - z_1)(z_2 - z_3)(z_2 - z_4)} \right] \\ &= \frac{\pi}{\sqrt{2}a^3} e^{-\alpha a/\sqrt{2}} \left(\cos \frac{\alpha a}{\sqrt{2}} + \sin \frac{\alpha a}{\sqrt{2}} \right) \\ I_2 &= \oint \frac{e^{-i\alpha z} dz}{(z - z_1)(z - z_2)(z - z_3)(z - z_4)} \end{aligned}$$

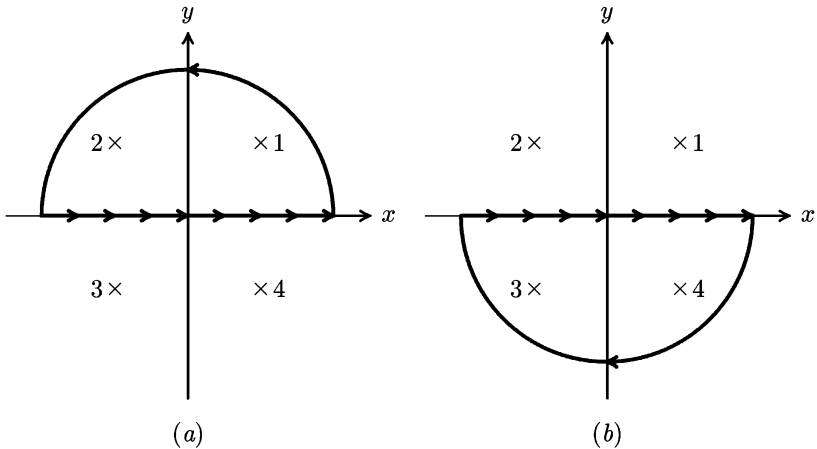


Figure A.1. (a) Contour for I_1 , closing above. (b) Contour for I_2 , closing below.

$$\begin{aligned}
 &= -2\pi i \left[\frac{e^{-i\alpha z_3}}{(z_3 - z_1)(z_3 - z_2)(z_3 - z_4)} + \frac{e^{-i\alpha z_4}}{(z_4 - z_1)(z_4 - z_2)(z_4 - z_3)} \right] \\
 &= \frac{\pi}{\sqrt{2}a^3} e^{-\alpha a/\sqrt{2}} \left(\cos \frac{\alpha a}{\sqrt{2}} + \sin \frac{\alpha a}{\sqrt{2}} \right)
 \end{aligned}$$

where for I_2 we have the negative of the sum of the residues because the contour goes clockwise (the portion of the contour between $-\infty$ and ∞ must be in the sense of the original integral in both cases). The final result is then (letting $a = \sqrt{2}b$ for convenience of expression)

$$I = \int_{-\infty}^{\infty} \frac{\cos \alpha x}{4b^4 + x^4} dx = \frac{\pi}{2b^3} e^{-\alpha b} (\cos \alpha b + \sin \alpha b).$$

A.2 Analytic continuation

In some cases, a function may be analytic in a specific domain, or contain a finite number of poles in that domain, but its properties in another domain are not initially known. For example, a function may be specified everywhere in the upper half-plane, or to the right or left of a vertical line in the complex plane, and the character of the function may be of interest in the undefined region. The specification of the properties of the function in the undefined region is called the *analytic continuation* of the function.

Suppose a function is defined, for example, by an integral over a specified contour C with the argument of the function establishing the location of a pole or poles relative to the specified contour, and the argument is defined only in a specified domain (e.g. real part positive, imaginary part greater than some

minimum value, etc). The analytic continuation would then give the recipe for establishing the value of the function as the argument leaves the specified domain. If none of the poles crosses the specified contour as the argument varies, then the analytic continuation is trivial, as the function is still analytic over that enlarged domain. If one of the poles crosses the specified contour, however, we must deform the contour so that the pole remains on the same side of the deformed contour as if the pole found the contour impenetrable and pushed the contour ahead of it. As long as the pole is not allowed to cross the contour, the integral along the deformed contour represents the analytic continuation of the integral into the originally undefined domain.

An example of analytic continuation is shown in [figure 4.3](#) on page 139 where the original contour was defined to be to the right of σ , or that $\operatorname{Re} p > \sigma$, as shown in the dashed curve. For the case shown, the analytic continuation, as the path is moved over to the left for convenience, is represented by the deformed contour which may not cross the pole in the left-hand half-plane so must double back in the neighborhood of the pole, leaving it to the left of the contour, and similarly must not cross the branch point, keeping both the branch point and branch cut to the left of the deformed contour. For this example, we effectively continued σ from positive and finite to negative and unbounded, making the evaluation of an integral over p trivial along the deformed contour, needing only to pick up contributions from circling the pole via the Cauchy integral theorem and from looping around the branch point, if any.

A.3 The method of steepest descents—saddle point method

The method of steepest descents, or the saddle point method which is the same thing, is a very powerful method for finding asymptotic expressions for integrals, and the recipe for the steepest descent contributions to an integral is relatively straightforward, but there is invariably a great deal of thought which must be given to the setting up of the problem before applying the recipe. This analysis which precedes the application of the recipe generally requires a good understanding of the physics of the problem (or it will lead to such an understanding), for each of the saddle points, if there are more than one, has an interpretation which must be understood if the proper evaluation is to take place. In this section, we shall first determine the recipe, and then do two examples to illustrate the method. The contour integrals in [chapter 6](#) will then serve as further examples which both use and describe the method.

A.3.1 Steepest descents with saddle points along the real axis

A simple but relatively general example of the method may be illustrated by the integral

$$F(t) = \int_A^B e^{th(x)} dx \quad (\text{A.3})$$

where $h(x)$ has a maximum (or several maxima) somewhere in the range $[A, B]$. In this problem, we are looking for an approximate expression for the integral in the limit where t is large, so we are looking for an asymptotic expression for $F(t)$.

We begin by expanding $h(x)$ in a series about the maximum (if there are several maxima, we treat them one at a time), such that

$$h(x) = h(x_0) + h'(x_0)(x - x_0) + \frac{h''(x_0)}{2!}(x - x_0)^2 + \frac{h'''(x_0)}{3!}(x - x_0)^3 + \dots$$

and we choose x_0 to be the maximum such that $h'(x_0) \equiv h'_0 = 0$ and $h''(x_0) \equiv h''_0 < 0$ (if $h''_0 = 0$, then require $h'''_0 = 0$ and $h^{iv}_0 < 0$). Then we have

$$\begin{aligned} F(t) &= e^{th_0} \int_A^B e^{\frac{1}{2}th''_0(x-x_0)^2} \left[1 + \frac{th'''_0}{3!}(x - x_0)^3 \right. \\ &\quad \left. + \frac{th^{iv}_0}{4!}(x - x_0)^4 + \dots \right] dx \end{aligned} \quad (\text{A.4})$$

$$\begin{aligned} &\simeq e^{th_0} \int_{-\infty}^{\infty} e^{\frac{1}{2}th''_0 u^2} \left[1 + \frac{th'''_0}{3!} u^3 + \frac{th^{iv}_0}{4!} u^4 \right. \\ &\quad \left. + \frac{1}{2!} \left(\frac{th'''_0}{3!} \right)^2 u^6 + \dots \right] du \end{aligned} \quad (\text{A.5})$$

$$\begin{aligned} &= e^{th_0} \left[\left(\frac{2\pi}{|h''_0|t} \right)^{\frac{1}{2}} + \frac{th^{iv}_0}{4!} \frac{3\sqrt{\pi}}{4} \left(\frac{2}{|h''_0|t} \right)^{5/2} \right. \\ &\quad \left. + \frac{1}{2!} \left(\frac{th'''_0}{3!} \right)^2 \frac{15\sqrt{\pi}}{8} \left(\frac{2}{|h''_0|t} \right)^{7/2} + \dots \right] \end{aligned} \quad (\text{A.6})$$

$$= \frac{\sqrt{2\pi} e^{th_0}}{[|h''_0|t]^{1/2}} \left[1 + \frac{h^{iv}_0}{8|h''_0|^2 t} + \frac{5[h'''_0]^3}{24|h''_0|^3 t} + \mathcal{O}\left(\frac{1}{t^2}\right) \right]. \quad (\text{A.7})$$

In equation (A.4) we have treated all the terms above h'' as small and expanded the exponent about the maximum. In equation (A.5), the largeness of t in the exponent guarantees that the principal contribution to the integral comes from the immediate vicinity of the maximum, since the width of the Gaussian gets narrower as t gets large, so we extend the limits of integration to infinity with little error. After performing these integrals, we collect the terms in equation (A.7), and note that all odd terms in u vanish, leaving only two terms of order $1/t$ from which we can estimate the range of validity of the approximations involved. In general, t must be large enough that the correction terms are small.

If the maximum should occur at an end point, then the extension is straightforward, since the integral would then be only semi-infinite, and we may even have $h'(0) < 0$, so the small terms are of order $t h''(0)$, etc.

The asymptotic narrowing of the Gaussian in the integral, in addition to the extension of the limits of integration to infinity, permits another variation which is frequently useful. If the original integral is, instead of equation (A.3), of the form

$$G(t) = \int_A^B g(x)e^{th(x)} dz$$

then the region near the maximum may be considered to be like a delta function, effectively evaluating $g(x)$ at that point and then moving it outside the integral, so that the result, following the same general procedures, may be expressed as

$$G(t) = \frac{\sqrt{2\pi}e^{th_0}}{[|h''_0|t]^{1/2}} \left\{ g_0 + \frac{1}{2t} \left[\frac{g''_0}{|h''_0|} + \frac{1}{|h''_0|^2} \left(\frac{h_0^{iv}g_0}{4} + h'''_0g'_0 + \frac{5(h''_0)^2g_0}{24|h''_0|} \right) \right] + \mathcal{O}\left(\frac{1}{t^2}\right) \right\}. \quad (\text{A.8})$$

Unfortunately, there is no unique way to determine which part of an integrand belongs to $g(u)$ and which part belong to $h(u)$ in the exponent, but generally any slowly varying function may be included in $g(u)$, while $h(u)$ includes as much as possible without becoming too complicated.

The gamma function demonstrates these arguments, such that

$$\Gamma(t+1) = \int_0^\infty e^{-u} u^t dt \quad t > -1 \quad (\text{A.9})$$

has an integrand which has a maximum value, but this maximum depends on t so that $u_0 = t$. We write the integrand as $e^{-u}u^t = \exp(-u + t \ln u) = \exp[th(u)]$ so $h(u) = \ln u - u/t$. Evaluating the various derivatives of $h(u)$ and evaluating them at $u = t$, equation (A.7) gives

$$\Gamma(t+1) = \sqrt{2\pi t} t^t e^{-t} \left[1 + \frac{1}{12t} + \dots \right] \quad (\text{A.10})$$

which is the Stirling formula for the large argument approximation to the gamma function.

Problem A.3.1. Modified bessel function. Show that

$$\begin{aligned} K_\nu(z) &= \int_0^\infty e^{-z \cosh t} \cosh(\nu t) dt \\ &\approx \sqrt{\frac{\pi}{2z}} e^{-z} \left[1 + \frac{4\nu^2 - 1}{8z} + \frac{(4\nu^2 - 1)(4\nu^2 - 9)}{2!(8z)^2} + \dots \right]. \end{aligned}$$

A.3.2 Saddle point method

In the complex plane, the statement of the problem is more general, such that we wish to evaluate

$$F(t) = \int_P \phi(z, t) dz \quad (\text{A.11})$$

and P represents some path from a point A to a point B in the complex plane. We solve this problem in two steps:

- (i) Find the best path between the prescribed end points. This involves scheming and conjecturing. This is the hard part.
- (ii) Execution of the integral. This is easy. Simply add the contributions from each saddle point (and perhaps from the end points).

A.3.2.1 General considerations

Suppose we only want an upper bound, which may be described by

$$|F(t)| \leq \int_P |\phi(z, t)| |dz| \leq \ell_P \max_P |\phi(z, t)|$$

where ℓ_P is the distance along the path and $\max_P |\phi(z, t)|$ is the maximum along the path. A better estimate may be found by choosing a different path with the same end points which does not leave the region of analyticity of $\phi(z, t)$. All such paths are admissible, and we label such paths C such that

$$|F(t)| \leq \ell_C \max_C |\phi(z, t)|$$

and we wish to choose C to minimize $\ell_C \max_C |\phi(z, t)|$.

Now if $\phi(z)$ behaves violently, then ℓ_C is unimportant, as the dominant contribution will come from short sections of the path. If $\phi(z)$ is *not* violent, then the saddle point method is of little use. Hence we ignore ℓ_C and look for a path C where $\max_C |\phi(z)|$ is minimal (if it exists). The strategy is to find a path from A to B along an admissible path C , the highest point of which is either an end point or a saddle point.

A.3.2.2 Steepest descent path

If the highest point is a saddle point, then we wish to cross it such as to minimize the path length. Thus we wish to use the steepest ascent and steepest descent, deforming the path as necessary to cross at the right point at the proper angle.

Suppose that in the neighborhood of the saddle point, $\psi'(\zeta) = 0$. (Analytic function theory guarantees us that $\psi' = 0$ is a saddle point if ψ is analytic.) Then

$$\psi(z) = \psi(\zeta) + \frac{1}{2}\psi''(\zeta)(z - \zeta)^2 + \dots$$

(and if $\psi''(\zeta) = 0$, go to $\psi'''(\zeta)$, etc). Then define an *axis* by a straight line through the saddle point oriented such that

$$\psi''(\zeta)(z - \zeta)^2 < 0 \text{ and real.}$$

We then let $\psi''(\zeta) = |\psi''(\zeta)|e^{i\arg\psi''}$ and define $\alpha x = (z - \zeta) = xe^{i\arg\alpha}$ where $|\alpha| = 1$. Then $\arg\psi'' + 2\arg\alpha = \pi$ guarantees the exponent will be real and negative along the path through the saddle at the angle defined by $\arg\alpha$. Solving for this crossing angle,

$$\arg\alpha = \frac{\pi}{2} - \frac{1}{2}\arg(\psi''). \quad (\text{A.12})$$

A.3.2.3 A general but simple case

We now take the case of evaluating

$$F(t) = \int_A^B g(z)e^{th(z)} dz \quad (\text{A.13})$$

where $g(z)$ and $h(z)$ are analytic in a domain that includes A and B , which are independent of t . Then we assume there exists a point ζ in the domain where $h'(\zeta) = 0$ and where $h''(\zeta) \neq 0$. In this case, ζ is a saddle point of $h(z)$, but not of $g(z)$, but this is sufficient provided $g(z)$ is slowly varying near the saddle point of $h(z)$. Then with $z = \zeta + \alpha x$ with x real,

$$F(t) = \int_A^B g(\zeta + \alpha x)e^{th(\zeta + \alpha x)} \alpha dx$$

and

$$h(\zeta + \alpha x) = h(\zeta) + \frac{1}{2}h''(\zeta)\alpha^2 x^2 + \dots$$

so

$$\begin{aligned} F(t) &= \alpha e^{th_0} g_0 \int_A^B e^{-t|h_0''|x^2/2} dx + \mathcal{O}(1/t) \\ &= \frac{\sqrt{2\pi}\alpha}{[t|h_0''|]^{1/2}} e^{th_0} [g_0 + f_1/t + \mathcal{O}(1/t^2)] \quad \text{as } t \rightarrow \infty \end{aligned} \quad (\text{A.14})$$

provided $g(\zeta) \equiv g_0 \neq 0$ where $h^{(n)}(\zeta) \equiv h_0^{(n)}$ and where

$$f_1 = \frac{\alpha^2 g_0''}{2|h_0''|} + \frac{\alpha^4}{|h_0''|^2} \left[\frac{g_0}{8} \left(h_0^{iv} + \frac{5\alpha^2(h_0''')^2}{3|h_0''|} \right) + \frac{g_0'h_0'''}{2} \right].$$

We note that $\alpha = \exp[i(\frac{\pi}{2} - \frac{1}{2}\arg h_0'')] = \exp[i(\frac{\pi}{2} - \arg h_0'')] = \exp[-i\arg h_0'']$ and that $th_0''\alpha^2 = -|th_0''|$.

A.3.3 Spatial Landau damping example

In addition to the temporal Landau damping found in [chapter 4](#), Landau showed that for spatial decay there is an additional term [33], whose inverse Laplace transform leads to an integral of the form

$$F(x) = \int_0^\infty g(k) e^{ikx - \omega^2/k^2 v^2} dk \quad (\text{Im}(x) > 0).$$

The positive imaginary part of x guarantees a maximum along the real axis, but the saddle point is displaced from the axis. Assuming $g(k)$ is slowly varying, we find from the exponent that $ikx - \omega^2/k^2 v^2 \equiv xh(k)$ gives

$$h(k) = ik - \frac{\omega^2}{k^2 v^2 x} \quad (\text{A.15})$$

$$h'(k) = i + \frac{2\omega^2}{k^3 v^2 x} \quad (\text{A.16})$$

$$h''(k) = -\frac{6\omega^2}{k^4 v^2 x}. \quad (\text{A.17})$$

We find then from equations (A.16) and (A.12) that the saddle points and crossing angles are located at $k_s = k_0 e^{i\phi}$ where

$$k_0 = \left(\frac{2\omega^2}{v^2 x} \right)^{1/3}$$

$$\phi = \frac{\pi}{6}, \frac{5\pi}{6}, -\frac{\pi}{2}$$

$$\alpha = \frac{\pi}{3}, \frac{2\pi}{3}, 0.$$

It is easy at this step to insert these pieces into equation (A.14) to obtain a result, but we have three different saddle points to choose from. Choosing the right saddle point(s) and the right sign is usually the hard part. For this example, it is relatively easy since only one saddle point is in the right half of the k -plane, as shown in [figure A.2](#) and the path should quite obviously be deformed to cross over this saddle point as in the figure, and the crossing is in the positive sense, so the result is

$$F(x) = \frac{2\sqrt{\pi}g(k_0)}{\sqrt{3}x^{2/3}} \left(\frac{\omega}{2v} \right)^{1/3} \exp \left[-\frac{3}{2} \left(\frac{\omega x}{2v} \right)^{2/3} (1 - i\sqrt{3}) + \frac{i\pi}{6} \right]. \quad (\text{A.18})$$

There is no contribution from the end points, so for large x , the spatial damping is exponential, but the exponential factor is not linear in x as one might expect from the time decay problem, but varies as $x^{2/3}$.

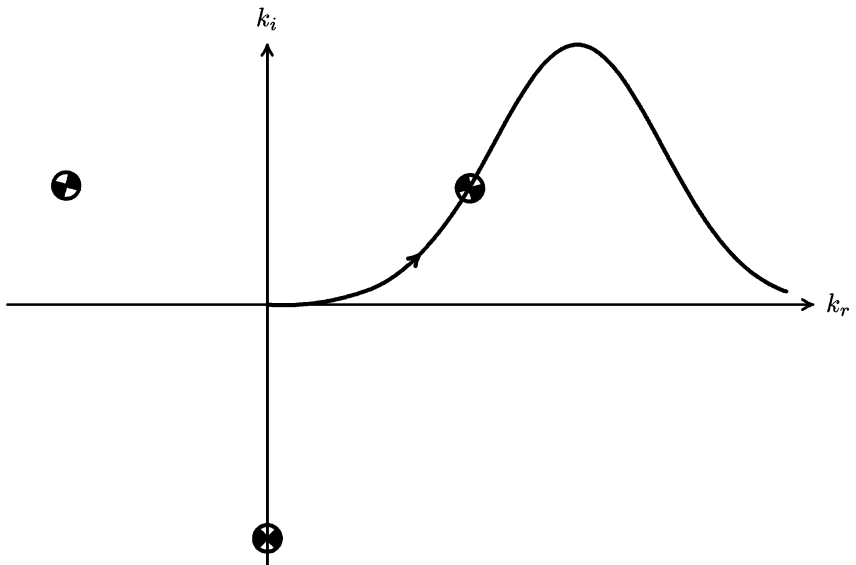


Figure A.2. Deformed contour for spatial Landau damping.

Problem A.3.2. Spatial Landau damping integral.

- (i) Fill in the steps leading to equation (A.18).
- (ii) Assuming $g(k)$ is a constant, calculate f_1 and from that estimate the minimum value of $|x|$ for which the asymptotic expression is useful, i.e. where $f_1(x)/x < g_0/3$.

When there are many saddle points, and especially when there are branch points and their associated branch cuts, the proper contour is the hardest part of the problem, as it requires the determination of the proper contour which connects the given end points without crossing any branch cuts. Occasionally, as in the contours of [chapter 6](#), the physical interpretation of each saddle point must be determined before the proper contour can be established, and although the end point is given, it may have to be approached at a specified angle so that one stays on a path which has no contribution *except* at the saddle points. Finally, if the function should be so perverse near its saddle point that it does not steepen and narrow even as the asymptotic parameter gets large, as in the case of the f_{\pm} saddle points in [figure 6.8](#) on page 275, then the steepest descents methods are not useful for the magnitude and phase of the contribution, but may still be useful in identifying the proper contour.

Appendix B

Special functions in plasma physics

B.1 Plasma dispersion function, $Z(\zeta)$

The plasma dispersion function is a commonly occurring function in thermal plasmas and is related to the error function for complex arguments and some other representations which occur commonly in the literature. Tabulated by Fried and Conte [31], we list here its properties and show its relationships to other common functions.

B.1.1 Properties of the plasma dispersion function

Definition of the plasma dispersion function:

$$Z(\zeta) \equiv \frac{1}{\sqrt{\pi}} \int_{-\infty}^{\infty} \frac{e^{-\xi^2} d\xi}{\xi - \zeta} \quad \text{Im}(\zeta) > 0. \quad (\text{B.1})$$

Differential equation:

$$Z'(\zeta) = -2[1 + \zeta Z(\zeta)]. \quad (\text{B.2})$$

Power series:

$$\begin{aligned} Z(\zeta) &= i\sqrt{\pi} \sum_{n=0}^{\infty} \frac{(i\zeta)^n}{\Gamma\left(\frac{n}{2} + 1\right)} = i\sqrt{\pi} e^{-\zeta^2} \\ &\quad - 2\zeta \left[1 - \frac{2}{3}\zeta^2 + \frac{4}{15}\zeta^4 \cdots \frac{(-2)^n \zeta^{2n}}{(2n+1)(2n-1)\cdots 3 \cdot 1} \right]. \end{aligned} \quad (\text{B.3})$$

Continued fraction expansion:

$$Z(\zeta) = \cfrac{\zeta}{\frac{1}{2} + \zeta^2 - \cfrac{\frac{1}{2}}{\frac{5}{2} + \zeta^2 - \cfrac{\frac{9}{2}}{\frac{13}{2} + \zeta^2 - \cdots}}}. \quad (\text{B.4})$$

This expression converges poorly as ζ approaches the real axis, but is very good for $\text{Im}(\zeta) \geq 1$.

Asymptotic series:

$$Z(\zeta) = -\frac{1}{\zeta} \sum_{n=0}^N \frac{(2n-1)!!}{(2\zeta^2)^n} + i\sigma\sqrt{\pi}e^{-\zeta^2} \quad (\text{B.5})$$

$$= -\frac{1}{\zeta} \left(1 + \frac{1}{2\zeta^2} + \frac{3}{4\zeta^4} + \dots \right) + i\sigma\sqrt{\pi}e^{-\zeta^2} \quad (\text{B.6})$$

where $(-1)!! = 1$, N indicates the series truncates when successive terms no longer decrease in magnitude, and

$$\sigma = \begin{cases} 0 & \text{Im}(\zeta) > 0 \\ 1 & \text{Im}(\zeta) = 0 \\ 2 & \text{Im}(\zeta) < 0. \end{cases}$$

The discontinuity due to the Stokes' phenomenon in the asymptotic series indicates an uncertainty of the same magnitude as the discontinuity in the asymptotic series expansion, since the smallest term is of the same order of magnitude as the pole term. For the asymptotic expansion, the imaginary part of $Z(\zeta)$ is exact only for real ζ .

Symmetry relations:

$$\begin{aligned} Z(-\zeta) &= 2i\sqrt{\pi}e^{-\zeta^2} - Z(\zeta) \\ Z(\zeta^*) &= [Z(\zeta) - 2i\sqrt{\pi}e^{-\zeta^2}]^* \\ \tilde{Z}(\zeta) &= Z(\zeta) - 2i\sqrt{\pi}e^{-\zeta^2} \quad \text{for } \text{Im}(\zeta) < 0. \end{aligned} \quad (\text{B.7})$$

Zeros of $Z(\zeta)$: An infinite number of zeros are located close to the negative 45° lines as illustrated in [figure B.1](#) where the first three zeros are shown. The first five zeros are located at

$$\zeta_1 = \pm 1.991\,466\,835 - 1.354\,810\,123i \quad (\text{B.8})$$

$$\zeta_2 = \pm 2.691\,149\,024 - 2.177\,044\,906i \quad (\text{B.9})$$

$$\zeta_3 = \pm 3.235\,330\,868 - 2.784\,387\,613i \quad (\text{B.10})$$

$$\zeta_4 = \pm 3.697\,309\,702 - 3.287\,410\,789i \quad (\text{B.11})$$

$$\zeta_5 = \pm 4.106\,107\,271 - 3.725\,948\,729i. \quad (\text{B.12})$$

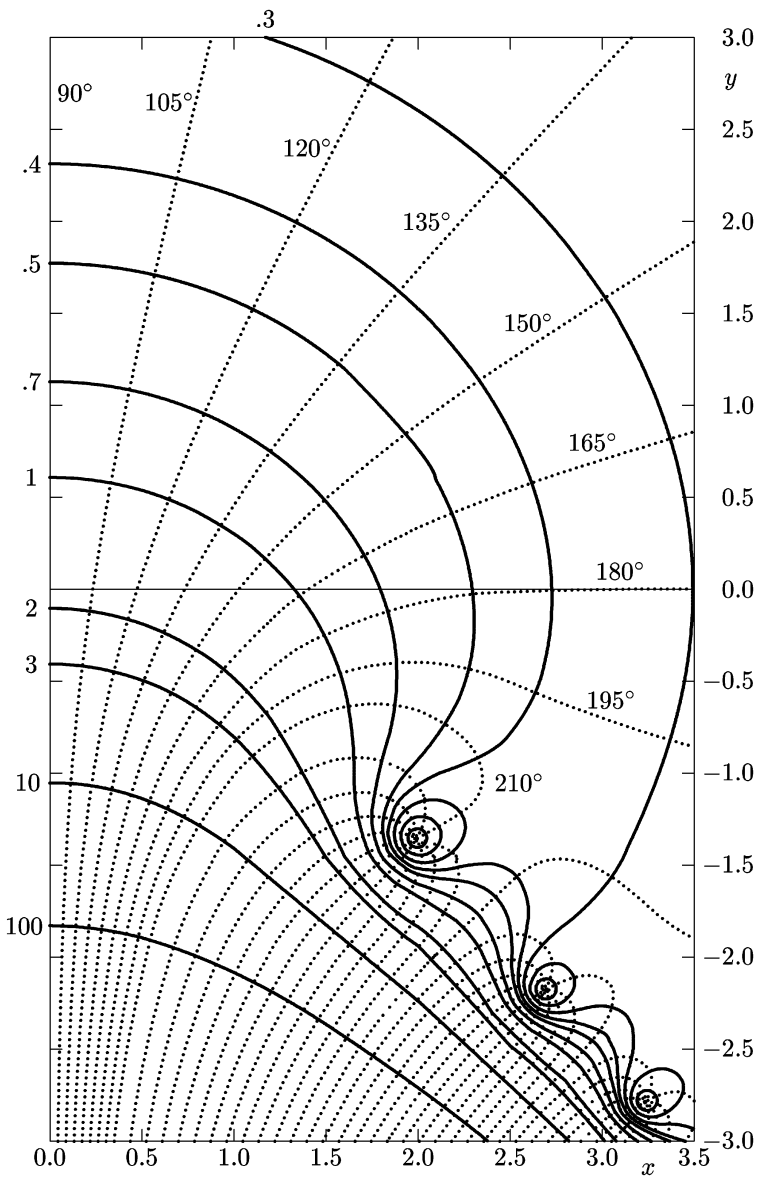


Figure B.1. Contours for $|Z(x + iy)| = 0.1, 0.2, 0.3, 0.4, 0.5, 0.7, 1, 2, 3, 10, 100$ for $x \geq 0$. The altitude contours are symmetric for $x < 0$ but the phase is not, tending toward 0° on the negative x -axis. The phase (\dots) is shown every 15° except in the vicinity of the zeros where the interval is 30° .

B.1.2 Generalized dispersion functions and the Gordeyev integrals

The generalized Gordeyev integrals may be defined by

$$I_n(\zeta) = -i \int_0^\infty \tau^n e^{i\zeta\tau - \tau^2/4} d\tau \quad (\text{B.13})$$

where $I_0(\zeta)$ is Gordeyev's integral. This integral is related to the generalized dispersion functions, defined by

$$Z_n(\zeta) = \frac{1}{\sqrt{\pi}} \mathcal{P} \int_C \frac{z^n e^{-z^2}}{z - \zeta} dz + i\sqrt{\pi} \frac{k_z}{|k_z|} \zeta^n e^{-\zeta^2} \quad (\text{B.14})$$

(where C is the integration path that goes through the singularity) through the relations $I_0(\zeta) = -Z_0(\zeta) = -Z(\zeta)$. The integrals of various orders are related by

$$I_n(\zeta) = (-i)^n \frac{d^n I_0(\zeta)}{d\zeta^n} \quad (\text{B.15})$$

and the $Z_n(\zeta)$ are related by

$$\frac{dZ_n(\zeta)}{d\zeta} = -2Z_{n+1}(\zeta) + nZ_{n-1}(\zeta). \quad (\text{B.16})$$

The $Z_n(\zeta)$ also have a recursion formula given by

$$Z_{n+1}(\zeta) = \zeta Z_n(\zeta) + \frac{(n-1)!!}{2^{n/2}} \varepsilon_n \quad (\text{B.17})$$

where $\varepsilon_n = 1$ for even n and $\varepsilon_n = 0$ for odd n . Several relations to the plasma dispersion function are

$$Z_0(\zeta) = Z(\zeta) \quad (\text{B.18})$$

$$Z_1(\zeta) = -\frac{1}{2} Z'(\zeta) \quad (\text{B.19})$$

$$Z_2(\zeta) = -\frac{\zeta}{2} Z'(\zeta) \quad (\text{B.20})$$

$$1 - 2Z_3(\zeta) = \zeta^2 Z'(\zeta) \quad (\text{B.21})$$

$$\frac{2Z_3(\zeta)}{Z_1(\zeta)} = 2\zeta^2 - \frac{2}{Z'(\zeta)}. \quad (\text{B.22})$$

B.1.2.1 Asymptotic series

The asymptotic expression for odd n is

$$Z_{2n-1}(\zeta) = -\sum_{j=0}^N \frac{(2(n+j)-1)!!}{2^{n+j} \zeta^{2(j+1)}} + i\sigma \sqrt{\pi} \frac{k_z}{|k_z|} \zeta^{2n-1} e^{-\zeta^2} \quad (\text{B.23})$$

where $N(\zeta)$ truncates the series when the terms no longer decrease in magnitude. The series with even n follows from equation (B.17) where $Z_{2n}(\zeta) = \zeta Z_{2n-1}(\zeta)$ for $n > 0$ while for $n = 0$, one uses equation (B.5).

B.1.2.2 Power series

For small arguments, one begins with equation (B.3) for $Z_0(\zeta) = Z(\zeta)$ as the starting point, and then equation (B.17) is used for higher n . Because the combination $2Z_3/Z_1$ appears together on some occasions, its series varies as

$$\frac{2Z_3(\zeta)}{Z_1(\zeta)} = 1 - i\sqrt{\pi}\zeta + (4 - \pi)\zeta^2 + i(\pi - 3)\sqrt{\pi}\zeta^3 + \mathcal{O}(\zeta^4). \quad (\text{B.24})$$

B.1.3 Relation to the error function for complex argument

We begin the analysis by examining the commonly occurring integral

$$I = \int_{-\infty}^{\infty} \frac{f_0(v) dv}{p + ikv} \quad \text{Re}(p) > 0 \quad (\text{B.25})$$

where the distribution function is a Maxwellian described by

$$f_0(v) = \frac{n_0}{\sqrt{\pi}v_0} \exp\left(-\frac{v^2}{v_0^2}\right)$$

and $v_0 = \sqrt{2kT/m}$. If we write

$$\frac{1}{p + ikv} = \int_0^{\infty} e^{(p+ikv)t} dt$$

then the original integral becomes

$$I = \frac{n_0}{\sqrt{\pi}v_0} \int_0^{\infty} dt e^{-pt} \int_{-\infty}^{\infty} dv e^{-v^2/v_0^2 - p + ikvt}.$$

Completing the square in the velocity integral, we obtain

$$\begin{aligned} I &= \frac{n_0}{\sqrt{\pi}v_0} \int_0^{\infty} dt e^{-pt - kv_0^2 t^2/4} \int_{-\infty}^{\infty} dv \exp\left[-\frac{1}{v_0^2} \left(v + \frac{ikv_0^2 t}{2}\right)^2\right] \\ &= n_0 \int_0^{\infty} dt e^{-pt - kv_0^2 t^2/4}. \end{aligned}$$

Completing the square again with $p = -ikv_0x$ so that $\text{Im}(x) > 0$, then

$$I = n_0 e^{-x^2} \int_0^{\infty} e^{(kv_0t/2 - ix)^2} dt.$$

Then let $kv_0t/2 - ix = u$ so that

$$I = \frac{2n_0}{kv_0} e^{-x^2} \int_{-ix}^{\infty} e^{-u^2} du = \frac{2n_0}{kv_0} e^{-x^2} \left(\int_{-ix}^0 e^{-u^2} du + \frac{\sqrt{\pi}}{2} \right)$$

and with the final variable change, we let $iu = \tau$ so that equation (B.25) may be written as

$$I = \frac{n_0\sqrt{\pi}}{kv_0} e^{-x^2} \left(1 + \frac{2i}{\sqrt{\pi}} \int_0^x e^{\tau^2} d\tau \right) \quad (\text{B.26})$$

and $x = ip/kv_0$ or $x = \omega/kv_0$ if $p = -i\omega$ so that $\text{Im}(\omega) > 0$. Equation (B.26) is in the form of the error function for a complex argument [71] such that

$$I = \frac{n_0\sqrt{\pi}}{kv_0} w(x)$$

and $w(x)$ is the tabulated function. Comparing this with the plasma dispersion function in chapter 4, we see that

$$Z(x) = i\sqrt{\pi}w(x) = i\sqrt{\pi}e^{-x^2}\text{Erfc}(-ix). \quad (\text{B.27})$$

B.1.4 Relation to the Y function

In Russian literature, the complex error function is tabulated as the Y function where

$$Y(z) \equiv i\sqrt{\pi}ze^{-z^2} \left(1 + \frac{2i}{\sqrt{\pi}} \int_0^z e^{t^2} dt \right) \quad (\text{B.28})$$

so that

$$\begin{aligned} Y &= i\sqrt{\pi}zw(z) \\ &= zZ(z). \end{aligned} \quad (\text{B.29})$$

Because the plasma dispersion function satisfies the differential equation

$$Z'(\zeta) = -2[1 + \zeta Z(\zeta)]$$

both the plasma dispersion function and its derivative may be simply expressed by means of the Y function as

$$Z(\zeta) = Y(\zeta)/\zeta \quad (\text{B.30})$$

$$Z'(\zeta) = -2[1 + Y(\zeta)]. \quad (\text{B.31})$$

B.1.5 Relation to the W function

Another equivalent function, similar to the Y function is the W function, which is defined by [118]

$$W(y) = \frac{1}{\sqrt{2\pi}} \int_{-\infty}^{\infty} \frac{x e^{-x^2/2}}{x - y} dx \quad \text{Im}(y) > 0. \quad (\text{B.32})$$

If we let $x = \sqrt{2}\xi$, this becomes

$$W(y) = \frac{1}{\sqrt{\pi}} \int_{-\infty}^{\infty} \frac{\xi e^{-\xi^2}}{\xi - y/\sqrt{2}} d\xi \quad (\text{B.33})$$

so it is related to the Z function either by

$$W(y) = 1 + \frac{y}{\sqrt{2}} Z\left(\frac{y}{\sqrt{2}}\right) = -\frac{1}{2} Z'\left(\frac{y}{\sqrt{2}}\right) \quad (\text{B.34})$$

or letting $y = \sqrt{2}\zeta$, by

$$W(\sqrt{2}\zeta) = 1 + \zeta Z(\zeta) = -\frac{1}{2} Z'(\zeta). \quad (\text{B.35})$$

The W function satisfies the differential equation

$$\frac{dW}{dy} = \frac{W - 1}{y} - y W. \quad (\text{B.36})$$

B.2 Weakly relativistic plasma dispersion function, $F_q(z)$

The weakly relativistic dispersion function (sometimes called the Dnestrovskii function) is defined by

$$F_q(z) \equiv -i \int_0^\infty \frac{e^{izt}}{(1-it)^q} dt. \quad (\text{B.37})$$

B.2.1 Relation to other functions

The properties of this function were described by Dnestrovskii *et al* [50], and its relation to other functions was noted by Lazzaro *et al* [119]. It is equivalent to the confluent hypergeometric function of the second kind by

$$F_q(z) = \psi(1, 2 - q, z) = z^{q-1} \psi(q, q, z) \quad (\text{B.38})$$

and this allows us to identify it with the error function so that for $q = \frac{1}{2}$,

$$F_{\frac{1}{2}}(x) = \sqrt{\pi/x} e^x [1 - \operatorname{erf}(\sqrt{x})] \quad (\text{B.39})$$

which establishes the connection noted by Shkarofsky [51] between $F_q(z)$ and the plasma dispersion function.

$$i F_{\frac{1}{2}}(z) = \int_0^\infty \frac{e^{izt}}{(1-it)^{1/2}} dt = \frac{1}{\sqrt{z}} Z(i\sqrt{z}). \quad (\text{B.40})$$

Integrating F_q by parts for $q > \frac{1}{2}$, we find

$$F_q = \sum_{p=0}^{q-3/2} (-z)^p \frac{\Gamma(q-p-1)}{\Gamma(q)} + \frac{\sqrt{\pi}}{\Gamma(q)} (-z)^{q-3/2} [i\sqrt{z} Z(i\sqrt{z})]. \quad (\text{B.41})$$

B.2.2 Properties of $F_q(z)$

A useful recursion relation for finding the properties of the higher order functions is

$$(q - 1)F_q(z) = 1 - zF_{q-1} \quad (\text{B.42})$$

so the first few of the functions are

$$F_{\frac{1}{2}} = \begin{cases} \frac{Z(i\sqrt{z})}{i\sqrt{z}} & z > 0 \\ \frac{Z^*(\sqrt{-z})}{\sqrt{-z}} & z < 0 \end{cases} \quad (\text{B.43})$$

$$F_{\frac{3}{2}} = -\tilde{Z}'(i\sqrt{z}) \quad (\text{B.44})$$

$$F_{\frac{5}{2}} = \frac{2}{3}[1 - zZ'(i\sqrt{z})]. \quad (\text{B.45})$$

For a large argument, the weakly relativistic dispersion function with half-integer order varies as

$$F_q(z) \simeq \frac{1}{z} \sum_{n=0}^N \frac{(-1)^N \Gamma(n+q)}{\Gamma(q) z^n} \quad N + q \leq |z| \quad (\text{B.46})$$

$$\simeq \frac{1}{z} \left(1 - \frac{q}{z} + \frac{q(q+1)}{z^2} - \dots \right). \quad (\text{B.47})$$

It is thus real for real argument.

For small arguments, we first note that for $F_{\frac{1}{2}}$, the function is real for positive real argument, since $Z(\zeta)$ is pure imaginary for pure imaginary $\zeta = i\sqrt{z}$. For $z < 0$, however, $i\sqrt{z}$ is real, and $Z(\zeta)$ is complex for real argument. Then using equation (B.41) for $q \geq \frac{3}{2}$, we may approximate

$$F_q(z) \simeq \frac{1}{q-1} - \frac{i\pi(-z)^{q-1} e^z}{\Gamma(q)} \quad (\text{B.48})$$

where the imaginary part is exact for $z < 0$ from equation (B.41).

B.3 Generalized relativistic plasma dispersion function, $\mathcal{F}_q(z, a)$

The weakly relativistic dispersion function $F_q(z)$ is for perpendicular propagation only, while the generalized function $\mathcal{F}_q(z, a)$ includes the effects of a parallel component through the parameter $a = \frac{1}{2}\mu n_{||}^2$, and $z_n = \mu(1 + n\omega_c/\omega)$ where $\mu = \kappa T_e/m_e c^2$.

B.3.1 Properties of $\mathcal{F}_q(z, a)$

Definition:

$$\mathcal{F}_q(z, a) \equiv -i \int_0^\infty \frac{\exp[izt - at^2/(1 - it)] dt}{(1 - it)^q}. \quad (\text{B.49})$$

Limiting form:

$$\lim_{a \rightarrow \infty} \mathcal{F}_q(z_n, a) = -Z(\zeta_n)/n_\parallel \beta. \quad (\text{B.50})$$

Recursion formula:

$$a\mathcal{F}_{q+2}(z, a) = 1 + (a - z)\mathcal{F}_q(z, a) - q\mathcal{F}_{q+1}(z, a). \quad (\text{B.51})$$

Differential equations:

$$\begin{aligned} \frac{\partial \mathcal{F}_q(z, a)}{\partial z} &= \mathcal{F}_q(z, a) - \mathcal{F}_{q-1}(z, a) \\ \frac{\partial \mathcal{F}_q(z, a)}{\partial a} &= \mathcal{F}_{q-1}(z, a) - 2\mathcal{F}_q(z, a) + \mathcal{F}_{q+1}(z, a). \end{aligned}$$

Asymptotic form:

$$\begin{aligned} \mathcal{F}_q(z, a) &= \frac{1}{z} \left[1 - \frac{q}{z} + \frac{q(q+1)+2a}{z^2} - \frac{q(q+1)(q+2)+6(q+1)a}{z^3} + \dots \right] \\ &= \frac{1}{z} \left[1 - \frac{A_1}{z} + \frac{A_2}{z^2} - \frac{A_3}{z^3} + \frac{A_4}{z^4} - \dots \right] \end{aligned} \quad (\text{B.52})$$

where $A_0 = 1$, $A_1(q) = q$, and the higher A_n are found from the recursion relation:

$$A_{n+1}(q) = qA_n(q+1) + a[A_n(q+2) - A_n(q)].$$

B.3.2 Relation to $Z(\xi)$

$$\mathcal{F}_{\frac{1}{2}}(z, a) = \begin{cases} \frac{1}{2i\sqrt{z-a}} [Z(\sqrt{a} + i\sqrt{z-a}) - Z^*(\sqrt{a} + i\sqrt{z-a})] & z > a \\ -\frac{1}{2\sqrt{a-z}} [Z(\sqrt{a} - \sqrt{a-z}) + Z(-\sqrt{a} - \sqrt{a-z})] & z < a \end{cases} \quad (\text{B.53})$$

$$\mathcal{F}_{\frac{3}{2}}(z, a) = \begin{cases} -\frac{1}{2\sqrt{a}} [Z(\sqrt{a} + i\sqrt{z-a}) + Z^*(\sqrt{a} + i\sqrt{z-a})] & z > a \\ -\frac{1}{2\sqrt{a}} [Z(\sqrt{a} - \sqrt{a-z}) - Z(-\sqrt{a} - \sqrt{a-z})] & z < a. \end{cases} \quad (\text{B.54})$$

B.4 Gamma function, $\Gamma(z)$

Definition: The gamma function, which for integer values is related to the factorial function, is defined by the integral

$$\Gamma(z) = \int_0^\infty t^{z-1} e^{-t} dt \quad \operatorname{Re} z > 0. \quad (\text{B.55})$$

Useful relations: Integrating by parts, it is easy to establish the recursion formula

$$\Gamma(z+1) = z\Gamma(z) \quad (\text{B.56})$$

which for integer values becomes

$$\Gamma(n+1) = n! \quad (\text{B.57})$$

since $\Gamma(1) = 1$. Some useful special values and relations are

$$\Gamma\left(\frac{1}{2}\right) = \sqrt{\pi} \quad \Gamma(1+iy)\Gamma(1-iy) = \frac{\pi y}{\sinh \pi y}.$$

Asymptotic expressions: For large arguments, Stirling's formula gives

$$\Gamma(z) = \sqrt{2\pi} z^{z-\frac{1}{2}} \exp\left(-z + \frac{1}{12z} - \frac{1}{360z^3} + \dots\right). \quad (\text{B.58})$$

For large half-integer values, it is convenient to use the alternate formula

$$\Gamma\left(z + \frac{1}{2}\right) = \sqrt{2\pi} z^z \exp\left(-z - \frac{1}{24z} + \frac{7}{2880z^3} - \dots\right). \quad (\text{B.59})$$

Hankel's contour integral:

$$\frac{1}{\Gamma(z)} = \frac{i}{2\pi} \int_C (-t)^{-z} e^{-t} dt \quad (|z| < \infty). \quad (\text{B.60})$$

The path of integration C starts at $+\infty$ on the real axis, circles the origin in the counterclockwise direction and returns to the starting point.

Incomplete gamma functions $\gamma(a, x)$ and $\Gamma(a, x)$: The incomplete gamma functions are defined by

$$\gamma(a, x) = \int_0^1 e^{-tx} x^{a-1} dx \quad \operatorname{Re}(a) > 0 \quad (\text{B.61})$$

$$\Gamma(a, x) = \Gamma(a) - \gamma(a, x) = \int_x^\infty e^{-tx} x^{a-1} dx. \quad (\text{B.62})$$

The recursion formula is

$$\gamma(a+1, x) = a\gamma(a, x) - x^a e^{-x}. \quad (\text{B.63})$$

The continued fraction expansion for $\Gamma(a, x)$ is

$$\Gamma(a, x) = e^{-x} x^a \left(\frac{1}{x+} \frac{1-a}{1+} \frac{1}{x+} \frac{2-a}{1+} \frac{2}{x+} \right) \quad x > 0. \quad (\text{B.64})$$

The error with this continued fraction does not decrease monotonically until a large number of terms is used, so it must be used with care. Also its accuracy is sensitive to relatively small changes in a . For large $|x|$, the asymptotic expression is

$$\Gamma(a, z) \sim e^{-z} z^{a-1} \left[1 + \frac{a-1}{z} + \frac{(a-1)(a-2)}{z^2} + \dots \right] \quad |\arg| < \frac{3\pi}{2}. \quad (\text{B.65})$$

B.5 Generalized hypergeometric functions

The generalized hypergeometric functions used in [chapter 4](#) are defined by the power series

$${}_1F_2(a; b_1, b_2; x) = \frac{\Gamma(b_1)\Gamma(b_2)}{\Gamma(a)} \sum_{k=0}^{\infty} \frac{\Gamma(a+k)}{\Gamma(b_1+k)\Gamma(b_2+k)} \frac{x^k}{k!} \quad (\text{B.66})$$

$$\begin{aligned} {}_2F_3(a_1, a_2; b_1, b_2, b_3; x) &= \frac{\Gamma(b_1)\Gamma(b_2)\Gamma(b_3)}{\Gamma(a_1)\Gamma(a_2)} \\ &\times \sum_{k=0}^{\infty} \frac{\Gamma(a_1+k)\Gamma(a_2+k)}{\Gamma(b_1+k)\Gamma(b_2+k)\Gamma(b_3+k)} \frac{x^k}{k!}. \end{aligned} \quad (\text{B.67})$$

B.5.1 Integrals leading to hypergeometric functions of the first type

Integrals over the angle that lead to the hypergeometric functions of the first type, ${}_1F_2(a_1; b_1, b_2, x)$, are:

$$\begin{aligned} &\int_0^\pi \sin \theta [J_n(b \sin \theta)]^2 d\theta \\ &= \frac{2b^{2n} {}_1F_2(n + \frac{1}{2}; n + \frac{3}{2}, 2n + 1; -b^2)}{(2n + 1)!} \end{aligned} \quad (\text{B.68})$$

$$\begin{aligned}
& \int_0^\pi \sin^2 \theta J_n(b \sin \theta) J'_n(b \sin \theta) d\theta \\
&= \frac{b^{2n-1} {}_1F_2(n + \frac{1}{2}; n + \frac{3}{2}, 2n; -b^2)}{(2n+1)(2n-1)!} \\
&\quad - \frac{b^{2n+1} {}_1F_2(n + \frac{3}{2}; n + \frac{5}{2}, 2n+2; -b^2)}{(2n+3)(2n+1)!}
\end{aligned} \tag{B.69}$$

$$\begin{aligned}
& \int_0^\pi \sin^2 \theta J_n(b \sin \theta) J_{n-1}(b \sin \theta) d\theta \\
&= \frac{2b^{2n-1} {}_1F_2(n + \frac{1}{2}; n + \frac{3}{2}, 2n; -b^2)}{(2n+1)(2n-1)!}
\end{aligned} \tag{B.70}$$

$$\begin{aligned}
& \int_0^\pi \sin^3 \theta [J_{n-1}(b \sin \theta)]^2 d\theta \\
&= \frac{4nb^{2n-2} {}_1F_2(n - \frac{1}{2}; n + \frac{3}{2}, 2n-1; -b^2)}{(2n+1)(2n-1)!} \\
&\quad - \frac{4b^{2n} {}_1F_2(n + \frac{1}{2}; n + \frac{5}{2}, 2n; -b^2)}{(2n+3)(2n+1)(2n-1)!}
\end{aligned} \tag{B.71}$$

$$\begin{aligned}
& \int_0^\pi \sin \theta \cos^2 \theta [J_n(b \sin \theta)]^2 d\theta \\
&= \frac{2b^{2n} {}_1F_2(n + \frac{1}{2}; n + \frac{5}{2}, 2n+1; -b^2)}{(2n+3)(2n+1)!}.
\end{aligned} \tag{B.72}$$

B.5.2 Integrals leading to hypergeometric functions of the second type

Integrals over the angle that lead to the hypergeometric functions of the second type, ${}_2F_3(a_1, a_2; b_1, b_2, b_3, x)$, are:

$$\begin{aligned}
& \int_0^\pi \sin \theta J_a(b \sin \theta) J_{-a}(b \sin \theta) d\theta \\
&= \frac{2 \sin \pi a}{\pi a} {}_2F_3\left(\frac{1}{2}, 1; \frac{3}{2}, 1-a, 1+a; -b^2\right)
\end{aligned} \tag{B.73}$$

$$\begin{aligned}
& \int_0^\pi \sin^2 \theta J_a(b \sin \theta) J'_{-a}(b \sin \theta) d\theta \\
&= \frac{b \sin \pi a}{3\pi a(a-1)} {}_2F_3\left(\frac{3}{2}, 1; \frac{5}{2}, 2-a, 1+a; -b^2\right) \\
&\quad - \frac{\sin \pi a}{\pi b} {}_2F_3\left(\frac{1}{2}, 1; \frac{3}{2}, -a, 1+a; -b^2\right)
\end{aligned} \tag{B.74}$$

$$\begin{aligned} & \int_0^\pi \sin^2 \theta J_a(b \sin \theta) J_{1-a}(b \sin \theta) d\theta \\ &= -\frac{2b \sin \pi a}{3\pi a(a-1)} {}_2F_3\left(\frac{3}{2}, 1; \frac{5}{2}, 2-a, 1+a; -b^2\right) \end{aligned} \quad (\text{B.75})$$

$$\begin{aligned} & \int_0^\pi \sin^2 \theta J_{a-1}(b \sin \theta) J_{-a}(b \sin \theta) d\theta \\ &= \frac{2 \sin \pi a}{\pi b} {}_2F_3\left(\frac{1}{2}, 1; \frac{3}{2}, 1-a, a; -b^2\right) \end{aligned} \quad (\text{B.76})$$

$$\begin{aligned} & \int_0^\pi \sin^3 \theta J_{a-1}(b \sin \theta) J_{1-a}(b \sin \theta) d\theta \\ &= -\frac{4 \sin \pi a}{3\pi(a-1)} {}_2F_3\left(\frac{1}{2}, 2; \frac{5}{2}, 2-a, a; -b^2\right) \end{aligned} \quad (\text{B.77})$$

$$\begin{aligned} & \int_0^\pi \sin \theta \cos^2 \theta J_a(b \sin \theta) J_{-a}(b \sin \theta) d\theta \\ &= \frac{2 \sin \pi a}{3a\pi} {}_2F_3\left(\frac{1}{2}, 1; \frac{5}{2}, 1-a, 1+a; -b^2\right). \end{aligned} \quad (\text{B.78})$$

Appendix C

The amplitude equations of geometric optics

In this appendix, we take an alternate approach to the equations of geometric optics in a slowly varying medium, and derive a specific set of amplitude equations which are ultimately equivalent to those in section 6 but more symmetric formally. The analysis here uses some of the formalism of Bernstein [90], but follows more closely the development of Bravo-Ortega [120].

C.1 The current density

We begin with the general expression for a nonlocal current density, where a disturbance at \mathbf{r}'', t'' induces a current at \mathbf{r}, t through the nonlocal conductivity such that

$$\mathbf{J}(\mathbf{r}, t) = \int d^3 r'' \int_{-\infty}^t dt'' \hat{\sigma}[\mathbf{r} - \mathbf{r}'', t - t''; \frac{1}{2}(\mathbf{r} + \mathbf{r}''), \frac{1}{2}(t + t'')] \cdot \mathbf{E}(\mathbf{r}'', t'') \quad (\text{C.1})$$

where in this appendix, we use the hat to denote a tensor. We note that in a homogeneous plasma, the difference terms remain, but the mean location and time terms disappear so that we expect relatively rapid variation from the difference terms and relatively slow variation from the mean terms. As in section 6.5, we represent the wave electric field as

$$\mathbf{E}(\mathbf{r}, t) = \mathbf{a}(\mathbf{r}, t) e^{i\psi(\mathbf{r}, t)} \quad (\text{C.2})$$

where $\psi(\mathbf{r}, t)$ is called the eikonal from which we define

$$\mathbf{k}(\mathbf{r}, t) \equiv \nabla \psi(\mathbf{r}, t) \quad \omega(\mathbf{r}, t) \equiv -\frac{\partial}{\partial t} \psi(\mathbf{r}, t). \quad (\text{C.3})$$

The phase function here is rapidly varying (over the scale length of a wavelength and period of the wave) and \mathbf{a} is slowly varying (over the scale length of the

plasma inhomogeneity) by assumption. Since geometric optics is essentially a local theory, the nonlocal effects in space and time will be treated to lowest nontrivial order. For simplicity, we introduce the change of variable

$$\mathbf{r}' \equiv \mathbf{r} - \mathbf{r}'' \quad t' = t - t''$$

so the current density becomes

$$\mathbf{J}(\mathbf{r}, t) = \int d^3 r' \int_0^\infty dt' \hat{\sigma}(\mathbf{r}', t'; \mathbf{r} - \frac{1}{2}\mathbf{r}', t - \frac{1}{2}t') \cdot \mathbf{a}(\mathbf{r} - \mathbf{r}', t - t') e^{i\psi(\mathbf{r}-\mathbf{r}', t-t')}.$$
(C.4)

We now expand the slow time dependence only in the conductivity tensor, so that

$$\begin{aligned} \hat{\sigma}(\mathbf{r}', t'; \mathbf{r} - \frac{1}{2}\mathbf{r}', t - \frac{1}{2}t') &= \left(1 - \frac{1}{2}\mathbf{r}' \cdot \nabla - \frac{1}{2}t' \frac{\partial}{\partial t} + \dots\right) \hat{\sigma}(\mathbf{r}', t'; \mathbf{r}, t) \\ \mathbf{a}(\mathbf{r} - \mathbf{r}', t - t') &= \left(1 - \mathbf{r}' \cdot \nabla - t' \frac{\partial}{\partial t} + \dots\right) \mathbf{a} \\ \psi(\mathbf{r} - \mathbf{r}', t - t') &= \psi - \mathbf{r}' \cdot \mathbf{k} + t' \omega + t' \mathbf{r}' \cdot \frac{\partial}{\partial t} \mathbf{k} \\ &\quad + \frac{1}{2} \mathbf{r}' \cdot (\mathbf{r}' \cdot \nabla) \mathbf{k} - \frac{1}{2} t'^2 \frac{\partial}{\partial t} \omega + \dots. \end{aligned}$$

Using the relation from equation (C.3) that $\partial \mathbf{k} / \partial t = -\nabla \omega$, along with the tensor identity for general tensor \hat{B} ,

$$\nabla \cdot (\phi \mathbf{A} B_{ij}) = (\mathbf{A} \cdot \phi + \phi \nabla \cdot \mathbf{A} + \phi \mathbf{A} \cdot \nabla) B_{ij}$$

from which we obtain

$$\nabla \cdot [e^{i(\omega t' - \mathbf{k} \cdot \mathbf{r}')} \mathbf{r}' \hat{\sigma}] = e^{i(\omega t' - \mathbf{k} \cdot \mathbf{r}')} \{ \mathbf{r}' \cdot \nabla \hat{\sigma} + i[t' \mathbf{r}' \cdot \nabla \omega - \mathbf{r}' \cdot (\mathbf{r}' \cdot \nabla) \mathbf{k}] \hat{\sigma} \}$$

we may write the current density as

$$\begin{aligned} \mathbf{J} &= e^{i\psi(\mathbf{r}, t)} \left\{ \int d^3 r' \int_0^\infty dt' e^{i(\omega t' - \mathbf{k} \cdot \mathbf{r}')} \left[\hat{\sigma} \cdot \mathbf{a} - \hat{\sigma} \cdot \left(\mathbf{r}' \cdot \nabla \mathbf{a} + t' \frac{\partial \mathbf{a}}{\partial t} \right) \right] \right. \\ &\quad - \frac{1}{2} \left[\frac{\partial}{\partial t} \int d^3 r' \int_0^\infty dt' e^{i(\omega t' - \mathbf{k} \cdot \mathbf{r}')} t' \hat{\sigma} \right] \cdot \mathbf{a} \\ &\quad \left. - \frac{1}{2} \left[\nabla \cdot \int d^3 r' \int_0^\infty dt' e^{i(\omega t' - \mathbf{k} \cdot \mathbf{r}')} \mathbf{r}' \hat{\sigma} \right] \cdot \mathbf{a} \right\}. \end{aligned}$$

We note that \mathbf{a} is outside the integrals since it depends on \mathbf{r}, t only.

We now define a Fourier transform in space and a Laplace transform in time such that

$$\hat{\sigma}_T(\mathbf{k}, \omega; \mathbf{r}, t) \equiv \int d^3 r' \int_0^\infty dt' e^{i(\omega t' - \mathbf{k} \cdot \mathbf{r}')} \hat{\sigma}$$
(C.5)

so that

$$\begin{aligned} i\nabla_k \hat{\sigma}_T &= \int d^3r' \int_0^\infty dt' e^{i(\omega t' - \mathbf{k} \cdot \mathbf{r}')} \mathbf{r}' \hat{\sigma} \\ -i\frac{\partial \hat{\sigma}_T}{\partial \omega} &= \int d^3r' \int_0^\infty dt' e^{i(\omega t' - \mathbf{k} \cdot \mathbf{r}')} t' \hat{\sigma}. \end{aligned}$$

Using this transform and the notation $\hat{\sigma} \cdot (\mathbf{r}' \cdot \nabla) \mathbf{a} \equiv \mathbf{r}' \hat{\sigma} : \nabla \mathbf{a}$, and introducing the tensor $\hat{\kappa}$ defined by

$$\hat{\kappa} \cdot \mathbf{a} \equiv -\frac{i}{2} \left[\nabla \cdot (\nabla_k \hat{\sigma}_T) - \frac{\partial}{\partial t} \left(\frac{\partial \hat{\sigma}_T}{\partial \omega} \right) \right] \cdot \mathbf{a} - i \left[\nabla_k \hat{\sigma}_T : \nabla \mathbf{a} - \frac{\partial \hat{\sigma}_T}{\partial \omega} \frac{\partial \mathbf{a}}{\partial t} \right] \quad (C.6)$$

the current density may be expressed as

$$\mathbf{J}(\mathbf{r}, t) = (\hat{\sigma}_T + \hat{\kappa}) \cdot \mathbf{a} e^{i\psi(\mathbf{r}, t)}. \quad (C.7)$$

C.2 The wave equation

Using the current density from the previous section, we wish to solve the wave equation

$$\nabla \times (\nabla \times \mathbf{E}) + \frac{1}{c^2} \frac{\partial^2 \mathbf{E}}{\partial t^2} + \mu_0 \frac{\partial \mathbf{J}}{\partial t}. \quad (C.8)$$

Then using equation (C.2) for \mathbf{E} and equation (C.7) for \mathbf{J} , the wave equation may be expressed as

$$\begin{aligned} \hat{\epsilon} \cdot \mathbf{a} &= \frac{c^2}{\omega^2} \{ \nabla \times (\nabla \times \mathbf{a}) + i[\mathbf{k} \times (\nabla \times \mathbf{a}) + \nabla \times (\mathbf{k} \times \mathbf{a})] \\ &\quad \times \frac{1}{\omega^2} \left\{ \frac{\partial^2 \mathbf{a}}{\partial t^2} - i \left[\omega \frac{\partial \mathbf{a}}{\partial t} + \frac{\partial}{\partial t}(\omega \mathbf{a}) + \frac{\partial}{\partial t}(\hat{Q} \cdot \mathbf{a}) \right] \right\} \\ &\quad + \frac{1}{\omega^2 \epsilon_0} \left[\frac{\partial}{\partial t}(\hat{\kappa} \cdot \mathbf{a}) - i\omega \hat{\kappa} \cdot \mathbf{a} \right] \end{aligned} \quad (C.9)$$

where we have introduced the definitions

$$\hat{Q} \equiv \frac{i\hat{\sigma}_T}{\epsilon_0} \quad \hat{\epsilon} \equiv \frac{c^2}{\omega^2} (\mathbf{k} \mathbf{k} - k^2 \hat{I}) + \hat{I} + \frac{\hat{Q}}{\omega}.$$

C.3 The amplitude equation

At this point we introduce the ordering where the amplitude has a dominant term and perturbations at various orders, so that we may write

$$\mathbf{a} = \mathbf{a}_0 + \delta \mathbf{a}_1 + \delta^2 \mathbf{a}_2 + \dots$$

where δ is a small expansion parameter. We now note that the quantities \mathbf{a} , \mathbf{k} , and ω are zero order quantities while ∇ and $\frac{\partial}{\partial t}$ (and hence $\hat{\kappa}$) are first order in δ . The zero order equation is then trivial since everything on the right-hand side of equation (C.9) is first order or higher. Hence,

$$\hat{\epsilon} \cdot \mathbf{a}_0 = 0 \quad (\text{C.10})$$

from which the basic ray equations were derived. The first order equation follows immediately as

$$\begin{aligned} \hat{\epsilon} \cdot \mathbf{a}_1 &= i \frac{c^2}{\omega^2} [\mathbf{k} \times (\nabla \times \mathbf{a}_0) + \nabla \times (\mathbf{k} \times \mathbf{a}_0)] \\ &\quad - \frac{i}{\omega^2} \left[\omega \frac{\partial \mathbf{a}_0}{\partial t} + \frac{\partial}{\partial t} (\omega \mathbf{a}_0) + \frac{\partial}{\partial t} (\hat{Q} \cdot \mathbf{a}_0) \right] \\ &\quad - \frac{i}{\epsilon_0 \omega} \omega \hat{\kappa} \cdot \mathbf{a}_0. \end{aligned} \quad (\text{C.11})$$

Expanding $\hat{\kappa}$ and using vector identities (and deleting the 0 subscript since it is no longer ambiguous) and the additional identities,

$$\begin{aligned} \omega \hat{\epsilon} &= \left(\omega - c^2 \frac{\mathbf{k}^2}{\omega} \right) \hat{I} + c^2 \frac{\mathbf{k}\mathbf{k}}{\omega} + \hat{Q} \\ \frac{\partial \omega \hat{\epsilon}}{\partial \omega} &= \left(1 + c^2 \frac{\mathbf{k}^2}{\omega^2} \right) \hat{I} - c^2 \frac{\mathbf{k}\mathbf{k}}{\omega^2} + \frac{\partial \hat{Q}}{\partial \omega} \\ \nabla_k(\omega \hat{\epsilon}) : \nabla \mathbf{a} &= \frac{c^2}{\omega} [-2(\mathbf{k} \cdot \nabla) \mathbf{a} + \nabla \mathbf{a} \cdot \mathbf{k} + \mathbf{k} \nabla \cdot \mathbf{a}] + \nabla_k \hat{Q} : \nabla \mathbf{a} \\ \nabla \cdot [\nabla_k(\omega \hat{\epsilon})] \cdot \mathbf{a} &= \frac{2c^2}{\omega} [\nabla \mathbf{k} \cdot \mathbf{a} - \mathbf{a} \nabla \cdot \mathbf{k}] + \nabla \cdot (\nabla_k \hat{Q}) \cdot \mathbf{a} \\ &\quad - \frac{c^2}{\omega^2} [\nabla(\omega \mathbf{k}) \cdot \mathbf{a} + \mathbf{k}(\mathbf{a} \cdot \nabla) \omega - 2(\mathbf{k} \cdot \nabla)(\omega \mathbf{a})] \\ \frac{\partial}{\partial t} \left[\frac{\partial(\omega \hat{\epsilon})}{\partial \omega} \right] &= \frac{2c^2}{\omega^3} (\mathbf{k}\mathbf{k} - k^2 \hat{I}) \frac{\partial \omega}{\partial t} + \left[\frac{\partial}{\partial t} \left(\frac{\partial \hat{Q}}{\partial \omega} \right) \right] \\ &\quad - \frac{c^2}{\omega^2} [2(\mathbf{k} \cdot \nabla \omega) \hat{I} - \nabla \omega (\mathbf{k} \cdot \hat{I}) - \mathbf{k}(\nabla \omega \cdot \hat{I})] \end{aligned}$$

this may also be written as

$$i\omega \hat{\epsilon} \cdot \mathbf{a}_1 = -\nabla_k(\omega \hat{\epsilon}) : \nabla \mathbf{a} - \frac{1}{2} \nabla \cdot [\nabla_k(\omega \hat{\epsilon})] \cdot \mathbf{a} + \frac{\partial(\omega \hat{\epsilon})}{\partial \omega} \cdot \frac{\partial \mathbf{a}}{\partial t} + \frac{1}{2} \left[\frac{\partial}{\partial t} \frac{\partial(\omega \hat{\epsilon})}{\partial \omega} \right] \cdot \mathbf{a}. \quad (\text{C.12})$$

The solution of the amplitude equations is implicit in equation (C.12), but this is still very difficult to solve in this form. In order to simplify the form of the

solution, we introduce \mathbf{b} , the null vector of $\hat{\epsilon}^\dagger$ which is defined such that

$$\hat{\epsilon}^\dagger \cdot \mathbf{b} = \mathbf{b}^\dagger \cdot \hat{\epsilon} = 0. \quad (\text{C.13})$$

Multiplying equation (C.12) on the left by $-2\mathbf{b}^\dagger$, we introduce the quantity

$$\begin{aligned} I &\equiv -2i\omega \mathbf{b}^\dagger \cdot \hat{\epsilon} \cdot \mathbf{a}_1 \\ &= -2\mathbf{b}^\dagger \cdot \left\{ -\nabla_k(\omega\hat{\epsilon}) : \nabla \mathbf{a} - \frac{1}{2}\nabla \cdot [\nabla_k(\omega\hat{\epsilon})] \cdot \mathbf{a} \right. \\ &\quad \left. + \frac{\partial(\omega\hat{\epsilon})}{\partial\omega} \cdot \frac{\partial \mathbf{a}}{\partial t} + \frac{1}{2} \left[\frac{\partial}{\partial t} \frac{\partial(\omega\hat{\epsilon})}{\partial\omega} \right] \cdot \mathbf{a} \right\} \\ &= -\frac{\partial}{\partial t} \left[\frac{\partial(\omega\hat{\epsilon})}{\partial\omega} : \mathbf{a}\mathbf{b}^\dagger \right] + \nabla \cdot [\nabla_k(\omega\hat{\epsilon}) : \mathbf{a}\mathbf{b}^\dagger] \\ &\quad - \frac{\partial(\omega\hat{\epsilon})}{\partial\omega} : \left[\frac{\partial \mathbf{a}}{\partial t} \mathbf{b}^\dagger - \mathbf{a} \frac{\partial \mathbf{b}^\dagger}{\partial t} \right] + \nabla_k(\omega\hat{\epsilon}) : [(\nabla \mathbf{a})\mathbf{b}^\dagger - \mathbf{a}\nabla \mathbf{b}^\dagger]. \end{aligned}$$

To avoid the complicated vector notation at this point, we introduce dummy indices such that

$$\frac{\partial}{\partial x_i} = \begin{cases} \nabla & i = 1, 2, 3 \\ \frac{\partial}{\partial t} & i = 4 \end{cases} \quad (\text{C.14})$$

$$\frac{\partial}{\partial k_i} = \begin{cases} \nabla_k & i = 1, 2, 3 \\ -\frac{\partial}{\partial\omega} & i = 4 \end{cases} \quad (\text{C.15})$$

in which case the amplitude equation becomes

$$I = \frac{\partial}{\partial x_i} \left[a_k b_j^\dagger \frac{\partial(\omega\epsilon_{jk})}{\partial k_i} \right] + \frac{\partial(\omega\epsilon_{jk})}{\partial k_i} \left(\frac{\partial a_k}{\partial x_i} b_j^\dagger - a_k \frac{\partial b_j^\dagger}{\partial x_i} \right). \quad (\text{C.16})$$

From equation (C.13), $b_j^\dagger \omega b \epsilon_{jk} a_k = 0$ so

$$\frac{\partial}{\partial x_i} \frac{\partial}{\partial k_i} (b_j^\dagger \omega b \epsilon_{jk} a_k) = \frac{\partial}{\partial x_i} \left[a_k b_j^\dagger \frac{\partial(\omega\epsilon_{jk})}{\partial k_i} \right] = 0 \quad (\text{C.17})$$

and $I = 0$, so we also have

$$\frac{\partial(\omega\epsilon_{jk})}{\partial k_i} \left(\frac{\partial a_k}{\partial x_i} b_j^\dagger - a_k \frac{\partial b_j^\dagger}{\partial x_i} \right) = 0. \quad (\text{C.18})$$

If we now separate $\mathbf{a} = \alpha \mathbf{A}$ and $\mathbf{b}^\dagger = \beta \mathbf{B}^\dagger$ where α and β represent the amplitude and \mathbf{A} and \mathbf{B}^\dagger are unit vectors, then equation (C.17) becomes

$$I_1 = \frac{\partial}{\partial x_i} \left[\alpha\beta \frac{\partial}{\partial k_i} (\omega\epsilon_{jk} A_k B_j^\dagger) \right] = 0. \quad (\text{C.19})$$

Since any factor multiplying the dispersion relation may be considered equivalent to a dispersion relation, so long as the distance along the ray characterized by the parameter τ is properly defined, we choose to define the dispersion relation as

$$D \equiv \omega\epsilon_{jk}A_kB_j^\dagger \quad (\text{C.20})$$

so that equation (C.19) becomes

$$I_1 = \frac{\partial D}{\partial k_i} \frac{\partial(\alpha\beta)}{\partial x_i} + \alpha\beta \frac{\partial}{\partial x_i} \left(\frac{\partial D}{\partial k_i} \right) = 0.$$

The corresponding parameter τ is defined then as

$$\frac{d}{d\tau} \equiv \frac{\partial D}{\partial k_i} \frac{\partial}{\partial x_i}$$

so that we obtain

$$\frac{d(\alpha\beta)}{d\tau} + \alpha\beta \frac{\partial}{\partial x_i} \left(\frac{\partial D}{\partial k_i} \right) = 0$$

or equivalently

$$\frac{d}{d\tau} \ln \alpha\beta = - \frac{\partial}{\partial x_i} \left(\frac{\partial D}{\partial k_i} \right). \quad (\text{C.21})$$

An alternate expression can be obtained from equation (C.18) such that

$$\begin{aligned} I_2 &= \frac{\partial(\omega\epsilon_{jk})}{\partial k_i} \left[A_k B_j^\dagger \left(\beta \frac{\partial\alpha}{\partial x_i} - \alpha \frac{\partial\beta}{\partial x_i} \right) + \alpha\beta \left(B_j^\dagger \frac{\partial A_k}{\partial x_i} - A_k \frac{\partial B_j^\dagger}{\partial x_i} \right) \right] \\ &= \frac{\partial D}{\partial k_i} \left(\beta \frac{\partial\alpha}{\partial x_i} - \alpha \frac{\partial\beta}{\partial x_i} \right) + \alpha\beta\omega\epsilon_{jk} \left(\frac{\partial A_k}{\partial k_i} \frac{\partial B_j^\dagger}{\partial x_i} - \frac{\partial B_j^\dagger}{\partial k_i} \frac{\partial A_k}{\partial x_i} \right) \\ &\quad + \alpha\beta \left[\frac{\partial}{\partial k_i} (\omega\epsilon_{jk} B_j^\dagger) \frac{\partial A_k}{\partial x_i} - \frac{\partial}{\partial k_i} (\omega\epsilon_{jk} A_k) \frac{\partial B_j^\dagger}{\partial x_i} \right] \\ &\quad - \omega\epsilon_{jk} \left[\frac{\partial}{\partial k_i} (A_k B_j^\dagger) \right] \left(\beta \frac{\partial\alpha}{\partial x_i} - \alpha \frac{\partial\beta}{\partial x_i} \right) \\ &= 0. \end{aligned}$$

From $\mathbf{b}^\dagger \cdot \hat{\epsilon} = \beta\epsilon_{jk}B_j^\dagger = 0$ and $\hat{\epsilon} \cdot \mathbf{a} = \alpha\omega\epsilon_{jk}A_k = 0$, the last terms vanish, and dividing by $\alpha\beta$, we have

$$\frac{d}{d\tau} \ln \frac{\alpha}{\beta} = \omega\epsilon_{jk} \left(\frac{\partial A_k}{\partial k_i} \frac{\partial B_j^\dagger}{\partial x_i} - \frac{\partial B_j^\dagger}{\partial k_i} \frac{\partial A_k}{\partial x_i} \right). \quad (\text{C.22})$$

Combining equations (C.21) and (C.22), the amplitude equations acquire their final symmetric form,

$$\frac{d}{dt} \ln \alpha^2 = - \frac{\partial}{\partial x_i} \left(\frac{\partial D}{\partial k_i} \right) - \omega \epsilon_{jk} \left(\frac{\partial A_k}{\partial k_i} \frac{\partial B_j^\dagger}{\partial x_i} - \frac{\partial B_j^\dagger}{\partial k_i} \frac{\partial A_k}{\partial x_i} \right) \quad (\text{C.23})$$

$$\frac{d}{dt} \ln \beta^2 = - \frac{\partial}{\partial x_i} \left(\frac{\partial D}{\partial k_i} \right) + \omega \epsilon_{jk} \left(\frac{\partial A_k}{\partial k_i} \frac{\partial B_j^\dagger}{\partial x_i} - \frac{\partial B_j^\dagger}{\partial k_i} \frac{\partial A_k}{\partial x_i} \right). \quad (\text{C.24})$$

We note that the first term in each expression is the four-dimensional divergence of the group velocity, and the Poisson brackets vanish for Hermitian dielectric tensors since then $\mathbf{a} = \mathbf{b}^*$.

We conclude the amplitude equations by noting that the components of \mathbf{a} are obtained from the minors of $\hat{\epsilon}$ with respect to any row and \mathbf{b}^\dagger is determined from the minors of $\hat{\epsilon}$ with respect to any column. Hence

$$\mathbf{a} \propto \begin{pmatrix} \epsilon_{22}\epsilon_{33} - \epsilon_{23}\epsilon_{32} \\ \epsilon_{23}\epsilon_{31} - \epsilon_{21}\epsilon_{33} \\ \epsilon_{21}\epsilon_{32} - \epsilon_{22}\epsilon_{31} \end{pmatrix} \quad (\text{C.25})$$

and

$$\mathbf{b}^\dagger \propto [(\epsilon_{22}\epsilon_{33} - \epsilon_{23}\epsilon_{32}), (\epsilon_{13}\epsilon_{32} - \epsilon_{12}\epsilon_{33}), (\epsilon_{12}\epsilon_{23} - \epsilon_{13}\epsilon_{22})]. \quad (\text{C.26})$$

Normalizing these vectors yields the unit vectors.

C.4 Energy density conservation

In order to cast the amplitude equations in a more useful form, we may recast equation (C.21) as

$$\frac{d}{dt} \ln \left(\alpha \beta \frac{\partial D}{\partial \omega} \right) = -\nabla \cdot \omega_{\mathbf{k}} \quad (\text{C.27})$$

where $\omega_{\mathbf{k}} = d\mathbf{r}/dt$ is the group velocity. If we then add equation (C.27) to its complex conjugate, and define the energy density \mathcal{U} by

$$\mathcal{U} = \frac{\epsilon_0}{2} \operatorname{Re} \left(\alpha \beta \frac{\partial D}{\partial \omega} \right)$$

then the energy density conservation law is

$$\frac{1}{\mathcal{U}} \frac{d\mathcal{U}}{dt} = -\operatorname{Re}(\nabla \cdot \omega_{\mathbf{k}}) \quad (\text{C.28})$$

whose solution is

$$\mathcal{U} = \mathcal{U}_0 \exp \left[- \int_0^t dt' \operatorname{Re}(\nabla \cdot \omega_{\mathbf{k}}) \right]. \quad (\text{C.29})$$

In the weak damping limit, it is useful to separate the energy density into the principal part which comes from the anti-Hermitian part of $\hat{\sigma}$ (the *Hermitian* part of $\hat{\epsilon}$), and the small part of order δ which comes from the Hermitian part of $\hat{\sigma}$. Letting $\mathcal{U} \equiv U + U_H$ where U_H is the small absorptive term, we may write equation (C.28) as

$$\begin{aligned}\frac{dU}{dt} &= -\frac{dU_H}{dt} - (U + U_H)\nabla \cdot \omega_{\mathbf{k}} \\ &\simeq -U\nabla \cdot \omega_{\mathbf{k}} + i\omega U_H.\end{aligned}$$

The energy density due the Hermitian part of the dielectric tensor is to lowest order given by

$$U_H \simeq \frac{i}{2\omega} \mathbf{a}^* \cdot \hat{\sigma}^H \cdot \mathbf{a}$$

so the result may be written as

$$\frac{dU}{dt} = -U\nabla \cdot \omega_{\mathbf{k}} - \frac{1}{2} \mathbf{a}^* \cdot \hat{\sigma}^H \cdot \mathbf{a}. \quad (\text{C.30})$$

Appendix D

Answers to selected problems

Chapter 2 Waves in a cold uniform plasma

Problem 2.1.2. Zeros of D .

(i) With only one ion species,

$$D = \frac{\omega_{ci}\omega_{pi}^2}{\omega(\omega^2 - \omega_{ci}^2)} - \frac{\omega_{ce}\omega_{pe}^2}{\omega(\omega^2 - \omega_{ce}^2)} = 0$$

so we have

$$\omega^2(\omega_{pi}^2\omega_{ci} - \omega_{ce}^2\omega_{pe}^2) = \omega_{pi}^2\omega_{ci}\omega_{ce}^2 - \omega_{pe}^2\omega_{ce}\omega_{ci}^2 = 0$$

because of charge neutrality. Hence either $\omega = 0$ or $\omega_{pi}^2 = \omega_{pe}^2 = 0$ or $\omega_{ci} = \omega_{ce} = 0$, all of which are forbidden by the problem statement.

(ii) Near each ion cyclotron resonance, the term in D due to that species will dominate sufficiently close to the resonance and will change sign as one passes through the resonance. This requires D to be positive just above each ion resonance and negative just below each ion resonance, and hence D must pass through zero between each adjacent pair of resonances.

Problem 2.2.1. The ordinary wave. From the dispersion relation for the O -wave, $n^2 = 1 - \omega_p^2/\omega^2$, we may solve for ω :

$$\omega = \sqrt{\omega_p^2 + k^2c^2}$$

so the phase velocity is

$$v_p = \frac{\omega}{k} = \frac{\sqrt{\omega_p^2 + k^2c^2}}{k}.$$

Similarly, the group velocity is given by

$$v_g = \frac{\partial \omega}{\partial k} = \frac{kc^2}{\sqrt{\omega_p^2 + k^2c^2}}$$

so the product is $v_p v_g = c^2$.

Problem 2.2.5. Change of polarization. Letting $\sin^2 \theta = P/S$, then the coefficients of equation (2.22) become

$$\begin{aligned} A &= P(2 - P/S) \\ B &= RLP/S + PS(2 - P/S) \\ C &= PRL \end{aligned}$$

and since the polarization changes when $n^2 = S$ from equation (2.49), we try this in equation (2.21) to get

$$P(2 - P/S)S^2 - [RLP/S + PS(2 - P/S)]S + PRL = 0$$

so $n^2 = S$ is a solution and E_x changes sign at that angle along with the polarization.

Problem 2.5.1. The whistler wave.

(i) Beginning with equation (2.79),

$$\tan \alpha = \frac{\frac{1}{k} \frac{\partial \omega}{\partial \theta}|_k}{\frac{\partial \omega}{\partial k}|_\theta} = -\frac{kc^2 \omega_{ce} \sin \theta / \omega_{pe}^2}{2kc^2 \omega_{ce} \cos \theta / \omega_{pe}^2} = -\frac{1}{2} \tan \theta$$

so

$$\frac{d}{d\theta} \left(\frac{\tan \theta}{2 + \tan^2 \theta} \right) = \frac{(2 + \tan^2 \theta) \sec^2 \theta - \tan \theta (2 \tan \theta \sec^2 \theta)}{(2 + \tan^2 \theta)^2} = 0$$

so $\tan^2 \theta = 2$ and the rest follows from the text.

(ii) The magnitude of the group velocity is given from equation (2.54) by

$$v_g = \sqrt{\left(\frac{\partial \omega}{\partial k} \Big|_\theta \right)^2 + \left(\frac{1}{k} \frac{\partial \omega}{\partial \theta} \Big|_k \right)^2} = \frac{kc^2 \omega_{ce}}{\omega_{pe}^2} \sqrt{1 + 3 \cos^2 \theta}$$

(iii) The plots are shown in figure D.1.

(iv) Eventually, as $\theta \rightarrow \pi/2$, it reaches the angle where $\tan^2 \theta_r = -P/S \gg 1$, so the wave ceases to propagate and $v_p \rightarrow 0$. The wave normal surfaces are not quite the perfect circles, then, that they appear to be in figure D.1 and the polar plot of v_g has a narrow tail reaching to the origin.

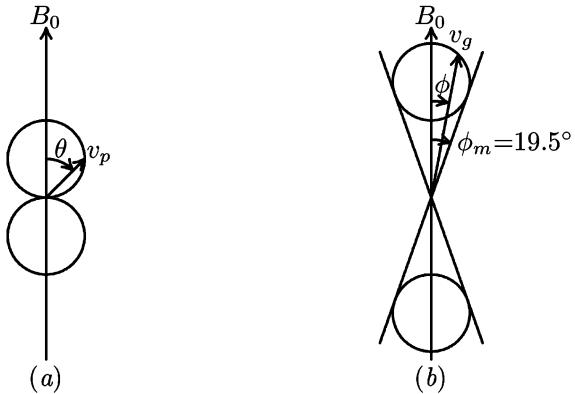


Figure D.1. (a) Wave normal surfaces $v_p(\theta)$ and (b) group velocity polar plot, $v_g(\phi)$ where $\phi = \theta + \alpha$, for the whistler mode.

Problem 2.6.1 Faraday rotation.

$$\omega_{pe}^2 = 9.16 \times 10^6 \rightarrow \bar{n} = 2.8 \times 10^3 / \text{m}^3.$$

Problem 2.7.1. Phase shift with nonuniform density profile.

(i)

$$\phi = \frac{\omega L}{2c} \left[\frac{a^2}{\alpha} \sinh^{-1} \left(\frac{\alpha}{a} \right) - 1 \right].$$

(ii)

$$\phi = \frac{\omega L}{c} \left[\frac{2}{\pi} E(\alpha^2) - 1 \right]$$

where E is the complete elliptic integral of the second kind.

Problem 2.8.1 Cold electrostatic waves. Since for the X -Wave, the dispersion relation is

$$n^2 = RL/S$$

and the hybrid resonances occur where $S \rightarrow 0$, then near the hybrid resonances, $n^2 \rightarrow \infty$ and neither P nor S is getting large. Thus the sufficient condition is satisfied.

Chapter 3 Waves in fluid plasmas

Problem 3.4.2. Low frequency dispersion relation with collisions.

(ii) equation (3.56) becomes

$$\omega \simeq k V_A \cos \theta \left[1 - \frac{ik^2 c^2}{2\omega_{pe}^2} (\epsilon_{\parallel} \sin^2 \theta + \epsilon_{\perp} \cos^2 \theta) \right]$$

equation (3.57) becomes

$$\omega^2 = k^2 [V_A^2 + c_s^2 \sin^2 \theta] (1 - ik^2 c^2 \epsilon_{\perp} / \omega_{pe}^2)$$

and equation (3.58) is unchanged to lowest order.

Chapter 4 Kinetic theory of plasma waves

Problem 4.2.1. Properties of the plasma dispersion function.

(iv)(b) For an eight-digit machine, $\zeta_c = 3.3$ for 4.7 digits accuracy. For the 14-digit machine, $\zeta_c = 4.3$ for 7.8 digits accuracy.

Problem 4.2.3. Landau damping with a Lorentzian distribution.

(i) $A = n_0 v_e / \pi$.

(ii) The potential and distribution function are given by

$$\begin{aligned} \tilde{\phi}_p(k, p) &= \frac{i\omega \omega_{pe}^2 \Delta m_e v_e (p + kv_e)}{ek^2 [(p + kv_e)^2 + \omega_{pe}^2]} \\ \tilde{f}_p(u, k, p) &= \frac{g(u)}{p + iku} \left\{ 1 - \frac{2\omega_{pe}^2 v_e (p + kv_e)}{k(u^2 + v_e^2)[(p + kv_e)^2 + \omega_{pe}^2]} \right\}. \end{aligned}$$

(iii) The potential is thus given by

$$\tilde{\phi}(k, t) = \frac{i\omega \omega_{pe}^2 \Delta m_e v_e}{ek^2} e^{-kv_e t} \cos(\omega_{pe} t).$$

The distribution function is more complicated, but is given by

$$\begin{aligned} \tilde{f} &= g(u) e^{-ikut} \left[1 - \frac{2\omega_{pe}^2 v_e}{A} k(u^2 + v_e^2) \right] \\ &\quad + \frac{2g(u)\omega_{pe}^2 v_e \bar{A}}{k(u^2 + v_e^2)} e^{-kv_e t} \left[\cos(\omega_{pe} t) - \frac{\omega_{pe}}{k(v_e - iu)} \sin(\omega_{pe} t) \right] \end{aligned}$$

where $\bar{A} = k(v_e - iu) / [k^2(v_e - iu)^2 + \omega_{pe}^2]$, so the leading term does not decay in time but the second term does.

Problem 4.2.4. The electrostatic picture of Landau damping.

- (iii) $I = n_0 k t \exp[-(k v_e t / 2)^2] \cos \omega t$. So $\kappa = (k v_e / 2)^2$.
- (iv) $I = n_0 k t e^{-k v_e t} \cos \omega t$.

Problem 4.2.5. The ordinary wave in a hot unmagnetized plasma. Even with the hot plasma corrections, $v_p > c$, so there cannot be any Landau damping of the type we have considered here. The theory here will imply some, since a Maxwellian has finite (but exponentially small) amplitude even for $v_p > c$, but the physical picture tells us this is a weakness in our analysis. A relativistic analysis requires a momentum distribution, $f(p) \sim \exp(-p^2/2m_0\kappa T)$ with $v < c$, and results in only slight changes in phase velocity.

Problem 4.3.9 Lorentz distribution.

- (i) With $v_0 \neq 0$, $F_m = (v_0 - i v_\ell)^m / k_z v_\ell (\zeta_n + i)$, and

$$\begin{aligned}\int_{-\infty}^{\infty} \frac{F'(v_z) dv_z}{\omega + n\omega_c - k_z v_z} &= - \frac{1}{k_z v_\ell^2 (\zeta_n + i)^2} \\ \int_{-\infty}^{\infty} \frac{v_z F'(v_z) dv_z}{\omega + n\omega_c - k_z v_z} &= - \frac{\zeta_n + v_0/v_\ell}{k_z v_\ell (\zeta_n + i)^2}.\end{aligned}$$

(ii) With $v_0 = 0$, simply let $v_0 \rightarrow 0$ in the previous expressions. Note that these results are equivalent to letting $Z(\zeta_n) \rightarrow -1/(\zeta_n + i)$.

Problem 4.3.10. Cold plasma limits.

- (i) As $T_\perp \rightarrow 0, \lambda \rightarrow 0$, so

$$\begin{aligned}K_0 &\rightarrow 0 \\ K_1 &\rightarrow 1 + \sum_j \frac{\omega_{pj}^2}{\omega k_z v_{\ell j}} \left\{ \frac{1}{2} [Z(\zeta_{+1j}) + Z(\zeta_{-1j})] \right. \\ &\quad \left. + \frac{k_z v_{\ell j}}{4\omega} [Z'(\zeta_{+1j}) + Z'(\zeta_{-1j})] \right\} \\ K_2 &\rightarrow i \sum_j \frac{\epsilon_j \omega_{pj}^2}{\omega k_z v_{\ell j}} \left\{ \frac{1}{2} [Z(\zeta_{-1j}) - Z(\zeta_{+1j})] + \frac{k_z v_{\ell j}}{4\omega} [Z'(\zeta_{-1j}) - Z'(\zeta_{+1j})] \right\} \\ K_3 &\rightarrow 1 - \sum_j \frac{\omega_{pj}^2}{\omega k_z v_{\ell j}} \left\{ \zeta_{0j} Z'(\zeta_{0j}) + \frac{k_\perp^2 v_\ell}{4k_z \omega \omega_{cj}} [(\omega - \omega_{cj}) Z'(\zeta_{-1j}) \right. \\ &\quad \left. - (\omega + \omega_{cj}) Z'(\zeta_{+1j})] \right\} \\ K_4 &\rightarrow - \sum_j \frac{k_\perp \omega_{pj}^2}{2\omega^2 k_z} \frac{1}{2} [Z'(\zeta_{+1j}) + Z'(\zeta_{-1j})]\end{aligned}$$

$$K_5 \rightarrow i \sum_j \frac{k_{\perp} \epsilon_j \omega_{pj}^2}{2\omega^2 k_z} \frac{1}{2} [Z'(\zeta_{+1j}) - Z'(\zeta_{-1j})].$$

(ii) As $T_{\parallel} \rightarrow 0$, $v_{\ell} \rightarrow 0$, so in this limit, $Z(\zeta_{nj})/k_z v_{\ell} \rightarrow -1/(\omega + n\omega_{cj})$ and $Z'(\zeta_{nj})/(k_z v_{\ell})^2 \rightarrow 1/(\omega + n\omega_{cj})^2$, and the tensor elements become

$$\begin{aligned} K_0 &\rightarrow 2 \sum_j \frac{\omega_{pj}^2 e^{-\lambda_j}}{\omega} \sum_{n=-\infty}^{\infty} \frac{\lambda_j(I'_n - I_n)}{\omega + n\omega_{cj}} \left[1 + \frac{k_z^2 v_{\perp j}^2}{\omega(\omega + n\omega_{cj})} \right] \\ K_1 &\rightarrow 1 - \sum_j \frac{\omega_{pj}^2 e^{-\lambda_j}}{\omega} \sum_{n=-\infty}^{\infty} \frac{n^2 I_n}{\lambda_j(\omega + n\omega_{cj})} \left[1 + \frac{k_z^2 v_{\perp j}^2}{\omega(\omega + n\omega_{cj})} \right] \\ K_2 &\rightarrow i \sum_j \frac{\epsilon_j \omega_{pj}^2 e^{-\lambda_j}}{\omega} \sum_{n=-\infty}^{\infty} \frac{n(I'_n - I_n)}{\omega + n\omega_{cj}} \left[1 + \frac{k_z^2 v_{\perp j}^2}{\omega(\omega + n\omega_{cj})} \right] \\ K_3 &\rightarrow 1 - \sum_j \frac{\omega_{pj}^2 e^{-\lambda_j}}{\omega^2} \sum_{n=-\infty}^{\infty} I_n = 1 - \sum_j \frac{\omega_{pj}^2}{\omega^2} \\ K_4 &\rightarrow \sum_j \frac{\omega_{pj}^2 k_z k_{\perp} v_{\perp j}^2 e^{-\lambda_j}}{2\omega^2 \omega_{cj}} \sum_{n=-\infty}^{\infty} \frac{n I_n}{\lambda_j(\omega + n\omega_{cj})} \\ K_5 &\rightarrow i \sum_j \frac{\epsilon_j \omega_{pj}^2 k_z k_{\perp} v_{\perp j}^2 e^{-\lambda_j}}{2\omega^2 \omega_{cj}} \sum_{n=-\infty}^{\infty} \frac{I_n - I'_n}{\omega + n\omega_{cj}}. \end{aligned}$$

(iii) Taking $T_{\parallel} \rightarrow 0$ last, or first taking $T_{\perp} = T_{\parallel} = T$ and then taking $T \rightarrow 0$, one recovers the cold plasma terms (and $K_0 = K_4 = K_5 = 0$). The order does not matter.

Problem 4.4.2. The unmagnetized ion dispersion relation.

(ii) Keeping the first warm plasma term, the result may be written as a quadratic in ω^2 of the form

$$a\omega^4 - b\omega^2 - c = 0$$

with

$$\begin{aligned} a &= k_z^2 + k_{\perp}^2 (1 + \omega_{pe}^2/\omega_{ce}^2) \\ b &= k_z^2 \omega_p^2 + k_{\perp}^2 \omega_{pi}^2 \\ c &= \frac{3}{2} k^4 v_i^2 \omega_{pi}^2. \end{aligned}$$

Since a , b , and c are all positive, one of the roots for ω^2 is negative, so that ω is imaginary for these roots. The other root is given approximately by

$$\omega^2 \simeq \frac{b}{a} + \frac{c}{b}$$

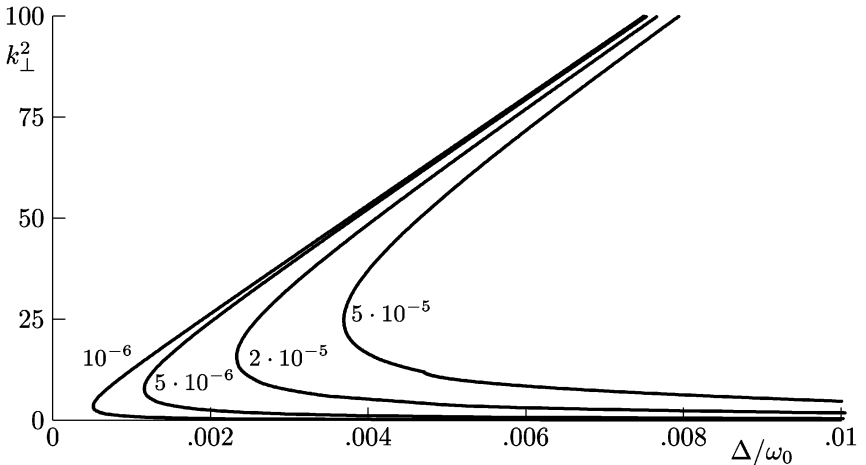


Figure D.2. Plot of k_{\perp}^2 versus fractional deviation from lower hybrid frequency, Δ/ω_0 with $k_z^2 = 10^{-6}, 5 \times 10^{-6}, 2 \times 10^{-5}, 5 \times 10^{-5}$ as a parameter with $v_i^2/\omega_0^2 = 10^{-4}$, $\omega_{pe} = \sqrt{2}\omega_{ce}$, and $m_i/m_e = 1836$.

$$= \omega_0^2 \left[\frac{1 + \mu\kappa}{1 + \kappa/(1 + \alpha)} + \frac{3(1 + \kappa)^2 k_z^2 v_i^2}{2(1 + \mu\kappa)\kappa\omega_0^2} \right]$$

where $\mu = m_i/m_e = 1836$, $\kappa = k_z^2/k_{\perp}^2$, and $\alpha = \omega_{pe}^2/\omega_{ce}^2$ so that $\omega_0^2 \equiv \omega_{pi}^2/(1 + \alpha)$. Letting $\omega = \omega_0 + \Delta$, then for $k_z = 0$, this leads to $\Delta/\omega_0 = \frac{3}{4}k_{\perp}^2 v_i^2/\omega_0^2$. For $k_z \neq 0$, we have

$$\frac{\Delta}{\omega_0} \simeq \frac{\kappa\mu}{2[1 + \kappa/(1 + \alpha)]} + \frac{3(1 + \kappa)^2}{\kappa(1 + \kappa\mu)} \frac{k_z^2 v_i^2}{\omega_0^2}.$$

Figure D.2 plots k_{\perp}^2 versus Δ/ω_0 for several values of k_z^2 .

Problem 4.4.3 The large- λ dispersion relation.

(iv) For $v = 40$, $\lambda = 100$, $a = 2.828$, $b = 0.0705 \simeq av^2/6\lambda^2 = 0.075$, $\eta = 0.390 \simeq v/\lambda = 0.4$, so the worst approximation is 6.4% error. $e^{b^2-a^2}Z(a)/Z(b) = 9.1 \times 10^{-4}$, hence it is neglectable. Since maximum of z is η , $\cosh\eta = 1.07605$ and $1 + \eta^2/2 = 1.07702$ so error is of the order of 0.1%.

Chapter 5 Bounded plasmas

Problem 5.2.2. Surface charge density at the plasma–vacuum interface.

$$\rho_s = \epsilon_0 \left(\frac{K_3}{n_{xp}} - \frac{1}{n_{xv}} \right) n_z E_z.$$

Problem 5.2.3. Second value of k_\perp .

$$k_{\perp 1}^2 k_{\perp 2}^2 = (\gamma^2 + \kappa_2^2) \frac{\kappa_3}{\kappa_1}$$

$$k_{\perp 1}^2 + k_{\perp 2}^2 = -\gamma \left(1 + \frac{\kappa_3}{\kappa_1} \right) + \frac{\kappa_2^2}{\kappa_1}$$

Problem 5.3.2. Glass boundary effect.

$$K_{\text{eff}} = K_g \left[\frac{(K_g + 1)b^2(c^2 + a^2) - (K_g - 1)(b^4 + a^2c^2)}{(K_g + 1)b^2(c^2 - a^2) - (K_g - 1)(b^4 - a^2c^2)} \right].$$

Problem 5.3.3. Estimates of the Tonks–Dattner resonances. We treat each resonance separately:

(i) For the main resonance, $\omega^2 = 0.39\omega_p^2$. This compares with $\omega^2 = 0.54\omega_p^2$ from [figure 5.5](#).

(ii) For the first resonance, $ka = 0$ and $\omega = \omega_p$ compared with $\omega^2 = 1.26\omega_p^2$ from [figure 5.5](#).

(iii) For the second resonance, $ka = x_0 - \epsilon$, $x_0 = 1.83$, $\epsilon \simeq 0.76$, leading to $\omega^2 = 1.0069\omega_p^2$. This compares with $\omega^2 = 1.89\omega_p^2$ from [figure 5.5](#).

Problem 5.3.7. The unbounded finite column. $1 - \omega_p^2/\omega^2 = -1.9677$ which leads to $\omega = 0.5805\omega_p$ and $\tau a = 2.236$. The values of $E_{1z}(r)/A$ for $r/a = 0.0, 0.5, 1.0, 1.5, 2.0$ are $0.370, 0.506, 1.0, 0.305, 0.098$ respectively so $E_{1z}(r)$ is sketched in [figure D.3](#).

Problem 5.4.1. The effects of ion motions.

$$\left(\frac{k_{\parallel}a}{p_{nv}} \right)^2 = -\frac{1 + \omega_{pe}^2/(\omega_{ce}^2 - \omega^2) + \omega_{pi}^2/(\omega_{ci}^2 - \omega^2)}{1 - \omega_p^2/\omega^2}.$$

Since $\omega_{LH} > \omega_{ci}$ always, the lower branch of the dispersion relation is modified (showing only the modifications to the lower branch, as the upper branches are unchanged) as in [figure D.4](#).

Problem 5.5.3. Waveguide cutoff frequencies.

(iii) For the first case ($B_z \neq 0$), $E_\theta(a) = 0$ so $J'_0 = -J_1(k_\perp a) = 0$, so $k_\perp a = p_{1v} = 3.83, 7.01, \dots$. For the second case ($E_z \neq 0$), $E_z(a) = 0$ so $k_\perp a = p_{0v} = 2.405, 5.52, \dots$

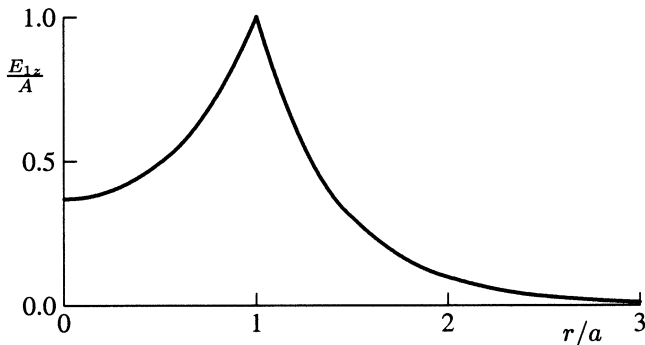


Figure D.3. Sketch of $E_{1z}(r)$ for an unmagnetized plasma column of radius a with $\tau_0 a = 2$ and $\omega_p a/c = 1$.

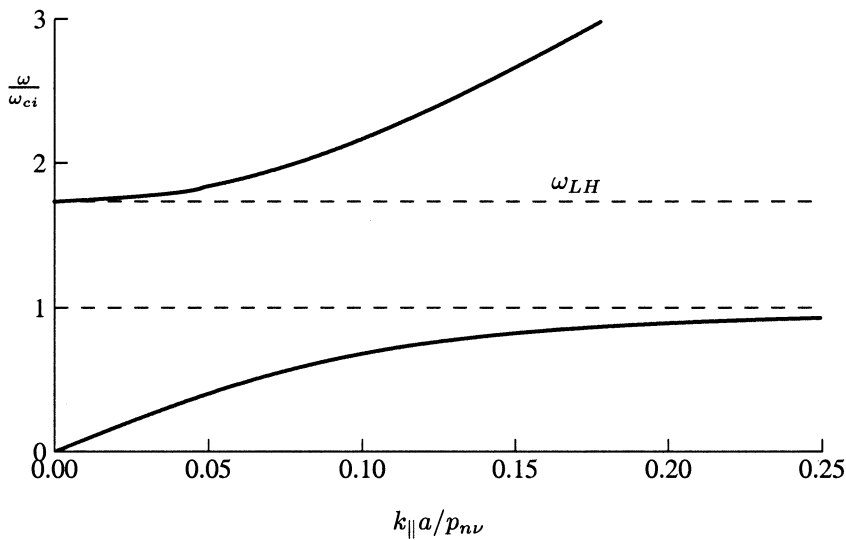


Figure D.4. Lower branch of the dispersion relation for electrostatic waves for the case where ion motions are important. This example has $m_i/m_e = 10$ and $\omega_{pi}^2/\omega_{ci}^2 = 2.52$.

(iv) The cutoff frequency is given by

$$\omega^2 = \omega_{pe}^2 + \frac{1}{2}(k_\perp^2 c^2 + \omega_{ce}^2) \pm \frac{1}{2}[(k_\perp^2 c^2 - \omega_{ce}^2)^2 + 4\omega_{pe}^2 \omega_{ce}^2]^{\frac{1}{2}}.$$

For the second case, $\kappa_3 = k_\perp^2 = \frac{\omega^2}{c^2}(1 - \omega_p^2/\omega^2)$ so $\omega^2 = \omega_{pe}^2 + k_\perp^2 c^2$ which is the same as the infinite magnetic field case.

Problem 5.5.6. Compressional mode excitation coefficients. $b/a = p_{11}/p_{12} =$

Table D.1. Amplitude ratios for fast wave modes for loop excitation.

n	p_{1n}	A_n/A_1
2	7.01	0
3	10.17	−4.52
4	13.32	1.96
5	16.47	11.01

$3.83/7.01 = 0.546$. For the relative amplitudes, the ratio is given by

$$\frac{A_n}{A_1} = \frac{p_{1n}}{p_{11}} \left(\frac{35}{36 - p_{1n}^2/p_{11}^2} \right)^{1/2} \frac{J_1(p_{1n}p_{11}/p_{12})}{J_1(p_{11}^2/p_{12})} \frac{J_0^2(p_{11})}{J_0^2(p_{1n})}$$

so the ratios are given in table D.1.

Problem 5.6.1. Boundary condition for vacuum layer in a conducting waveguide.

$$U(k_{\perp 1}) - U(k_{\perp 2}) = 0$$

where

$$U(k_{\perp j}) = \frac{\frac{J'_m(k_{\perp j}a)}{k_{\perp j}J_m(k_{\perp j}a)} + \frac{g'(Ta)}{Tg(Ta)} - \frac{im[(\kappa_1 - \frac{\omega^2}{c^2})(\gamma + k_{\perp j}^2) - \kappa_2^2]}{a\kappa_2 T^2 k_{\perp j}^2}}{\frac{\beta_j J'_m(k_{\perp j}a)}{k_{\perp j}J_m(k_{\perp j}a)} + \frac{\omega^2 \beta_j}{c^2 \kappa_3} \frac{f'(Ta)}{Tf(Ta)} + \frac{im k_z^2 \kappa_2}{a\kappa_1 T^2} \left(1 + \frac{T^2}{k_{\perp j}^2} \right)}$$

where in the vacuum region, we defined

$$E_{zv} = B_m \left[I_m(Tr) - \frac{I_m(Tb)}{K_m(Tb)} K_m(Tr) \right] \equiv B_m f(Tr)$$

$$B_{zv} = D_m \left[I_m(Tr) - \frac{I'_m(Tb)}{K'_m(Tb)} K_m(Tr) \right] \equiv D_m g(Tr).$$

Problem 5.7.1. The Poynting vector profile. See [figure D.5](#).

$$S_z = \omega k_{\parallel} \epsilon_0 |A|^2 k_{\perp}^2 [J_1(k_{\perp} r)]^2 / \gamma^2.$$

Problem 5.7.2. Thermal corrections. The dispersion relation is

$$k_{\perp}^2 = \frac{p_{nv}^2}{a^2} = \left(\frac{\omega^2}{c^2} - k_{\parallel}^2 \right) \left(1 - \frac{\omega_p^2}{\omega^2 - k_{\parallel}^2 v_s^2} \right)$$

where $v_s^2 = \gamma k_B T / m_e$. This dispersion relation has the same cutoff as [figure 5.17](#), but there is no longer a resonance. The slope near the origin is unchanged, but now as k_{\parallel} gets large, there remains a finite slope of $\omega/k_{\parallel} \simeq v_s$ which is the sound speed. See [figure D.6](#).

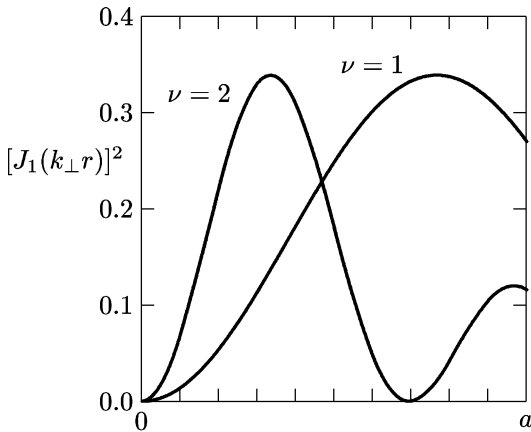


Figure D.5. Power flow versus radius for a plasma-filled waveguide in a magnetic field.

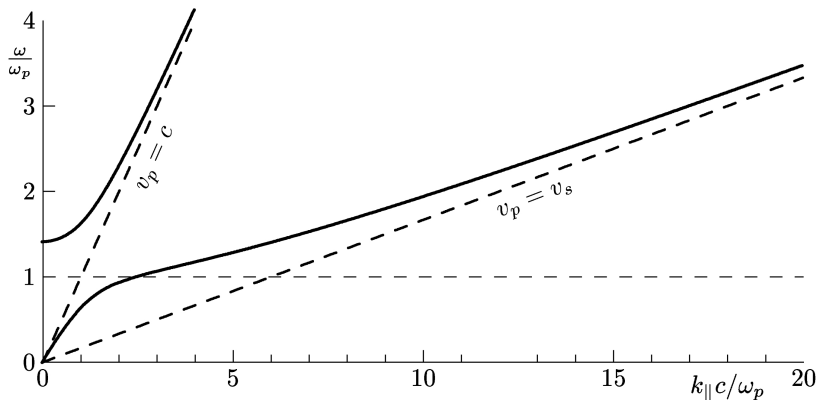


Figure D.6. Dispersion relation for the plasma-filled waveguide in an infinite magnetic field with finite temperature. For this example, $\omega_0 = \omega_p$ and $c/v_s = 6$.

Chapter 6 Inhomogeneous plasmas

Problem 6.2.1. WKB approximation. The approximations are that $|\eta''|$ can be ignored, that

$$\left| \frac{1}{2} \frac{k'^2}{k^3} \right| \ll \left| \left(\frac{k'}{k^2} \right)' \right|$$

and finally that $|k'/k^2| \ll 1$.

Problem 6.2.2. Validity of linear matching to WKB solutions.

- (i) $k^2(x) = \alpha k_0^2 x / 4 + \mathcal{O}(x^2)$.
- (ii) $u = \frac{3}{2} \left(\frac{3\alpha}{k_0}\right)^{2/3}$.
- (iii) $2kdk/dx = \frac{1}{4}\alpha k_0^2 \operatorname{sech}^2 u$, so

$$\frac{1}{k^2} \frac{dk}{dx} = \frac{\alpha}{k_0 (\cosh u)^{1/2} (2 \sinh u)^{3/2}}.$$

- (iv) The condition $|\zeta| \geq 3$ may be written

$$\frac{\alpha}{k_0} \leq \frac{(2u)^{3/2}}{9} \quad (\text{Airy asymptotic condition}) \quad (\text{D.1})$$

and the limit on k'/k^2 may be written

$$\frac{\alpha}{k_0} \leq 0.1 (\cosh u)^{1/2} (2 \sinh u)^{3/2} \quad (\text{WKB condition}) \quad (\text{D.2})$$

and these are both monotonically increasing functions of u , so there always exists a value of α/k_0 which is small enough for validity for any value of u .

(v) The percentage error between the linear approximation and the exact expression may be found from

$$\% \text{ error} = \left| \frac{k^2(u) - \frac{1}{2}k_0^2 u}{k^2(u)} \right| \times 100\% = |1 - uctnhu| \times 100\%. \quad (\text{D.3})$$

Calculating the percentage error from equation (D.3), the Airy limit on α/k_0 from equation (D.1) and the WKB limit from equation (D.2), all as a function of u , the results may be expressed as in [table D.2](#), and then plotting the *smaller* limit versus the error, the result may be expressed as in [figure D.7](#). Hence if one limits the error in the linear approximation, one limits the value of α/k_0 where the matching is valid.

Problem 6.3.1. Changing to dimensionless variables. For $b_0 \neq 0$, $\lambda^2 = b_2^{5/2}/b_0^{3/2}$, $z_0 = a_2 b_0^{1/2}/b_2^{3/2}$, and $\gamma = b_2(a_0 b_2 - a_2 b_0)/b_0^2$.

For $b_0 = 0$, $\lambda^2 = b_2$, $z_0 = a_2/b_2$, and $\beta = a_0/b_2$.

Problem 6.3.2. The case for $\lambda^2 < 0$.

- (i) The roots of $k^4 + \lambda_0^2 z k^2 - \lambda_0^2 \beta = 0$ are plotted in [figure D.8](#).
- (ii) The roots of $k^4 - \lambda_0^2 x k^2 + \lambda_0^2 x - \gamma_0 = 0$ are plotted in [figure D.9](#).

Table D.2. Errors in wkb matching.

u	% Error	Airy limit	WKB limit
0.1	0.33	0.010	0.009
0.2	1.3	0.028	0.026
0.3	3.0	0.052	0.049
0.4	5.3	0.080	0.077
0.5	8.2	0.111	0.113
0.6	11.7	0.146	0.156
0.7	15.8	0.184	0.209
0.8	20.5	0.225	0.274

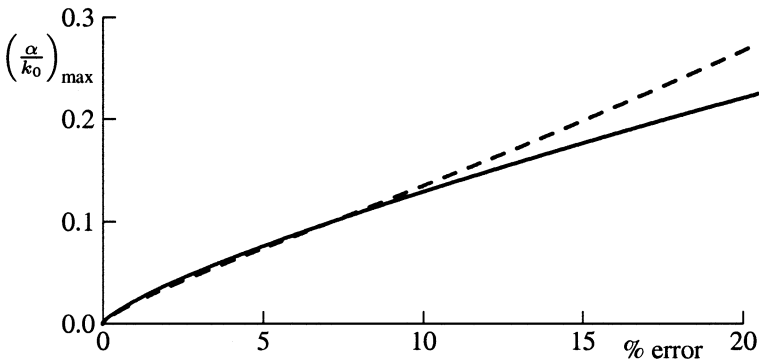


Figure D.7. α/k_0 limits versus percentage error: dashes, from WKB condition; full curve, from Airy asymptotic condition.

Problem 6.3.3. Conservation laws.

(ii) The expression for $P(s_{\pm})$ is straightforward, and is dominated by the first term only in the asymptotic limit. For the fast wave, the first two terms cancel and the last two add so that

$$P(f_{\pm}) \rightarrow \mp 2i(1 + \gamma)|f_{\pm}|^2 = \mp 2\pi i\lambda^2(1 - e^{-2\eta})$$

where the identity $|\Gamma(1 \pm iy)|^2 = \pi y / \sinh \pi y$ has been used.

(iii) The connection formula for solution y_1 is

$$T_1 f_- \leftarrow e^{-\eta} y_1 \rightarrow f_- + C_1 s_-$$

so the conserved quantities give

$$T_1^2 P(f_-) = P(f_-) + C_1^2 P(s_-)$$

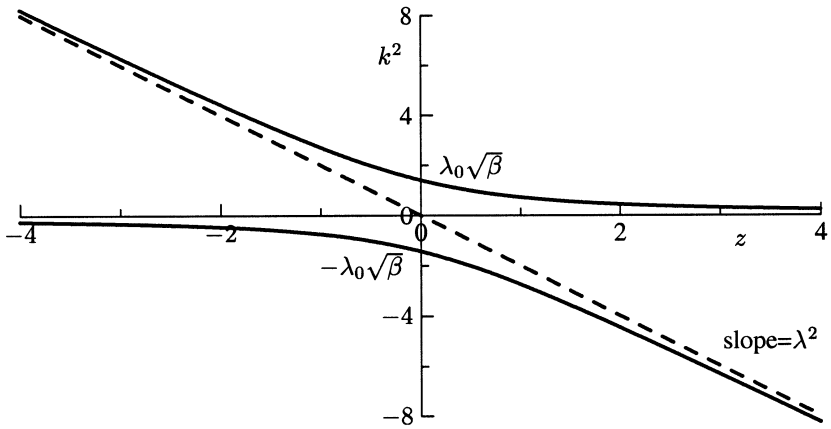


Figure D.8. Dispersion relation for $\lambda^2 < 0$ for Wasow equation with $\lambda^2 = -2$, $\beta = 1$.

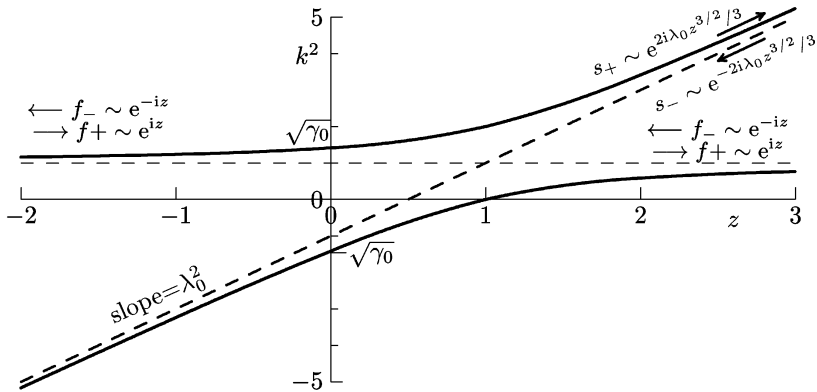


Figure D.9. Dispersion relation for $\lambda^2 < 0$ and $1 + \gamma < 0$ for the tunneling equation with $\lambda^2 = -2$, $\gamma = -2$.

or

$$T_1^2 = 1 + C_1^2 / (1 - e^{-2\eta}) = 1 + \rho C_1^2$$

so $\rho = (1 - e^{-2\eta})^{-1}$ as for solution y_2 .

Problem 6.3.4. Connection formulas for the case $\gamma < -1$. The solution equation (6.32) is still exact, but it is now convenient to use $\eta = \frac{\pi}{2}|1+\gamma|/\lambda^2 > 0$. But the location and orientation of the fast-wave saddle points is different. The saddle points are located where $h'(u_0) = 0$ with $u_0 = u_f, u_s$. Hence,

$$\tan u_f = \pm i \left(1 - \frac{2\eta}{\pi z} \right)$$

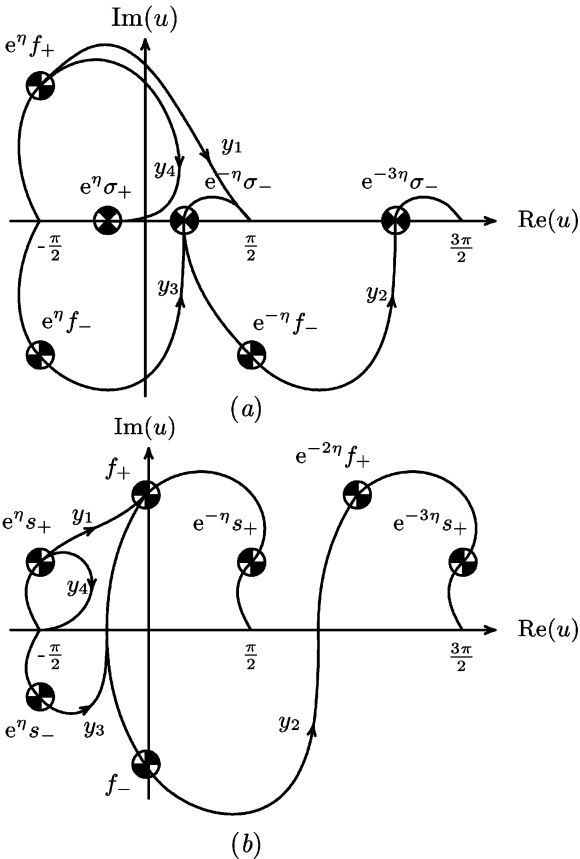


Figure D.10. Saddle points and asymptotic contours for solutions of the tunneling equation with $1+\gamma < 0$; (a) locations and paths as $z \rightarrow -\infty$; and (b) locations and paths as $z \rightarrow \infty$.

$$u_f = \begin{cases} n\pi \pm \frac{i}{2} \ln \left| \frac{4\lambda^2 z}{1+\gamma} \right| & z > 0 \\ (2n+1)\frac{\pi}{2} \pm \frac{i}{2} \ln \left(\frac{4\lambda^2 z}{1+\gamma} \right) & z < 0 \end{cases}$$

so that the saddle points and asymptotic contours for $z \rightarrow \pm\infty$ are given in figure D.10, and the corresponding solutions in table 6.3 and the coupling coefficients in table 6.4. In order to construct the relevant contours, it must be noted that e^{iz} is still incoming from the left and e^{-iz} is incoming from the right ($z > 0$). This is because switching from $x = -\alpha(z - z_0)$ switches both the phase velocity and the group velocity for the fast waves, but now the outgoing slow wave is s_+ .

Problem 6.3.5. The Wasow equation for $\lambda^2 > 0$.

(i) The exact solution is

$$y(z) = \int_C \exp\left(-ikz + \frac{ik^3}{3\lambda^2} - \frac{i\beta}{k}\right) \frac{1}{k^2} dk.$$

(ii) The end point condition is

$$\exp\left(-ikz + \frac{ik^3}{3\lambda^2} - \frac{i\beta}{k}\right) \Big|_C = 0$$

so the contours must end where $|k| \rightarrow \infty$ along the angles $\pi/6, 5\pi/6$, or $-\pi/2$ with an additional end point at the origin, approached along the positive imaginary axis (for $\beta > 0$). The contours are sketched in [figure D.11](#).

(iii) The saddle points are located approximately at $\pm i\sqrt{z}$ and at $\pm \sqrt{\beta/z}$ as $z \rightarrow \infty$ and at $\pm i\lambda\sqrt{|z|}$ and $\pm i\sqrt{\beta/|z|}$ as $z \rightarrow -\infty$ (see [figure D.12](#)).

(iv) The fast-wave saddle point contributions from $k_0 \simeq \pm \sqrt{\beta/z}$ are not accurate because of the singularity at the origin near the saddle point. Using the integral expression for the Hankel function [67]

$$H_1^{(2)}(x) = \frac{i}{\pi} \int_{-\infty}^{\infty-i\pi} e^{x \sinh t - t} dt$$

with suitable variable changes (let $k \rightarrow iu$ first, $0 < u < \infty$ for f_- , then neglect t^3 term in exponent (why?), and in the Hankel integral, let $t = \ln(2\tau/x)$, and compare), the result is

$$f_- = -\sqrt{z/\beta}\pi H_1^{(2)}\left(2\sqrt{\beta z}\right).$$

As $z \rightarrow -\infty$, the slow-wave saddle points at $k_0 = \pm i\lambda\sqrt{|z|}$ lead to

$$s_- = \frac{\sqrt{\pi}}{\lambda^{3/2}|z|^{5/4}} \exp\left(-\frac{2\lambda|z|^{3/2}}{3}\right)$$

$$s_+ = \frac{i\sqrt{\pi}}{\lambda^{3/2}|z|^{5/4}} \exp\left(\frac{2\lambda|z|^{3/2}}{3}\right)$$

respectively. For the fast wave contributions from $k_0 = \pm i\sqrt{\beta/z}$, the corresponding results vary as

$$f_+ \propto \sqrt{\beta|z|} I_1\left(2\sqrt{\beta|z|}\right) \quad \text{and} \quad f_- \propto \sqrt{\beta|z|} K_1\left(2\sqrt{\beta|z|}\right).$$

(v) For $z \rightarrow \infty$, f_- is an incoming fast wave and f_+ is outgoing. For the slow waves, s_- is outgoing and s_+ is incoming. As $z \rightarrow -\infty$, s_- and f_- are decaying away from the resonance and s_+ and f_+ are growing slow and fast waves respectively.

(vi) The contours are sketched in [figure D.12](#).

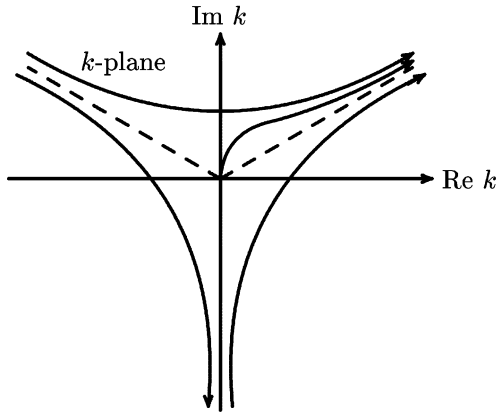


Figure D.11. Independent contours for the Wasow equation in the k -plane.

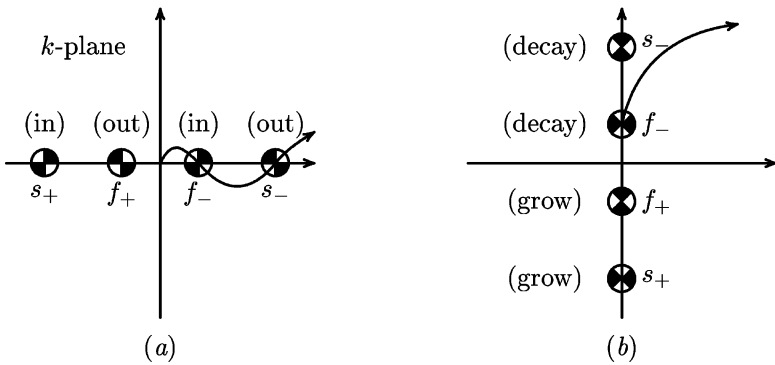


Figure D.12. Saddle points and contour for (a) $z \rightarrow \infty$ and (b) $z \rightarrow -\infty$.

Problem 6.3.9. The energy-conserving tunneling equation. As $k \rightarrow 0$, $\zeta \rightarrow \infty$, so $Z(\zeta) \rightarrow -1/\zeta = -kv_i/(\omega - 2\omega_{ci}) \rightarrow kv_i L/\omega x$.

(i) In this limit, factoring out kv_i/ω , the result is

$$E_y^{iv} - \frac{1}{x} E_y''' + \left[\frac{16(\frac{1}{3} + p^2)x}{\rho_L^2 L} - \frac{1}{Lx} + \frac{2\omega^2(\frac{1}{3} - p^2)}{V_A^2} \right] E_y'' - \frac{2\omega^2(\frac{1}{3} - p^2)}{V_A^2 x} E_y' + \frac{2\omega^2(\frac{1}{3} - p^2)}{V_A^2} \left[\frac{8(1 + p^2)x}{\rho_L^2 L} - \frac{1}{Lx} \right] E_y = 0$$

which still has all the odd derivative terms.

(ii) With $E_y = u\phi$, the differential equation becomes

$$\phi^{iv} + f_3\phi''' + f_2\phi'' + f_1\phi' + f_0\phi = 0$$

with

$$\begin{aligned}
 f_3 &= \left(\frac{4u'}{u} - \frac{1}{x} \right) \\
 f_2 &= \frac{6u''}{u} - \frac{3u'}{ux} + \frac{16(\frac{1}{3} + p^2)x}{\rho_L^2 L} + \frac{2\omega^2(\frac{1}{3} - p^2)}{V_A^2} \\
 f_1 &= \frac{4u'''}{u} - \frac{3u''}{ux} + \frac{32(\frac{1}{3} + p^2)xu'}{\rho_L^2 Lu} + \frac{2\omega^2(\frac{1}{3} - p^2)}{V_A^2} \left(\frac{2u'}{u} - \frac{1}{x} \right) \\
 f_0 &= \frac{u^{iv}}{u} - \frac{u'''}{ux} + \frac{16(\frac{1}{3} + p^2)xu''}{\rho_L^2 Lu} + \frac{4\omega^2(\frac{1}{3} - p^2)}{V_A^2} \left(\frac{u''}{u} - \frac{u'}{xu} \right) \\
 &\quad + \frac{16\omega^2(1 + p^2)(\frac{1}{3} - p^2)x}{LV_A^2 \rho_L^2}
 \end{aligned}$$

so we require $u'/u = 1/4x$ so that $u = x^{1/4}$.

(iii) Changing variables to $z - z_0 = \mu x \omega / V_A$, this becomes

$$\phi^{iv} + \lambda^2 z \phi'' + \frac{1}{2} \lambda^2 \phi' + (\lambda^2 z + \gamma) \phi \simeq 0$$

where terms in $(z - z_0)^{-1}$ or smaller have been discarded for the asymptotic equation. Note that even though the first and third derivative coefficients were asymptotically vanishing in the original equation for E_y , the substitution that formally eliminated the third derivative resulted in a nonvanishing coefficient for the first derivative term.

(iv) From the *Handbook of Plasma Physics* [71], we have the case with $\alpha = \frac{1}{2}$, and the fast and slow wave solutions vary as

$$s_- \sim (\lambda^2 z)^{\alpha/2} z^{-5/4} \exp\left(-i\frac{2}{3}\lambda z^{3/2}\right) \quad f_{\pm} \sim \left(\frac{1+\gamma}{\lambda^2 z}\right)^{\alpha/2} \exp(\pm iz)$$

so for the slow wave, $\phi \sim z^{-1} \exp(-2i\lambda z^{3/2}/3)$ so $E_y \sim z^{-3/4} \exp(-2i\lambda z^{3/2}/3)$. For the fast wave, since $\phi \sim z^{-1/4} \exp(\pm iz)$, then $E_y \sim \exp(\pm iz)$.

Problem 6.3.10. Kinetic flux and power conservation.

(i)

$$E_+ = \left[2 + \frac{1}{k^2 - \frac{\omega^2}{c^2} R} \frac{d^2}{dx^2} \right] i E_y.$$

(ii) From problem 6.3.9 and the result above, $E_+ \sim E_y'' \simeq z^{1/4} \exp(-2i\lambda z^{3/2}/3)$. Hence, $E_+'^* E_+ \sim z$ and since $K_H \sim 1/z$, then $E_+'^* K_H E_+ \sim \text{constant}$.

(iii) With $\alpha = 0$, $E_+ \sim E_y'' \simeq z^{-1/4} \exp(-2i\lambda z^{3/2}/3)$. Hence, $E_+'^* E_+ \sim \text{constant}$ and since $K_H \sim 1/z$, then $E_+'^* K_H E_+ \sim 1/z$.

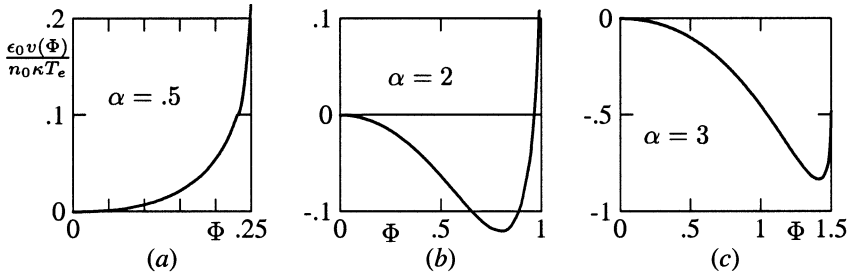


Figure D.13. $V(\Phi)$ versus Φ for (a) $\alpha = 0.5$, (b) $\alpha = 2.0$, and (c) $\alpha = 3.0$.

Problem 6.6.1. Drift instability growth rate.

- (iii) Maximum growth rate occurs when $\alpha_m = 4.12$.

Chapter 7 Weak turbulence theory

Problem 7.3.1. Plasma wave echo damping.

$$\frac{\gamma_2}{\gamma_3} = \frac{k_3^3}{k_2^3} \exp \left(\frac{1}{2k_2^2 \lambda_D^2} - \frac{1}{2k_3^2 \lambda_D^2} \right)$$

so since $k_2 \simeq 2k_3$,

$$\frac{\gamma_2}{\gamma_3} \simeq \frac{1}{8} \exp \left(\frac{3}{8k_3 \lambda_D^2} \right).$$

Since wave 2 is presumed to be weakly damped, $1/2k_2^2 \lambda_D^2 > 8$ so $1/8k_3^2 \lambda_D^2 > 8$, and $\gamma_2/\gamma_3 > 10^9$.

Chapter 8 Nonlinear plasma waves

Problem 8.2.1. The solitary wave ‘pseudopotential’. If we define $\Phi = e\phi/\kappa T_e$, then we may write the pseudopotential $v(\Phi)$ as

$$v(\Phi) = -\frac{n_0 \kappa T_e}{\epsilon_0} \left[\alpha \left(\sqrt{1 - \frac{2\Phi}{\alpha}} - 1 \right) + e^\Phi - 1 \right]$$

so we can plot v versus Φ for the three cases which are shown in figures D.13(a)–(c).

α_c must satisfy

$$-\alpha_c + e^{\alpha_c/2} - 1 = 0$$

whose root is $\alpha_c = 2.513$.

Problem 8.2.2. Small (but finite) amplitude solitary wave solution. $\ell = 2$, $\Delta = 2\lambda_D/\sqrt{1 - 1/\alpha(\Phi_m)}$, and $\Phi_m = e\phi_m/\kappa T_e = 3\alpha(\alpha - 1)/(3 - \alpha^2)$ with $1 < \alpha^2 < 3$, or inverting,

$$\alpha(\Phi_m) = \frac{1 + \sqrt{1 + 4\Phi_m(1 + \Phi_m/3)}}{2(1 + \Phi_m/3)}$$

so that $U = c_s \sqrt{\alpha(\Phi_m)}$.

Problem 8.2.4. Ion acoustic solitons.

- (ii) $k = \sqrt{A/6}$, $U = A/3$.
- (iii) $\phi = \phi_m \operatorname{sech}^2[K(x - vt)]$ with $v = c_s/(1 - \Phi_m/3)$, $K = \sqrt{\Phi_m/6}(1 - \Phi_m/3)/\lambda_D$.

References

- [1] Jeffreys H 1923 *Proc. London Math. Soc.* **23** 428
- [2] Wentzel G 1926 *Z. Phys.* **38** 518
Kramers H A 1926 *Z. Phys.* **39** 828
Brillouin L *Comput. Rend.* **183** 24
- [3] Appleton E V 1928 *URSI Proc., Washington Assembly (Brussels)*
- [4] Appleton E V 1932 *J. Inst. Electr. Engr.* **71** 642
- [5] Gillmor C and Stewart 1982 *Proc. Am. Phil. Soc.* **126** 395
- [6] Stix T H 1962 *The Theory of Plasma Waves* (New York: McGraw-Hill)
- [7] Astrom E O 1950 *Arkiv. Fysik* **2** 443
- [8] Allis W P 1959 *Sherwood Conf. Contr. Fusion, Gatlinburg* p 32
See also Allis W P, Buchsbaum S J and Bers A 1962 *Waves in Plasmas* (New York: Wiley)
- [9] Alfvén H 1950 *Cosmical Electrodynamics* (New York: Oxford University Press)
- [10] Barkhausen H 1919 *Physik. Z.* **20** 401
- [11] Barkhausen H 1930 *Proc. IRE* **18** 1155
- [12] Kuehl H H 1962 *Phys. Fluids* **5** 1095
1973 *Phys. Fluids* **16** 1311
- [13] Fisher R K and Gould R W 1969 *Phys. Rev. Lett.* **22** 1093
1971 *Phys. Fluids* **14** 857
- [14] Swanson D G 1996 ‘Plasma Waves and Instabilities’ *Encyclopedia of Applied Physics* vol 14 (New York: VCH) p 237
- [15] Bohm D and Gross E P 1949 *Phys. Rev.* **75** 1851
- [16] Stringer T E 1963 *Plasma Physics (J. Nucl. Energy)* C **5** 89
- [17] Braginskii S I 1957 *Sov. Phys. Dokl.* **2** 345
- [18] Braginskii S I 1965 *Review of Plasma Physics* vol 1, ed M A Leontovich (New York: Consultants Bureau) p 205
- [19] Twiss R Q 1951 *Proc. Phys. Soc. B* **64** 654
1952 *Phys. Rev.* **88** 1392
- [20] Landau L D and Lifshitz E M 1953 *Electrodynamics of Continuous Media* (Moscow: GITTL) p 141 (in Russian only)
- [21] Sturrock P A 1958 *Phys. Rev.* **112** 1488
- [22] Briggs R J 1964 *Electron-Stream Interaction with Plasmas* (Cambridge: MIT Press)
- [23] Johnson H R 1955 *Proc. IRE* **43** 684
- [24] Montgomery D C and Tidman D A 1964 *Plasma Kinetic Theory* (New York: McGraw-Hill)
- [25] Vlasov A A 1945 *J. Phys. (USSR)* **9** 25

- [26] Spitzer L 1956 *Physics of Fully Ionized Gases* (New York: Interscience)
- [27] Krall N A and Trivelpiece A W 1973 *Principles of Plasma Physics* (New York: McGraw-Hill)
- [28] Balescu R 1960 *Phys. Fluids* **3** 52
Lenard A 1960 *Ann. Phys., NY* **3** 390
Rostoker N and Rosenbluth M N 1960 *Phys. Fluids* **3** 1
- [29] Hinton F L 1983 *Handbook of Plasma Physics* vol 1, ed A Galeev and R N Sudan (Amsterdam: North-Holland) p 147
- [30] Bogolyubov N N 1946 *Problems of a Dynamical Theory in Statistical Physics* (Moscow: State Technical Press) (also included in deBoer J and Uhlenbeck G E (eds) 1962 *Studies in Statistical Mechanics I* (Amsterdam: North-Holland)
Born M and Green H S 1949 *A General Kinetic Theory of Liquids* (London: Cambridge University Press)
Kirkwood J G 1946 *J. Chem. Phys.* **14** 180
1947 *J. Chem. Phys.* **15** 72
Yvon J 1935 *La Théorie des Fluides et l'équation d'état; Actualités Scientifiques et Industrielles* (Paris: Hermann)
- [31] Fried B D and Conte S D 1961 *The Plasma Dispersion Function* (New York: Academic)
- [32] Stubbe P and Sukhorukov A I 1999 *Phys. Plasmas* **6** 2976
- [33] Landau L D 1946 *J. Phys. (USSR)* **10** 25
- [34] Malmberg J H and Wharton C B 1964 *Phys. Rev. Lett.* **13** 184
- [35] Stubbe P 1990 *Phys. Fluids B* **2** 22
- [36] Meyer E and Sessler G 1957 *Z. Phys.* **149** 15
- [37] Hammett G W and Perkins F W 1990 *Phys. Rev. Lett.* **64** 3019
- [38] Lenard A and Bernstein I B 1958 *Phys. Rev.* **112** 1456
- [39] Short R W and Simon A 2002 *Phys. Plasmas* **9** 3245
- [40] Ng C S, Bhattacharjee A and Skiff F 1999 *Phys. Rev. Lett.* **83** 1974
- [41] Drummond J E 1958 *Phys. Rev.* **110** 293
- [42] Sagdeev R Z and Shafranov V D 1958 *Proc. 2nd Int. Conf., (Geneva)* **31** 118
- [43] Rosenbluth M N and Rostoker R 1958 *Proc. 2nd Int. Conf., (Geneva)* **31** 144
- [44] Newberger B S 1982 *J. Math. Phys.* **23** 1278
1983 *J. Math. Phys.* **24** 2250(E)
- [45] Bernstein I B 1958 *Phys. Rev.* **109** 10
- [46] 1962 *The Theory of Plasma Waves* (New York: McGraw-Hill) p 240
1958 *Phys. Fluids* **1** 308
Stix T H and Palladino R W 1958 *Proc. 2nd Int. Conf., Geneva* **31** 282
- [47] Yamoto H, Iiyoshi A, Rothman M A, Sinclair R M and Yoshikawa S 1967 *Phys. Fluids* **10** 756
- [48] Trubnikov B A 1959 *Plasma Physics and the Problem of Controlled Thermonuclear Reactions* vol III, ed M A Leontovich (Oxford: Pergamon) p 122
- [49] Brambilla M 1998 *Kinetic Theory of Plasma Waves* (Oxford: Clarendon) p 138
- [50] Dnestrovskii Yu N, Kostomarov D P and Skrydlov N V 1964 *Sov. Phys.–Tech. Phys.* **8** 691
- [51] Shkarofsky I P 1966 *Phys. Fluids* **9** 561
- [52] Swanson D G 2002 *Plasma Phys. Control. Fusion* **44** 1329
- [53] Tonks L 1931 *Phys. Rev.* **37** 1458
- [54] Trivelpiece A W and Gould R W 1959 *J. Appl. Phys.* **30** 1784

- see also Krall N A and Trivelpiece A W 1973 *Principles of Plasma Physics* (New York: McGraw-Hill)
- [55] Swanson D G, Gould R W and Hertel R H 1964 *Phys. Fluids* **7** 269
- [56] Jephcott D F and Malein A 1964 *Proc. R. Soc. A* **28** 243
- [57] Allis W P, Buchsbaum S J and Bers A 1963 *Waves in Anisotropic Plasmas* (Cambridge, MA: MIT Press)
- [58] Dattner A 1957 *Ericsson Technics* **2** 309
1963 *Ericsson Technics* **8** 1
- [59] Parker J V, Nickel J C and Gould R W 1964 *Phys. Fluids* **7** 1489
- [60] Baldwin D E 1969 *Phys. Fluids* **12** 279
- [61] Gould R W 1959 *Proc. of the Linde Conf. on Plasma Oscillations, Indianapolis*
See also 1960 *Bull. Am. Phys. Soc.* **5** 322
- [62] Lehnert Bo 1954 *Phys. Rev.* **94** 815
- [63] Wilcox J M, Boley F I and De Silva A W 1960 *Phys. Fluids* **3** 15
Wilcox J M, De Silva A W and Cooper III W S 1961 *Phys. Fluids* **4** 1506
- [64] Takahashi H 1977 *J. Physique* **38** Coll. C6 171
- [65] Paoloni F J 1975 *Phys. Fluids* **18** 640
- [66] Kuehl H H, Stewart G E and Yeh C 1965 *Phys. Fluids* **8** 723
- [67] Abramowitz M and Stegun I 1964 *Handbook of Mathematical Functions* (Washington, DC: National Bureau of Standards)
- [68] Stix T H 1965 *Phys. Rev. Lett.* **15** 878
- [69] Wasow W 1950 *Ann. Math.* **52** 350
- [70] Rabenstein A L 1958 *Arch. Ration. Mech. Anal.* **1** 418
- [71] Stix T H and Swanson D G 1983 *Handbook of Plasma Physics* vol 1, ed A Galeev and R A Sudan (Amsterdam: North Holland) p 335
- [72] Budden K G 1961 *Radio Waves in the Ionosphere* (Cambridge: Cambridge University Press)
- [73] Swanson D G 1985 *Phys. Fluids* **28** 2645
- [74] Erokhin N S 1969 *Ukr. Fiz. Zh.* **14** 2055
reviewed by Erokhin N S and Moiseev S S 1979 *Reviews of Plasma Physics* vol 7, ed M A Leontovich (New York: Consultants Bureau) p 181
- [75] Ngan Y C and Swanson D G 1977 *Phys. Fluids* **20** 1920
- [76] Faulconer D W 1980 *Phys. Lett. A* **75** 355
- [77] Gambier D J D and Schmitt J P M 1983 *Phys. Fluids* **26** 2200
Gambier D J and Swanson D G 1985 *Phys. Fluids* **28** 145
- [78] Cairns R A and Lashmore-Davies C N 1983 *Phys. Fluids* **26** 1268
- [79] Swanson D G and Shvets V F 1963 *J. Math. Phys.* **50** 163
- [80] Swanson D G 1998 *Theory of Mode Conversion and Tunneling in Inhomogeneous Plasmas* (New York: Wiley)
- [81] Swanson D G 2002 *Phys. Plasmas* **9** 2854
- [82] Park H, Lee P S, Peebles W A and Luhmann N C Jr 1984 *Phys. Rev. Lett.* **52** 1609
- [83] Jacquinot J, McVey B D and Scharer J E 1977 *Phys. Rev. Lett.* **39** 88
- [84] Kuehl H H 1967 *Phys. Rev.* **154** 124
Kuehl H H, O'Brien B B and Stewart G E 1970 *Phys. Fluids* **13** 1595
- [85] Swanson D G 1981 *Phys. Fluids* **24** 2035
- [86] Colesstock P L and Kashuba R J 1983 *Nucl. Fusion* **23** 763
- [87] Bekefi G 1966 *Radiation Processes in Plasmas* (New York: Wiley)
- [88] Swanson D G and Cho Suwon 1989 *Phys. Rev. Lett.* **63** 1386

- [89] Weinberg S 1962 *Phys. Rev.* **126** 1899
- [90] Bernstein I B 1975 *Phys. Fluids* **18** 320
- [91] Mikhailovskii A B 1983 *Handbook of Plasma Physics* vol 1, ed A Galeev and R N Sudan (Amsterdam: North Holland) p 587
- [92] Krall N A 1968 *Advances in Plasma Physics* vol 1, ed A Simon and W B Thompson (New York: Interscience) p 153
- [93] Drummond W E and Pines D 1962 *Nucl. Fusion Suppl.* **3** 1049
- [94] Vedenov A A, Velikhov E P and Sagdeev R Z 1961 *Nucl. Fusion* **1** 82
1962 *Nucl. Fusion Suppl.* **2** 423
- [95] Kadomtsev B B 1966 *Plasma Turbulence* (London: Academic)
1964 *Voprosy Teorii Plasmy* ed M A Leontovich (Moscow: Atomizdat) p 188
- [96] Kennel C F and Fengelmann F 1966 *Phys. Fluids* **9** 2377
- [97] Davidson R C 1972 *Nonlinear Plasma Theory* (New York: Academic)
- [98] Galeev A A and Sagdeev R Z 1983 *Handbook of Plasma Physics* vol 1, ed A Galeev and R N Sudan (Amsterdam: North-Holland) p 677
- [99] Landau L 1936 *Phys. Z. Sowjetunion* **10** 154
- [100] Gould R W, O'Neil T M and Malmberg J H 1967 *Phys. Rev. Lett.* **19** 219
O'Neil T M and Gould R W 1968 *Phys. Fluids* **11** 134
- [101] Malmberg J H, Wharton C B, Gould R W and O'Neil T M 1968 *Phys. Fluids* **11** 1147
- [102] Ablowitz M and Segur H 1981 *Solitons and the Inverse Scattering Transform* (Philadelphia: SIAM)
- [103] Lamb G L 1980 *Elements of Soliton Theory* (New York: Wiley)
- [104] Washimi H and Taniuti T *Phys. Rev. Lett.* **17** 996
- [105] Gardner C S and Morikawa G K 1960 Rep. NYU-9082 (Courant Inst. of Math. Sci., New York University)
- [106] Morton K W 1964 *Phys. Fluids* **7** 1800
- [107] Zakharov V E and Shabat A B 1972 *Sov. Phys.-JETP* **34** 62
- [108] Morales G J, Lee Y C and White R B 1974 *Phys. Rev. Lett.* **32** 457
- [109] Kaup D J 1988 *Phys. Fluids* **31** 1465
- [110] O'Neil T M 1965 *Phys. Fluids* **8** 2255
- [111] Palmadesso P and Schmidt G 1971 *Phys. Fluids* **14** 1411
- [112] Oei I H and Swanson D G 1972 *Phys. Fluids* **15** 2218
- [113] Canosa J and Gazdag J 1974 *Phys. Fluids* **17** 2030
- [114] Morales G J and O'Neil T M 1972 *Phys. Rev. Lett.* **28** 417
- [115] Bernstein I B, Greene J M and Kruskal M D 1957 *Phys. Rev.* **108** 546
- [116] Lord Rayleigh 1883 *Phil. Mag.* **15** 229
- [117] Kaw P K, Kruer W L, Liu C S and Nishikawa Kyoji 1976 *Advances in Plasma Physics* vol 6, ed A Simon and W B Thompson (New York: Interscience) pp 1–269
- [118] Ichimaru S 1973 *Basic Principles of Plasma Physics* (Reading, MA: Benjamin)
- [119] Lazzaro E, Ramponi G and Giruzzi G 1982 *Phys. Fluids* **25** 1220
- [120] Bravo-Ortega A 1988 *PhD Thesis* Auburn University